FENDER FORCES IN SHIP BERTHING

Part I: Text

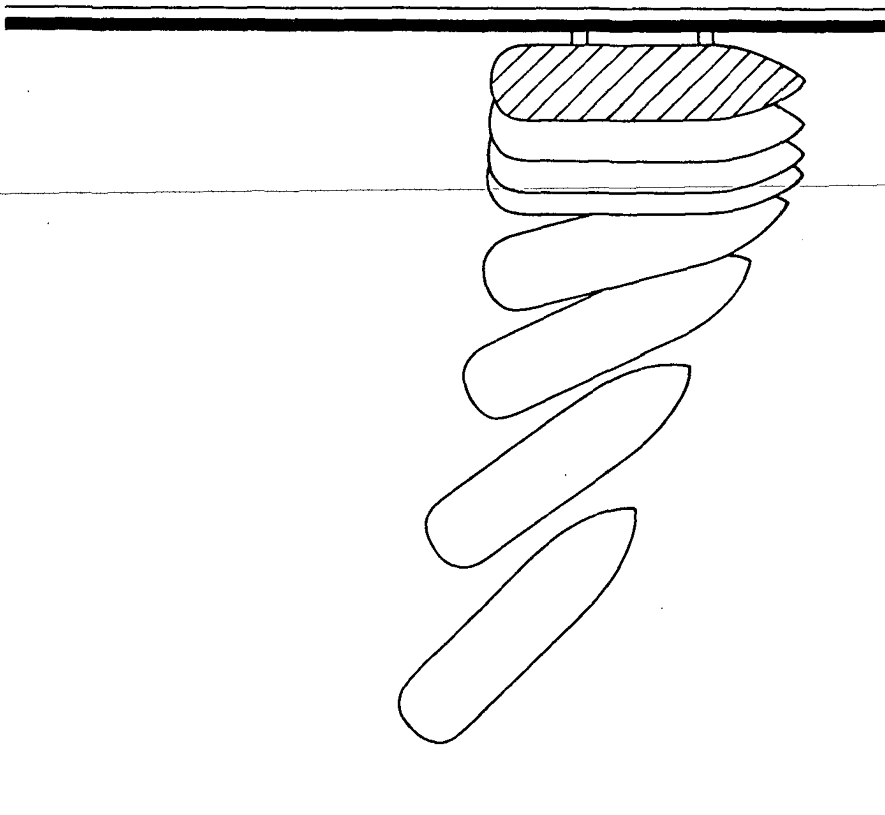

H. L. Fontijn

This thesis is also published in the series 'Communications on Hydraulic and Geotechnical Engineering' of the Department of Civil Engineering, Delft University of Technology, as Report No. 88-2.

FENDER FORCES IN SHIP BERTHING

Part I: Text

Proefschrift

ter verkrijging van de graad van doctor aan de Technische Universiteit Delft, op gezag van de Rector Magnificus, prof. drs. P. A. Schenck, in het openbaar te verdedigen ten overstaan van een commissie door het College van Dekanen daartoe aangewezen, op donderdag 15 december 1988 te 14.00 uur, door

Henri Lodewijk Fontijn,

geboren te Amsterdam,
civiel ingenieur.

Dit proefschrift is goedgekeurd door de promotor
prof. dr. ir. J. P. Th. Kalkwijk

Meae meisque

ABSTRACT

Mathematical formulations are presented that aim at describing the behaviour of a ship berthing to an open or closed structure and at predicting the related fender forces. To both berthing situations the impulse-reponse-function technique is applied requiring a linear and time-invariant ship-fluid system. In case of the closed berth also a direct-time approach is used, in which non-linearities can be taken into account. Both approaches enable the inclusion of arbitrary external forces and -maintaining all essential features- produce results of sufficient accuracy for practical applications. For verification experiments were carried out on a scale model. Comparison of theory and experiments shows a satisfactory agreement for the method(s) applied.

CONTENTS (part I)

CONTENTS (part II)

SUMMARY

This study deals with the behaviour of a ship berthing to a fender structure and the related fender forces. A mathematical formulation is applied containing all essential features and yielding quantitative results of sufficient accuracy for most practical applications. The investigation was actuated by the fact that theoretically founded criteria for designing berthing facilities are hardly available.
Two principal types of berthing structure can be distinguished, viz. the open berth (jetty type) and the closed berth (quay-wall), either fitted with fenders. The open berth does not interfere with flow and pressure fields around the ship, the closed berth does.

The method developed is based on a time-domain approach in which the fluid reactive forces are represented appropriately and the remaining forces are taken into account over their entire time histories (Section 1). The combination of ship and fluid is conceived as a linear system with time-independent properties; the external forces upon the ship may be non-linear and of arbitrary nature. The linear ship-fluid system can be described both in the frequency domain and in the time domain; these representations are equivalent and related by Fourier transforms. For the present investigation use is made of the i(mpulse) r(esponse) f(unction)-technique.

In Section 2 the i.r.f.-technique as related to ship motions is dealt with in a general mathematical formulation. The forcing function(s) (e.g. fender forces) act as input signal(s) and the ship motion as output signal. The coupling between the respective modes of motion is taken into consideration. The linearity concept implies that merely small ship motions are considered with respect to an initial state of equilibrium (i.e. rest or uniform motion). The requirement of stability of the system leads to a choice of the velocity as output signal.
A description is given of the ship-fluid system in the frequency domain. The fluid reactive effects are represented by the hydrodynamic coefficients, which -because of the free water-surface- are frequency dependent and define the frequency response function (f.r.f.). This frequency dependence reflects the 'memory effect' of the system and generates a time-domain description containing convolution integrals. In the time domain the ship-fluid system is fully characterized by the i.r.f.

Section 3 deals with ship berthing to an open structure fitted with one single fender without mass of its own. The fender characteristics are represented by a (non-)linear, undamped spring. The ship is schematized to a rigid, prismatic body with a rectangular cross-section and a symmetrical distribution of mass. During the berthing operation the ship has a zero forward speed and the transverse velocity of approach towards the berth is constant. Both centric and eccentric impacts are considered. The i.r.f.-technique now is applied to the horizontal modes of motion (swaying and yawing) of the schematized ship in (shallow) water with relatively large horizontal dimensions.
Since the description of transient ship motions in the time domain requires knowledge of the i.r.f., which are related to the f.r.f., first of all the hydrodynamic coefficients are determined, theoretically -applying strip theory- as well as experimentally. For moderate to high frequencies the agreement between theory and experiments is satisfactory; the differences occurring in the lower-frequency range are accounted for and the values of the hydrodynamic coefficients are adapted.
With the hydrodynamic coefficients known the corresponding i.r.f. are calculated.
Then the mathematical model to simulate the berthing operation and to determine the relevant related quantities is presented. To examine its adequacy an extensive series of (model) experiments was carried out. For the numerical simulation typical test situations were selected. Generally it holds good that the agreement between theory and experiment is satisfactory.

The berthing of a ship to a closed structure is dealt with in Section 4. The berthing facility consists of a straight, impervious, vertical wall, fitted with one single fender of the same type as at the open berth. The ship is schematized in the same way as before. In berthing it maintains a lateral motion with its longitudinal axis of symmetry parallel to the face of the berth; the forward speed is zero and the transverse velocity of approach towards the berth is constant. This implies a centric impact in which only the sway motion plays a part.
A set of governing equations is formulated describing -in the time domain- the transverse motion of the schematized ship in shallow water at zero forward speed, alongside of and parallel to a vertical wall. In order to solve these governing equations two procedures are followed.
The first approach, requiring a linearization, makes use of the i.r.f.-technique. The hydrodynamic coefficients are determined theoretically as well as

experimentally. The agreement between theory and experiment is satisfactory; the influence of the underkeel friction appears to be significant. Then the corresponding i.r.f. are calculated, after which the berthing can be simulated theoretically. For verification again (model) tests were carried out. Comparison of theory and experiments shows that application of the i.r.f.-technique leads to satisfactory results only if underkeel friction is incorporated in the hydrodynamic coefficients.

In the second procedure, being a 'direct-time approach' (d.t.a.), the influence of non-linearities can be evaluated. The governing equations are simplified to a two-dimensional situation (strip theory) and solved directly in the time domain. The d.t.a. presents a satisfactory agreement between theory and experiment provided that the underkeel friction, at least, is modelled properly. In general, the influence of the non-linearities is small.

Finally, Section 5 resumes the most important conclusions.

SAMENVATTING

Krachten op fenders t.g.v. het afmeren van schepen

Deze studie gaat over het afmeren van een schip en de daarbij optredende fenderkrachten. Er wordt een mathematische formulering gebruikt die alle essentiële elementen bevat en voor de meeste practische toepassingen voldoend nauwkeurige resultaten oplevert. De aanleiding voor het onderzoek werd gevormd door het feit dat theoretisch gefundeerde criteria voor het ontwerpen van afmeerfaciliteiten nauwelijks beschikbaar zijn.

In principe kan er onderscheid worden gemaakt tussen twee typen afmeervoorzieningen, te weten open constructies (steigers) en gesloten constructies (kademuren), beide voorzien van fenders. De open afmeerconstructie interfereert niet met de stroming en de drukken rondom het schip, de gesloten afmeerconstructie wel.

De ontwikkelde methode is gebaseerd op een aanpak in het tijdsdomein, waarbij de reactiekrachten van de vloeistof op passende wijze worden weergegeven en de overige krachten in rekening worden gebracht over hun gehele tijdsverloop (Hoofdstuk 1). De combinatie schip-vloeistof wordt opgevat als een lineair systeem met tijdsonafhankelijke eigenschappen; de externe krachten op het schip mogen niet-lineair zijn en een willekeurig karakter hebben. Het lineaire schip-vloeistof systeem kan zowel in het frequentiedomein beschreven worden als in het tijdsdomein; deze voorstellingswijzen zijn equivalent en gerelateerd via Fourier-transformaties. Voor het huidige onderzoek wordt gebruik gemaakt van de i(mpuls)r(espons)f(unctie)-techniek.

In Hoofdstuk 2 wordt de i.r.f.-techniek betrokken op scheepsbewegingen en in algemene zin mathematisch geformuleerd. De krachtfuncties (e.g. fenderkrachten) fungeren als ingangssignalen en de scheepsbeweging als uitgangssignaal. De koppeling tussen de respectieve bewegingsvormen wordt in aanmerking genomen. Het lineariteitsconcept houdt in dat alleen kleine scheepsbewegingen worden beschouwd t.o.v. een initiële evenwichtstoestand (i.e. rust of eenparige beweging). De vereiste stabiliteit van het systeem leidt ertoe dat de snelheid als uitgangssignaal wordt gekozen.

Er wordt een beschrijving gegeven van het systeem schip-vloeistof in het frequentiedomein. De reactie van de vloeistof komt tot uiting in de hydrodynamische coëfficiënten, die -vanwege het vrije wateroppervlak- frequentie-afhankelijk zijn en de frequentieresponsfunctie (f.r.f.) bepalen. Deze frequentie-

afhankelijkheid geeft het 'geheugeneffect' van het systeem weer en genereert een beschrijving in het tijdsdomein die convolutie-integralen bevat. In het tijdsdomein wordt het systeem schip-vloeistof volledig gekarakteriseerd door de i.r.f.'s.

Hoofdstuk 3 gaat over het afmeren van een schip aan een open constructie voorzien van een enkele fender zonder eigen massa. De fenderkarakteristieken worden weergegeven door een (niet-)lineaire, ongedempte veer. Het schip wordt geschematiseerd tot een onvervormbaar, prismatisch lichaam met een rechthoekige dwarsdoorsnede en een symmetrische massaverdeling. Tijdens de afmeeroperatie heeft het schip geen voorwaartse snelheid en is de dwarsscheepse snelheid waarmee de fenderconstructie genaderd wordt, constant. Er worden zowel centrische als excentrische botsingen beschouwd. De i.r.f.-techniek wordt nu toegepast op de horizontale bewegingsvormen (verzetten en gieren) van het geschematiseerde schip op (ondiep) water met relatief grote horizontale afmetingen.
Aangezien voor de beschrijving van kortdurende scheepsbewegingen in het tijdsdomein kennis vereist is van de i.r.f.'s, die weer gerelateerd zijn aan de f.r.f.'s, worden allereerst de hydrodynamische coëfficiënten bepaald; dit gebeurt zowel theoretisch -met toepassing van de striptheorie- als experimenteel. Voor middelmatige tot hoge frequenties is de overeenstemming tussen theorie en experimenten bevredigend; de verschillen die voorkomen bij lagere frequenties worden verklaard en de waarden van de hydrodynamische coëfficiënten aangepast.
Nu de hydrodynamische coëfficiënten bekend zijn, worden de bijbehorende i.r.f.'s berekend.
Dan volgt de presentatie van het mathematische model om de afmeeroperatie te simuleren en de daarmee verband houdende relevante grootheden te bepalen. De geschiktheid ervan is onderzocht aan de hand van een uitgebreide serie (model)experimenten. Voor de numerieke simulatie zijn karakteristieke proefsituaties uitgekozen. In het algemeen geldt dat de overeenstemming tussen theorie en experiment bevredigend is.

Het afmeren van een schip aan een gesloten constructie wordt behandeld in Hoofdstuk 4. De afmeerfaciliteit bestaat uit een rechte, ondoorlatende, verticale wand, met een enkele fender van hetzelfde type als bij de open afmeerconstructie. Het schip is op identieke wijze geschematiseerd als in het voorgaande. Bij het afmeren handhaaft het een laterale beweging met zijn longitudinale symmetrie-as evenwijdig aan de voorzijde van de afmeerconstruc-

tie; de voorwaartse snelheid is nul en de dwarsscheepse snelheid waarmee het de afmeerconstructie nadert is constant. Dit impliceert een centrische botsing, waarbij alleen de verzetbeweging een rol speelt.
Er wordt een stelsel basisvergelijkingen geformuleerd dat in het tijdsdomein -bij afwezigheid van voorwaartse snelheid- de dwarsscheepse beweging van het geschematiseerde schip beschrijft op ondiep water, langszij en evenwijdig aan een verticale wand. Om deze basisvergelijkingen op te lossen worden twee werkwijzen gevolgd.
De eerste aanpak, die een linearisering vereist, maakt gebruik van de i.r.f.-techniek. De hydrodynamische coëfficiënten worden zowel theoretisch als experimenteel bepaald. De overeenstemming tussen theorie en experiment is bevredigend; de invloed van de wrijving in het gebied onder het schip blijkt belangrijk te zijn. Vervolgens worden de bijbehorende i.r.f.'s berekend, waarna het afmeren theoretisch gesimuleerd kan worden. Ter verificatie zijn wederom (model)proeven uitgevoerd. Vergelijking van theorie en experimenten laat zien dat toepassing van de i.r.f.-techniek alleen tot bevredigende resultaten leidt, indien de invloed van de wrijving onder het schip in de hydrodynamische coëfficiënten wordt verwerkt.
De tweede werkwijze is een 'directe tijdsdomein-aanpak' (d.t.a.) en maakt het mogelijk om de invloed van niet-lineariteiten te evalueren. De basisvergelijkingen worden vereenvoudigd tot een tweedimensionale situatie (striptheorie) en rechtstreeks opgelost in het tijdsdomein. De d.t.a. vertoont een bevredigende overeenstemming tussen theorie en experiment, op voorwaarde dat de wrijving onder het schip op passende wijze wordt gemodelleerd. In het algemeen is de invloed van niet-lineariteiten klein.

Tot slot worden in Hoofdstuk 5 de belangrijkste conclusies samengevat.

1. INTRODUCTION

1.1. General description of berthing-ship phenomenon

During the last decades ships have grown larger and larger. As a consequence berthing facilities had to be newly constructed or adapted to the larger units. Nowadays, mainly for economical reasons, the growth of ship's dimensions appears to have come to an end.

With respect to the construction of berthing facilities, the increased proportions in shipping necessitate the application of reliable, theoretically founded design criteria. However, up to now these are hardly available. The investigation to be presented was primarily actuated by the lack of good design criteria, and as such it deals with the experimental and/or theoretical determination of berthing forces.

Generally a berthing facility consists of one or more elastic elements (fenders) attached to a rigid structure (finger pier, caisson-type jetty, quay-wall, etc.). The fenders absorb the berthing forces and form a protection for ship and berthing structure. As the maximum permissible berthing force against the side of e.g. a mammoth tanker is distinctly lower than what is acceptable for the berthing structure, the ship is therefore the prevailing factor for fender design. Ref. [1] gives a review of various types of open berthing structures; besides it presents a classification of the countless systems of fenders with special regard to their properties and applicabilities. For an inventory of fender systems it further is referred to ref. [2].

The phenomena occurring during the berthing manoeuvre of a ship are complicated and the fender loads are influenced by a lot of parameters: the configuration of the berthing site, the geometry and the rigidity of the (hull of the) ship, the mechanical properties of the fender(s), the speed of approach, the forces exerted by tugs, wind, current and waves, the mode of motion (in general translation in the horizontal plane combined with rotation), the keel clearance.

In ref. [2] some information can be found on ship-berthing manoeuvres.

As far as the lay-out of the berthing site is concerned, two situations can be distinguished:

a - a situation of water with relatively large horizontal dimensions; this implies an open jetty-type berthing facility, which is supposed not to interfere with flow and pressure fields around the ship; and b - a situation with a closed berth, i.e. a berthing structure with a solid front; now the berth does interfere with the flow and pressure fields around the ship, so that the hydrodynamic phenomena are more complicated than in the situation mentioned sub a.

The laterally moving ship pushes ahead of itself a positive pressure field, more or less noticeable as a raised water level. In case of a closed berth this pressure field is reflected by the solid front of the structure, further raising the water level between ship and wall. The rise in water level becomes larger the nearer the ship gets to the berth. When the ship slows down and stops on the berth, the underkeel flow, which keeps going for a time, sucks water out of the gap between berth and ship (i.e. the quay clearance) thus drawing down the water level there. In case of a berthing structure with a solid front there thus appears to be two opposing effects:

1) as the ship closes on the berth, the reflected pressure wave increasingly cushions the impact by raising the water level in the quay clearance,
2) as the ship slows down on the fender, the inertia of the underkeel flow draws down the water level in the quay clearance and 'sucks' the ship harder onto the berth.

In advance it is not simply clear which effect will dominate: it requires careful analytical and experimental research to establish the net effect on ship motions and fender loads.

The behaviour of a berthing ship and the resulting fender loads can be determined beforehand either by means of experiments with scale models or by way of an analytical treatment of the phenomenon. Of course a combination of both methods is possible as well.

On the one hand model testing has a few drawbacks. Model tests are expensive and time consuming. The test set-up is complicated; it is essential that the elastic properties of the fenders are simulated very carefully and, sometimes, sophisticated facilities are needed to simulate the relevant environmental conditions. For these reasons test programs are usually restricted to those final design configurations and selected conditions which are assumed to be the most critical. Besides, the insight gained from model tests into the fundamentals of the problem remains limited: only the resulting output is measured without yielding much knowledge of the mechanism which causes the output. On the other hand a general mathematical treatment of the problem is rather complicated.

1.2. Review of previous studies

When designing a berthing structure generally an approach is used in which it is assumed that the energy to be absorbed by the fender(s) equals the kinetic energy of the ship. Usually the mode of motion of the ship then consists of a translation -with or without forward speed- combined with a rotation. To include the effect of the entrained water a certain constant added mass(-moment of inertia) is introduced (see e.g. refs. [1 through 29] for the open jetty-type berthing facility and refs. [1 through 4, 6, 8, 12, 15, 16, 23, 27, 29 through 34] for the closed berthing structure). This is also the case in refs. [35, 36] where, in addition, an account is given of research on the slowing down of a ship in approaching laterally a closed quay-wall. Refs. [2, 37] present a review of the most common expressions for the added mass. In this context, guidelines for fender-system design are given in ref. [2].

This approach, in fact, involves the use of Newton's second law

$$\frac{d}{dt}(m\dot{x}) = f(t) \quad , \tag{1.1^a}$$

describing the motion(s) x(t) of a freely floating ship with mass(-moment of inertia) m in response to some external force or moment f(t); t represents the time co-ordinate. Since m may be regarded as a constant, the equations of motion become:

$$m\ddot{x} = f(t) \quad . \tag{1.1^b}$$

In the following the concept 'force' has to be understood in a generalized sense meaning force or moment. In general the external force f(t) in ($1.1^{a,b}$) is composed of:

- forces, e.g. due to waves, varying arbitrarily in time,
- hydrodynamic and hydrostatic restoring forces, which are a function of the motion of the ship,
- (restoring) forces due to the fender and/or mooring system, which are a function of the instantaneous position of the ship.

In the classical theory of ship motions it is common practice to formulate the equations (of motion) as follows:

$$(m+a)\ddot{x} + b\dot{x} + cx = f(t) \quad , \tag{1.2}$$

where a is the added mass(-moment of inertia), b the hydrodynamic coefficient of the damping force and c the hydrostatic restoring coefficient; the coefficients a and b represent the hydrodynamic effects. (1.2) has the form of a linear differential equation of the second order with constant coefficients; due to its linear character it can only reflect linearized hydrodynamic phenomena.

Applying the assumption of linearity, it is obvious that a ship, under the action of a harmonically oscillating force at one specific frequency, will perform a harmonic motion with the same frequency as that of the excitation. The distribution of the hydrodynamic stresses on the wet ship hull then also presents a harmonic behaviour with the same frequency. Experimentally and theoretically it can be shown that harmonic ship motions lead to frequency-dependent coefficients a and b, the so-called hydrodynamic coefficients; the coefficient c is considered to represent the hydrostatic restoring effects and is defined as being independent of the frequency (see e.g. refs. [38 through 66]. The frequency dependence of a and b only emerges, when a free water-surface is present; in absence of a free water-surface the hydrodynamic coefficients are constants. Therefore, it is stated that the occurrence of frequency dependence of the hydrodynamic coefficients can be completely ascribed to the existence of a boundary in the form of a free water-surface.

In Section 1.3 it will be shown that the introduction of hydrodynamic coefficients with a frequency-dependent behaviour generates a formulation in the time domain, which differs fundamentally from (1.2): instead of forces acting only instantaneously in time, now (also) a 'memory effect' appears on the scene, i.e. each occurrence becomes, in fact, dependent on all preceding occurrences. Actually the 'memory effect' reflects the dissipative property of the free water-surface (wave radiation), which can be illustrated as follows. Surface waves, once generated, continue to move about for a very long time; if the fluid were not viscous, they even would appear forever. On the other hand, in case of a body moving through an ideal fluid filling all space, all motion stops instantly if the body stops.

With frequency-dependent hydrodynamic coefficients (1.2) takes the form:

$$\{m+a(\omega)\}\ddot{x} + b(\omega)\dot{x} + cx = f(t) \quad , \tag{1.3}$$

where ω represents the circular frequency. (1.3) states that a harmonically oscillating excitation with $f(t) = \hat{f}\exp(i\omega t)$ has a harmonic response as well, viz. $x(t) = \hat{x}\exp(i\omega t)$; the circumflex means 'amplitude of', $i = \sqrt{-1}$. Now (1.3) is not any longer a real equation of motion in the sense that it relates the variables of the instantaneous motion to the instantaneous values of the exciting forces. On the contrary, (1.3) merely represents a set of algebraic equations fixing the amplitudes and phases of the (six) oscillations of the ship under the action of an exciting oscillating force at one specific frequency; in other words, this set of equations is valid only if the right-hand sides all vary sinusoidally at a single frequency and if the 'constant' coefficients a and b on the left have the values appropriate to that frequency. Therefore (1.3) can only be used as a representation in the frequency domain of a steady oscillating motion, since the hydrodynamic coefficients a and b depend on the frequency of the motion itself. Substitution of $f(t) = \hat{f}(\omega)\exp(i\omega t)$ and $x(t) = \hat{x}(\omega)\exp(i\omega t)$ into (1.3) yields an expression which has to be considered as a description of the ship-fluid system in the frequency domain:

$$\left[-\omega^2\{m+a(\omega)\} + i\omega b(\omega) + c\right]\hat{x}(\omega) = \hat{f}(\omega) \quad . \tag{1.4}$$

This can be rewritten as

$$R(\omega)\ \hat{x}(\omega) = \hat{f}(\omega) \tag{1.5}$$

with

$$R(\omega) = -\omega^2\{m+a(\omega)\} + i\omega b(\omega) + c \quad ; \tag{1.6}$$

$R(\omega)$ relates the harmonically oscillating excitation with its response. The analytical (and experimental) work dealing with the berthing of ships, as mentioned in refs. [1 through 36], in principle is based on (1.3). In these investigations the coefficient a is supposed to be independent of the frequency c.q. constant during the motion of the ship, while the coefficient b is neglected. Since berthing manoeuvres mainly take place in the horizontal plane, the hydrostatic restoring coefficient c is left out of consideration. (1.3) then reduces to a simplified form of (1.2):

$$(m+a)\ddot{x} = f(t) \quad . \tag{1.7}$$

(1.7) can be regarded as a differential equation, representing a set of equations of motion, which is only adequate to describe the motion of a body in a fluid without a free water-surface. However, when a free water-surface is present, (1.7) will yield incorrect results due to the non-negligible 'memory effect'. In (1.7) the hydrodynamic influences are reflected only by the constant added mass(-moment of inertia). Besides, the choice of a proper value for a is a problem, the more so as it appears from literature (see e.g. refs. [38 through 66]) that the hydrodynamic coefficients are very much dependent on the frequency, especially in shallow water and in the vicinity of a closed wall: generally it holds true that the concept of constant hydrodynamic coefficients is not justifiable. Consequently, to determine fender forces as a result of the berthing of a ship, a time-domain description of the behaviour of the moving ship is needed, which is able to make allowance for the frequency dependence of the fluid reaction forces, i.e. a method has to be used in which the hydrodynamic coefficients are taken into account as functions of the frequency.

1.3. The present research

1.3.1. Objective of investigation

The present investigation aims at the formulation of a mathematical model which is sufficiently accurate both to describe the behaviour of a ship berthing to an open jetty-type facility or a closed structure (either fitted with fenders) and to determine the response of the fenders themselves in a theoretical way; all essential features are to be maintained and quantitative results of sufficient accuracy are to be produced for most practical applications.

To achieve this end, a system approach is followed, which has the restriction that the combination of ship and fluid is supposed to be linear. In addition to the fender loads other (external) forces upon the ship, such as forces exerted by wind, waves, current, tugs and mooring lines can be incorporated in the model as well.

1.3.2. Ship-fluid system and linearity concept

When applying a system approach to the problem under consideration, for obvious reasons the combination of ship, fluid and fender structure has not to be taken for 'the system'. By isolating the freely floating ship in still water, ship and fluid combined can be conceived as the system to be considered. The fender loads then are thought to belong to the category of external forces.

On account of several investigations (see e.g. refs. [43, 46, 50, 54, 58]) it can be stated that the ship-fluid system is linear. In addition to the references mentioned, a good survey on this point as well as a (comprehensive) description of character and behaviour of the linear ship-fluid system is given in ref. [67]. All (experimental) data indicate that this basic linearity-assumption is a well-working approximation for small to moderate displacements of real ship forms. Therefore it is hypothesized that the assumption of linearity of the ship-fluid system holds absolutely.
With regard to fluid idealization the facts point into two directions. While it is sure that the restriction to a homogeneous, incompressible fluid, free from surface tension, is acceptable, the viscosity may lead to complications, notwithstanding the fact that viscous terms are basically linear. On the one hand, in dealing with (ship) motions it is of great advantage and in some cases (e.g. a ship in waves) necessary to consider the water as an inviscid, c.q. ideal fluid. On the other hand, due to interaction between the viscosity and the (non-linear) convective terms flow separation and consequent eddy formation may occur, which phenomena are distinctly perceptible, especially with larger ship motions. It makes itself primarily felt in additional damping and in a change in the hydrodynamic coefficients which couple the motions mutually. In principle, the combination of fluid viscosity and non-linear terms also underlies the occurrence of turbulence, which may lead to non-linear frictional effects. However, as long as the ship motions (i.e. displacements or velocities, or both) remain small, viscous effects can be taken into account without violating the basic linearity-concept of the ship-fluid system.
Beside linearity, the further requirements to be made upon this system approach are time independence of the system parameters and stability.

1.3.3. Approach to be followed

The berthing-ship problem is concerned with fixing those quantities as functions of time, which are essential for the motion of the ship and, especially, the interaction between ship and fender. In order to be able to represent correctly the time-dependent ship-water interaction with its 'memory effect' due to the free surface, the full information embedded in the frequency dependence of the hydrodynamic coefficients has to be taken into account; in literature -though for non-horizontal ship motions- this is confirmed theoretically and experimentally (see e.g. ref. [67]). Particularly the keel clearance and the vicinity of a closed wall do highly affect the sensitivity of the ship-fluid interaction to frequencies. By means of a Fourier-transform technique a formally correct representation of the ship-fluid interaction in the time domain can be drawn up, which is equivalent to its formulation in the frequency domain. This representation in the time domain holds good for external forces arbitrarily varying in time (in the sense of transient disturbances of restricted duration). The condition attached is that the ship-fluid system behaves linearly.

Considering the above assertions now two approaches can be followed, starting from (1.4) and its equivalent form (1.5),(1.6), respectively:

I - The description of the linear ship-fluid system in the time domain can be determined by the inverse Fourier transform of (1.4). On certain conditions with respect to the transformed functions, this yields an equation of motion for the variable x(t) in the form of an integro-differential equation, viz.:

$$m\ddot{x} + \int_{-\infty}^{t} \ddot{x}(\tau)A(t-\tau)d\tau + \int_{-\infty}^{t} \dot{x}(\tau)B(t-\tau)d\tau + cx = f(t) \qquad , \qquad (1.8)$$

where τ represents an integration variable (time). This expression includes convolution integrals containing the so-called retardation functions A(t) and B(t), which are the inverse Fourier transforms of $a(\omega)$ and $b(\omega)$, respectively. The convolution products thus arise from the frequency dependence of the hydrodynamic coefficients and, therefore, represent the memory effect as generated by the free water-surface (see further refs. [68, 67, 58]).

II - Starting from (1.5),(1.6) the inverse Fourier transform takes -on certain conditions- the form

$$f(t) = \int_{-\infty}^{t} x(\tau)\, r(t-\tau)d\tau \qquad , \qquad (1.9)$$

where r(t), with $r(t) \equiv 0$ for $t < 0$, is the inverse Fourier transform of $R(\omega)$. In (1.9) the response of the ship to arbitrary motions is fully characterized by the function r(t). This compact formulation supposes a generalized-function concept: $r(t)$ consists, among other things, of contributions from delta or Dirac functions and their derivatives. According to the specific notation (1.9) the system of the ship-fluid interaction is regarded as a black box, relating the excitation (input signal) and the response (output signal) of the system without reflecting the governing physical processes. In this, $r(t)$ has to be conceived as the impulse response function of the system, i.e. the response to a unit pulse, on the understanding that response and excitation represent force and motion, respectively. The requirement that $r(t) \equiv 0$ for $t < 0$, ensues from the fact that the ship-fluid system -like each physical system- is causal.

The motion of the ship is produced by external forces, one of them, the fender force, being a function of the ship motion itself. Therefore, with regard to the interaction between berthing ship and fender(s) it is obvious -contrary to the above- to interchange response and excitation: now the forces $f(t)$, exerted somewhere upon the ship, are conceived as input signals (excitation), whereas the ship motion $x(t)$ (displacement and rotation or derived quantities) is considered to be the output signal (response). Then -provided the ship-fluid system is linear- input signal and output signal are connected by means of a convolution integral over the entire time history of the forcing function(s) according to

$$x(t) = \int_{-\infty}^{t} f(\tau)\, k(t-\tau) d\tau \quad , \tag{1.10}$$

where $k(t)$ represents the impulse response function, i.e. the response to a unit pulse (Dirac function at $t = 0$). Naturally (1.10) has a similar form as (1.9); $k(t)$, with $k(t) \equiv 0$ for $t < 0$, is the inverse Fourier transform of $1/R(\omega)$. The linear ship-fluid system is fully characterized if $k(t)$ is known, i.e. the response $x(t)$ to an arbitrary forcing function $f(t)$ can be found in terms of $k(t)$. The external forces, e.g. fender loads, may be linear or non-linear and can be incorporated in the forcing function. According to (1.10) the ship-fluid interaction again is regarded as a black box (see fig. 1.1).

Approach II, as outlined above, is denominated as 'impulse response function'-technique.

With respect to the linearity concept the following observation may be added. Linearity of the system means much more than the linearity of

(1.3). In that case, linearity implied that if the ship were subjected to a sum of two excitations both harmonically oscillating at the same frequency, the total response would be the sum of the separate responses. Now the assumption of linearity is extended to cover excitations of any nature. In particular, if a ship is given a pulse of some kind, it will have a certain response lasting much longer than the duration of the pulse itself. If the ship experiences a succession of pulses, its response at any time is assumed to be the sum of its responses to the individual pulses, each response being calculated with an appropriate time lag from the instant of the corresponding pulse. These pulses can be considered as occurring closer and closer together, until finally one integrates the responses, rather than summing them.

For approach I as well as approach II the respective descriptions of the linear ship-fluid system in time and frequency domain are related by means of Fourier transforms. From a mathematical point of view the respective time-domain formulations according to approach I and approach II are one another's variants: (1.8) and (1.9) c.q. (1.10) are fully equivalent, since they originate from one and the same system description in the frequency domain. A good review of the ship-fluid system in the time domain and the frequency domain is given in ref. [67]; further reference can be made to refs. [69, 68].

When the hydrodynamic coefficients in the frequency domain are known, both approach I and approach II is appropriate to apply to time-dependent problems: the situation of a ship being initially at rest as well as the situation of a ship with a uniform motion can be considered. For, both situations are to be conceived as initial states of equilibrium, from which -according to the supposed linearity- small disturbances are occurring. The hydrodynamic influence of a given, initial velocity finds merely expression in $a(\omega)$, $b(\omega)$ and c, and consequently is only reflected by the retardation functions (approach I) and the impulse response function (approach II).

Practical applications of approach I are presented in refs. [70, 58], which are concerned with ship motions on water with relatively large, horizontal dimensions. Ref. [70] deals with ship berthing, viz. a centric impact to a jetty fitted with a linear, undamped fender. In a more universal way the motions of a moored ship in waves are described in ref. [58].

Due to its black-box formulation the 'impulse response function'-technique (approach II) is less appropriate to analyse the response (i.e. the motion) of the ship than approach I: for, making use of approach II it is difficult to discriminate in the time domain between the respective contributions of inertia and damping effects. If it is only a question of the response itself and not of its analysis, then the 'impulse response function'-technique is an appropriate approach, offering the possibility to incorporate in an efficient way all kind of factors which are of importance for the ship-fluid system. In ship berthing the main point is with the resulting course of the ship motion and its related history of the load on the berthing facility. That is the reason why in the present investigation a choice is made for applying the 'impulse response function'-technique with the forcing function(s) as input signal and the ship motion as output signal.

1.3.4. Simplification of problem

For the specific case of a ship berthing to a fender structure the following assumptions and simplifications are made.

The open berth is of the jetty-type; the closed berth consists of a straight, impervious, vertical wall of infinite length. Both berthing facilities are fitted with one single fender without mass of its own, or at most with a mass which is small with respect to that of the ship. The fender has a horizontal line of action situated in the plane of the water surface at rest; for the closed berth the line of action is perpendicular to the front side of the (quay-)wall.

The characteristics of the fender are assumed to be undamped and (non-)linear.

The frictional force between the hull of the ship and the fender is neglected.

Only berthing operations on sheltered locations (e.g. harbours) are considered, i.e. the influences of waves, current and wind are not taken into account.

As berthing manoeuvres and the ship-fender interactions take place mainly in the horizontal plane, only the surge, sway and yaw motions of the ship play a part; so, in this context it is assumed explicitly that dynamic effects due to any possible vertical ship motions (heaving and pitching) and rolling -which in a way do occur in reality- are of minor importance and do not influence the motion in the horizontal plane.

The vessel is considered as a rigid, prismatic body with a rectangular cross-section and a symmetrical distribution of mass. This schematization is justified by the fact that many sea-going vessels and most inland ships have a more or less box-like shape, being slightly streamlined at bow and stern.

The ship's forward speed is supposed to be zero or negligibly small, which ensues from the fact that during a berthing operation the forward speed is indeed small or zero, particularly for large (sea-going) ships.
Further, in case of a closed berthing facility it is assumed that the ship maintains a lateral motion with its longitudinal axis of symmetry parallel to the face of the berth. It implies a centric impact in which only the sway motion plays a part, and no rotation. This assumption arises from the geometrical situation of berthing manoeuvres at closed structures in general and the fact that the influence of the sway motion on fender loads predominates the effect of surging and yawing.
Diffraction phenomena and flow around bow and stern are not considered.
Special attention is paid to the case when shallowness of the water is of dominant importance, for, berthing facilities are often located in shallow water. The bottom is horizontal and impervious. In case of the open jetty-type berth the fluid domain is supposed to be relatively large in the horizontal directions; the same applies to the fluid domain in front of the (quay-)wall. Besides it is assumed that the fluid is incompressible.
As stated above, a very important starting-point with respect to the ship is that displacements and rotations or derived quantities remain so small that the ship-motion problem can be regarded as linear, thus leading to the concept of a linear ship-fluid system; further, this system must have time-independent parameters and behave stably.
The two berthing situations distinguished (open and closed berth) are represented schematically in figs. 1.2^a and 1.2^b; each situation can be considered to reflect in an adequate way the berthing of, notably, large (sea-going) ships.

With the supposed linearity of the ship-fluid system and under the simplifications mentioned above the problem of a ship berthing to a fender structure now has been reduced to some essential points. It has to be recognized that all simplifications and assumptions -with the except of the adoption of the linearity concept- are not absolutely necessary; they are only carried through to put the ship-berthing problem as clearly and unambiguously as possible and do not derogate from the generality of its formulation. What then remains is the formulation of a mathematical model based on the linearity of the ship-fluid system, which is able to describe the force(s) exerted upon some fender facility as a result of the berthing of a (schematized) ship with a horizontal motion (swaying and yawing), at calm, shallow water with relatively large, horizontal dimensions. In essence it all amounts to a time-domain description of the ship motion, making use of the 'impulse response function'-technique. As such this approach is more sophisticated and diametrically opposed to the method usually applied, in which the berthing forces are determined by supposing that the energy to be absorbed by the fenders equals the kinetic energy of the ship: it is not only to be regarded as a more reliable and theoretically founded way of determining berthing forces, but -in a general sense- it also contributes to an enlargement of the existing knowledge of the subject under consideration.

1.4. Outline of successive Sections

In Section 2 the 'impulse response function'-technique is dealt with in a general mathematical formulation and its features are discussed. For reasons of completeness the approach is generalized to systems with six degrees of freedom. The linear ship-fluid system is described in the frequency domain as well as in the time domain. Both the stability of the system and the causality condition is considered. Then expressions are derived for the respective impulse response functions.

Section 3 is concerned with ship berthing to open fender structures. The 'impulse response function'-technique is applied to the horizontal modes of motion of a schematized ship on shallow water with relatively large horizontal dimensions. At first the hydrodynamic coefficients are determined, theoretically as well as experimentally, from which the corresponding impulse response functions are calculated. Then a mathematical approach is presented to simulate the berthing of the ship to a jetty and to determine the relevant quantities. For certain situations the results of theoretical and experimental investigations are compared and discussed.

The berthing of a ship to a closed fender structure is dealt with in Section 4. Starting from a general time-domain description of the sway motion of a schematized ship on shallow water and parallel to a vertical wall, two procedures are followed. In the first approach again the 'impulse response function'-technique is applied: the hydrodynamic coefficients are determined both theoretically and experimentally yielding the corresponding impulse response function; then the berthing operation is simulated in a similar way as in Section 3. The second procedure is a 'direct-time approach', in which nonlinearities (in the hydrodynamics) can be taken into account. For certain berthing situations the theoretical results from each of the two approaches are compared with experiments and discussed.

Section 5 closes with some conclusions.

This study mainly is based on the results of research published as refs. [54, 66, 71, 72, 73, 74, 75, 76].

2. THE 'IMPULSE RESPONSE FUNCTION'-TECHNIQUE

2.1. Introduction

This section deals with the mathematical formulation of the 'impulse response function'-technique as related to ship motions. For reasons of completeness, the approach is generalized to motions with six degrees of freedom, while the coupling between the respective modes of motion is taken into account. The result applies to deep as well as shallow water; the effect of a vertical wall can be included. A theoretical derivation of the relevant formulae is provided.

As stated before, the two important assumptions made are that the ship behaves as a rigid body and that its motions remain small. The effects governed by rigid-body characteristics and by hydrodynamics must be incorporated separately, since they are controlled by different parameters.

Before starting the formal formulation of the ship-motion problem, three further restrictions are made: a) - the ship's form is transversely symmetric with respect to its vertical centre plane, longitudinal symmetry is not assumed; b) - at rest the ship is floating upright in stable equilibrium; and c) - the ship has a constant (mean) velocity with two components, viz. a forward speed and a transverse speed, parallel and perpendicular to the above plane of symmetry, respectively. In principle these three simplifications are not essential to the general formulation of the problem, but they facilitate it greatly; besides they correspond to what is common practice in naval hydrodynamics (real ship forms).

First of all the co-ordinate systems to be used are defined. On account of the linearity concept small ship motions are considered with respect to a co-ordinate system, which translates at a constant speed and as such acts as (initial) state of equilibrium.

Next a description is given of the ship-fluid system in the frequency domain. The fluid reactive effects are represented by the hydrodynamic coefficients, which are frequency dependent because of the free water-surface. These coefficients define the frequency response functions and can be determined by means of a harmonic analysis of the system.

The frequency-dependent behaviour of the hydrodynamic coefficients reflects the 'memory effect' of the ship-fluid system and generates a formulation in the time domain containing convolution integrals. Within the scope of the 'impulse response function'-technique this implies that the ship-fluid interaction is conceived as a 'black box' with the external forces upon the ship as input signals and the ship motion as output signal. This time-domain description is fully characterized by the impulse response functions. The respective descriptions of the system in frequency domain and time domain are fully equivalent and related by means of Fourier transforms: the impulse response function is the inverse Fourier transform of the corresponding frequency response function on the condition that this inverse Fourier transform exists in terms of the generalized function theory.

It is necessary that the ship-fluid system is stable and causal. Since each physical system is causal, in this case the principle of causality holds unconditionally. With respect to the requirement of stability of the system, an appropriate choice has to be made for the output signal. In case of ship motions with a restoring force (heave, roll and pitch) the ship-fluid system simply is always stable, regardless whether the displacement/rotation, the velocity or the acceleration is taken as the output signal. For ship motions without a restoring force (surge, sway and yaw) the stability is dependent on the existence of damping in the system for the steady equilibrium situation: in case of zero damping only the velocity or the acceleration as output signal yields a stable system, whereas in case of non-zero damping also the displacement/rotation is qualified to bring about this. One thing and another leads to a choice for the velocity as output signal, since the ship-fluid system then behaves stably for all modes of motion.

Thereupon expressions are derived for the respective impulse response functions.

Further some remarks are made on the significance of the causality of the system.

2.2. Co-ordinate systems

Analogous to ref. [46] the following co-ordinate systems are introduced:

$OX_1X_2X_3$ = space-fixed right-handed system of Cartesian co-ordinates with origin O; OX_1X_2 coincides with the water surface at rest; the vertical OX_3-axis is positive upwards; the forward speed V_1 and the transverse speed V_2 of the ship is parallel to the positive OX_1-axis and the positive OX_2-axis, respectively.

$ox_1x_2x_3$ = right-handed Cartesian co-ordinate system parallel with $OX_1X_2X_3$, but translating with the (constant) ship's speeds V_1,V_2; at rest the origin o coincides with the ship's centre of gravity G; the longitudinal ox_1-axis is positive in forward direction, the ox_2-axis is positive to port-side, the ox_3-axis is positive upwards.

Gxyz = moving right-handed Cartesian co-ordinate system with origin G and fixed with respect to the ship; Gxz coincides with the longitudinal plane of symmetry of the ship; the Gy-axis is positive to port-side, the Gz-axis is positive upwards.

The relations between the first two co-ordinate systems are:

$$X_1 = x_1 + V_1t \quad , \quad X_2 = x_2 + V_2t \quad , \quad X_3 = x_3 + a_3 \quad ,$$

where a_3 represents the distance of G below the plane of the water-line. In the following a_3 is supposed to be zero.

On account of its definition $ox_1x_2x_3$ is an inertial system. In principle, within the linearity concept small disturbances are considered from an initial state of motion of the ship. Relating to berthing this implies small ship motions with respect to the translating $ox_1x_2x_3$-co-ordinate system, which acts as state of equilibrium.

The motions of the ship now can be represented by the motion variable $x_j(t)$, where $j = 1, 2, \ldots, 6$; x_1, x_2 and x_3 stand for the translations surge, sway and heave, while x_4, x_5 and x_6 denote the rotations around the ox_1-axis, the ox_2-axis and the ox_3-axis, respectively. In naval hydrodynamics it is usual to introduce a set of three independent angular displacements, the so-called Eulerian angles, viz.: yawing, being around the absolutely vertical ox_3-axis, pitching around the rotated position of the ox_2-axis, which remains in the horizontal plane, and rolling around the position of the ox_1-axis after the previous two rotations. Only the latter axis coincides with a body axis. The rotational vectors are not directed along $ox_1x_2x_3$, but in considering small motion amplitudes and linearizing consequently these Eulerian angles coincide with the angular displacements around the space-fixed axes (see ref. [46]).

The displacements $x_j(t)$ in the six respective directions then are:

$x_1(t)$ = translation in the X_1-direction = surge motion (positive forwards),

$x_2(t)$ = translation in the X_2-direction = sway motion (positive to port-side),

$x_3(t)$ = translation in the X_3-direction = heave motion (positive upwards),

$x_4(t)$ = rotation around the OX_1-axis	=	roll motion (positive from deck to starboard-side),
$x_5(t)$ = rotation around the OX_2-axis	=	pitch motion (positive with bow moving downwards),
$x_6(t)$ = rotation around the OX_3-axis	=	yaw motion (positive with bow moving to port-side).

In consequence of the ship's rotation formally virtual forces (due to Coriolis and centrifugal effects) as well as an inertial contribution (due to the angular acceleration) are introduced. These influences can be neglected, since -within the context of the linear approach- they become small of the second order. If these effects nevertheless should be taken into account, they are to be classed in the forcing function (i.e. input signal) of the ship-fluid system.

Fig. 2.1 shows the respective co-ordinate systems in case merely the ship motions in the horizontal plane are considered.

2.3. Ship-fluid system in frequency domain

Due to the linearity of the ship-fluid system, (1.3) can be extended for the general case of coupled ship motions; i.e. the mass, damping and restoring forces resulting from the distinct directions of motion may be superimposed to counterbalance the exciting force in the relevant direction (see refs. [68, 67]):

$$\sum_{j=1}^{6} \left[\{m_{jk}+a_{jk}(\omega)\}\ddot{x}_j + b_{jk}(\omega)\dot{x}_j + c_{jk}x_j \right] = f_k(t) \quad , \quad k = 1,2,\ldots,6, \qquad (2.1)$$

where m_{jk} = inertia matrix (i.e. generalized mass) of the ship,

$a_{jk}(\omega)$ = hydrodynamic coefficient of the mass term in the k-equation as a result of motion in the j-direction,

$b_{jk}(\omega)$ = hydrodynamic coefficient of the damping force in the k-equation as a result of motion in the j-direction,

c_{jk} = hydrostatic restoring coefficient in the k-equation as a result of a static displacement in the j-direction at zero speed,

$f_k(t)$ = external exciting harmonic force upon the ship in the k-direction,

ω = circular frequency;

the double subscript j,k relates the force in the k-direction to the motion in the j-direction. $a_{jk}(\omega)$, $b_{jk}(\omega)$ and c_{jk} are elements in an a_{jk}-, b_{jk}- and c_{jk}-matrix, respectively. In case of diagonal matrices hydrodynamic coupling between the respective modes of motion does not occur; then i = j = k. As -at rest- the co-ordinate origin o of $ox_1x_2x_3$ coincides with G, due to the symmetry of the ship, in a first-order approximation all non-diagonal elements in m_{jk} vanish, except m_{46}; m_{46} = 0 in case of fore and aft symmetry.
Expression (2.1) is a description of the linear ship-fluid system in the frequency domain. Accordingly it is not a set of real differential equations in the time, and it does not represent a set of equations of motion in the sense that instantaneous quantities of the motion are related to instantaneous values of the external force. (2.1) exclusively holds good for steady harmonic oscillations at a specific frequency and their corresponding 'constants' on the left-hand side (see also refs. [69, 68, 67]).

The exciting harmonic force $f_k(t)$ has the form

$$f_k(t) = \hat{f}_k(\omega) \exp(i\omega t) \quad , \tag{2.2}$$

with

$$\hat{f}_k(\omega) = |\hat{f}_k(\omega)| \exp\{i\varepsilon_k(\omega)\} \quad , \tag{2.3}$$

where $\varepsilon_k(\omega)$ = phase angle of the harmonic force in the k-direction.
Then the motion variable $x_j(t)$ has to be written as:

$$x_j(t) = \hat{x}_j(\omega) \exp(i\omega t) \quad , \tag{2.4}$$

with

$$\hat{x}_j(\omega) = |\hat{x}_j(\omega)| \exp\{i\varepsilon_j(\omega)\} \quad , \tag{2.5}$$

where $\varepsilon_j(\omega)$ = phase angle of the harmonic motion in the j-direction.
Substitution of (2.2) and (2.4) into (2.1) yields

$$\sum_{j=1}^{6} R_{jk}(\omega)\, \hat{x}_j(\omega) = \hat{f}_k(\omega) \quad , \tag{2.6}$$

with

$$R_{jk}(\omega) = -\omega^2\{m_{jk} + a_{jk}(\omega)\} + i\omega b_{jk}(\omega) + c_{jk} \quad . \tag{2.7}$$

Now consider the motion in one direction, say the i-direction; then $\hat{x}_j(\omega) = 0$ for $i \neq j$. The subscript i indicating a direction should not be mixed up with the symbol i representing $\sqrt{-1}$. From (2.6) combined with (2.2), (2.3) and (2.4),(2.5) it subsequently can be derived

$$R_{ik}(\omega) = |R_{ik}(\omega)| \exp\{-i\theta_{ik}(\omega)\}, \quad \text{provided} \quad \hat{x}_j(\omega) = 0 \quad \text{for} \quad i \neq j \quad , \tag{2.8}$$

with

$$\left.\begin{aligned} |R_{ik}(\omega)| &= \frac{|\hat{f}_k(\omega)|}{|\hat{x}_i(\omega)|} \quad , \\ \theta_{ik}(\omega) &= \arg\{R_{ik}(\omega)\} = \varepsilon_i(\omega) - \varepsilon_k(\omega) \quad , \end{aligned}\right\} \tag{2.9}$$

where $R_{ik}(\omega)$ = harmonic transfer function for the k-direction in response to a harmonic (motion) excitation in the i-direction,

$\theta_{ik}(\omega)$ = phase shift between the harmonic motion and its (force) response;

the symbolic notation arg{...} means 'argument of'. $|R_{ik}(\omega)|$ represents the amplification factor.

As a result of the condition $\hat{x}_j(\omega) = 0$ for $i \neq j$, it can be stated that with respect to (1.3) -in a formal sense- excitation and response have been interchanged: now $x_i(t)$ is to be considered as the excitation and $f_k(t)$ as its response. This view corresponds with the common practice in forced harmonic oscillation experiments.

From (2.7) it then follows for $a_{ik}(\omega)$ and $b_{ik}(\omega)$:

$$\left.\begin{aligned} a_{ik}(\omega) &= \frac{1}{\omega^2}\{c_{ik} - \mathrm{Re}[R_{ik}(\omega)]\} - m_{ik}, \\ b_{ik}(\omega) &= \frac{1}{\omega}\,\mathrm{Im}[R_{ik}(\omega)] \quad , \end{aligned}\right\} \text{provided } \hat{x}_j(\omega) = 0 \text{ for } i \neq j, \tag{2.10}$$

where on account of (2.9),

$$\left.\begin{aligned}\mathrm{Re}[R_{ik}(\omega)] &= \frac{|\hat{f}_k(\omega)|}{|\hat{x}_i(\omega)|}\cos(\theta_{ik}),\\ \mathrm{Im}[R_{ik}(\omega)] &= -\frac{|\hat{f}_k(\omega)|}{|\hat{x}_i(\omega)|}\sin(\theta_{ik});\end{aligned}\right\} \qquad (2.11)$$

the symbolic notation Re[...] and Im[...] means 'real part of' and 'imaginary part of', respectively.

(2.10) and (2.11) combined can be applied in case of an experimental determination of the hydrodynamic coefficients (forced oscillation tests; see e.g. ref. [42]).

Due to linearity it holds good for a ship with $V_1, V_2 = 0$ that (ref. [46])

$$a_{jk}(\omega) = a_{kj}(\omega) \quad , \quad b_{jk}(\omega) = b_{kj}(\omega) \quad , \quad c_{jk} = c_{kj} \quad . \qquad (2.12^a)$$

Under these conditions c_{jk} -on account of its definition- can be further particularized as

$$c_{j1} = c_{1k} = 0 \qquad \text{for all } j \text{ and } k. \qquad (2.12^b)$$

In the event of a ship with a given speed, in principle also in the horizontal plane hydrodynamic effects of the form $c_{jk}x_j$ can occur, so that in this case $c_{jk} \neq 0$ for $j,k = 1,2,6$.

In consequence of the extant symmetry of the ship form it generally applies that

$$\left.\begin{aligned} a_{jk}(\omega) = b_{jk}(\omega) = c_{jk} = 0 \quad &\text{for } j = 2,4,6 \text{ and } k = 1,3,5,\\ &\phantom{\text{for }} j = 1,3,5 \text{ and } k = 2,4,6, \text{ respectively.}\end{aligned}\right\} (2.12^c)$$

It has to be emphasized here that the expressions (2.12^a), (2.12^b) and (2.12^c) exclusively hold good for a ship with $V_1, V_2 = 0$.

If $V_1 \neq 0$ and $V_2 = 0$ it further can be stated (refs. [77, 78]):

$$b_{15}(\omega) = b_{51}(\omega) \ , \ b_{24}(\omega) = b_{42}(\omega) \ , \ b_{jk}(\omega) = -b_{kj}(\omega) \text{ for all other } j \neq k. \qquad (2.12^d)$$

The respective hydrodynamic coefficients in fact represent in-phase (i.e. in phase with x_i and $\ddot{x}_i$) and out-of-phase (i.e. in phase with $\dot{x}_i$) components of the hydrodynamic force. For the hydrodynamic damping coefficient $b_{ik}(\omega)$ -which proceeds from the out-of-phase component of the hydrodynamic force- this simply is obvious: see (2.10) and (2.11). The in-phase component includes two contributions: the added mass and the restoring force coefficient. In order to avoid ambiguity with respect to the determination of added mass and restoring force coefficient, c_{ik} now is conceived as being frequency independent. The c_{ik}-coefficient by definition is considered to be apart from the hydrodynamic phenomenon, and therefore it is not associated with the harmonically oscillating motion: c_{ik} is determined in the first place by the geometry of the hull of the ship, and further it may vary with the ship's speed. So, the indication of 'hydrostatic coefficient' for c_{jk} is not altogether right, since at a given ship's speed in general hydrostatic as well as hydrodynamic effects play a part. Nevertheless, in the generalized expression (2.1) c_{jk} in principle is maintained as a frequency-independent quantity. Accordingly c_{jk} is a characteristic of the ship itself. $a_{jk}(\omega)$ and $b_{jk}(\omega)$ are in the first place characteristics of the flow around the ship and therefore can be influenced by external conditions, such as the position of the bottom, the presence of a quay-wall, etc. With the linear approach various external conditions, which do influence hydrodynamics, are not taken into account in these coefficients, but they are classed in external forcing functions (e.g. wave forces). Further, $a_{jk}(\omega)$, $b_{jk}(\omega)$ and c_{jk} in principle are dependent on the velocities V_1, V_2 of the ship.
Now the hydrodynamic coefficients $a_{jk}(\omega)$ and $b_{jk}(\omega)$ formally can be determined by means of a harmonic analysis of the linear ship-fluid system making use of (2.10) and (2.11).

In case of coupled ship motions the nomenclature with respect to $a_{jk}(\omega)$, $b_{jk}(\omega)$ and c_{jk} is only formal and has no physical background: if two or more harmonic motions occur simultaneously, in principle it is possible (dependent on the phase shift between the respective coupled motions) that contributions of say the form $a_{jk}(\omega)\ddot{x}_j$ do not merely represent inertial forces but also damping forces.

2.4. Ship-fluid system in time domain

2.4.1. General description

Any linear, time-independent, stable, physical system can be described by (see refs. [79, 80]):

$$u(t) = \int_{-\infty}^{+\infty} f(\tau)\, k(t-\tau) d\tau \quad , \tag{2.13}$$

where $f(t)$ = excitation of the system = input signal,

$k(t)$ = response to a unit pulse (i.e. Dirac function at $t = 0$) = = impulse response function (i.r.f.),

$u(t)$ = response of the system to the input signal $f(t)$ = = output signal.

If $f(t) = \delta(t)$, with

$\delta(t)$ = delta function or Dirac function,

then $u(t) = k(t)$. The symbol $k(t)$ representing the i.r.f. should not be mixed up with the subscript k indicating a direction.

The time independence of the system implies that the system parameters do not depend on t, i.e. the input-output relation does not change in time. The 'black-box' approach according to (2.13) defines the characteristic features of the system by means of the relation between input signal and output signal.

Since a physical system is causal, it must hold good that

$$k(t-\tau) \equiv 0 \qquad \text{for } \tau > t \quad , \tag{2.14}$$

i.e. the future behaviour of $f(t)$ for $\tau > t$ does not affect $u(t)$ at time t. Then (2.13) can be written as

$$u(t) = \int_{-\infty}^{t} f(\tau)\, k(t-\tau) d\tau \quad . \tag{2.15}$$

With $k(t)$ known, the properties of the system are fixed, i.e. for any arbitrary excitation the corresponding response can be determined.

The requirement of stability implies that the difference between the responses of the system to distinct excitations, for $t \to \infty$ always converges to a finite value. If $\lim\limits_{t\to\infty} k(t)$ = constant $\neq 0$, the system is stable; if $\lim\limits_{t\to\infty} k(t) = 0$, the system is so much as asymptotically stable. In addition to the stability of the system, it is naturally required that $f(t)$ remains bounded; then u(t) is bounded too.

The combination of ship plus fluid can be conceived as an arbitrary, time-invariant, stable, causal system: the forces exerted somewhere upon the ship are regarded as input signals, whereas the motion of the ship (displacement and rotation or derived quantities) is considered to be the output signal. In consequence of the 'memory effect' associated with the influence of the free surface (and the vorticity), it is necessary to represent the transient ship motion -arising from a set of forces- in terms of a convolution integral over the entire time history of the forcing functions. Thus the six components of the motion have to be considered to be of the general form (see refs. [79, 80, 81]):

$$u_j(t) = \int_{-\infty}^{t} k_j[f_i(\tau), t-\tau]d\tau, \qquad i,j = 1,2,\ldots,6 \quad , \tag{2.16}$$

where k_j = kernel for motion in the j-direction,
$u_j(t)$ = response of the system in the j-direction to the set of input signals $\{f_i(t)\}$.

The kernel k_j depends on the set of forcing functions $\{f_i(t)\}$, on the retarded time $t - \tau$, on the geometry of the ship and on the physical properties of the fluid.

If it is allowed to consider the ship and the fluid combined as a linear system, (2.16) changes into a more familiar and simple form (refs. [79, 80, 81]):

$$u_j(t) = \sum_{i=1}^{6} \int_{-\infty}^{t} f_i(\tau)\, k_{ij}(t-\tau)d\tau = \sum_{i=1}^{6} \int_{0}^{\infty} k_{ij}(\tau)\, f_i(t-\tau)d\tau, \; j=1,2,\ldots,6, \tag{2.17}$$

where $k_{ij}(t)$ = response for the j-direction to a unit pulse (i.e. Dirac function at $t = 0$) in the i-direction =
= impulse response function.

It has to be noted that (2.17) is the extension of (2.15) for six degrees of freedom.

On account of the above definition for $k_{ij}(t)$ it holds good that (principle of causality):

$$k_{ij}(t) \equiv 0 \qquad \text{for } t < 0 \quad . \tag{2.18}$$

The i.r.f. $k_{ij}(t)$ is a real function of t which depends on the geometry of the

ship as well as on the boundaries of the fluid domain and its physical properties. The matrix $\{k_{ij}(t)\}$ represents the 'memory effect' due to the presence of the free surface and fully characterizes the response of the ship to an arbitrary excitation. Apart from convergence of the (convolution) integrals, the only assumption required in this is that the ship-fluid system behaves linearly. The input signals need not be linear.
As an example of the necessity for the representation given above, it can be noted that in the case of a captive model which is given a short 'pulse' disturbance and then returned to its original, steady, restrained condition, an unsteady fluid motion -visible especially in the disturbance of the free surface- and an associated force will persist thereafter, in principle ad infinitum.

Consistent with the hypothesis of linearity of the ship-fluid system it is assumed that $|f_i(t)|$ remains bounded. This assumption is closely linked up with the demand for stability of the system: if $f_i(t)$ is bounded in time, then $u_j(t)$ will be bounded in time as well.

2.4.2. Stability

The ship-fluid system behaves stably, if at least the following condition is met:

$$\lim_{t\to\infty} k_{ij}(t) = \text{constant} \quad . \tag{2.19}$$

As far as the ship motions are concerned then distinction can be made between
a- ship motions with a restoring force (heave, roll and pitch motion), and
b- ship motions without a restoring force (surge, sway and yaw motion).

Ad a: Let the ship motion in the j-direction be attended with a restoring force in the same direction, $c_{jj}x_j \neq 0$. In response to a unit pulse at $t = 0$ the ship will return to its original position, so that for $t \to \infty$ $x_j(t) \to 0$ and $\dot{x}_j(t) \to 0$. With $u_j(t) = x_j(t)$ (i.e. output signal = displacement) then it holds for the relevant i.r.f. $\lim_{t\to\infty} k_{ij}(t) = 0$, i.e. the system is unconditionally asymptotically stable in all suitable modes of motion, independent of the fact whether the displacement/rotation or the velocity or the acceleration is conceived as output signal. (2.17) now can be written as:

$$x_j(t) = \sum_{i=1}^{6} \int_{-\infty}^{t} f_i(\tau)\, k_{ij}^{*}(t-\tau)d\tau =$$

$$= \sum_{i=1}^{6} \int_{0}^{\infty} k_{ij}^{*}(\tau)\, f_i(t-\tau)d\tau \quad , \quad j = 3,4,5, \qquad (2.17^a)$$

where $k_{ij}^{*}(t)$ = i.r.f. based on the displacement/rotation as output signal.

Ad b: A ship motion in the j-direction now has not any longer a restoring force $c_{jj}x_j \neq 0$, so that the ship -in response to a unit pulse at $t = 0$- does not return to its original position. Dependent on the existence of damping in the system for the steady equilibrium situation ($t \rightarrow \infty$), two cases can be distinguished.

- Zero damping from the fluid for $t \rightarrow \infty$: the velocity of the ship in the j-direction -in response to a unit pulse in the i-direction at $t = 0$- aproaches asymptotically to a constant value in conformity with a certain equilibrium situation; the displacement in the j-direction does not remain bounded anymore for $t \rightarrow \infty$.
- Non-zero damping from the fluid for $t \rightarrow \infty$: the velocity of the ship in the j-direction approaches to 0 for $t \rightarrow \infty$; the corresponding displacement then approaches asymptotically to a certain constant $\neq 0$.

Therefore in this case the ship-fluid system anyhow behaves stably, if the velocity (or the acceleration) is considered to be the output signal. Displacements or rotations can be measured in a much easier way than velocities and accelerations. Besides the calculation of the velocity from displacements/rotations is more accurate than the calculation of the acceleration. With the velocity as output signal (2.17) then becomes:

$$\dot{x}_j(t) = \sum_{i=1}^{6} \int_{-\infty}^{t} f_i(\tau)\, k_{ij}(t-\tau)d\tau =$$

$$= \sum_{i=1}^{6} \int_{0}^{\infty} k_{ij}(\tau)\, f_i(t-\tau)d\tau \quad , \quad j = 1,2,\ldots,6, \qquad (2.17^b)$$

where $k_{ij}(t)$ = i.r.f. based on the velocity as output signal.

On behalf of the generality of the following dissertation the velocity will be conceived as output signal throughout, i.e.

$$u_j(t) = \dot{x}_j(t) \qquad ; \tag{2.20}$$

for all modes of motion considered the ship-fluid system then is at least stable.

For an elaborate definition and a further explanation of the concept 'stability' in case of the linear ship-fluid system it is referred to Appendix A.

The i.r.f. $k^*_{ij}(t)$ and $k_{ij}(t)$ are related as follows. According to (2.17[a]) $x_j(t)$ is:

$$x_j(t) = \sum_{i=1}^{6} \int_{-\infty}^{t} f_i(\tau)\, k^*_{ij}(t-\tau)d\tau \qquad ;$$

further it can be derived that:

$$\dot{x}_j(t) = \sum_{i=1}^{6} \frac{d}{dt}\int_{-\infty}^{t} f_i(\tau)\, k^*_{ij}(t-\tau)d\tau = \sum_{i=1}^{6} \int_{-\infty}^{t} f_i(\tau)\, \frac{d}{dt}k^*_{ij}(t-\tau)d\tau + \sum_{i=1}^{6} f_i(\tau)\, k^*_{ij}(0) \; ;$$

$$k^*_{ij}(0) = 0 \quad , \quad \text{so that}$$

$$\dot{x}_j(t) = \sum_{i=1}^{6} \int_{-\infty}^{t} f_i(\tau)\, \frac{d}{dt}k^*_{ij}(t-\tau)d\tau \qquad ;$$

being equivalent with (2.17[b]) this expression yields:

$$k_{ij}(t) = \frac{d}{dt}k^*_{ij}(t) \qquad . \tag{2.21}$$

2.4.3. <u>Frequency response versus impulse response</u>

The Fourier transform of (2.17[b]) yields a description of the linear ship-fluid system in the frequency domain of the form:

$$F\{\dot{x}_j(t)\} = i\omega F\{x_j(t)\} = \sum_{i=1}^{6} F\{f_i(t)\}\; F\{k_{ij}(t)\} \qquad , \tag{2.22}$$

where $F\{f(t)\} = \int_{-\infty}^{\infty} f(\tau)\,\exp(-i\omega\tau)d\tau$ = Fourier transform of $f(t)$,

$F\{k_{ij}(t)\} = K_{ij}(\omega)$ = harmonic transfer function for the j-direction in response to a (harmonic force) excitation in the i-direction = frequency response function (f.r.f.).

As long as response and excitation can be considered as transient quantities, (2.22) represents per Fourier component the equations for arbitrary ship motions as a result of an arbitrary external force. (2.22) is only then a meaningful expression, if $f_i(t)$ is bounded in time and the ship-fluid system is stable, i.e. $k_{ij}(t\to\infty)$ = constant $\neq 0$, c.q. = 0 and $\dot{x}_j(t\to\infty)$ = constant $\neq 0$, c.q. = 0. These very properties of $f_i(t)$, $k_{ij}(t)$ and $\dot{x}_j(t)$ are an absolute requirement for the existence of their corresponding Fourier transforms in (2.22).

The description of the ship-fluid system in the frequency domain by (2.22) is equivalent to that by (2.6). As a result of the mapping per Fourier component by (2.22), in (2.22) and (2.6) $F\{f_i(t)\}$ and $\hat{f}_k(\omega)$ for k = i as well as $F\{x_j(t)\}$ and $\hat{x}_j(\omega)$ are identical. This can also be shown by substituting $x_j(t)$ according to (2.4) and $f_k(t)$ according to (2.2) with $\hat{f}_k(\omega) = 0$ for $k \neq i$ into (2.17^b), yielding directly (2.22) without summation operator. Now by putting

$$\left.\begin{aligned} U_j(\omega) &= F\{\dot{x}_j(t)\} = i\omega F\{x_j(t)\} = i\omega\hat{x}_j(\omega) \quad , \\ F_k(\omega) &= F\{f_k(t)\} = \hat{f}_k(\omega) \quad , \end{aligned}\right\} \tag{2.23}$$

the following set of equations is generated:

$$\left.\begin{aligned} U_j(\omega) &= \sum_{i=1}^{6} F_i(\omega)\ K_{ij}(\omega) \quad , \\ i\omega F_k(\omega) &= \sum_{j=1}^{6} R_{jk}(\omega)\ U_j(\omega) \quad , \\ F_k(\omega) &= 0 \text{ for } k \neq i \quad , \end{aligned}\right\} \quad k = 1,2,\ldots,6 \quad . \tag{2.24}$$

As indicated in ref. [74] in principle $K_{ij}(\omega)$ is to be solved from (2.24) and expressed in $R_{jk}(\omega)$, so that $K_{ij}(\omega)$ becomes a function of $a_{jk}(\omega)$, $b_{jk}(\omega)$ and c_{jk}. The i.r.f. $k_{ij}(t)$ then can be determined as the inverse Fourier transform of $K_{ij}(\omega)$. If this inverse Fourier transform exists in a general sense, i.e. in terms of the generalized function theory, the f.r.f. and the i.r.f. are related by a Fourier transform (refs. [83, 84]):

$$K_{ij}(\omega) = \int_{-\infty}^{\infty} k_{ij}(\tau)\ \exp(-i\omega\tau)d\tau = \int_{0}^{\infty} k_{ij}(\tau)\ \exp(-i\omega\tau)d\tau \quad , \tag{2.25^a}$$

or,

$$k_{ij}(t) = \frac{1}{2\pi}\int_{-\infty}^{\infty} K_{ij}(\omega)\exp(i\omega t)d\omega \qquad . \qquad (2.25^b)$$

The f.r.f. $K_{ij}(\omega)$ can be written as:

$$K_{ij}(\omega) = \int_0^{\infty} k_{ij}(\tau)\exp(-i\omega\tau)d\tau = \mathrm{Re}[K_{ij}(\omega)] + i\mathrm{Im}[K_{ij}(\omega)] \qquad ,$$

where $\mathrm{Re}[K_{ij}(\omega)] = \int_0^{\infty} k_{ij}(\tau)\cos(\omega\tau)d\tau$ = even function of ω ,

$$\mathrm{Im}[K_{ij}(\omega)] = -\int_0^{\infty} k_{ij}(\tau)\sin(\omega\tau)d\tau = \text{odd function of } \omega \qquad .$$

With these expressions (2.25^b) becomes:

$$k_{ij}(t) = \frac{1}{2\pi}\int_{-\infty}^{\infty}\{\mathrm{Re}[K_{ij}(\omega)]\cos(\omega t) - \mathrm{Im}[K_{ij}(\omega)]\sin(\omega t)\}d\omega +$$

$$+ \frac{i}{2\pi}\int_{-\infty}^{\infty}\{\mathrm{Re}[K_{ij}(\omega)]\sin(\omega t) + \mathrm{Im}[K_{ij}(\omega)]\cos(\omega t)\}d\omega \qquad ;$$

$k_{ij}(t)$ is a real, causal time function, $\mathrm{Re}[K_{ij}(\omega)]$ and $\cos(\omega t)$ are even functions of ω, and $\mathrm{Im}[K_{ij}(\omega)]$ and $\sin(\omega t)$ are odd functions of ω; therefore:

$$\int_{-\infty}^{\infty}\mathrm{Re}[K_{ij}(\omega)]\sin(\omega t)d\omega = -\int_{-\infty}^{\infty}\mathrm{Im}[K_{ij}(\omega)]\cos(\omega t)d\omega = 0 \qquad ,$$

so that

$$k_{ij}(t) = \frac{1}{2\pi}\int_{-\infty}^{\infty}\mathrm{Re}[K_{ij}(\omega)]\cos(\omega t)d\omega - \frac{1}{2\pi}\int_{-\infty}^{\infty}\mathrm{Im}[K_{ij}(\omega)]\sin(\omega t)d\omega =$$

$$= \frac{1}{\pi}\int_0^{\infty}\mathrm{Re}[K_{ij}(\omega)]\cos(\omega t)d\omega - \frac{1}{\pi}\int_0^{\infty}\mathrm{Im}[K_{ij}(\omega)]\sin(\omega t)d\omega \qquad .$$

Since the first term on the right-hand side of this expression is an even function of t and the second term an odd function, while at the same time $k_{ij}(t) \equiv 0$ for $t < 0$, it follows for $k_{ij}(t)$:

$$\left.\begin{aligned}
k_{ij}(t) &= \frac{2}{\pi}\int_0^\infty \mathrm{Re}[K_{ij}(\omega)]\cos(\omega t)d\omega = \\
&= -\frac{2}{\pi}\int_0^\infty \mathrm{Im}[K_{ij}(\omega)]\sin(\omega t)d\omega \quad \text{for } t>0 \quad , \\
k_{ij}(0) &= \frac{1}{\pi}\int_0^\infty \mathrm{Re}[K_{ij}(\omega)]d\omega = \frac{1}{2}\,k_{ij}(0^+) \quad , \\
k_{ij}(t) &\equiv 0 \quad \text{for} \quad t<0 \quad .
\end{aligned}\right\} \tag{2.25^c}$$

In determining the integrals in (2.25^c) any singularities occurring in the functions $K_{ij}(\omega)$ may play a part. To illustrate this the case with $V_1,V_2 = 0$ and exclusively uncoupled ship motions is considered. Then, using (2.12^a), it holds good that

$$a_{jk}(\omega) = a_{kj}(\omega) = 0, \quad b_{jk}(\omega) = b_{kj}(\omega) = 0, \quad c_{jk} = c_{kj} = 0 \quad \text{for } k \neq j, \tag{2.26^a}$$

and therefore, on account of (2.7):

$$R_{jk}(\omega) = R_{kj}(\omega) = 0 \quad \text{for } j \neq k \quad . \tag{2.26^b}$$

From (2.24) it now can be derived:

$$K_{ij}(\omega) = K_{ji}(\omega) = 0 \quad \text{for } i \neq j \tag{2.26^c}$$

and

$$K_{ii}(\omega) = \frac{i\omega}{R_{ii}(\omega)} \quad , \tag{2.26^d}$$

with

$$R_{ii}(\omega) = -\omega^2\{m_{ii} + a_{ii}(\omega)\} + i\omega b_{ii}(\omega) + c_{ii} \quad . \tag{2.26^e}$$

The steady state as attained for $t \to \infty$ in case of transient motions corresponds in the frequency domain with $\omega = 0$. For $c_{ii} \neq 0$, implying ship motions with a restoring force, $K_{ii}(\omega)$ is a regular function for which the inverse transformation to the time domain is always possible. The ship-fluid system is asymptotically stable with $\dot{x}_i(t\to\infty) = 0$, $x_i(t\to\infty) = 0$. On the contrary, for $c_{ii} = 0$ -which means ship motions without a restoring force- $K_{ii}(\omega)$ may show a singular behaviour dependent on the existence of damping in the system for $\omega \to 0$. With zero damping from the water for $\omega \to 0$, i.e. $b_{ii}(\omega \to 0) = 0$, $K_{ii}(\omega)$ behaves singularly for $\omega = 0$; the system is stable with $\dot{x}_i(t \to \infty) = \text{constant} \neq 0$. With non-zero damping from the water for $\omega \to 0$, i.e. $b_{ii}(\omega \to 0) \neq 0$, $K_{ii}(\omega)$ is a regular function; the system is asymptotically stable with $\dot{x}_i(t \to \infty) = 0$.

The complete set of i.r.f. forms a so-called i.r.f. matrix, which in principle can be determined experimentally.

Successively now the two respective cases of ship motions with and ship motions without a restoring force are dealt with. In regard to the behaviour of the i.r.f. at infinity, the first case corresponds with $k_{ij}(\infty) = 0$, i.e. $\int_0^\infty |k_{ij}(t)| dt$ does exist, and the latter case corresponds with $k_{ij}(\infty) = \text{constant} \neq 0$, i.e. $\int_0^\infty |k_{ij}(t)| dt$ does not exist, or with $k_{ij}(\infty) = 0$, respectively, dependent on the existence of damping in the ship-fluid system for the steady equilibrium state $(t \to \infty)$.

2.5. Determination of impulse response function

2.5.1. Ship motions with restoring force

It is supposed that $f_i(t)$ has the characteristic of a harmonic (force) excitation in the i-direction with a form in accordance with (2.2),(2.3). Substitution of these expressions with $k = i$ into (2.17^b) yields for $\dot{x}_j(t)$:

$$\dot{x}_j(t) = |\hat{f}_i(\omega)| \{K_{ij}^{(c)}(\omega) - iK_{ij}^{(s)}(\omega)\} \exp[i\{\omega t + \varepsilon_i(\omega)\}] \quad , \qquad (2.27^a)$$

where

$$K_{ij}^{(c)}(\omega) = \int_{-\infty}^{\infty} k_{ij}(\tau) \cos(\omega\tau) d\tau = \int_0^{\infty} k_{ij}(\tau) \cos(\omega\tau) d\tau \qquad (2.28^a)$$

and

$$K_{ij}^{(s)}(\omega) = \int_{-\infty}^{\infty} k_{ij}(\tau) \sin(\omega\tau) d\tau = \int_0^{\infty} k_{ij}(\tau) \sin(\omega\tau) d\tau \qquad (2.28^b)$$

represent the Fourier cosine transform and the Fourier sine transform of $k_{ij}(t)$, respectively (see refs. [84, 85, 86]). Hereby it should be borne in mind that $k_{ij}(t) \equiv 0$ for $t < 0$ (i.e. (2.18)). The i.r.f. $k_{ij}(t)$ is related to $K_{ij}^{(c)}(\omega)$ and $K_{ij}^{(s)}(\omega)$ by the inverse Fourier transforms (refs. [84, 85, 86]):

$$k_{ij}(t) = \frac{2}{\pi}\int_0^\infty K_{ij}^{(c)}(\omega)\cos(\omega t)d\omega = \frac{2}{\pi}\int_0^\infty K_{ij}^{(s)}(\omega)\sin(\omega t)d\omega \quad . \qquad (2.29^{a,b})$$

The relation between $K_{ij}^{(c)}(\omega)$ and $K_{ij}^{(s)}(\omega)$ is unique: if one of the two functions is known, then the other can be determined by means of ($2.29^{a,b}$) and ($2.28^{a,b}$).

An other way of representing (2.27^{a}) is:

$$\frac{\dot{x}_j(t)}{f_i(t)} = K_{ij}(\omega) \quad ,$$

where the f.r.f. $K_{ij}(\omega)$ is a complex quantity given as:

$$K_{ij}(\omega) = K_{ij}^{(c)}(\omega) - iK_{ij}^{(s)}(\omega) \quad , \qquad (2.30)$$

with

$$K_{ij}^{(c)}(\omega) = \mathrm{Re}[K_{ij}(\omega)] \quad , \quad K_{ij}^{(s)}(\omega) = -\mathrm{Im}[K_{ij}(\omega)] \quad . \qquad (2.31^{a,b})$$

On account of (2.30) and refs. [79, 80, 84, 85, 86] it can be stated in a more general way that the i.r.f. and the f.r.f. are related through a Fourier transform by (2.25^{a}) and ($2.25^{b,c}$). By (2.27^{a}) it can be seen that $K_{ij}^{(c)}(\omega)$ and $K_{ij}^{(s)}(\omega)$ are the respective amplitudes of the in-phase and out-of-phase components of the response in the j-direction to a harmonic forcing function -with unit amplitude and circular frequency ω- in the i-direction. In this context (2.27^{a}) can be written as:

$$\dot{x}_j(t) = |\hat{f}_i(\omega)| \sqrt{\{K_{ij}^{(c)}(\omega)\}^2 + \{K_{ij}^{(s)}(\omega)\}^2}\, \exp(i\{\omega t+\varepsilon_i(\omega)+\theta_j(\omega)\}) \quad , \qquad (2.27^{b})$$

where $\quad \tan\{\theta_j(\omega)\} = \dfrac{K_{ij}^{(s)}(\omega)}{K_{ij}^{(c)}(\omega)} \quad .$

This expression shows that the response of the ship-fluid system to a harmonic (force) excitation with unit amplitude has the amplitude

$$\sqrt{\{K_{ij}^{(c)}(\omega)\}^2 + \{K_{ij}^{(s)}(\omega)\}^2} \qquad (2.32^{a})$$

and follows the excitation by the phase

$$\arctan\{K^{(s)}_{ij}(\omega)/K^{(c)}_{ij}(\omega)\} \quad . \tag{2.32^b}$$

For the case under consideration with $k_{ij}(\infty) = 0$ it holds good in (2.1) that $c_{jk} > 0$. By substitution of (2.27^a) and (2.2) into (2.1) a system of equations can be formed for the unknown functions $a_{jk}(\omega)$ and $b_{jk}(\omega)$; the coefficients c_{jk} are supposed to be known, e.g. as being determined from static measurements. In order to determine the unknown hydrodynamic coefficients it is necessary to consider the responses to excitations in each of the modes of motion separately. If the in-phase and out-of-phase components of the responses are separated, then sufficient equations are obtained to determine the hydrodynamic coefficients.

In principle the hydrodynamic coefficients can be determined from the set of i.r.f. $\{k_{ij}(t)\}$; therefore they contain no information which is not derivable from these functions.

The response for a given frequency, as determined by the pair of functions (2.32^a) and (2.32^b) or alternatively by the pair of functions $K^{(c)}_{ij}(\omega)$ and $K^{(s)}_{ij}(\omega)$ in (2.27^a), represents a mapping in the frequency domain of the unit response function, which is defined in the time domain. Since by means of (2.27^{a,b}) it is permitted to pass from either domain to the other, the two representations (in frequency and time domain) of the linear ship-fluid system are fully equivalent.

In berthing operations horizontal motions are predominant, and these very modes of motion lack restoring forces. Supposing that there is no coupling between motions in the horizontal plane (i.e. $(i,j,k) = 1,2,6$) and motions in the vertical plane (i.e. $(i,j,k) = 3,4,5$), it suffices here to state that for $(i,j,k) = 3,4,5$ $K_{ij}(\omega)$ can be solved from (2.24) and expressed in $R_{jk}(\omega)$, so that $K_{ij}(\omega)$ becomes a function of the hydrodynamic coefficients $a_{jk}(\omega)$, $b_{jk}(\omega)$ and of c_{jk}. With these last quantities known the i.r.f. $k_{ij}(t)$ then simply is to be determined as the inverse Fourier transform of $K_{ij}(\omega)$ by means of (2.25^c).

2.5.2. Ship motions without restoring force

As stated above ship motions without a restoring force exclusively occur in the horizontal plane. This implies that only surge, sway and yaw modes of motion are of importance, so that

$$\begin{pmatrix} i \\ j \\ k \end{pmatrix} = 1,2,6 \qquad \text{and} \qquad c_{jk} = 0 \quad . \tag{2.33}$$

The description of the linear ship-fluid system in the frequency domain, as represented in its general form by (2.1) then reduces to

$$\sum_{j}^{1,2,6} \left[\{m_{jk} + a_{jk}(\omega)\}\ddot{x}_j + b_{jk}(\omega)\dot{x}_j \right] = f_k(t) \quad . \tag{2.34}$$

Likewise, the original description of the system in the time domain, as given by (2.17^b) changes into

$$\dot{x}_j(t) = \sum_{i}^{1,2,6} \int_{-\infty}^{t} f_i(\tau)\, k_{ij}(t-\tau)d\tau = \sum_{i}^{1,2,6} \int_{0}^{\infty} k_{ij}(\tau)\, f_i(t-\tau)d\tau \quad . \tag{2.35}$$

With (2.33) now (2.24) takes the form

$$\left.\begin{aligned} U_j(\omega) &= \sum_{i}^{1,2,6} F_i(\omega)\, K_{ij}(\omega) \quad , \\ F_k(\omega) &= \sum_{j}^{1,2,6} R^*_{jk}(\omega)\, U_j(\omega) \quad , \\ F_k(\omega) &= 0 \quad \text{for} \quad k \neq i \quad , \end{aligned}\right\} \quad k = 1,2,6 \quad , \tag{2.36}$$

where on account of (2.7) and (2.33)

$$R^*_{jk}(\omega) = i\omega\{m_{jk}\delta_{jk} + a_{jk}(\omega)\} + b_{jk}(\omega) \qquad , \quad j,k = 1,2,6 \quad , \tag{2.37^a}$$

with δ_{jk} = Kronecker delta: $\delta_{jk} = 1$ for $j = k$, $\delta_{jk} = 0$ for $j \neq k$; the superscript * indicates that the quantity concerned is a reduced version of its original. Then $K_{ij}(\omega)$ can be solved from (2.36) and expressed in terms of $R^*_{jk}(\omega)$. To that end at first $U_j(\omega)$ is eliminated for the respective cases $i = k = 1$, $i = k = 2$ and $i = k = 6$, yielding

$$\left.\begin{aligned} R^*_{11}(\omega)\, K_{i1}(\omega) + R^*_{21}(\omega)\, K_{i2}(\omega) + R^*_{61}(\omega)\, K_{i6}(\omega) &= \delta_{i1} \ , \\ R^*_{12}(\omega)\, K_{i1}(\omega) + R^*_{22}(\omega)\, K_{i2}(\omega) + R^*_{62}(\omega)\, K_{i6}(\omega) &= \delta_{i2} \ , \\ R^*_{16}(\omega)\, K_{i1}(\omega) + R^*_{26}(\omega)\, K_{i2}(\omega) + R^*_{66}(\omega)\, K_{i6}(\omega) &= \delta_{i6} \ , \end{aligned}\right\} \ i = 1,2,6 \quad . \tag{2.38}$$

Due to the extant symmetry of usual ship forms there is only a coupling between swaying and yawing, which means:

$$\left.\begin{aligned} a_{12}(\omega) = a_{21}(\omega) = a_{16}(\omega) = a_{61}(\omega) = 0 \quad , \\ b_{12}(\omega) = b_{21}(\omega) = b_{16}(\omega) = b_{61}(\omega) = 0 \quad , \end{aligned}\right\} \tag{2.39}$$

so that it follows from (2.37^a):

$$R^*_{12}(\omega) = R^*_{21}(\omega) = R^*_{16}(\omega) = R^*_{61}(\omega) = 0 \quad . \tag{2.37^b}$$

Combining (2.38) and (2.37^b) it then can be derived for $K_{ij}(\omega)$:

$$\left.\begin{aligned} & K_{11}(\omega) = \frac{1}{R^*_{11}(\omega)} \quad \text{provided} \quad R^*_{11}(\omega) \neq 0 \quad , \\ & \left.\begin{aligned} & K_{1i}(\omega) = K_{1j}(\omega) = 0 \text{ provided } R^*_{ii}(\omega)R^*_{jj}(\omega) - R^*_{ij}(\omega)R^*_{ji}(\omega) \neq 0 \ , \\ & K_{i1}(\omega) = K_{j1}(\omega) = 0 \text{ provided } R^*_{11}(\omega) \neq 0 \ , \end{aligned}\right\} \text{for } i=2, \ j=6, \\ & \left.\begin{aligned} & K_{ii}(\omega) = \cfrac{1}{R^*_{ii}(\omega) - \cfrac{R^*_{ij}(\omega)R^*_{ji}(\omega)}{R^*_{jj}(\omega)}} \ , \\ & K_{ij}(\omega) = \cfrac{1}{R^*_{ji}(\omega) - \cfrac{R^*_{ii}(\omega)R^*_{jj}(\omega)}{R^*_{ij}(\omega)}} \ , \end{aligned}\right\} \text{ for } i=2,j=6 \text{ and } i=6,j=2 \quad . \end{aligned}\right\} \tag{2.40}$$

Dependent on the values of the respective hydrodynamic coefficients of the damping force, $b_{jk}(\omega)$, for $\omega = 0$, $K_{ij}(\omega)$ may show a singularity (pole) in $\omega = 0$. Any possible singularities in $K_{ij}(\omega)$ for $\omega \neq 0$ due to particular combinations of the hydrodynamic coefficients $a_{jk}(\omega)$ and $b_{jk}(\omega)$ are beforehand excluded. From a physical point of view $a_{jk}(\omega)$ and $b_{jk}(\omega)$ must be even functions of ω. In a more general sense this can be derived mathematically from the fact that $Re[K_{ij}(\omega)]$ is an even function of ω and $Im[K_{ij}(\omega)]$ an odd function. It is an obvious supposition, affirmed by refs. [46, 54, 58, 66] that $a_{jk}(0) = \text{finite} \neq 0$ and $b_{jk}(0) = 0$. For (very) small values of ω, $a_{jk}(\omega)$ and $b_{jk}(\omega)$ then can be represented by

$$\left.\begin{aligned} a_{jk}(\omega) &= a_{jk}(0) + a_{jk}^{(2)}\omega^2 + O(\omega^4) \quad , \\ b_{jk}(\omega) &= \qquad\qquad b_{jk}^{(2)}\omega^2 + O(\omega^4) \quad , \end{aligned}\right\} \text{ for } \omega \to 0 \quad , \tag{2.41}$$

respectively,

where $a_{jk}^{(n)}$ = coefficient of term with order n in power series development for $a_{jk}(\omega)$,

$b_{jk}^{(n)}$ = coefficient of term with order n in power series development for $b_{jk}(\omega)$.

With the generalized mass of the ship, m_{jk}, remaining finite, it then holds good that

$$\lim_{\omega\to 0} R^{*}_{ij}(\omega) = 0 \quad , \tag{2.42}$$

so that $K_{ij}(\omega\to 0)$ behaves singularly, i.e. shows a pole. If there should be further any poles, these probably lie in the left half-plane; the presence of hydrodynamic damping points that way.

The integrals in (2.17^b) and (2.25^a) have to be convergent. As $|f_i(t)|$ is supposed to be bounded in time, these conditions are fulfilled only if $\int_{-\infty}^{\infty}|k_{ij}(t)|dt$ does exist; considering the behaviour of the i.r.f. at infinity this should imply that $k_{ij}(\infty) = 0$.

However, the case in which $k_{ij}(t)$ approaches some non-zero but finite limit as t tends to infinity can be treated too.

If $\lim_{t\to\infty} k_{ij}(t) = k_{ij}(\infty) = \text{constant} \neq 0$, the ordinary Fourier transform of $k_{ij}(t)$ does not exist. This difficulty can be overcome, if in such a case use is made of the generalized function theory (see refs. [84, 86]).

The i.r.f. $k_{ij}(t)$ can be written as:

$$k_{ij}(t) = \{k_{ij}(t) - k_{ij}(\infty)U(t)\} + k_{ij}(\infty)U(t) \quad ,$$

where U(t) is the unit step or Heaviside function, defined as:

$$U(t) = \begin{cases} 0 \text{ for } t < 0 & , \\ \frac{1}{2} \text{ for } t = 0 & , \\ 1 \text{ for } t > 0 & . \end{cases} \tag{2.43}$$

The Fourier transform of $\{k_{ij}(t) - k_{ij}(\infty)U(t)\}$ does exist:

$$\int_{-\infty}^{\infty}\{k_{ij}(\tau) - k_{ij}(\infty)U(\tau)\}\exp(-i\omega\tau)d\tau = -\frac{1}{i\omega}\exp(-i\omega\tau)\{k_{ij}(\tau) - k_{ij}(\infty)U(\tau)\}\Big|_{-\infty}^{\infty} +$$

$$+\frac{1}{i\omega}\int_{-\infty}^{\infty}\{\dot{k}_{ij}(\tau) - k_{ij}(\infty)\delta(\tau)\}\exp(-i\omega\tau)d\tau =$$

$$= \frac{1}{i\omega}\int_{-\infty}^{\infty}\dot{k}_{ij}(\tau)\exp(-i\omega\tau)d\tau - \frac{1}{i\omega}k_{ij}(\infty) \quad .$$

For $t < 0$ is $k_{ij}(t) = \dot{k}_{ij}(t) = 0$, so that it can be written:

$$\int_{-\infty}^{\infty}\{k_{ij}(\tau) - k_{ij}(\infty)U(\tau)\}\exp(-i\omega\tau)d\tau = \frac{1}{i\omega}\{\int_{0}^{\infty}\dot{k}_{ij}(\tau)\exp(-i\omega\tau)d\tau - k_{ij}(\infty)\} \quad .$$

From the generalized function theory it is known that

$$\int_{-\infty}^{\infty}U(\tau)\exp(-i\omega\tau)d\tau = \frac{1}{i\omega} + \pi\delta(\omega) \quad .$$

The Fourier transform of $k_{ij}(t)$ then takes the following form:

$$K_{ij}(\omega) = \int_{-\infty}^{\infty}k_{ij}(\tau)\exp(-i\omega\tau)d\tau = \int_{0}^{\infty}k_{ij}(\tau)\exp(-i\omega\tau)d\tau =$$

$$= \pi\delta(\omega)k_{ij}(\infty) + \frac{1}{i\omega}\int_{0}^{\infty}\dot{k}_{ij}(\tau)\exp(-i\omega\tau)d\tau \quad . \qquad (2.44)$$

This expression contains a singularity for $\omega = 0$; if this singularity is excluded, $K_{ij}(\omega)$ changes into

$$K_{ij}(\omega) = \frac{1}{i\omega}\int_{0}^{\infty}\dot{k}_{ij}(\tau)\exp(-i\omega\tau)d\tau \quad , \quad \omega \neq 0 \quad ,$$

which can be written as:

$$K_{ij}(\omega) = \int_{0}^{\infty}k_{ij}(\tau)\cos(\omega\tau)d\tau - i\int_{0}^{\infty}k_{ij}(\tau)\sin(\omega\tau)d\tau =$$

$$= -\frac{i}{\omega}\{\int_{0}^{\infty}\dot{k}_{ij}(\tau)\cos(\omega\tau)d\tau - i\int_{0}^{\infty}\dot{k}_{ij}(\tau)\sin(\omega\tau)d\tau\} \quad , \qquad (2.45)$$

or otherwise:

$$K_{ij}^{(c)}(\omega) - iK_{ij}^{(s)}(\omega) = -\frac{i}{\omega}\dot{K}_{ij}^{(c)}(\omega) - \frac{1}{\omega}\dot{K}_{ij}^{(s)}(\omega) \quad ,$$

where $\dot{K}_{ij}^{(s)}(\omega)$ and $\dot{K}_{ij}^{(c)}(\omega)$ are the Fourier sine transform and the Fourier cosine transform of $\dot{k}_{ij}(t)$, respectively (see refs. [85, 84, 86]). From this it follows finally:

$$K_{ij}^{(c)}(\omega) = -\frac{1}{\omega}\dot{K}_{ij}^{(s)}(\omega) \quad , \quad K_{ij}^{(s)}(\omega) = \frac{1}{\omega}\dot{K}_{ij}^{(c)}(\omega) \quad \text{with } \omega \neq 0 \quad . \tag{2.46^{a,b}}$$

If use is made of these expressions for $K_{ij}^{(c)}(\omega)$ and $K_{ij}^{(s)}(\omega)$, then (2.27^{a,b}) and (2.30) keep their validity setting beforehand in (2.3), for $k = i$, $|\hat{f}_k(\omega)| = 1$ and $\varepsilon_k(\omega) = 0$.

It has to be noted that $K_{ij}^{(c)}(\omega)$ and $K_{ij}^{(s)}(\omega)$ in the case under consideration are no longer Fourier transforms of $k_{ij}(t)$, because these do not exist. Nevertheless an inverse Fourier transform is still possible. To that end the following expression is considered:

$$\int_{-\infty}^{\infty}\{k_{ij}(\tau) - k_{ij}(\infty)U(\tau)\}\cos(\omega\tau)d\tau =$$

$$= \frac{1}{\omega}\{k_{ij}(\tau) - k_{ij}(\infty)U(\tau)\}\sin(\omega\tau)\Big|_{-\infty}^{\infty} - \frac{1}{\omega}\int_{-\infty}^{\infty}\{\dot{k}_{ij}(\tau) - k_{ij}(\infty)\delta(\tau)\}\sin(\omega\tau)d\tau =$$

$$= -\frac{1}{\omega}\int_{-\infty}^{\infty}\dot{k}_{ij}(\tau)\sin(\omega\tau)d\tau + \frac{1}{\omega}k_{ij}(\infty)\int_{-\infty}^{\infty}\delta(\tau)\sin(\omega\tau)d\tau =$$

$$= -\frac{1}{\omega}\int_{0}^{\infty}\dot{k}_{ij}(\tau)\sin(\omega\tau)d\tau = -\frac{1}{\omega}\dot{K}_{ij}^{(s)}(\omega) = K_{ij}^{(c)}(\omega) \quad ,$$

or, for $t > 0$ $K_{ij}^{(c)}(\omega)$ is the Fourier cosine transform of $\{k_{ij}(t) - k_{ij}(\infty)\}$; for the inverse Fourier transform it can be written (refs. [85, 84, 86]):

$$k_{ij}(t) = k_{ij}(\infty) + \frac{2}{\pi}\int_{0}^{\infty}K_{ij}^{(c)}(\omega)\cos(\omega t)d\omega \quad , \quad \text{for } t > 0 \quad . \tag{2.47^{a}}$$

When $k_{ij}(\infty) = 0$, (2.47^a) is identical with (2.29^a).

In an analogous way as above it can be considered:

$$\int_{-\infty}^{\infty}\{k_{ij}(\tau) - k_{ij}(\infty)U(\tau)\}\sin(\omega\tau)d\tau =$$

$$= -\frac{1}{\omega}\{k_{ij}(\tau) - k_{ij}(\infty)U(\tau)\}\cos(\omega\tau)\Big|_{-\infty}^{\infty} + \frac{1}{\omega}\int_{-\infty}^{\infty}\{\dot{k}_{ij}(\tau) - k_{ij}(\infty)\delta(\tau)\}\cos(\omega\tau)d\tau =$$

$$= \frac{1}{\omega}\int_{-\infty}^{\infty}\dot{k}_{ij}(\tau)\cos(\omega\tau)d\tau - \frac{1}{\omega}k_{ij}(\infty)\int_{-\infty}^{\infty}\delta(\tau)\cos(\omega\tau)d\tau =$$

$$= -\frac{1}{\omega}k_{ij}(\infty) + \frac{1}{\omega}\int_{0}^{\infty}\dot{k}_{ij}(\tau)\cos(\omega\tau)d\tau = \frac{1}{\omega}\{\dot{K}_{ij}^{(c)}(\omega) - k_{ij}(\infty)\} =$$

$$= K_{ij}^{(s)}(\omega) - \frac{1}{\omega}k_{ij}(\infty) \quad ,$$

or, for $t > 0$ $\quad K_{ij}^{(s)}(\omega) - \frac{1}{\omega} k_{ij}(\infty)$ is the Fourier sine transform of $\{k_{ij}(t) - k_{ij}(\infty)\}$; for the inverse Fourier transform it holds good that (refs. [85, 84, 86]):

$$k_{ij}(t) = k_{ij}(\infty) + \frac{2}{\pi} \int_0^\infty \{K_{ij}^{(s)}(\omega) - \frac{1}{\omega} k_{ij}(\infty)\} \sin(\omega t) d\omega =$$

$$= k_{ij}(\infty)\{1 - \frac{2}{\pi} \int_0^\infty \frac{\sin(\omega t)}{\omega} d\omega\} + \frac{2}{\pi} \int_0^\infty K_{ij}^{(s)}(\omega) \sin(\omega t) d\omega \qquad ;$$

since

$$\int_0^\infty \frac{\sin(\omega t)}{\omega} d\omega = \frac{\pi}{2} \quad \text{for } t > 0 \qquad ,$$

$k_{ij}(t)$ then takes the form:

$$k_{ij}(t) = \frac{2}{\pi} \int_0^\infty K_{ij}^{(s)}(\omega) \sin(\omega t) d\omega \quad \text{for } t > 0 \qquad . \tag{2.47^b}$$

Bearing in mind that $k_{ij}(\infty)$ is a real quantity, combination of (2.44), (2.45) and (2.46^{a,b}) yields

$$\left.\begin{aligned} \mathrm{Re}[K_{ij}(\omega)] &= \pi\delta(\omega)k_{ij}(\infty) + K_{ij}^{(c)}(\omega) \quad , \\ \mathrm{Im}[K_{ij}(\omega)] &= - K_{ij}^{(s)}(\omega) \quad , \end{aligned}\right\} \tag{2.48}$$

which expressions have a form analogous to (2.31^{a,b}). As

$$\int_0^\infty \delta(\omega) \cos(\omega t) d\omega = \frac{1}{2} \qquad ,$$

it can be stated that (2.25^c) holds generally whether $k_{ij}(\infty) = 0$ or $k_{ij}(\infty) = \text{constant} \neq 0$, provided $\mathrm{Re}[K_{ij}(\omega)]$ and $\mathrm{Im}[K_{ij}(\omega)]$ are applied according to (2.48). Within this concept $K_{ij}(\omega)$ as presented by (2.40) has to be conceived as the non-generalized f.r.f. with $K_{ij}^{(c)}(\omega)$ and $-K_{ij}^{(s)}(\omega)$ as its respective real and imaginary parts. Apparently, for ship motions without restoring force a correct mapping between frequency and time domain can only be obtained by adding to the original, non-generalized f.r.f. $K_{ij}(\omega)$ (2.40), which behaves singularly in $\omega = 0$, a contribution from a delta function in

$\omega = 0$. The thus generalized f.r.f. with real and imaginary parts according to (2.48) then can be subjected to an inverse Fourier transformation in the usual way.

If $K_{ij}^{(c)}(\omega)$ and $K_{ij}^{(s)}(\omega)$ are known, it is not difficult to determine whether $k_{ij}(\infty)$ equals zero or not. Using (2.47^b) $k_{ij}(\infty)$ can be written as

$$k_{ij}(\infty) = \lim_{t\to\infty} \frac{2}{\pi} \int_0^\infty K_{ij}^{(s)}(\omega) \sin(\omega t) d\omega \quad .$$

By substitution of (2.46^b) this expression takes the form:

$$k_{ij}(\infty) = \lim_{t\to\infty} \frac{2}{\pi} \int_0^\infty \dot{K}_{ij}^{(c)}(\omega) \frac{\sin(\omega t)}{\omega} d\omega \quad .$$

If a function $f(\omega)$ on an interval $(0,a)$ satisfies the Dirichlet conditions, then it holds good for positive values of a that (see refs. [85, 87]):

$$\lim_{t\to\infty} \int_0^a f(\omega) \frac{\sin(\omega t)}{\omega} d\omega = \frac{1}{2}\pi f(0^+) \quad , \quad a > 0 \quad .$$

Making use of this theorem $k_{ij}(\infty)$ changes into:

$$k_{ij}(\infty) = \dot{K}_{ij}^{(c)}(0^+) = \lim_{\omega\to 0} \omega K_{ij}^{(s)}(\omega) \quad . \tag{2.49}$$

From (2.40) and (2.48) in combination with (2.41) it is to be derived that

$$\lim_{\omega\to 0} K_{ij}^{(c)}(\omega) = \text{finite} \quad \text{and} \quad \lim_{\omega\to 0} K_{ij}^{(s)}(\omega) = \infty \quad ;$$

since for $\omega \to \infty$ it can be shown that $a_{jk}(\infty)$ remains finite and $b_{jk}(\omega)$ asymptotically tends to zero (see e.g. refs. [89, 88, 90, 54, 60, 73]), it holds at the same time

$$\lim_{\omega\to\infty} K_{ij}^{(c)}(\omega) = 0 \quad \text{and} \quad \lim_{\omega\to\infty} K_{ij}^{(s)}(\omega) = 0 \quad ;$$

therefore ${}_0\int^\infty \mathrm{Re}[K_{ij}(\omega)]d\omega$ does converge absolutely and ${}_0\int^\infty \mathrm{Im}[K_{ij}(\omega)]d\omega$ does not. This applies as far as ship motions without restoring force are dealt with. Then, on account of the lemma of Riemann-Lebesgue (refs. [91, 87]) it holds good that

$$\lim_{t\to\infty} \int_0^\infty K_{ij}^{(c)}(\omega) \cos(\omega t)d\omega = 0 \quad ,$$

so that indeed (2.47^a) leads to

$$\lim_{t\to\infty} k_{ij}(t) = k_{ij}(\infty) = \text{constant} \quad .$$

Due to the behaviour of $K_{ij}^{(s)}(\omega)$ for $\omega \to 0$, the determination of $k_{ij}(t)$ using the integral in (2.47^b) requires an asymptotic expansion of its integrand for small values of ω. In evaluating the i.r.f., therefore in (2.25^c) the expression containing $Im[K_{ij}(\omega)]$ is further left out of consideration. Naturally, in the limit for $t \to \infty$ (2.47^b) also must yield $k_{ij}(\infty)$ = constant $\neq 0$.

N.B. For ship motions with a restoring force, which implies $k_{ij}(\infty) = 0$, $_0\int^\infty Im[K_{ij}(\omega)]d\omega$ on the contrary is absolutely convergent, so that in this case the lemma of Riemann-Lebesgue does apply and indeed $k_{ij}(\infty) = 0$.

Besides by means of the above approach (ref. [73]), expressions for the generalized f.r.f. and the i.r.f. can also be determined in a more obvious and direct way by applying certain aspects of the theory of Laplace transforms related to the Fourier integral of a causal function (ref. [74]).

Let the Laplace transform associated with the generalized f.r.f. $K_{ij}(\omega)$ be denoted by $H_{ij}(s)$, which function on account of ref. [79] can be understood as the general transfer function for the j-direction in response to a (force) excitation in the i-direction:

$$H_{ij}(s) = L\{k_{ij}(t)\} = \int_0^\infty k_{ij}(\tau) \exp(-s\tau)d\tau \quad , \tag{2.50}$$

where $s = \lambda + i\omega$ = complex variable with $Re[s] = \lambda$, $Im[s] = \omega$,

$L\{f(t)\} = \int_0^\infty f(\tau) \exp(-s\tau)d\tau$ = unilateral Laplace transform of $f(t)$ with region of existence $Re[s] > Re[s_1]$,

s_1 = certain complex number.

If $L\{f(t)\}$ exists and $f(t)$ has a limit for $t \to \infty$ then it holds (ref. [87]):

$$\lim_{s\downarrow 0} sL\{f(t)\} = \lim_{t\to\infty} f(t) \quad .$$

Making use of this lemma one obtains:

$$\lim_{t\to\infty} k_{ij}(t) = k_{ij}(\infty) = \lim_{s\downarrow 0} sL\{k_{ij}(t)\} = \lim_{s\downarrow 0} sH_{ij}(s) \quad . \tag{2.51}$$

Now the Fourier transforms in (2.36) can be replaced by Laplace transforms. Hereby it has to be borne in mind that only then a set of meaningful expressions is generated, if the respective Laplace transforms of $\dot{x}_j(t)$, $f_i(t)$ and $k_{ij}(t)$ exist and at least whether the Laplace transform of $f_i(t)$ or that of $k_{ij}(t)$ on the right-hand side of the Laplace-transformed convolution integral converges absolutely. Then the $H_{ij}(s)$-function can be determined in a similar way as done for the non-generalized f.r.f. (2.40), yielding

$$\left.\begin{array}{ll}
H_{11}(s) = \dfrac{1}{R^*_{11}(s)} \quad , & \\[2ex]
\left.\begin{array}{l} H_{1i}(s) = H_{1j}(s) = 0 \quad , \\[2ex] H_{i1}(s) = H_{j1}(s) = 0 \quad , \end{array}\right\} & \text{for } i=2, j=6 \quad , \\[4ex]
\left.\begin{array}{l} H_{ii}(s) = \dfrac{1}{R^*_{ii}(s) - \dfrac{R^*_{ij}(s)\, R^*_{ji}(s)}{R^*_{jj}(s)}} \quad , \\[6ex] H_{ij}(s) = \dfrac{1}{R^*_{ji}(s) - \dfrac{R^*_{ii}(s)\, R^*_{jj}(s)}{R^*_{ij}(s)}} \quad , \end{array}\right\} & \text{for } i=2, j=6 \text{ and } i=6, j=2 \quad ,
\end{array}\right\} \quad (2.52)$$

where on account of (2.37[a,b]) $R^*_{ij}(s)$ has the form:

$$\left.\begin{array}{l}
R^*_{ij}(s) = s\{m_{ij}\delta_{ij} + a_{ij}(s)\} + b_{ij}(s) \quad , \\[1ex]
R^*_{12}(s) = R^*_{21}(s) = R^*_{16}(s) = R^*_{61}(s) = 0 \quad ,
\end{array}\right\} \quad i,j = 1,2,6 \quad . \qquad (2.53)$$

Since (2.34) describes the ship-fluid system in the 'real frequency' or ω-domain, formally $H_{ij}(s)$ -being a function of the 'complex frequency' s- is only known for $s = i\omega$. Therefore it is obvious to work with its related (generalized) Fourier transform of $k_{ij}(t)$, viz. $K_{ij}(\omega)$.

With respect to the relation between $H_{ij}(s)$ and $K_{ij}(\omega)$ generally three cases can be considered. The region of existence of $H_{ij}(s)$ is denoted by $Re[s] > Re[s_1]$. If the region of convergence of $H_{ij}(s)$ contains the $i\omega$-axis in its interior, i.e. if $Re[s_1] < 0$ (first case), then

$$K_{ij}(\omega) = H_{ij}(s)\Big|_{s=i\omega} \quad . \tag{2.54}$$

This case applies generally to modes of motion with a restoring force, implies that $k_{ij}(\infty) = 0$ and is further left out of consideration.
If the $i\omega$-axis is outside the region of convergence of $H_{ij}(s)$, i.e. if $Re[s_1] > 0$ (second case), then $K_{ij}(\omega)$ does not exist: the function $k_{ij}(t)$ has no Fourier transform in terms of the generalized function theory and the linear ship-fluid system behaves unstably.
The last case is $Re[s_1] = 0$; the function $H_{ij}(s)$ is analytic for $Re[s] > 0$, but at least one of the singular points lies on the $i\omega$-axis. This case applies to modes of motion without restoring force, implies that $k_{ij}(\infty)$ = constant $\neq 0$ and is connected with singularities (poles) in $H_{ij}(s)$ for $s = 0$, i.e. $\lambda = 0$, $i\omega = 0$. In this context, now, a function $H_{ij}(s)$ is considered with n simple poles $i\omega_1$, $i\omega_2$, ..., $i\omega_n$ and no other singularities in the half plane $Re[s] \geq 0$. This function then can be written as (ref. [83])

$$H_{ij}(s) = G_{ij}(s) + \sum_{m=1}^{n} \alpha_{ij}^{(m)} (s-i\omega_m)^{-1} \quad ,$$

in which $G_{ij}(s)$ = a function free from singularities for $Re[s] \geq 0$,

$$\alpha_{ij}^{(m)} = \lim_{s \to i\omega_m} (s-i\omega_m)\, H_{ij}(s) \quad .$$

From (2.54) it follows that the Fourier transform corresponding to $G_{ij}(s)$ is given by $G_{ij}(i\omega)$; therefore (ref. [83])

$$K_{ij}(\omega) = H_{ij}(s)\Big|_{s=i\omega} + \pi \sum_{m=1}^{n} \alpha_{ij}^{(m)}\, \delta(\omega-\omega_m) \quad .$$

With $i\omega_m = 0$ and $n = 1$ this leads directly to an expression for the generalized f.r.f., viz.

$$K_{ij}(\omega) = H_{ij}(i\omega) + \pi\alpha_{ij}\delta(\omega) \quad , \tag{2.55}$$

where

$$H_{ij}(i\omega) = H_{ij}(s)\Big|_{s=i\omega} \quad , \tag{2.56^a}$$

$$\alpha_{ij} = \lim_{s \downarrow 0} sH_{ij}(s) \quad . \tag{2.56^b}$$

On account of (2.51) it also holds good that

$$\alpha_{ij} = k_{ij}(\infty) \qquad . \tag{2.56^c}$$

In this context $H_{ij}(i\omega)$ is to be conceived as the non-generalized f.r.f. From (2.52), (2.53) and (2.56[a]) it can be derived for $H_{ij}(i\omega)$:

$$\left.\begin{aligned}
&H_{11}(i\omega) = \frac{b_{11}(\omega)}{\{m_{11}+a_{11}(\omega)\}^2\omega^2 + b_{11}^2(\omega)} - i\,\frac{\omega\{m_{11}+a_{11}(\omega)\}}{\{m_{11}+a_{11}(\omega)\}^2\omega^2 + b_{11}^2(\omega)} \quad ,\\
&\left.\begin{aligned}
&H_{1i}(i\omega) = H_{1j}(i\omega) = 0 \quad ,\\
&H_{i1}(i\omega) = H_{j1}(i\omega) = 0 \quad ,
\end{aligned}\right\} \text{ for } i=2, j=6 \quad ,\\
&\left.\begin{aligned}
H_{ii}(i\omega) &= \frac{p_{ii}(\omega)b_{jj}(\omega) + \omega q_{ii}(\omega)\{m_{jj}+a_{jj}(\omega)\}}{p_{ii}^2(\omega) + q_{ii}^2(\omega)} + \\
&\quad - i\,\frac{q_{ii}(\omega)b_{jj}(\omega) - \omega p_{ii}(\omega)\{m_{jj}+a_{jj}(\omega)\}}{p_{ii}^2(\omega) + q_{ii}^2(\omega)} \quad ,\\
H_{ij}(i\omega) &= \frac{p_{ij}(\omega)b_{ij}(\omega) + \omega q_{ij}(\omega)a_{ij}(\omega)}{p_{ij}^2(\omega) + q_{ij}^2(\omega)} + \\
&\quad - i\,\frac{q_{ij}(\omega)b_{ij}(\omega) - \omega p_{ij}(\omega)a_{ij}(\omega)}{p_{ij}^2(\omega) + q_{ij}^2(\omega)} \quad ,
\end{aligned}\right\} \begin{array}{l}\text{for } i=2, j=6\\ \text{and } i=6, j=2\end{array} \quad ,
\end{aligned}\right\} \tag{2.57}$$

with

$$\begin{aligned}
p_{ii}(\omega) &= b_{ii}(\omega)b_{jj}(\omega) - b_{ij}(\omega)b_{ji}(\omega) + \\
&\quad -\omega^2\left[\{m_{ii}+a_{ii}(\omega)\}\{m_{jj}+a_{jj}(\omega)\} - a_{ij}(\omega)a_{ji}(\omega)\right],\\
q_{ii}(\omega) &= \omega\left[b_{ii}(\omega)\{m_{jj}+a_{jj}(\omega)\} + b_{jj}(\omega)\{m_{ii}+a_{ii}(\omega)\} + \right.\\
&\quad \left.-\{a_{ji}(\omega)b_{ij}(\omega) + a_{ij}(\omega)b_{ji}(\omega)\}\right] \quad ,
\end{aligned}$$

$$\left.\begin{aligned}
&p_{ii}(\omega) = p_{jj}(\omega) \quad ,\\
&q_{ii}(\omega) = q_{jj}(\omega) \quad ,\\
&p_{ij}(\omega) = p_{ji}(\omega) = -p_{ii}(\omega) \quad ,\\
&q_{ij}(\omega) = q_{ji}(\omega) = -q_{ii}(\omega) \quad ,
\end{aligned}\right\} \text{for } i=2,j=6 \; ; \qquad (2.58)$$

further $m_{11} = m_{22}$.

On account of (2.41) -bearing in mind that $k_{ij}(t)$ and $b_{ij}(\omega)$ are real functions- it must hold good that

$$\lim_{s \downarrow 0} \frac{b_{ij}(s)}{s} = 0 \quad .$$

Applying this result, combination of (2.52), (2.53) and ($2.56^{b,c}$) yields for α_{ij}:

$$\left.\begin{aligned}
&\alpha_{11} = k_{11}(\infty) = \frac{1}{m_{11} + a_{11}(0)} \quad ,\\
&\left.\begin{aligned}
&\alpha_{1i} = k_{1i}(\infty) = \alpha_{1j} = k_{1j}(\infty) = 0 \quad ,\\
&\alpha_{i1} = k_{i1}(\infty) = \alpha_{j1} = k_{j1}(\infty) = 0 \quad ,
\end{aligned}\right\} \text{for } i=2,j=6 \quad ,\\
&\left.\begin{aligned}
&\alpha_{ii} = k_{ii}(\infty) = \frac{m_{jj} + a_{jj}(0)}{\{m_{ii} + a_{ii}(0)\}\{m_{jj} + a_{jj}(0)\} - a_{ij}(0)a_{ji}(0)} \; ,\\
&\alpha_{ij} = k_{ij}(\infty) = \frac{-a_{ij}(0)}{\{m_{ii} + a_{ii}(0)\}\{m_{jj} + a_{jj}(0)\} - a_{ij}(0)a_{ji}(0)} \; ,
\end{aligned}\right\} \begin{aligned}&\text{for } i=2,j=6\\ &\text{and } i=6,j=2.\end{aligned}
\end{aligned}\right\} (2.59)$$

The fact that the respective expressions for $\alpha_{ij} = k_{ij}(\infty)$ are independent of b_{ij} is caused by the parabolic behaviour of $b_{ij}(\omega)$ near by the point $\omega = 0$. Since it hold good that $k_{ij}(\infty) = \text{constant} \neq 0$, the linear ship-fluid system indeed behaves stably in the case under consideration (see Appendix A).

The real and imaginary part of the generalized f.r.f. $K_{ij}(\omega)$ presented in (2.55) reads as

$$\left.\begin{aligned} Re[K_{ij}(\omega)] &= Re[H_{ij}(i\omega)] + \pi\alpha_{ij}\delta(\omega) \quad , \\ Im[K_{ij}(\omega)] &= Im[H_{ij}(i\omega)] \quad , \end{aligned}\right\} \tag{2.60}$$

respectively, which expressions are identical to those in (2.48).

The i.r.f. $k_{ij}(t)$ now can be evaluated by means of (2.25^c) with $Re[K_{ij}(\omega)]$ given by (2.60); for reasons already mentioned, the integral expression in (2.25^c) containing $Im[K_{ij}(\omega)]$ is left out of consideration. $Re[H_{ij}(i\omega)]$ and $\alpha_{ij} = k_{ij}(\infty)$ occurring in the expression for $Re[K_{ij}(\omega)]$ are to be determined according to (2.57),(2.58) and (2.59), respectively. A necessary condition then is that the hydrodynamic coefficients $a_{ij}(\omega)$ and $b_{ij}(\omega)$ are known functions of ω.

For a physical interpretation and an explanation of the behaviour of the i.r.f. at infinity in case of (uncoupled) ship motions without restoring force, reference is made to Appendix B.

2.5.2.1. Special cases

A special case arises when the hydrodynamic coefficients are independent of the (constant) forward speed V_1 and the (constant) lateral speed V_2; this situation occurs, for instance, with (very) small values of V_1 and V_2. A further simplification is achieved, if the modes of motion of the ship are supposed to be uncoupled.

In case of a negligible influence of V_1,V_2 on the hydrodynamic coefficients it can be written (see also (2.12^a)):

$$a_{ij}(\omega) = a_{ji}(\omega) \quad , \quad b_{ij}(\omega) = b_{ji}(\omega) \quad . \tag{2.61^a}$$

With these expressions (2.57),(2.58) and (2.59) lead to

$$H_{ij}(i\omega) = H_{ji}(i\omega) \tag{2.61^b}$$

and

$$\alpha_{ij} = k_{ij}(\infty) = \alpha_{ji} = k_{ji}(\infty) \quad , \tag{2.61^c}$$

respectively. From (2.55) it then follows

$$K_{ij}(\omega) = K_{ji}(\omega) \qquad , \tag{2.61^d}$$

so that (2.60) and (2.25^c) combined yield

$$k_{ij}(t) = k_{ji}(t) \qquad . \tag{2.61^e}$$

In other words, for the case under consideration the sequence of the respective subscripts i,j -representing directions- may be mutually interchanged, which eventually induces simplified expressions for the i.r.f.

When at the same time the modes of motion of the ship are uncoupled, it holds good for the hydrodynamic coefficients (see also (2.26^a))

$$a_{ij}(\omega) = a_{ji}(\omega) = 0 \quad , \quad b_{ij}(\omega) = b_{ji}(\omega) = 0 \quad , \quad \text{for } i \neq j \quad , \tag{2.62^a}$$

and therefore, from the respective expressions (2.57),(2.58) and (2.59),

$$H_{ij}(i\omega) = H_{ji}(i\omega) = 0 \quad \text{for } i \neq j \tag{2.62^b}$$

and

$$\alpha_{ij} = k_{ij}(\infty) = \alpha_{ji} = k_{ji}(\infty) = 0 \quad \text{for } i \neq j \qquad . \tag{2.62^c}$$

Due to (2.55) the generalized f.r.f. then reads as

$$K_{ii}(\omega) = H_{ii}(i\omega) + \pi\alpha_{ii}\delta(\omega) \qquad , \tag{2.63}$$

where, on account of (2.57),(2.58) and (2.59),

$$H_{ii}(i\omega) = \frac{b_{ii}(\omega)}{\{m_{ii} + a_{ii}(\omega)\}^2\omega^2 + b_{ii}^2(\omega)} - i\,\frac{\omega\{m_{ii} + a_{ii}(\omega)\}}{\{m_{ii} + a_{ii}(\omega)\}^2\omega^2 + b_{ii}^2(\omega)} \quad , \tag{2.64}$$

and

$$\alpha_{ii} = k_{ii}(\infty) = \frac{1}{m_{ii} + a_{ii}(0)} \qquad , \tag{2.65}$$

respectively, for i = 1,2,6. Since (2.60) now takes the form

$$\left.\begin{aligned} Re[K_{ii}(\omega)] &= Re[H_{ii}(i\omega)] + \pi\alpha_{ii}\delta(\omega) \quad , \\ Im[K_{ii}(\omega)] &= Im[H_{ii}(i\omega)] \quad , \end{aligned}\right\} \text{for } i = 1,2,6 \quad , \tag{2.66}$$

the expression for the i.r.f. (2.25^c) finally reduces to

$$\left.\begin{aligned} k_{ii}(t) &= \frac{2}{\pi}\int_0^\infty Re[K_{ii}(\omega)]\cos(\omega t)d\omega = \\ &= -\frac{2}{\pi}\int_0^\infty Im[K_{ii}(\omega)]\sin(\omega t)d\omega \quad \text{for } t > 0 \quad , \\ k_{ii}(0) &= \frac{1}{\pi}\int_0^\infty Re[K_{ii}(\omega)]d\omega = \frac{1}{2}\,k_{ii}(0^+) \quad , \\ k_{ii}(t) &\equiv 0 \quad \text{for } t < 0 \quad . \end{aligned}\right\} (i = 1,2,6) \tag{2.67}$$

For the case of uncoupled, horizontal ship motions the descriptions of the ship-fluid system in the frequency and the time domain, as given by (2.34) and (2.35), respectively, now take a simpler form, viz.:

$$\{m_{ii} + a_{ii}(\omega)\}\ddot{x}_i + b_{ii}(\omega)\dot{x}_i = f_i(t) \quad (i = 1,2,6) \tag{2.68}$$

and

$$\dot{x}_i(t) = \int_{-\infty}^{t} f_i(\tau)\,k_{ii}(t-\tau)d\tau = \int_0^\infty k_{ii}(\tau)\,f_i(t-\tau)d\tau \quad (i = 1,2,6) \quad . \tag{2.69}$$

Using (2.66), (2.64) and (2.65) combined with (2.41) for $j = k = i$ it can be shown in a simple way that the integral $_0\int^\infty Re[K_{ii}(\omega)]d\omega$ indeed converges absolutely. Further,

$$\lim_{\omega\to 0} Im[K_{ii}(\omega)] = -\frac{1}{m_{ii} + a_{ii}(0)}\left.\frac{1}{\omega}\right|_{\omega\to 0} \quad ,$$

i.e. $Im[K_{ii}(\omega)]$ shows a singular point for $\omega = 0$. Although $_0\int^\infty Im[K_{ii}(\omega)]d\omega$ consequently does not converge absolutely, the expression for the i.r.f. as given by

$$k_{ii}(t) = -\frac{2}{\pi}\int_0^\infty \mathrm{Im}[K_{ii}(\omega)]\sin(\omega t)d\omega \quad \text{for } t > 0$$

still does exist, since it can be written for sin(ωt):

$$\sin(\omega t) = \omega t - \frac{(\omega t)^3}{3!} + O(\omega^5 t^5) \quad .$$

The above expression for $k_{ii}(t)$ also leads directly to:

$$\alpha_{ii} = k_{ii}(\infty) = \lim_{t\to\infty} k_{ii}(t) = -\frac{2}{\pi}\lim_{t\to\infty}\int_0^\infty \mathrm{Im}[K_{ii}(\omega)]\sin(\omega t)d\omega =$$

$$= -\frac{2}{\pi}\lim_{t\to\infty}\int_0^\infty \omega\ \mathrm{Im}[K_{ii}(\omega)]\frac{\sin(\omega t)}{\omega}\ d\omega =$$

$$= -\lim_{\omega\to 0} \omega\ \mathrm{Im}[K_{ii}(\omega)] = \frac{1}{m_{ii} + a_{ii}(0)} \quad ,$$

provided $\omega \mathrm{Im}[K_{ii}(\omega)]$ satisfies the Dirichlet conditions on the interval $(0,\infty)$.

For the case under consideration, with negligible influence of V_1, V_2 on the hydrodynamic coefficients, the uncoupling of the ship motions can be materialized by schematizing the ship to a rigid, prismatic body with a rectangular cross-section and a symmetrical distribution of mass. Besides, in case of shallow water the uncoupling of the motions requires a horizontal bottom. When a closed wall is present, the ship motions are only uncoupled if one of the horizontal body axes of the (schematized) ship is parallel to the wall.

In addition to the method already dealt with, there are two further methods to derive an expression for $k_{ii}(t)$ as given in (2.67). These methods, in which use is made of Laplace transforms, are not specifically different, but they are more direct. For an explanation in this it is referred to Appendix C.

N.B.1. If, for uncoupled, horizontal ship motions, the hydrodynamic coefficients $a_{ii}(\omega)$ and $b_{ii}(\omega)$ were constants with $b_{ii} \neq 0$, (2.67) can be solved analytically using (2.66) -where α_{ii} vanishes- and (2.64), yielding

$$k_{ii}(t) = \frac{1}{m_{ii} + a_{ii}} \exp\left(-\frac{b_{ii}}{m_{ii} + a_{ii}} t\right) U(t) \quad ;$$

in this expression a_{ii} and b_{ii} have to be conceived as constant quantities independent of the circular frequency ω.
With $b_{ii} = 0$ the i.r.f. can be derived to be

$$k_{ii}(t) = \frac{1}{m_{ii} + a_{ii}} U(t) \quad .$$

N.B.2. If the hydrodynamic effects -i.e. the influence of the water- are left out of consideration, it holds good that

$$a_{ij}(\omega) = 0 \quad , \quad b_{ij}(\omega) = 0 \quad , \quad i,j = 1,2,6 \quad .$$

Anyhow, the coupling between the respective modes of motion then vanishes and (2.57),(2.58) and (2.59) change into

$$\left.\begin{aligned} H_{ii}(i\omega) &= - i \frac{1}{\omega m_{ii}} \quad , \\ H_{ij}(i\omega) &= H_{ji}(i\omega) \quad \text{for } i \neq j \quad , \end{aligned}\right\}$$

and

$$\left.\begin{aligned} \alpha_{ii} &= k_{ii}(\infty) = \frac{1}{m_{ii}} \quad , \\ \alpha_{ij} &= k_{ij}(\infty) = \alpha_{ji} = k_{ji}(\infty) = 0 \quad \text{for } i \neq j \quad , \end{aligned}\right\}$$

respectively, so that by way of (2.66) the i.r.f. gets a form as presented in (2.67). Substitution of the above expressions into (2.66) and subsequent combination of (2.67) and (2.66) yields

$$\left.\begin{aligned} k_{ii}(t) &= \frac{1}{m_{ii}} = \frac{2}{\pi} \int_0^\infty \frac{\sin(\omega t)}{m_{ii}\omega} d\omega \quad \text{for } t > 0 \quad , \\ k_{ii}(0) &= \frac{1}{2m_{ii}} \quad , \\ k_{ii}(t) &\equiv 0 \quad \text{for } t < 0 \quad . \end{aligned}\right\}$$

Since

$$\int_0^\infty \frac{\sin(\omega t)}{\omega}\,d\omega = \frac{\pi}{2} \qquad \text{for } t > 0 \quad ,$$

it can be written for $k_{ii}(t)$:

$$k_{ii}(t) = \frac{1}{m_{ii}}\,U(t) \qquad (i = 1,2,6) \quad .$$

For the situation under consideration again the ship-fluid system in the time domain is described by (2.69). Substituting the above expression for $k_{ii}(t)$ into (2.69) one obtains

$$\dot{x}_i(t) = \frac{1}{m_{ii}} \int_{-\infty}^{t} f_i(\tau)d\tau \quad ,$$

or

$$m_{ii}\ddot{x}_i(t) = f_i(t) \quad ,$$

i.e. Newton's second law. Naturally this obvious result also can be derived directly from (2.34), c.q. (2.68), representing the ship-fluid system in the frequency domain.

2.6. Causality

Like each physical system also the linear ship-fluid system is a causal system, which finds expression both in the frequency domain and in the time domain.

The respective hydrodynamic coefficients of the mass term and the damping force are mutually dependent, since they are to be derived from one and the same physical quantity, viz. the distribution of the hydrodynamic stress on the wet ship hull. Considering, for instance, a ship-fluid system with a total number of n hydrodynamic coefficients, this implies that n/2 relations exist to be satisfied by $a_{ij}(\omega)$ and $b_{ij}(\omega)$. The mutual dependence in the frequency domain mentioned above is equivalent to the causal behaviour of the ship-fluid system in the time domain. This very attribute gives rise to the so-called 'memory effect' materialized by the wave radiation at the free water-surface: only waves already generated (i.e. 'the past') do influence the interaction between the moving ship and the surrounding water, the waves to be generated (i.e. 'the future') do not. It can be established that the memory effect in the frequency domain is expressed by the frequency dependence of the hydrodynamic coefficients, and that this frequency dependence in its turn is due to the wave radiation at the free water-surface.

Regarding the general description of the linear ship-fluid system in the time domain (2.17^b), it is observed that the memory effect is represented by means of the convolution integrals and especially by the i.r.f. $k_{ij}(t)$. Of great importance for the relation between the respective system descriptions in the frequency domain and the time domain is the property that the system behaves causally, which finds expression in the real, causal time function $k_{ij}(t)$, viz. $k_{ij}(t) \equiv 0$ for $t < 0$. In this context the following remark has to be made. In fact, causality conditions for the real and imaginary part of $K_{ij}(\omega)$ should be introduced as from the first expression in (2.24), since this expression in itself passes over the information embedded in (2.18). These very conditions should be taken along throughout all further derivations until (2.25^c), where they allow the inverse Fourier transform applied. (2.25^c) then directly expresses the causality conditions and is equivalent to the explicit relations between the real and imaginary part of the (generalized) f.r.f. of a causal system referred to as the so-called Hilbert transforms.
So, for a causal function, say $k_{ij}(t)$, there exists a relation between the real and imaginary part of its Fourier transform $K_{ij}(\omega)$. For convenience' sake omitting the subscripts it can be written for $K_{ij}(\omega)$:

$$K(\omega) = P(\omega) + iQ(\omega) \quad , \tag{2.70^a}$$

with

$$P(\omega) = \mathrm{Re}[K(\omega)] \quad \text{and} \quad Q(\omega) = \mathrm{Im}[K(\omega)] \quad . \tag{2.70^b}$$

The Hilbert transforms in their usual and modified form then read as (refs. [83, 84])

$$\left.\begin{aligned} P(\omega) &= P(\infty) + \frac{1}{\pi} \int_{-\infty}^{\infty} \frac{Q(\xi)}{\omega - \xi}\, d\xi = P(\infty) - \frac{2}{\pi} \int_{0}^{\infty} \frac{\xi Q(\xi)}{\xi^2 - \omega^2}\, d\xi \quad , \\[2ex] Q(\omega) &= - \frac{1}{\pi} \int_{-\infty}^{\infty} \frac{P(\xi)}{\omega - \xi}\, d\xi = \frac{2\omega}{\pi} \int_{0}^{\infty} \frac{P(\xi)}{\xi^2 - \omega^2}\, d\xi \quad , \end{aligned}\right\} \tag{2.71}$$

respectively,

where $P(\infty) = \lim_{\omega\to\infty} K(\omega)$,

ξ = integration variable (circular frequency),

$⨍ f(\xi)d\xi$ = Cauchy principal-value integral of $f(\xi)$.

The term $P(\infty) \neq 0$ is generated if the inverse Fourier transform of $K(\omega)$, i.e. $k(t)$, contains singularities in the origin in the form of impulses. The first expressions for $P(\omega)$ and $Q(\omega)$ in (2.71) represent the usual Hilbert transforms, the second expressions their modified forms. (2.71) is also referred to as the Kramers-Kronig relations (refs. [67, 46]); see just as well refs. [92, 93]. Such formulae are obtainable whenever the system response obeys a linear law and there is a clear causality relation between input and output. Generally the (numerical) evaluation of (2.71) is complicated. However, by a change in the independent variable a simple set of equations, known as the Wiener-Lee transforms, can be derived (see further ref. [83]). This method will also permit the direct evaluation of the causal time function $k(t)$ in terms of $P(\omega)$ and $Q(\omega)$. If the real and imaginary part of the Fourier transform of $k(t)$ satisfy (2.71), then $k(t)$ is a causal function. Therefore (2.71) has also to be considered as a causality relation.

It is stated that for the physical (and consequently causal) linear ship-fluid system, represented in the frequency domain by (2.6) and (2.7), the real and imaginary part of $R_{ik}(\omega)$ have to satisfy the Hilbert transforms too. Then $K_{ij}(\omega)$ has to be replaced by $R_{ik}(\omega)$, whereas $P(\omega) = \mathrm{Re}[R(\omega)]$ and $Q(\omega) = \mathrm{Im}[R(\omega)]$. The causal time function associated with $R(\omega)$ is now indicated as retardation function and the description of the ship-fluid system in the time domain has the form of an integro-differential equation for the motion variable $x(t)$ (see (1.8) and further refs. [68, 67, 58]). This illustrates that the eventual form of the causality relations (2.71) is dependent on the way of describing the ship-fluid system in the time domain.

According to (2.71), for each ω $P(\omega)$ can be evaluated from $Q(\omega)$ provided $Q(\omega)$ is known for the entire frequency domain, and vice versa. This implies, $P(\omega) = \mathrm{Re}[R(\omega)]$ and $Q(\omega) = \mathrm{Im}[R(\omega)]$ being explicit functions of the hydrodynamic coefficients (see (2.10)), that $b_{ik}(\omega)$ can be determined directly, if $a_{ik}(\omega)$ is known for the entire frequency range and $b_{ik}(\omega)$ for one single frequency, and conversely. c_{ik} is frequency independent and has in the frequency domain as well as in the time domain the same value. For the expressions here aimed at, presenting explicit relations between $a_{ik}(\omega)$ and $b_{ik}(\omega)$, it is referred to refs. [67, 46].

Due to its black-box approach, the impulse response function-technique does not yield explicit relations between the respective hydrodynamic coefficients.

Since on account of (2.25^c) it must hold good mathematically that

$$\frac{2}{\pi}\int_0^\infty \mathrm{Re}[K_{ij}(\omega)]\cos(\omega t)d\omega = -\frac{2}{\pi}\int_0^\infty \mathrm{Im}[K_{ij}(\omega)]\sin(\omega t)d\omega \quad , \text{ for } t > 0 \quad ,$$

this expression could be used as a test function for the causality of the linear ship-fluid system.

2.7. Recapitulation of governing equations

In case of exclusively horizontal motions without restoring force the following expressions apply.

Coupled modes of motion: $(i,j,k) = 1,2,6$.

- description of the linear ship-fluid system in the frequency domain:

$$\sum_{j}^{1,2,6} \left[\{m_{jk} + a_{jk}(\omega)\}\ddot{x}_j + b_{jk}(\omega)\dot{x}_j\right] = f_k(t) \quad ; \tag{2.34}$$

- description of the linear ship-fluid system in the time domain:

$$\dot{x}_j(t) = \sum_{i}^{1,2,6} \int_{-\infty}^{t} f_i(\tau)\, k_{ij}(t-\tau)d\tau = \sum_{i}^{1,2,6} \int_0^\infty k_{ij}(\tau)\, f_i(t-\tau)d\tau \quad ; \tag{2.35}$$

- impulse response function:

$$\left.\begin{aligned}
k_{ij}(t) &= \frac{2}{\pi}\int_0^\infty \mathrm{Re}[K_{ij}(\omega)]\cos(\omega t)d\omega = \\
&= -\frac{2}{\pi}\int_0^\infty \mathrm{Im}[K_{ij}(\omega)]\sin(\omega t)d\omega \quad \text{for } t > 0 \quad , \\
k_{ij}(0) &= \frac{1}{\pi}\int_0^\infty \mathrm{Re}[K_{ij}(\omega)]d\omega = \frac{1}{2}\,k_{ij}(0^+) \quad , \\
k_{ij}(t) &\equiv 0 \quad \text{for } t < 0 \quad ;
\end{aligned}\right\} \tag{2.25^c}$$

- generalized frequency response function:

$$K_{ij}(\omega) = H_{ij}(i\omega) + \pi\alpha_{ij}\delta(\omega) \quad , \tag{2.55}$$

with

$$\left.\begin{aligned} Re[K_{ij}(\omega)] &= Re[H_{ij}(i\omega)] + \pi\alpha_{ij}\delta(\omega) \quad , \\ Im[K_{ij}(\omega)] &= Im[H_{ij}(i\omega)] \quad ; \end{aligned}\right\} \tag{2.60}$$

- non-generalized frequency response function:

$$\left.\begin{aligned}
&H_{11}(i\omega) = \frac{b_{11}(\omega)}{\{m_{11}+ a_{11}(\omega)\}^2\omega^2+ b_{11}^2(\omega)} - i\,\frac{\omega\{m_{11}+ a_{11}(\omega)\}}{\{m_{11}+ a_{11}(\omega)\}^2\omega^2+ b_{11}^2(\omega)} \,, \\
&\left.\begin{aligned} H_{1i}(i\omega) &= H_{1j}(i\omega) = 0 \quad , \\ H_{i1}(i\omega) &= H_{j1}(i\omega) = 0 \quad , \end{aligned}\right\} \text{for } i=2, j=6 \quad , \\
&\left.\begin{aligned} H_{ii}(i\omega) &= \frac{p_{ii}(\omega)b_{jj}(\omega) + \omega q_{ii}(\omega)\{m_{jj}+ a_{jj}(\omega)\}}{p_{ii}^2(\omega) + q_{ii}^2(\omega)} + \\ &\quad - i\,\frac{q_{ii}(\omega)b_{jj}(\omega) - \omega p_{ii}(\omega)\{m_{jj}+ a_{jj}(\omega)\}}{p_{ii}^2(\omega) + q_{ii}^2(\omega)} \,, \\ H_{ij}(i\omega) &= \frac{p_{ij}(\omega)b_{ij}(\omega) + \omega q_{ij}(\omega)a_{ij}(\omega)}{p_{ij}^2(\omega) + q_{ij}^2(\omega)} + \\ &\quad - i\,\frac{q_{ij}(\omega)b_{ij}(\omega) - \omega p_{ij}(\omega)a_{ij}(\omega)}{p_{ij}^2(\omega) + q_{ij}^2(\omega)} \,, \end{aligned}\right\} \begin{aligned}&\text{for } i=2, j=6 \\ &\text{and } i=6, j=2,\end{aligned}
\end{aligned}\right\} \tag{2.57}$$

with

$$\left.\begin{aligned}
p_{ii}(\omega) &= b_{ii}(\omega)b_{jj}(\omega) - b_{ij}(\omega)b_{ji}(\omega) + \\
&\quad - \omega^2\left[\{m_{ii}+ a_{ii}(\omega)\}\{m_{jj}+ a_{jj}(\omega)\} - a_{ij}(\omega)a_{ji}(\omega)\right] \,, \\
q_{ii}(\omega) &= \omega\left[b_{ii}(\omega)\{m_{jj}+ a_{jj}(\omega)\} + b_{jj}(\omega)\{m_{ii}+ a_{ii}(\omega)\} + \right. \\
&\quad \left. - \{a_{ji}(\omega)b_{ij}(\omega) + a_{ij}(\omega)b_{ji}(\omega)\}\right] \,, \\
p_{ii}(\omega) &= p_{jj}(\omega) \quad ,
\end{aligned}\right\} \begin{aligned}&\text{for} \\ &i=2, j=6;\end{aligned} \tag{2.58}$$

$$\left.\begin{array}{l} q_{ii}(\omega) = q_{jj}(\omega) \quad , \\ p_{ij}(\omega) = p_{ji}(\omega) = -p_{ii}(\omega) \quad , \\ q_{ij}(\omega) = q_{ji}(\omega) = -\, q_{ii}(\omega) \quad , \end{array}\right\}$$

- $\alpha_{ij} = k_{ij}(\infty)$:

$$\left.\begin{array}{l} \alpha_{11} = k_{11}(\infty) = \dfrac{1}{m_{11} + a_{11}(0)} \quad , \\ \left.\begin{array}{l} \alpha_{1i} = k_{1i}(\infty) = \alpha_{1j} = k_{1j}(\infty) = 0 \quad , \\ \alpha_{i1} = k_{i1}(\infty) = \alpha_{j1} = k_{j1}(\infty) = 0 \quad , \end{array}\right\} \text{for } i=2, j=6 \quad , \\ \left.\begin{array}{l} \alpha_{ii} = k_{ii}(\infty) = \dfrac{m_{jj} + a_{jj}(0)}{\{m_{ii} + a_{ii}(0)\}\{m_{jj} + a_{jj}(0)\} - a_{ij}(0)a_{ji}(0)} , \\ \alpha_{ij} = k_{ij}(\infty) = \dfrac{-a_{ij}(0)}{\{m_{ii} + a_{ii}(0)\}\{m_{jj} + a_{jj}(0)\} - a_{ij}(0)a_{ji}(0)} , \end{array}\right\} \begin{array}{l}\text{for } i=2, j=6 \\ \text{and } i=6, j=2;\end{array} \end{array}\right\} (2.59)$$

- if V_1 and V_2 are negligibly small, the sequence of the respective subscripts in j,k and i,j may be mutually interchanged.

Uncoupled modes of motion: $V_1, V_2 = 0$, $i = 1,2,6$.

- description of the linear ship-fluid system in the frequency domain:

$$\{m_{ii} + a_{ii}(\omega)\}\ddot{x}_i + b_{ii}(\omega)\dot{x}_i = f_i(t) \quad ; \tag{2.68}$$

- description of the linear ship-fluid system in the time domain:

$$\dot{x}_i(t) = \int_{-\infty}^{t} f_i(\tau)\, k_{ii}(t-\tau)d\tau = \int_0^{\infty} k_{ii}(\tau)\, f_i(t-\tau)d\tau \quad ; \tag{2.69}$$

- impulse response function:

$$\left.\begin{array}{l} k_{ii}(t) = \dfrac{2}{\pi}\displaystyle\int_0^{\infty} \mathrm{Re}[K_{ii}(\omega)]\cos(\omega t)d\omega = \\ \qquad = -\dfrac{2}{\pi}\displaystyle\int_0^{\infty} \mathrm{Im}[K_{ii}(\omega)]\sin(\omega t)d\omega \quad \text{for } t > 0 \quad , \end{array}\right|$$

$$\left.\begin{aligned} k_{ii}(0) &= \frac{1}{\pi}\int_0^{\infty} \mathrm{Re}[K_{ii}(\omega)]d\omega = \frac{1}{2}\, k_{ii}(0^+) \quad , \\ k_{ii}(t) &\equiv 0 \quad \text{for } t < 0 \quad ; \end{aligned}\right\} \tag{2.67}$$

- generalized frequency response function:

$$K_{ii}(\omega) = H_{ii}(i\omega) + \pi\alpha_{ii}\delta(\omega) \quad , \tag{2.63}$$

with

$$\left.\begin{aligned} \mathrm{Re}[K_{ii}(\omega)] &= \mathrm{Re}[H_{ii}(i\omega)] + \pi\alpha_{ii}\delta(\omega) \quad , \\ \mathrm{Im}[K_{ii}(\omega)] &= \mathrm{Im}[H_{ii}(i\omega)] \quad ; \end{aligned}\right\} \tag{2.66}$$

- non-generalized frequency response function:

$$H_{ii}(i\omega) = \frac{b_{ii}(\omega)}{\{m_{ii} + a_{ii}(\omega)\}^2\omega^2 + b_{ii}^2(\omega)} - i\,\frac{\omega\{m_{ii} + a_{ii}(\omega)\}}{\{m_{ii} + a_{ii}(\omega)\}^2\omega^2 + b_{ii}^2(\omega)} \; ; \tag{2.64}$$

- $\alpha_{ii} = k_{ii}(\infty)$:

$$\alpha_{ii} = k_{ii}(\infty) = \frac{1}{m_{ii} + a_{ii}(0)} \quad . \tag{2.65}$$

2.8. Concluding remarks

From the foregoing it is obvious that the main interest concerns the i.r.f., since the determination of transient ship motions requires knowledge of the behaviour of this very quantity. With regard to the question whether the i.r.f. have to be determined theoretically or experimentally, in general the following can be remarked.

The respective descriptions of the linear ship-fluid system in the time domain and the frequency domain are completely equivalent. Both methods of description can be used in order to define the response to transient disturbances; there is no specific advantage attached to either of them. If the ship-fluid system has been formulated mathematically the i.r.f. or the f.r.f. can be evaluated, but if this is not possible they can also be determined in an experimental way.

The f.r.f. can be determined experimentally using a harmonically varying input signal. The measured output signal contains only one single frequency due to the linearity of the ship-fluid system. Therefore it is sufficiently characterized by its amplitude and phase, which are represented in the f.r.f. in a complex way.

Since the i.r.f. and the f.r.f. are related by means of a Fourier transform, a mere determination of the f.r.f. is sufficient. Direct determination of an i.r.f., however, would be far more efficient than direct determination of a f.r.f. In the first case a few experiments, using a pulse or/and an arbitrary function of time, are sufficient, whereas in the second case many tests have to be carried out in order to find the f.r.f. over a sufficiently long interval of the frequency. In this context, by way of example, refs. [94, 95] may be mentioned: in ref. [94] the f.r.f. for heave and pitch are determined by means of transient (force) pulse tests, in ref. [95] the i.r.f. for sway and yaw are calculated from measured f.r.f.; both references concern mainly ships with non-zero forward speed. Compared with transient pulse tests, experiments to determine f.r.f. are much easier, since the pulse technique presents more specific problems and demands a higher degree of accuracy of the measuring equipment.

For these reasons the choice in favour of a determination of the f.r.f. -what actually amounts to direct determination of the hydrodynamic coefficients as functions of the frequency- is obvious. Consequently, if the hydrodynamic coefficients are known along a frequency range which is sufficiently large, then the corresponding i.r.f. can be determined making use of the expressions derived in the preceding sections.

3. SHIP BERTHING TO AN OPEN FENDER STRUCTURE

3.1. Introduction

This section deals with the application of the impulse response function-technique to the situation of a ship berthing to an open jetty-type fender structure.

The assumptions and simplifications made for this specific case have already been presented in Section 1.3.4; in this context it has to be noted that, due to the schematization of the ship, any coupling between the sway and yaw mode of motion does not exist.

Since the description of transient ship motions in the time domain requires knowledge of the i.r.f., which in its turn can be determined from the f.r.f. c.q. the hydrodynamic coefficients, first of all these last-mentioned quantities have to be known. Hence the hydrodynamic coefficients are determined theoretically as well as experimentally for the respective cases of pure swaying and yawing at zero forward and transverse speed (i.e. $V_1, V_2 = 0$). Hereby it is assumed implicitly that in berthing the transverse velocity of the ship is so small that it does not affect the hydrodynamic coefficients and a restoring force is not generated. With regard to the theoretical determination of the hydrodynamic coefficients, the fluid motion is supposed to be two-dimensional (strip-theory); further it is assumed that the fluid is inviscid and moves irrotationally. The mathematical approach is formulated in terms of a velocity potential, which -subject to appropriate boundary conditions- is applied to the respective fluid domains adjoining the sides of the ship. Coupling of the fields of flow on both sides of the ship then is done by applying the law of conservation of momentum to the mass of water under the ship. Friction in the underkeel region is taken into account. The results from theory and experiment, for swaying as well as for yawing, are compared and discussed.

With the hydrodynamic coefficients known the corresponding i.r.f. can be calculated.

Then the mathematical model to simulate the berthing of the schematized ship to the fender structure and to determine the relevant related quantities is presented. Both centric and eccentric impacts are considered, the initial eccentricity giving rise to rotation of the ship after the first moment of contact between ship and fender. As a consequence of this rotation formally virtual forces (due to Coriolis and centrifugal effects) as well as an inertial contribution (due to the angular acceleration) have to be introduced. These effects are classed in the (external) forcing function (i.e. the input signal) of the ship-fluid system. To examine the adequacy of the theoretical simulation of berthing operations in case of an open fender structure, an extensive series of (model) experiments was carried out, applying fenders with linear and non-linear behaviour. Typical test situations are selected for the numerical simulation in order to see whether and to what extent the observed phenomena are reproduced by means of the theoretical approach presented: theoretical results are compared with the results from experiments and discussed, the influence of the rotational effects is evaluated.

3.2. Determination of hydrodynamic coefficients

3.2.1. Theoretical approach

3.2.1.1. Governing equations

The ship motions take place with respect to the $ox_1x_2x_3$-co-ordinate system, which is now space-fixed. The vertical ox_3-axis coincides with the starting-position of the ship's longitudinal plane of symmetry. In rest and during motion the keel clearance of the ship is supposed to be constant and the side-walls maintain a vertical position. The assumption of a two-dimensional fluid motion implies that merely motions in planes perpendicular to the ship's longitudinal plane of symmetry are considered and that the calculations relate to the unit length, i.e. a strip-theory approach is applied.
The water depth at rest (i.e. the mean water level) is represented by h, the draught, the beam and the length of the ship by D, B and L, respectively. The respective fluid velocities in the x_2- and x_3-direction are denoted by v and w. The fluid domain can be divided into three regions; the subscripts a, b and c are used to indicate that the dependent variables concerned must be related to these respective regions.
For a definition sketch see fig. 3.1.

On account of the assumptions stated above the mathematical approach may be formulated in terms of a velocity potential $\Phi = \Phi(x_2,x_3,t)$. The horizontal and vertical velocity component of a fluid particle with co-ordinates x_2,x_3 at time t is

$$v = \frac{\partial \Phi}{\partial x_2} \quad , \quad w = \frac{\partial \Phi}{\partial x_3} \quad , \tag{3.1}$$

respectively. The velocity potential must satisfy the Laplace equation

$$\nabla^2\Phi = \frac{\partial^2\Phi}{\partial x_2^2} + \frac{\partial^2\Phi}{\partial x_3^2} = 0 \qquad (3.2)$$

in the field of flow, subject to relevant boundary conditions on all boundary surfaces and at infinity.

On each side of the ship a velocity potential exists. As only small ship motions are considered, it can be stated that these respective velocity potentials are antimetric. Coupling of the fields of flow on both sides of the ship is done by applying the law of conservation of momentum to the mass of water in the keel clearance. As a consequence, it is sufficient to determine the velocity potential only on one side of the ship.

Now define a fluid region R coinciding with region c, in which the Laplace equation is to be solved:

$$\left.\begin{array}{lll} x_2 > \frac{1}{2}B \quad , & -h \leq x_3 \leq 0 \quad , & \\ x_2 = \frac{1}{2}B \quad , & -D \leq x_3 \leq 0 \quad , & -h \leq x_3 < -D \quad . \end{array}\right\} R \qquad (3.3)$$

Ignoring surface tension the free-surface boundary condition reads -in linearized form- as:

$$\frac{\partial^2\Phi}{\partial t^2} + g\frac{\partial\Phi}{\partial x_3} = 0 \qquad \text{on} \qquad x_2 \geq \frac{1}{2}B \ , \ x_3 = 0 \quad , \qquad (3.4)$$

where g = acceleration due to gravity.

At the side of the ship the horizontal fluid velocity in the normal direction equals the velocity of the ship itself. Due to the small displacements of the ship from its starting-position, the boundary condition for the velocities at the ship's side applies at $x_2 = \frac{1}{2}B$ and can be written as:

$$\frac{\partial\Phi}{\partial x_2} = \{U(x_3+D) - U(x_3)\}\dot{x}_2 \qquad \text{on} \qquad x_2 = \frac{1}{2}B \quad . \qquad (3.5^a)$$

In region b, the keel clearance, it is assumed that B >> h-D. Pressure gradients or accelerations in the x_2-direction then being large as compared with the corresponding quantities in the x_3-direction, this leads to $w_b = 0$, a hydrostatic pressure and a uniform velocity distribution over the height. The boundary condition for the velocities across the keel clearance now becomes:

$$\frac{\partial\Phi}{\partial x_2} = \{U(x_3+h) - U(x_3+D)\}v_b \qquad \text{on} \qquad x_2 = \tfrac{1}{2}B \quad , \tag{3.5^b}$$

where v_b = fluid velocity in x_2-direction in region b.
At this stage the motion variable of the ship $x_2(t)$ and the underkeel velocity $v_b(t)$ are not yet specified. Defining the velocity potential for a specific case relevant expressions for x_2 and v_b are to be prescribed. The full boundary condition on the plane $x_2 = \frac{1}{2}B$ then can be written as:

$$\frac{\partial\Phi}{\partial x_2} = \{U(x_3+D) - U(x_3)\}\dot{x}_2 + \{U(x_3+h) - U(x_3+D)\}v_b \qquad \text{on} \qquad x_2 = \tfrac{1}{2}B \quad . \tag{3.5}$$

The assumption of an impervious bottom leads to the boundary condition:

$$\frac{\partial\Phi}{\partial x_3} = 0 \qquad \text{on} \qquad x_2 \geqq \tfrac{1}{2}B \ , \ x_3 = -h \qquad . \tag{3.6}$$

The boundary condition at infinity states that

$$\Phi(x_2,x_3,t)\Big|_{x_2\to\infty} \longrightarrow \text{outgoing dispersive wave} \quad , \tag{3.7}$$

or, at infinity only simple-harmonic waves propagating in positive x_2-direction are permissible.
As a supplementary condition it is supposed that in region R the function $\Phi(x_2,x_3,t)$ together with its respective first partial derivatives remain finite:

$$\Phi(x_2,x_3,t),\ \Phi^1(x_2,x_3,t) \quad \text{being finite in R} \quad ; \tag{3.8}$$

the superscript 1 means first partial derivative.

Summarizing it can be stated: the velocity potential $\Phi(x_2,x_3,t)$ has to satisfy the homogeneous, linear, partial differential equation (3.2) plus a set of non-homogeneous, linearized boundary conditions (3.4), (3.5), (3.6) and (3.7) and the supplementary condition (3.8). The solution of (3.4), (3.5), (3.6) and (3.7) specifies a mixed boundary-value problem for the Laplacian (3.2).

3.2.1.2. Solution of mixed boundary-value problem

The hydrodynamic problem as formulated above now is solved for the specific case that a simple-harmonic motion is imposed on the ship, viz.

$$x_2(t) = -i\hat{x}_2 \exp(i\omega t) \quad , \tag{3.9}$$

where $\hat{x}_2$ = amplitude of the ship motion in sway ($\hat{x}_2 > 0$, limited and real). Since the ship motion is harmonic in time, the fluid velocity in the underkeel clearance becomes of the form:

$$v_b(t) = \hat{v}_b \exp\{i(\omega t-\theta)\} \quad , \tag{3.10}$$

where $\hat{v}_b$ = amplitude of the underkeel fluid velocity v_b ($\hat{v}_b > 0$, limited and real),

θ = phase shift between the underkeel fluid velocity v_b and the sway velocity of the ship (θ real).

It is essential to note that so far $\hat{v}_b$ and θ are unknown quantities. In determining the velocity potential, however, it is necessary to suppose that $\hat{v}_b$ and θ are known constants. Once having determined $\Phi(x_2,x_3,t)$ on basis of this supposition, $\hat{v}_b$ and θ can be defined by applying the law of conservation of momentum to the mass of water underneath the ship.

Now it can be stated that the velocity potential $\Phi(x_2,x_3,t)$ is a simple-harmonic function of time, which has to satisfy the Laplacian (3.2) plus the set of non-homogeneous boundary conditions (3.4), (3.5), (3.6) and (3.7) and the supplementary condition (3.8), with $x_2(t)$ and $v_b(t)$ prescribed according to (3.9) and (3.10), respectively. The determination of this velocity potential is outlined in Appendix D, from which the general solution for $\Phi(x_2,x_3,t)$ is seen to be given by:

$$\Phi(x_2,x_3,t) = i\frac{\omega}{m_0}\{A_0+B_0\exp(-i\theta)\} \cosh\{m_0(x_3+h)\} \exp\{i(\omega t-m_0x_2+ \frac{m_0B}{2})\} +$$

$$- \sum_{n=1}^{\infty} \frac{\omega}{m_n}\{A_n+B_n\exp(-i\theta)\} \exp(-m_nx_2+ \frac{m_nB}{2}) \cos\{m_n(x_3+h)\} \exp(i\omega t) \quad , \tag{3.11}$$

where

$$m_0 = \text{positive root of} \quad \omega^2 = gm_0 \tanh(m_0h) \quad , \tag{3.12a}$$

$$m_n = \text{positive roots of} \quad \omega^2 = -gm_n \tan(m_nh) \quad ,$$

$$m_1 < m_2 < \ldots\ldots < m_n < \ldots\ldots \quad , \tag{3.12b}$$

$$\frac{A_0}{\hat{x}_2} = A_0' = 2\,\frac{\sinh(m_0h) - \sinh\{m_0(h-D)\}}{m_0h + \sinh(m_0h)\cosh(m_0h)} \quad , \qquad (3.13^a)$$

$$\frac{A_n}{\hat{x}_2} = A_n' = 2\,\frac{\sin(m_nh) - \sin\{m_n(h-D)\}}{m_nh + \sin(m_nh)\cos(m_nh)} \quad , \qquad (3.13^b)$$

$$\frac{B_0\omega}{\hat{v}_b} = B_0' = \frac{2\sinh\{m_0(h-D)\}}{m_0h + \sinh(m_0h)\cosh(m_0h)} \quad , \qquad (3.14^a)$$

$$\frac{B_n\omega}{\hat{v}_b} = B_n' = \frac{2\sin\{m_n(h-D)\}}{m_nh + \sin(m_nh)\cos(m_nh)} \quad ; \qquad (3.14^b)$$

the superscript ' indicates that the quantity concerned is dimensionless. (3.12^a) and (3.12^b) are the expressions for the wave numbers: m_0 is the usual wave number and m_n satisfies $(n - \frac{1}{2})\pi < m_nh < n\pi$.

3.2.1.3. Hydrodynamic forces and coupling of fluid regions

The fluid pressure can be obtained from the linearized equation of Bernoulli for unsteady flow

$$\frac{\partial\Phi}{\partial t} + \frac{p}{\rho} + gx_3 = 0 \quad , \qquad (3.15)$$

where $p = p_c(x_2,x_3,t)$ = fluid pressure in region c,

ρ = specific mass density of the fluid.

Substitution of $\Phi(x_2,x_3,t)$ as represented by (3.11) into (3.15) yields for the fluid pressure in the vertical plane $x_2 = \frac{1}{2}B$:

$$p_c(\tfrac{1}{2}B,x_3,t) = \rho\frac{\omega^2}{m_0}\{A_0+B_0\exp(-i\theta)\}\cosh\{m_0(x_3+h)\}\exp(i\omega t) + $$
$$+ \rho\sum_{n=1}^{\infty} i\frac{\omega^2}{m_n}\{A_n+B_n\exp(-i\theta)\}\cos\{m_n(x_3+h)\}\exp(i\omega t) - \rho g x_3 \ . \qquad (3.16)$$

The horizontal force per unit length as exerted by the fluid on the ship-wall in question, then is:

$$-\int_{-D}^{0} p_c(\tfrac{1}{2}B,x_3,t)dx_3 = -\rho\frac{\omega^2}{m_0^2}\{A_0+B_0\exp(-i\theta)\}\left[\sinh(m_0h)-\sinh\{m_0(h-D)\}\right]\exp(i\omega t) +$$
$$-\rho\sum_{n=1}^{\infty} i\frac{\omega^2}{m_n^2}\{A_n+B_n\exp(-i\theta)\}\left[\sin(m_nh)-\sin\{m_n(h-D)\}\right]\exp(i\omega t) +$$
$$- \frac{1}{2}\rho g D^2 \quad ;$$

the first two terms on the right-hand side of this expression represent the hydrodynamic part of the force, the last term is the hydrostatic part.
On each side of the ship a velocity potential exists. These respective velocity potentials are antimetric. The antimetry of the fields of flow on both sides of the ship is the cause of the fact that -in determining the total horizontal force- the hydrostatic contributions to the individual horizontal forces on each wall of the ship cancel. Then the total horizontal (hydrodynamic) force on the ship per unit length, $f_{2,s}(t)$, becomes twice the hydrodynamic force on a single wall of the ship:

$$f_{2,s}(t) = -2\rho\frac{\omega^2}{m_0^2}\{A_0+B_0\exp(-i\theta)\}\left[\sinh(m_0h)-\sinh\{m_0(h-D)\}\right]\exp(i\omega t) +$$

$$-2\rho\sum_{n=1}^{\infty} i\frac{\omega^2}{m_n^2}\{A_n+B_n\exp(-i\theta)\}\left[\sin(m_nh)-\sin\{m_n(h-D)\}\right]\exp(i\omega t) \quad . \tag{3.17}$$

In a similar way it can be derived for the total horizontal (hydrodynamic) force on the mass of water in the keel clearance per unit length, i.e. $f_{2,kc}(t)$:

$$f_{2,kc}(t) = -2\rho\frac{\omega^2}{m_0^2}\{A_0+B_0\exp(-i\theta)\}\sinh\{m_0(h-D)\}\exp(i\omega t) +$$

$$-2\rho\sum_{n=1}^{\infty} i\frac{\omega^2}{m_n^2}\{A_n+B_n\exp(-i\theta)\}\sin\{m_n(h-D)\}\exp(i\omega t) \quad . \tag{3.18}$$

The subscripts s and kc indicate that the quantity concerned relates to the 'ship' and the 'keel clearance', respectively.

The so far unknown quantities $\hat{v}_b$ and θ are determined by coupling the fields of flow on both sides of the ship. To that end the law of conservation of momentum is applied to the mass of water in the underkeel clearance:

$$f_{2,kc}(t) = \rho B(h-D)\frac{dv_b}{dt} \quad . \tag{3.19^a}$$

To introduce eventual (linear) friction effects in the underkeel clearance, the flow in region b is supposed to be laminar, i.e.

$$Re = \frac{(h-D)|v_b|}{\nu} < 1100 \text{ to } 1200 \qquad \text{(pressure flow between two parallel walls)},$$

and/or

$$Re = \frac{(h-D)|\dot{x}_2|}{\nu} < 1900 \qquad \text{(Couette flow)}$$

(see ref. [97]). Then the friction force in the x_2-direction per unit length as acting on the fluid in region b due to the presence of the moving ship can be represented by

$$-\tau_{2,b}\big|_{ship}\, B \qquad \text{with} \qquad \tau_{2,b}\big|_{ship} = \gamma(v_b - \dot{x}_2) \qquad ;$$

analogously the corresponding friction force due to the presence of the fixed bottom has the form

$$-\tau_{2,b}\big|_{bottom}\, B \qquad \text{with} \qquad \tau_{2,b}\big|_{bottom} = \gamma v_b \qquad ;$$

in this Re = Reynolds number,

ν = (coefficient of) kinematic viscosity of the fluid,

$\tau_{2,b}\big|_{ship}$ = shear stress in the x_2-direction in region b at the ship-fluid interface,

$\tau_{2,b}\big|_{bottom}$ = shear stress in the x_2-direction in region b at the fluid-bottom interface,

γ = proportionality coefficient for the shear stress in case of laminar flow.

The total friction force in the x_2-direction per unit length of the ship as acting on the fluid in region b then becomes

$$-2\gamma B(v_b - \tfrac{1}{2}\,\dot{x}_2) \qquad ,$$

i.e. in order to incorporate the friction effect for laminar flow in the keel clearance, the left-hand side of (3.19^a) has to be extended with the above expression, yielding

$$f_{2,kc}(t) - 2\gamma B(v_b - \tfrac{1}{2}\,\dot{x}_2) = \rho B(h-D)\,\frac{dv_b}{dt} \qquad . \qquad (3.19^b)$$

In case of a predominantly oscillating flow in the keel clearance with a relatively thin laminar boundary layer (i.e. thickness of laminar boundary layer << h-D) a Stokes' type friction formula can be used, implying

$$\gamma = \rho \sqrt{\nu\omega} \tag{3.20a}$$

(see ref. [98]). For smooth walls the boundary layer is considered to be laminar when (see ref. [99])

$$\mathrm{Re} = \frac{\hat{v}_b\sqrt{\frac{\nu}{\omega}}}{\nu} = \frac{\hat{v}_b}{\sqrt{\nu\omega}} < 200 \text{ to } 300 \quad .$$

In case of (steady) laminar flow in the underkeel clearance γ -for pressure flow between two parallel plates- is determined to be (see ref. [100]):

$$\gamma = \frac{6\rho\nu}{h-D} \quad . \tag{3.20b}$$

By substitution of $x_2(t)$, $v_b(t)$, $f_{2,kc}(t)$ and γ according to (3.9), (3.10), (3.18) and (3.20^a), respectively, into (3.19^b) one obtains ($\omega \neq 0$);

$$\frac{2}{m_0^2}\,(A_0 + B_0 e^{-i\theta})\,\sinh\{m_0(h-D)\} + \sum_{n=1}^{\infty} i\,\frac{2}{m_n^2}\,(A_n + B_n e^{-i\theta})\,\sin\{m_n(h-D)\} +$$
$$+ 2B\sqrt{\frac{\nu}{\omega}}\,\left(\frac{\hat{v}_b}{\omega}\,e^{-i\theta} - \frac{1}{2}\,\hat{x}_2\right) = -\,iB\,(h-D)\,\frac{\hat{v}_b}{\omega}\,e^{-i\theta} \quad . \tag{3.21}$$

From the respective real and imaginary part of (3.21) it can be derived, using (3.13^{a,b}) and (3.14^{a,b}):

$$\frac{\omega\hat{x}_2}{\hat{v}_b}\,\left(a_0 - B\sqrt{\frac{\nu}{\omega}}\right) + \left(b_0 + 2B\sqrt{\frac{\nu}{\omega}}\right)\cos(\theta) + (b_n + c)\,\sin(\theta) = 0 \quad , \tag{3.22a}$$

$$\frac{\omega\hat{x}_2}{\hat{v}_b}\,a_n + (b_n + c)\cos(\theta) - \left(b_0 + 2B\sqrt{\frac{\nu}{\omega}}\right)\sin(\theta) = 0 \quad , \tag{3.22b}$$

where

$$a_0 = \frac{2A_0'}{m_0^2}\,\sinh\{m_0(h-D)\} \quad , \qquad a_n = \sum_{n=1}^{\infty}\frac{2A_n'}{m_n^2}\,\sin\{m_n(h-D)\} \quad , \tag{3.23a}$$

$$b_0 = \frac{2B_0'}{m_0^2}\,\sinh\{m_0(h-D)\} \quad , \qquad b_n = \sum_{n=1}^{\infty}\frac{2B_n'}{m_n^2}\,\sin\{m_n(h-D)\} \quad , \tag{3.23b}$$

$$c = B(h-D) \quad . \tag{3.23c}$$

The expressions (3.22^a) and (3.22^b) represent a set of two equations with two unknowns, viz. θ and $\hat{v}_b$; for, a_0, a_n, b_0, b_n and c in principle are known quantities, since A_0' through A_n' and B_0' through B_n' can be determined for all values of ω from ($3.13^{a,b}$) and ($3.14^{a,b}$) in combination with (3.12^a) and (3.12^b). The solution for θ and $\hat{v}_b$ can be written in the (dimensionless) form

$$\tan(\theta) = \frac{-(a_0 - B\sqrt{\frac{\nu}{\omega}})(b_n + c) + a_n(b_0 + 2B\sqrt{\frac{\nu}{\omega}})}{-(a_0 - B\sqrt{\frac{\nu}{\omega}})(b_0 + 2B\sqrt{\frac{\nu}{\omega}}) - a_n(b_n + c)} \quad , \qquad (3.24^a)$$

$$\frac{\hat{v}_b}{\omega\hat{x}_2} = \frac{-(a_0 - B\sqrt{\frac{\nu}{\omega}})}{(b_0 + 2B\sqrt{\frac{\nu}{\omega}})\cos(\theta) + (b_n + c)\sin(\theta)} =$$

$$= \frac{a_n}{(b_0 + 2B\sqrt{\frac{\nu}{\omega}})\sin(\theta) - (b_n + c)\cos(\theta)} \quad . \qquad (3.25^a)$$

In case of zero underkeel friction (i.e. $\nu = 0$) (3.24^a) and (3.25^a) reduce to

$$\tan(\theta) = \frac{-a_0(b_n+c) + a_nb_0}{-a_0b_0 - a_n(b_n+c)} \quad , \qquad (3.24^b)$$

$$\frac{\hat{v}_b}{\omega\hat{x}_2} = \frac{-a_0}{b_0\cos(\theta) + (b_n+c)\sin(\theta)} = \frac{a_n}{b_0\sin(\theta) - (b_n+c)\cos(\theta)} \quad , \qquad (3.25^b)$$

respectively.

3.2.1.4. Swaying and yawing

On the ship a simple-harmonic sway motion has been imposed of a form according to (3.9). This requires an external exciting force in the x_2-direction, viz. $f_2(t)$. The 'equation of motion' in the x_2-direction for the oscillating ship then is:

$$m_{22}\ddot{x}_2 = \int_L f_{2,s}(t)\,dx_1 + \int_L \gamma B(v_b - \dot{x}_2)\,dx_1 + f_2(t) \quad , \qquad (3.26^a)$$

where $f_{2,s}(t)$ is given by (3.17) and the second term on the right-hand side represents the (linear) friction force upon the underside of the moving ship. On account of (2.34) the description of the ship-fluid system in the frequency domain for the sway and yaw motion reads in case of a real ship form and to the neglect of the surge motion (see also refs. [46, 101]):

$$\{m_{22} + a_{22}(\omega)\}\ddot{x}_2 + b_{22}(\omega)\,\dot{x}_2 + a_{62}(\omega)\,\ddot{x}_6 + b_{62}(\omega)\,\dot{x}_6 = f_2(t) \quad , \tag{3.27}$$

$$a_{26}(\omega)\,\ddot{x}_2 + b_{26}(\omega)\,\dot{x}_2 + \{m_{66} + a_{66}(\omega)\}\ddot{x}_6 + b_{66}(\omega)\,\dot{x}_6 = f_6(t) \quad , \tag{3.28}$$

respectively. The expressions for pure swaying can be derived from (3.27) and (3.28) by putting $\dot{x}_6 = \ddot{x}_6 = 0$:

$$\left.\begin{aligned} &\{m_{22} + a_{22}(\omega)\}\ddot{x}_2 + b_{22}(\omega)\,\dot{x}_2 = f_2(t) \quad , \\ &a_{26}(\omega)\,\ddot{x}_2 + b_{26}(\omega)\,\dot{x}_2 = f_6(t) \quad . \end{aligned}\right\} \quad \text{(pure swaying)} \qquad (3.29^a)$$

Likewise it holds good for pure yawing (i.e. $\dot{x}_2 = \ddot{x}_2 = 0$):

$$\left.\begin{aligned} &a_{62}(\omega)\,\ddot{x}_6 + b_{62}(\omega)\,\dot{x}_6 = f_2(t) \quad , \\ &\{m_{66} + a_{66}(\omega)\}\ddot{x}_6 + b_{66}(\omega)\,\dot{x}_6 = f_6(t) \quad . \end{aligned}\right\} \quad \text{(pure yawing)} \qquad (3.30^a)$$

The hydrodynamic coefficients are independent of the distribution of the mass along the ship; they depend on the geometry of the hull. Supposing that in case of pure swaying $a_{22}(\omega)$ and $b_{22}(\omega)$ are known for every transverse section of the hull (at x_1), then -on account of the strip-theory approach- the hydrodynamic coefficients for the entire ship can be obtained by integration over the length:

$$\left.\begin{aligned} &\begin{pmatrix} a_{22}(\omega) \\ a_{66}(\omega) \end{pmatrix} = \int_L \begin{pmatrix} 1 \\ x_1^2 \end{pmatrix} a_{22}^{(x_1)}(\omega)\,dx_1 \ , \qquad \begin{pmatrix} b_{22}(\omega) \\ b_{66}(\omega) \end{pmatrix} = \int_L \begin{pmatrix} 1 \\ x_1^2 \end{pmatrix} b_{22}^{(x_1)}(\omega)\,dx_1 \ , \\ &\begin{pmatrix} a_{26}(\omega) \\ b_{26}(\omega) \end{pmatrix} = \begin{pmatrix} a_{62}(\omega) \\ b_{62}(\omega) \end{pmatrix} = \int_L x_1 \begin{pmatrix} a_{22}^{(x_1)}(\omega) \\ b_{22}^{(x_1)}(\omega) \end{pmatrix} dx_1 \quad , \end{aligned}\right\} \tag{3.31}$$

where the superscript (x_1) indicates that the quantity concerned applies to the transverse section of the hull at x_1. For the schematized ship it follows directly from (3.31) that

$$a_{26}(\omega) = a_{62}(\omega) = 0 \quad , \qquad b_{26}(\omega) = b_{62}(\omega) = 0 \quad , \tag{3.32}$$

$$\left.\begin{aligned} a_{22}(\omega) &= L\, a_{22}^{(x_1)}(\omega) \quad , \\ b_{22}(\omega) &= L\, b_{22}^{(x_1)}(\omega) \quad , \end{aligned}\right\} \tag{3.33}$$

and

$$\left.\begin{aligned} a_{66}(\omega) &= \frac{1}{12} L^2\, a_{22}(\omega) \quad , \\ b_{66}(\omega) &= \frac{1}{12} L^2\, b_{22}(\omega) \quad . \end{aligned}\right\} \tag{3.34^{a,b}}$$

For the respective pure sway and yaw motion as presented in (3.29^a) and (3.30^a) it then applies:

$$\{m_{22} + a_{22}(\omega)\}\ddot{x}_2 + b_{22}(\omega)\,\dot{x}_2 = f_2(t) \quad , \tag{3.29^b}$$

$$\{m_{66} + a_{66}(\omega)\}\ddot{x}_6 + b_{66}(\omega)\,\dot{x}_6 = f_6(t) \quad , \tag{3.30^b}$$

which results for $i = 2,6$ also directly can be derived from (2.68).
The expressions ($3.34^{a,b}$) hold for all ω. The specific denomination of $a_{22}(\omega)$ and $a_{66}(\omega)$ is added mass for swaying motion and added mass-moment of inertia for yawing motion, respectively; $b_{22}(\omega)$ is denoted as the sway damping force coefficient and $b_{66}(\omega)$ as the yaw damping moment coefficient.
For the schematized ship (3.26^a) takes the form

$$m_{22}\,\ddot{x}_2 = L\, f_{2,s}(t) + \gamma BL(v_b - \dot{x}_2) + f_2(t) \quad . \tag{3.26^b}$$

Elimination of $f_2(t)$ from (3.26^b) and (3.29^b) yields:

$$a_{22}(\omega)\,\ddot{x}_2 + b_{22}(\omega)\,\dot{x}_2 = -L\, f_{2,s}(t) - \gamma BL(v_b - \dot{x}_2) \quad . \tag{3.35}$$

By substitution of $x_2(t)$, $v_b(t)$, $f_{2,s}(t)$ and γ according to (3.9), (3.10), (3.17) and (3.20^a), respectively, into (3.35) and subsequently equating the imaginary and real parts, one obtains:

$$a_{22}(\omega) = 2\rho L\Big(-\frac{1}{m_0^2}\frac{\hat{v}_b}{\omega\hat{x}_2} B_0' \sin(\theta)\left[\sinh(m_0 h) - \sinh\{m_0(h-D)\}\right] +$$

$$+ \sum_{n=1}^{\infty} \frac{1}{m_n^2}\{A_n' + \frac{\hat{v}_b}{\omega\hat{x}_2} B_n' \cos(\theta)\}\left[\sin(m_n h) - \sin\{m_n(h-D)\}\right]\Big) +$$

$$+ \rho BL\sqrt{\frac{\nu}{\omega}}\frac{\hat{v}_b}{\omega\hat{x}_2}\sin(\theta) \quad , \qquad (3.36^a)$$

$$b_{22}(\omega) = 2\rho L\Big(\frac{\omega}{m_0^2}\{A_0' + \frac{\hat{v}_b}{\omega\hat{x}_2} B_0' \cos(\theta)\}\left[\sinh(m_0 h) - \sinh\{m_0(h-D)\}\right] +$$

$$+ \sum_{n=1}^{\infty} \frac{\omega}{m_n^2}\frac{\hat{v}_b}{\omega\hat{x}_2} B_n' \sin(\theta)\left[\sin(m_n h) - \sin\{m_n(h-D)\}\right]\Big) +$$

$$-\rho BL\omega\sqrt{\frac{\nu}{\omega}}\{\frac{\hat{v}_b}{\omega\hat{x}_2}\cos(\theta) - 1\} \quad . \qquad (3.37^a)$$

The last term on the right-hand side of the respective expressions (3.36^a) and (3.37^a) vanishes in case of zero underkeel friction (i.e. $\nu = 0$). For the sake of simplicity the friction effect in the underkeel clearance is further left out of consideration.

In the cases that $\omega \to 0$ and $\omega \to \infty$ the relevant transitions to the limit for the sway added-mass and the sway damping force coefficient yield:

$$a_{22}(0) = 2\rho L\Big(\frac{BD^2}{2(h-D)} + 2\frac{h^4}{(h-D)^2}\sum_{n=1}^{\infty}\frac{1}{(n\pi)^3}\sin^2\{n\pi\,\frac{h-D}{h}\}\Big) \quad , \qquad (3.38)$$

$$b_{22}(0) = 0 \quad , \qquad (3.39)$$

and

$$a_{22}(\infty) = 4\rho Lh^2\Big(\sum_{n=1}^{\infty}\{(-1)^n + P_n\}^2 Q_n^{-3} +$$

$$- \Big[\sum_{n=1}^{\infty}\{(-1)^n + P_n\}P_n Q_n^{-3}\Big]^2 \Big[\frac{B(h-D)}{4h^2} + \sum_{n=1}^{\infty} P_n^2 Q_n^{-3}\Big]^{-1}\Big) \quad , \qquad (3.40)$$

$$b_{22}(\infty) = 0 \quad , \qquad (3.41)$$

with $\quad P_n = \sin(\frac{h-D}{h}\,Q_n) \quad , \quad Q_n = (2n-1)\frac{\pi}{2} \quad .$

A special case arises when the keel clearance becomes zero. The hydrodynamic sway coefficients for this particular situation can be derived to be:

$$a_{22}(\omega)\Big|_{h\to D} = 2\rho L \sum_{n=1}^{\infty} \frac{1}{m_n^2} \frac{2\sin^2(m_n h)}{m_n h + \sin(m_n h)\cos(m_n h)} \quad , \tag{3.42}$$

$$b_{22}(\omega)\Big|_{h\to D} = 2\rho L \frac{\omega}{m_0^2} \frac{2\sinh^2(m_0 h)}{m_0 h + \sinh(m_0 h)\cosh(m_0 h)} \quad , \tag{3.43}$$

$$a_{22}(0)\Big|_{h\to D} = 0 \quad , \tag{3.44}$$

$$b_{22}(0)\Big|_{h\to D} = 2\rho Lh\sqrt{gh} \quad , \tag{3.45}$$

$$a_{22}(\infty)\Big|_{h\to D} = 4\rho Lh^2 \sum_{n=1}^{\infty} \frac{1}{\{(2n-1)\frac{\pi}{2}\}^3} \quad , \tag{3.46}$$

$$b_{22}(\infty)\Big|_{h\to D} = 0 \quad . \tag{3.47}$$

The series occurring in (3.36^a), (3.37^a), (3.23^a), (3.23^b), (3.38), (3.40), (3.42) and (3.46) can be proved to be convergent; consequently it is possible to develop a break-off criterion for these series.

In Appendix E the hydrodynamic sway coefficients $a_{22}(\omega)$ and $b_{22}(\omega)$ for the schematized ship are derived using a long-wave approximation for the motion of the water.

3.2.1.5. Recapitulation of most important formulae

The hydrodynamic sway coefficients for the schematized ship in case of zero underkeel friction and non-zero keel clearance read as follows:

- added mass for swaying motion:

$$a_{22}(\omega) = 2\rho L\Big(-\frac{1}{m_0^2}\frac{\hat{v}_b}{\omega\hat{x}_2} B_0' \sin(\theta)\,\big[\sinh(m_0 h) - \sinh\{m_0(h-D)\}\big] + \sum_{n=1}^{\infty}\frac{1}{m_n^2}\Big\{A_n' + \frac{\hat{v}_b}{\omega\hat{x}_2} B_n'\cos(\theta)\Big\}\big[\sin(m_n h) - \sin\{m_n(h-D)\}\big]\Big) \tag{3.36^b}$$

with the limit cases

$$a_{22}(0) = 2\rho L\Big(\frac{BD^2}{2(h-D)} + 2\frac{h^4}{(h-D)^2}\sum_{n=1}^{\infty}\frac{1}{(n\pi)^3}\sin^2\{n\pi\frac{h-D}{h}\}\Big) \tag{3.38}$$

and

$$a_{22}(\infty) = 4\rho Lh^2 \Big(\sum_{n=1}^{\infty} \{(-1)^n + P_n\}^2 Q_n^{-3} +$$

$$-\Big[\sum_{n=1}^{\infty} \{(-1)^n + P_n\} P_n Q_n^{-3} \Big]^2 \Big[\frac{B(h-D)}{4h^2} + \sum_{n=1}^{\infty} P_n^2 Q_n^{-3} \Big]^{-1} \Big) \quad , \qquad (3.40)$$

where $\quad P_n = \sin(\frac{h-D}{h} Q_n) \quad , \quad Q_n = (2n-1)\frac{\pi}{2} \quad ;$

- sway damping force coefficient:

$$b_{22}(\omega) = 2\rho L\Big(\frac{\omega}{m_0^2} \{A_0' + \frac{\hat{v}_b}{\omega \hat{x}_2} B_0' \cos(\theta)\} \left[\sinh(m_0 h) - \sinh\{m_0(h-D)\}\right] +$$

$$+ \sum_{n=1}^{\infty} \frac{\omega}{m_n^2} \frac{\hat{v}_b}{\omega \hat{x}_2} B_n' \sin(\theta) \left[\sin(m_n h) - \sin\{m_n(h-D)\}\right] \Big) \qquad (3.37^b)$$

with the limit cases

$$b_{22}(0) = 0 \qquad (3.39)$$

and

$$b_{22}(\infty) = 0 \quad ; \qquad (3.41)$$

- the relevant quantities in these expressions are:

$$m_0 = \text{positive root of} \quad \omega^2 = g m_0 \tanh(m_0 h) \quad , \qquad (3.12^a)$$

$$m_n = \text{positive roots of} \quad \omega^2 = -g m_n \tan(m_n h) \;,\; m_1 < m_2 < \cdots < m_n < \cdots \;, \qquad (3.12^b)$$

$$A_0' = 2\,\frac{\sinh(m_0 h) - \sinh\{m_0(h-D)\}}{m_0 h + \sinh(m_0 h)\cosh(m_0 h)} \;,\quad A_n' = 2\,\frac{\sin(m_n h) - \sin\{m_n(h-D)\}}{m_n h + \sin(m_n h)\cos(m_n h)} \;, \qquad (3.13^{a,b})$$

$$B_0' = \frac{2\sinh\{m_0(h-D)\}}{m_0 h + \sinh(m_0 h)\cosh(m_0 h)} \;,\quad B_n' = \frac{2\sin\{m_n(h-D)\}}{m_n h + \sin(m_n h)\cos(m_n h)} \;, \qquad (3.14^{a,b})$$

$$\tan(\theta) = \frac{-a_0(b_n + c) + a_n b_0}{-a_0 b_0 - a_n(b_n + c)} \quad , \qquad (3.24^b)$$

$$\frac{\hat{v}_b}{\omega\hat{x}_2} = \frac{-a_0}{b_0\cos(\theta) + (b_n+c)\sin(\theta)} = \frac{a_n}{b_0\sin(\theta) - (b_n+c)\cos(\theta)} \quad , \tag{3.25^b}$$

$$a_0 = \frac{2A_0'}{m_0^2}\sinh\{m_0(h-D)\} \quad , \quad a_n = \sum_{n=1}^{\infty}\frac{2A_n'}{m_n^2}\sin\{m_n(h-D)\} \quad , \tag{3.23^a}$$

$$b_0 = \frac{2B_0'}{m_0^2}\sinh\{m_0(h-D)\} \quad , \quad b_n = \sum_{n=1}^{\infty}\frac{2B_n'}{m_n^2}\sin\{m_n(h-D)\} \quad , \tag{3.23^b}$$

$$c = B(h-D) \quad . \tag{3.23^c}$$

In case of zero underkeel friction and zero keel clearance the hydrodynamic sway coefficients for the schematized ship have the following form:

- added mass for swaying motion:

$$a_{22}(\omega)\Big|_{h\to D} = 2\rho L \sum_{n=1}^{\infty}\frac{1}{m_n^2}\,\frac{2\sin^2(m_n h)}{m_n h + \sin(m_n h)\cos(m_n h)} \tag{3.42}$$

with the limit cases

$$a_{22}(0)\Big|_{h\to D} = 0 \tag{3.44}$$

and

$$a_{22}(\infty)\Big|_{h\to D} = 4\rho L h^2 \sum_{n=1}^{\infty}\frac{1}{\{(2n-1)\frac{\pi}{2}\}^3} \quad ; \tag{3.46}$$

- sway damping force coefficient:

$$b_{22}(\omega)\Big|_{h\to D} = 2\rho L\,\frac{\omega}{m_0^2}\,\frac{2\sinh^2(m_0 h)}{m_0 h + \sinh(m_0 h)\cos(m_0 h)} \tag{3.43}$$

with the limit cases

$$b_{22}(0)\Big|_{h\to D} = 2\rho L h\sqrt{gh} \tag{3.45}$$

and

$$b_{22}(\infty)\Big|_{h\to D} = 0 \quad . \tag{3.47}$$

In case of yawing it generally holds for the schematized ship:

- added mass-moment of inertia for yawing motion:

$$a_{66}(\omega) = \frac{1}{12} L^2 a_{22}(\omega) \quad ; \qquad (3.34^a)$$

- yaw damping moment coefficient:

$$b_{66}(\omega) = \frac{1}{12} L^2 b_{22}(\omega) \quad . \qquad (3.34^b)$$

3.2.2. Experiments

3.2.2.1. Description of experimental set-up

In order to verify the theoretical results as presented by the expressions derived in the preceding Section 3.2.1, a series of model experiments was carried out in the Laboratory of Fluid Mechanics of the Department of Civil Engineering, Delft University of Technology (as a matter of fact, all experimental work further to be described in this thesis was also carried out in this laboratory). The experiments comprised forced oscillation tests to determine the hydrodynamic coefficients of the schematized ship (model) in case of pure swaying and yawing at zero forward and transverse speed on calm, shallow water with relatively large, horizontal dimensions.

The schematized ship model was made of wood and the outside sheathed with polyester. Its main particulars are given in Table 1.

Since shallowness of the water is of dominant importance for the hydrodynamic coefficients, two water depths were chosen, viz. h = 0.175 m and h = 0.200 m. The water was calm, i.e. no waves and no current.
Further, in the following is: $\rho = 1000$ kg m^{-3} and $g = 9.81$ m s^{-2}.

The hydrodynamic coefficients for the respective sway and yaw mode of motion were determined experimentally by means of the so-called planar-motion mechanism (P.M.M.) from the Shipbuilding Laboratory of the Department of Naval Architecture, Delft University of Technology. This P.M.M. consists of a horizontal ships's excitator with a coupled measuring system. The main component of the excitator is a Scotch-yoke mechanism. The excitator has two struts, spaced 1.0000 m apart which both can perform a harmonically oscillating, translatory motion either in phase or with a certain phase difference. The motions of the struts are measured and an electronic control system is used to keep the number of revolutions of the driving motor unit constant, which is necessary to achieve a purely harmonic motion. With this experimental equip-

length (on the water-line)	L	2.438	m
beam	B	0.375	m
draught	D	0.150	m
volume of displacement	L.B.D	0.1371	m^3
area of cross-section	B.D	0.056	m^2
water-line area	L.B	0.924	m^2
lateral plane area	L.D	0.366	m^2
block coefficient		1.000	
centre of gravity (with respect to frame 10)		0	m
centre of gravity in height (with respect to keel point)		0.140	m
mass for horizontal motions in case of berthing operations	m_{11}, m_{22}	137.24	kg
mass-moment of inertia around Gz-axis	m_{66}	50.99	kg m^2
radius of gyration with respect to Gz-axis		0.610	m

Table 1. Main particulars of ship model.

ment -in the horizontal plane- an arbitrary, harmonically oscillating motion can be imposed on a ship model with a prescribed amplitude and frequency, while at the same time the excited forces are measured. For more (general) details on (the use of) the P.M.M. see ref. [102] and also ref. [54]. Unlike the P.M.M. as described in ref. [102] the version used in these experiments had an option for a degree of freedom in vertical direction, achieved by means of a ball-bushing construction in the struts of the horizontal excitator. This implied that the ship model was allowed to move -without restraint- in the vertical direction during the forced oscillation tests.
The excited forces were measured by means of two strain-gauge dynamometers. These dynamometers -mounted in the ship model's longitudinal plane of symmetry at equal distances from the centre of gravity- connected (the struts of) the excitator to the ship model. Only forces in the plane of the water-line with a direction perpendicular to the longitudinal plane of symmetry of the ship model were measured. The distance between the centre-lines of the dynamometers

was 1.0000 m. The measuring system forming part of the P.M.M. was able to measure first, second and third harmonic components of the sway and yaw forces, in amplitude- as well as in phase-relation to the motion of the ship model. This was done by a mechanical-electronical Fourier-analyzer. For further details see refs. [102, 54].

For the version of the P.M.M. used in the experiments, the amplitude of the sway motion was adjustable from 0.0000 m to 0.2500 m and the amplitude of the yaw motion from 0.0000 rad. to 0.4636 rad. (i.e. atan(0.5000)). The circular frequency of the oscillatory motions could vary continuously between 0.196 rad.s^{-1} and 3.927 rad.s^{-1}, which corresponds with a period range from 32.0 s to 1.6 s.

The maximum capacity of the dynamometers was about 100 N each. The accuracy of the P.M.M. as a measuring device depended mainly on the occurrence of adequately large forces, which had to exceed values of 0.2 N. Therefore the dimensions of the ship model had to be chosen such that particularly for combinations of low frequency and small amplitude measurable forces occurred.

The mass of the ship model as based on the volume of displacement amounted to 137.10 kg; the mass for horizontal motion as used in the dynamic tests, however, was 133.82 kg. This difference can be explained by the presence of the ball-bushing constructions in the struts of the excitator: the weight of the shafts of the ball-bushing constructions plus two times half the weight of the dynamometers did contribute to the weight (or rather the volume of displacement) of the ship model, but they did not contribute to the mass forces on the dynamometers.

The pure sway and yaw tests with zero forward and transverse speed were executed in the middle of a rectangular basin with relatively large, horizontal dimensions, viz. length = 32.34 m and breadth = 13.98 m. The basin had a horizontal bottom and was bounded by vertical walls.

The P.M.M. was stiffly mounted on a rectangular steel frame, which was as rigid as possible; this frame had four legs, stood in a fixed position in the basin and was adjustable in height. The dimensions of the horizontal cross-section of the legs were relatively small with respect to the main dimensions of the ship model. The longitudinal plane of symmetry of the ship model in its state of rest (i.e. the equilibrium position) coincided with the respective breadthwise axes of symmetry of the basin and the frame. The distances of the legs of the frame to the ship model were relatively large, even during the oscillations. As a result of the oscillatory motions of the ship model during the dynamic tests waves were generated. Therefore the model was placed in the basin in such a position that the generated waves travelled as much as possible in the longitudinal direction of the basin; these waves were reflected against the opposite short side-walls of the basin. In order to attain faster wave damping each opposite short side of the basin was provided with a simple wave damping construction in the form of a wall of perforated bricks with a relatively great percentage of holes. The wave damping properties of these perforated walls were rather good for short-period waves, but fairly bad for long-period waves.

For a schematical representation of the model installation it is referred to fig. 3.2.

The natural frequencies of the combination frame-P.M.M. in both horizontal and vertical direction turned out to be at least many times higher than the frequencies considered in the experiments; the same applied to the natural frequencies of the strain-gauge dynamometers for different directions.

3.2.2.2. Execution of model experiments

For the dynamic tests the circular frequency and the amplitude of motion had to be considered as independent variables; for a certain dynamic test they were fixed quantities.

The hydrodynamic coefficients for the sway and yaw modes of motion could be determined -as functions of circular frequency and amplitude of motion- from the measurement of the first harmonic components of the excited lateral forces in a way as pointed out in ref. [54].

The tests were carried out in accordance with Froude's law of similitude. Because of the limitations of the experimental equipment no data could be obtained for frequencies smaller than 0.196 rad.s^{-1}.

Some combinations of the independent variables (viz. high frequency together with large amplitude) set upper limits to the dynamic tests. One absolute upper limit was the maximum capacity of the dynamometers. Another more relative upper limit was formed by the vertical degree of freedom of the ship model. By this the oscillating ship model could run the risk of touching the bottom for certain combinations of amplitude and frequency. This phenomenon was caused by the velocity effect: the ship model could sink deeper into the water during the oscillatory motions than its draught as indicated for the state of rest. For obvious reasons this could not be accepted.

Each experiment was started with the water level at rest; it had to be terminated at the moment when the first (partial) wave reflections against the opposite (short) basin walls were expected at the (exposed) sides of the ship model; for, reflected waves arriving at the ship model during a measurement should influence the test results.
The minimum length of time required for the execution of one dynamic test was equal to the duration of the transient phenomena of the experimental equipment plus the period time.
The vast majority of the dynamic tests could be carried out before the reflected waves arrived at the ship model. In a few cases, however, the model experiments were possibly disturbed by reflected waves, viz. for $\omega < 0.4$ rad.s^{-1} roughly: this had to be understood in this sense that -also considering the accuracy- only the test results for $\omega \geq 0.4$ rad.s^{-1} could be reproduced in a satisfactory way. Although the disturbance of the model experiments by the reflection phenomena was very small, the test results for $\omega < 0.4$ rad.s^{-1} have to be considered with some reserve, because they might be not completely reliable.

Despite the fact that a perfectly horizontal bottom was tried for, the part of the bottom of the basin covered by the oscillatory motions of the ship model showed differences in height. The water depth as well as the position in height of the bottom were determined with respect to the centre of the basin: the bottom under the fore-part of the ship model was tolerably horizontal, whereas the bottom under the aft-part sloped downwards, starting from and mainly in a direction perpendicular to the lengthwise axis of the basin, with a maximum difference in height of $0.5*10^{-2}$ m. The (possible) inaccuracies in the test results in consequence of this uneveness of the bottom were accepted. In case of a perfectly horizontal bottom the respective hydrodynamic forces on the fore-part and the aft-part of the ship model have to be equal to one another for reasons of symmetry. Therefore the hydrodynamic coupling coefficients a_{26}, b_{26}, a_{62} and b_{62} then have to be equal to zero. As a result of the non-horizontal bottom, however, the (absolute) values of the hydrodynamic forces on the fore-part of the ship model turned out to be systematically larger than those on the aft-part. This held good for the in-phase components of the forces as well as for the ninety degrees out-of-phase components. For $h = 0.175$ m these differences were stronger than for $h = 0.200$ m. The hydrodynamic coupling coefficients were (slightly) different from zero. From the test results it can be verified that in case of a perfectly horizontal bottom, for the frequency range considered in the experiments and for both water depths, the (real) values of a_{22}, b_{22}, a_{66} and b_{66} generally will be (slightly) larger than the measured values: this holds good for b_{22} and b_{66}, whereas for a_{22} and a_{66} this roughly holds good up to $\omega = 2.3$ rad.s^{-1} and $\omega = 2.9$ rad.s^{-1}, respectively. The differences from the measured values in case of h = 0.175 m will be somewhat stronger than in case of h = 0.200 m; for both water depths the differences in case of b_{22} and b_{66} will be more significant than in case of a_{22} and a_{66}, especially for small amplitudes of motion.

During the oscillatory motions the vertical degree of freedom of the ship model -due to the velocity effect- led to a reduction of the original keel clearance. For a certain ω a larger amplitude of motion yielded a larger amplitude of (angular) velocity and as a consequence a deeper sinking of the ship model with respect to the undisturbed water level. The influence of this temporary (i.e. only during the oscillatory motions) reduction of the keel clearance on the test results, however, could not be determined distinctly and unambiguously, the more so as the phenomena of vortex shedding and separation of flow at the 'bow', the 'stern' and the 'bilges' of the ship model came through more explicitly as the amplitude of motion increased.

3.2.3. Comparison of theory and experiment

3.2.3.1. Results in case of pure swaying

The hydrodynamic coefficients for the case of pure swaying with zero forward and transverse speed, as determined theoretically and experimentally, are represented in dimensionless form by

$\frac{a_{22}}{\rho LBD}$ = dimensionless added mass for swaying

and

$\frac{b_{22}}{\rho LBD}\sqrt{\frac{B}{g}}$ = dimensionless sway damping force coefficient.

The results are plotted as functions of the dimensionless circular frequency $\omega\sqrt{B/g}$ with the dimensionless water depth h/D as parameter. Only the most representative results of the dynamic tests are given together with the corresponding results of the calculations. The experimental results are plotted as centred symbols, whereas the curves represent the theoretical results.

Figs. 3.3, 3.4 and 3.5 show the theoretical results for a_{22} and b_{22} as function of ω with the water depth h as parameter; the friction effect in the underkeel clearance is not included. Generally both a_{22} and b_{22} appear to be strongly dependent on the frequency. For large values of ω, a_{22} and b_{22} approach asymptotically to a constant value $\neq 0$ and the zero-value, respectively. The graphs of b_{22} for the respective values of h are going to coincide for large ω; generally it may be stated that for large values of $\omega\sqrt{B/g}$ (say > 3.9) b_{22} becomes independent of the water depth (see also Appendix F; at the same time this appendix comprises supplementary information on the behaviour of $a_{22}(\omega)$ for $\omega \to 0$ as well as $\omega \to \infty$ and on a_{66}, b_{66}). The relation between the curves of a_{22} versus ω for non-zero and zero keel clearance can be understood as follows. For decreasing h the 'image' of the a_{22}-curve shifts to the left; the branch of the curve on the left of the minimum value of a_{22} becomes steeper, the $a_{22}(0)$-value moves along the vertical axis in upward direction, the minimum value of a_{22} sags down and shifts to smaller ω, the $a_{22}(\infty)$-value increases slightly. A limit case is attained for h = D: the (now degenerated) branch of the curve on the left of the minimum value of a_{22} coincides with the vertical $a_{22}/(\rho LBD)$-axis, and the branch on the right touches the horizontal axis in the origin.

A similar observation applies to the relation between the curves of b_{22} versus ω for non-zero and zero underkeel clearance.

Complementary information on the influence of the amplitude of the fluid velocity in the keel clearance and its phase difference with respect to the ship motion is given in ref. [54].

From the expressions for a_{22} and b_{22} as based on a long-wave approximation for the motion of the water (see Appendix E), it simply can be shown that -for the water depths considered- the influence of the underkeel friction is small, viz. up to a few per cent. of the values of a_{22}, b_{22} determined without friction, on the understanding that b_{22} is more affected than a_{22}. As far as the frequency range considered in the dynamic tests is concerned, a_{22} slightly decreases and b_{22} increases. This trend -also being corroborated by a valuation of the friction terms on the respective right-hand sides of (3.36^a) and (3.37^a)- forms a justification for a full neglect of underkeel friction effects.

The experimental results for a_{22} and b_{22} are presented in figs. $3.6^{a,b}$ and $3.7^{a,b}$. For clearness' sake the amplitude of motion, originally indicated as $\hat{x}_2$, is represented by $\hat{a}$. In these figures also the relevant theoretical values of a_{22}, b_{22} as derived in Section 3.2.1 are given as well as the results from Appendix E.

For both values of h/D the test results for a_{22} and b_{22} are subject to large changes when ω increases. In case of the smaller water depth, up to $\omega\sqrt{B/g} = 0.45$, a_{22} is larger than for the situation with deeper water; for $\omega\sqrt{B/g} > 0.45$ a_{22} in case of h/D = 1.167 seems to be somewhat smaller than in case of h/D = 1.333. For h/D = 1.167 b_{22} is larger than for h/D = 1.333.

For that part of the frequency range where the test results are not influenced by reflected waves (i.e. $\omega\sqrt{B/g} > 0.08$ or $\omega > 0.4$ rad.s^{-1}) -for certain ω- a_{22} slightly decreases and b_{22} slightly increases in case of increasing $\hat{a}$. Generally this holds good up to $\hat{a} = 0.05$ m for both water depths; in case of h/D = 1.167 this is more significant than in case of h/D = 1.333, particularly for lower frequencies. Probably this phenomenon is caused by friction in the underkeel clearance. Assuming a friction force proportional to certain (positive) power of the underkeel velocity, its influence on a_{22}, b_{22} becomes greater as $\hat{a}$ increases; a_{22} will be affected to a less extent than b_{22}. One thing and another is conformable to the influence of the underkeel friction on a_{22}, b_{22} as indicated above for the long-wave approximation. The underkeel friction effect increases in case of a reduction of the keel clearance, which reduction is greater as the amplitude of motion (and consequently the friction force) is larger.

During the sway experiments it was observed that for $\hat{a} \geq 0.05$ m the phenomena of vortex shedding and separation of flow at the 'bow', the 'stern' and the 'bilges' of the ship model were going to play an increasingly important part, such that an extension of the preceding observations to larger amplitudes of motion does not seem to be justified.

The results of the dynamic sway tests indicate that the system ship-fluid may be considered as being linear (i.e. independent of the amplitude of motion), at least within the frequency range considered in the experiments. The assumption of linearity of the system ship-fluid in case of swaying is a well-working approximation notably for small to moderate amplitudes (say up to $\hat{a} = 0.05$ m) of model ship forms as used.

Making allowance for the fact that -as a result of the non-fully horizontal bottom in the dynamic tests- the (real) values of a_{22} and b_{22} generally will be (slightly) larger than their measured values, the agreement between theory and experiments is quite satisfactory; notably this holds for moderate to high frequencies (i.e. for $0.15 < \omega\sqrt{B/g} < 0.58$) for both values of h/D.

For the low-frequency range (say $\omega\sqrt{B/g} < 0.15$) the theoretical and experimental results do not agree. This is caused by the fact that in the theoretical determination of the hydrodynamic coefficients the respective effects of strip theory and neglect of viscosity as well as the so-called end effects are not taken into account. In addition to this the experimental results for $\omega\sqrt{B/g} < 0.08$ were influenced by (reflected) waves. It is very difficult to evaluate to what extent the reflection phenomenon influences the test results; anyhow, for $\omega\sqrt{B/g} < 0.08$ these have to be considered with some reserve.

Application of the strip theory implies a neglect of the mutual interactions between the various cross-sections of the ship (model); the influence of this on the hydrodynamic coefficients derived theoretically finds expression mainly in the low-frequency range, because there the length of the waves generated by the oscillating ship motions is relatively large with respect to the size of the hull; the influence of the ends of the hull ('bow' and 'stern') on the hydrodynamic phenomena then may become relatively important.

For the low-frequency range the viscous effects in themselves come into play rather than the free-surface effects and may present an increasing influence on the hydrodynamic phenomena as the frequency decreases.

For $h/D = 1.333$ the agreement between theory and experiment turns out to be slightly better than for $h/D = 1.167$. This is caused by the fact that for $h/D = 1.167$ the keel clearance underneath the ship is smaller than for $h/D = 1.333$. In case of a smaller keel clearance the circulation effect is stronger.

For very low frequencies a good agreement should be expected between the theoretical results as derived in Section 3.2.1 and the results of the long-wave approximation for the motion of the water (Appendix E). However, the contrary is the case. As cause might be mentioned the supposition -inherent to the long-wave approximation- that already in vertical planes at extremely short distances from the ship's walls the horizontal fluid velocities are uniformly distributed over the height, what is generally not the case in the theoretical approach in Section 3.2.1. In this latter case there will be only question of a uniform velocity distribution in vertical planes very close to the ship's wall, if the keel clearance tends to zero. Therefore, the relevant results of the theory as presented in Section 3.2.1 and the long-wave approximation are only allowed to be compared if both ω tends to zero (i.e. pure long-wave approximation) and h tends to D (i.e. zero keel clearance). Indeed it can be ascertained that (3.44) and (E.15) as well as (3.45) and (E.16) do agree.

Likewise, the above explains why there exists in case of h/D = 1.167 a better agreement between the theoretical results from Section 3.2.1 and the results of the long-wave approximation than in case of h/D = 1.333.

3.2.3.2. Results in case of pure yawing

The hydrodynamic coefficients for the case of pure yawing with zero forward and transverse speed, as determined theoretically and experimentally, are represented in dimensionless form by

$\dfrac{a_{66}}{\frac{1}{12}L^2\rho LBD}$ = dimensionless added mass-moment of inertia for yawing motion

and

$\dfrac{b_{66}}{\frac{1}{12}L^2\rho LBD}\sqrt{\dfrac{B}{g}}$ = dimensionless yaw damping moment coefficient.

The results are plotted in the same way as done for the hydrodynamic sway coefficients.

The experimental results for a_{66} and b_{66} are presented in figs. $3.8^{a,b}$ and $3.9^{a,b}$. The amplitude of motion is denoted by $\psi_0 = \frac{\hat{a}}{l}$, where l = half the distance between the two struts of the P.M.M. (l = 0.5000 m). In these figures also the relevant theoretical values of a_{66} and b_{66} as based on (3.34^a) and (3.34^b), respectively, are given.

For both values of h/D the test results for a_{66} remain nearly constant, whereas those for b_{66} are subject to large changes when ω increases. In case of the smaller water depth, up to $\omega\sqrt{B/g} = 0.56$, a_{66} is larger than for the situation with deeper water; for $\omega\sqrt{B/g} > 0.56$ a_{66} in case of h/D = 1.167 seems to be somewhat smaller than in case of h/D = 1.333. For h/D = 1.167 b_{66} is larger than for h/D = 1.333.

For that part of the frequency domain where the experimental results are not influenced by reflected waves (i.e. $\omega\sqrt{B/g} > 0.08$ or $\omega > 0.4$ rad.s^{-1}) -for certain ω- the values of a_{66} for the various amplitudes of motion ψ_0 coincide reasonably well; generally this holds good up to ψ_0 = 0.10 rad. for both water depths. During the yaw experiments it was observed that for $\psi_0 \geq 0.10$ rad. the phenomena of vortex shedding and separation of flow at the 'bow', the 'stern' and the 'bilges' of the ship model were going to play an increasingly impor-

tant part. This last fact seems to affirm that the influence of the smaller amplitudes of motion on a_{66} is of secondary importance.
For $\omega\sqrt{B/g} > 0.08$ b_{66} for certain ω (slightly) increases as ψ_0 increases; generally this holds good for both water depths. This phenomenon may be explained in a similar way as in the case of pure swaying, viz. by friction in the keel clearance. For b_{66} an extension of this explanation to amplitudes of motion $\psi_0 \geqq 0.10$ rad. does not seem justified for reasons of the increasingly important part played by vortex shedding and separation of flow.
The results of the dynamic yaw tests indicate that the added mass-moment of inertia for yawing motion -unlike the yaw damping moment coefficient- may be considered as independent of the amplitude of motion, at least within the frequency range considered in the experiments. Nevertheless it will be supposed that the system ship-fluid also in case of yawing is linear, and that this supposition is a well-working approximation notably for (very) small amplitudes of motion (say up to $\psi_0 = 0.06$ rad.) of model ship forms as used.

Even when regard is paid to the fact that -as a result of the non-fully horizontal bottom in the dynamic tests- the (real) values of a_{66} and b_{66} generally will be (slightly) larger than their measured values, there is no agreement between theory and experiments, at least as far as the considered frequency domain is concerned; notably this holds good for a_{66}, in case of b_{66} the theoretical and experimental results present the same trend. The effect of the neglect of viscosity yields no satisfactory explanation. Therefore it is obvious to think of an explanation in terms of the effect of the strip theory in combination with the so-called end effects.
Essentially the strip theory is two-dimensional; consequently the solution for the three-dimensional yawing is obtained by hypothesizing that locally this rotational motion is equivalent to a transverse translatory motion of angle times the distance from the axis of rotation. Besides, in the strip theory the mutual interactions between the various cross-sections are neglected, while another complicating aspect is formed by the phase relation of the motions of the various cross-sections. In addition to the effects of the strip theory another complicating factor is formed by the fact that the strip theory cannot account for (the side force and) the yaw moment associated with a small keel clearance, because in this case circulation (i.e. the lengthwise motion of fluid, passing around the ends of the ship) belongs to the eventualities.
It will be obvious by now that the effects of the strip theory together with the circulation effect are responsible for the general disagreement between

the theoretically derived and the experimentally determined results for the hydrodynamic coefficients in case of yawing.

3.2.4. Complementary observations

3.2.4.1. General remarks

To conclude with Section 3.2 a number of complementary observations can be made.

One is tempted to suppose that the values of the various hydrodynamic coefficients for zero frequency will be the same as those for (very) low frequencies, but particularly with respect to a_{22} and a_{66} one has to be careful with this extrapolation. Concerning the hydrodynamic damping coefficients the problem seems to be less complicated.

It looks like that the symmetry relations $a_{62} = a_{26}$, $b_{62} = b_{26}$ are confirmed by experiments only in the low-frequency domain. At higher frequencies the inequality of the respective hydrodynamic cross-coupling coefficients is probably due to the shedding of vorticity and separation of flow (see also ref. [46]).

Apart from the model experiments as carried out the question remains whether at higher frequencies the respective linear expressions for pure swaying and yawing (3.29^a) and (3.30^a), would satisfy to describe the lateral ship motions. There seem to be objections to the use of the independent variables $\hat{a}$ c.q. ψ_0 and ω. It might be better to carry out the dynamic tests for constant values of the velocity and acceleration amplitudes, respectively, for these are the variables which are considered in (3.29^a) and (3.30^a). In that case suitable combinations of $\hat{a}$ c.q. ψ_0 and ω have to be chosen. A plot of the various hydrodynamic coefficients on a basis of velocity and acceleration amplitudes, respectively, could be useful to judge the separate effects of both these variables.

The frequency dependence of the hydrodynamic coefficients is caused by the wave effects associated with the unsteady motion of the ship (model) at the free surface and by the vorticity shedding from the hull (the latter phenomenon -within the linearity concept- being of minor importance). There is some evidence to suggest that the presence of the free surface plays a more important role in the damping components of force and moment than in the corresponding added mass(-moment of inertia) components. This is to be expected since in an ideal unbounded fluid the hydrodynamic force (moment) is entirely

in phase with the (angular) acceleration.
For the low-frequency range viscous effects come into play rather than free-surface effects.
For sufficiently small frequencies the pseudo-steady-state analysis is valid (i.e. pertaining to steady-state hydrodynamic forces and moments acting on a ship).

The hydrodynamic coefficients for the three-dimensional ship form were obtained by combining the contributions from the separate cross-sections in a simple stripwise manner. If the hydrodynamic quantities, calculated in this way, are in agreement with test results, then this is an obvious support to two propositions: firstly, that the separate contributions for all cross-sections of the ship have been predicted correctly, and secondly, that the measure in which the cross-sections influence one another is negligible. Beside the consequences of the stripwise approach, also the influence of viscosity and the end effects (i.e. the circulation around 'bow' and 'stern') have not been taken into account. Hence, in a general sense, successively the effects of the strip theory, the neglect of viscosity and the end effects will be discussed below.

3.2.4.2. Effect of strip theory

By strip theory is simply understood the stringing of a series of two-dimensional elements to construct an approximative solution for a three-dimensional problem: each cross-section of the ship (model) is considered to be part of an infinitely long prismatic body and each two-dimensional problem so constructed is solved separately, after which the solutions are combined in some way to yield a solution for the entire ship. Consequently two stages can be distinguished in the strip-theory approach. Firstly, the solution of the two-dimensional problem of oscillating prisms: in this stage the elementary local values of the hydrodynamic coefficients must be determined. Secondly, the combination of these values to approximate the three-dimensional coefficients (at zero forward and transverse speed): here physically three-dimensional effects come into play, but only as far as the strip theory neglects them.
Using strip theory it is obvious that the longitudinal translation (surge) cannot be dealt with; however, this motion has been left out of consideration. In the two-dimensional theoretical problem as dealt with in Section 3.2.1 the

cross-section can only perform swaying. A solution for the three-dimensional yawing has been obtained by making the hypothesis that locally this rotational motion is equivalent to a transverse translatory motion of angle times the distance from the axis of rotation.
The strip theory has the great drawback that it neglects the mutual interactions between the various cross-sections. For slender bodies strip theory results logically from the truely three-dimensional theory for high frequencies of motion. Therefore it may be expected that the correctness of this neglect depends primarily on the range of frequencies involved in relation to the size of the body or, in physical terms, on the relative length of the waves generated by the oscillations and the dimensions of the body: short waves will not be affected distinctly by parts of the body being many wave lengths away (and vice versa), but for long waves the same parts are close to the source of the disturbance and will directly attribute to the hydrodynamic phenomena.
Looking at the matter in this physical way another aspect is formed by the phase relation of the motions of the various sections. A phase identity for all sections as with swaying resembles two-dimensional conditions, while a phase transition of π radians at mid-length as with yawing promotes interference effects.
Naturally the basic principle of strip theory breaks down at the ends of the body.

The above is only a qualitative evaluation; it is very difficult to say where the limits of relatively high frequencies or of long waves are, or to what extent the end effects influence the ultimate results.

3.2.4.3. Effect of neglect of viscosity

Viscous contributions appear in two forms: skin friction and separation of flow. Usually these viscous components are of a non-linear nature.
Skin friction is proportional to some positive power of a velocity (gradient) and will contribute mainly to the damping coefficients, while separation of flow changes the flow pattern around the body to a certain extent, so that it may influence both the damping and the added mass(-moment of inertia). Skin friction may be left out of consideration since, probably, it will be small with respect to flow separation, although in unsteady flow motions large velocity gradients and consequently large shear forces may occur.
Separation of flow occurs at relatively sharp edges of the ship (model). This

is a source of energy loss due to eddy formation which contributes mainly to the damping coefficients: probably, the shedding of eddies does not seriously affect that part of the pressure distribution which is in phase with the body acceleration (ref. [46]). In cases where the damping due to wave radiation is small, the influence of separation of flow cannot be neglected, however; such cases are e.g. the hydrodynamic forces at the ends of the ship in transverse motion, maybe the (local) forces on the bilges.

The viscous contributions at the ends of the ship (model) in swaying and yawing may be locally significant, but probably they are negligible with respect to the magnitude of the total damping.

3.2.4.4. End effects

Strip theory cannot account for the side force and the yaw moment associated with a small keel clearance, because in this case the circulation around 'bow' and 'stern', i.e. the end effects, may become important. It may be expected that the influence(s) of the ends of the ship does (do) not dominate the integrated pressures due to two-dimensional potential flow, if the ratios of ship's length to wave length are large enough and as long as there is no forward and transverse speed: at least the circulation effects will relatively diminish. For short(er) ships and/or long(er) waves deviations can be expected.

In physical terms one thing and another implies the following. Using a two-dimensional theory it is not possible to obtain results always reliable, because three-dimensional effects can be of crucial importance.
In swaying distinction must be made between situations in which fluid easily can pass under the keel of the ship (model), and situations in which most of the fluid must move lengthwise, passing around the ends of the ship. Only in the former situation added mass and damping coefficients may be calculated in a simple stripwise manner, neglecting three-dimensional effects. In the latter situation, which has as its extreme case that of a grounded ship touching the bottom along its whole length, the given theory holds good only for an infinitely long ship (model) and, as a consequence, the results must be regarded with utmost care. Therefore it is possible to state in advance that for a ship with finite keel clearance and finite length a two-dimensional theory produces values for the hydrodynamic coefficients in case of swaying which are too high.

The hydrodynamic coefficients for yawing are determined from those for swaying in a simple stripwise manner. In yawing the lengthwise motion of fluid passing around the ends of the ship (i.e. circulation) is rather important -certainly in case of a finite keel clearance- so that (very) inaccurate or even wrong results for the hydrodynamic coefficients can be expected from a two-dimensional theory.

3.3. Calculation of impulse response function

3.3.1. Introductory considerations

In Section 3.2 the hydrodynamic coefficients were determined both in an experimental and in an analytical way. As a consequence of the restricted possibilities of the experimental facilities the hydrodynamic coefficients could only be measured in a limited frequency range. Therefore an analytical determination of the hydrodynamic coefficients was necessary in order to obtain information concerning $a_{ii}(\omega)$ and $b_{ii}(\omega)$ ($i = 2,6$) along a sufficiently long frequency range. As the theoretical results for the hydrodynamic coefficients were derived using strip theory (i.e. a two-dimensional approach), three-dimensional effects, such as the circulation around 'bow' and 'stern' could not be taken into account. This is the main cause of the discrepancy between the theoretical and the experimental results for the hydrodynamic coefficients in the lower-frequency range. In case of higher frequencies the theory is sufficiently accurate -also on shallow water- to determine the hydrodynamic coefficients in a (two-dimensional) stripwise manner (see further Appendix F).
Since the hydrodynamic coefficients for the lower frequencies have a relatively greater influence on the behaviour of the i.r.f. than those for the higher frequencies, especially in the lower-frequency range $a_{ii}(\omega)$ and $b_{ii}(\omega)$ must be known as accurate as possible.

The respective i.r.f. for the sway motion and the yaw motion are calculated making use of the set of equations (2.67), (2.66), (2.64) and (2.65). For an outline and an elucidation of the method used for this numerical calculation, reference is made to Appendix G. The calculation was done starting from values for the hydrodynamic coefficients $a_{ii}(\omega)$ and $b_{ii}(\omega)$ given at the following frequencies: for $0 \leq \omega \leq 25\ s^{-1}$ with frequency step = $0.1\ s^{-1}$, for $25 \leq \omega \leq 50\ s^{-1}$ with frequency step = $0.5\ s^{-1}$, for $50 \leq \omega \leq 80\ s^{-1}$ with frequency step = $1.0\ s^{-1}$. In all cases considered, the combined influence of the truncation of the numerical process of integration and the discretization error remained -for all $t > 0$- smaller than 0.01 % of the corresponding value calculated for $k_{ii}(t)$. By systematic variation of the upper bound of ω in the relevant integral represented by (2.67), it was found that the influence of the hydrodynamic coefficients at higher frequencies on the i.r.f. indeed is of minor importance. When, for instance, this upper bound is set to $\omega = 30.0\ s^{-1}$, the combined effect of truncation and discretization error -for all $t > 0$- is still smaller than 1 % of the value calculated for $k_{ii}(t)$.

For $k_{ii}(t)$ at $t = 0$ the estimated value of the discretization error remained smaller than 0.01 % of the values as calculated for $k_{ii}(0)$. It was not possible to give an estimate for the truncation error. However, systematic variation of the upper bound of ω in the relevant integral (2.67) showed that as long as this upper bound was larger than $30.0\ s^{-1}$ -for all cases considered- the combined influence of the truncation of the numerical process of integration and the discretization error is amply within 1 % of the values calculated for $k_{ii}(0)$.

The i.r.f. $k_{ii}(t)$ was calculated numerically at intervals of time amounting to 0.01 s. The upper limit of the calculations was taken at $t = 7.50$ s; this time range was regarded to be sufficiently long, since it was found that for $t > 7.50$ s $k_{ii}(t) \approx k_{ii}(\infty)$.

3.3.2. Sway mode of motion

In figs. $3.6^{a,b}$ and $3.7^{a,b}$ the hydrodynamic coefficients for the sway motion are represented for that part of the frequency domain, for which also experimental results are available. As a consequence of the discrepancy between theory and experiment in case of low frequencies, the relevant hydrodynamic sway coeffients calculated two-dimensionally have been fitted to the (three-dimensional) experimental values; for the higher frequencies they are maintained. To avoid a possible non-linear distortion of the f.r.f. (i.e. the hydrodynamic coefficients) this local adjustment of theory to experiment is based on the smallest amplitudes of the harmonically oscillating sway motion.

Starting from the hydrodynamic coefficients $a_{22}(\omega)$ and $b_{22}(\omega)$ as given in figs. $3.6^{a,b}$ and $3.7^{a,b}$ and further in Section 3.2.1.5, the i.r.f. for the sway motion $k_{22}(t)$ can then be calculated numerically (see Appendix G). The results are presented in the dimensionless form $\rho LBDk_{22}$ in figs. 3.10 and 3.11 as function of the dimensionless time $t\sqrt{g/B}$ with the dimensionless water depth h/D as a parameter. The figs. 3.10 and 3.11 each show three curves:

- the dot-and-dash line represents $k_{22}(t)$ as calculated from hydrodynamic coefficients determined theoretically (i.e. two-dimensionally) along the whole frequency-range;
- the full line represents $k_{22}(t)$ as calculated from hydrodynamic coefficients which in case of higher frequencies were determined theoretically (i.e. two-dimensionally) and in case of low frequencies were fitted to experimental (i.e. three-dimensional) values;
- the broken line represents $k_{22}(t)$ as calculated from an expression which can be derived analytically using a long-wave approximation for the motion of the water; this long-wave approximation is basically one-dimensional (see Appendix H).

From figs. 3.10 and 3.11 it can be seen that the i.r.f. $k_{22}(t)$ approximates rather quickly to a constant value as t increases; this means that in the convolution integral (2.69) -representing for $i = 2$ the motion of the ship in the sway direction- much emphasis is laid on the very near past of the time history of the forcing function.

3.3.3. Yaw mode of motion

Figs. $3.8^{a,b}$ and $3.9^{a,b}$ show the hydrodynamic coefficients for the yaw motion along that part of the frequency range, for which also experimental values are available. Since theory and experiment do not agree in the frequency domain considered, the hydrodynamic yaw coefficients calculated two-dimensionally have been fitted to the (three-dimensional) experimental values; they are maintained for the higher frequencies. To avoid a possible non-linear distortion of the f.r.f. (i.e. hydrodynamic coefficients) this local adjustment of theory to experiment is based on the smallest amplitudes of the harmonically oscillating yaw motion.

Concerning the values of $a_{66}(\omega)$ and $b_{66}(\omega)$ as actually used, the following additional remarks have to be made. In case $h/D = 1.333$, for $\omega\sqrt{B/g} \leqq 0.567$ (i.e. $\omega \leqq 2.9\ s^{-1}$) $a_{66}(\omega)$ as well as $b_{66}(\omega)$ have been fitted to their corresponding experimental values; for $2.9 \leqq \omega \leqq 5.9\ s^{-1}$ $a_{66}(\omega)$ was extrapolated by means of a straight line according to $a_{66}(\omega) = -34.32\omega + 217.22$, which was faired into the curve at $\omega = 2.9\ s^{-1}$; for $\omega > 5.9\ s^{-1}$, it was applied $a_{66}(\omega) = \frac{1}{12}L^2 a_{22}(\omega)$ (see Appendix F); for $2.9 \leqq \omega \leqq 3.3\ s^{-1}$ $b_{66}(\omega)$ was extrapolated by means of a straight line according to $b_{66}(\omega) = 235.36\omega - 436.89$, which was faired into the curve at $\omega = 2.9\ s^{-1}$; for $\omega > 3.3.\ s^{-1}$ it was applied $b_{66}(\omega) = \frac{1}{12}L^2 b_{22}(\omega)$ (see Appendix F). In case h/D = 1.167, for $\omega\sqrt{B/g} \leq 0.567$ $a_{66}(\omega)$ as well as $b_{66}(\omega)$ have been fitted to their corresponding values; for $2.9 \leq \omega \leq 3.9\ s^{-1}$ $a_{66}(\omega)$ was extrapolated by means of a straight line according to $a_{66}(\omega) = -88.26\omega + 367.75$, which was faired into the curve at $\omega = 2.9\ s^{-1}$; for $\omega > 3.9\ s^{-1}$ it was applied $a_{66}(\omega) = \frac{1}{12}L^2 a_{22}(\omega)$ and for $\omega > 2.9\ s^{-1}$ $b_{66}(\omega) = \frac{1}{12}L^2 b_{22}(\omega)$ (see Appendix F).

Starting from the hydrodynamic coefficients $a_{66}(\omega)$ and $b_{66}(\omega)$, as given in figs. $3.8^{a,b}$ and $3.9^{a,b}$ and further above and in Section 3.2.1.5, the i.r.f. for the yaw motion $k_{66}(t)$ then can be calculated numerically (see Appendix G). The results are presented in the dimensionless form $m_{66}k_{66}$ in figs. 3.12 and 3.13 as function of the dimensionless time $t\sqrt{g/B}$ with the dimensionless water depth h/D as a parameter. The figs. 3.12 and 3.13 each show two curves:

- the dot-and-dash line represents $k_{66}(t)$ as calculated from hydrodynamic coefficients determined theoretically (i.e. two-dimensionally) along the whole frequency range;
- the full line represents $k_{66}(t)$ as calculated from hydrodynamic coefficients which in case of low frequencies were fitted to experimental (i.e. three-dimensional) values and further were extrapolated linearly, and which in case of higher frequencies were determined theoretically (i.e. two-dimensionally).

From figs. 3.12 and 3.13 it can be seen that the i.r.f. $k_{66}(t)$, just like $k_{22}(t)$, approximates rather quickly to a constant value as t increases; this means that in the convolution integral (2.69) -representing for i = 6 the motion of the ship in the yaw direction- much emphasis is laid on the very near past of the time history of the forcing function.

3.4. Application of i.r.f.-technique to berthing ship

3.4.1. Outline of mathematical approach

Consider the schematized ship berthing to an open jetty fitted with one single fender. The characteristics of the fender are assumed to be represented by an undamped spring with a horizontal line of action situated in the plane of the water surface at rest. The mass of the fender is supposed to be small with respect to the mass of the ship. This implies that the effect of the initial impact may be neglected, i.e. the given state of motion does not change. If the mass of the fender is not negligibly small with respect to that of the

ship, then the fender gets a sudden acceleration at the first moment of contact; the initial impact between ship and fender can be considered as non-elastic. Just after the first moment of contact ship and fender combined move as a whole. Due to a redistribution of the momentum of the approaching ship, in that case a new initial value for the joint velocity of ship and fender arises, without any change of the initial position of the ship. Application of the law of conservation of momentum for this situation to ship as well as fender, then leads to expressions for both their initial joint velocity and the initial impact load. Further the frictional force between the hull of the ship and the fender is neglected.
As only horizontal motions are involved, the position of the ship's centre of gravity G in height is of no importance. Consequently, for the sake of simplicity, G is assumed to be situated in the free water-surface at rest.
Initially, i.e. before the first contact between ship and fender, the ship moves laterally towards the berth with a zero forward speed (i.e. $V_1 = 0$), a constant speed of approach $V_2 = v_A$ and without rotation. The first contact between ship and fender is supposed to take place at point of time $t = 0$. Then the line of action of the fender is perpendicular to the longitudinal axis of symmetry of the ship; its initial distance to the ship's centre of gravity G is denoted by e_0. At $t = 0$ the space-fixed $OX_1X_2X_3$-co-ordinate system is assumed to coincide with the translating $ox_1x_2x_3$-co-ordinate system; the ship-fixed Gxyz-co-ordinate system then also coincides with $OX_1X_2X_3$. When $e_0 \neq 0$, at $t = 0$ the ship starts rotating, so that for $t > 0$ the motion of the ship consists of a translation and a rotation around the OX_3-axis. The co-ordinates of the ship's centre of gravity G at point of time t are indicated by $X_{1G}(t)$ and $X_{2G}(t)$; the angle of rotation of the ship's longitudinal axis of symmetry around the OX_3-axis then is $X_6(t) = \psi(t)$. The co-ordinates of the point of the fender are $X_{1f}(t) = -e_0$ for all t, and $X_{2f}(t)$ with $X_{2f}(t) = \frac{1}{2}B$ for $t \leqq 0$. The added subscripts G and f indicate that the quantity concerned must be related to the ship's centre of gravity G and the fender, respectively. The deflexion of the fender is denoted by $\Delta X_{2f}(t) = X_{2f}(t) - \frac{1}{2}B$. With the position of the ship given by $X_{1G}(t), X_{2G}(t)$ and its orientation by $\psi(t)$ the deflexion of the fender can be expressed as:

$$\Delta X_{2f}(t) = X_{2G} - \frac{1}{2}B\{1-\cos(\psi)\} + \{X_{1f} - X_{1G} + \frac{1}{2}B \sin(\psi)\}\tan(\psi) \quad ,$$

$$\Delta X_{2f}(t) \geqq 0 \quad . \qquad (3.48)$$

for a sketch of the berthing lay-out see fig. 3.14.

The relation between the deflexion of the fender $\Delta X_{2f}(t)$ at a certain point of time $t > 0$ and the corresponding reaction force in the fender $F_{2f}(t)$ can be represented as:

$$F_{2f}(t) = f(\Delta X_{2f}) \qquad \text{for} \qquad t \geqq 0 \quad . \tag{3.49}$$

The resulting force and moment, as acting in and around the ship's centre of gravity, then become:

$$\left.\begin{aligned} f_2(t) &= F_{2f}\cos(\psi) \quad , \\ f_6(t) &= -\overline{AG}\,F_{2f}\cos(\psi) \quad , \end{aligned}\right\} t \geqq 0 \tag{3.50^{a,b}}$$

respectively, where

$$\overline{AG} = \frac{X_{1G} - X_{1f}}{\cos(\psi)} - \frac{1}{2}B\tan(\psi)$$

with $\quad X_{1f} = -e_0 \quad , \quad \psi < \frac{\pi}{2} \quad , \quad |\overline{AG}| \leqq \frac{1}{2}L \quad .$

According to (2.69) the (transient) velocities of the ship are described with respect to the $ox_1x_2x_3$-co-ordinate system, which translates with a constant forward speed V_1 and a constant transverse speed V_2, and -in the case under consideration- for $t > 0$ also rotates with an angular velocity $\dot{\psi}(t)$. Due to the rotation $ox_1x_2x_3$ cannot longer be considered as an inertial system, so that formally a correction has to be made in order to implicate its effect. Within the context given above (2.69) can be rewritten as:

$$\dot{x}_i(t) = \int_0^t f_i(\tau)\,k_{ii}(t-\tau)d\tau \quad , \quad i = 1,2,6 \quad . \tag{3.51^{a,b,c}}$$

The initial values of the berthing problem are given at $t = 0$ and read as:

$$\left.\begin{array}{lll} X_{1G}(0) = 0 \quad , & & X_{2G}(0) = 0 \quad , \\ \dot{X}_{1G}(0) = V_1 = 0 \quad , & & \dot{X}_{2G}(0) = V_2 = v_A \quad , \\ X_{2f}(0) = \frac{1}{2}B \quad , & & \\ x_6(0) = \psi(0) = 0 \quad , & & \\ f_1(0) = 0 \; , & f_2(0) = 0 \quad , & f_6(0) = 0 \quad . \end{array}\right\} \tag{3.52}$$

$\dot{X}_{1G}(0) = V_1 = 0$ and $\dot{X}_{2G}(0) = V_2 = v_A$ describe the uniform translational motion of the $ox_1x_2x_3$-system.

Now let $f_6(t)$ be known until the point of time t. Then $\dot{x}_6(t) = \dot{\psi}(t)$ can be evaluated by means of

$$\dot{\psi}(t) = \int_0^t f_6(\tau)\, k_{66}(t-\tau)d\tau \qquad (3.51^c)$$

in order to get the ship into its proper orientation given by $\psi(t)$. Under these conditions the absolute velocities of the ship's centre of gravity are (see fig. 3.15):

$$\left.\begin{aligned} \dot{X}_{1G}(t) &= \dot{x}_1(t)\cos\{\psi(t)\} - \dot{x}_2(t)\sin\{\psi(t)\} + V_1 - X_{2o}(t)\dot{\psi}(t) \quad , \\ \dot{X}_{2G}(t) &= \dot{x}_1(t)\sin\{\psi(t)\} + \dot{x}_2(t)\cos\{\psi(t)\} + V_2 + X_{1o}(t)\dot{\psi}(t) \quad , \end{aligned}\right\} \qquad (3.53)$$

where $X_{1o}(t)$, $X_{2o}(t)$ = distance covered by G in the X_1- and X_2-direction, respectively, with respect to the uniformly travelling origin of $ox_1x_2x_3$;

the subscript o is added to indicate that the quantity concerned must be related to the origin of the $ox_1x_2x_3$-co-ordinate system; in (3.53) it holds good:

$$X_{1o}(0) = 0 \ , \ X_{2o}(0) = 0 \ ; \ X_{1o}(t) \leqq 0 \ , \ X_{2o}(t) \geqq 0 \ ; \ V_1 = 0 \ , \ V_2 = v_A \ . \qquad (3.54)$$

Supposing that $f_1(t)$ and $f_2(t)$ are known functions until point of time t, $\dot{x}_1(t)$ and $\dot{x}_2(t)$ are to be evaluated by

$$\dot{x}_1(t) = \int_0^t f_1(\tau)\, k_{11}(t-\tau)d\tau \quad , \qquad (3.51^a)$$

and

$$\dot{x}_2(t) = \int_0^t f_2(\tau)\, k_{22}(t-\tau)d\tau \quad , \qquad (3.51^b)$$

respectively. The first two terms on the right-hand sides of (3.53) represent the relative velocities of the ship in the $ox_1x_2x_3$-system resolved in the absolute $OX_1X_2X_3$-system; the third and the fourth term are corrections due to the uniform translation of $ox_1x_2x_3$ and its rotational velocity, respectively. Introducing $x_{1G}(t)$ and $x_{2G}(t)$, defined as the co-ordinates of G within the travelling $ox_1x_2x_3$-system, it can be written:

$$\left.\begin{aligned} X_{1o}(t) &= x_{1G}(t)\cos\{\psi(t)\} - x_{2G}(t)\sin\{\psi(t)\} \quad , \\ X_{2o}(t) &= x_{1G}(t)\sin\{\psi(t)\} + x_{2G}(t)\cos\{\psi(t)\} \quad . \end{aligned}\right\} \qquad (3.55^a)$$

Concerning the co-ordinates of the origin of $ox_1x_2x_3$ it can be stated that

$$V_1t = X_{1G}(t) - X_{1o}(t) \qquad \text{and} \qquad V_2t = X_{2G}(t) - X_{2o}(t) \quad ,$$

from which it follows:

$$\left.\begin{aligned} X_{1o}(t) &= X_{1G}(t) \quad , \\ X_{2o}(t) &= X_{2G}(t) - v_At \quad . \end{aligned}\right\} \qquad (3.56)$$

Due to the rotation of the $ox_1x_2x_3$-system formally additional forces have to be introduced into the description of the force balance. These additional forces can be determined by relating the accelerations in the $ox_1x_2x_3$-system to a new co-ordinate system $o\underline{x}_1\underline{x}_2\underline{x}_3$, which merely translates. Then it formally holds good that

$$\left.\begin{aligned} \ddot{x}_1(t) &= \ddot{\underline{x}}_1(t)\cos\{\psi(t)\} + \ddot{\underline{x}}_2(t)\sin\{\psi(t)\} + a_{1r}(t) \quad , \\ \ddot{x}_2(t) &= -\ddot{\underline{x}}_1(t)\sin\{\psi(t)\} + \ddot{\underline{x}}_2(t)\cos\{\psi(t)\} + a_{2r}(t) \quad , \end{aligned}\right\} \qquad (3.57^a)$$

where $a_{1r}(t)$, $a_{2r}(t)$ = additional accelerations in $ox_1x_2x_3$ to be introduced due to the rotation of $ox_1x_2x_3$ with respect to $o\underline{x}_1\underline{x}_2\underline{x}_3$;

the subscript r indicates that the quantity concerned is due to the rotation. The first two terms on the right hand sides of (3.57) represent the instantaneous components of $\ddot{\underline{x}}_1$ and $\ddot{\underline{x}}_2$ in the respective x_1- and x_2-direction. Now $a_{1r}(t)$ and $a_{2r}(t)$ can be put into the form

$$\left.\begin{aligned} -a_{1r}(t) &= -2\dot{x}_2(t)\,\dot{\psi}(t) - x_{1G}(t)\,\dot{\psi}^2(t) - x_{2G}(t)\,\ddot{\psi}(t) \quad , \\ -a_{2r}(t) &= 2\dot{x}_1(t)\,\dot{\psi}(t) - x_{2G}(t)\,\dot{\psi}^2(t) + x_{1G}(t)\,\ddot{\psi}(t) \quad , \end{aligned}\right\} \qquad (3.58^a)$$

respectively, where the first term on each right-hand side represents the

Coriolis-effect and the second term the centrifugal effect -both due to the angular velocity- , whereas the third term stands for the inertial contribution due to the angular acceleration. $x_{1G}(t)$ and $x_{2G}(t)$ can be expressed into $X_{1o}(t)$ and $X_{2o}(t)$ by

$$\left.\begin{aligned} x_{1G}(t) &= X_{1o}(t)\cos\{\psi(t)\} + X_{2o}(t)\sin\{\psi(t)\} \quad , \\ x_{2G}(t) &= -X_{1o}(t)\sin\{\psi(t)\} + X_{2o}(t)\cos\{\psi(t)\} \quad , \end{aligned}\right\} \qquad (3.55^{b})$$

being equivalent to (3.55^{a}). For (3.57^{a}) it can be written:

$$\left.\begin{aligned} m_{11}\ddot{x}_1(t) &= m_{11}[\ddot{\underline{x}}_1(t)\cos\{\psi(t)\} + \ddot{\underline{x}}_2(t)\sin\{\psi(t)\}] + m_{11}a_{1r}(t) \quad , \\ m_{22}\ddot{x}_2(t) &= m_{22}[-\ddot{\underline{x}}_1(t)\sin\{\psi(t)\} + \ddot{\underline{x}}_2(t)\cos\{\psi(t)\}] + m_{22}a_{2r}(t) \quad . \end{aligned}\right\} \qquad (3.57^{b})$$

The additional forces in the x_1- and x_2-direction, as a result of the rotation of $ox_1x_2x_3$, consequently are

$$\left.\begin{aligned} f_{1r}(t) &= m_{11}a_{1r}(t) = m_{11}\dot{\psi}(t)\{2\dot{x}_2(t) + x_{1G}(t)\,\dot{\psi}(t)\} + m_{11}x_{2G}(t)\,\ddot{\psi}(t) \ , \\ f_{2r}(t) &= m_{22}a_{2r}(t) = m_{22}\dot{\psi}(t)\{-2\dot{x}_1(t) + x_{2G}(t)\,\dot{\psi}(t)\} - m_{22}x_{1G}(t)\,\ddot{\psi}(t) . \end{aligned}\right\} \ (3.58^{b})$$

In other words, the respective additional force in the x_1- and the x_2-direction due to the rotation is the sum of the so-called virtual forces (consisting of the Coriolis-force and the centrifugal force) and the inertial force (resulting from the angular acceleration). If these additional forces are taken into account, they are to be classed in the relevant (external) forcing function $f_i(t)$ of the ship-fluid system.

Using the set of equations (3.48) through ($3.58^{a,b}$) as presented above, it is possible -in a formal way- to determine the fender force and to describe the ship trajectory during the berthing operation.

Within the linearity concept of the i.r.f.-technique (dealing with small disturbances with respect to a given uniform ship motion) the virtual forces as given in (3.58^{b}) represent a second-order effect. Further the berthing situation under consideration leads to the supposition that $x_{1G}(t)$ and $x_{2G}(t)$ (and therefore $X_{1o}(t)$ and $X_{2o}(t)$, see ($3.55^{a,b}$)) remain small quantities, so that the inertial forces due to the angular acceleration also are to be considered as a second-order effect. Consequently the additional forces

$f_{1r}(t)$ and $f_{2r}(t)$ may be neglected. With this simplification it can be stated that $f_1(t) = 0$ for all t, so that on account of (3.51[a]) also $\dot{x}_1(t) = 0$. The contribution to $\dot{X}_{1G}(t)$ and $\dot{X}_{2G}(t)$, respectively, in (3.53) due to the rotational velocity of $ox_1x_2x_3$ just as well may be considered as a second-order effect, so that (3.53) eventually takes the form

$$\left.\begin{aligned} \dot{X}_{1G}(t) &= -\dot{x}_2(t)\sin\{\psi(t)\} \quad , \\ \dot{X}_{2G}(t) &= v_A + \dot{x}_2(t)\cos\{\psi(t)\} \quad , \end{aligned}\right\} \qquad (3.59^{a,b})$$

whereby it has to be borne in mind that according to (3.59[a]) $\dot{X}_{1G}(t)$ likewise will remain small of the second order.

With these simplifications the mathematical formulation of the berthing problem now has been reduced to a set of equations consisting of (3.48), (3.49), (3.50[a,b]), (3.52), (3.51[b,c]) and (3.59[a,b]). Actually this (simplified) approach amounts to a formulation related to an $ox_1x_2x_3$-co-ordinate system travelling along with the given initial velocities V_1, V_2 and without rotation.

Since in (3.51[b,c]) the forcing functions $f_2(t)$ and $f_6(t)$, as acting during the contact between ship and fender, are functions of the displacements of the ship as well as of the deflexion of the fender, (3.48), (3.49), (3.50[a,b]), (3.51[b,c]) and (3.59[a,b]) combined form a closed-loop system; (3.51[b,c]) represents a set of two integro-differential equations. Then, provided the relevant i.r.f. are known, it is possible to determine fender loads and ship trajectories; naturally this can only be done if the fender characteristics are given too.

Two kinds of fenders are considered: a linear fender represented by

$$F_{2f}(t) = \begin{cases} 0 & \text{for} \quad \Delta X_{2f}(t) < 0 \quad , \\ -c_0 \Delta X_{2f}(t) & \text{for} \quad \Delta X_{2f}(t) \geq 0 \quad , \end{cases} \qquad (3.60^{a})$$

and a non-linear fender represented by

$$F_{2f}(t) = \begin{cases} 0 & \text{for} \quad \Delta X_{2f}(t) < 0 \quad , \\ -c_1 \Delta X_{2f}(t) & \text{for} \quad 0 \leq \Delta X_{2f}(t) \leq d_{sc} \quad , \\ -c_1 \Delta X_{2f}(t) - c_2\{\Delta X_{2f}(t) - d_{sc}\} & \text{for} \quad \Delta X_{2f}(t) \geq d_{sc} \quad , \end{cases} \qquad (3.60^{b})$$

where c_0 = spring rate of linear fender,

c_1, c_2 = respective spring rates of the two linear springs which combined form the non-linear fender,

d_{sc} = initial distance (i.e. at rest) between the two linear spring elements of the non-linear fender.

A distinction can be made between two types of berthing operations, viz. berthing operations in which $e_0 = 0$ ('centric impacts') and berthing operations in which $e_0 \neq 0$ ('eccentric impacts').

The combined equations (3.48), (3.49), ($3.50^{a,b}$), ($3.51^{b,c}$) and ($3.59^{a,b}$) with initial values (3.52) and the fender characteristics given by ($3.60^{a,b}$) now have to be solved (numerically).

3.4.2. Numerical solution

The numerical solution is carried through according to the following procedure.

Suppose that the (mathematical) simulation of the berthing of the schematized ship to the jetty has arrived to the point of time t. Δt is the time increment applied, so the set of equations derived above has to be solved for the point of time $t + \Delta t$. First of all the velocities for $t + \Delta t$ are predicted:

$$\dot{\psi}(t+\Delta t) = \dot{\psi}(t) \quad , \quad \dot{X}_{1G}(t+\Delta t) = \dot{X}_{1G}(t) \quad , \quad \dot{X}_{2G}(t+\Delta t) = \dot{X}_{2G}(t) \quad .$$

Subsequently the new orientation and the new position of the ship are determined by numerical integration of the velocities, applying the trapezoidal rule:

$$\psi(t+\Delta t) = \psi(t) + \frac{\dot{\psi}(t) + \dot{\psi}(t+\Delta t)}{2}\,\Delta t \quad ,$$

$$X_{1G}(t+\Delta t) = X_{1G}(t) - \Delta t\,\frac{\dot{x}_2(t) + \dot{x}_2(t+\Delta t)}{2}\,\sin\{\bar{\psi}(t+\Delta t)\} \quad ,$$

$$X_{2G}(t+\Delta t) = X_{2G}(t) + v_A\Delta t + \Delta t\,\frac{\dot{x}_2(t) + \dot{x}_2(t+\Delta t)}{2}\,\cos\{\bar{\psi}(t+\Delta t)\} \quad ,$$

where $\quad \bar{\psi}(t+\Delta t) = \dfrac{\psi(t) + \psi(t+\Delta t)}{2} \quad ,$

representing the mean value of $\psi(t)$ on the interval of time considered. For time $t + \Delta t$ (3.48) then yields the displacement of the fender $\Delta X_{2f}(t+\Delta t)$ and (3.49) and ($3.60^{a,b}$) combined the fender force $F_{2f}(t+\Delta t)$; the resulting force and moment, as acting in and around the ship's centre of gravity G - $f_2(t+\Delta t)$ and $f_6(t+\Delta t)$, respectively- can be predicted by means of ($3.50^{a,b}$). Now the time history of the forcing functions is known until the time $t + \Delta t$; therefore the convolution integrals in (3.51^b) and (3.51^c) can be calculated. The numerical integration of these convolution integrals is carried out by means of the trapezoidal rule, using a time increment equal to the time step Δt. In doing so one obtains new, corrected, values for the relative velocity $\dot{x}_2$ and the angular velocity at $t + \Delta t$. Again $\psi(t+\Delta t)$ is approximated and thereupon -by means of ($3.59^{a,b}$)- $\dot{X}_{1G}(t+\Delta t)$ and $\dot{X}_{2G}(t+\Delta t)$. Finally these three corrected values are compared with the corresponding values predicted at the beginning of the calculation. If the respective differences are acceptable (i.e. in case the predicted and the calculated velocities at $t + \Delta t$ are in satisfactory agreement), the calculation continues for the next time step; if not, the calculation is repeated with the new corrected velocities $\dot{\psi}(t+\Delta t)$, $\dot{X}_{1G}(t+\Delta t)$ and $\dot{X}_{2G}(t+\Delta t)$ (iteration procedure). The criterion for the continuation of the calculation for the next time step is based on the absolute value of the difference between the predicted and the calculated velocities (expressed in $rad.s^{-1}$, c.q. $m\ s^{-1}$): it is assumed that this absolute value has to be smaller than 10^{-7}. The calculation is finished when the ship loses the contact with the fender; this is the case when $\Delta X_{2f}(t+\Delta t)$ becomes zero or negative.
For the case of a berthing operation in which $X_{1f} = - e_0 = 0$ (i.e. a 'centric impact') to a linear fender, a criterion can be derived for the convergence of the computational scheme (see Appendix I), viz.:

$$\Delta t < 2\sqrt{\frac{1}{c_0 k_{22}(0^+)}} \quad . \tag{3.61}$$

3.4.3. <u>Examples of berthing operations: experiment and theory</u>

3.4.3.1. <u>Experimental set-up and model tests</u>

In order to examine the adequacy of the mathematical approach to the simulation of berthing operations as described in Section 3.4.1, an extensive experimental program was carried out. Afterwards typical test situations were selected for the numerical simulation to see whether the observed phenomena could be reproduced by means of the mathematical model.

The experimental study was executed with a schematized ship model berthing to an open jetty fitted with one single fender, in water with respective depths amounting to 1.333 and 1.167 times the draught of the vessel. The schematized ship model and the water depths were the same as described in Section 3.2.2.1. The lay-out of the test set-up and the conditions under which the berthing operations took place, corresponded with the situation as described in Sections 1.3.4 and 3.4.1.

In the experiments the following quantities were measured as functions of the time: the deflexion of the fender (and therefore the fender load), the position of the ship's centre of gravity G and the angle of rotation of the ship's longitudinal plane of symmetry.

The test facility was situated in the middle of a rectangular basin with relatively large, horizontal dimensions -effective length = 33.15 m, effective breadth = 13.95 m- and a horizontal bottom. It consisted of the following principal parts (the numbers refer to fig. 3.16):

1 - the schematized ship model;
2 - the fender;
3 - an open structure, fixed to the bottom of the basin, which acted as support for the fender; the value of e_0 could be varied by moving the fender along the structure (for instance to the places indicated by A, B, C and D);
4 - an open structure, fixed to the bottom of the basin, to fasten the ship in a fixed position when at rest; this fixed position acted as starting-position for the berthing operation;
5 - a facility to give the ship model the proper constant lateral speed of approach;
6 - a 'position follower' to measure the 'X,Y-co-ordinates' of the ship's centre of gravity G;
7 - a facility mounted on the bottom of the ship to measure the angle of rotation of the ship's longitudinal plane of symmetry.

Fig. 3.17^a shows a general view of the test facility.

The longitudinal plane of symmetry of the ship model in its starting-position (i.e. when at rest) coincided with the breadthwise axis of symmetry of the basin. The trajectory of the ship's centre of gravity G before the contact between ship and fender coincided with the lengthwise axis of symmetry of the basin.

The 'position follower' was mounted horizontally on a frame which was adjustable in height. In principle it was a mechanical X/Y-recorder and consisted of a carriage and a routing carrier. The carriage -measuring the motions of G in the 'Y-direction'- moved along two parallel, horizontal shafts, had a span of 0.70 m and could cover a distance of 0.90 m. It was composed of two parallel, horizontal shafts along which the routing carrier could move; the routing carrier measured the motions of G in the 'X-direction' and could cover a distance of 0.60 m. The alignment of the carriage was such that the 'X-' and 'Y-directions' were orthogonal. The direction of motion of the carriage was chosen parallel to the lateral speed of approach of the ship. The 'X-' and 'Y-co-ordinates' were measured by means of two independent string-driven potentiometers of high precision, one for each axis (see figs. 3.18[a] and 3.18[b]). The horizontal motions of the ship's centre of gravity G were transferred to the routing carrier via a shaft. This shaft was connected with the routing carrier in such a way that it -while in upright position- only could move vertically without restraint, and rotation (around its lengthwise axis) with respect to the carrier was impossible. By a universal joint, situated in the plane of the water-line just above the ship's centre of gravity G, this vertically movable, non-rotatable shaft was coupled to a second shaft which coincided with the Gz-axis of the moving, ship-fixed Gxyz-co-ordinate system. This second shaft was by means of a gear-wheel transmission -mounted on the bottom of the ship- connected with a precision potentiometer, by which the angle of rotation of the ship's longitudinal plane of symmetry could be measured. In order to prevent that during a berthing operation too vehement roll motions -if any- yet were transferred to the routing carrier, c.q. carriage, the absolutely vertical shaft (i.e. the upper one) was supported elastically with respect to the sides of the ship (see fig. 3.17[b]). A measuring arrangement of this type implied that the ship model was allowed to heave, to roll and to pitch without any restraint, whereas the motions in the horizontal plane (i.e. translations as well as rotation) could be measured without being influenced. The 'position follower' was constructed as light and rigid as possible. The friction in the moving parts was minimized by applying eminent materials, such as precision ball-bearings, ball-bushing constructions, special extruded and hardened shafts, etc.

According to Section 3.2.2.1 the mass of the ship model, as based on the volume of displacement, amounted to 137.10 kg, whereas the mass for horizontal motions as used in the tests and the calculations, m_{22}, was 137.24 kg. This difference was caused by the presence of the 'position follower' (carriage with routing carrier), which contributed to the (moving) mass of the ship. Otherwise, the contribution of the mass of the 'position follower' to that of the ship model -just as the frictional effects in the moving parts- could be considered as negligible (less than 0.5 per cent., i.e. within the accuracy of the measurements).

To give the ship model the proper constant speed of approach two equal horizontal forces were applied to the fore and aft end of the ship model such that rotational motions did not arise. These forces were exerted by a weight connected to the ship model via lines and pulleys. At the beginning of a test the ship model was released from its starting-position at a distance of about 0.50 m from the fender. Then it was accelerated gradually until the distance to the fender was about 0.10 m, at which moment the weight reached a cantilever. Till the fender was touched the only external force acting on the ship model was the fluid resistance. It appeared that in this phase the lateral speed of approach remained almost constant. The following constant lateral speeds of approach were applied in the tests: circa 0.01 m s^{-1}, 0.02 m s^{-1} and 0.03 m s^{-1}. Their actual values were determined by (numerical) differentiation of the displacement of the ship's centre of gravity G in the 'Y-direction' as measured by the 'position follower'.

Several fenders were used. The elasticity of these fenders was simulated by means of two or more undamped leaf springs, as shown in fig. 3.17^c and fig. 3.17^d. The frictional force between the hull of the ship and the fender was minimized by using a (small) horizontal wheel which was fitted on a precision ball-bearing at the extreme end of the fender. The fender was attached to its supporting structure in such a way that this horizontal wheel was situated in the water surface at rest and the line of action of the fender was perpendicular to the longitudinal plane of symmetry of the ship when approaching laterally. The reaction forces (or strictly speaking the deflexions) of the fender were measured by means of strain-gauge transducers. The own mass of the fender could be neglected with respect to the mass of the ship model. The natural period of the respective fenders was many times smaller than the length of time of their deflexion. The 'centric impacts' were carried out with three linear fenders (c_0= 2146 kg s^{-2}; c_0= 1373 kg s^{-2}; c_0= 576 kg s^{-2}) and with one non-linear fender (c_1= 625 kg s^{-2}, c_2= 1108 kg s^{-2}, d_{sc}= 0.664 * 10^{-2} m). The 'eccentric impacts' were carried out with one linear fender (c_0= 637 kg s^{-2}) for three values of e_0 (e_0= 0.406 m; e_0= 0.813 m; e_0= 1.219 m).

All signals were recorded simultaneously on paper chart.

3.4.3.2. Calculation of berthing operations

For the numerical simulation of the berthing operations those test situations were selected from the experiments, which were in agreement with the conditions and the situation as described in Sections 1.3.4 and 3.4.1. This implied that the calculations were carried out for the same schematized ship (model), for the same constant lateral speeds of approach, for the same water depths, for the same fenders and for the same values of e_0 as in the tests. Since the schematized ship model and the water depths were the same as described in Section 3.2.2.1, in the numerical calculations use could be made of the relevant i.r.f. as determined in Section 3.3.

In the numerical simulation of the berthing operations the following quantities were calculated as functions of the time (see also fig. 3.14):
the rotational velocity of the ship, $\dot{x}_6(t) = \dot{\psi}(t)$;
the velocity components of the ship's centre of gravity G, $\dot{X}_{1G}(t)$ and $\dot{X}_{2G}(t)$;
the co-ordinates of the ship's centre of gravity G, $X_{1G}(t)$ and $X_{2G}(t)$;
the angle of rotation of the ship's longitudinal axis of symmetry around the OX_3-axis, $x_6(t) = \psi(t)$;
the deflexion of the fender, $\Delta X_{2f}(t)$;
the reaction force in the fender, $F_{2f}(t)$;
in the relevant cases these quantities were determined only for the length of time, during which there was contact between ship and fender.

The results of the calculations showed that generally $X_{1G}(t)$ was very small with respect to $X_{2G}(t)$; in all cases considered $X_{1G}(t)$ remained smaller than $0.4 * 10^{-3}$ m. Besides, the values of $X_{1G}(t)$ as determined experimentally fell within the accuracy of the measurements. For these reasons $X_{1G}(t)$ further is left out of consideration. Otherwise, from a (rough) estimation of the rotational influences as formally introduced in Section 3.4.1, it appeared that these -when fully taken into account- indeed can be neglected as being second-order effects, at least for the berthing situation under consideration.
Fluid reactive forces from viscous origin have been neglected. The greatest influence can be expected in the sway mode of motion. An estimate of these forces was made by using the empirical formula:

$$F_{2,viscous} = -\frac{1}{2}\rho C_D \, LD \, \dot{X}_{2G}|\dot{X}_{2G}| \quad ,$$

where $F_{2,viscous}$ = fluid reactive force on the ship from viscous origin in the sway mode of motion,

C_D = drag coefficient.

Inclusion of this force in the mathematical model for berthing situations without rotation did not change the results significantly.

According to criterion (3.61) yielding a condition for the convergence of the computational scheme in case of a 'centric impact' against a linear fender, the time step of the calculations, Δt, -for the situations considered- has to be smaller than 0.4 s. On the one side the computing time roughly is linearly proportional to the inverse of the time step Δt. On the other hand, systematic calculations with varying time step have shown that the accuracy of the calculations decreases with increasing values of Δt. To arrive at an accuracy as great as possible all calculations were carried out with a time step Δt = 0.01 s.

Using a long-wave approximation for the motion of the water, the expressions describing the berthing of the schematized ship (model) to a linear fender can be derived analytically (see Appendix J).

3.4.4. Presentation of results

3.4.4.1. General remarks

Merely the most representative results of the tests are given together with the corresponding results of the calculations.

Since the berthing operation can be described completely by the reaction force in the fender and the position and orientation of the (schematized) ship during its contact with it, in the following only $F_{2f}(t)$, $X_{2G}(t)$ and $\psi(t)$ are considered. In order to bring about a 'collapse of data' these quantities are represented in dimensionless form by

$\dfrac{F_{2f}}{v_A\sqrt{c_0 M_0}}$ = dimensionless reaction force in the (linear) fender,

$\dfrac{X_{2G}}{v_A}\sqrt{\dfrac{c_0}{M_0}}$ = dimensionless translation of the ship's centre of gravity G during the contact between ship and (linear) fender,

$\dfrac{\psi m_{66}}{v_A e_0 M_0}\sqrt{\dfrac{c_0}{M_0}}$ = dimensionless angle of rotation of the ship's longitudinal axis of symmetry during the contact between ship and (linear) fender, where $$\frac{1}{M_0} = \frac{e_0^2}{m_{66}} + \frac{1}{\rho LBD} \quad ;$$

M_0 has to be interpreted as the reduced or effective mass of the ship (model) for horizontal motion. The results are presented as functions of the dimensionless time

$$t\sqrt{\frac{c_0}{M_0}} \quad .$$

The respective expressions with which $F_{2f}(t)$, $X_{2G}(t)$, $\psi(t)$ and t are made dimensionless can be determined analytically by solving the problem of the schematized ship berthing to a linear fender, for the case of motion in an ideal medium to the neglect of the hydrodynamic effects.
The dimensionless representation above applies to the case of the ship berthing to a linear fender. For berthing to the non-linear fender c_0 has to be replaced by c_1.
The parameters which further play a part in the presentation of the experimental and theoretical results are the (dimensionless) water depth, the (dimensionless) characteristics of the fender, the (dimensionless) initial distance of the line of action of the fender to the ship's centre of gravity G and -for the tests- the (dimensionless) constant lateral speed of approach.

In addition to the experimental results which are plotted as centred symbols, the figures to be presented each show three curves representing the theoretical results (see also Sections 3.3.2 and 3.3.3):

- the dot-and-dash line represents the results as calculated by means of i.r.f. which have to be considered as two-dimensional;
- the full line represents the results as calculated by means of i.r.f. which can be considered as three-dimensional;
- the broken line represents the results as determined (analytically) by making use of a long-wave approximation for the motion of the water (see Appendix J); these results are basically one-dimensional.

Therefore, the theoretical results as given by the broken lines and the dot-and-dash lines have to be considered as one-dimensional and two-dimensional, respectively, whereas the theoretical results as given by the full lines have to be considered as three-dimensional.

Successively now berthing operations are considered in which $e_0 = 0$ (i.e. 'centric impacts') and berthing operations in which $e_0 \neq 0$ (i.e. 'eccentric impacts').

3.4.4.2. Centric impacts

Since in case of a 'centric impact' $\psi(t) = 0$, $X_{2G}(t) = \Delta X_{2f}(t)$ and $F_{2f}(t) = f(\Delta X_{2f})$, it suffices to present only the results for $F_{2f}(t)$.

Figs. 3.19 through 3.24 show $F_{2f}v_A^{-1}(c_0M_0)^{-1/2}$ versus $t(c_0/M_0)^{1/2}$ for the case of a linear fender, with the dimensionless water depth h/D and the dimensionless fender characteristic $c_0(\rho g D^2)^{-1}$ as parameters. As could be expected, the calculated fender forces are proportional to the constant lateral speed of approach. Further it can be seen from these figures that in case of increasing fender stiffness the (maximum value of the) fender force also increases, whereas the length of time of the contact between ship and fender decreases and the point of time at which the fender force reaches its maximum occurs earlier. In case of a larger water depth -at constant fender stiffness- the (maximum value of the) fender force as well as the length of time of the contact between ship and fender is smaller, while the point of time at which the fender force reaches its maximum occurs earlier.

Figs. 3.25 through 3.28 show $F_{2f}v_A^{-1}(c_1M_0)^{-1/2}$ versus $t(c_1/M_0)^{1/2}$ for the case of the non-linear fender, with the dimensionless water depth and the dimensionless constant lateral speed of approach, $v_A(gh)^{-1/2}$, as parameters. The dimensionless fender characteristics are represented by $c_1(\rho g D^2)^{-1}$, c_1/c_2 and d_{sc}/B. From figs. 3.25 through 3.28 it appears that a larger lateral speed of approach causes an increase of the (maximum value of the) fender force and a decrease of the length of time of the contact between ship and fender; likewise, the point of time at which the fender force reaches its maximum occurs earlier in case of a larger lateral speed of approach. Further, in case of increasing water depth the (maximum value of the) fender force as well as the length of time of the contact between ship and fender decreases, while the point of time at which the fender force reaches its maximum occurs earlier.

The total amount of energy E absorbed by a fender with linear behaviour is given by

$$E = \int_0^{(\Delta X_{2f})_{max}} F_{2f}(t)\, d(\Delta X_{2f}) = \tfrac{1}{2}c_0(\Delta X_{2f})^2_{max} \qquad ,$$

where $(\Delta X_{2f})_{max}$ = maximum deflexion of the (linear) fender.

By means of this expression the influence of the fender stiffness in case of a linear fender on the absorption of energy can be represented. However, problems arise when the fender is infinitely stiff (i.e. $c_0 \to \infty$) and when the fender is infinitely soft (i.e. $c_0 = 0$). The kinetic energy of the schematized ship at the first moment of contact between ship and fender in case of a constant lateral speed of approach v_A -this implies $\omega = 0$- is:

$$\frac{1}{2}\{\rho LBD + a_{22}(0)\}v_A^2 \quad .$$

In case $c_0 \to \infty$, the total kinetic energy of the schematized ship is transferred -during the impact- to the '(linear) fender' in a length of time $\Delta t = 0$; the hydrodynamic damping then can be neglected. As small lengths of time correspond with high (circular) frequencies -i.e. $\omega = \infty$ is predominant-, the total amount of energy absorbed by the '(linear) fender' in case $c_0 \to \infty$ becomes:

$$\frac{1}{2}c_0(\Delta X_{2f})^2_{max} \longrightarrow \frac{1}{2}\{\rho LBD + a_{22}(\infty)\}v_A^2 \qquad \text{for } c_0 \to \infty \quad .$$

In case $c_0 = 0$ the presence of the fender is not palpable. During the 'impact' the kinetic energy of the schematized ship is transferred to the '(linear) fender' in a length of time $\Delta t \to \infty$; the hydrodynamic damping does not play any part since the lateral speed of the ship does not change: v_A is maintained. The energy 'absorbed by the (linear) fender' equals the kinetic energy of the ship at the first moment of 'contact' between ship and fender, and becomes:

$$\frac{1}{2}c_0(\Delta X_{2f})^2_{max} \longrightarrow \frac{1}{2}\{\rho LBD + a_{22}(0)\}v_A^2 \qquad \text{for } c_0 \downarrow 0.$$

Figs. 3.29 and 3.30 show the dimensionless absorbed energy, $c_0(\Delta X_{2f})^2_{max}(\rho LBD)^{-1}v_A^{-2}$, versus the dimensionless fender characteristic $c_0(\rho g D^2)^{-1}$, with the dimensionless water depth h/D as parameter. In these figures the total amount of absorbed energy, $\frac{1}{2}c_0(\Delta X_{2f})^2_{max}$, was made dimensionless with the kinetic energy as possessed by the schematized ship before and during the first contact between ship and fender in case of the absence of water, viz. $\frac{1}{2}\rho LBDv_A^2$. From figs. 3.29 and 3.30 it can be seen that -at constant water depth- a stiff fender absorbs less energy to stop the ship than a soft fender. This effect is caused by the greater wave radiation in case of a stiffer fender. Further, in case of a smaller water depth the total amount of energy as absorbed by the (linear) fender increases.

3.4.4.3. Eccentric impacts

In case of an 'eccentric impact' the results for $F_{2f}(t)$ as well as the results for $X_{2G}(t)$ and $\psi(t)$ have to be presented.

Figs. 3.31 through 3.38 show $F_{2f}v_A^{-1}(c_0M_0)^{-1/2}$, $X_{2G}v_A^{-1}(c_0/M_0)^{1/2}$ and $\psi m_{66}(v_Ae_0M_0)^{-1}(c_0/M_0)^{1/2}$ versus $t(c_0/M_0)^{1/2}$ for the case of one linear fender, with the dimensionless water depth and the dimensionless initial distance of the line of action of the fender to the ship's centre of gravity, e_0/L, as parameters. Although for the case $e_0 = 0$ experimental results are not available, for the sake of completeness the calculated results are presented (figs. 3.31 and 3.32). As expected the calculated fender forces, translations of the ship's centre of gravity G and angles of rotation of the ship's longitudinal axis of symmetry can be considered to be proportional to the constant lateral speed of approach.

From figs. 3.31 through 3.38 it can be seen that in case of increasing value of e_0 the (maximum value of the) fender force as well as the length of time of the contact between ship and fender decreases, while the point of time at which the fender force reaches its maximum occurs earlier. This general trend does not apply to the length of time of the contact between ship and fender as calculated by means of the two-dimensional theory for the case with e_0/L = 0.500 and h/D = 1.167. Further, in case of a larger water depth the (maximum value of the) fender force as well as the length of time of the contact between ship and fender is smaller, and the point of time at which the fender force reaches its maximum value occurs earlier. Froms figs. 3.31 through 3.38 it also appears that in case of a larger water depth the maximum value of the translation of the ship's centre of gravity G as well as the total angle of rotation of the ship's longitudinal axis of symmetry is smaller; mainly this is due to the influence of the shorter length of time of the contact between ship and fender.

In case of increasing value of e_0 it is not possible to describe in general terms the trend of the maximum value of the translation of G and the total angle of rotation of the ship's longitudinal axis of symmetry: this is a consequence of the fact that the values of these both quantities are influenced by the length of time of the contact between ship and fender. So far as the maximum value of the translation of the ship's centre of gravity G is concerned, the results as calculated by means of the long-wave approximation and the theory adapted to the three-dimensional situation show -for both water depths- the same trend. Further, all calculated results for the total angle of

rotation of the ship's longitudinal axis of symmetry show the same features, for both water depths; the result calculated by means of the two-dimensional theory for the case with $e_0/L = 0.500$ and $h/D = 1.167$ has to be excluded.
The test results for $\psi(t)$ at the smallest speed of approach may show (locally) some discrepancies with respect to the test results at the higher speeds of approach. This is caused by the relative weak signals combined with tolerance(s) in the gear-wheel transmission which transfers the angle of rotation of the ship's longitudinal plane of symmetry to the recording potentiometer. These tolerances have a greater influence on the measured results as the signals are weaker.

3.5. Discussion and conclusions

3.5.1. Qualitative analysis of results

With regard to the simulation of ship berthing to an open fender structure the (quantitative) agreement between the results of mathematical approach and physical model appears to be very reasonable. Yet some discrepancies remain. On the one side these differences are produced by experimental imperfections, on the other hand they are due to the restrictions of the mathematical formulation.

The experimental errors may have the undermentioned origins:

- imperfections of the experimental set-up, such as
  - . the restricted horizontal dimensions of the rectangular basin in which the model tests were carried out;
  - . small deviations from the horizontal position of that part of the bottom of the basin covered by the motions of the ship model;
  - . frictional effects between ship model and fender in case of berthing with an initial eccentricity, actually intended to be absent;
  - . flexibility of the fender support;
  - . a transverse speed of approach of the ship model which is not exactly a constant (at the moment of first contact between ship and fender);
  - . the possibility that the line of action of the fender is not precisely perpendicular to the longitudinal axis of symmetry of the ship at its first contact with the fender;
  - . deviations from the intended values of the initial 'eccentricity' in case of centric as well as eccentric impacts;
  - . dynamic effects, damping, friction and tolerances in both the 'position

follower' and the facility to measure the angle of rotation of the ship's longitudinal plane of symmetry;

- measuring errors resulting from the limited accuracy of the electronic measuring and recording equipment;
- evaluation errors due to the process of converting analogue signals recorded on paper chart into proper figures.

The magnitude of this first category of errors is hard to estimate, but the total effect of measuring and evaluation inaccuracies is valued at amply less than five per cent. An exception to this is formed by the error in measuring the angle of rotation, which may go up to five per cent. due to the mechanical imperfections of the relevant measuring device.

Concerning the accuracy of the mathematical description the following can be observed.

- The i.r.f.-technique applied is based on the concept that the ship-fluid system is linear. The (experimental) investigations indicate that this basic linearity-assumption is a well-working approximation in case of small to moderate transient displacements of the (schematized) ship (model).
- In a general sense mention can be made of the application of the strip theory and the neglect of both the diffraction phenomena and the flow around 'bow' and 'stern' of the ship. In this respect it is to be expected that a general three-dimensional determination of the hydrodynamic coefficients -especially in the lower-frequency range- yields a better agreement between theory and experiment.

Comparison of experimental results with results as calculated on the one side by means of the two-dimensional theory and on the other hand by means of the theory adapted to the three-dimensional situation indeed shows that the accuracy of the hydrodynamic coefficients in the lower-frequency range may be an important factor. Nevertheless, fairly large differences in the hydrodynamic coefficients at lower frequencies may occur without the result of a too significant change in the (maximum value of the) fender force, the point of time at which the fender force reaches its maximum, the length of time of the contact between ship and fender, the translation of the ship's centre of gravity and the angle of rotation of the ship's longitudinal axis of symmetry.
The two-dimensional theory and the long-wave approximation yield lengths of time of contact between ship and fender being systematically too large; in this context the long-wave approximation presents a better prediction than the two-dimensional approach. One thing and another can be explained from the re-

spective accuracies with which the hydrodynamic coefficients in the lower-frequency range are determined.

- Certain approximations are involved in the numerical calculation of the hydrodynamic coefficients, the i.r.f. and the mathematical simulation of the berthing operations, affecting in principle the accuracy of the results.
- A mathematical approach using the i.r.f.-technique is only appropriate to describe transient ship motions and does certainly not apply to (nearly) steady motions. In the latter case the (non-)linear viscous effects are not any longer negligibly small, and they may change the picture entirely.

3.5.2. Conclusions

Generally it can be stated that the agreement between theory and experiment is satisfactory. Notably by means of the theory adapted to the three-dimensional situation the (maximum values of the) fender forces as well as the lengths of time of the contact between ship and fender, and the points of time at which the fender forces reach their maxima are predicted well. The same holds good with respect to the maximum values of the translation of the ship's centre of gravity and the total angles of rotation of the ship's longitudinal axis of symmetry. This applies for both water depths investigated.

For a first estimate of the maximum value of the fender force use can be made of the long-wave approximation or -with less accuracy- of the two-dimensional theory. The same holds in case of a first valuation of the points of time at which the fender forces reach their maxima. Generally the two-dimensional theory does not provide a proper prediction of the length of time of the contact between ship and fender; the same applies with respect to the long-wave approximation in case of a centric impact at the smaller water depth. Further, in case of an eccentric impact, by means of the long-wave approximation a rather reliable estimate can be made of the maximum value of the translation of the ship's centre of gravity as well as of the total angle of rotation of its longitudinal axis of symmetry.

For both water depths considered, underkeel friction is of secondary importance.

Viscous effects have not been taken into account. Since in model tests these effects are overestimated, it may be concluded from the good agreement between calculated and measured results that the viscosity of the fluid does not influence the relevant quantities which play a part in berthing.

The experimental and theoretical results demonstrate that the mathematical approach presented provides a good foundation for the description and the determination of the relevant quantities which figure in the problem of a ship berthing to some open structure fitted with linear or non-linear fenders.

4. SHIP BERTHING TO A CLOSED FENDER STRUCTURE

4.1. Introduction

In this section a mathematical model is presented that aims to describe the behaviour of a ship berthing to a closed fender structure and the prediction of the fender forces.

For the assumptions and simplifications made it is referred to Section 1.3.4. On account of the results for the open berth (see Section 3.4.4) the idealization of the berthing situation under consideration, with merely centric impacts, is supposed to lead to conservative fender forces.

In order to determine the fender loads as a result of ship berthing also in this specific situation a time-domain description of the moving ship is needed which makes allowance for the frequency dependence of the fluid reactive forces. To this end a set of governing equations is formulated describing the transverse (i.e. sway) motion of the schematized ship in shallow water at zero forward speed, alongside of and parallel to a vertical wall. Nonlinearities in the displacement of the ship, vertical acceleration of the water particles in the fluid domain between ship and quay-wall (i.e. the quay clearance), and fluid friction and flow separation in the underkeel region are taken into account. As during berthing manoeuvres low frequencies (are supposed to) play a dominant part, a long-wave approximation for the motion of the water is applied to the fluid domain situated at that side of the ship not facing the quay-wall.

To solve the governing equations two separate procedures are followed. The first approach, requiring a linearization, makes use of the i.r.f.-technique as dealt with in Section 2 and already applied to the case of a ship berthing to an open fender structure (see Section 3). In this context yet some remarks have to be made. On account of the linearity concept formally small disturbances were considered from an initial state of equilibrium represented by the uniform transverse motion of the approaching ship, the i.r.f. being determined with respect to this steady state. For the case under consideration this implies not only that during a berthing operation -as distinct from the situation with an open berth- it has to be doubted whether the initial steady state of motion can be maintained without exerting external forces, but also that the i.r.f. in fact becomes a function of the clearance between ship and quay-wall. Since this might lead to an ambiguous and, at least, complicated situation, the i.r.f.-technique now is going to be applied on the understanding that for a certain berthing operation an i.r.f. is used based on the (fixed) initial quay clearance as occurring at the moment of first contact between ship and fender. The underlying suppositions are that the motion of the ship during its contact with the fender is considered to be a disturbance from a state of rest and that its displacement remains small with respect to the initial quay clearance. The hydrodynamic coefficients for the swaying motion are determined theoretically as well as experimentally at zero forward and transverse speed (i.e. $V_1,V_2 = 0$). Thereupon the corresponding i.r.f. can be calculated. Just as in Section 3, it is hereby assumed implicitly that in berthing the (transverse) velocity of the ship remains so small that it does not affect the hydrodynamic coefficients and a restoring force is not generated. The berthing of the schematized ship to the closed fender structure then can be simulated -apart from the rotation- in a similar way as done in case of the open fender structure, and the relevant related quantities can be determined.

In the second procedure, being a direct-time approach, the influences of the respective non-linearities can be evaluated. The governing equations then are simplified to a two-dimensional situation (strip theory) and solved directly in the time domain.

To examine the adequacy of the theoretical simulation of berthing operations in case of a closed fender structure, again an extensive series of (model) experiments was carried out. Typical test situations are selected for the numerical simulation in order to see whether and to what extent the observed phenomena are reproduced by means of the two respective approaches to solve the governing equations: theoretical results are compared with the results from experiments and discussed.

4.2. Mathematical formulation of hydrodynamic model

4.2.1. Governing equations

The ship motion is regarded with respect to the $ox_1x_2x_3$-co-ordinate system, which -until further notice- is taken to be space fixed. In accordance with Section 2.2, ox_1x_2 and Gxy are situated in the water surface at rest; the ox_3- and Gz-axes are positive upwards. The coinciding ox_2- and Gy-axes are at right angles to the vertical wall and positive outwards. The origin o lies at $d_{sq}+ \frac{1}{2}B$ in front of the wall, where d_{sq} is the distance c.q. clearance between

ship and wall when G coincides with o. In rest and during motion the keel clearance of the ship remains constant. The sway-motion variable of the ship again is represented by $x_2(t)$. The fluid velocities in the x_1-, x_2- and x_3-direction are u, v and w, respectively. ζ stands for the elevation of the water surface and η for the height of a long wave, both with respect to the water depth at rest. The fluid domain can be divided into four regions: the subscripts a, b, c and d indicate that the dependent variables concerned must be related to these respective regions.
For a definition sketch see fig. 4.1.

For region a, representing the quay clearance, it is supposed that $d_{sq} + x_2 << \frac{1}{2}L$ and $d_{sq} + x_2 << D$. The pressure gradients or accelerations acting in the x_1- and x_3-direction can now be considered as large in comparison with the corresponding quantities in the x_2-direction. This implies a uniform velocity distribution along the x_2-direction.
The law of conservation of mass as applied to region a then reads

$$\frac{\partial u_a}{\partial x_1} + \frac{\partial w_a}{\partial x_3} + \frac{\dot{x}_2}{d_{sq} + x_2} = 0 \qquad , \qquad (4.1^a)$$

where $u_a = u_a(x_1,x_3,t) =$ fluid velocity in x_1-direction in region a,
$w_a = w_a(x_1,x_3,t) =$ fluid velocity in x_3-direction in region a.
Application of the law of conservation of momentum in the x_1-direction to region a yields

$$\frac{\partial u_a}{\partial t} + \frac{\partial (u_a^2)}{\partial x_1} + \frac{\partial (u_a w_a)}{\partial x_3} + \frac{\dot{x}_2 u_a}{d_{sq} + x_2} + \frac{1}{\rho}\frac{\partial p_a}{\partial x_1} = 0 \qquad , \qquad (4.2)$$

where $p_a = p_a(x_1,x_3,t) =$ fluid pressure in region a.
Combination of (4.1^a) and (4.2) in order to eliminate $\dot{x}_2$ results in the equation of motion in the x_1-direction for region a:

$$\frac{\partial u_a}{\partial t} + u_a \frac{\partial u_a}{\partial x_1} + w_a \frac{\partial u_a}{\partial x_3} + \frac{1}{\rho}\frac{\partial p_a}{\partial x_1} = 0 \qquad ; \qquad (4.3^a)$$

with $\quad u_a \dfrac{\partial u_a}{\partial x_1} << \dfrac{\partial u_a}{\partial t} \quad$ and $\quad w_a \dfrac{\partial u_a}{\partial x_3} << \dfrac{\partial u_a}{\partial t}$

this expression becomes

$$\frac{\partial u_a}{\partial t} + \frac{1}{\rho}\frac{\partial p_a}{\partial x_1} = 0 \quad . \tag{4.3^b}$$

The law of conservation of momentum in the x_3-direction for region a can be represented by

$$\frac{\partial w_a}{\partial t} + \frac{\partial(u_a w_a)}{\partial x_1} + \frac{\partial(w_a^2)}{\partial x_3} + \frac{w_a \dot{x}_2}{d_{sq} + x_2} + g + \frac{1}{\rho}\frac{\partial p_a}{\partial x_3} = 0 \quad . \tag{4.4}$$

Elimination of $\dot{x}_2$ from (4.1^a) and (4.4) yields the equation of motion in the x_3-direction for region a:

$$\frac{\partial w_a}{\partial t} + u_a \frac{\partial w_a}{\partial x_1} + w_a \frac{\partial w_a}{\partial x_3} + g + \frac{1}{\rho}\frac{\partial p_a}{\partial x_3} = 0 \quad ; \tag{4.5^a}$$

with $\quad u_a \dfrac{\partial w_a}{\partial x_1} << \dfrac{\partial w_a}{\partial t} \quad$ and $\quad w_a \dfrac{\partial w_a}{\partial x_3} << \dfrac{\partial w_a}{\partial t}$

(4.5^a) takes the form

$$\frac{\partial w_a}{\partial t} + \frac{1}{\rho}\frac{\partial p_a}{\partial x_3} + g = 0 \quad . \tag{4.5^b}$$

A further simplification is carried through by averaging the horizontal velocity u_a over the depth according to

$$(D+\zeta_a)\bar{u}_a = \int_{-D}^{\zeta_a} u_a dx_3 \quad ,$$

where $\bar{u}_a = \bar{u}_a(x_1,t)$ = depth-averaged fluid velocity in x_1-direction in region a,

$\zeta_a = \zeta_a(x_1,t)$ = elevation of water surface in region a with respect to mean water level;

a bar over a quantity means 'average value of'. Using Leibniz' rule (4.1^a) then can be rewritten as

$$\frac{\partial \bar{u}_a}{\partial x_1} + \frac{\partial w_a}{\partial x_3} + \frac{\dot{x}_2}{d_{sq} + x_2} = 0 \qquad (4.1^b)$$

and (4.3^b) as

$$\frac{\partial \bar{u}_a}{\partial t} + \frac{1}{\rho D} \int_{-D}^{\zeta_a} \frac{\partial p_a}{\partial x_1} dx_3 = 0 \quad ; \qquad (4.3^c)$$

in deriving (4.1^b) and (4.3^c) it is assumed that

$$\bar{u}_a \frac{\partial \zeta_a}{\partial x_1} << (D+\zeta_a) \frac{\partial \bar{u}_a}{\partial x_1} \quad , \quad u_a(x_1,\zeta_a,t) \frac{\partial \zeta_a}{\partial x_1} << (D+\zeta_a) \frac{\partial \bar{u}_a}{\partial x_1}$$

and

$$\bar{u}_a \frac{\partial \zeta_a}{\partial t} << (D+\zeta_a) \frac{\partial \bar{u}_a}{\partial t} \quad , \quad u_a(x_1,\zeta_a,t) \frac{\partial \zeta_a}{\partial t} << (D+\zeta_a) \frac{\partial \bar{u}_a}{\partial t} \quad , \quad \zeta_a << D \quad ,$$

respectively.

It can be stated now that, apart from the initial values and the boundary conditions, the motion of the fluid in the quay clearance is described by (4.1^b), (4.3^c) and (4.5^b) combined. With respect to these expressions it holds that in a general sense only small values of u_a, $\bar{u}_a$, w_a, ζ_a and their derivatives have been considered. In the following the same line is taken.

For reasons of symmetry the boundary condition for region a at $x_1 = 0$ reads as

$$\bar{u}_a(x_1,t)\Big|_{x_1=0} = 0 \quad . \qquad (4.6^a)$$

As boundary condition for region a at $x_1 = \pm \frac{1}{2}L$ it is taken:

$$\zeta_a(x_1,t)\Big|_{x_1=\pm\frac{1}{2}L} = 0 \quad . \qquad (4.6^b)$$

The boundary condition for the vertical velocity at the free water-surface in the quay clearance has the form

$$w_a(x_1,x_3,t)\Big|_{x_3=\zeta_a} = \frac{\partial \zeta_a}{\partial t} + \bar{u}_a \frac{\partial \zeta_a}{\partial x_1} \quad ;$$

with $\bar{u}_a \dfrac{\partial\zeta_a}{\partial x_1} << \dfrac{\partial\zeta_a}{\partial t}$

this expression becomes

$$w_a(x_1,x_3,t)\Big|_{x_3=\zeta_a} = \frac{\partial\zeta_a}{\partial t} \quad . \tag{4.6^c}$$

The boundary condition for the fluid pressure at the free water-surface in region a can be written as:

$$p_a(x_1,x_3,t)\Big|_{x_3=\zeta_a} = 0 \quad . \tag{4.6^d}$$

Concerning the underkeel region b it is assumed $B << L$ and $h-D << B$. Pressure gradients or accelerations in the x_2-direction then being large as compared with the corresponding quantities in the x_1- and x_3-direction, this leads to $u_b = w_b = 0$, a hydrostatic pressure and a uniform velocity distribution over the height. The quantities u_b and w_b represent the respective fluid velocities in x_1- and x_3-direction in the underkeel region.
Suppressing until further notice friction effects and flow separation, the equation of motion in the x_2-direction for the keel clearance then reads as

$$\frac{\partial v_b}{\partial t} + \frac{1}{\rho}\frac{\partial p_b}{\partial x_2} = 0 \quad , \tag{4.7^a}$$

where $v_b = v_b(x_1,x_3,t)$,
$p_b = p_b(x_1,x_2,x_3,t)$ = fluid pressure in region b.
Averaging the horizontal velocity v_b over the height h-D according to

$$(h-D)\bar{v}_b = \int_{-h}^{-D} v_b dx_3 \quad ,$$

in which $\bar{v}_b = \bar{v}_b(x_1,t)$ = height-averaged fluid velocity in x_2-direction in region b,
(4.7^a) takes the form

$$(h-D)\frac{\partial\bar{v}_b}{\partial t} + \frac{1}{\rho}\int_{-h}^{-D}\frac{\partial p_b}{\partial x_2}dx_3 = 0 \quad . \tag{4.7^b}$$

From the equation of motion in the x_3-direction in region b it follows directly that the pressure distribution is hydrostatic, i.e.

$$p_b(x_1,x_2,x_3,t) = -\rho g x_3 + p_b^{(1)}(x_1,x_2,t) \quad , \tag{4.8}$$

where $p_b^{(1)}(x_1,x_2,t)$ = fluctuating part of fluid pressure in region b; the superscript (1) indicates that the quantity concerned represents the fluctuating part of its original. Substitution of p_b into (4.7^b) and successive integration with respect to x_2 over the interval $[-\frac{1}{2}B + x_2 \ , \ \frac{1}{2}B + x_2]$ yields

$$\rho B \frac{\partial \bar{v}_b}{\partial t} + p_b^{(1)}(x_1,\tfrac{1}{2}B+x_2,t) - p_b^{(1)}(x_1,-\tfrac{1}{2}B+x_2,t) = 0 \quad . \tag{4.7^c}$$

Since

$$p_b^{(1)}(x_1,\tfrac{1}{2}B+x_2,t) = \rho g(D + \eta_c) - \rho g D = \rho g \eta_c$$

and

$$p_b^{(1)}(x_1,-\tfrac{1}{2}B+x_2,t) = p_a(x_1,-D,t) - \rho g D \quad ,$$

in which $\eta_c = \eta_c(x_1,t)$,
(4.7^c) now can be written as:

$$B \frac{\partial \bar{v}_b}{\partial t} = -g(\eta_c + D) + \frac{1}{\rho} p_a(x_1,-D,t) \quad . \tag{4.7^d}$$

According to Section 3.2.1.3, the total friction force in the x_2-direction per unit length of the ship as acting on the fluid in region b in case of laminar flow has the form

$$-2\gamma B(\bar{v}_b - \tfrac{1}{2}\dot{x}_2) = -\alpha_1 \frac{\rho g(h-D)}{c_w} B\,(\bar{v}_b - \tfrac{1}{2}\dot{x}_2) \quad , \quad c_w = \sqrt{gh} \quad ,$$

with

$$\alpha_1 = \frac{2\gamma c_w}{\rho g(h-D)} \quad ; \tag{4.9}$$

in this α_l = dimensionless friction coefficient relating to laminar flow in the x_2-direction in region b;

the subscript l indicates that the quantity concerned must be related to a laminar flow regime. In case of turbulent flow in the keel clearance the total friction force in the x_2-direction per unit length of the ship as acting on the fluid in region b can be written as:

$$-(\tau_{2,b}\big|_{ship} + \tau_{2,b}\big|_{bottom})\ B$$

with

$$\tau_{2,b}\big|_{ship} = \alpha_t \rho(\bar{v}_b - \dot{x}_2)|\bar{v}_b - \dot{x}_2| \quad ,$$

$$\tau_{2,b}\big|_{bottom} = \alpha_t \rho\ \bar{v}_b|\bar{v}_b| \quad ,$$

where α_t = dimensionless friction coefficient relating to turbulent flow in the x_2-direction in region b;

the subscript t is used to indicate a turbulent flow regime. The friction effect in the underkeel region then is taken into account by extending the right-hand side of (4.7^d) with a term $-R_{2,b}(x_1,t)$, where

$$R_{2,b}(x_1,t) = \alpha_l \frac{Bg}{c_w}(\bar{v}_b - \frac{1}{2}\dot{x}_2) \quad \text{for laminar flow} \quad , \qquad (4.10^a)$$

$$R_{2,b}(x_1,t) = \alpha_t \frac{B}{h-D}\{(\bar{v}_b - \dot{x}_2)|\bar{v}_b - \dot{x}_2| + \bar{v}_b|\bar{v}_b|\} \quad \text{for turbulent flow,} \qquad (4.10^b)$$

respectively. With respect to (4.10^b) it can be remarked that using Blasius' law the following generalization can be put through (see ref. [100]): in case of (steady) laminar flow in the underkeel region α_t can be represented by

$$\alpha_t = \frac{12}{Re} \quad , \quad Re \leq 2300 \qquad (4.11^a)$$

and in case of (steady) turbulent flow by

$$\alpha_t = \frac{1}{8}\frac{0.3164}{Re^{1/4}} \quad , \quad 2300 < Re < 10^6 \quad , \qquad (4.11^b)$$

where the Reynolds number Re is defined as

$$Re = \frac{2|\bar{v}_b|(h-D)}{\nu} \quad ; \tag{4.12}$$

(4.11^a) corresponds with the expression for γ as given by (3.20^b).
The loss of energy in region b due to the abrupt contraction of the flow at the entrance and the sudden expansion at the outlet can be taken into account by adding the term $-gH_{2,b}(x_1,t)$ to the right-hand side of (4.7^d), with

$$H_{2,b}(x_1,t) = \lambda_b \frac{(\bar{v}_b - \dot{x}_2)|\bar{v}_b - \dot{x}_2|}{2g} \quad , \tag{4.13}$$

$$\lambda_b = \xi_{b,e} + \xi_{b,o} \quad , \quad \xi_{b,e} = \left(\frac{1}{\mu} - 1\right)^2 \quad , \tag{4.14^a}$$

where $H_{2,b}(x_1,t)$ = loss of energy head in region b due to contraction and separation of flow in x_2-direction,

λ_b = general head-loss coefficient referring to contraction and flow separation in region b,

$\xi_{b,e}$ = head-loss coefficient in region b due to abrupt contraction at entrance,

$\xi_{b,o}$ = head-loss coefficient in region b due to sudden expansion at outlet,

μ = contraction coefficient;

the added subscripts e and o are used to indicate entrance and outlet, respectively. With μ = 0.611 (applying to very sharp edges, see ref. [98]) and $\xi_{b,o}$ = 1 (Borda-Carnot approach) λ_b is calculated to be

$$\lambda_b = 1.44 \quad . \tag{4.14^b}$$

With the two extra terms as stated above the equation of motion in the x_2-direction for the underkeel region eventually takes the form:

$$B \frac{\partial \bar{v}_b}{\partial t} = -g(\eta_c + D) + \frac{1}{\rho} p_a(x_1,-D,t) - R_{2,b}(x_1,t) - gH_{2,b}(x_1,t) \quad , \tag{4.7^e}$$

in which $R_{2,b}(x_1,t)$ is given by (4.10^a) and (4.10^b), respectively, and $H_{2,b}(x_1,t)$ by (4.13). As the underkeel flow in principle can be laminar or turbulent, two expressions for $R_{2,b}(x_1,t)$ have been introduced (with the comment that under full-scale conditions the occurrence of a laminar flow regime is not very likely). Apart from the type of underkeel flow, the transient ship motion in berthing suggests the existence of a relatively thin boundary layer with large velocity gradients. This implies that application of a steady-state friction law has to be considered with some reserve.

Region d, forming a transition between the regions a and b, is supposed to be small with respect to these domains, which results in a hydrodynamic pressure not depending on x_2 and x_3. Application of the law of conservation of mass then yields

$$\frac{\partial u_d}{\partial x_1} + \frac{\partial w_d}{\partial x_3} + \frac{v_b(x_1,x_3,t)}{d_{sq} + x_2} = 0 \quad , \tag{4.15^a}$$

where $u_d = u_d(x_1,x_3,t)$ = fluid velocity in x_1-direction in region d,
$w_d = w_d(x_1,x_3,t)$ = fluid velocity in x_3-direction in region d.

Averaging the horizontal velocity u_d over the height h-D by means of

$$(h-D)\bar{u}_d = \int_{-h}^{-D} u_d dx_3 \quad ,$$

where $\bar{u}_d = \bar{u}_d(x_1,t)$ = height-averaged fluid velocity in x_1-direction in region d,

and considering that $w_d(x_1,-D,t) = w_a(x_1,-D,t)$, (4.15^a) can be rewritten as

$$\frac{\partial \bar{u}_d}{\partial x_1} + \frac{w_a(x_1,-D,t)}{h - D} + \frac{\bar{v}_b(x_1,t)}{d_{sq} + x_2} = 0 \quad . \tag{4.15^b}$$

At the same time assuming that

$$\frac{\partial \bar{u}_d}{\partial x_1} << \frac{w_a(x_1,-D,t)}{h - D} \quad \text{and} \quad \frac{\partial \bar{u}_d}{\partial x_1} << \frac{\bar{v}_b(x_1,t)}{d_{sq} + x_2} \quad ,$$

this last expression becomes

$$(d_{sq} + x_2)\, w_a(x_1,-D,t) + (h-D)\, \bar{v}_b(x_1,t) = 0 \quad . \tag{4.15^c}$$

By applying in the x_2-direction a one-dimensional long-wave approximation to the motion of the water in region c, which implies a hydrostatic pressure distribution and $u_c = w_c = 0$, it can be derived that

$$(h-D)\bar{v}_b + (D+\eta_c)\dot{x}_2 - c_w\eta_c = 0 \quad ; \tag{4.16^a}$$

u_c and w_c represent the respective fluid velocities in x_1- and x_3-direction in region c. On the assumption that $\eta_c << D$ (4.16[a]) takes the form:

$$(h-D)\bar{v}_b + D\dot{x}_2 - c_w\eta_c = 0 \quad . \tag{4.16^b}$$

The equation of motion in the x_2-direction for the ship reads as

$$\rho LBD\ddot{x}_2 = 2\int_0^{L/2}\int_{-D}^{\zeta_a} p_a(x_1,x_3,t)dx_3dx_1 - \rho g\int_0^{L/2}(\eta_c + D)^2dx_1 +$$

$$+ R_{2,b,s}(t) + f_2(t) \quad , \tag{4.17}$$

where $R_{2,b,s}(t)$ = friction force in x_2-direction upon the bottom of the moving ship.

$R_{2,b,s}(t)$ can be expressed as

$$R_{2,b,s}(t) = 2B\int_0^{L/2}\tau_{2,b}\big|_{ship}\,dx_1 \quad ,$$

so that this quantity, with $\tau_{2,b}\big|_{ship}$ being known (see Section 3.2.1.3 and above), can be put into the respective forms

$$R_{2,b,s}(t) = \alpha_1\frac{h-D}{h}c_w\rho B\int_0^{L/2}(\bar{v}_b - \dot{x}_2)dx_1 \quad \text{for laminar flow in region b,} \tag{4.18^a}$$

and

$$R_{2,b,s}(t) = 2\alpha_t\rho B\int_0^{L/2}(\bar{v}_b - \dot{x}_2)|\bar{v}_b - \dot{x}_2|dx_1 \quad \text{for turbulent flow in region b.} \tag{4.18^b}$$

Under the assumptions and simplifications made, the set of seven governing equations (4.1[b]), (4.3[c]), (4.5[b]), (4.7[e]), (4.15[c]), (4.16[b]) and (4.17) together with the boundary conditions (4.6[a,b,c,d]) represents -apart from the initial values- a general formulation in the time domain of the motion characteristics of ship and fluid.

4.2.2. Further elaboration

On the assumption that

$$\left(\frac{\partial \bar{u}_a}{\partial x_1} + \frac{\dot{x}_2}{d_{sq} + x_2}\right)\zeta_a << \frac{\partial \zeta_a}{\partial t} \quad ,$$

for w_a it can be derived from (4.1^b) and boundary condition (4.6^c):

$$w_a(x_1,x_3,t) = \frac{\partial \zeta_a}{\partial t} - \left(\frac{\partial \bar{u}_a}{\partial x_1} + \frac{\dot{x}_2}{d_{sq} + x_2}\right)x_3 \quad . \tag{4.19}$$

One thing and another implies that now also with respect to $\dot{x}_2$ only small values are considered and that $\zeta_a << d_{sq} + x_2$. Eliminating w_a from (4.19) and (4.5^b) and introducing boundary condition (4.6^d) the fluid pressure p_a can be expressed as:

$$p_a(x_1,x_3,t) = \rho g(\zeta_a - x_3) - \rho \frac{\partial^2 \zeta_a}{\partial t^2} x_3 + \\ + \frac{1}{2}\rho\left\{\frac{\partial^2 \bar{u}_a}{\partial x_1 \partial t} + \frac{(d_{sq} + x_2)\ddot{x}_2 - \dot{x}_2^2}{(d_{sq} + x_2)^2}\right\}x_3^2 \quad ; \tag{4.20}$$

in this it was assumed that

$$\frac{\partial^2 \zeta_a}{\partial t^2} << g \quad \text{and} \quad \frac{1}{2}\left\{\frac{\partial^2 \bar{u}_a}{\partial x_1 \partial t} + \frac{(d_{sq} + x_2)\ddot{x}_2 - \dot{x}_2^2}{(d_{sq} + x_2)^2}\right\}\zeta_a << g \quad .$$

The last two terms on the right-hand side of (4.20) represent the non-hydrostatic part of the fluid pressure in region a due to the acceleration of the fluid particles in the x_3-direction. Substitution of p_a according to (4.20) into (4.3^c) yields -with $\zeta_a << D$-:

$$\frac{\partial \bar{u}_a}{\partial t} + g\frac{\partial \zeta_a}{\partial x_1} + \frac{1}{2}f_{w_a} D\left\{\frac{\partial^3 \zeta_a}{\partial x_1 \partial t^2} + \frac{1}{3}D\frac{\partial^3 \bar{u}_a}{\partial x_1^2 \partial t}\right\} = 0 \quad , \tag{4.21}$$

where f_{w_a} = switch parameter with value either 0 or +1 representing the influence of the vertical acceleration of the fluid in region a;

$$f_{w_a} = \left.\begin{array}{l} 0\text{: zero} \\ \\ +1\text{: non-zero} \end{array}\right\} \text{ vertical acceleration of fluid in region } a.$$

Elimination of $w_a(x_1,-D,t)$ from (4.15^c) by means of (4.19) gives:

$$(d_{sq}+ x_2)\{\frac{\partial\zeta_a}{\partial t} + D\,\frac{\partial\bar{u}_a}{\partial x_1}\} + D\dot{x}_2 + (h-D)\bar{v}_b = 0 \quad . \tag{4.22}$$

Using (4.20), now (4.7^e) can be written as

$$B\,\frac{\partial\bar{v}_b}{\partial t} = g(\zeta_a - \eta_c) + f_{w_a} D[\frac{\partial^2\zeta_a}{\partial t^2} + \frac{1}{2}D\{\frac{\partial^2\bar{u}_a}{\partial x_1\partial t} + \frac{(d_{sq}+ x_2)\ddot{x}_2 - \dot{x}_2^{\,2}}{(d_{sq}+ x_2)^2}\}] +$$

$$- R_{2,b}(x_1,t) - gH_{2,b}(x_1,t) \quad , \tag{4.23}$$

and (4.17) with $\zeta_a << D$ and $\eta_c << D$ as

$$\rho LBD\ddot{x}_2 = \rho D\int_0^{L/2} [2g(\zeta_a - \eta_c) + f_{w_a} D\,\frac{\partial^2\zeta_a}{\partial t^2} +$$

$$+ \frac{1}{3}f_{w_a} D^2\{\frac{\partial^2\bar{u}_a}{\partial x_1\partial t} + \frac{(d_{sq}+ x_2)\ddot{x}_2 - \dot{x}_2^{\,2}}{(d_{sq}+ x_2)^2}\}]dx_1 + R_{2,b,s}(t) + f_2(t) \quad . \tag{4.24}$$

Elimination of $\bar{v}_b$ and η_c from (4.16^b), (4.22), (4.23) and (4.24) yields

$$\{\frac{d_{sq}+ x_2}{h - D} + f_{w_a}\,\frac{D}{B}\}\,\frac{\partial^2\zeta_a}{\partial t^2} + \{\frac{\dot{x}_2}{h - D} + \frac{g(d_{sq}+ x_2)}{Bc_w}\}\,\frac{\partial\zeta_a}{\partial t} + \frac{g}{B}\,\zeta_a +$$

$$+ D\{\frac{d_{sq}+ x_2}{h - D} + \frac{1}{2}f_{w_a}\,\frac{D}{B}\}\,\frac{\partial^2\bar{u}_a}{\partial x_1\partial t} + D\{\frac{\dot{x}_2}{h - D} + \frac{g(d_{sq}+ x_2)}{Bc_w}\}\,\frac{\partial\bar{u}_a}{\partial x_1} =$$

$$= -D\{\frac{1}{h - D} + \frac{1}{2}f_{w_a}\,\frac{D}{B(d_{sq}+ x_2)}\}\ddot{x}_2 + \frac{1}{2}f_{w_a}\,\frac{D^2}{B(d_{sq}+ x_2)^2}\,\dot{x}_2^{\,2} +$$

$$+ \frac{1}{B}\,R_{2,b}(x_1,t) + \frac{g}{B}\,H_{2,b}(x_1,t) \tag{4.25}$$

and

$$\{1 - \frac{1}{6}f_{w_a} \frac{D^2}{B(d_{sq} + x_2)}\}\ddot{x}_2 + \frac{1}{6}f_{w_a} \frac{D^2}{B} \frac{\dot{x}_2^{\,2}}{(d_{sq} + x_2)^2} =$$

$$= \frac{2g}{LB} \int_0^{L/2} \{\zeta_a + \frac{d_{sq} + x_2}{c_w} \frac{\partial \zeta_a}{\partial t} + \frac{1}{2}f_{w_a} \frac{D}{g} \frac{\partial^2 \zeta_a}{\partial t^2} + \frac{D(d_{sq} + x_2)}{c_w} \frac{\partial \bar{u}_a}{\partial x_1} +$$

$$+ \frac{1}{6}f_{w_a} \frac{D^2}{g} \frac{\partial^2 \bar{u}_a}{\partial x_1 \partial t}\}dx_1 + \frac{1}{\rho LBD} R_{2,b,s}(t) + \frac{1}{\rho LBD} f_2(t) \quad , \qquad (4.26)$$

in which $R_{2,b}(x_1,t)$, $H_{2,b}(x_1,t)$ and $R_{2,b,s}(t)$ represent the modified expressions (4.10^{a,b}), (4.13) and (4.18^{a,b}), respectively:

$$R_{2,b}(x_1,t) = -\alpha_1 \frac{gB}{c_w(h-D)}\{Z_0(x_1,t) - \frac{1}{2}(h-D)\dot{x}_2\} \quad \text{for laminar flow in region b,} \qquad (4.27^a)$$

$$R_{2,b}(x_1,t) = -\alpha_t \frac{B}{(h-D)^3}[Z_0^2(x_1,t)\,\mathrm{sgn}\{Z_0(x_1,t)\} +$$

$$+ \{Z_0(x_1,t) - (h-D)\dot{x}_2\}^2\,\mathrm{sgn}\{Z_0(x_1,t) - (h-D)\dot{x}_2\}] \quad \text{for turbulent flow in region b} \quad , \qquad (4.27^b)$$

$$H_{2,b}(x_1,t) = -\frac{\lambda_b}{2g(h-D)^2} Z_0^2(x_1,t)\,\mathrm{sgn}\{Z_0(x_1,t)\} \quad , \qquad (4.28)$$

$$R_{2,b,s}(t) = -\alpha_1 \frac{B}{h} \rho c_w \int_0^{L/2} Z_0(x_1,t)dx_1 \quad \text{for laminar flow in region b,} \qquad (4.29^a)$$

$$R_{2,b,s}(t) = -\alpha_t \frac{2\rho B}{(h-D)^2} \int_0^{L/2} Z_0^2(x_1,t)\,\mathrm{sgn}\{Z_0(x_1,t)\}dx_1 \quad \text{for turbulent flow in region b} \; ; \qquad (4.29^b)$$

$Z_0(x_1,t)$ is a real function of x_1 and t, given as

$$Z_0(x_1,t) = (d_{sq} + x_2)\{\frac{\partial \zeta_a}{\partial t} + D \frac{\partial \bar{u}_a}{\partial x_1}\} + h\dot{x}_2 \quad , \qquad (4.30)$$

and

$$\mathrm{sgn}(Z_0) = \begin{cases} +1 & \text{for } Z_0 > 0 \\ -1 & \text{for } Z_0 < 0 \end{cases} \quad \text{, i.e. the 'signum' operator.}$$

The original set of seven governing equations with four boundary conditions now has been reduced to a set of three equations, viz. (4.21), (4.25) and (4.26), with the two boundary conditions (4.6^a) and (4.6^b). The new set of equations contains the four unknown quantities $\bar{u}_a(x_1,t)$, $\zeta_a(x_1,t)$, $x_2(t)$ and $f_2(t)$; this implies that either the ship motion $x_2(t)$ or the external (exciting) force $f_2(t)$ must be known beforehand. If necessary $\bar{v}_b(x_1,t)$ can be determined by means of (4.22).

4.2.3. Recapitulation of relevant formulae

The general mathematical description in the time domain of the transverse motion of the schematized ship in shallow water alongside of and parallel to a vertical, closed wall can -apart from the initial values- be formulated by means of the three equations

$$\frac{\partial \bar{u}_a}{\partial t} + g\frac{\partial \zeta_a}{\partial x_1} + \frac{1}{2}f_{w_a} D\{\frac{\partial^3 \zeta_a}{\partial x_1 \partial t^2} + \frac{1}{3}D\frac{\partial^3 \bar{u}_a}{\partial x_1^2 \partial t}\} = 0 \quad , \qquad (4.21)$$

$$\{\frac{d_{sq} + x_2}{h - D} + f_{w_a}\frac{D}{B}\}\frac{\partial^2 \zeta_a}{\partial t^2} + \{\frac{\dot{x}_2}{h - D} + \frac{g(d_{sq} + x_2)}{Bc_w}\}\frac{\partial \zeta_a}{\partial t} + \frac{g}{B}\zeta_a +$$

$$+ D\{\frac{d_{sq} + x_2}{h - D} + \frac{1}{2}f_{w_a}\frac{D}{B}\}\frac{\partial^2 \bar{u}_a}{\partial x_1 \partial t} + D\{\frac{\dot{x}_2}{h - D} + \frac{g(d_{sq} + x_2)}{Bc_w}\}\frac{\partial \bar{u}_a}{\partial x_1} =$$

$$= -D\{\frac{1}{h - D} + \frac{1}{2}f_{w_a}\frac{D}{B(d_{sq} + x_2)}\}\ddot{x}_2 + \frac{1}{2}f_{w_a}\frac{D^2}{B(d_{sq} + x_2)^2}\dot{x}_2^2 +$$

$$+ \frac{1}{B}R_{2,b}(x_1,t) + \frac{g}{B}H_{2,b}(x_1,t) \quad , \qquad (4.25)$$

$$\{1 - \frac{1}{6}f_{w_a}\frac{D^2}{B(d_{sq} + x_2)}\}\ddot{x}_2 + \frac{1}{6}f_{w_a}\frac{D^2}{B}\frac{\dot{x}_2^2}{(d_{sq} + x_2)^2} =$$

$$= \frac{2g}{LB} \int_0^{L/2} \{\zeta_a + \frac{d_{sq} + x_2}{c_w} \frac{\partial \zeta_a}{\partial t} + \frac{1}{2} f_{w_a} \frac{D}{g} \frac{\partial^2 \zeta_a}{\partial t^2} + \frac{D(d_{sq} + x_2)}{c_w} \frac{\partial \bar{u}_a}{\partial x_1} +$$

$$+ \frac{1}{6} f_{w_a} \frac{D^2}{g} \frac{\partial^2 \bar{u}_a}{\partial x_1 \partial t}\} dx_1 + \frac{1}{\rho LBD} R_{2,b,s}(t) + \frac{1}{\rho LBD} f_2(t) \quad , \qquad (4.26)$$

with boundary conditions

$$\bar{u}_a(x_1,t)\big|_{x_1=0} = 0 \quad , \qquad (4.6^a)$$

$$\zeta_a(x_1,t)\big|_{x_1=\pm\frac{1}{2}L} = 0 \quad ; \qquad (4.6^b)$$

either the ship motion $x_2(t)$ or the external (exciting) force $f_2(t)$ has to be known beforehand.

In these expressions it applies:

$$f_{w_a} = \left.\begin{matrix} 0\text{: zero} \\ +1\text{: non-zero} \end{matrix}\right\} \text{vertical acceleration of fluid in region a} \quad ,$$

$$c_w = \sqrt{gh} \quad ,$$

$$R_{2,b}(x_1,t) = -\alpha_1 \frac{gB}{c_w(h-D)} \{Z_0(x_1,t) - \tfrac{1}{2}(h-D)\dot{x}_2\} \quad \text{for laminar flow in region b,} \qquad (4.27^a)$$

$$R_{2,b}(x_1,t) = -\alpha_t \frac{B}{(h-D)^3} [Z_0^2(x_1,t)\ \mathrm{sgn}\{Z_0(x_1,t)\} +$$

$$+ \{Z_0(x_1,t) - (h-D)\dot{x}_2\}^2\ \mathrm{sgn}\{Z_0(x_1,t) - (h-D)\dot{x}_2\}] \quad \text{for turbulent flow in region b,} \qquad (4.27^b)$$

$$H_{2,b}(x_1,t) = -\frac{\lambda_b}{2g(h-D)^2} Z_0^2(x_1,t)\ \mathrm{sgn}\{Z_0(x_1,t)\} \quad , \qquad (4.28)$$

$$R_{2,b,s}(t) = -\alpha_1 \frac{B}{h} \rho c_w \int_0^{L/2} Z_0(x_1,t) dx_1 \quad \text{for laminar flow in region b,} \qquad (4.29^a)$$

$$R_{2,b,s}(t) = -\alpha_t \frac{2\rho B}{(h-D)^2} \int_0^{L/2} Z_0^2(x_1,t)\, \mathrm{sgn}\{Z_0(x_1,t)\} dx_1 \quad \text{for turbulent flow in region b} \quad , \qquad (4.29^b)$$

where

$$\alpha_1 = \frac{2\gamma c_w}{\rho g(h-D)} \quad , \qquad (4.9)$$

$$\lambda_b = 1.44 \quad , \qquad (4.14^b)$$

$$Z_0(x_1,t) = (d_{sq} + x_2)\{\frac{\partial \zeta_a}{\partial t} + D\,\frac{\partial \bar{u}_a}{\partial x_1}\} + h\dot{x}_2 \quad ; \qquad (4.30)$$

using Blasius' law to model the frictional effect in the underkeel region α_t is given to be

$$\alpha_t = \begin{cases} \dfrac{12}{Re} & \text{for} \quad Re \leq 2300 \quad , \qquad (4.11^a) \\[2ex] \dfrac{1}{8}\,\dfrac{0.3164}{Re^{1/4}} & \text{for} \quad 2300 < Re < 10^6 \quad , \qquad (4.11^b) \end{cases}$$

with

$$Re = \frac{2|\bar{v}_b|(h-D)}{\nu} \qquad (4.12)$$

and $\bar{v}_b$ to be determined from

$$(d_{sq} + x_2)\{\frac{\partial \zeta_a}{\partial t} + D\,\frac{\partial \bar{u}_a}{\partial x_1}\} + D\dot{x}_2 + (h-D)\bar{v}_b = 0 \quad . \qquad (4.22)$$

4.3. Application of i.r.f.-technique

4.3.1. Determination of hydrodynamic sway coefficients

4.3.1.1. Theoretical approximation

4.3.1.1.1. Derivation of general expressions

Since application of the i.r.f.-technique requires a linear and time-invariant ship-fluid system, the resulting equations as compiled in Section 4.2.3 must be linearized. This implies that the displacement of the ship has to remain small with respect to a mean value, i.e.

$x_2 << d_{sq}$,

and that the non-linear terms

$$\dot{x}_2 \frac{\partial \zeta_a}{\partial t} \quad , \quad \dot{x}_2 \frac{\partial \bar{u}_a}{\partial x_1} \quad , \quad \dot{x}_2^{\,2} \quad , \quad \left(\frac{\partial \zeta_a}{\partial t}\right)^2 \quad , \quad \frac{\partial \zeta_a}{\partial t}\frac{\partial \bar{u}_a}{\partial x_1} \quad , \quad \left(\frac{\partial \bar{u}_a}{\partial x_1}\right)^2$$

are neglected under the assumption of being small of the second order. The linearization then leads to the following set of equations:

$$\frac{\partial \bar{u}_a}{\partial t} + g \frac{\partial \zeta_a}{\partial x_1} + \frac{1}{2} f_{w_a} D\left\{\frac{\partial^3 \zeta_a}{\partial x_1 \partial t^2} + \frac{1}{3} D \frac{\partial^3 \bar{u}_a}{\partial x_1^{\,2} \partial t}\right\} = 0 \quad , \tag{4.21}$$

$$\left\{\frac{d_{sq}}{h-D} + f_{w_a} \frac{D}{B}\right\} \frac{\partial^2 \zeta_a}{\partial t^2} + \frac{g d_{sq}}{B c_w} \frac{\partial \zeta_a}{\partial t} + \frac{g}{B} \zeta_a + D\left\{\frac{d_{sq}}{h-D} + \frac{1}{2} f_{w_a} \frac{D}{B}\right\} \frac{\partial^2 \bar{u}_a}{\partial x_1 \partial t} +$$

$$+ \frac{g D d_{sq}}{B c_w} \frac{\partial \bar{u}_a}{\partial x_1} = - \frac{D}{d_{sq}}\left\{\frac{d_{sq}}{h-D} + \frac{1}{2} f_{w_a} \frac{D}{B}\right\} \ddot{x}_2 +$$

$$- \alpha_1 \frac{g}{c_w (h-D)} \left\{d_{sq}\left(\frac{\partial \zeta_a}{\partial t} + D \frac{\partial \bar{u}_a}{\partial x_1}\right) + \frac{1}{2}(h+D)\dot{x}_2\right\} \quad , \tag{4.31}$$

$$\left\{1 - \frac{1}{6} f_{w_a} \frac{D^2}{B d_{sq}}\right\} \ddot{x}_2 =$$

$$= \frac{2g}{LB} \int_0^{L/2} \left\{\zeta_a + \frac{d_{sq}}{c_w} \frac{\partial \zeta_a}{\partial t} + \frac{1}{2} f_{w_a} \frac{D}{g} \frac{\partial^2 \zeta_a}{\partial t^2} + \frac{D d_{sq}}{c_w} \frac{\partial \bar{u}_a}{\partial x_1} + \frac{1}{6} f_{w_a} \frac{D^2}{g} \frac{\partial^2 \bar{u}_a}{\partial x_1 \partial t}\right\} dx_1 +$$

$$- \alpha_1 \frac{g}{c_w L D} \int_0^{L/2} \left\{d_{sq}\left(\frac{\partial \zeta_a}{\partial t} + D \frac{\partial \bar{u}_a}{\partial x_1}\right) + h \dot{x}_2\right\} dx_1 + \frac{1}{\rho L B D} f_2(t) \quad . \tag{4.32}$$

As expected, in the underkeel region only the influence of the linear(ized) friction can be maintained; the effect of contraction and separation of flow has vanished due to its non-linear character.

The hydrodynamic sway coefficients can be determined by means of a harmonic analysis of the ship-fluid system. To that end a simple-harmonic sway motion

$$x_2(t) = \hat{x}_2 \exp(i\omega t) \quad , \tag{4.33^a}$$

is imposed on the ship, which requires an external exciting force in the x_2-direction of the form

$$f_2(t) = \hat{f}_2 \exp(i\omega t) \quad . \tag{4.33b}$$

This just as well implies

$$\bar{u}_a(x_1,t) = \hat{\bar{u}}(x_1) \exp(i\omega t) \quad , \quad \zeta_a(x_1,t) = \hat{\zeta}_a(x_1) \exp(i\omega t) \quad . \tag{4.34a,b}$$

Substitution of these time-harmonic expressions for $x_2(t)$, $f_2(t)$, $\bar{u}_a(x_1,t)$ and $\zeta_a(x_1,t)$ into (4.21), (4.31) and (4.32) yields

$$\frac{d\hat{\zeta}_a}{dx_1} = -i\omega\{\hat{\bar{u}}_a + \tfrac{1}{6}f_{w_a} D^2 \frac{d^2\hat{\bar{u}}_a}{dx_1^2}\} \left(g - \tfrac{1}{2}f_{w_a} D\omega^2\right)^{-1} \quad , \tag{4.35}$$

$$P\hat{\zeta}_a + Q \frac{d\hat{\bar{u}}_a}{dx_1} - R\hat{x}_2 = 0 \quad , \tag{4.36}$$

$$-\omega^2\{1 - \tfrac{1}{6}f_{w_a} \frac{D^2}{Bd_{sq}}\}\hat{x}_2 = \frac{2}{LB} \int_0^{L/2} \{T\hat{\zeta}_a + D(\frac{gd_{sq}}{c_w} + \tfrac{1}{6}f_{w_a} i\omega D) \frac{d\hat{\bar{u}}_a}{dx_1}\}dx_1 +$$

$$-\alpha_1 \frac{g}{c_w LD} \int_0^{L/2} \{d_{sq}(i\omega\hat{\zeta}_a + D \frac{d\hat{\bar{u}}_a}{dx_1}) + i\omega h\hat{x}_2\}dx_1 + \frac{1}{\rho LBD} \hat{f}_2 \quad , \tag{4.37}$$

respectively, in which

$$P = -\omega^2\{\frac{d_{sq}}{h - D} + f_{w_a} \frac{D}{B}\} + i\omega \frac{gd_{sq}}{Bc_w} + \frac{g}{B} + \alpha_1 \frac{i\omega g d_{sq}}{c_w(h-D)} \quad ,$$

$$Q = i\omega D\{\frac{d_{sq}}{h - D} + \tfrac{1}{2}f_{w_a} \frac{D}{B}\} + \frac{gDd_{sq}}{Bc_w} + \alpha_1 \frac{gDd_{sq}}{c_w(h-D)} \quad ,$$

$$R = \frac{\omega^2 D}{d_{sq}}\{\frac{d_{sq}}{h - D} + \tfrac{1}{2}f_{w_a} \frac{D}{B}\} - \tfrac{1}{2}\alpha_1 \frac{i\omega g(h+D)}{c_w(h-D)} \quad ,$$

$$T = g\left(1 + i\omega \frac{d_{sq}}{c_w}\right) - \tfrac{1}{2}f_{w_a} \omega^2 D \quad .$$

By elimination of $\hat{\zeta}_a$ from (4.35) and (4.36) it can be written

$$S \frac{d^2\hat{\hat{u}}_a}{dx_1^2} - \hat{\hat{u}}_a = 0 \qquad , \tag{4.38}$$

with

$$S = \frac{g - \frac{1}{2}f_{w_a} D\omega^2}{i\omega} \frac{Q}{P} - \frac{1}{6}f_{w_a} D^2 \qquad .$$

The solution of (4.38) reads as

$$\hat{\hat{u}}_a(x_1) = C_1\exp(rx_1) + C_2\exp(-rx_1) \qquad , \tag{4.39}$$

where C_1, C_2 = constant of integration,

$$r = + S^{-1/2} \qquad .$$

Substituting this expression for $\hat{\hat{u}}_a$ into (4.36) it can be derived for $\hat{\zeta}_a$:

$$\hat{\zeta}_a(x_1) = - \frac{rQ}{P}\{C_1\exp(rx_1) - C_2\exp(-rx_1)\} + \frac{R}{P}\,\hat{x}_2 \qquad . \tag{4.40}$$

With (4.34^{a,b}) the respective boundary conditions (4.6^a) and (4.6^b) become

$$\hat{\hat{u}}_a(x_1)\Big|_{x_1=0} = 0 \tag{4.41^a}$$

and

$$\hat{\zeta}_a(x_1)\Big|_{x_1=\pm\frac{1}{2}L} = 0 \qquad . \tag{4.41^b}$$

Combining (4.39) with (4.41^a) and (4.40) with (4.41^b) C_1 and C_2 then are determined to be

$$C_1 = -C_2 = \frac{R}{2rQ\,\cosh(\frac{1}{2}rL)}\,\hat{x}_2 \qquad ,$$

so that (4.39) can be written as:

$$\hat{\hat{u}}_a(x_1) = f_{u_a} \frac{R}{rQ} \frac{\sinh(rx_1)}{\cosh(\frac{1}{2}rL)} \hat{x}_2 \quad , \tag{4.42}$$

where f_{u_a} = switch parameter with value either 0 or + 1 representing the influence of the horizontal velocity of the fluid in region a;

$$f_{u_a} = \left.\begin{matrix} 0\text{: zero} \\ \\ +1\text{: non-zero} \end{matrix}\right\} \text{horizontal velocity of fluid in region a;}$$

$f_{u_a} = 0$ actually implies independence of x_1, i.e. strip theory. By means of (4.36) and (4.42) $\hat{\zeta}_a$ can be put into the form

$$\hat{\zeta}_a(x_1) = \frac{R}{P}\{1 - f_{u_a} \frac{\cosh(rx_1)}{\cosh(\frac{1}{2}rL)}\}\hat{x}_2 \quad . \tag{4.43}$$

Using (4.42) and (4.43) now $\hat{\hat{u}}$ and $\hat{\zeta}_a$ can be eliminated from (4.37) yielding

$$\frac{\hat{f}_2}{\rho\hat{x}_2} = LD\left(-B + \frac{1}{6}f_{w_a}\frac{D^2}{d_{sq}}\right)\omega^2 - LD\frac{TR}{P} +$$

$$- 2f_{u_a} D\frac{R}{rQ}\left\{\frac{gDd_{sq}}{c_w} + \frac{1}{6}f_{w_a} i\omega D^2 - \frac{TQ}{P}\right\}\tanh(\tfrac{1}{2}rL) +$$

$$+ \frac{1}{2}\alpha_1 \frac{gB}{c_w}\left\{i\omega L\left(d_{sq}\frac{R}{P} + h\right) + 2f_{u_a} d_{sq}\frac{R}{rQ}\left(-i\omega\frac{Q}{P} + D\right)\tanh(\tfrac{1}{2}rL)\right\} \quad . \tag{4.44}$$

According to (3.29^b), where now $m_{22} = \rho LBD$, the behaviour of the ship-fluid system in the frequency domain in case of a pure sway mode of motion is described by

$$\{\rho LBD + a_{22}(\omega)\}\ddot{x}_2 + b_{22}(\omega)\dot{x}_2 = f_2(t) \quad ; \tag{4.45^a}$$

with (4.33^a) and (4.33^b) this expression takes the form

$$\frac{\hat{f}_2}{\rho\hat{x}_2} = - \frac{1}{\rho}\{\rho LBD + a_{22}(\omega)\}\omega^2 + i\frac{\omega}{\rho}\, b_{22}(\omega) \quad , \tag{4.45^b}$$

from which it follows for the hydrodynamic sway coefficients $a_{22}(\omega)$ and $b_{22}(\omega)$:

$$a_{22}(\omega) = -\rho LBD - \frac{\rho}{\omega^2}\,\mathrm{Re}\left[\frac{\hat{f}_2}{\rho\hat{x}_2}\right] \quad , \tag{4.46}$$

$$b_{22}(\omega) = \frac{\rho}{\omega}\,\mathrm{Im}\left[\frac{\hat{f}_2}{\rho\hat{x}_2}\right] \quad . \tag{4.47}$$

In the case that $\omega \to 0$ the relevant transitions to the limit for $a_{22}(\omega)$ and $b_{22}(\omega)$ yield

$$\frac{a_{22}(0)}{\rho LBD} = (1-f_{u_a})\frac{D}{h-D} + \frac{1}{6}f_{w_a}(2-3f_{u_a})\frac{D^2}{Bd_{sq}} - \frac{1}{4}(1-f_{u_a})\,\alpha_1^2\,\frac{gBd_{sq}(h+D)^2}{c_w^{\,2}D(h-D)^2} +$$

$$+ f_{u_a}(1-\frac{1}{2}\alpha_1\frac{B}{D})^2\left\{\frac{D}{h-D} + \frac{1}{2}f_{w_a}\frac{D^2}{Bd_{sq}}\right\}\left\{1+\alpha_1\frac{B}{h-D}\right\}^{-2} +$$

$$+ \frac{1}{12}f_{w_a}f_{u_a}\alpha_1\frac{D(h+D)}{d_{sq}(h-D)}\left\{1+\alpha_1\frac{B}{h-D}\right\}^{-1} \tag{4.48^a}$$

and

$$\frac{b_{22}(0)}{\rho LBD}\frac{c_w}{g} = \frac{1}{2}\alpha_1\left[\left\{(1-f_{u_a})\frac{h+D}{h-D} + \frac{h}{D}\right\} + f_{u_a}\frac{h+D}{h-D}\left\{1-\frac{1}{2}\alpha_1\frac{B}{D}\right\}\left\{1+\alpha_1\frac{B}{h-D}\right\}^{-1}\right] \quad , \tag{4.49^a}$$

on condition that the proportionality coefficient for the shear stress, γ, as occurring in

$$\alpha_1 = \frac{2\gamma c_w}{\rho g(h-D)} \quad , \tag{4.9}$$

is taken to be a constant.
If, with respect to the underkeel frictional effect -just as in Section 3.2.1.3- a Stokes' type friction formula is used for a predominantly oscillating flow with a relatively thin boundary layer, so that again

$$\gamma = \rho\sqrt{\nu\omega} \quad , \tag{3.20^a}$$

(4.48^{a}) and (4.49^{a}) become

$$a_{22}(0) = \rho LBD\{\frac{D}{h-D} + \frac{1}{3}f_{w_a}\frac{D^2}{Bd_{sq}}\} \quad , \qquad (4.48^b)$$

$$b_{22}(0) = 0 \quad , \qquad (4.49^b)$$

respectively.

Some specific cases allow -using (4.44) and (4.46) through ($4.49^{a,b}$)- a rather simple derivation of direct expressions for the hydrodynamic sway coefficients; see for this, Appendix K.

4.3.1.1.2. Survey of most important formulae

The hydrodynamic coefficients for the schematized ship in case of a pure sway mode of motion near a vertical wall read as follows:

- added mass for swaying motion:

$$a_{22}(\omega) = -\rho LBD - \frac{\rho}{\omega^2}\,\mathrm{Re}[\frac{\hat{f}_2}{\rho\hat{x}_2}] \quad , \qquad (4.46)$$

with the limit case

$$a_{22}(0) = \rho LBD\{\frac{D}{h-D} + \frac{1}{3}f_{w_a}\frac{D^2}{Bd_{sq}}\} \quad ; \qquad (4.48^b)$$

- sway damping force coefficient:

$$b_{22}(\omega) = \frac{\rho}{\omega}\,\mathrm{Im}[\frac{\hat{f}_2}{\rho\hat{x}_2}] \quad , \qquad (4.47)$$

with the limit case

$$b_{22}(0) = 0 \quad ; \qquad (4.49^b)$$

- in these expressions is

$$\frac{\hat{f}_2}{\rho\hat{x}_2} = LD(-B + \frac{1}{6}f_{w_a}\frac{D^2}{d_{sq}})\omega^2 - LD\frac{TR}{P} +$$

$$- 2f_{u_a}D\frac{R}{rQ}\{\frac{gDd_{sq}}{c_w} + \frac{1}{6}f_{w_a}i\omega D^2 - \frac{TQ}{P}\}\tanh(\frac{1}{2}rL) +$$

$$+ \tfrac{1}{2}\alpha_1 \frac{gB}{c_w}\{i\omega L\left(d_{sq} \frac{R}{P} + h\right) + 2f_{u_a} d_{sq} \frac{R}{rQ}\left(-i\omega\frac{Q}{P} + D\right)\tanh(\tfrac{1}{2}rL)\} \quad , \quad (4.44)$$

where

$$P = -\omega^2\left\{\frac{d_{sq}}{h - D} + f_{w_a} \frac{D}{B}\right\} + i\omega \frac{gd_{sq}}{Bc_w} + \frac{g}{B} + \alpha_1 \frac{i\omega g d_{sq}}{c_w(h-D)} \quad ,$$

$$Q = i\omega D\left\{\frac{d_{sq}}{h - D} + \tfrac{1}{2}f_{w_a} \frac{D}{B}\right\} + \frac{gDd_{sq}}{Bc_w} + \alpha_1 \frac{gDd_{sq}}{c_w(h-D)} \quad ,$$

$$R = \frac{\omega^2 D}{d_{sq}}\left\{\frac{d_{sq}}{h - D} + \tfrac{1}{2}f_{w_a} \frac{D}{B}\right\} - \tfrac{1}{2}\alpha_1 \frac{i\omega g(h+D)}{c_w(h-D)} \quad ,$$

$$S = \frac{g - \tfrac{1}{2}f_{w_a} D\omega^2}{i\omega} \frac{Q}{P} - \tfrac{1}{6}f_{w_a} D^2 \quad ,$$

$$T = g\left(1 + i\omega \frac{d_{sq}}{c_w}\right) - \tfrac{1}{2}f_{w_a} \omega^2 D \quad ,$$

$$r = + S^{-1/2} \quad ,$$

$$\alpha_1 = \frac{2\gamma c_w}{\rho g(h-D)} \quad , \qquad (4.9)$$

$$\gamma = \rho\sqrt{\nu\omega} \quad , \qquad (3.20^a)$$

$$c_w = \sqrt{gh} \quad ;$$

- further it applies:

$$f_{u_a} = \left.\begin{matrix} 0: \text{zero} \\ \\ +1: \text{non-zero} \end{matrix}\right\} \text{horizontal velocity of fluid in region a,}$$

$$f_{w_a} = \left.\begin{matrix} 0: \text{zero} \\ \\ +1: \text{non-zero} \end{matrix}\right\} \text{vertical acceleration of fluid in region a.}$$

4.3.1.2. Experiments

4.3.1.2.1. Description of experimental set-up

Just as in the case of horizontally unrestricted water a series of model tests was carried out in order to verify the theoretical results as presented by the expressions derived in the preceding Section 4.3.1.1. The experiments comprised forced oscillation tests to determine (the influence of a vertical wall parallel to the ship's longitudinal centre-line on) the hydrodynamic coefficients in case of pure swaying at zero forward speed.

The same schematized ship model was used as described in Section 3.2.2.1.

Four water depths were involved, viz. $h = 0.160$ m, $h = 0.175$ m, $h = 0.200$ m and $h = 0.250$ m. Again the water was calm, i.e. absence of waves and current.

The straight and impervious (quay-)wall was made up of concrete elements with a smooth, vertical front side. Four values of the distance/clearance between ship and wall were considered, viz. $d_{sq} = 0.043$ m, $d_{sq} = 0.063$ m, $d_{sq} = 0.086$ m and $d_{sq} = 0.129$ m.

The hydrodynamic coefficients for the sway mode of motion were determined experimentally by means of a P.M.M. as set out in Section 3.2.2.1. For the version used in these experiments the circular frequency of the oscillatory motions could vary continuously between 0.1 rad.s^{-1} and 11.5 rad.s^{-1}, which corresponds with a period range from 62.8 s to 0.55 s. The maximum capacity of the dynamometers applied was about 800 N each.

The pure sway tests at zero forward speed were executed near one of the short sides of a rectangular basin with relatively large horizontal dimensions: effective length = 32.00 m, effective breadth = 13.95 m. The basin had a horizontal bottom and was bounded by vertical walls.
The P.M.M. was stiffly mounted on a rectangular steel frame with the same qualifications as the frame described in Section 3.2.2.1. The longitudinal plane of symmetry of the ship model was parallel to the vertical quay-wall as well as to the breadthwise axes of symmetry of basin and frame. The distances of the legs of the frame to the ship model were relatively large.
The test set-up was situated in the basin such that the generated waves travelled as much as possible in the longitudinal direction of the basin. In order to attain faster wave damping the opposite short side of the basin was provided with a slope of coarse gravel. For a schematical representation of the model installation it is referred to fig. 4.2.

4.3.1.2.2. Execution of model experiments

With respect to the execution of the model tests generally the same applies as stated in Section 3.2.2.2.
For values of the circular frequency lower than 0.1 rad.s^{-1} no data could be obtained.

In the experiments the ship model was not allowed to move freely in the vertical direction in order to prevent uncontrolled heave motions (due to combined action of pressure fluctuations in quay clearance and underkeel region) and to maintain a constant value of the draught; also the risk of touching the bottom for certain combinations of amplitude and frequency thus was eliminated.
For obvious reasons the amplitude of the sway motion had to be small with respect to the distance between ship model and vertical quay-wall. To be assured yet of reasonably measurable forces -especially for the lower frequencies- a choice was made for $\hat{x}_2 = \hat{a} = 0.0025$ m. As a consequence of this option for a small motion-amplitude the sum of all tolerances in the mechanical part of the P.M.M. might influence the (accuracy of the) measurements, especially in case of smaller values of the forces. To eliminate the effect of these tolerances each strut of the excitator was separately pretensioned by means of a weight of about 200 N, which could follow its oscillatory motion. Both weights had a horizontal line of action perpendicular to the ship's longitudinal axis of symmetry and a point of application above the dynamometer, so that the measured values were not affected. A second, larger amplitude was applied to check the linearity, viz. $\hat{a} = 0.005$ m. From the results it appeared that the hydrodynamic forces for the sway mode of motion are linearly depending on the sway motion-amplitude, at least in the range of amplitudes tested.

As pointed out in Section 3.2.2.2, the test results might be affected by reflected waves arriving at the ship model during a measurement. Roughly this occured for $\omega < 0.18$ rad.s^{-1}. Although the disturbance of the model experiments by the reflection phenomena was very small, it implies that the test results for $\omega < 0.2$ rad.s^{-1} have to be considered with some reserve.

4.3.1.3. Comparison of theory and experiment

The hydrodynamic coefficients -determined both theoretically and experimentally- for the case of pure swaying at zero forward and transverse speed, are represented in a similar way as in Section 3.2.3.1. In addition to h/D now also the dimensionless distance between ship and vertical quay-wall, d_{sq}/B, acts as a parameter.

Figs. 4.3 through 4.10 show calculated and measured results for various values of the water depth and the distance between ship and quay-wall. The calculational results include the respective influences of the vertical acceleration and the horizontal velocity in the quay clearance as well as the underkeel friction, the latter effect being based on a Stokes' type friction formula for predominantly oscillating flow with a relatively thin boundary layer.

In general the agreement between theory and experiment can be considered everyway as quite reasonable. As expected, the results show a better fit as the water depth and the quay clearance are smaller. The differences may be explained by the assumptions and simplifications made in formulating the hydrodynamic model. For instance, the circulation around 'bow' and 'stern' has not been taken into account; further the concept used for modelling the underkeel friction might play a part.

The absolute value of the added mass increases with decreasing keel clearance in the low-frequency range, while -to a smaller extent- the reverse seems to be the case at higher frequencies. The slope of the curves increases with decreasing water depth and the peaks shift towards lower frequencies. In shallow water the sway damping force coefficient is also larger and the respective peaks occur at lower frequencies; in the higher-frequency domain the curves do not approach each other as in the case of horizontally unrestricted water. A larger distance between ship and quay-wall has a reducing effect on the (absolute) values of added mass and damping force coefficient, while the peaks shift towards lower frequencies.

In formulating the hydrodynamic model a long-wave approximation was applied to the motion of the water in region c, which formally means $\omega \ll 2\pi\sqrt{g/h}$. This implies that the values of the hydrodynamic coefficients in case of high frequencies, say $\omega \gg 0.7\sqrt{g/h}$, maybe have to be considered with some reserve.

From figs. 4.3 through 4.10 it can be seen that the presence of the quay-wall has a remarkable effect on the hydrodynamic sway coefficients of the ship.

Comparison of figs. 4.5 and 4.6 with the corresponding fig. 3.3 for horizontally unrestricted water shows that the effect of the quay-wall on the added mass disappears, or at least gets minimal for very low and very high frequencies. In the range of frequencies, however, which is of interest for ship molinear underkeel friction as introduced in the application of the i.r.f.-technique has to be conceived as a general damping mechanism.

4.3.3. Outline of mathematical approach to berthing ship

Consider the schematized ship berthing to a closed structure; the geometrical situation and the conditions are as described in Section 1.3.4. The berth is fitted with one single fender, represented by an undamped, linear spring; its horizontal line of action is situated in the plane of the water surface at rest and perpendicular to the face of the berth. A plan and cross-section of the closed berthing lay-out are given in fig. 4.18. Just as in the case of ship berthing to an open jetty-type structure (see Section 3.4.1), the mass of the fender is again supposed to be small with respect to that of the ship.

Shortly before the first contact between ship and fender the laterally moving ship (i.e. $V_1 = 0$) has a certain constant speed of approach $V_2 = -v_A$ towards the berth. The first contact between ship and fender takes place at point of time $t = 0$. Then the clearance between the vertical quay-wall and the ship is d_{sq}. At $t = 0$ the space-fixed $OX_1X_2X_3$-co-ordinate system is assumed to coincide with the translating $ox_1x_2x_3$-system; the ship-fixed Gxyz-system then also coincides with $OX_1X_2X_3$. During the berthing operation the ship maintains a translational motion with its longitudinal axis of symmetry parallel to the face of the berth (i.e. uncoupled ship motions and a 'centric impact').

Now a berthing situation has come about, which -apart from the rotation- is comparable to that dealt with in Section 3.4.1. The deflexion of the fender has the form $\Delta X_{2f}(t) = X_{2f}(t) + \frac{1}{2}B$ and can -see also (3.48)- be expressed as:

$$\Delta X_{2f}(t) = X_{2G} \quad , \quad \Delta X_{2f}(t) \leqq 0 \qquad . \tag{4.53}$$

The relation between $\Delta X_{2f}(t)$ and the corresponding reaction force in the fender $F_{2f}(t)$ again is given by

$$F_{2f}(t) = f(\Delta X_{2f}) \qquad \text{for} \qquad t \geqq 0 \qquad , \tag{3.49}$$

while the resulting force upon the ship, as acting in G, becomes (see (3.50^{a,b}))

tions, the added mass is influenced significantly. Most interesting feature is the occurrence of (sharp) peaks and negative values for the added mass. Observations during the tests revealed that the peak values may be associated with the occurrence of standing waves between ship and quay-wall with nodal lines perpendicular to the quay-wall.
A physical interpretation of negative (sway) added-'mass' is difficult. However, this quantity is just the in-phase component of the fluid reactive force in the frequency-domain description of the ship-fluid system (see Section 2.3). Instead of combining this component with the inertia term (which is common practice and underlies the denomination 'added mass'), it could also be considered as a displacement term and defined then as 'hydrodynamic spring coefficient'. On account of this view it can be put that, in the frequency range where the sway added-mass is negative, the water between quay-wall and ship acts like a spring.

From comparison of figs. 4.6 and 4.8 with the corresponding fig. 3.4 for horizontally unrestricted water it appears that the hydrodynamic damping increases considerably near a quay-wall.

The ω-value of the first zero-crossing between the two main peaks in the sway added-mass curve can be shown to equal approximately the natural frequency of the mass of water in a domain consisting of the successive regions a, d, b and c (i.e. 'surge tank' analogon). This natural frequency also nearly coincides with the ω-value of the main peak in the corresponding curve for the hydrodynamic sway damping force coefficient. A rough estimate of the natural frequency can be derived from (4.31). The smaller peaks in the added mass and hydrodynamic damping curves figure at frequencies which may be associated with the occurrence of standing wave patterns in the quay clearance.

Further it is remarked that the trends shown in figs. 4.3 through 4.10 are confirmed by similar results from ref. [58] for a real, i.e. non-schematized, ship in case of an analogous situation.

Resuming the data obtained, it may be concluded that the theoretical results -derived from the mathematical model describing the sway motion in case of shallow water and a relatively small distance between ship and quay-wall- show a satisfactory agreement with experimental values. The theoretical approach is considered to be sufficient for a prediction of the hydrodynamic coefficients in the frequency range which is of practical interest for ship motions. The frequency dependence of the hydrodynamic sway coefficients is striking, especially in (very) shallow water. It also appears that the influence of water depth and distance between ship and quay-wall, respectively, on the sway added-mass and the sway damping force coefficient is extremely important.

In figs. 4.11 and 4.12 theoretical data are presented for the combination $h/D = 1.067$, $d_{sq}/B = 0.115$, where separately the respective influences are shown of the horizontal velocity and the vertical acceleration in the quay clearance, and the friction effect in the underkeel region. As distinct from the situation with horizontally unrestricted water, now especially the influence of the underkeel friction does appear to be significant. The incorporation in the quay clearance of the horizontal velocity has also a noticeable effect, whereas the influence of the vertical acceleration is much less pronounced. The underkeel friction effect as introduced into the theoretical approximation of the hydrodynamic coefficients induces a considerable attenuation of the peaks. Comparison of figs. 4.3 and 4.4 with figs. 4.11 and 4.12, respectively, shows that the experimental values of each of both hydrodynamic coefficients approximately lie in between the complete, theoretical curve and the curve for $f_{u_a} = 0$, which implies that the schematization of the influence of the horizontal velocity in the quay clearance possibly is too strong. The four figs. last-mentioned also suggest that in the theoretical approach the friction effect in the underkeel region is reasonably well modelled.

Finally it is observed that in refs. [111] through [117] data are presented on the two-dimensional sway added-mass of rectangular profiles in shallow water near a vertical wall (i.e. strip theory). In these the free surface has been treated as a rigid plane, on the assumption that the frequency of motion is infinitesimal, which means that the results are solely valid for the case $\omega = 0$. Applying these data to the geometrical situation under consideration, one arrives at values which are comparable and have the same order of magnitude as those found in this study.

4.3.2. Calculation of impulse response function for sway motion

The i.r.f. for the sway mode of motion, $k_{22}(t)$, in principle can be determined analytically from the set of linearized equations (4.21), (4.31) and (4.32).

For the situation under consideration the description of the linear ship-fluid system in the time domain reads as (see (2.69))

$$\dot{x}_2(t) = \int_{-\infty}^{t} f_2(\tau)\; k_{22}(t-\tau)d\tau \qquad . \tag{4.50}$$

Let there be a state of rest for $t < t_0$. At the time $t = t_0$ an arbitrary, centric unit pulse is exerted upon the ship in the sway direction:

$$f_i(t) = \zeta_i\; \delta_i(t-t_0) \quad , \quad \zeta_i = 1 \quad , \quad t_0 > 0 \quad , \quad i = 2 \qquad , \tag{4.51}$$

where t_0 = point of time.
From these two equations it can be derived:

$$\dot{x}_2(t) = \zeta_2\; k_{22}(t-t_0) \quad , \quad \zeta_2 = 1 \qquad , \tag{4.52}$$

with $\qquad \dot{x}_2(t) = \zeta_2\; k_{22}(t-t_0) = 0 \quad$ for $t < t_0 \qquad .$

In order to determine $k_{22}(t)$ the following procedure has to be pursued:
- using (4.51) $f_2(t)$ is substituted into (4.32);
- then the unilateral Laplace transforms (with respect to t) are taken of the set of linearized equations (4.21), (4.31) and (4.32);
- from the three equations thus generated the Laplace transforms $L\{\bar{u}_a(x_1,t)\}$ and $L\{\zeta_a(x_1,t)\}$ are eliminated, so that an expression arises with the remaining Laplace transform $L\{\dot{x}_2(t)\}$;
- by taking the inverse Laplace transform of $L\{\dot{x}_2(t)\}$ then $\dot{x}_2(t)$ can be determined, which -by means of (4.52)- finally yields $k_{22}(t)$.

However, this procedure is rather laborious and it yet remains to be seen whether the derivation of an analytical expression for $k_{22}(t)$ is feasible. In the simplified case of zero horizontal velocity in the quay clearance, implying independence of x_1 (i.e. strip theory), an analytical expression for $k_{22}(t)$ still can be determined; this is done in Appendix L.

Since the derivation of an analytical expression for $k_{22}(t)$ appears to grow problematic when taking into account the influence of $\bar{u}_a$, it is passed on to a direct numerical calculation from theoretical data for the hydrodynamic sway coefficients $a_{22}(\omega)$ and $b_{22}(\omega)$. In this an identical procedure is applied as described in Section 3.3.1, inclusive of the estimations for the truncation error and the discretization error. The calculation was done starting from values for the hydrodynamic coefficients given at the following frequencies: for $0 \leq \omega \leq 10\ s^{-1}$ with frequency step = $0.01\ s^{-1}$, for $10 \leq \omega \leq 25\ s^{-1}$ with frequency step = $0.1\ s^{-1}$, for $25 \leq \omega \leq 100\ s^{-1}$ with frequency step = $1.0\ s^{-1}$.

In all cases considered, the combined effect of the truncation of the numerical process of integration and the discretization error remained -for all t- amply within 1 % of the corresponding value calculated for $k_{22}(t)$.
Again the i.r.f. was calculated numerically at intervals of time amounting to 0.01 s, and the upper limit of the calculation was taken at $t = 7.50$ s; this time range was regarded to be sufficiently long, since it was found once more that $k_{22}(t)$ tends to $k_{22}(\infty)$ for $t > 7.50$ s.

Figs. 4.13 through 4.16 show the i.r.f. for the sway motion near a vertical wall in case of zero forward and transverse speed; the results are plotted in a similar way as in Section 3.3.2, on the understanding that besides h/D now also d_{sq}/B acts as a parameter. In the results presented the influences of the vertical acceleration and the horizontal velocity in the quay clearance as well as the underkeel friction effect are included. From figs. 4.13 through 4.16 it can be seen that the i.r.f. $k_{22}(t)$ approximates (rather quickly) to a constant value as t increases; this means that in the convolution integral (4.50) -representing the motion of the ship in the sway direction- much emphasis is laid on the (very) near past of the time history of the forcing function. In this connection it once again is pointed out that the i.r.f. is dependent on the geometrical configuration: each i.r.f. applies to a certain (initial) quay clearance in respect of which only small displacements may occur. On the curves representing the i.r.f. a fast oscillation can be discerned: its (circular) frequency can be estimated by means of the expressions derived in Appendix L.
In fig. 4.17 data are presented for the combination $h/D = 1.067$, $d_{sq}/B = 0.115$, where the respective influences are shown of the horizontal velocity and the vertical acceleration in the quay clearance and the friction effect in the underkeel region. It appears that especially the influence of the underkeel friction is significant, whereas the influences of the horizontal velocity and the vertical acceleration in the quay clearance are much less pronounced. In fig. 4.17 it can be seen that the i.r.f.-curve for $f_{u_a} = 0$ lies lower than the complete curve, but to a less extent than in the case with zero friction in the underkeel region.
It is questionable whether the linear friction mechanism in the underkeel region as introduced in determining the hydrodynamic coefficients, also holds good for the type of motion represented by the i.r.f. During oscillatory motions the underkeel friction mechanism may be different from that during the transient motion in response to an external (impulsive) force. Therefore the

$$f_2(t) = F_{2f}(t) \quad , \quad t \geq 0 \quad . \tag{4.54}$$

The initial values of the berthing problem are given at $t = 0$ and read as:

$$\left.\begin{array}{ll} X_{2G}(0) = 0 \quad , & \dot{X}_{2G}(0) = V_2 = -v_A \ , \\ X_{2f}(0) = -\frac{1}{2}B \ , & f_2(0) = 0 \quad . \end{array}\right\} \tag{4.55}$$

Since there is no rotational motion at all, it is obvious that the absolute velocity of the ship's centre of gravity -on account of $(3.59^{a,b})$- becomes of the form

$$\dot{X}_{2G}(t) = -v_A + \dot{x}_2(t) \tag{4.56}$$

with $\dot{x}_2(t)$ given according to (3.51^b),

$$\dot{x}_2(t) = \int_0^t f_2(\tau)\ k_{22}(t-\tau)d\tau \quad . \tag{3.51^b}$$

The i.r.f. $k_{22}(t)$ to be applied is based on the (fixed) initial quay clearance as occurring at the moment of first contact between ship and fender.
The linear fender is represented by

$$F_{2f}(t) = \begin{cases} 0 & \text{for} \quad \Delta X_{2f}(t) > 0 \quad , \\ -c_0 \Delta X_{2f}(t) & \text{for} \quad \Delta X_{2f}(t) \leq 0 \quad . \end{cases} \tag{4.57}$$

Now it is possible to determine the fender force (and the ship trajectory), provided the relevant i.r.f. is known. The combined equations (4.53), (3.49), (4.54), (4.56) and (3.51^b) with initial conditions (4.55) and the fender characteristics given by (4.57) form a closed-loop system and represent the mathematical formulation of the berthing situation under consideration; (3.51^b) is an integro-differential equation.
The solution of the above set of equations is carried through following a similar numerical procedure as outlined in Section 3.4.2.

4.3.4. Examples of berthing operations: experiment and theory

4.3.4.1. Experimental set-up and model tests

Again an extensive series of model tests was carried out to verify the adequacy of the i.r.f.-technique for the simulation of berthing operations under conditions as described in Sections 1.3.4 and 4.3.3.

The experimental study was executed with a schematized ship model laterally berthing to a closed structure fitted with one single, linear fender, in water with respective depths amounting to 1.067, 1.167, 1.333 and 1.667 times the draught of the vessel. The ship model and the water depths were the same as in Section 4.3.1.2.1. With respect to the distance between ship model and (vertical) quay-wall at the moment of first contact between ship and fender two values were considered, viz. $d_{sq}/B = 0.115$ and $d_{sq}/B = 0.168$.

In the experiments the following quantities were measured as functions of the time: the deflexion of the fender (and so the fender load), the position of the ship's centre of gravity G and the angle of rotation of the ship's longitudinal plane of symmetry (merely to determine the lateral speed of approach and to check whether the ship model is moving into the X_1-direction and/or is rotating), the vertical motion of the water level in the quay clearance.

The experimental facility for the model tests was situated near a short side of the same rectangular basin where also the forced oscillation tests were carried out (see Section 4.3.1.2.1). Apart from the quay-wall and its connected provisions the same experimental set-up was applied as described in Section 3.4.3.1.

The test facility consisted of the following principal parts (the numbers refer to fig. 4.19):

1 - the schematized ship model;

2 - the straight, impervious (quay-)wall with vertical front side;

3 - the (linear) fender, mounted before a rectangular recess in the (quay-)wall in order to have some space available for its deflexion;

4 - an (open) structure fixed to the bottom of the basin behind the (quay-)wall, which acted as support for the fender; the value of d_{sq} could be varied by moving this structure into the Y-direction (= X_2-direction);

5 - a facility to give the ship model the proper lateral speed of approach;

6 - a device to lead the towing lines through the (quay-)wall with a minimum of friction and leakage of water;

7 - an open structure, fixed to the bottom of the basin, to fasten the ship in a fixed position when at rest; this fixed position acted as starting-position for the berthing operation;

8 - a 'position follower' to measure the 'X,Y-co-ordinates' of the ship's centre of gravity G;

9 - a facility mounted on the bottom of the ship model to measure the angle of rotation of the ship's longitudinal plane of symmetry;

10 - a wave height meter, situated at 0.45 m from the centre of the fender, to measure the vertical motion of the water level in the quay clearance.

The longitudinal plane of symmetry of the ship model in its starting-position was parallel to the breadthwise axis of symmetry of the basin as well as to the vertical quay-wall. The trajectory of the ship's centre of gravity before, during and after the contact between ship and fender coincided with the lengthwise axis of symmetry of the basin.

For a description of the 'position follower' and the facility to measure the rotation as well as for an explanation of their respective working principles and implications it is referred to Section 3.4.3.1.

In order to give the ship model the proper (constant) speed of approach the same procedure was followed as applied in the case of horizontally unrestricted water (see Section 3.4.3.1). In a number of cases it appeared to be slightly problematical to impose a constant velocity of approach onto the ship model. This was a consequence of the so-called 'cushioning effect' (i.e. the rise of the water level) in the quay clearance: the ship model -freely floating along a distance of about 0.10 m immediately before its first contact with the fender- somewhat slowed down when approaching the fender c.q. the quay-wall, especially in case of small water depths. With the values of d_{sq} applied this was, however, not a serious problem: from the test results it appeared that the speed of approach at the moment of first contact between ship and fender practically could be considered as being constant. The lateral speeds of approach applied in the tests were between 0.005 m s^{-1} and 0.03 m s^{-1}. Their actual values again were determined by (numerical) differentiation of the displacement of the ship's centre of gravity G in the 'Y-direction' as measured by the 'position follower'.

Three linear, undamped fenders were used, which were of the same type and working principle as described in Section 3.4.3.1; also the way of attaching the fender to its supporting structure was identical. The spring rates of the three linear fenders were c_0 = 4817 kg s^{-2} , c_0 = 2095 kg s^{-2} and

$c_0 = 1275\ kg\ s^{-2}$, respectively.

All signals were recorded simultaneously on paper chart.

4.3.4.2. Calculation of berthing operations

From the experiments test situations were selected for the numerical simulation of the berthing operations; starting-point was that they had to be in conformity with the conditions and the situation described in Sections 1.3.4 and 4.3.3. This implied that the calculations not only were carried out for the same schematized ship (model) and the same fenders as in the tests, but that also identical values were used for the (constant) lateral speed of approach, the water depth and d_{sq}. Since the ship model, the water depths and the values of d_{sq} were the same as applied in Section 4.3.2, in the numerical calculations use could be made of the relevant i.r.f. as determined at that place.

In the numerical simulation of the berthing operations the following quantities were calculated as functions of the time (see also fig. 4.18):
the velocity of the ship's centre of gravity G in the relevant (i.e. sway) direction, $\dot{X}_{2G}(t)$;
the relevant co-ordinate of the ship's centre of gravity G, $X_{2G}(t)$;
the deflexion of the fender, $\Delta X_{2f}(t)$;
the reaction force in the fender, $F_{2f}(t)$;
in the cases considered these quantities were determined only for the length of time, during which there was contact between ship and fender.
It could be shown that fluid reactive forces from viscous origin, with a form as given in Section 3.4.3.2, did not affect the results significantly.

In order to satisfy criterion (3.61) yielding a condition for the convergence of the computational scheme, the time step of the calculations, Δt, has to be smaller than 0.3 s. All calculations were carried out with a time step $\Delta t = 0.01$ s, since this led to a combination of accuracy and computing time which was as favourable as possible.

4.3.5. Presentation of results

Merely the most representative results of the model tests are given together with the corresponding results of the i.r.f.-technique.

Under the conditions mentioned, the berthing operation of the (schematized) ship to a certain fender can be described completely by the reaction force in the fender. Therefore, in the following only $F_{2f}(t)$ will be considered. Analogous to Section 3.4.4.1 this quantity is represented here in dimensionless form by

$$\frac{F_{2f}}{v_A\sqrt{c_0 \rho LBD}} = \text{dimensionless reaction force in the linear fender,}$$

while the results are presented as function of the dimensionless time

$$t\sqrt{\frac{c_0}{\rho LBD}} \quad .$$

N.B. Since the i.r.f.-technique as applied in this context does not yield results with respect to the vertical motions of the water level in the quay clearance, the quantity $\zeta_a(x_1,t)$ is left out of consideration here.

The parameters which further play a part in the presentation of the results are the (dimensionless) water depth, the (dimensionless) characteristic of the linear fender, the (dimensionless) distance between ship and quay-wall at the moment of first contact between ship and fender, and -for the model tests- the (dimensionless) lateral speed of approach.

Figs. 4.20 through 4.35 show a selection from the theoretical and experimental results: $F_{2f}v_A^{-1}(c_0\rho LBD)^{-1/2}$ versus $t\{c_0/(\rho LBD)\}^{1/2}$ with h/D, $c_0/(\rho g D^2)$ and d_{sq}/B as parameters. As could be expected on account of the application of the i.r.f.-technique, the calculated fender forces are proportional to the lateral speed of approach v_A. Within the range of values applied for v_A the experimental results also point that way. Further it can be seen from these figures that in case of increasing fender stiffness the (maximum value of the) fender force also increases, whereas the duration of the contact between ship and fender decreases and the point of time at which the fender force reaches its maximum occurs earlier. In case of a larger water depth the (maximum value of the) fender force as well as the duration of the contact between ship and fender is smaller, while the point of time at which the fender force reaches its maximum occurs earlier. These trends were also found with corresponding results for horizontally unrestricted water (see Section 3.4.4.2). An increase of the initial distance between ship and quay-wall, d_{sq}, results in a smaller (maximum value of the) fender force.

It has to be observed that the theoretical values for the duration of the contact between ship and fender are systematically too small, on the understanding that the experimental values are approximated better as the water depth increases.

In figs. 4.36 and 4.37 time histories of fender forces are presented for the combination $h/D = 1.067$, $d_{sq}/B = 0.115$ with $c_0/(\rho g D^2) = 21.831$ and $c_0/(\rho g D^2) = 5.778$, respectively; in these two figures the respective influences are shown of the horizontal velocity and the vertical acceleration in the quay clearance, and the friction effect in the underkeel region. It appears that especially the influence of the frictional effect in the keel clearance is significant, whereas the influences of the horizontal velocity and the vertical acceleration in the quay clearance are much less pronounced; the influence of the vertical acceleration in the quay clearance is even next to negligible. The results in case of zero underkeel friction seem to yield a better prediction for the duration of the contact between ship and fender.

Figs. 4.38 and 4.39 present the influence of the fender stiffness on the absorption of energy. These figures have come about in an analogous way as in Section 3.4.4.2, on the understanding that now also the (dimensionless) initial distance between ship and quay-wall plays a part. It has to be noted that the situation of an infinitely soft fender (i.e. $c_0 = 0$) cannot occur, since the deflexion of the fender always must be smaller than d_{sq}. As from a theoretical point of view the displacement of the ship (and therefore the deflexion of the fender) has to remain small with respect to the (initial) quay clearance, the results for very soft fenders should be considered with some reserve. Just as with horizontally unrestricted water -though to a less extent- it can be seen that a soft fender absorbs more energy to stop the ship than a stiff fender. Again this is due to the greater wave radiation in case of a stiffer fender. Further, in case of a smaller water depth or a smaller initial distance between ship and quay-wall the total amount of energy as absorbed by the linear fender increases.

4.4. Direct-time approach

4.4.1. General observations

The i.r.f.-technique as applied requires a time-invariant and linear ship-fluid system. With respect to the mathematical formulation of the hydrodynamic model this implies that merely linear(ized) terms can be taken into account; only the external (exciting) force(s) may be non-linear.

If the ship-fluid combination has to be considered as being essentially non-linear, in principle the ship-motion problem just as well can be dealt

with by a system approach, viz. by means of a non-linear i.r.f.-technique in which use is made of a Volterra series. Using a Volterra series, of which the respective kernels in addition to the ordinary i.r.f. are to be conceived as higher-order i.r.f., it is possible to characterize a non-linear process. The method of solution has the advantage of presenting a non-linear system as a rather straightforward generalization of the linear case; the higher-order i.r.f. are the kernels of the Volterra series expansion.
The main advantages of a Volterra-series approach to a non-linear system are its simplicity of structure, its generality and the relatively modest knowledge needed: with little more than knowledge of ordinary multi-dimensional Laplace transforms and the convolution integral it is possible to determine the kernels. The main disadvantages are the potential non-convergence of the Volterra series, the practical limitation to non-linearities of a rather simple structure, and the divergence in case of large input signals and/or large non-linearities.
To get an impression of the application of Volterra series to non-linear processes it is referred to refs. [118] through [120].

Because of the disadvantages associated with the Volterra-series representation of a non-linear process and the good deal of tedious work involved, this method is not applied. To get, nevertheless, an insight into the influence of non-linearities on the berthing of a schematized ship in the vicinity of a closed wall, an approach is followed of solving the ship-motion problem directly in the time domain.
Within the framework of this 'direct-time approach' (d.t.a.) -in a general sense- non-linearities (in the hydrodynamics) can be taken into account in an appropriate way. For reasons of simplicity the influence of the horizontal velocity in the quay clearance -as being of minor importance (see Section 4.3.5) - is left out of consideration, which actually implies a two-dimensional approach, or strip theory. Subject to this assumption the relevant berthing operations are simulated; the outcome is compared with the corresponding experimental results from Section 4.3 and discussed.

4.4.2. Mathematical approach

The general mathematical formulation in the time domain of the transverse motion of the schematized ship in shallow water alongside of and parallel to a vertical, closed wall is represented by the set of equations as recapitulated in Section 4.2.3. Deleting $\bar{u}_a(x_1,t)$, supposing independence of x_1 (i.e. strip theory) and using Blasius' law to model the underkeel friction these equations reduce to:

$$\left\{\frac{d_{sq}+x_2}{h-D} + f_{w_a}\frac{D}{B}\right\}\ddot{\zeta}_a + \left\{\frac{\dot{x}_2}{h-D} + \frac{g(d_{sq}+x_2)}{Bc_w}\right\}\dot{\zeta}_a + \frac{g}{B}\zeta_a =$$

$$= -D\left\{\frac{1}{h-D} + \frac{1}{2}f_{w_a}\frac{D}{B(d_{sq}+x_2)}\right\}\ddot{x}_2 + \frac{1}{2}f_{w_a}\frac{D^2}{B(d_{sq}+x_2)^2}\dot{x}_2^{\,2} +$$

$$- \frac{1}{h-D}\{X_0(t) + Y_0(t)\} - \frac{\lambda_b}{2B(h-D)^2} Z_0^2(t)\,\mathrm{sgn}\{Z_0(t)\} \quad , \qquad (4.58)$$

$$\left\{1 - \frac{1}{6}f_{w_a}\frac{D^2}{B(d_{sq}+x_2)}\right\}\ddot{x}_2 + \frac{1}{6}f_{w_a}\frac{D^2}{B}\frac{\dot{x}_2^{\,2}}{(d_{sq}+x_2)^2} =$$

$$= \frac{g}{B}\left\{\zeta_a + \frac{d_{sq}+x_2}{c_w}\dot{\zeta}_a + \frac{1}{2}f_{w_a}\frac{D}{g}\ddot{\zeta}_a\right\} - \frac{1}{D}X_0(t) + \frac{1}{\rho LBD}f_2(t) \;, \qquad (4.59)$$

with

$$X_0(t) = \alpha_t \frac{1}{(h-D)^2} Z_0^2(t)\,\mathrm{sgn}\{Z_0(t)\} \quad , \qquad (4.60^a)$$

$$Y_0(t) = \alpha_t \frac{1}{(h-D)^2}\{Z_0(t) - (h-D)\dot{x}_2\}^2 \mathrm{sgn}\{Z_0(t) - (h-D)\dot{x}_2\} \quad , \qquad (4.61^a)$$

$$Z_0(t) = (d_{sq}+x_2)\dot{\zeta}_a + h\dot{x}_2 \quad , \qquad (4.62)$$

$$\alpha_t = \begin{cases} \dfrac{12}{Re} & \text{for} \quad Re \leq 2300 \quad , & (4.11^a) \\[2ex] \dfrac{1}{8}\dfrac{0.3164}{Re^{1/4}} & \text{for} \quad 2300 < Re < 10^6 \quad , & (4.11^b) \end{cases}$$

$$Re = \frac{2|\bar{v}_b|(h-D)}{\nu} \quad , \qquad (4.12)$$

$$\lambda_b = 1.44 \quad , \tag{4.14^b}$$

and $\bar{v}_b(t)$ to be determined from

$$(d_{sq} + x_2)\dot{\zeta}_a + D\dot{x}_2 + (h-D)\bar{v}_b = 0 \quad ; \tag{4.63}$$

the terms containing the real time functions $X_0(t)$ and $Y_0(t)$ can be conceived as representing the underkeel friction effect.
Substitution of α_t into (4.60^a) and (4.61^a) using a Reynolds number adapted to the specific form of $X_0(t)$ and $Y_0(t)$, respectively, yields in case of laminar flow in the underkeel region

$$\left.\begin{aligned} X_0(t) &= f_l \frac{6\nu}{(h-D)^2} Z_0(t) \quad , && (4.60^b) \\ Y_0(t) &= f_l \frac{6\nu}{(h-D)^2}\{Z_0(t) - (h-D)\dot{x}_2\} \quad , && (4.61^b) \end{aligned}\right\} \text{ for } \quad Re \leqq 2300 \ ,$$

and in case of turbulent flow

$$\left.\begin{aligned} X_0(t) &= f_t \frac{0.03326\ \nu^{1/4}}{(h-D)^2}\left|Z_0(t)\right|^{7/4}\mathrm{sgn}\{Z_0(t)\} \ , && (4.60^c) \\ Y_0(t) &= f_t \frac{0.03326\ \nu^{1/4}}{(h-D)^2}\left|Z_0(t) - (h-D)\dot{x}_2\right|^{7/4} \cdot \\ &\qquad \cdot \mathrm{sgn}\{Z_0(t) - (h-D)\dot{x}_2\} \ , && (4.61^c) \end{aligned}\right\} \text{ for } \quad 2300 < Re < 10^6;$$

f_l and f_t are multiplication factors (with standard values $\equiv 1$) in order to be able to modify -if necessary- the underkeel friction effect in the respective cases of a laminar and turbulent flow regime. The transition between both regimes is supposed to take place at a Reynolds number Re = 2300 with Re defined as:

$$Re = 2\nu^{-1}\left|\bar{v}_b - \tfrac{1}{2}\dot{x}_2\right|(h-D) = \nu^{-1}\left|2Z_0(t) - (h-D)\dot{x}_2\right| \quad . \tag{4.64}$$

The external forcing function upon the ship again is the (linear) fender force, now -on the analogy of (4.53), (3.49), (4.54) and (4.57) combined- to be represented by

$$f_2(t) = F_{2f}(t) = \begin{cases} 0 & \text{for} \quad x_2(t) > 0\ , \\ -c_0 x_2(t) & \text{for} \quad x_2(t) \leqq 0\ . \end{cases} \tag{4.65}$$

The initial values of the problem are:

$$\left.\begin{aligned} \zeta_a(0) &= 0\ , & \dot{\zeta}_a(0) &= 0\ , \\ x_2(0) &= 0\ , & \dot{x}_2(0) &= -v_a\ . \end{aligned}\right\} \tag{4.66}$$

The equations (4.58), (4.59) and (4.65) combined, with initial conditions (4.66), now have to be solved for the case that the underkeel friction effect is modelled in conformity with ($4.60^{b,c}$) and ($4.61^{b,c}$).

In order to facilitate the further procedure (4.58) and (4.59) are linked up to:

$$\begin{aligned} \left\{\frac{d_{sq} + x_2}{h - D} + \frac{1}{2} f_{w_a} \frac{D}{B}\right\}\ddot{\zeta}_a + \frac{\dot{x}_2}{h - D}\dot{\zeta}_a = &- \left\{1 + \frac{D}{h-D} + \frac{1}{3} f_{w_a} \frac{D^2}{B(d_{sq} + x_2)}\right\}\ddot{x}_2 + \\ &+ \frac{1}{3} f_{w_a} \frac{D^2}{B(d_{sq} + x_2)^2}\dot{x}_2{}^2 - \frac{1}{h-D}\{X_0(t) + Y_0(t)\} - \frac{1}{D} X_0(t) + \\ &- \frac{\lambda_b}{2B(h-D)^2} Z_0^2(t)\ \mathrm{sgn}\{Z_0(t)\} + \frac{1}{\rho LBD} f_2(t). \end{aligned} \tag{4.67}$$

Combination of (4.58) and (4.67) finally leads to the expressions:

$$\ddot{x}_2 = \frac{-g_2(t)\ P_0(t) + g_1(t)\ Q_0(t)}{g_1(t)\ g_4(t) - g_2(t)\ g_3(t)}\ , \tag{4.68^a}$$

$$\ddot{\zeta}_a = \frac{g_4(t)\ P_0(t) - g_3(t)\ Q_0(t)}{g_1(t)\ g_4(t) - g_2(t)\ g_3(t)}\ , \tag{4.69^a}$$

where $P_0(t)$, $Q_0(t)$ = function of x_2, $\dot{x}_2$, ζ_a, $\dot{\zeta}_a$,
$g_1(t)$, $g_2(t)$, $g_3(t)$, $g_4(t)$ = function of x_2 ,
with the respective form

$$P_0(t) = -\left\{\frac{g(d_{sq}+x_2)}{Bc_w} + \frac{\dot{x}_2}{h-D}\right\}\dot{\zeta}_a - \frac{g}{B}\zeta_a + \frac{1}{2}g_5(t)\,\dot{x}_2^{\,2} +$$

$$- \frac{1}{h-D}\{X_0(t) + Y_0(t)\} - \frac{\lambda_b}{2B(h-D)^2} Z_0^2(t)\,\mathrm{sgn}\{Z_0(t)\} ,$$

$$Q_0(t) = -\frac{\dot{x}_2\dot{\zeta}_a}{h-D} + \frac{1}{3}g_5(t)\,\dot{x}_2^{\,2} - \frac{1}{h-D}\{X_0(t) + Y_0(t)\} - \frac{1}{D}X_0(t) +$$

$$- \frac{\lambda_b}{2B(h-D)^2} Z_0^2(t)\,\mathrm{sgn}\{Z_0(t)\} + \frac{1}{\rho LBD} f_2(t) ,$$

$$g_1(t) = \frac{d_{sq}+x_2}{h-D} + f_{w_a}\frac{D}{B} ,$$

$$g_2(t) = \frac{d_{sq}+x_2}{h-D} + \frac{1}{2}f_{w_a}\frac{D}{B} ,$$

$$g_3(t) = \frac{D}{h-D} + \frac{1}{2}f_{w_a}\frac{D^2}{B(d_{sq}+x_2)} ,$$

$$g_4(t) = 1 + \frac{D}{h-D} + \frac{1}{3}f_{w_a}\frac{D^2}{B(d_{sq}+x_2)} ,$$

$$g_5(t) = f_{w_a}\frac{D^2}{B(d_{sq}+x_2)^2} ;$$

further, $X_0(t)$ and $Y_0(t)$ are represented by (4.60^{b,c}) and (4.61^{b,c}), respectively, and $Z_0(t)$ is given by (4.62), while $\lambda_b = 1.44$ according to (4.14^b).

For the sake of completeness the linearized forms of (4.68^a) and (4.69^a) are presented just as well. Linearization with regard to terms containing combinations of x_2 and $\dot{\zeta}_a$ and/or their respective derivatives yields:

$$\ddot{x}_2 = \frac{-g_2^* P_0^*(t) + g_1^* Q_0^*(t)}{g_1^* g_4^* - g_2^* g_3^*} \quad , \tag{4.68^b}$$

$$\ddot{\zeta}_a = \frac{g_4^* P_0^*(t) - g_3^* Q_0^*(t)}{g_1^* g_4^* - g_2^* g_3^*} \quad , \tag{4.69^b}$$

with

$$P_0^*(t) = - \frac{gd_{sq}}{Bc_w} \dot{\zeta}_a - \frac{g}{B} \zeta_a - \frac{1}{h-D}\{X_0^*(t) + Y_0^*(t)\} \quad ,$$

$$Q_0^*(t) = - \frac{1}{h-D}\{X_0^*(t) + Y_0^*(t)\} - \frac{1}{D} X_0^*(t) + \frac{1}{\rho LBD} f_2(t) \quad ,$$

$$g_1^* = \frac{d_{sq}}{h - D} + f_{w_a} \frac{D}{B} \quad ,$$

$$g_2^* = \frac{d_{sq}}{h - D} + \frac{1}{2} f_{w_a} \frac{D}{B} \quad ,$$

$$g_3^* = \frac{D}{h-D} + \frac{1}{2} f_{w_a} \frac{D^2}{Bd_{sq}} \quad ,$$

$$g_4^* = 1 + \frac{D}{h-D} + \frac{1}{3} f_{w_a} \frac{D^2}{Bd_{sq}} \quad ,$$

$$\left.\begin{aligned} X_0^*(t) &= f_1 \frac{6\nu}{(h-D)^2} Z_0^*(t) \quad , && (4.70) \\ Y_0^*(t) &= f_1 \frac{6\nu}{(h-D)^2}\{Z_0^*(t) - (h-D)\dot{x}_2\} \quad , && (4.71) \end{aligned}\right\}$$

$$Z_0^*(t) = d_{sq}\dot{\zeta}_a + h\dot{x}_2 \quad ; \tag{4.72}$$

the superscript * indicates that the quantity concerned is a linearized version of its original.

The two sets of differential equations (4.68^a),(4.69^a) and (4.68^b), (4.69^b) -each with $f_2(t)$ given by (4.65) and with initial conditions (4.66)- are to be solved numerically.

The initial condition for $\zeta_a(t)$ as stated in (4.66), viz. $\zeta_a(0) = 0$, actually has to be considered as an approximative value. It is possible, however, to give a better estimate of $\zeta_a(0)$.

A constant, lateral speed of approach of the ship towards the berth, i.e.

$$\dot{x}_2(t) = -v_A \quad \text{for} \quad t \leq 0 \quad ,$$

supposes a steady state for which it holds good that

$$\bar{v}_b = - \frac{D}{h-D} \dot{x}_2 \qquad \text{with} \qquad \dot{x}_2 = -v_A \quad .$$

Under these circumstances there is a difference in water level across the ship: the water level at the side of the ship nearest the berth is higher. The loss of energy head in the underkeel region due to contraction and separation of flow is (see (4.13)):

$$H_{2,b} = \lambda_b \frac{(\bar{v}_b - \dot{x}_2)|\bar{v}_b - \dot{x}_2|}{2g} \qquad \text{with} \qquad \lambda_b = 1.44 \quad ;$$

the loss of energy head due to the friction in the keel clearance can be written as (see (4.10^b)):

$$\frac{R_{2,b}}{g} = \alpha_t \frac{B}{g(h-D)}\{(\bar{v}_b - \dot{x}_2)|\bar{v}_b - \dot{x}_2| + \bar{v}_b|\bar{v}_b|\} \quad .$$

Introduction of α_t as given by ($4.11^{a,b}$) -again using an adapted Reynolds number- yields in case of laminar flow in the underkeel region

$$\frac{R_{2,b}}{g} = \frac{12\nu B}{g(h-D)^2} (\bar{v} - \tfrac{1}{2}\dot{x}_2) \qquad \text{for} \quad Re \leq 2300 \quad ,$$

and in case of turbulent flow

$$\frac{R_{2,b}}{g} = \frac{0.03326 \; B\nu^{1/4}}{g(h-D)^{5/4}} \{|\bar{v}_b - \dot{x}_2|^{7/4}\mathrm{sgn}(\bar{v}_b - \dot{x}_2) + |\bar{v}_b|^{7/4}\mathrm{sgn}(\bar{v}_b)\}$$

$$\text{for} \quad 2300 < Re < 10^6 .$$

The total loss of energy head in the underkeel region during the steady state before the first contact between ship and fender now is

$$H_{2,b} + \frac{R_{2,b}}{g} \quad .$$

If $(H_{2,b} + R_{2,b}/g) \ll h$ one thing and another implies that this total loss of energy head can be applied as an estimate for the elevation of the water level at that side of the ship which is the nearest to the berth, so that the actual value of the initial condition for $\zeta_a(t)$ becomes:

$$\zeta_a(0) = H_{2,b} + \frac{R_{2,b}}{g} \quad . \qquad (4.73^a)$$

Elimination of $\bar{v}_b$ and $\dot{x}_2$ finally yields for $\zeta_a(0)$

$$\zeta_a(0) = \lambda_b \frac{h^2}{(h-D)^2} \frac{v_A^2}{2g} + \frac{6\nu B(h+D)}{g(h-D)^3} v_A \quad , \quad \lambda_b = 1.44 \quad , \text{ for } \quad Re \leqq 2300, \qquad (4.73^b)$$

and

$$\zeta_a(0) = \lambda_b \frac{h^2}{(h-D)^2} \frac{v_A^2}{2g} + \frac{0.03326\ B\nu^{1/4}}{g(h-D)^3} (h^{7/4} + D^{7/4}) v_A^{7/4} \quad , \ \lambda_b = 1.44,$$

$$\text{for} \quad 2300 < Re < 10^6, \qquad (4.73^c)$$

where -according to (4.64)- Re is defined as:

$$Re = \frac{(h+D)v_A}{\nu} \quad . \qquad (4.74)$$

4.4.3. Calculation of berthing operations

The numerical solution of the set of differential equations (4.68^a) and (4.69^a), with $f_2(t)$ given by (4.65) and with initial conditions (4.66), is carried through by means of a fourth-order Runge-Kutta computational scheme (see ref. [109]). The underkeel friction effect is introduced in conformity with ($4.60^{b,c}$) and ($4.61^{b,c}$), where the distinction between laminar and turbulent flow is based on a critical Reynolds number Re = 2300, with Re defined by (4.64). The calculation is finished at the point of time the ship loses its contact with the fender; this is the case when $x_2(t)$ becomes zero and $\dot{x}_2(t) > 0$.

The set of linearized differential equations (4.68^b) and (4.69^b) -again with $f_2(t)$ and the initial conditions according to (4.65) and (4.66), respectively- is solved in an identical way.

For the numerical simulation of the berthing operations the same (test) situations were chosen as in Section 4.3.4.2. The following quantities were calculated as functions of the time:
the velocity of the ship's centre of gravity G in the sway direction, $\dot{x}_2(t)$;
the relevant co-ordinate of G, $x_2(t)$;
the deflexion of the fender, $x_2(t) = \Delta X_{2f}(t)$;
the reaction force in the fender, $f_2(t) = F_{2f}(t)$;
the elevation of the water surface in the quay clearance with respect to the mean water level, $\zeta_a(t)$;
in the cases considered these quantities were determined only for the length of time during which there was contact between ship and fender.

For all calculations a time step $\Delta t = 0.01$ s was found to be more than adequate to give reliable results without taking too much computing time.

4.4.4. Presentation of results

For the numerical simulation the same berthing situations were selected as used in applying the i.r.f.-technique: the results of the model tests already given in Section 4.3.5 now are presented together with the corresponding calculational results of the d.t.a. In addition to the displacement and the velocity of the ship, the deflexion of the fender and the fender force, now also $\zeta_a(t)$ can be calculated. Further, the same parameters apply as in Section 4.3.5, on the understanding that each berthing situation has to be calculated with its own specific lateral speed of approach, since in the d.t.a. non-linear effects are taken into account.
The representation of the time history of the reaction force in the (linear) fender is identical to that in Section 4.3.5; the time history of the water-surface elevation in the quay clearance is represented -likewise as function of the dimensionless time- by

$\frac{\zeta_a}{v_A}\sqrt{\frac{c_0}{\rho LBD}}$ = dimensionless elevation of the water surface in region a with respect to the mean water level.

In addition to the experimental results which are plotted as centred symbols, the figures to be presented each show three curves:
- the full line and the dashed line represent the results as calculated from the d.t.a. taking into account non-linearities, for two different lateral speeds of approach: the full line refers to a lower value of v_A than the

dashed line;

- the dot-and-dash line represents the results as calculated from the linearized version of the d.t.a.

By means of an appropriate choice for the values of the respective multiplication factors f_l and f_t, for each combination of water depth and fender stiffness, the influence of the underkeel friction was adapted such that the theoretical results in broad outline fit the experimental results. For the sake of simplicity a choice was made for $f_l = f_t$. In the linear version of the d.t.a. the same value of f_l was applied as in the non-linear version.

Figs. 4.40 through 4.55 show the theoretical and experimental results: $F_{2f}v_A^{-1}(c_0\rho LBD)^{-1/2}$ and $\zeta_a v_A^{-1}\{c_0/(\rho LBD)\}^{1/2}$ versus $t\{c_0/(\rho LBD)\}^{1/2}$ with h/D, $c_0/(\rho g D^2)$, d_{sq}/B and $v_A/(gh)^{1/2}$ as parameters. As could be expected, $F_{2f}(t)$ and $\zeta_a(t)$, as calculated from the non-linear version, generally are not proportional to v_A; naturally the principle of proportionality does hold good for the linearized version. Within the range of values applied for v_A, the test results -as already observed in Section 4.3.5- do point in the direction of proportionality to this quantity. Further it can be seen from these figures that the behaviour of $F_{2f}(t)$ when varying c_0, h and d_{sq}, shows the same trends as found with applying the i.r.f.-technique (see Section 4.3.5); the same was observed in the case of ship berthing on horizontally unrestricted water, but then with regard to c_0 and h (see Section 3.4.4.2). The (minimum) value of $\zeta_a(t)$ falls with increasing c_0 and decreasing d_{sq} and shows a rising trend in case of larger h. As far as the non-linear version of the d.t.a. is concerned, a larger lateral speed of approach -within the range of values applied- leads to a smaller (maximum value of the) dimensionless fender force and an increase of the (minimum value of the) dimensionless water-surface elevation in the quay clearance. Although the theoretical curves show the same trend as the experimental results, now the theoretical values for the duration of the contact between ship and fender are systematically too large; but again, just as with applying the i.r.f.-technique, a larger water depth yields a better approximation.

In figs. 4.56 through 4.59 time histories are presented of fender forces and water-surface elevations in the quay clearance for the combination $h/D = 1.067$, $d_{sq}/B = 0.115$ with $c_0/(\rho g D^2) = 21.831$ and $c_0/(\rho g D^2) = 5.778$, respectively; in these figures the influences are shown of the vertical acceleration in the quay clearance as well as of the friction in the keel clearance and the underkeel contraction and flow separation. Figs. 4.56 and 4.57

refer to the non-linear version of the d.t.a. and figs. 4.58 and 4.59 to the linearized version. It appears that especially the underkeel frictional effect is significant, whereas the respective influences of the vertical acceleration in the quay clearance and the contraction and flow separation in the underkeel region are much less pronounced.

The observations above apply to all values of h, c_0, d_{sq} and v_A investigated.

Starting from the linearized version of the d.t.a., in Appendix M a rough estimation is made of the main (circular) frequencies playing a part in the berthing-ship phenomenon. Calculations showed that all suppositions and assumptions made are acceptable. It appears that the circular frequency ω_I (see $(M.12^b)$) indeed corresponds with a period time approximately equalling twice the duration of the contact between ship and fender; the other circular frequency, ω_{II} (see $(M.14^b)$) -if perceptible- can be discerned as a faster, small oscillation on the curves representing the time histories of $F_{2f}(t)$ and, particularly, $\zeta_a(t)$. This oscillation comes through the more explicitly as the fender stiffness is larger and is primarily caused by the inertia of the fluid in quay clearance and underkeel region.
Further, calculation of the berthing operations using an initial condition $\zeta_a(0) \neq 0$ as evaluated by $(4.73^{b,c})$ does not yield substantially differing results; for the berthing situations under discussion this could already be expected on account of the form of these very formulae. As a matter of fact, the experimental values of $\zeta_a(0)$ were also found to be approximately equal to zero and to fall as such within the accuracy of the measurements.

4.5. Discussion and conclusions

With regard to the simulation of ship berthing to a closed fender structure the same general observations on the experiments apply as in Section 3.5.1. Only the enumeration of the experimental errors now has to be completed with two items, viz.:

- the perviousness of the straight, vertical wall representing the closed front of the berth, and
- the possibility that the line of action of the fender is not precisely perpendicular to the front side of the vertical quay-wall.

The general remarks in Section 3.5.1 relating to the accuracy of the mathematical description of the berthing-ship phenomenon also hold in this case.

Concerning the application of the i.r.f.-technique it generally can be stated that both the qualitative and the quantitative agreement between theory and experiment is satisfactory, if anyhow use is made of i.r.f. determined from theoretical data for the hydrodynamic coefficients inclusive of (linear) friction in the underkeel region. Especially the leading slope of the fender force as function of time, its peak value and the point of time at which it reaches its maximum are predicted well; the theoretical values for the duration of the contact between ship and fender are systematically too small. The influences of the horizontal velocity and the vertical acceleration in the quay clearance are not at all predominant and could be left out of consideration.

With respect to the d.t.a. it can be put that in case of a properly modelled underkeel friction the theoretical results are in satisfactory agreement with the experiments: leading slope and peak value of the fender force are represented reasonably well, the descending rear side shows a less convincing agreement: the theory yields lengths of time of contact between ship and fender being systematically too large. In judging the theoretical results for ζ_a it has to be considered that the influence of the strip theory on the vertical motion of the water surface in the quay clearance is relatively strong. The respective influences of the vertical acceleration in the quay clearance and the contraction and separation of flow in the underkeel region are small and could be neglected. In comparison with the non-linear version of the d.t.a. the linearized version shows consistently conservative values for $F_{2f}(t)$ and $\zeta_a(t)$, but -within the range of values applied for v_A- the effect of the non-linearities can be considered to be small.

With the d.t.a., the friction formula used in the underkeel region actually applies only to steady flow with fully developed boundary layers between parallel smooth walls. During berthing operations, however, the underkeel water motion has a transient character, which implies developing thin boundary layers with large velocity gradients not influenced by the height of the keel clearance. As the boundary layer controls the shear stress, this explains why the values of f_l,f_t as chosen for curve fitting differ substantially from their standard value 1 and grow larger with increasing h (and c_0). Moreover, it must be recognized that calibrating the theory with experimental results in terms of the selection of the friction factors covers any errors arising from the two-dimensional approach adopted and other theoretical (and experimental) imperfections in addition to its effect on the underkeel friction. In Appendix

N an attempt is made to derive a more appropriate expression for the shear stress in the underkeel region in case of transient fluid motion.

The experimental and theoretical results demonstrate that application of both the i.r.f.-technique and the d.t.a. can provide a workable foundation for the description and the determination of the relevant quantities which figure in the problem of a ship berthing to some closed structure fitted with (linear) fenders.

A basic linearity-assumption yields a practical approximation in case the transient displacements of the (schematized) ship (model) remain small with respect to the initial quay clearance.

5. CONCLUSIONS

The description of a ship berthing to an open or a closed fender structure as well as the determination of the associated fender forces necessitates a time-domain approach, in which the fluid reactive forces are represented in an appropriate way and the remaining forces are taken into account over their entire time histories. The mathematical formulations presented refer primarily to ship motions in the horizontal plane. As such they satisfy the above requirements and enable the inclusion of external forces of arbitrary nature; this implies that the fenders may be damped, undamped, linear or non-linear, and also may have a mass of their own. A practical and sufficiently accurate foundation is provided for the description and determination of the relevant quantities figuring in ship berthing.

The respective mathematical approaches are applied to the simplified case of a schematized ship, that on calm, shallow water at zero forward speed berthes to an open jetty-type structure or a closed, straight, vertical quay-wall, each fitted with one undamped, (non-)linear fender without mass of its own. For verification experiments were carried out on a scale model.

In case of ship berthing to the open fender structure both centric and eccentric impacts are considered. This berthing situation is tackled by means of the i.r.f.-technique, which has the restrictions that the ship-fluid system is supposed to be linear and time-invariant; the (linear) fluid reactive forces then are described by way of the frequency-dependent hydrodynamic coefficients. Underkeel friction appears to be of secondary importance. Comparison of theoretical and experimental results for the time histories of fender force and ship motion shows a good agreement. For a first estimation of the maximum value of the fender force use can be made of a long-wave approximation for the motion of the water.

With regard to ship berthing to the closed fender structure only centric impacts are dealt with. Two methods are used, namely the i.r.f.-technique and a d.t.a., both of them ensueing from the same mathematical model. Application of the i.r.f.-technique now leads to satisfactory results only if underkeel friction is incorporated in the hydrodynamic coefficients; similarly, the d.t.a. is merely able to present a satisfactory agreement between theory and experiment provided that the underkeel friction, at least, is modelled properly. In the quay clearance the influence of the (longitudinal) horizontal velocity is not very pronounced and the vertical acceleration plays a minor part. An option of the d.t.a. is that (hydrodynamic) non-linearities can be taken into account; however, their influence is small.

For both berthing situations, the respective mathematical formulations presented are sufficiently accurate for the qualitative and quantitative description of the typical behaviour of a berthing ship as well as for the determination of the response of the fender(s). The calculated results from berthing simulations are in satisfactory agreement with values obtained from measurements on a scale model, especially up to the point of time where the maximum value of the fender force is reached: leading slope and peak value of the fender force are predicted well. This applies for all water depths, fender stiffnesses, eccentricities of the fender force (, initial clearances between ship and quay-wall) and lateral speeds of approach investigated.

Further, the assumption of linearity for the ship-fluid system in both berthing situations appears to yield a very well acceptable and practical approximation for the quantitative analysis of transient motions of shiplike bodies.

Viscous effects of the fluid do not influence significantly the relevant quantities that play a part in berthing.

REFERENCES

1. Rupert, D.
'Zur Bemessung und Konstruktion von Fendern und Dalben', Mitteilungen des Franzius-Instituts für Wasserbau und Küsteningenieurwesen der Technischen Universität Hannover, H. 44, Hannover, 1976, pp. 112-288.

2. Report of the International Commission for Improving the Design of Fender Systems, P.I.A.N.C., suppl. to Bull. No. 45, 1984.

3. Pagès, M.
'Etude mécanique du choc se produisant lors de l'accostage d'un navire à un quai', Annales des Ponts et Chaussées, 122^{e} année, mars-avril 1952, pp. 205-217.

4. Eggink, A.
XVIIIth Intern. Navigation Congress, P.I.A.N.C., Rome, 1953, S.II-2, pp. 167-187.

5. Grim, O.
'Das Schiff und der Dalben', Schiff und Hafen, H. 9, 1955, pp. 535-545.

6. Abbett, W./Levington, Z.
'Design and construction of terminals for large ships', XXth Intern. Navigation Congress, P.I.A.N.C., Baltimore, 1961, S.II-1, pp. 307-328.

7. Gillespie, J.H.H./et al.
XXth Intern. Navigation Congress, P.I.A.N.C., Baltimore, 1961, S.II-1, pp 89-118.

8. Greco, L./et al.
XXth Intern. Navigation Congress, P.I.A.N.C., Baltimore, 1961, S.II-1, pp. 131-155.

9. Woodruff, G.B.
'Berthing and mooring forces', Journ. of the Waterways and Harbors Division, Proc. A.S.C.E., Vol. 88, No. WW1, Febr. 1962, pp. 71-82. Discussion: idem, Vol. 88, No. WW3, Aug. 1962, pp. 189-193.

10. Saurin, B.F.
'Berthing forces of large tankers', Proc. of the Sixth World Petroleum Congress, Frankfurt/Main, 1963, S.VII, Paper 10, pp. 63-73.

11. Vasco Costa, F.
'The berthing ship. The effect of impact on the design of fenders and other structures', The Dock & Harbour Authority, Vol. XLV, Nos. 523, 524,

525, May, June, July 1964, pp. 22-26, 49-52, 90-94.

12. Proc. of the NATO Advanced Study Institute on 'Analytical treatment of problems of Berthing and Mooring Ships', Lisbon, 1965 (publ. A.S.C.E., New York, 1970).

13. Giraudet, P.
'Recherches expérimentales sur l'énergie d'accostage des navires', Annales des Ponts et Chaussées, 136^{e} année, no. II, mars-avril 1966, pp. 103-127.

14. Tyrrell, B.G.
'Mooring dolphins. Evaluation of forces and principles of design', The Dock & Harbour Authority, Vol. XLVII, No. 550, August 1966, pp. 115-120, No. 551, Sept. 1966, pp. 161-166.

15. Vasco Costa, F.
'Berthing manoeuvres of large ships', The Dock & Harbour Authority, Vol. XLVII, No. 569, March 1968, pp. 351-358.

16. Lee, T.T.
'Design criteria recommended for marine fender systems', Proc. 11th Conf. on Coastal Engineering, London, 1968 (publ. A.S.C.E., 1969, Part 3, pp. 1159-1184).

17. Nagai, S./et al.
'Impacts exerted on the dolphins of sea-berths by roll, sway and drift of supertankers subjected to waves and swells', XXIInd Intern. Navigation Congress, P.I.A.N.C., Paris, 1969, S.II-3, pp. 63-90.

18. Reese, L.C./et al.
'Rational design concept for breasting dolphins', Journ. of the Waterways and Harbors Division, Proc. A.S.C.E., Vol. 96, No. WW2, May 1970, pp. 433-450.

19. Shu-t'ien Li/Venkataswamy Ramakrishnan
'Ultimate energy design of prestressed concrete fender piling', Journ. of the Waterways, Harbors and Coastal Engineering Division, Proc. A.S.C.E., Vol. 97, No. WW4, Nov. 1971, pp. 647-662.

20. Komatsu, S./Salman, A.H.
'Dynamic response of the ship and the berthing fender system after impact', Trans. Japanese Soc. of Civil Engineers, Vol. 4, 1972, pp. 18-19.

21. Papers presented at NATO Advanced Study Institute on 'Analytical treatment of problems in the berthing and mooring of ships', Wallingford, 1973

(publ. Hydraulics Research Station, Wallingford, U.K.).

22. Sakharov, S.M./et al.
XXIIIrd Intern. Navigation Congress, P.I.A.N.C., Ottawa, 1973, S.II-1, pp. 289-311.

23. Taubert, A.
'Belastung von Bauwerken durch Schiffsstosz', HANSA, 110, No. 21, 1973, pp. 1864-1868.

24. Dubois, J./Langlet, M.
'Etudes relatives aux conditions d'accostage et d'amarrage au terminal d'Antifer', 6th Intern. Harbour Congress, Antwerpen, 1974, S.2.29, pp. 2.29/1-2.29/6.

25. Lee, T.T./et al.
'On the determination of impact forces, mooring forces and motions of supertankers at marine terminal', 7th Annual Offshore Technology Conf., Houston, 1975, Paper OTC 2211, pp. 661-678.

26. Fischer, J.
'Conception of the fendering systems for the (very) large ships berthing', 24th Intern. Navigation Congress, P.I.A.N.C., Leningrad, 1977, S.II-4, pp. 15-31.

27. Wirsbitzki, B.
'Criteria for economical design of fender systems', 24th Intern. Navigation Congress, P.I.A.N.C., Leningrad, 1977, S.II-4, pp. 33-46.

28. Patrick, J.G.
'The design of jetties for large ships', Trans. Inst. Mar. Engrs. (C), Vol. 92, Conf. no. 6, 1980, Paper C48, pp. 19-24.

29. Nikerov, P.S./et al.
'Improving the methods of determining the loads applied by berthing ships, the effect of wave disturbance, and examination of flexible fender systems', XXVth Intern. Navigation Congress, P.I.A.N.C., Edinburgh, 1981, S.II, Vol. I, Pergamon Press, Oxford, 1981, pp. 195-208.

30. Callet, P.
XVIIIth Intern. Navigation Congress, P.I.A.N.C., Rome, 1953, S.II-Q.2, pp. 87-109.

31. Visioli, F./et al.
XVIIIth Intern. Navigation Congress, P.I.A.N.C., Rome, 1953, S.II-2, pp. 143-165.

32. Girgrah, M.
'Practical aspects of dock fender design', 24th Intern. Navigation Congress, P.I.A.N.C., Leningrad, 1977, S.II-4, pp. 5-14.

33. Brolsma, J.U./et al.
'On fender design and berthing velocities', 24th Intern. Navigation Congress, P.I.A.N.C., Leningrad, 1977, S.II-4, pp. 87-100.

34. Piaseckyj, P.J.
'Fender design in North America for large ships .....', 24th Intern. Navigation Congress, P.I.A.N.C., Leningrad, 1977, S.II-4, pp. 133-145.

35. Leclercq, R.
'Résultats d'essais sur modèles réduits de dérive latérale des navires', Annales des Ponts et Chaussées, 130[e] année, mars-avril 1960, pp. 181-215.

36. Deschennes, H./Dubois, J.
XXth Intern. Navigation Congress, P.I.A.N.C., Baltimore, 1961, S.II-1, pp. 65-88.

37. Blok, J.J./Dekker, J.N.
'On hydrodynamic aspects of ship collision with rigid or non-rigid structures', 11th Annual Offshore Technology Conf., Houston, 1979, Proc. Vol. IV, Paper OTC 3664, pp. 2683-2697.

38. Yu, Y.S./Ursell, F.
'Surface waves generated by an oscillating circular cylinder on water of finite depth: theory and experiment', Journ. of Fluid Mech., Vol. 11, 1961, pp. 529-551.

39. Newman, J.N.
'The damping of an oscillating ellipsoid near a free surface', Journ. of Ship Research, Vol. 5, No. 3, Dec. 1961, pp. 44-58.

40. Joosen, W.P.A.
'Slender body theory for an oscillating ship at forward speed', Proc. 5th O.N.R. Symp. on Naval Hydrodynamics, Bergen, 1964, pp. 167-183.

41. Newman, J.N./Tuck, E.O.
'Current progress in the slender body theory for ship motions', Proc. 5th O.N.R. Symp. on Naval Hydrodynamics, Bergen, 1964, pp. 129-166.

42. Leeuwen, G. van
'The lateral damping and added mass of a horizontally oscillating ship model', Rep. no. 65S, Netherlands Research Centre T.N.O. for Shipbuilding and Navigation, Delft, The Netherlands, Dec. 1964.

43. Vugts, J.H.
'The hydrodynamic coefficients for swaying, heaving and rolling cylinders in a free surface', Rep. no. 112S, Netherlands Ship Research Center T.N.O., Shipbuilding Department, Delft, The Netherlands, May 1968.

44. Tasai, F./Kim, C.H.
'Effect of shallow water on the natural period of heave', Reports of Research Institute for Applied Mechanics, Kyushu University, Japan, Vol. XVI, No. 54, 1968, pp. 223-229.

45. Kim, C.H.
'Hydrodynamic forces and moments for heaving, swaying, and rolling cylinders on water of finite depth', Journ. of Ship Research, Vol. 13, No. 3, June 1969, pp. 137-154.

46. Vugts, J.H.
'The hydrodynamic forces and ship motions in waves', Thesis Delft University of Technology, Uitgeverij Waltman, Delft, The Netherlands, 1970.

47. Garrison, C.J.
'Hydrodynamics of large objects in the sea. Part I - Hydrodynamic analysis', Journ. of Hydronautics, Vol. 8, No. 1, Jan. 1974, pp. 5-12.

48. Keil, H.
'Die hydrodynamische Kräfte bei der periodischen Bewegung zweidimensionaler Körper an der Oberfläche flacher Gewässer', Institut für Schiffbau der Universität Hamburg, B.R.D., Bericht Nr. 305, Febr. 1974.

49. Garrison, C.J.
'Dynamic response of floating bodies', 6th Annual Offshore Technology Conf., Houston, 1974, Paper OTC 2067, pp. 365-377.

50. Gerritsma, J./et al.
'The effects of beam on the hydrodynamic characteristics of ship hulls', Proc. 10th O.N.R. Symp. on Naval Hydrodynamics, Cambridge, Mass., 1974, pp. 3-33.

51. Newton, R.E.
'Finite element analysis of two-dimensional added mass and damping', Ch. 11 in 'Finite elements in fluids, Vol. 1, Viscous flow and hydrodynamics', ed. by Gallagher, R.H. et al., John Wiley & Sons, London, 1975.

52. Visser, W./Wilt, M. van der
'A numerical approach to the study of irregular ship motions', Ch. 12 in 'Finite elements in fluids, Vol. 1, Viscous flow and hydrodynamics', ed. by Gallagher, R.H. et al., John Wiley & Sons, London 1975.

53. Chung, Y.K./Coleman, M.I.
'Hydrodynamic forces and moments for oscillatory cylinders', Proc. Civil Engineering in the Oceans III, 1975, Univ. of Delaware, Newark, Vol. 2 (publ. A.S.C.E., New York, 1975), pp. 899-913.

54. Fontijn, H.L.
'An approximative method for the determination of the hydrodynamic coefficients of a ship in case of swaying and yawing on shallow water', Communications on Hydraulics, Rep. no. 75-4, Dept. of Civil Engineering, Delft University of Technology, Delft, The Netherlands, 1975.

55. Keil, H.
'Hydrodynamische Masse und Dämpfungskonstante tauchender Zylinder auf flachem Wasser', Schiffstechnik, Bd. 23, 1976, pp. 186-188.

56. Ursell, F.
'On the virtual-mass and damping coefficients for long waves in water of finite depth', Journ. of Fluid Mech., Vol. 76, part 1, 1976, pp. 17-28.

57. Rhodes-Robinson, P.F.
'Note on the long-wave limit of the virtual-mass coefficient for a half-immersed circular cylinder heaving on water of finite depth', Journ. of Fluid Mech., Vol. 76, part 1, 1976, pp. 29-33.

58. Oortmerssen, G. van
'The motions of a moored ship in waves', Thesis Delft University of Technology, H. Veenman en zonen n.v., Wageningen, The Netherlands, 1976.

59. Takaki, M.
'On the hydrodynamic forces and moments acting on the two-dimensional bodies oscillating in shallow water', Reports of Research Institute for Applied Mechanics, Vol. XXIV, No. 78, Kyushu University, Japan, 1977.

60. Kan, M.
'The added mass coefficient of a cylinder oscillating in shallow water in the limit $k \to 0$ and $k \to \infty$', Papers of Ship Research Institute, No. 52, Tokyo, Japan, 1977.

61. Plotkin, A.
'Heave and pitch motions in shallow water including the effect of forward speed', Journ. of Fluid Mech., Vol. 80, part 3, 1977, pp. 433-441.

62. Chung, J.S.
'Forces on submerged cylinders oscillating near a free surface', Journ. of Hydronautics, Vol. 11, No. 3, July 1977, pp. 100-106.

63. Keuning, J.A./Beukelman, W.
'Hydrodynamic coefficients of rectangular barges in shallow water', BOSS '79, 2nd Int. Conf. Behavior Off-Shore Struct., London, 1979, Cranfield, B.H.R.A. Fluid Eng., 1979, Vol. 2, Paper 55, pp. 105-124.

64. Sayer, P.
'The long-wave behaviour of the virtual mass in water of finite depth', Proc. R. Soc. London, A, 372, 1980, pp. 65-91.

65. Sayer, P.
'An integral-equation method for determining the fluid motion due to a cylinder heaving on water of finite depth', Proc. R. Soc. London, A, 372, 1980, pp. 93-110.

66. Fontijn, H.L.
'Ship berthing to a vertical quay-wall: fender forces and ship motion', Communications on Hydraulics, Rep. no. 83-4, Dept. of Civil Engineering, Delft University of Technology, Delft, The Netherlands, 1983.

67. Ogilvie, T.F.
'Recent progress toward the understanding and prediction of ship motions', Proc. 5th O.N.R. Symp. on Naval Hydrodynamics, Bergen, 1964, pp. 3-80.

68. Cummins, W.E.
'The impulse response function and ship motions', Schiffstechnik, Bd. 9, H. 47, 1962, pp. 101-109.

69. Tick, L.J.
'Differential equations with frequency-dependent coefficients', Journ. of Ship Research, Techn. Note, Vol. 3, No. 2, Oct. 1959, pp. 45-46.

70. Oortmerssen, G. van
'The berthing of a large tanker to a jetty', 6th Annual Offshore Technology Conf., Houston, 1974, Paper OTC 2100, pp. 665-676.

71. Fontijn, H.L.
'Impact forces on berthing facilities resulting from moving ships', 6th Int. Harbour Congress, Antwerpen, 1974, S.2.24, pp. 2.24.1/2.24.6.

72. Fontijn, H.L.
'Forces on berthing structures from moving ships', Proc. XVIIth I.A.H.R. Congress, Baden-Baden, 1977, Paper C16, pp. 119-126.

73. Fontijn, H.L.
'The berthing ship problem: forces on berthing structures from moving ships', Rep. no. 78-2, Communications on Hydraulics, Dept. of Civil Engi-

neering, Delft University of Technology, Delft, The Netherlands, 1978.

74. Fontijn, H.L.
'The berthing of a ship to a jetty', Journ of the Waterway, Port, Coastal and Ocean Division, Proc. A.S.C.E., Vol. 106, No. WW2, May 1980, pp. 239-259.
Errata in Vol. 106, No. WW4, Nov. 1980, pp. 509-510.

75. Fontijn, H.L.
'On the determination of berthing forces', Int. Conf. on Numerical and Hydraulic Modelling of Ports and Harbours, Birmingham, U.K., 1985, Paper G1, pp. 187-193.

76. Fontijn, H.L./Kalkwijk, J.P.Th.
'Prediction of fender loads at a closed berthing structure', Proc. Instn Civ. Engrs, Part 2, Vol. 81, Dec. 1986, pp. 511-534.

77. Timman, R./Newman, J.N.
'The coupled damping coefficients of a symmetric ship', Journ. of Ship Research, Vol. 5, No. 4, March 1962, pp. 1-7.

78. Newman, J.N.
'The exciting forces on a moving body in waves', Journ. of Ship Research, Vol. 9, No. 3, Dec. 1965, pp. 190-199.

79. Wunsch, G.
'Moderne Systemtheorie', Akademische Verlagsgesellschaft, Geest & Portig K.G., Leipzig, 1962.

80. Wunsch, G.
'Systemanalyse', B.1 1969, B.2 1970, Verlag Technik, Berlin.

81. Newman, J.N.
'Some hydrodynamic aspects of ship maneuverability', Proc. 6th O.N.R. Symp. on Naval Hydrodynamics, Washington, 1966, pp. 203-237.

82. Timman, R.
'Lecture notes a84 - Stability' (in Dutch, unpublished), Delft University of Technology, Delft, The Netherlands, 1968-1969.

83. Papoulis, A.
'The Fourier integral and its applications', McGraw-Hill Book Company, Inc., New York, 1962.

84. Hwei P. Hsu
'Fourier analysis', revised ed., Simon and Schuster, New York, 1970.

85. Sneddon, I.N.
'Fourier transforms', McGraw-Hill Book Company, Inc., 1951.

86. Lighthill, M.J.
'Fourier analysis and generalized functions', Cambridge University Press, 1970.

87. Kuipers, L./Timman, R. (eds.)
'Handbook of mathematics - Ch. XIII, Cohen, J.W.: The Laplace transform', Intern. series of monographs in pure and applied mathematics, Vol. 99, Oxford, Pergamon Press, 1969.

88. Todd, F.H.
'Ship hull vibration', Edward Arnold (Publishers) Ltd, London, 1961.

89. Koch, J.J.
'Eine experimentelle Methode zur Bestimmung der reduzierten Masse des mitschwingenden Wassers bei Schiffsschwingungen', Ingenieur-Archiv, IV. Band, 2. Heft, 1933, pp. 103-109.

90. Newman, J.N.
'The exciting forces on fixed bodies in waves', Journ. of Ship Research, Vol. 6, No. 3, Dec. 1962, pp. 10-17.

91. Whittaker, E.T./Watson, G.N.
'A course of modern analysis', 4th ed., Cambridge University Press, 1965.

92. Kotik, J./Mangulis, V.
'On the Kramers-Kronig relations for ship motions', Intern. Shipbuilding Progress, Vol. 9, No. 97, Sept. 1962, pp. 361-368.

93. Kotik, J./Lurye, J.
'Some topics in the theory of coupled ship motions', Proc. 5th O.N.R. Symp. on Naval Hydrodynamics, Bergen, 1964, pp. 407-424.

94. Smith, W.E./Cummins, W.E.
'Force pulse testing of ship models', Proc. 5th O.N.R. Symp. on Naval Hydrodynamics, Bergen, 1964, pp. 439-457, disc. pp. 457-459.

95. Bishop, R.E.D./et al.
'Oscillatory testing for the assessment of ship maneuverability', Proc. 10th O.N.R. Symp. on Naval Hydrodynamics, Cambridge, Mass., 1974, pp. 109-121, disc. pp. 122-130.

96. Biesel, F./Suquet, F.
'Les appareils générateurs de houle en laboratoire', La Houille Blanche, Vol. 6, 1951, No. II (mars-avril, pp. 147-165, 1re partie), No. IV (juillet-août, pp. 475-496, 2e partie), No. V (sept.-oct., pp. 723-737, 3e partie).

97. Hinze, J.O.
'Turbulence', McGraw-Hill Book Company, New York, 2nd ed., 1975.

98. Lamb, H.
'Hydrodynamics', Cambridge University Press, Cambridge, 6th ed., 1932.

99. Li, H.
'Stability of oscillatory laminar flow along a wall', B.E.B., T.M. 47, 1954.

100. Schlichting, H.
'Boundary-layer theory', McGraw-Hill Book Company, New York, 6th ed., 1968.

101. Abkowitz, M.A.
'Lectures on ship hydrodynamics, steering and manoeverability', Rep. no. HY-5, Hydrodynamics Department Hydro- og Aerodynamisk Laboratorium, Lyngby, Denmark, 1964.

102. Zunderdorp, H.J./Buitenhek, M.
'Oscillator-techniques at the Shipbuilding Laboratory', Rep. no. 111, Shipbuilding Laboratory, Dept. of Naval Architecture, Delft University of Technology, Delft, The Netherlands, 1963.

103. Flagg, C.N./Newman, J.N.
'Sway added-mass coefficients for rectangular profiles in shallow water', Journ. of Ship Research, Dec. 1971, pp. 257-265.

104. Ursell, F./et al.
'Forced small-amplitude water waves: a comparison of theory and experiment', Journ. of Fluid Mech., Vol. 7, part 1, 1960, pp. 33-52.

105. Wendel, K.
'Hydrodynamische Massen und hydrodynamische Massenträgheitsmomente', Jahrbuch der Schiffbautechnische Gesellschaft, Vol. 44, 1950, pp. 207-255.

106. Zienkiewicz, O.C./Nath, B.
'Analogue procedure for determination of virtual mass', Journ. of the Hydraulics Division, Proc. A.S.C.E., No. HY5, Sept. 1964, pp. 69-81.

107. Lai, R.Y.S./Karadi, G.M.
'Die Impedanz eines axial oszillierenden Sphäroids in einem nicht-zusammendrückbaren viskosen Medium', Mitteilungen Versuchsanstalt für Wasserbau und Kulturtechnik, Theodor Rehbock Fluszbaulaboratorium, Universität Fridericiana, Karlsruhe, B.R.D., H. 162, 1974, pp. 333-350.

108. Brennen, C.E.
'A review of added mass and fluid inertial forces', Naval Civil Engineering Laboratory, Port Hueneme, California, U.S.A., Rep. no. CR 82.010, 1982.
109. Abramowitz, M./Stegun, I.A. (eds.)
'Handbook of mathematical functions', Ch. 25, Dover Publications, Inc., New York.
110. Smirnow, W.I.
'Lehrgang der höheren Mathematik', Teil 1, Deutscher Verlag der Wissenschaften, Berlin, 1. Auflage, 1953.
111. Newman, J.N.
'Some theories for ship manoeuvring', Int. Symp. on Dir. Stab. & Control of Bodies Moving in Water, Journ. of Mech. Eng. Sci., Vol. 14, No. 7, 1972, Suppl. Issue, pp. 34-42.
112. Fujino, M.
'On the added mass of a rectangular cylinder moving in a rectangular channel', Int. Shipbuilding Progress, Vol. 22, No. 248, 1975, pp. 115-131.
113. Fujino, M.
'The effects of the restricted waters on the added mass of a rectangular cylinder', Proc. of the 11th O.N.R. Symp. on Naval Hydrodynamics, London, 1976, pp. 655-670.
114. Bai, K.J.
Disc. on ref. [113], Proc. of the 11th O.N.R. Symp. on Naval Hydrodynamics, London, 1976, pp. 706-713.
115. Bai, K.J.
'Sway added-mass of cylinders in a canal using dual-extremum principles', Journ. of Ship Research, Vol. 21, No. 4, Dec. 1977, pp. 193-199.
116. Bai, K.J.
'Added mass of a rectangular cylinder in a rectangular canal', Journ. of Hydronautics, Vol. 11, No. 1, Jan. 1977, pp. 29-32.
117. Kim, C.H./Chen, N.
'The effect of a vertical wall on the sway-added mass of a Lewis-form section in shallow water', Trans. A.S.M.E., Journ. Energy Resour. Technol., 104(1982)4, pp. 357-362.
118. Alper, P./Poortvliet, D.C.J.
'On the use of Volterra series representation and higher order impulse

responses for nonlinear systems', Electronics Laboratory, Delft University of Technology, Delft, The Netherlands, 1963.

119. Alper, P.
'Some aspects of the Volterra series', Electronics Laboratory, Delft University of Technology, Delft, The Netherlands, 1964.

120. Eijkhoff, P.
'System identification', John Wiley & Sons, 1979, Chicester, New York.

NOMENCLATURE

1. General conventions

- A bar over a quantity means 'average value of'.
- A circumflex over a quantity means 'amplitude of'.
- Dots over a quantity mean derivatives with respect to time.

- Subscripts:

a,b,c,d indicates that the quantities concerned (i.e. dependent variables and -when stated explicitly- constants) must be related to the regions a,b,c,d, respectively;

e added to indicate that the quantity concerned must be related to the 'entrance';

f indicates that the quantity concerned must be related to the fender;

i,j,k are used for a direction or a degree of freedom in a Cartesian co-ordinate system; in general they vary from 1 to 6, unless specified otherwise;

kc indicates that the quantity concerned relates to the (motion of the mass of water in the) 'keel clearance';

l indicates that the quantity concerned must be taken at $\tau = l\Delta t$, c.q. must be related to a laminar flow regime;

m (running index representing a) real, positive integer;

n (running index representing a) real, positive integer; indicates that the quantity concerned must be taken at $t = n\Delta t$;

o indicates that the quantity concerned must be related to the origin of the $ox_1x_2x_3$-co-ordinate system, c.q. added to indicate that the quantity concerned must be related to the 'outlet';

r indicates that the quantity concerned is due to the rotation of $ox_1x_2x_3$;

s indicates that the quantity concerned relates to the (motion of the) 'ship';

t indicates that the quantity concerned must be related to a turbulent flow regime;

G indicates that the quantity concerned must be related to the ship's centre of gravity G;

M real, positive, even integer;

N indicates that the quantity concerned must be taken at $t = N\Delta t$.

- Superscripts:
  - (c) is used to indicate a Fourier cosine transform;
  - (m) indicates consecutive order, c.q. that (in an iteration procedure) the m^{th}-approximation is taken of the quantity concerned;
  - (n) indicates order in power series development;
  - (p) indicates that the quantity concerned contains a pole;
  - (r) indicates that the quantity concerned is free from poles;
  - (s) is used to indicate a Fourier sine transform;
  - (x_1) indicates that the quantity concerned applies to the transverse section of the hull at x_1;
  - 1 means first partial derivative;
  - (1) indicates that the quantity concerned represents the fluctuating part of its original;
  - * indicates that
    - . the i.r.f. concerned is based on the displacement/rotation as output signal;
    - . the harmonic transfer function concerned is a reduced version of its original;
    - . the quantity concerned is a linearized version of its original;
  - ' indicates that the quantity concerned is dimensionless;
  - '' indicates that the quantity concerned is given per unit length.

- Abbreviations:
  - f.r.f. frequency response function;
  - i.r.f. impulse response function;
  - d.t.a. direct-time approach;
  - P.M.M. planar motion mechanism.

2. Co-ordinate systems

$OX_1X_2X_3$ space-fixed right-handed system of Cartesian co-ordinates with origin O; OX_1X_2 coincides with the water surface at rest; the vertical OX_3-axis is positive upwards; the forward speed V_1 and the transverse speed V_2 of the ship is parallel to the positive OX_1-axis and the positive OX_2-axis, respectively.

$ox_1x_2x_3$ right-handed Cartesian co-ordinate system parallel with $OX_1X_2X_3$, but translating with the (constant) ship's speeds V_1,V_2; at rest the origin o coincides with the ship's centre of gravity G; the longitudinal ox_1-axis is positive in forward direction, the ox_2-axis is positive to port-side, the ox_3-axis is positive upwards; in case the system is subjected to a rotation, formally additional forces have to be introduced.

$o\underline{x}_1\underline{x}_2\underline{x}_3$ co-ordinate system which is fully identical to and coincides with $ox_1x_2x_3$ provided the latter system does not rotate.

Gxyz moving right-handed Cartesian co-ordinate system with origin G and fixed with respect to the ship; Gxz coincides with the longitudinal plane of symmetry of the ship; the Gy-axis is positive to port-side, the Gz-axis is positive upwards.

3. List of symbols

Symbols not included in the list below are only used at a specific place and are explained where they occur.

a	real function of ω;
$\hat{a}$	amplitude of sway motion (= amplitude of motion of struts of P.M.M.);
a_0, a_n	real constant (coefficient) (n = 1,2,...);
a_α	real constant;
$a_{jk}(\omega)$	hydrodynamic coefficient of mass term in k-equation as a result of motion in j-direction;
$a_{22}(\omega)$	added mass for swaying motion;
$a_{66}(\omega)$	added mass-moment of inertia for yawing motion;
$a_{jk}^{(n)}$	coefficient of term with order n in power series development for $a_{jk}(\omega)$;
$a_{1r}(t), a_{2r}(t)$	additional accelerations in $ox_1x_2x_3$ to be introduced due to rotation of $ox_1x_2x_3$ with respect to $o\underline{x}_1\underline{x}_2\underline{x}_3$;
$\arg\{...\}$	argument of ...
b	real function of ω;
b_0, b_n	real constant (coefficient) (n = 1,2,...);
b_α	real constant;
$b_{jk}(\omega)$	hydrodynamic coefficient of damping force in k-equation as a re-

	sult of motion in j-direction;
$b_{22}(\omega)$	sway damping force coefficient;
$b_{66}(\omega)$	yaw damping moment coefficient;
$b_{jk}^{(n)}$	coefficient of term with order n in power series development for $b_{jk}(\omega)$;
c, c_n	real constant (coefficient) ($n = 1,2,\ldots$);
c_0	spring rate of linear fender;
c_1, c_2	respective spring rates of the two linear springs which combined form the non-linear fender;
c_w	velocity of propagation of long wave;
c_{jk}	hydrostatic restoring coefficient in k-equation as a result of static displacement in j-direction at zero speed;
d_1, d_2	real constant coefficient;
d_{sc}	initial distance (i.e. at rest) between the two linear spring elements of the non-linear fender;
d_{sq}	distance/clearance between ship and vertical (quay-)wall when G coincides with o;
e_0	(initial) distance of line of action of fender to ship's centre of gravity G before and during the first contact between ship and fender;
f_l, f_t	multiplication factors for underkeel friction effect in case of laminar or turbulent flow regime (standard values $\equiv 1$);
f_n	value of $f(\omega)$ at $\omega = \omega_n$;
f_{u_a}	switch parameter with value 0 or +1 representing influence of horizontal velocity of fluid in region a;
f_{w_a}	switch parameter with value 0 or +1 representing influence of vertical acceleration of fluid in region a;
$f(t)$	excitation of system (input signal); general expression for function of t;
$f_i(t)$	(external) forcing function upon ship in i-direction;
$f_{1_r}(t), f_{2_r}(t)$	additional forces resulting from $a_{1_r}(t)$ and $a_{2_r}(t)$, respectively;
$f_{2,kc}(t)$	hydrodynamic force in x_2-direction upon mass of water in keel clearance (per unit length);
$f_{2,s}(t)$	hydrodynamic force in x_2-direction upon ship (per unit length);
g	acceleration due to gravity;
$g_n(t)$	real function of time ($n = 1,2,\ldots,5$);

g_n^*	real constant, linearized version of $g_n(t)$ $(n = 1,2,.,4)$;
h	water depth at rest (mean water level);
i	$\sqrt{-1}$;
$k(t)$	impulse response function; simplified notation for $k_{22}(t)$;
$k_{ij}(t)$	response for j-direction to a unit pulse (i.e. Dirac function at $t = 0$) in i-direction = impulse response function (i.r.f.); $k_{ij}(t)$ = i.r.f. based on velocity as output signal; $k_{ij}^*(t)$ = i.r.f. based on displacement/rotation as output signal;
l	half the distance between struts of P.M.M.; real positive integer;
m_0	usual wave number;
m_n	wave number satisfying $(n-1/2)\pi < m_n h < n\pi$ $(n = 1,2,...)$;
m_{jk}	inertia matrix (i.e. generalized mass) of ship;
m_{11}	mass of ship for horizontal (surge) motion;
m_{22}	mass of ship for horizontal (sway) motion;
m_{66}	mass-moment of inertia of ship around Gz-axis;
n	real positive integer;
p	fluid pressure;
p_0,p_1	real constant (coefficient);
p_a	fluid pressure in region a;
p_b	fluid pressure in region b;
$p_b^{(1)}$	fluctuating part of p_b;
p_c	fluid pressure in region c;
$p_{ij}(\omega)$	real function of ω;
q_0,q_1	real constant (coefficient);
q_i	constant in approximative expression for $b_{ii}(\omega)$ in case $\omega \to \infty$;
$q_{ij}(\omega)$	real function of ω;
r	radius of (semi-)circle around origin; modulus of s; complex function of ω;
r_0,r_n	real constant (coefficient) $(n = 1,2,3,4)$;
r_α	real constant;
s	complex variable;
s_m	certain complex number $(m = 1,2,3)$;
$\mathrm{sgn}\{...\}$	signum operator;
t	time co-ordinate;
t_0,t_1	point of time;
t_*	time scale;

u	fluid velocity in x_1-direction;
u_a	fluid velocity in x_1-direction in region a;
$\bar{u}_a$	depth-averaged fluid velocity in x_1-direction in region a;
u_b	fluid velocity in x_1-direction in region b;
u_d	fluid velocity in x_1-direction in region d;
$\bar{u}_d$	height-averaged fluid velocity in x_1-direction in region d;
u_c	fluid velocity in x_1-direction in region c;
$u(t)$	response of system (output signal);
$u_j(t)$	response of ship-fluid system in j-direction to set of forcing functions $\{f_i(t)\}$;
v	fluid velocity in x_2-direction;
v_a	fluid velocity in x_2-direction in region a;
v_b	fluid velocity in x_2-direction in region b;
$\bar{v}_b$	height-averaged fluid velocity in x_2-direction in region b;
v_c	fluid velocity in x_2-direction in region c;
v_A	constant, lateral speed of approach of ship towards berth;
v_{oi}	constant velocity of ship in i-direction;
v_{b*}	variation of $\bar{v}_b$ at time scale t_*;
w	fluid velocity in x_3-direction;
w_a	fluid velocity in x_3-direction in region a;
w_b	fluid velocity in x_3-direction in region b;
w_c	fluid velocity in x_3-direction in region c;
w_d	fluid velocity in x_3-direction in region d;
w_m	root of characteristic equation ($m = 1,2,3$);
$x_j(t)$	j-th mode of motion of ship;
$x_1(t)$	surge motion of ship;
$x_2(t)$	sway motion of ship;
$x_3(t)$	heave motion of ship;
$x_4(t)$	roll motion of ship (Eulerian angle);
$x_5(t)$	pitch motion of ship (Eulerian angle);
$x_6(t)$	yaw motion of ship (Eulerian angle);
$x_{1G}(t), x_{2G}(t)$	co-ordinates of G within travelling $ox_1x_2x_3$-system;
$y_{n-1,n,n+1}(\omega)$	approximative expression for $f(\omega)$ on closed interval $[\omega_{n-1}, \omega_{n+1}]$ based on Lagrange three point interpolation for equally spaced abscissas;
A	real constant coefficient;
A_0, A_n	real coefficient c.q. real constant ($n = 1,2,\ldots$);

A'_0, A'_n	dimensionless form of A_0, A_n;
A_c	real constant;
$A(s)$	constant of integration;
B	beam of ship;
B_0, B_n	real coefficient ($n = 1,2,\ldots$);
B'_0, B'_n	dimensionless form of B_0, B_n;
B_c	real constant;
$B(s)$	constant of integration;
C_1, C_2	real constant; constant of integration;
C_3, C_4	real constant;
C_m	constant of integration ($m = 1,2,3$);
D	draught of ship;
D_n	(complex) constant ($n = 1,2,\ldots,6$);
E	total amount of energy absorbed by (linear) fender;
$E_{n-1,n,n+1}(\omega)$	discretization error on closed interval $[\omega_{n-1}, \omega_{n+1}]$ as result of approximation $y_{n-1,n,n+1}(\omega)$ for $f(\omega)$;
$F(s)$	Laplace transform of $f(t)$;
$F_k(\omega)$	Fourier transform of $f_k(t)$;
$F_{2f}(t)$	reaction force in fender acting in X_2-direction;
$F\{f(t)\}$	Fourier transform of function $f(t)$;
G	centre of gravity of ship;
G_n	real constant ($n = 0,1,..,4$);
$G_{ij}(s)$	function corresponding with $H_{ij}(s)$ free from singularities;
$H_{ij}(s)$	Laplace transform of $k_{ij}(t)$; general transfer function for j-direction in response to (force) excitation in i-direction;
$H_{2,b}(x_1,t)$	loss of energy head in region b due to contraction and separation of flow in x_2-direction;
$I_M(t)$	result of numerical integration along closed interval $[0, \omega_M]$;
I_I, I_{II}, I_{III}	symbolic notation of (Laplace) integral;
$Im[\ldots]$	imaginary part of ...;
$K_{ij}(\omega)$	Fourier transform of $k_{ij}(t)$ = harmonic transfer function for j-direction in response to (harmonic force) excitation in i-direction = frequency response function (f.r.f.);
$K_{ij}^{(c)}(\omega)$	Fourier cosine transform of $k_{ij}(t)$;
$\dot{K}_{ij}^{(c)}(\omega)$	Fourier cosine transform of $\dot{k}_{ij}(t)$;
$K_{ij}^{(s)}(\omega)$	Fourier sine transform of $k_{ij}(t)$;

$\dot{K}_{ij}^{(s)}(\omega)$	Fourier sine transform of $\dot{k}_{ij}(t)$;
$K_{ii}(s)$	Laplace transform of $k_{ii}(t)$; transfer function for i-direction in response to (force) excitation in i-direction;
$K_{ii}^{(r)}(s)$	part of $K_{ii}(s)$ without poles;
$K_{ii}^{(p)}(\omega)$	part of $K_{ii}(\omega)$ containing a pole for $\omega = 0$;
$K_{ii}^{(r)}(\omega)$	part of $K_{ii}(\omega)$ without poles;
K_α	real constant;
L	length of ship;
$L\{f(t)\}$	unilateral Laplace transform of $f(t)$;
$L^{-1}\{F(s)\}$	inverse Laplace transform of $F(s)$;
M	real constant;
M_0	reduced or effective mass of ship for horizontal motion;
M_{ii}	representation of 'mass effect' of ship in equation(s) of motion in case of uncoupled motions ($M_{ii} = m_{ii}+$ added mass(-moment of inertia));
N	real positive integer representing the number of time steps of the total durance of contact between ship and fender; real constant;
P	real constant; real or complex function of ω;
P_n	real constant ($n = 1,2,\ldots$);
$P(x_2,s)$	unilateral, one-dimensional Laplace transform of $p(x_2,t)$ with respect to t;
$P_0(t)$	real function of t;
$P_0^*(t)$	real function of t, linearized version of $P_0(t)$;
Q	real constant; real or complex function of ω;
Q_n	real constant ($n = 1,2,\ldots$);
$Q_0(t)$	real function of t;
$Q_0^*(t)$	real function of t, linearized version of $Q_0(t)$;
R	fluid region in which the Laplacian is (to be) solved; real constant; complex function of ω;
R_1	real constant;
$R_i(\omega)$	wave making coefficient for (ship) motion in i-direction = ratio of amplitude of radiated waves at infinity to amplitude of (ship) motion in i-direction;
$R_M(t)$	discretization (i.e. process) error in consequence of numerical integration along closed interval $[0, \omega_M]$;

$R_{ij}(\omega)$	harmonic transfer function for j-direction in response to a harmonic (motion) excitation in i-direction;
$R^*_{ij}(\omega)$	reduced form of $R_{ij}(\omega)$;
$R_{2,b}(x_1,t)$	term representing frictional effect in equation of motion in x_2-direction for fluid in region b;
$R_{2,b,s}(t)$	friction force in x_2-direction upon bottom of moving ship;
Re	Reynolds number;
Re[...]	real part of ...;
S	real constant; complex function of ω;
S_0,S_n	real function of ω ($n = 1,2,\ldots,5$);
T	real constant; complex function of ω;
T_I,T_{II}	certain period time of harmonic oscillation corresponding with ω_I,ω_{II};
$T_{s,kc}(t)$	simple-harmonic function of time;
U(t)	unit step or Heaviside function;
$U_j(\omega)$	Fourier transform of $\dot{x}_j(t)$;
V_1	constant forward speed of ship;
V_2	constant transverse speed of ship;
V_n	value of V(t) at $t = n\Delta t$;
V(t)	simplified notation for $\dot{X}_{2G}(t)$;
$V(x_3,s)$	unilateral, one-dimensional Laplace transform of $v(x_3,t)$ with respect to t;
$X_{1f}(t),X_{2f}(t)$	abscissa (= constant for all t) and ordinate of point of fender, respectively;
$X_{1o}(t),X_{2o}(t)$	distance covered by G in X_1- and X_2-direction, respectively, with respect to uniformly travelling origin of $ox_1x_2x_3$;
$X_{1G}(t),X_{2G}(t)$	abscissa and ordinate of ship's centre of gravity G, respectively;
X,Y	abscissa and ordinate, respectively, of ship's centre of gravity G in the horizontal plane as measured during berthing operation by 'position follower';
$X_0(t),Y_0(t)$	real functions of t representing underkeel friction in case of strip theory;
$X^*_0(t),Y^*_0(t)$	real functions of t representing underkeel friction in case of strip theory, linearized versions of $X_0(t),Y_0(t)$;
$Y_{s,kc}(x_2)$	function of x_2 only;
$Z_0(t)$	real function of t;

$Z_0^*(t)$	real function of t, linearized version of $Z_0(t)$;
$Z_0(x_1,t)$	real function of x_1 and t;
$Z_{s,kc}(x_3)$	function of x_3 only;
α	square root of constant of separation; main dimension of body with elementary form; real function of ω;
α_0, α_n	real constant (coefficient) (n = 1,2,3);
α_i	$\mathrm{Im}[\alpha]$;
α_l	dimensionless friction coefficient relating to laminar flow in x_2-direction in region b;
α_r	$\mathrm{Re}[\alpha]$;
α_t	dimensionless friction coefficient relating to turbulent flow in x_2-direction in region b;
α_{ij}	quantity equivalent to $k_{ij}(\infty)$;
β	main dimension of body with elementary form; real function of ω;
β_0	real constant coefficient;
β_I, β_{II}	certain damping constant;
γ	proportionality coefficient for shear stress in case of laminar flow;
γ_0	real constant coefficient;
δ_{jk}	Kronecker delta: $\delta_{jk} = 1$ for $j = k$, $\delta_{jk} = 0$ for $j \neq k$;
$\delta(t)$	delta function or Dirac function;
$\delta_i(t)$	unit pulse (i.e. delta or Dirac function) in i-direction;
ε	certain complex number; small (complex) parameter;
$\varepsilon_i(\omega)$	phase angle of harmonic force c.q. motion in i-direction;
ζ	elevation of water surface with respect to mean water level;
ζ_a	elevation of water surface in region a with respect to mean water level;
ζ_i	(arbitrary) coefficient specifying magnitude of $\delta_i(t)$;
η	height of long wave with respect to mean water level;
η_a	height of long wave in region a with respect to mean water level;
η_c	height of long wave in region c with respect to mean water level;
η_i	(arbitrary) coefficient specifying magnitude of $\delta_i(t)$;
θ	phase shift between underkeel fluid velocity v_b and sway velocity of ship;
$\theta_{ij}(\omega)$	phase shift between harmonic motion and its (force) response;

κ_m	root of second-degree (characteristic) equation (m = 1,2);
λ	real part of s;
λ_b	general head-loss coefficient referring to contraction and flow separation in region b;
μ	contraction coefficient;
ν	(coefficient of) kinematic viscosity of fluid;
ξ	integration variable (circular frequency); certain value of ω on the closed interval $[\omega_{n-1}, \omega_{n+1}]$;
ξ_m	root of cubic equation (m = 1,2,3);
$\xi_{b,e}$	head-loss coefficient in region b due to abrupt contraction at entrance;
$\xi_{b,o}$	head-loss coefficient in region b due to sudden expansion at outlet;
ρ	specific mass density of fluid;
τ	integration variable (time);
$\tau_{2,b}\vert_{bottom}$	shear stress in x_2-direction in region b at fluid-bottom interface;
$\tau_{2,b}\vert_{ship}$	shear stress in x_2-direction in region b at ship-fluid interface;
ϕ	argument of s; (real) angle;
$\phi_{s,kc}(x_2,x_3)$	harmonic function of place;
χ_m	root of fourth-degree (characteristic) equation (m = 1,2,3,4);
ψ_0	amplitude of pure yaw motion;
$\psi(t)$	angle of rotation of ship's longitudinal axis of symmetry around OX_3-axis (during contact between ship and fender);
$\bar{\psi}(t+\Delta t)$	mean value of $\psi(t)$ on interval of time Δt;
ω	circular frequency; imaginary part of s;
$\omega_1,\omega_n,\omega_M$	certain (circular) frequency;
ω_I,ω_{II}	certain (circular) frequency corresponding with T_I,T_{II};
Δt	interval of time; time increment; time step;
$\Delta X_{2f}(t)$	deflexion of fender in X_2-direction;
$(\Delta X_{2f})_{max}$	maximum deflexion of (linear) fender;
$\Delta Y_1,\Delta Y_n$	value of $\Delta Y(t)$ at $\tau = 1\Delta t$, $t = n\Delta t$, respectively;
$\Delta Y(t)$	simplified notation for $\Delta X_{2f}(t)$;
$(\Delta\omega)_n$	interval between successive, equally spaced abscissas ω_{n-1}, ω_n and ω_{n+1} (n = 1,3,5,...);
$\Phi(x_2,x_3,t)$	velocity potential;

$\Phi_{kc}(x_2,x_3,t)$ velocity potential resulting from motion of mass of water in keel clearance;

$\Phi_s(x_2,x_3,t)$ velocity potential resulting from motion of ship.

Curriculum Vitae

Henri L. Fontijn werd op 26 januari 1942 in Amsterdam geboren. In deze plaats werden ook het lager en voorbereidend wetenschappelijk onderwijs genoten. Het einddiploma Gymnasium β werd behaald in 1960.

Vervolgens werd 'Weg- en Waterbouwkunde' gestudeerd aan de toentertijd gelijknamige Afdeling van de Technische Hogeschool Delft. In 1969 werd deze studie 'met lof' afgerond.

Sinds 1 september 1969 is H. L. Fontijn medewerker aan de -zoals de huidige benaming luidt- Faculteit der Civiele Techniek van de Technische Universiteit Delft. Op het gebied van de Vloeistofmechanica wordt onderwijs gegeven en worden bijdragen geleverd aan het onderzoek. Vanaf medio 1975 is hij tevens belast met de dagelijkse leiding van het Laboratorium voor Vloeistofmechanica.

Stellingen

behorende bij het proefschrift

FENDER FORCES IN SHIP BERTHING

H.L. Fontijn

15 december 1988

1. Voor de correcte bepaling van de afmeerkrachten op een constructie is het noodzakelijk dat de bewegingen van het schip tijdens de aanlegmanoeuvre beschreven worden in het tijddomein.

2. Afmeerkrachten bepaald met behulp van een energiebeschouwing -waarbij verondersteld wordt dat de door de fenderconstructie te absorberen energie gelijk is aan een aantal malen de kinetische energie van het naderende schipdienen met het nodige voorbehoud geïnterpreteerd te worden.

3. Het gebruik van het begrip 'toegevoegde massa' zou, indien gehanteerd als frequentie-afhankelijke grootheid, zoveel mogelijk vermeden moeten worden.

4. De onzekerheid met betrekking tot de keuze van waarden voor sommige ontwerpparameters van een aanlegconstructie rechtvaardigt een probabilistische aanpak van het ontwerpproces.

5. Bij de samenstelling van de Noordzee Reductiekaart is het gebruik van een via numerieke simulatie verkregen bestand van getijgegevens aanbevelenswaardig.

6. Ondanks de groeiende toepassing van numerieke simulatietechnieken binnen het vakgebied van de waterbouwkunde, kan het gebruik van fysische modellen niet gemist worden: in algemene zin zijn deze modelleringsvormen complementair.

7. De belangstelling van studenten voor een bepaalde universitaire studierichting mag niet tot de enige basis worden gemaakt voor het toewijzingsbeleid inzake personele en financiële middelen, omdat dan het risico wordt gelopen dat de noodzakelijke continuïteit in onderwijs en onderzoek verstoord wordt.

8. Het niet onbeperkt toegankelijk laten zijn van de eerste fase van een academische opleiding door aan de universiteiten de vrijheid te geven zelf te selecteren, dient ernstig overwogen te worden. Deze mogelijkheid impliceert dat de selectie in mindere mate dan nu het geval is een organiek onderdeel behoeft te zijn van de studie; tevens kan zij gebruikt worden om te komen tot een (gewenste) verhoging van status en niveau van de opleiding en een reductie van overbodige doctorandi.

9. Door de geleidelijke verwording van de universiteit van Alma Mater tot beroepsopleiding, waarin geen plaats is voor algemene culturele vorming en zeker niet voor de humaniora, dreigt er een generatie te ontstaan van aculturele, niet-idealistische no-nonsense beleidsmakers en carrièristen zonder levensbeschouwelijke diepgang.

10. Om analytisch te leren denken is het volgen van wiskundeonderwijs niet beslist noodzakelijk. Dit doel kan ook bereikt worden door het bestuderen van een goed gestructureerde taal, met als bijkomend voordeel bij het lezen c.q. vertalen van literatuur de aanwezigheid van een inhoud.
In dit verband kunnen de klassieke talen een belangrijke rol spelen. Door hun nogal van het Nederlands afwijkende structuur dwingt bestudering ervan tot een bezinning op de moedertaal: het beroep dat wordt gedaan om (andermans) gedachten adequaat te verwoorden is uitermate geschikt om de geest te scherpen.

11. In de media en de politiek fungeert het begrip antizionisme in sommige gevallen als een moderne verpakking van het getaboeiseerde begrip antisemitisme.

12. De geringe bereidheid van de mens om zich te verdiepen in de fundamentele oorzaken van het ontstaan en bestaan van totalitaire systemen met hun drang tot het uitroeien van potentiële vijanden, alsmede zijn grote geneigdheid tot vergeten en verdringen van het verleden, kan niet alleen leiden tot intellectuele maar ook tot fysieke zelfvernietiging.

13. Het milieubeheer in Nederland kan gekarakteriseerd worden als symptoombestrijding en is als zodanig te vergelijken met de manier waarop in de Middeleeuwen de wateroverlast werd aangepakt.

14. Het beoefenen van de kunst van het vioolspel kan door het daarvoor vereiste concentratievermogen en de benodigde inzet een goede remedie vormen tegen eventuele spanningen die ontstaan tijdens het schrijven van een dissertatie.

15. Het gebruik om de laatste stellingen bij een academisch proefschrift het karakter te geven van een hyperbolische bewering, een retorische constatering, een ludieke aanbeveling, een paradoxale uitlating of een aforisme, dient in het Promotiereglement te worden vastgelegd.

FENDER FORCES IN SHIP BERTHING

Part II: Figures

Appendices

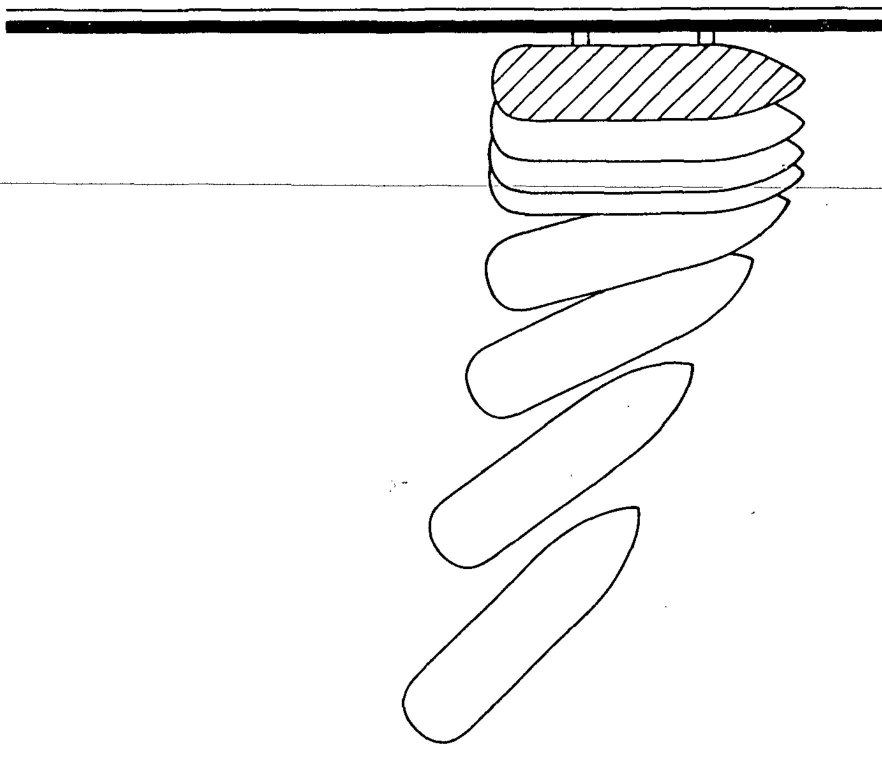

H. L. Fontijn

FENDER FORCES IN SHIP BERTHING

Part II: Figures
Appendices

Proefschrift

ter verkrijging van de graad van doctor aan de Technische Universiteit Delft, op gezag van de Rector Magnificus, prof. drs. P. A. Schenck, in het openbaar te verdedigen ten overstaan van een commissie door het College van Dekanen daartoe aangewezen, op donderdag 15 december 1988 te 14.00 uur, door

Henri Lodewijk Fontijn,

geboren te Amsterdam,
civiel ingenieur.

Dit proefschrift is goedgekeurd door de promotor
prof. dr. ir. J. P. Th. Kalkwijk

CONTENTS (part II)

LIST OF FIGURES

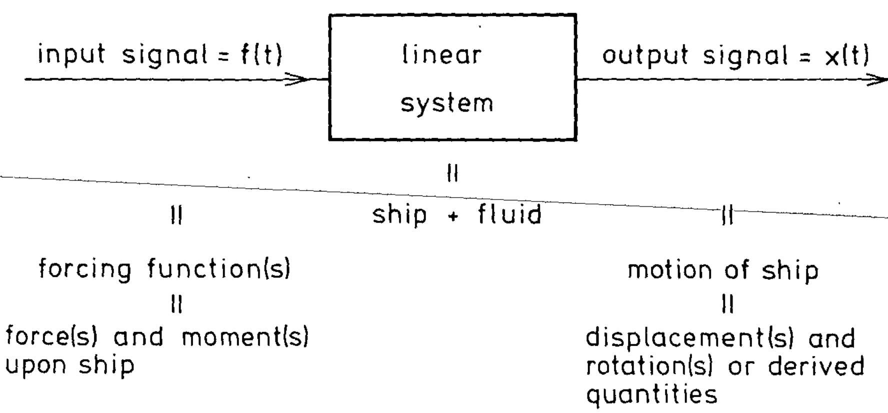

Fig. 1.1 - Schematic representation of ship-fluid system ('black box')

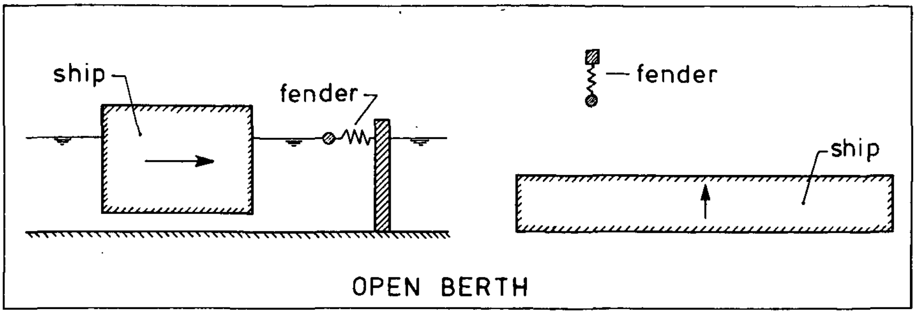

Fig. 1.2[a] - Sketch of open berthing lay-out

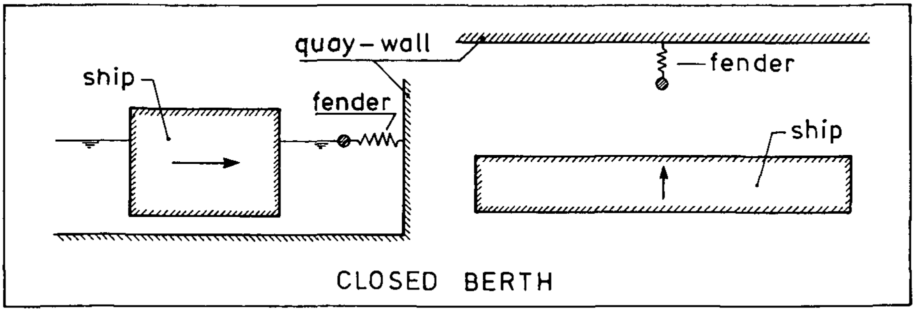

Fig. 1.2[b] - Sketch of closed berthing lay-out

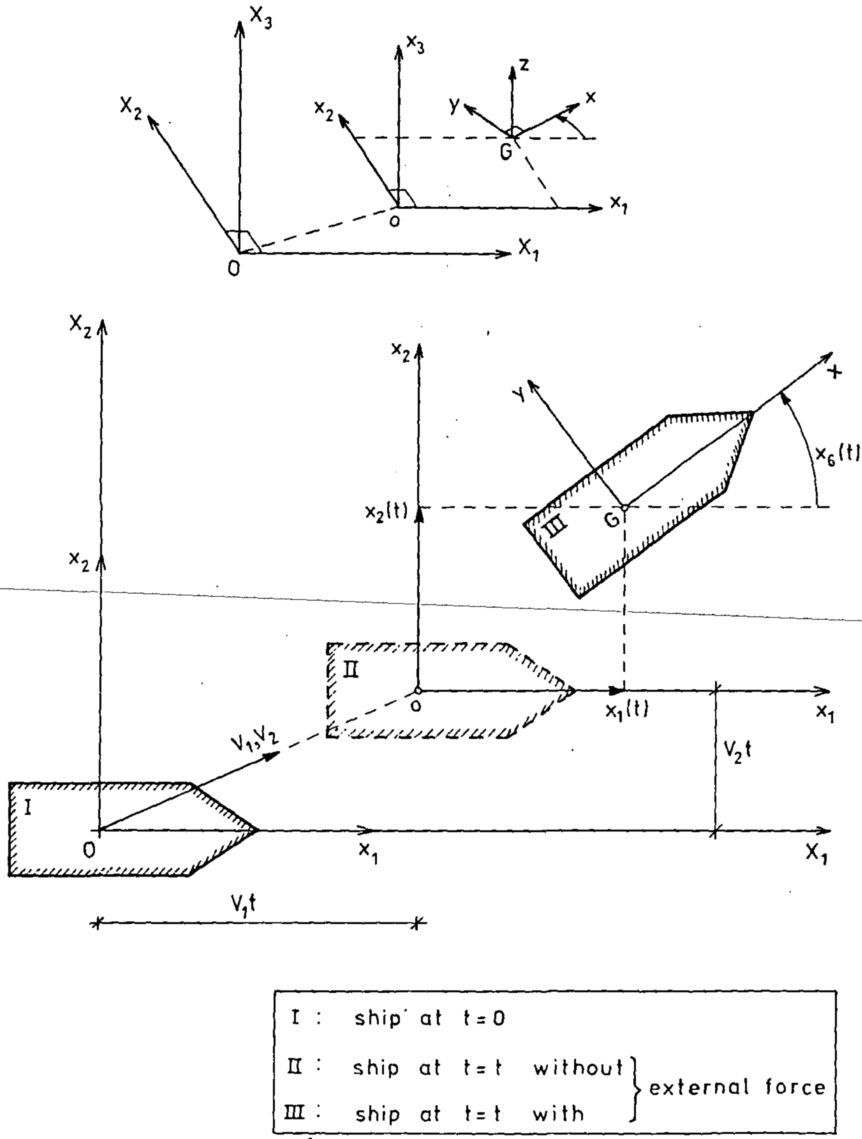

Fig. 2.1 - Co-ordinate systems for horizontal ship motion

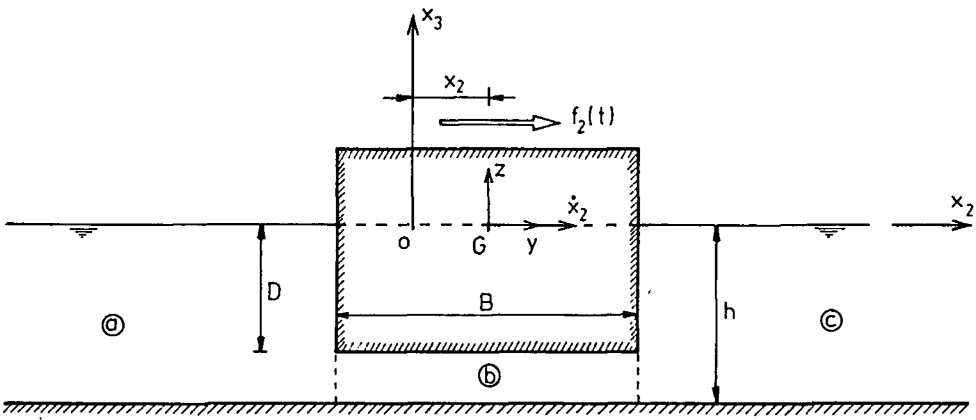

Fig. 3.1 - Definition sketch for sway motion on horizontally unrestricted water

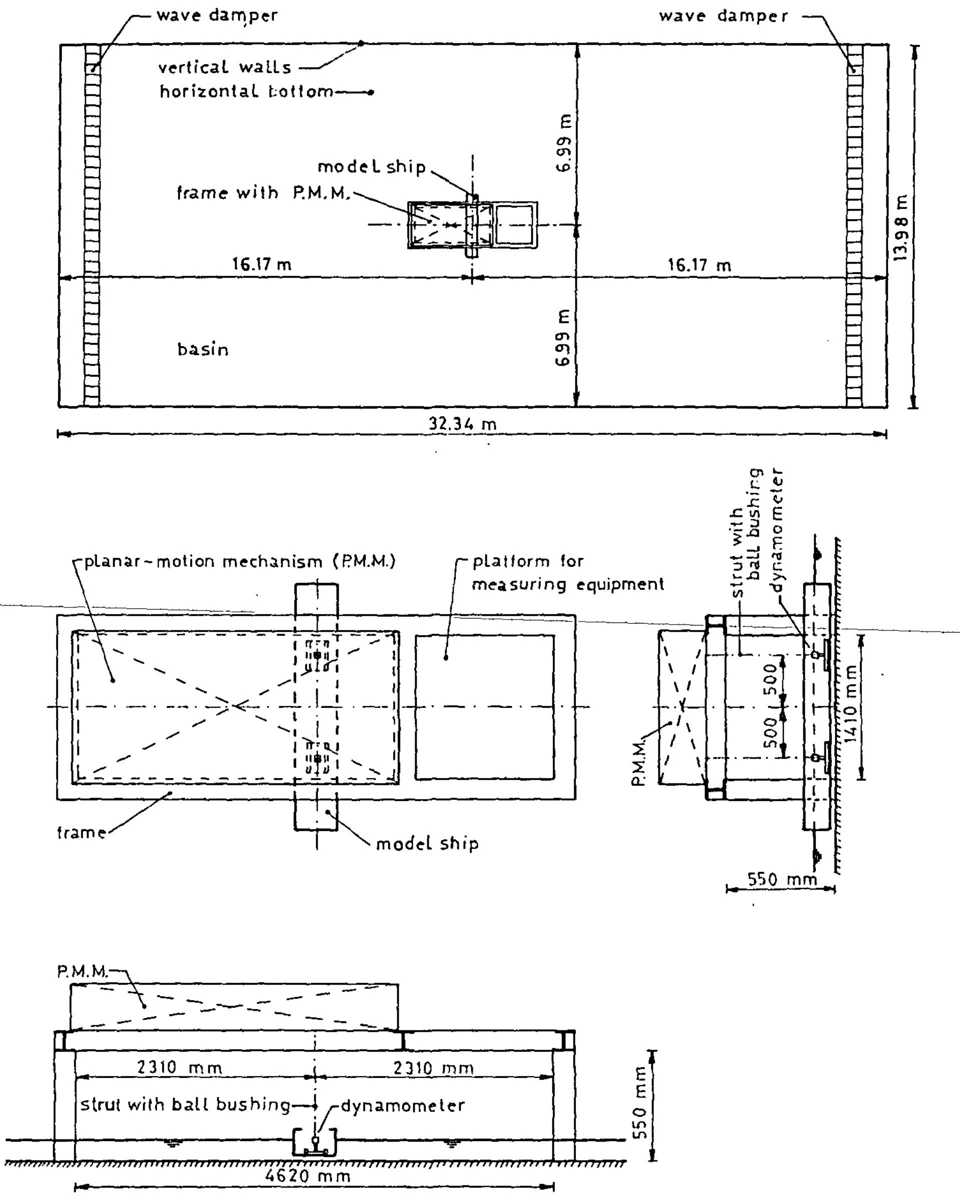

Fig. 3.2 - Schematic representation of experimental set-up for harmonic sway and yaw tests on horizontally unrestricted water

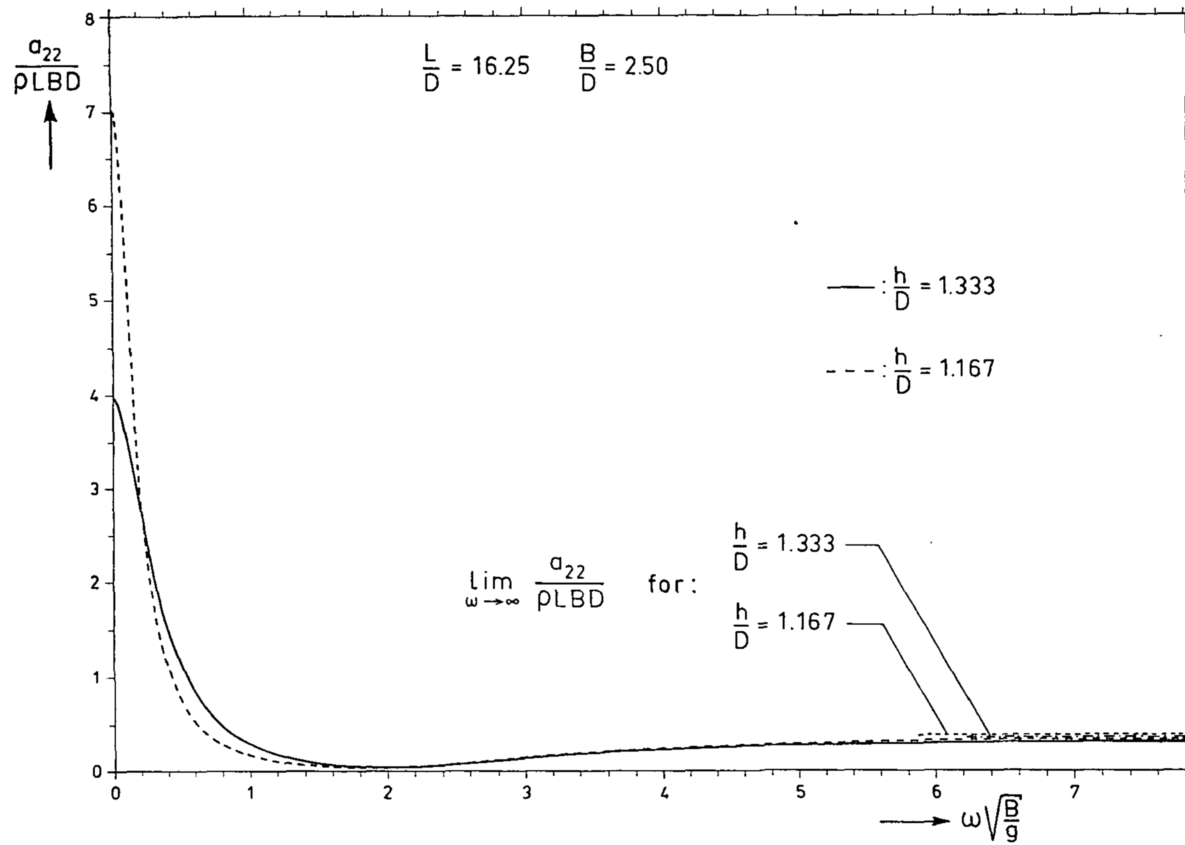

Fig. 3.3 - Added mass for swaying motion on horizontally unrestricted water (non-zero keel clearance)

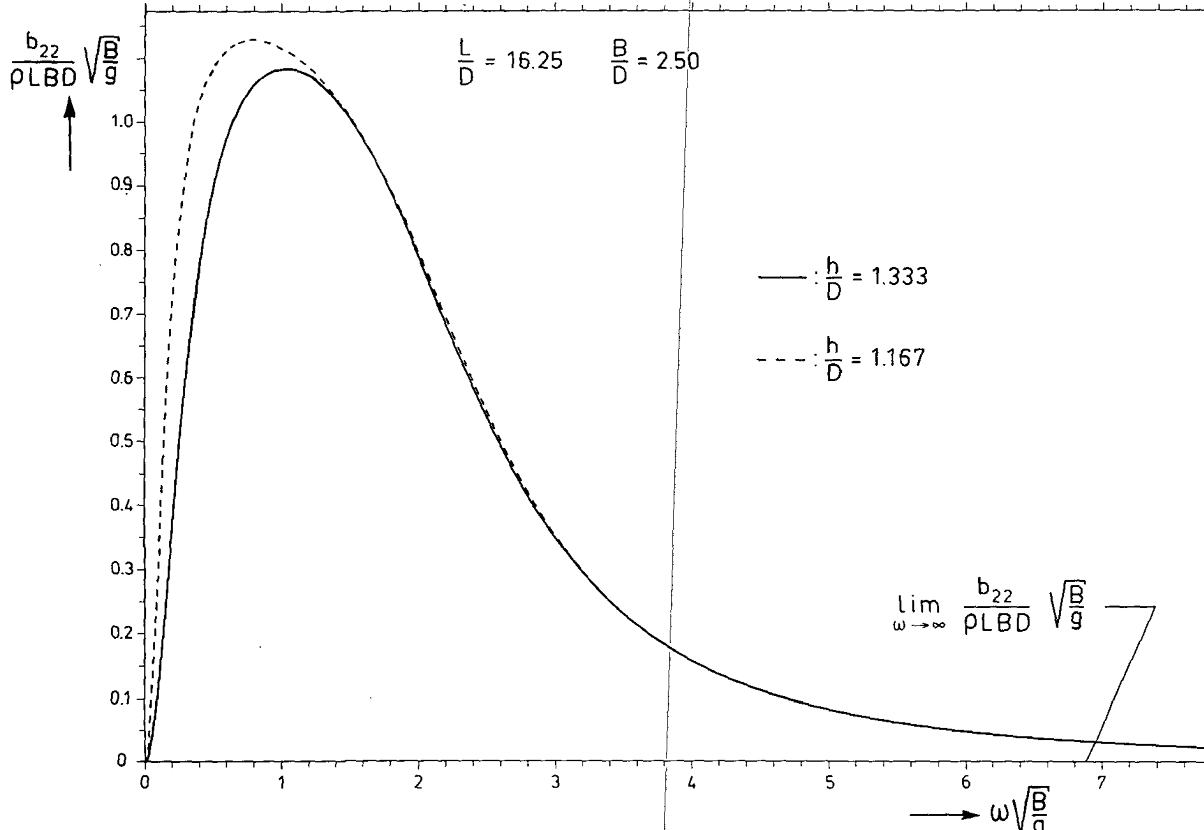

Fig. 3.4 - Sway damping force coefficient on horizontally unrestricted water (non-zero keel clearance)

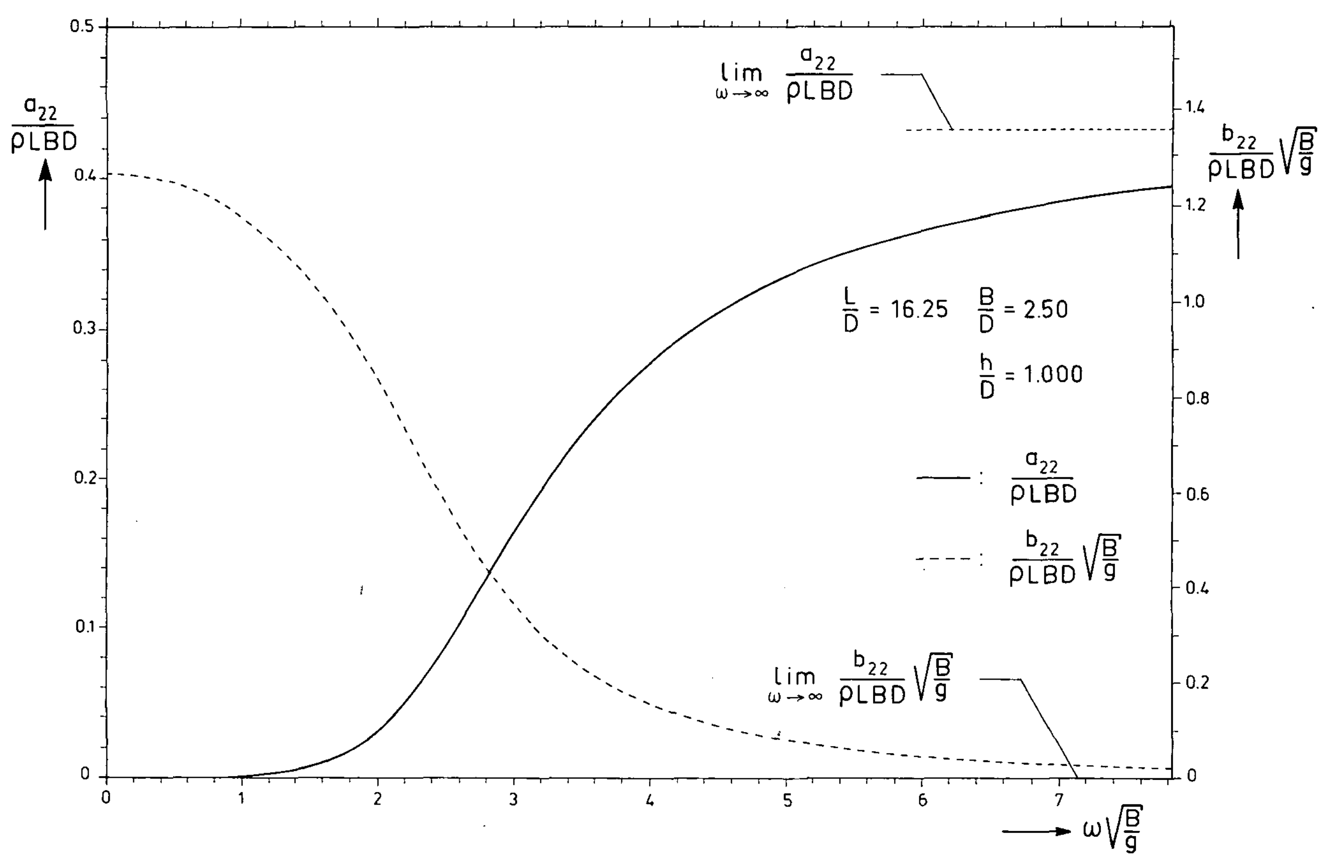

Fig. 3.5 - Sway added-mass and sway damping force coefficient on horizontally unrestricted water (zero keel clearance)

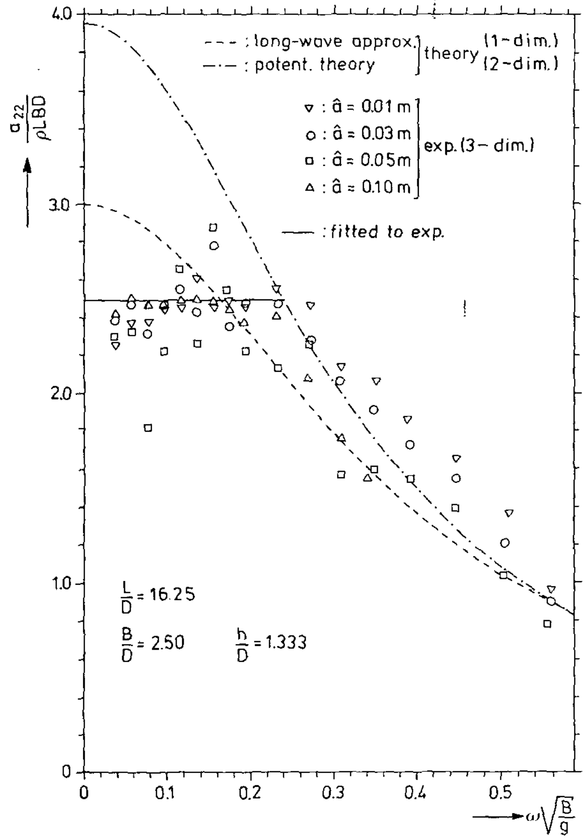

Fig. 3.6[a] - Added mass for swaying motion on horizontally unrestricted water (h/D = 1.333)

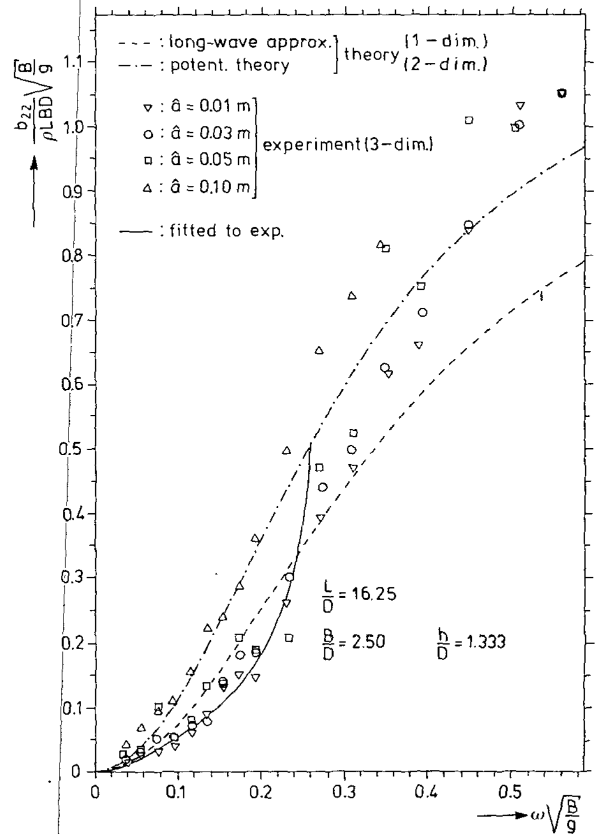

Fig. 3.6[b] - Sway damping force coefficient on horizontally unrestricted water (h/D = 1.333)

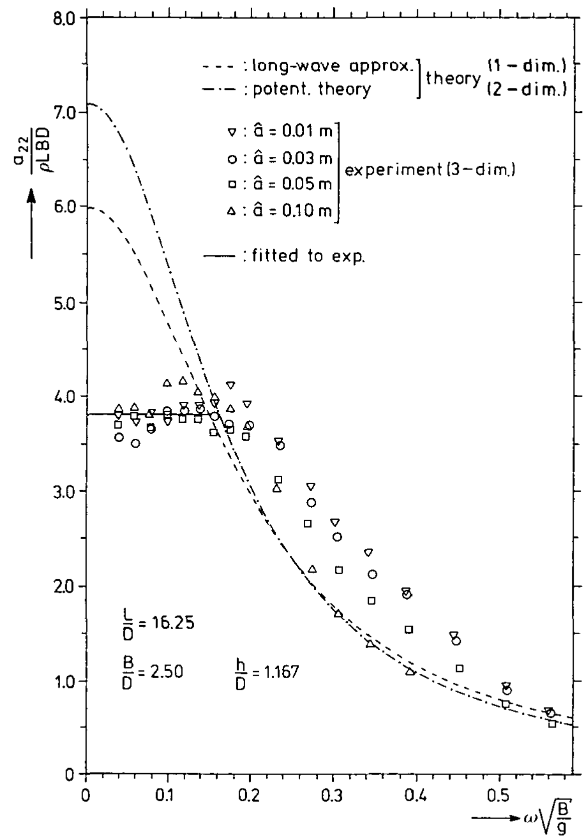

Fig. 3.7[a] - Added mass for swaying motion on horizontally unrestricted water (h/D = 1.167)

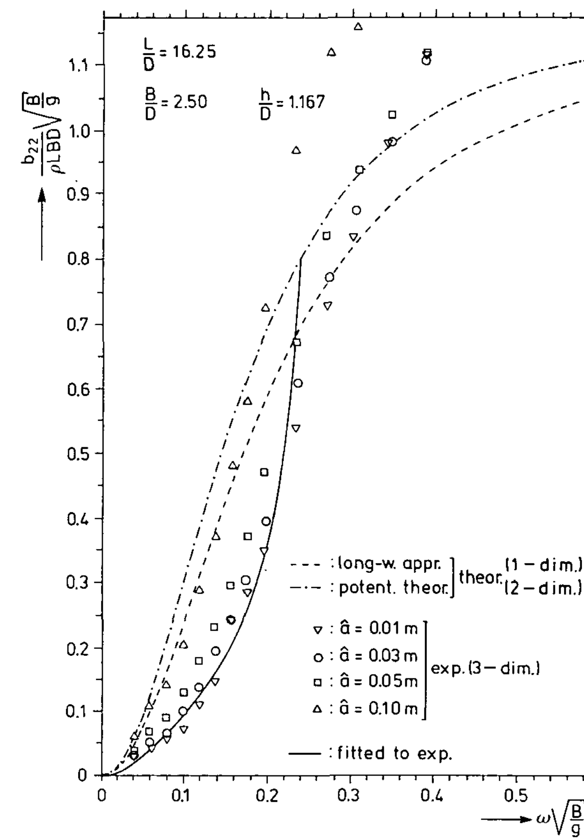

Fig. 3.7[b] - Sway damping force coefficient on horizontally unrestricted water (h/D = 1.167)

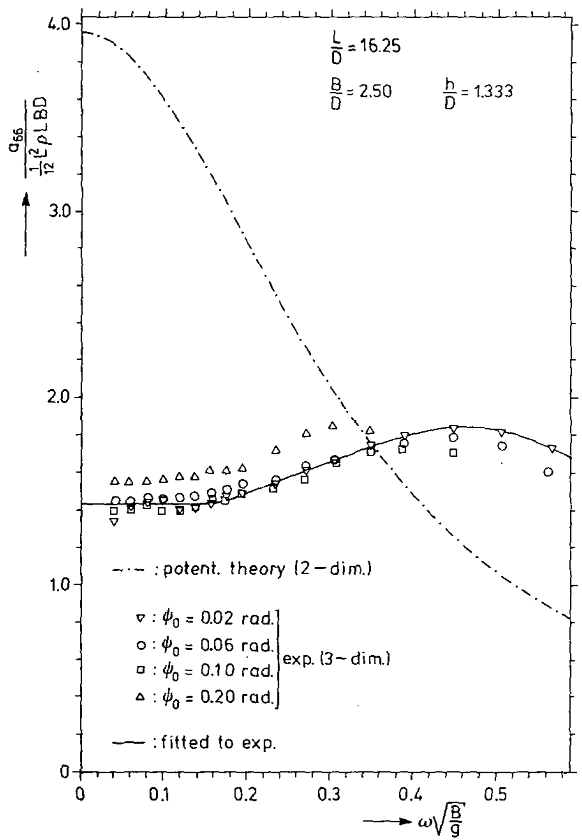

Fig. 3.8[a] - Added mass-moment of inertia for yawing motion on horizontally unrestricted water (h/D = 1.333)

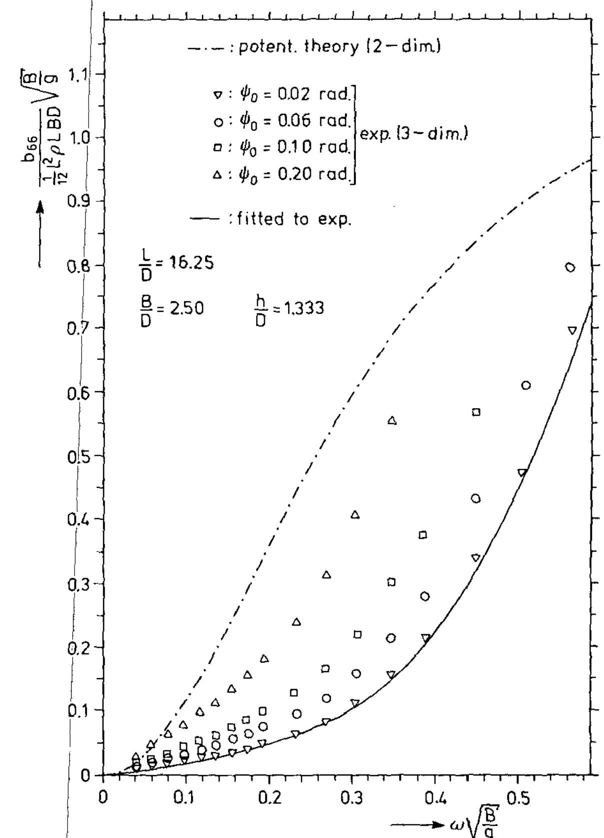

Fig. 3.8[b] - Yaw damping moment coefficient on horizontally unrestricted water (h/D = 1.333)

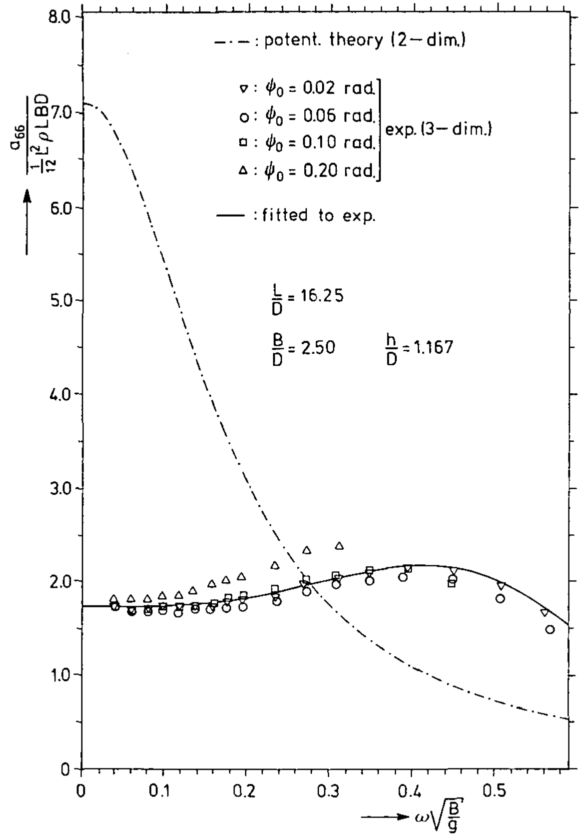

Fig. 3.9[a] - Added mass-moment of inertia for yawing motion on horizontally unrestricted water (h/D = 1.167)

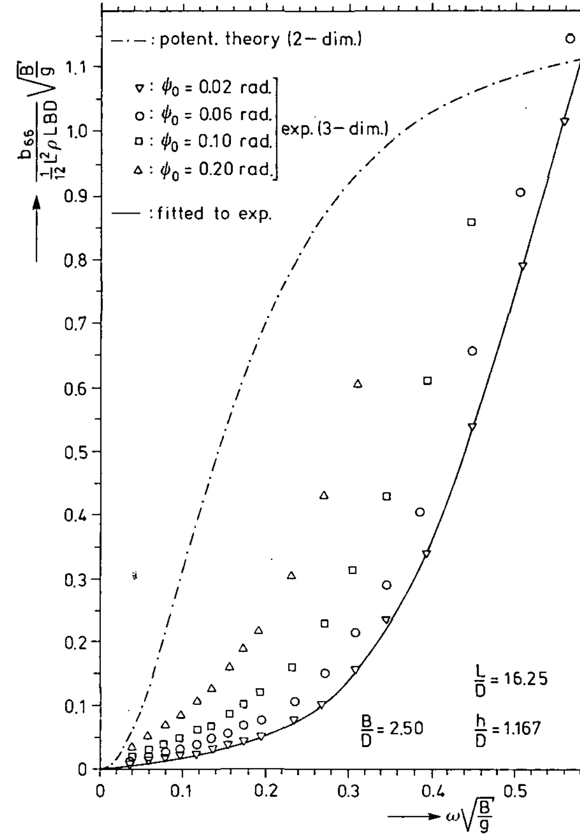

Fig. 3.9[b] - Yaw damping moment coefficient on horizontally unrestricted water (h/D = 1.167)

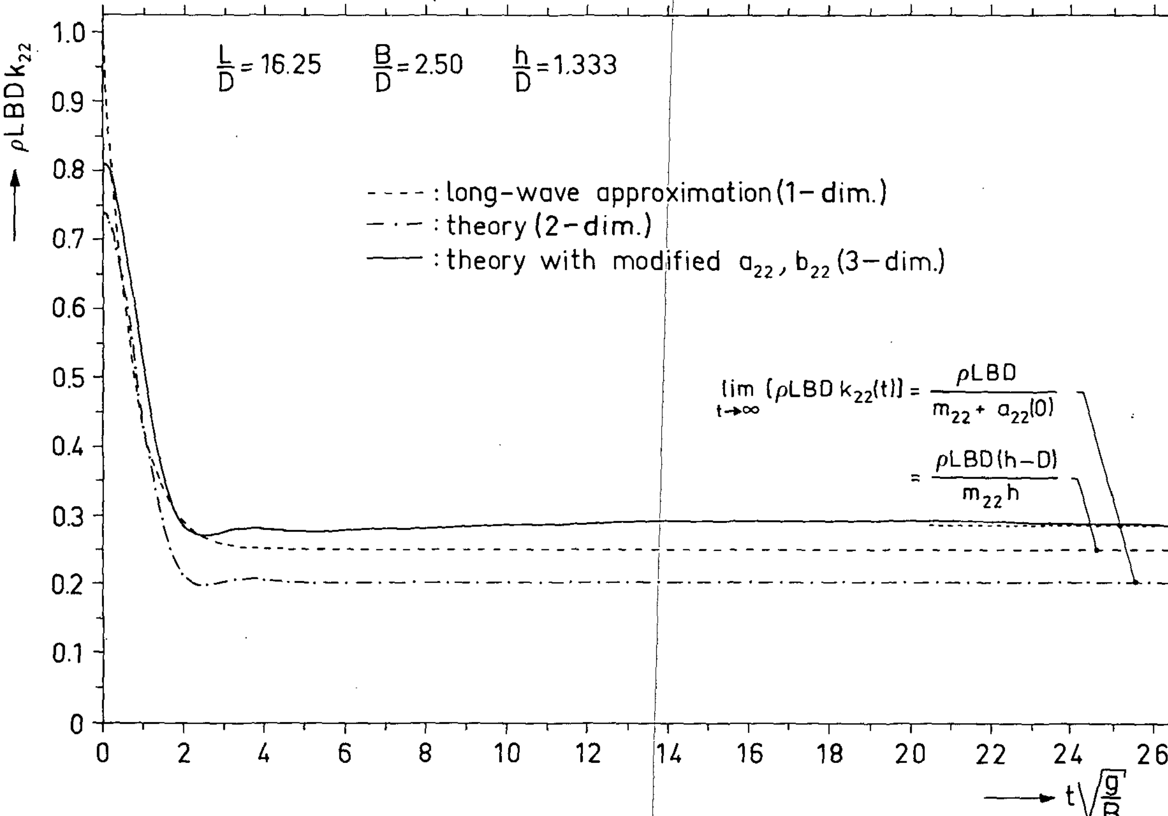

Fig. 3.10 - Impulse response function for sway motion on horizontally unrestricted water (h/D = 1.333)

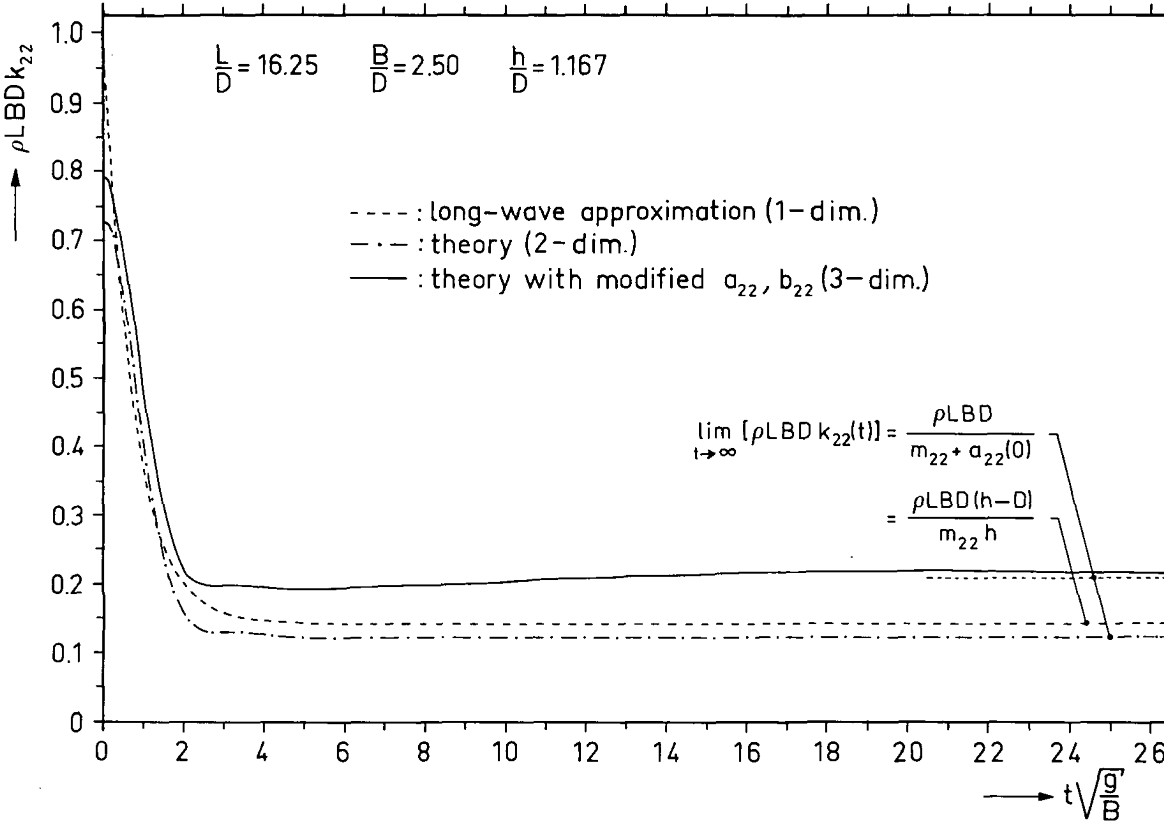

Fig. 3.11 - Impulse response function for sway motion on horizontally unrestricted water (h/D = 1.167)

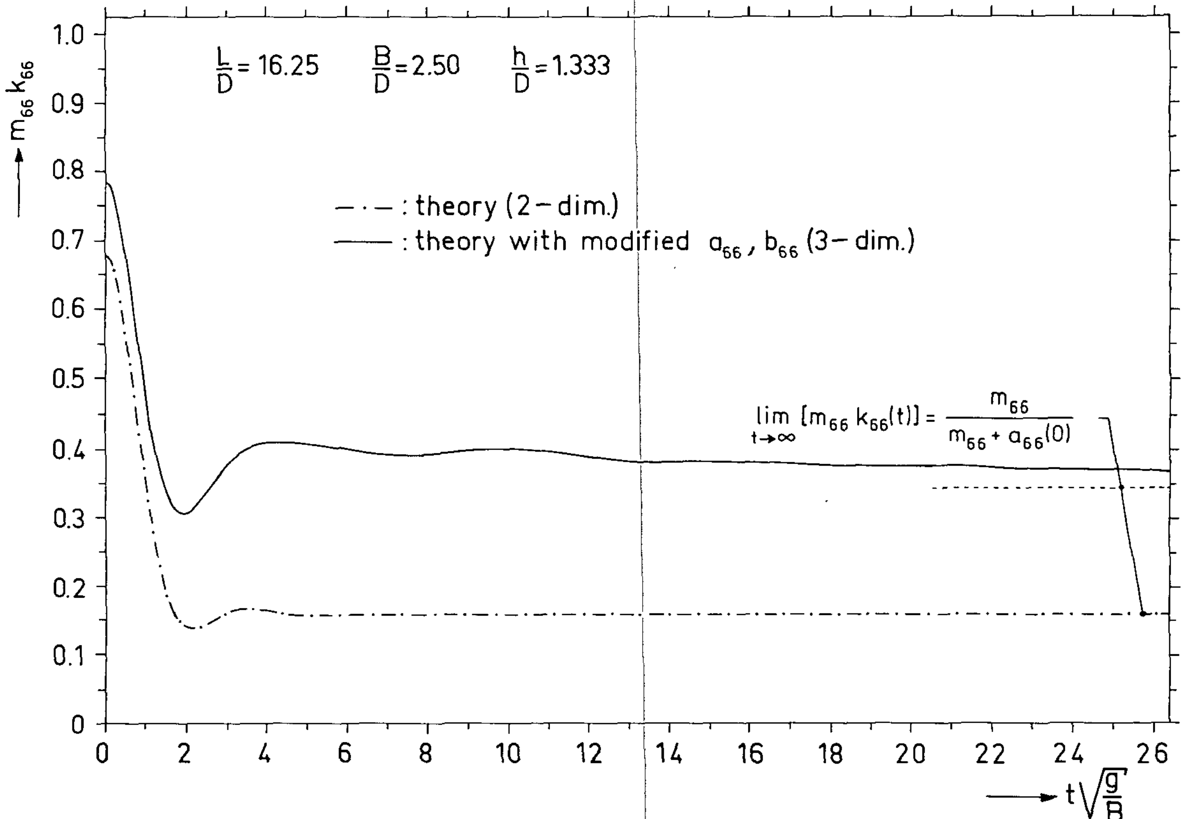

Fig. 3.12 - Impulse response function for yaw motion on horizontally unrestricted water ($h/D = 1.333$)

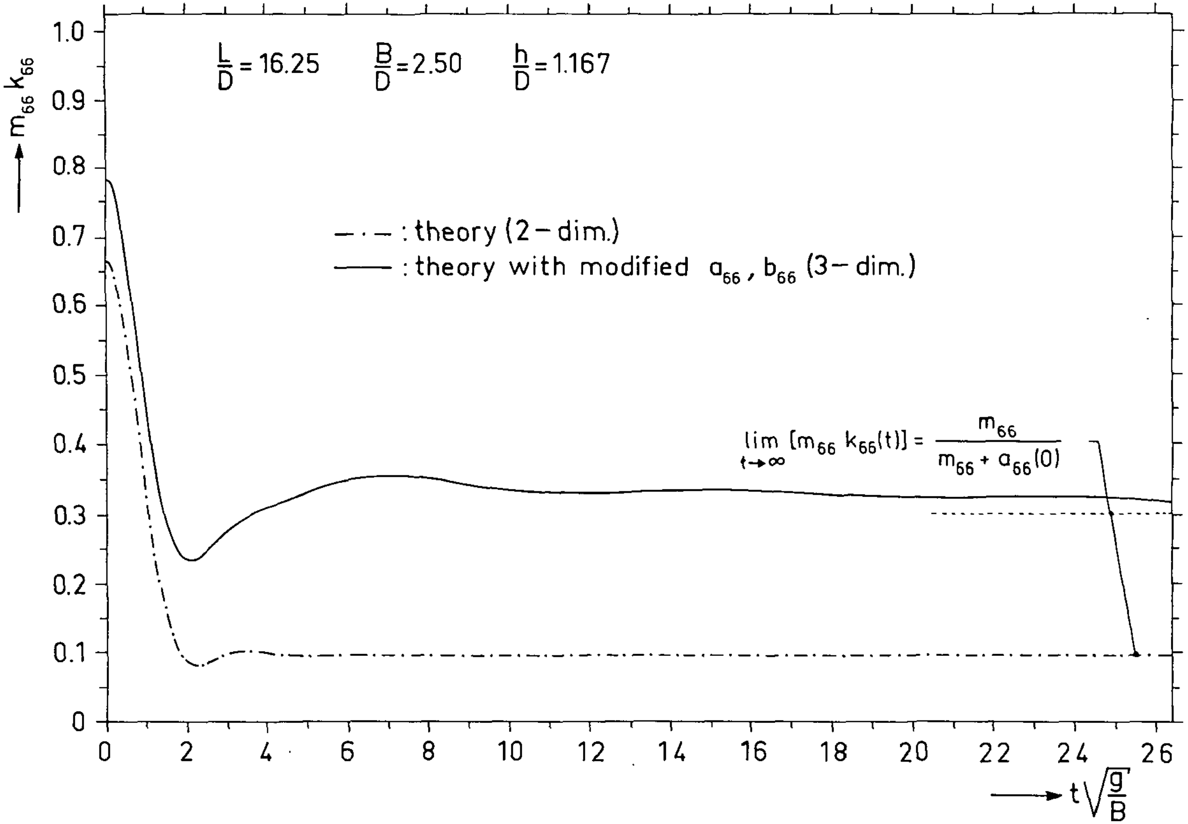

Fig. 3.13 - Impulse response function for yaw motion on horizontally unrestricted water (h/D = 1.167)

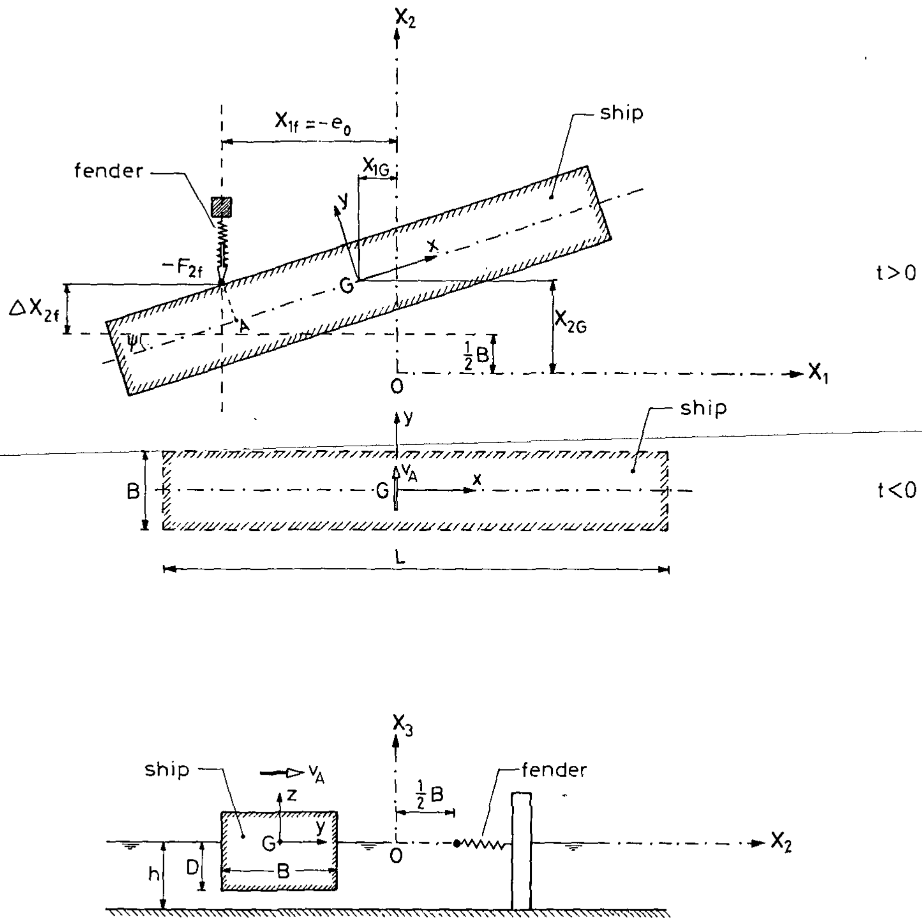

Fig. 3.14 - Plan and cross-section of open berthing lay-out

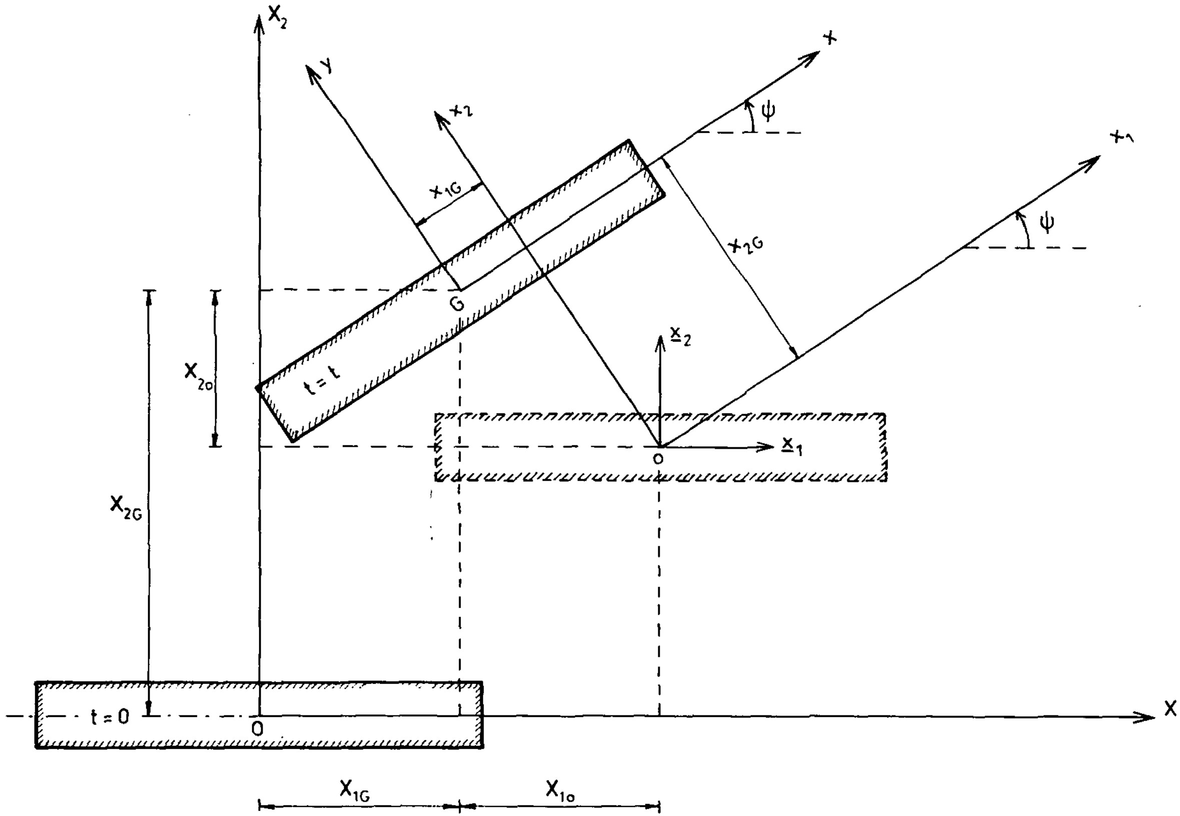

Fig. 3.15 - Definition sketch of ship motion during berthing operation

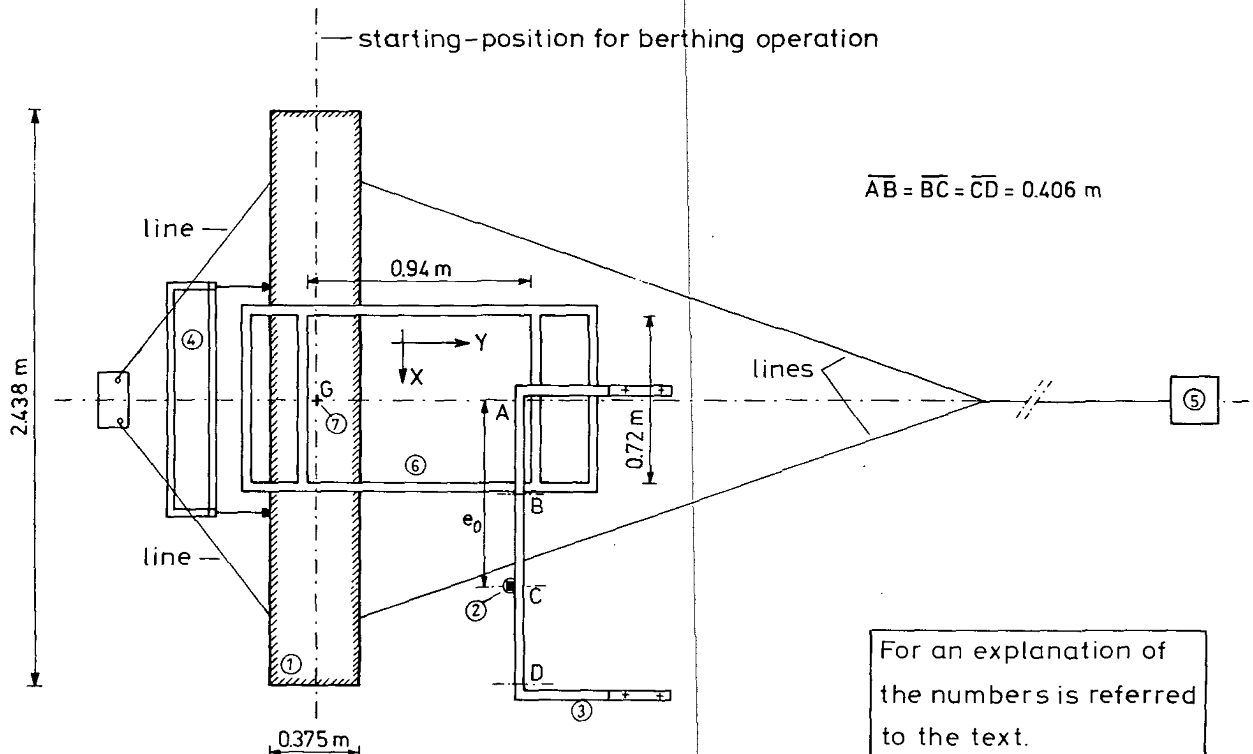

Fig. 3.16 - Plan of berthing lay-out for experiments: open berth

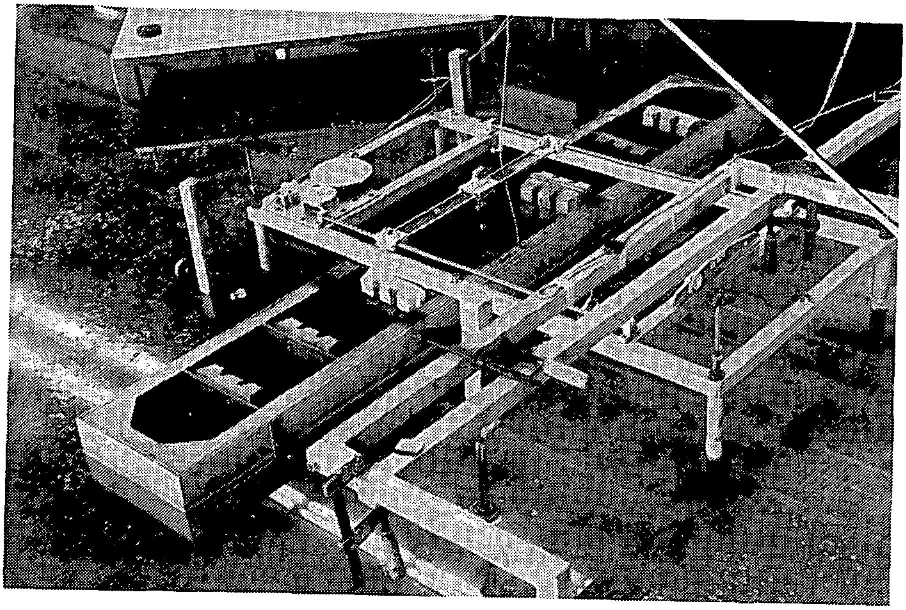

Fig. 3.17^{a} - General view of experimental facility

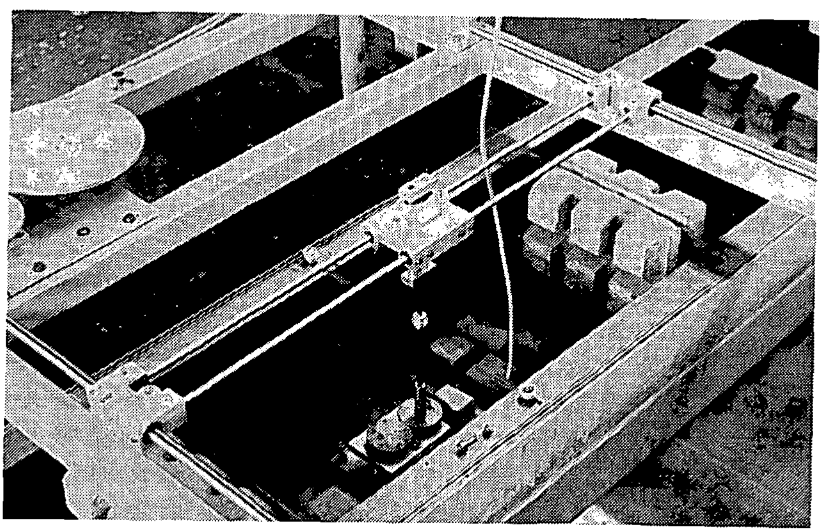

Fig. 3.17^{b} - Connection between ship model and 'position follower'

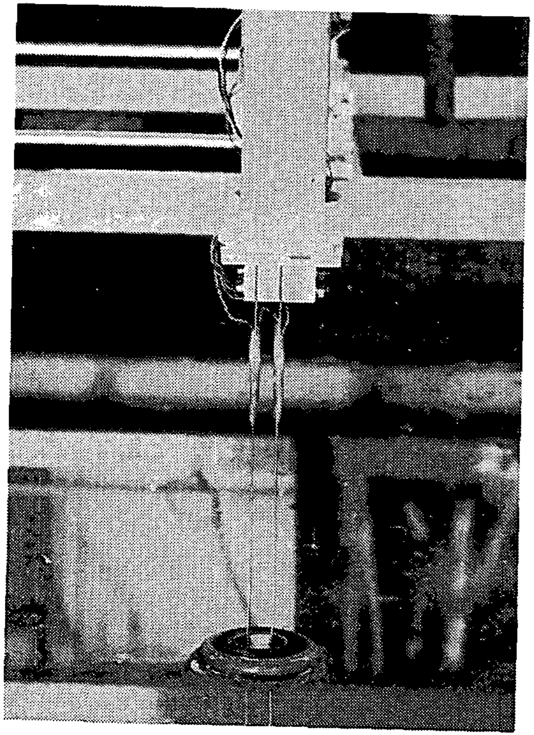

Fig. 3.17^{c} - Simulation of linear fender

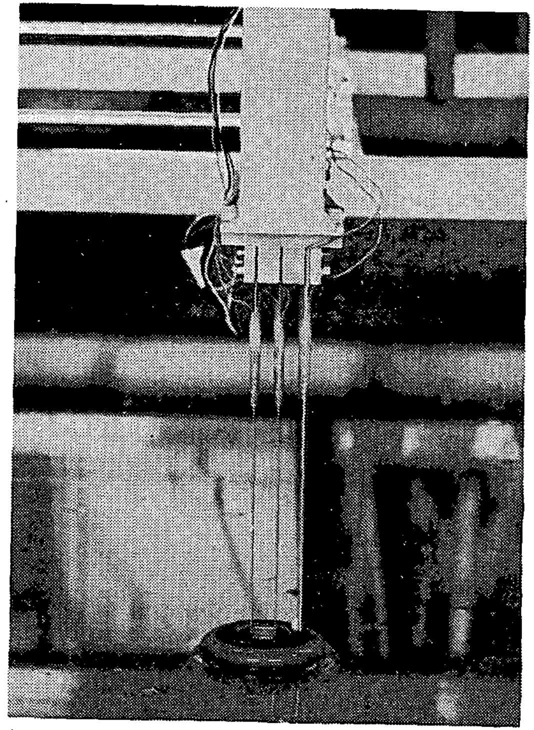

Fig. 3.17^{d} - Simulation of non-linear fender

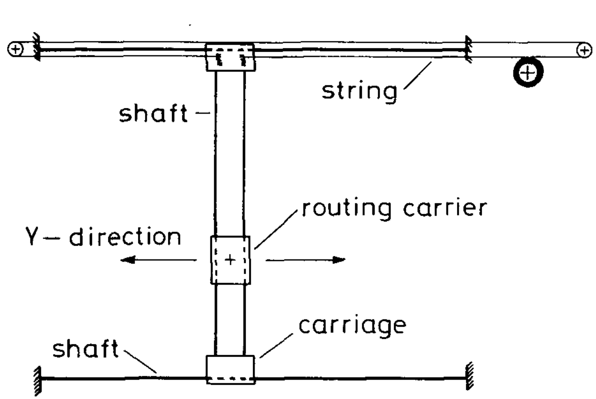

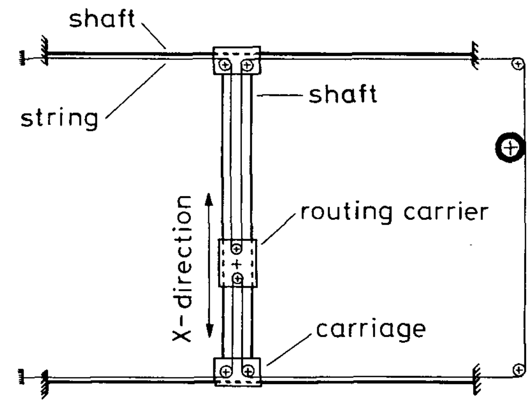

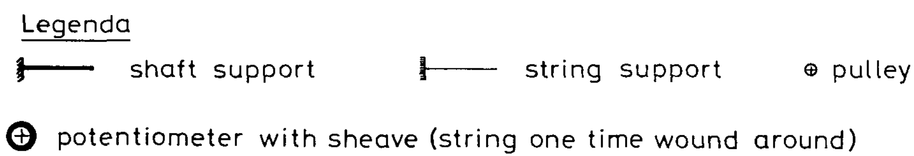

Fig. 3.18[a] - Plan of carriage (= 'Y'-)axis string driven potentiometer circuit

Fig. 3.18[b] - Plan of routing carrier (= 'X'-)axis string driven potentiometer cicuit

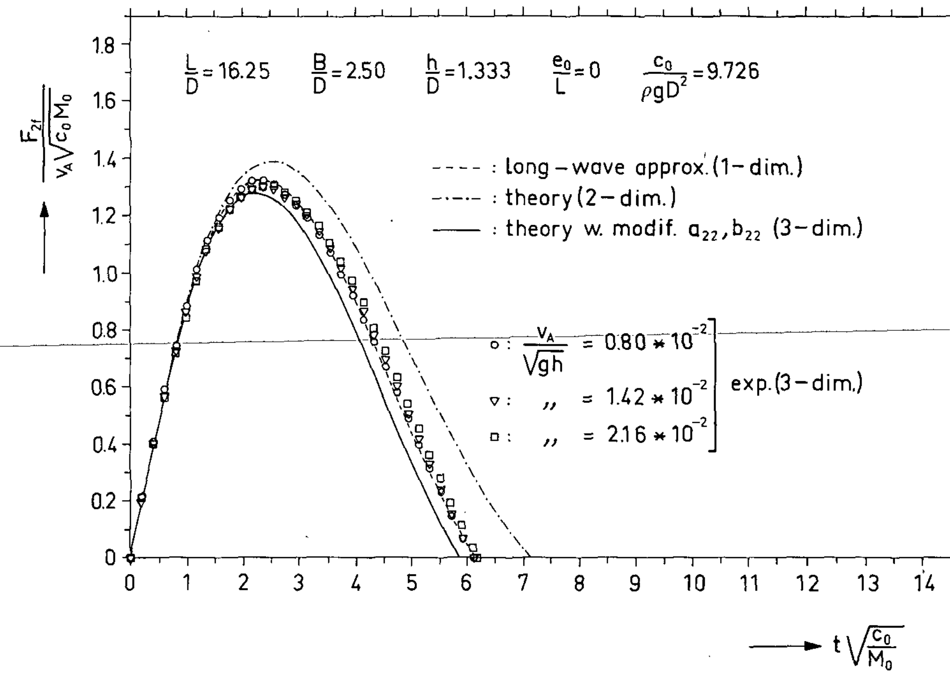

Fig. 3.19 - Time history of fender force: open berth, linear fender, centric impact (h/D = 1.333)

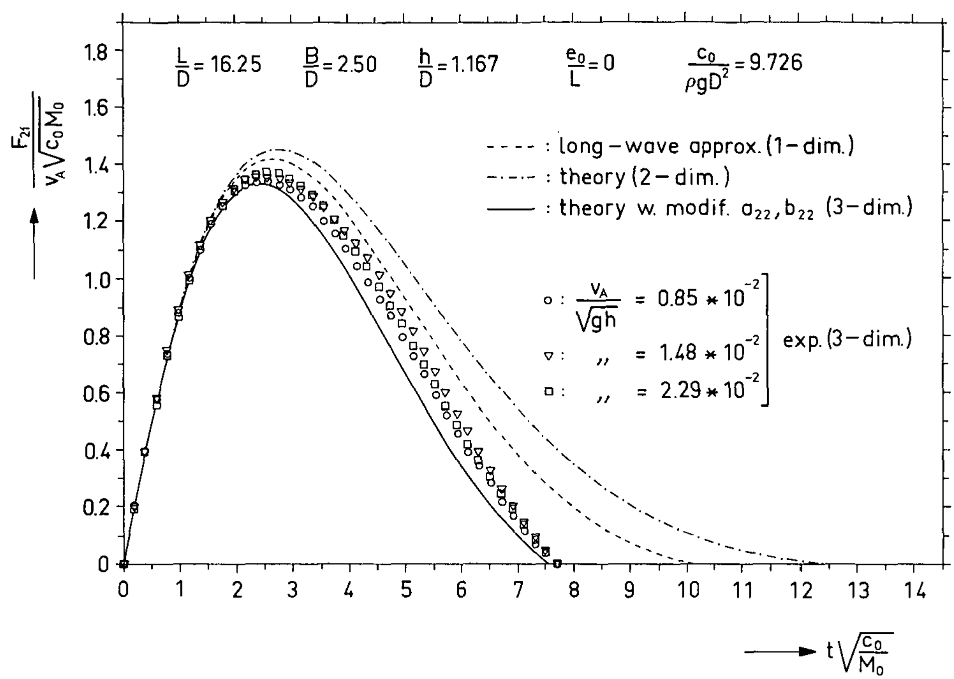

Fig. 3.20 - Time history of fender force: open berth, linear fender, centric impact (h/D = 1.167)

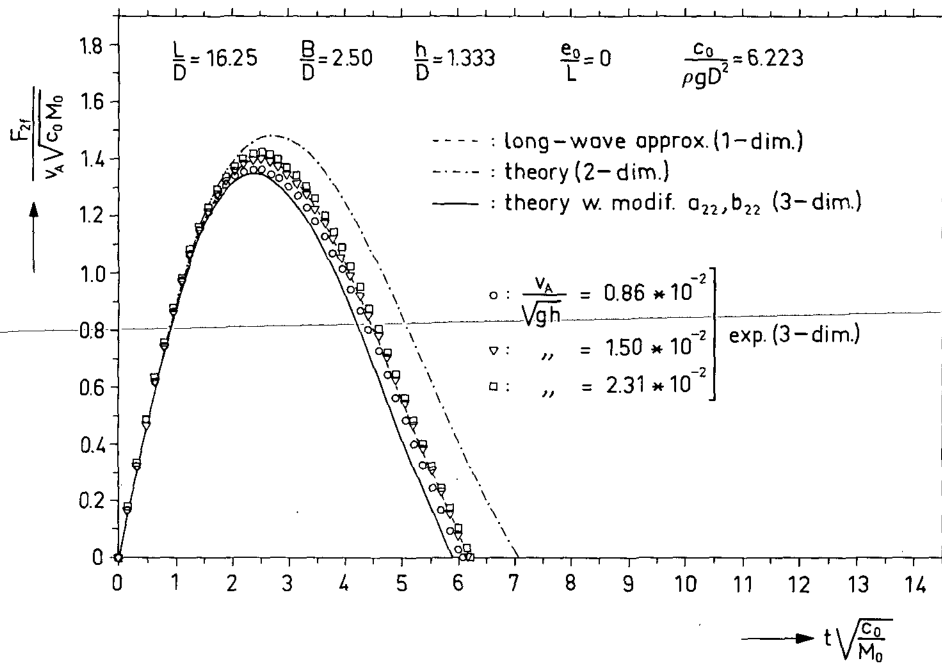

Fig. 3.21 - Time history of fender force: open berth, linear fender, centric impact (h/D = 1.333)

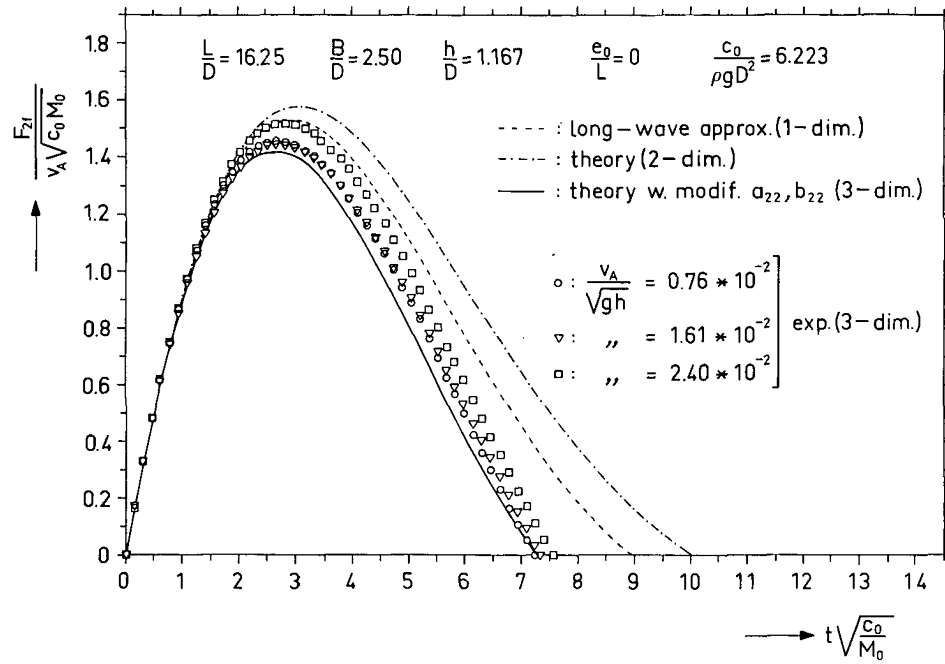

Fig. 3.22 - Time history of fender force: open berth, linear fender, centric impact (h/D = 1.167)

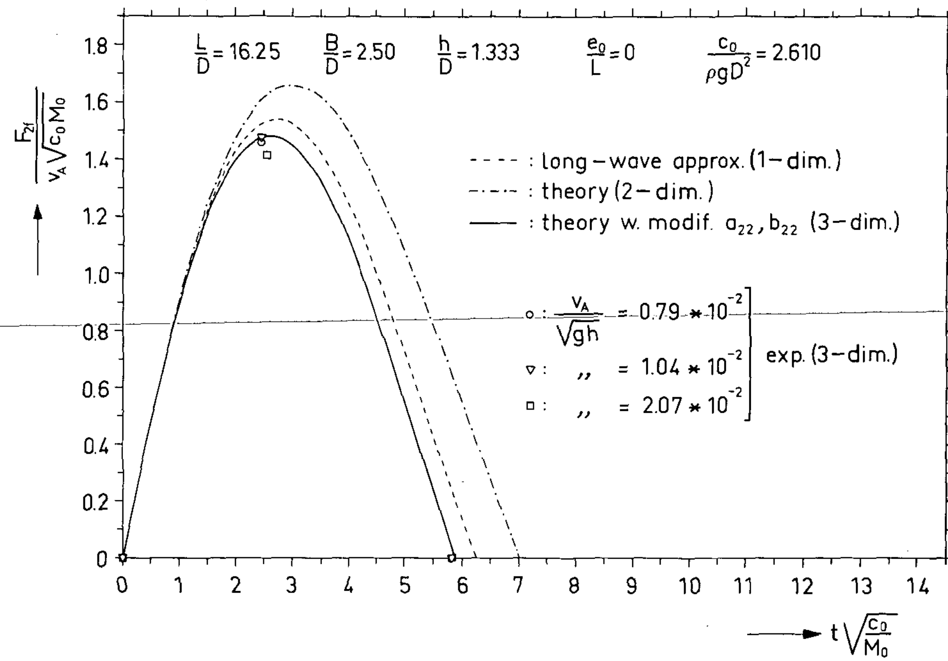

Fig. 3.23 - Time history of fender force: open berth, linear fender, centric impact (h/D = 1.333)

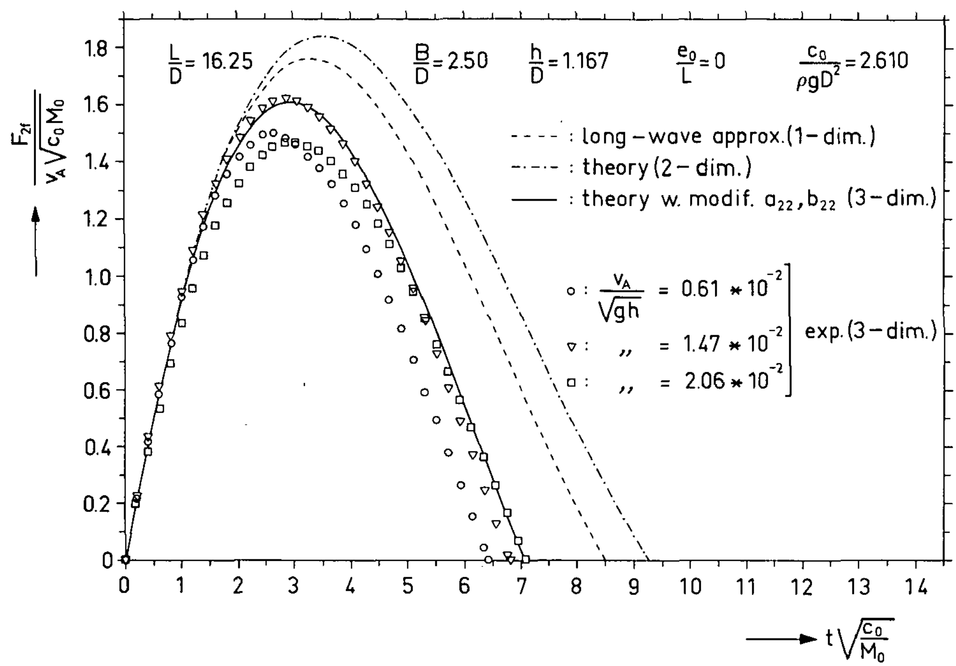

Fig. 3.24 - Time history of fender force: open berth, linear fender, centric impact (h/D = 1.167)

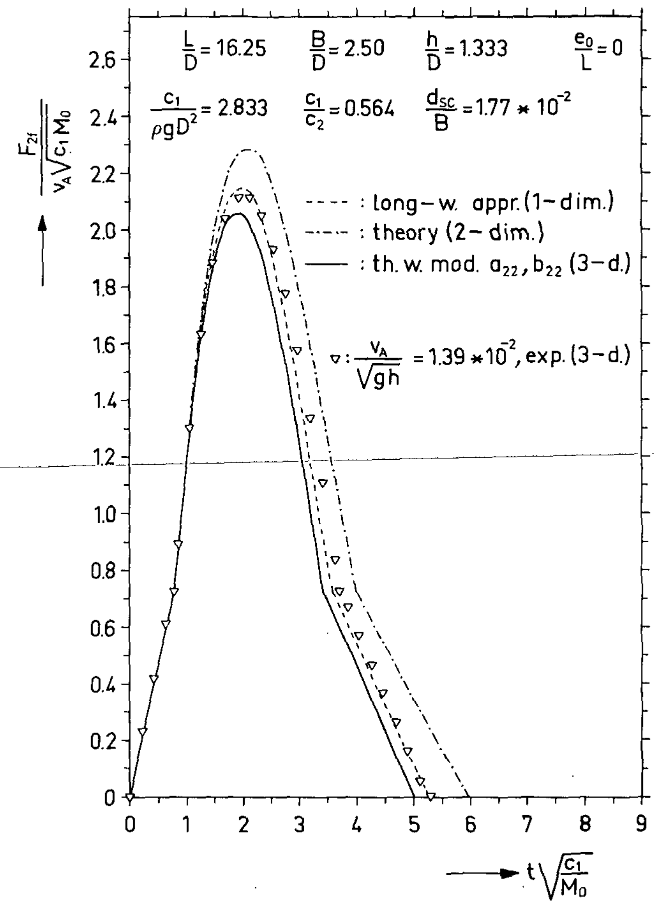

Fig. 3.25 - Time history of fender force: open berth, non-linear fender, centric impact (h/D = 1.333)

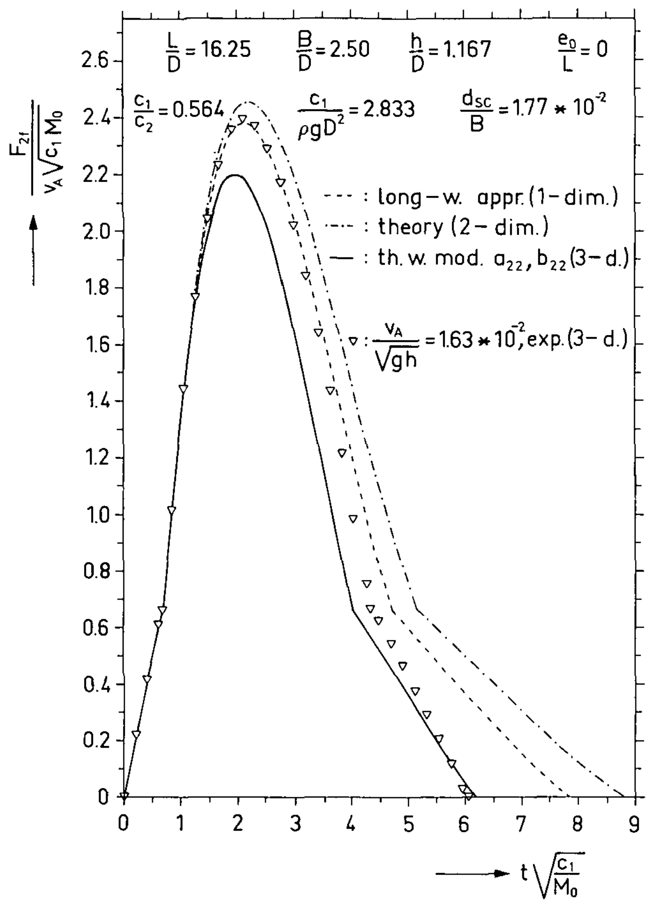

Fig. 3.26 - Time history of fender force: open berth, non-linear fender, centric impact (h/D = 1.167)

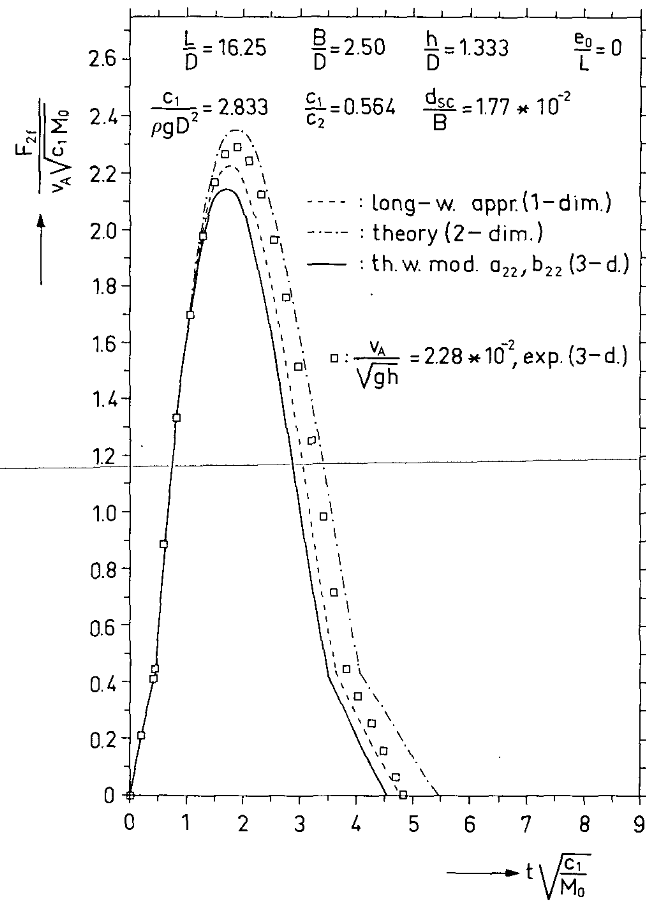

Fig. 3.27 - Time history of fender force: open berth, non-linear fender, centric impact (h/D = 1.333)

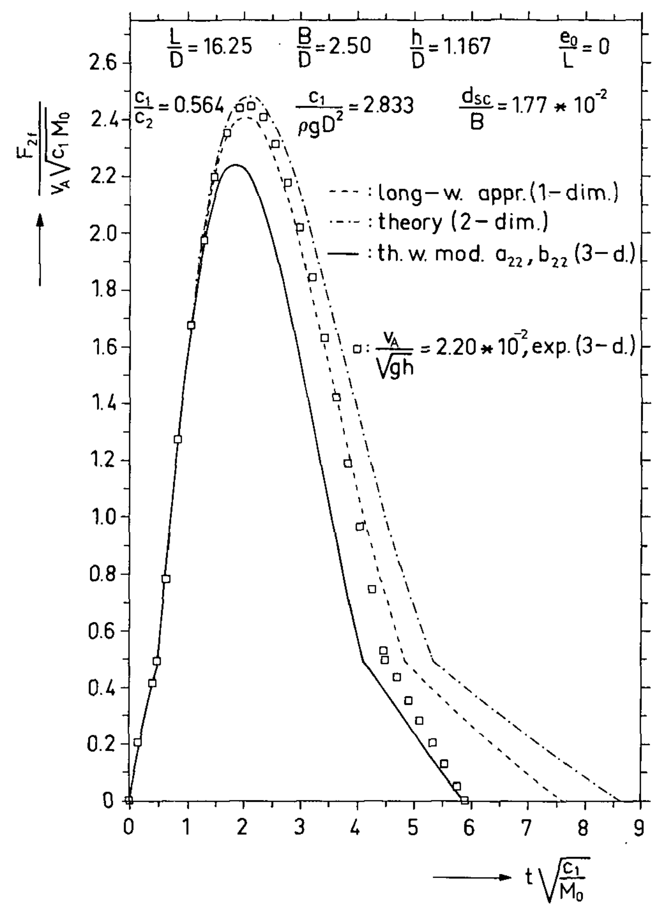

Fig. 3.28 - Time history of fender force: open berth, non-linear fender, centric impact (h/D = 1.167)

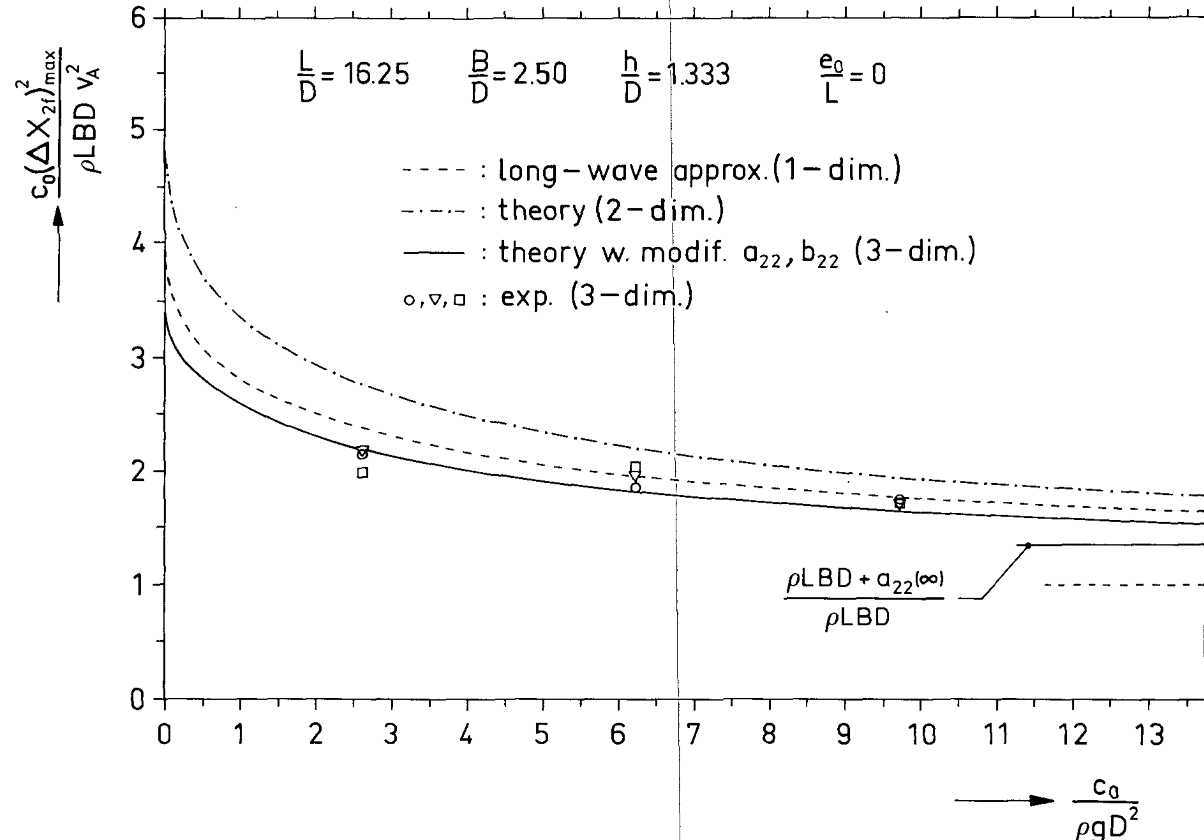

Fig. 3.29 - Influence of fender elasticity on absorbed energy: open berth, linear fender, centric impact (h/D = 1.333)

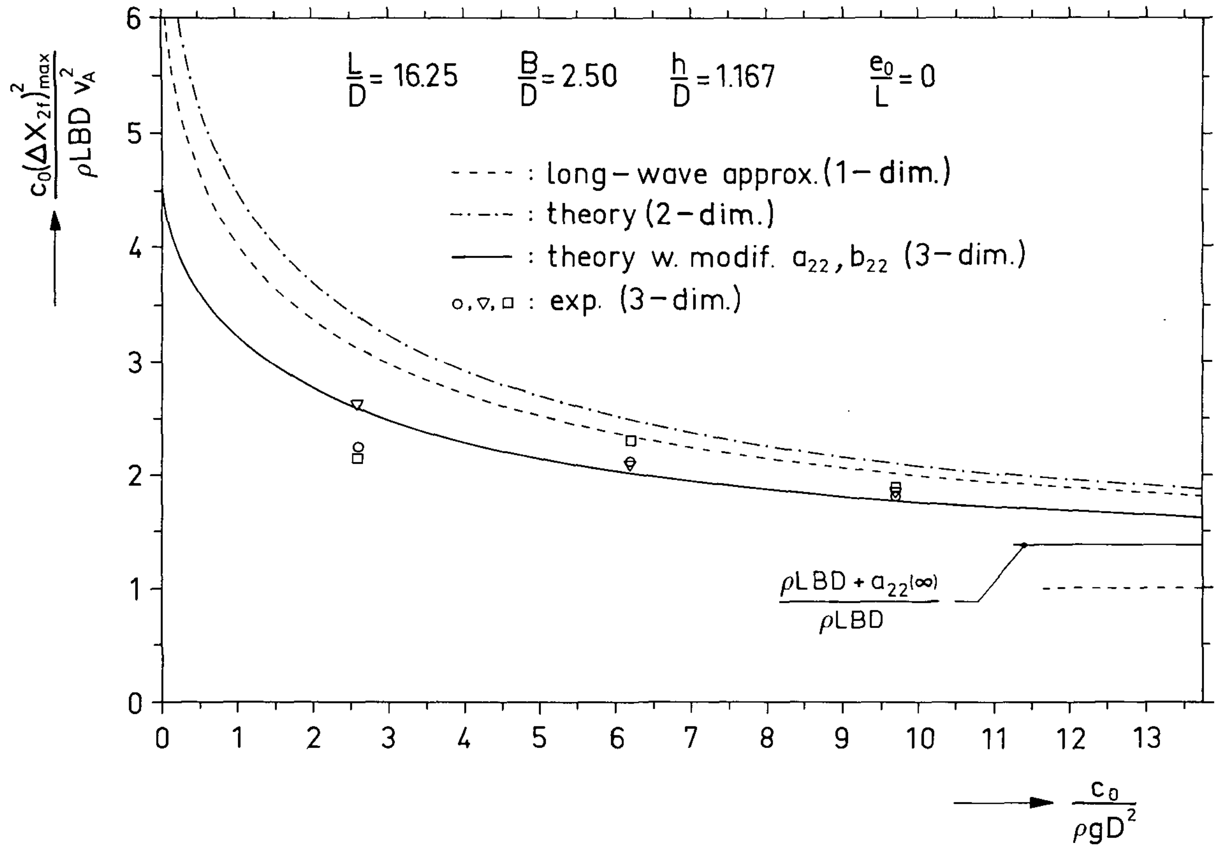

Fig. 3.30 - Influence of fender elasticity on absorbed energy: open berth, linear fender, centric impact (h/D = 1.167)

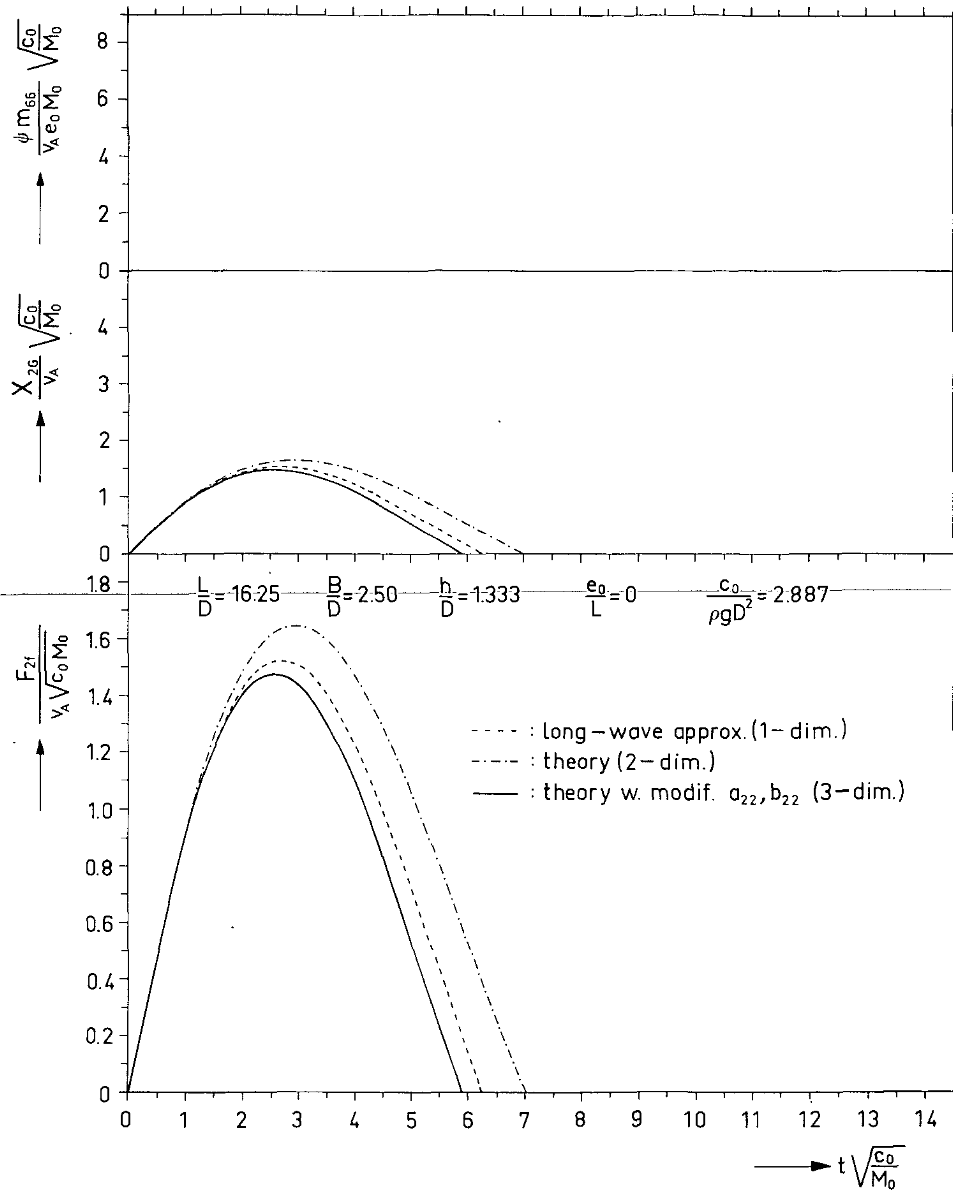

Fig. 3.31 - Time histories of fender force, translation of G and angle of rotation: open berth, linear fender, centric impact (h/D = 1.333)

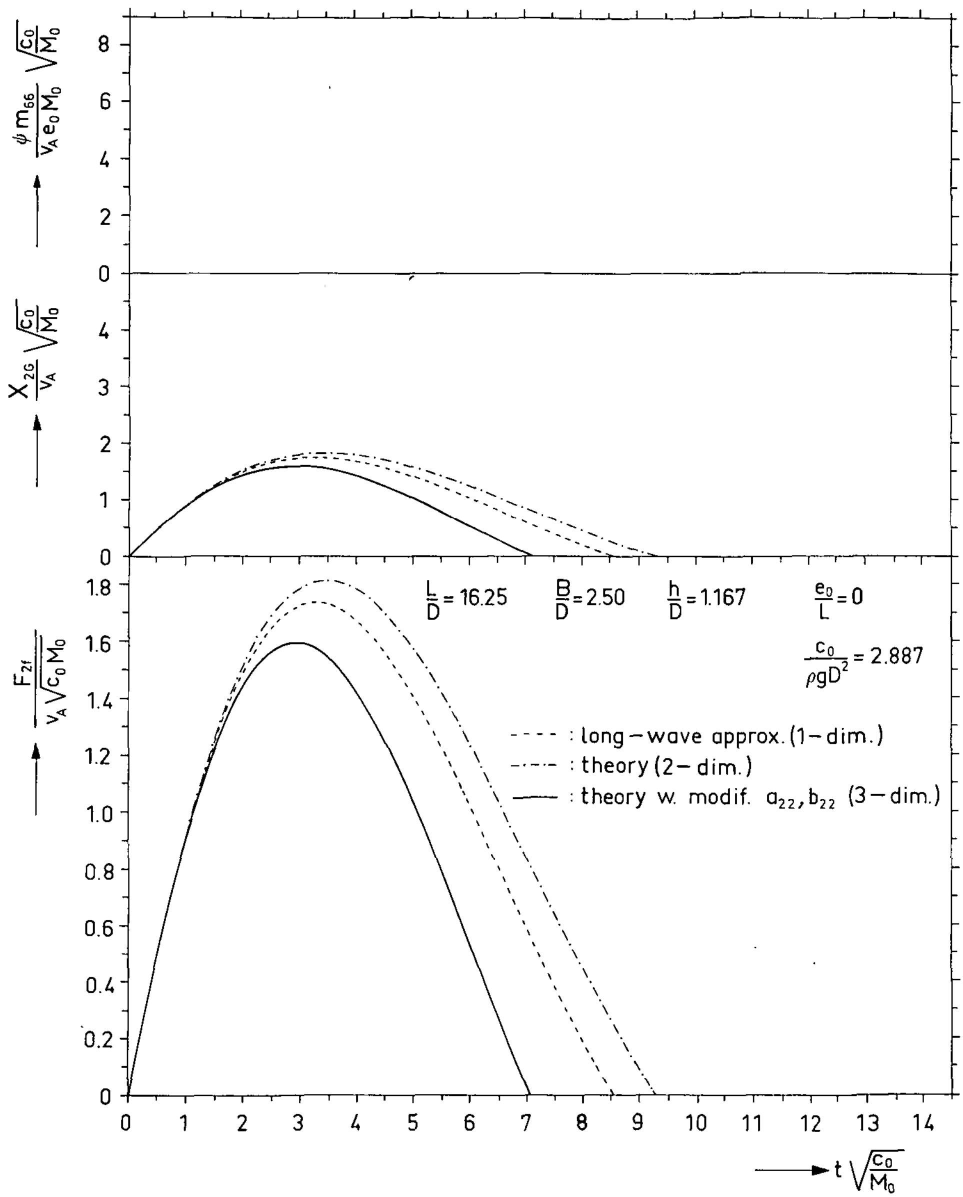

Fig. 3.32 - Time histories of fender force, translation of G and angle of rotation: open berth, linear fender, centric impact (h/D = 1.167)

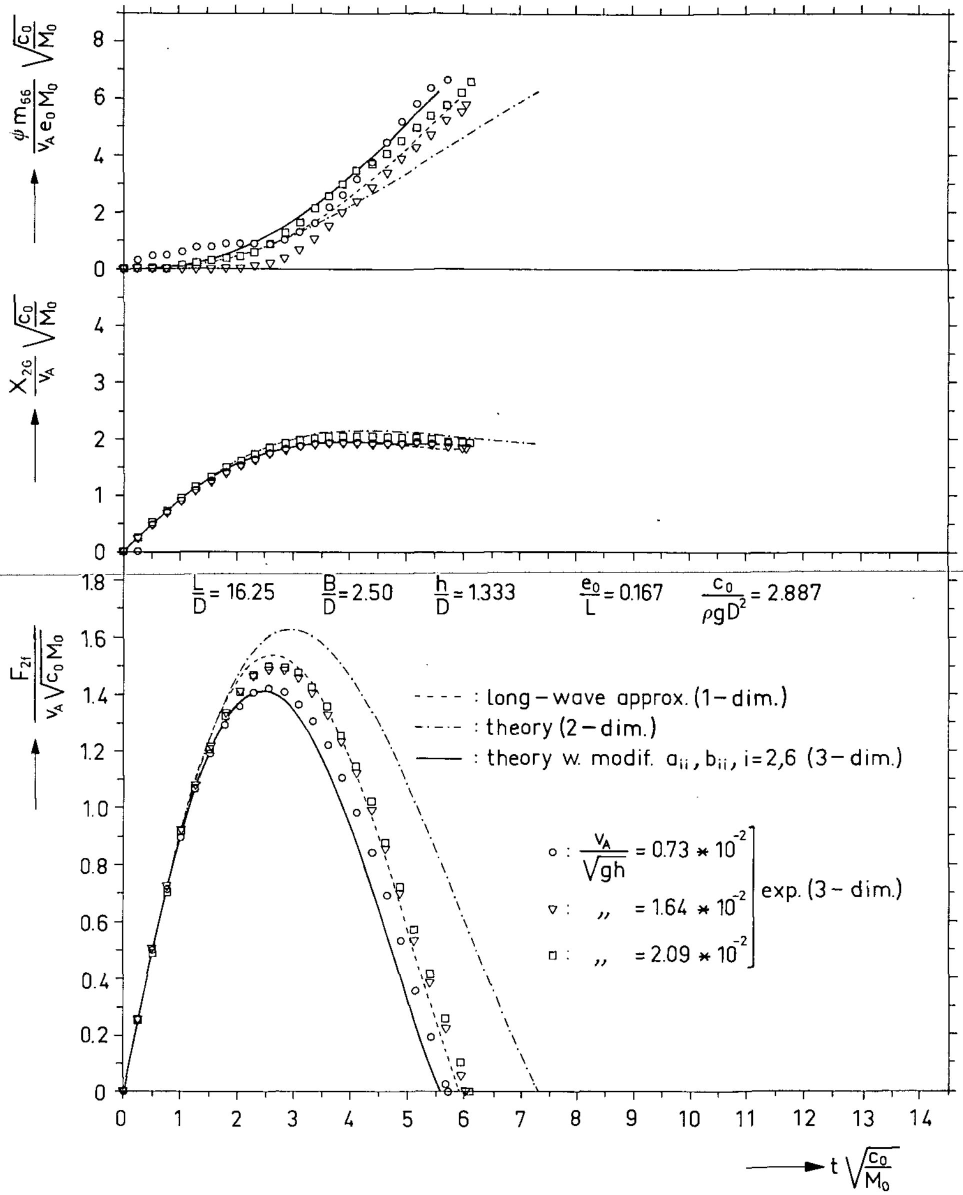

Fig. 3.33 - Time histories of fender force, translation of G and angle of rotation: open berth, linear fender, eccentric impact (h/D = 1.333)

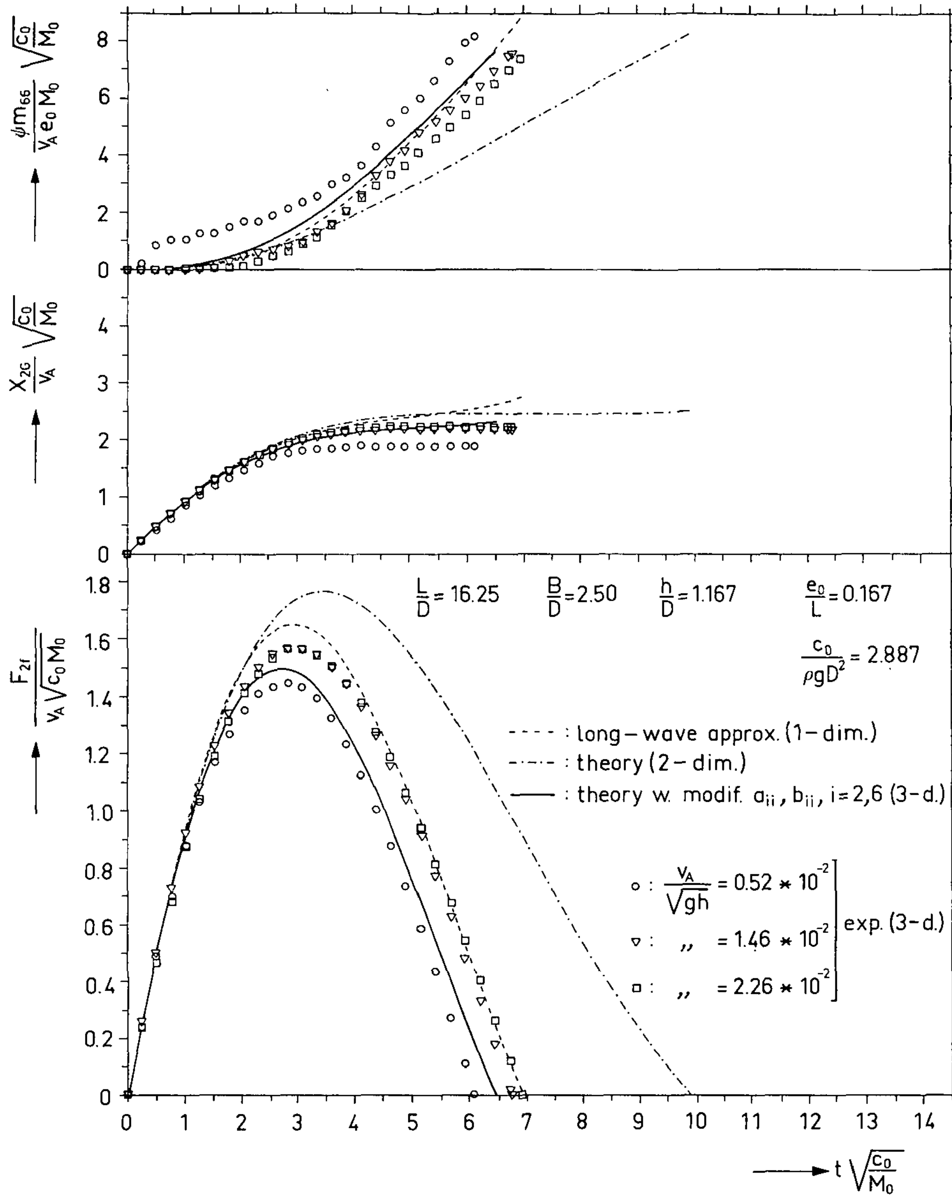

Fig. 3.34 - Time histories of fender force, translation of G and angle of rotation: open berth, linear fender, eccentric impact (h/D = 1.167)

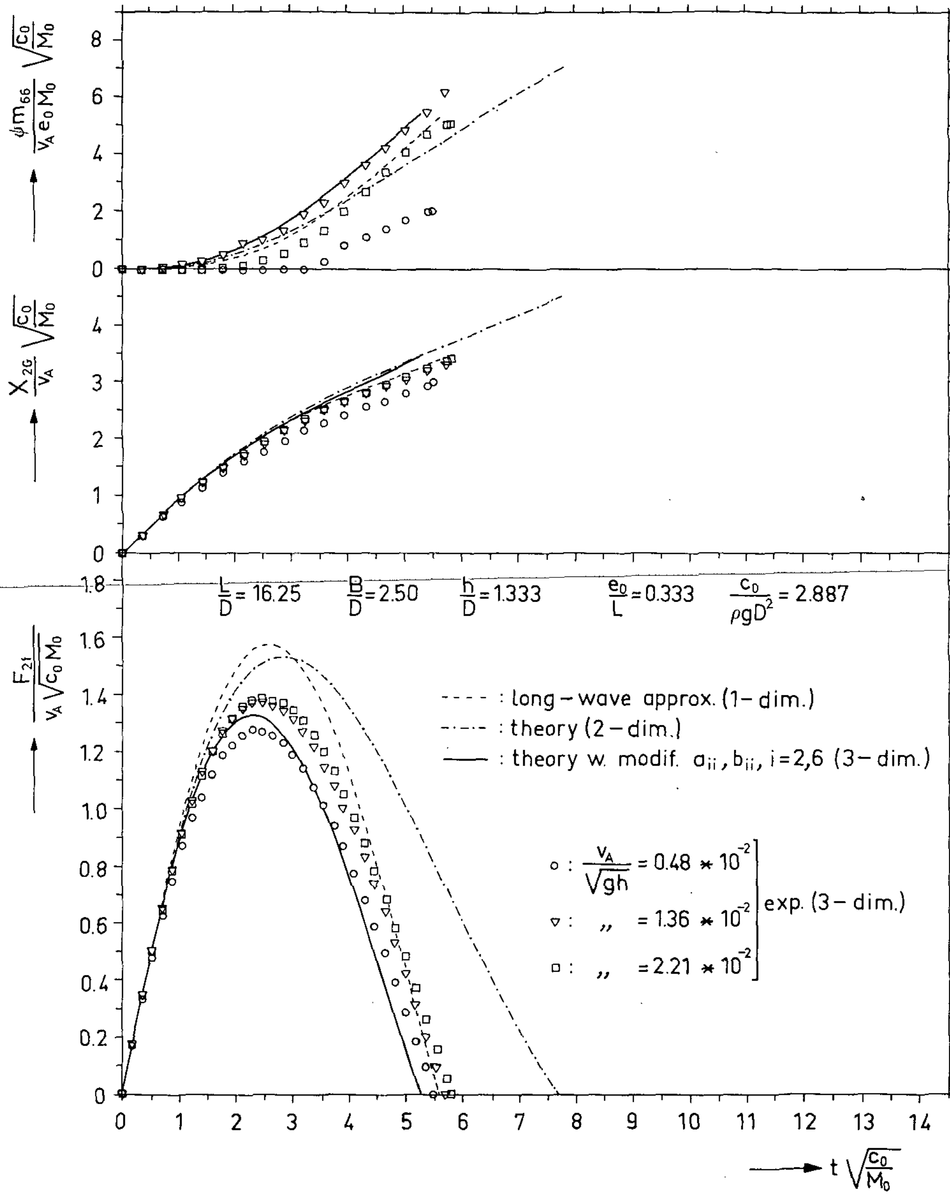

Fig. 3.35 - Time histories of fender force, translation of G and angle of rotation: open berth, linear fender, eccentric impact (h/D = 1.333)

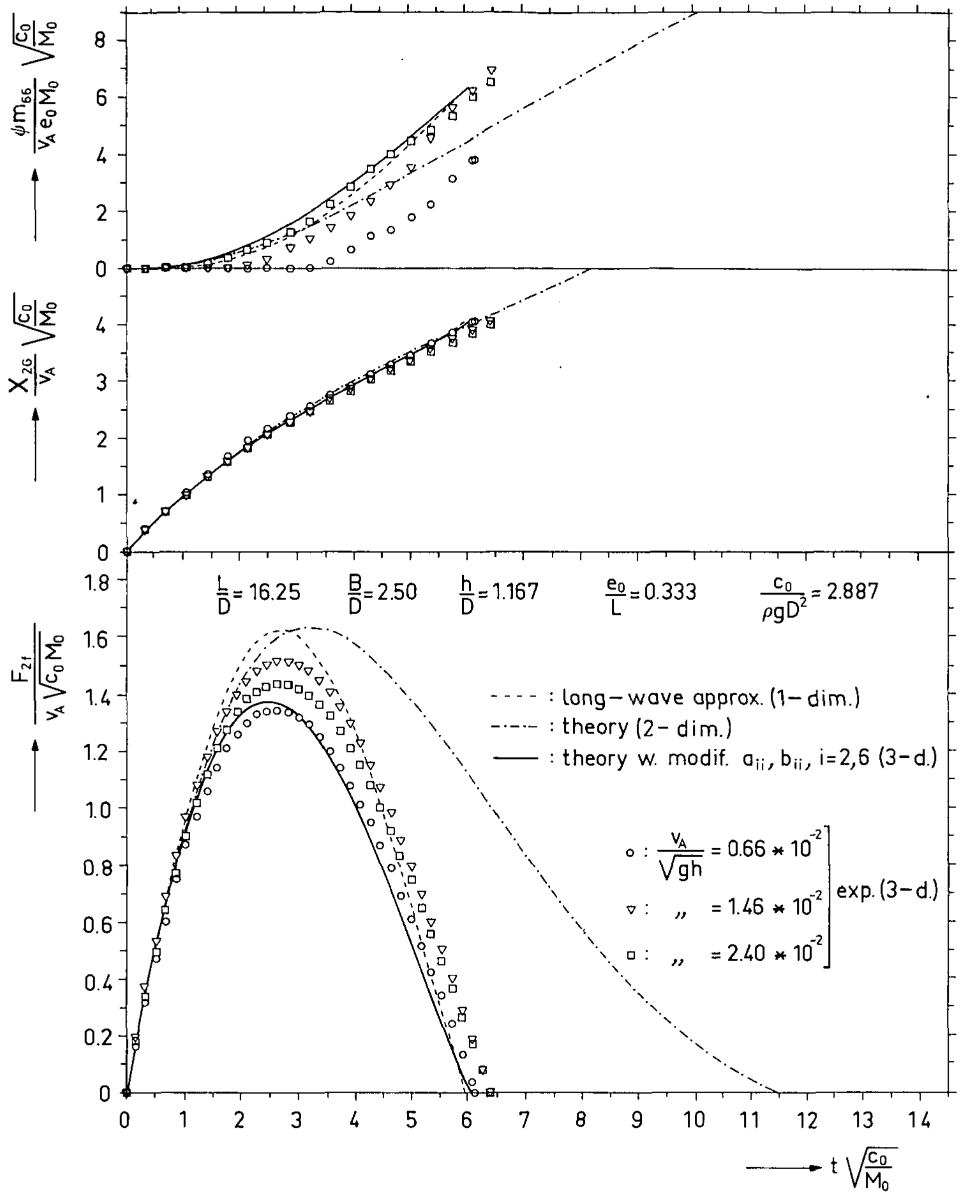

Fig. 3.36 - Time histories of fender force, translation of G and angle of rotation: open berth, linear fender, eccentric impact (h/D = 1.167)

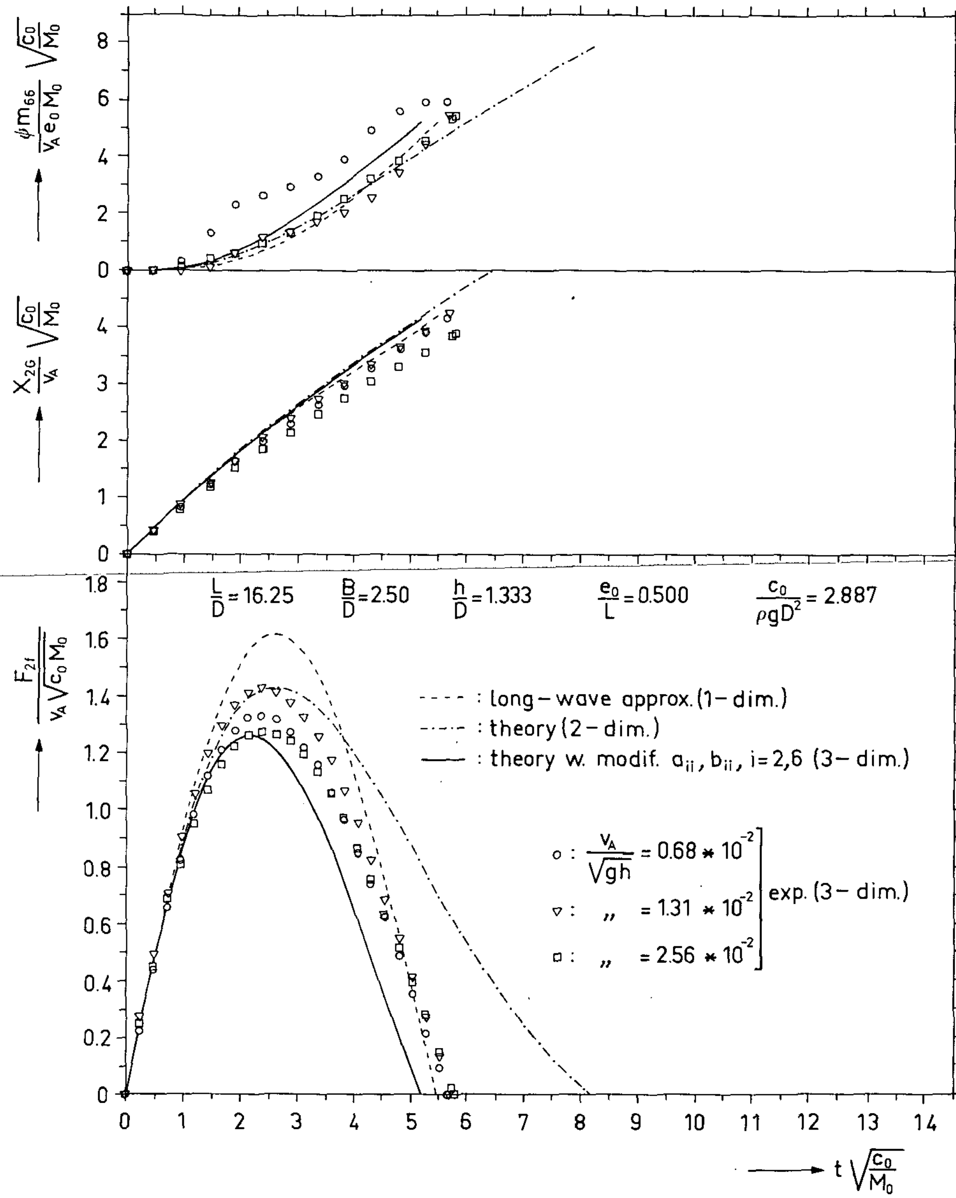

Fig. 3.37 - Time histories of fender force, translation of G and angle of rotation: open berth, linear fender, eccentric impact (h/D = 1.333)

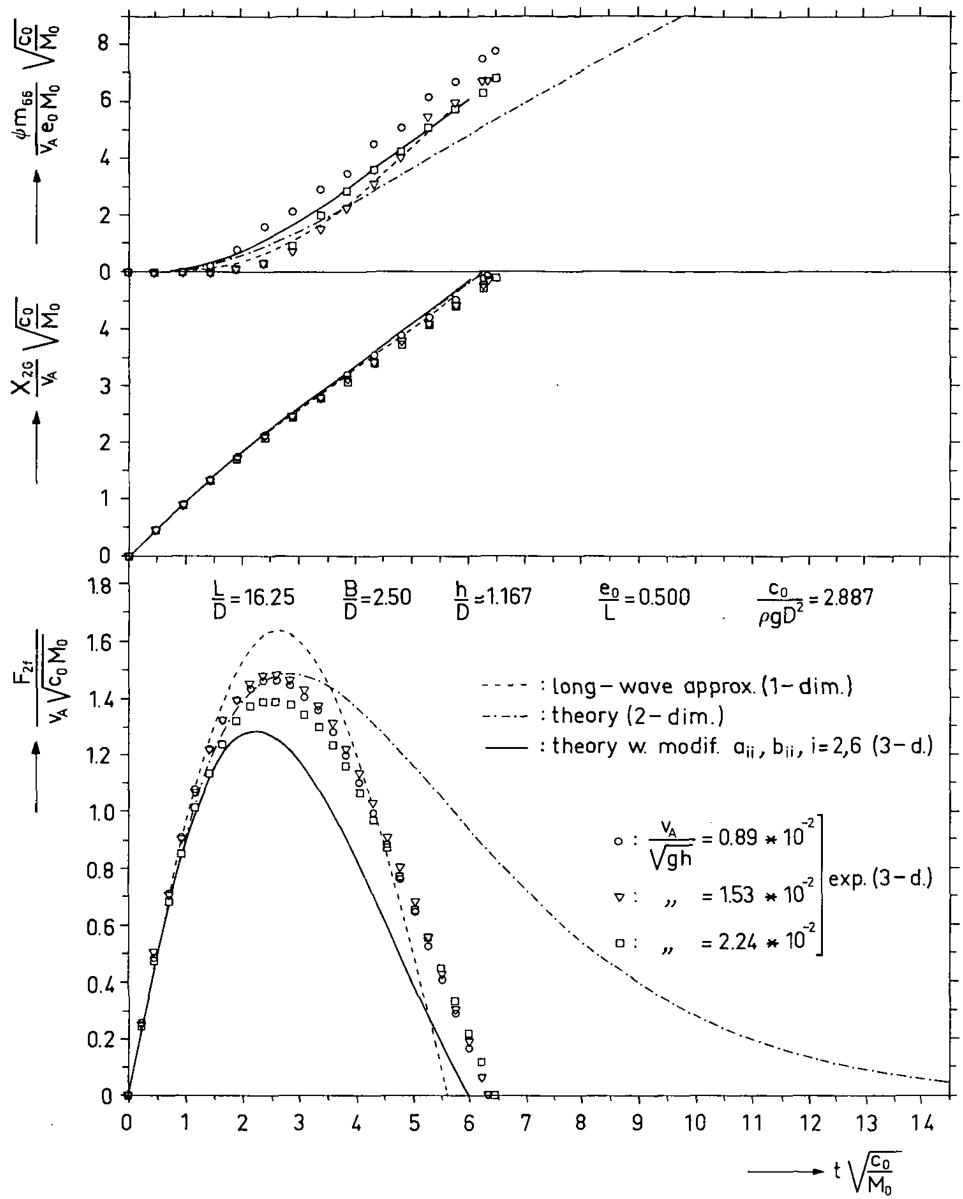

Fig. 3.38 - Time histories of fender force, translation of G and angle of rotation: open berth, linear fender, eccentric impact (h/D = 1.167)

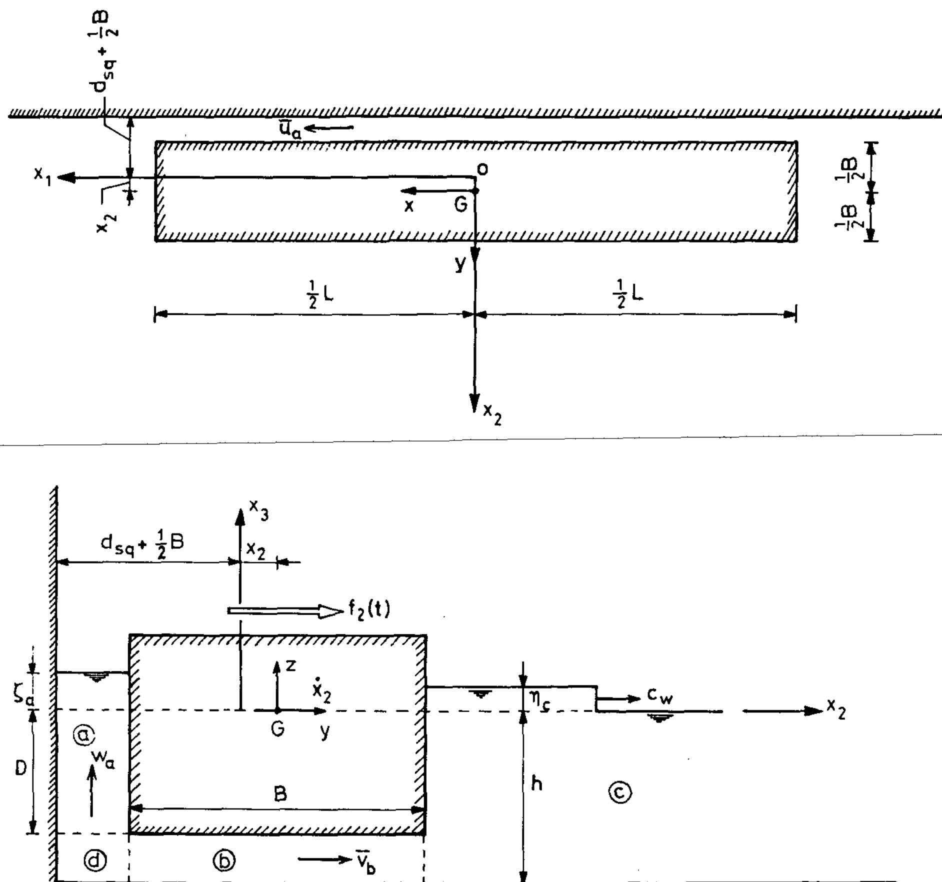

Fig. 4.1 - Definition sketch for sway motion near a vertical wall

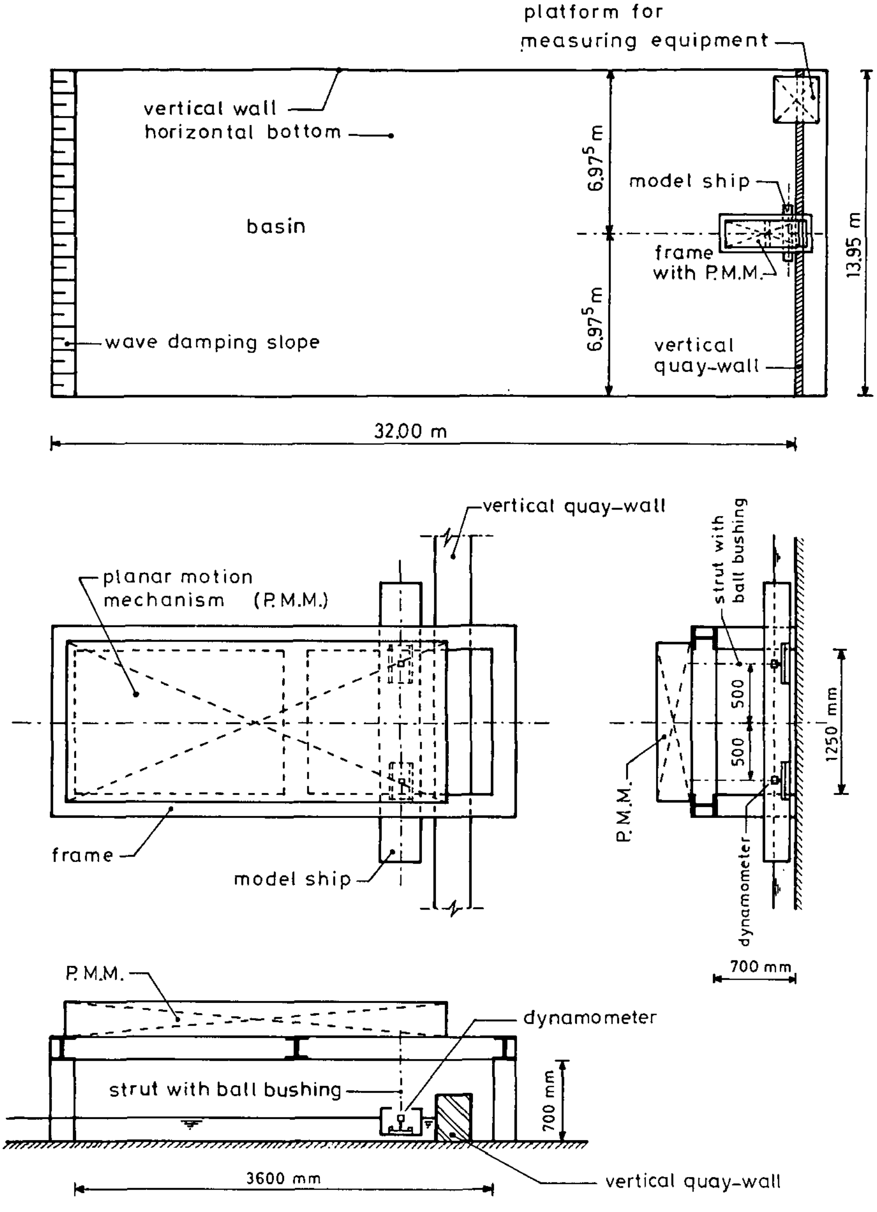

Fig. 4.2 - Schematic representation of experimental set-up for harmonic sway tests near a vertical wall

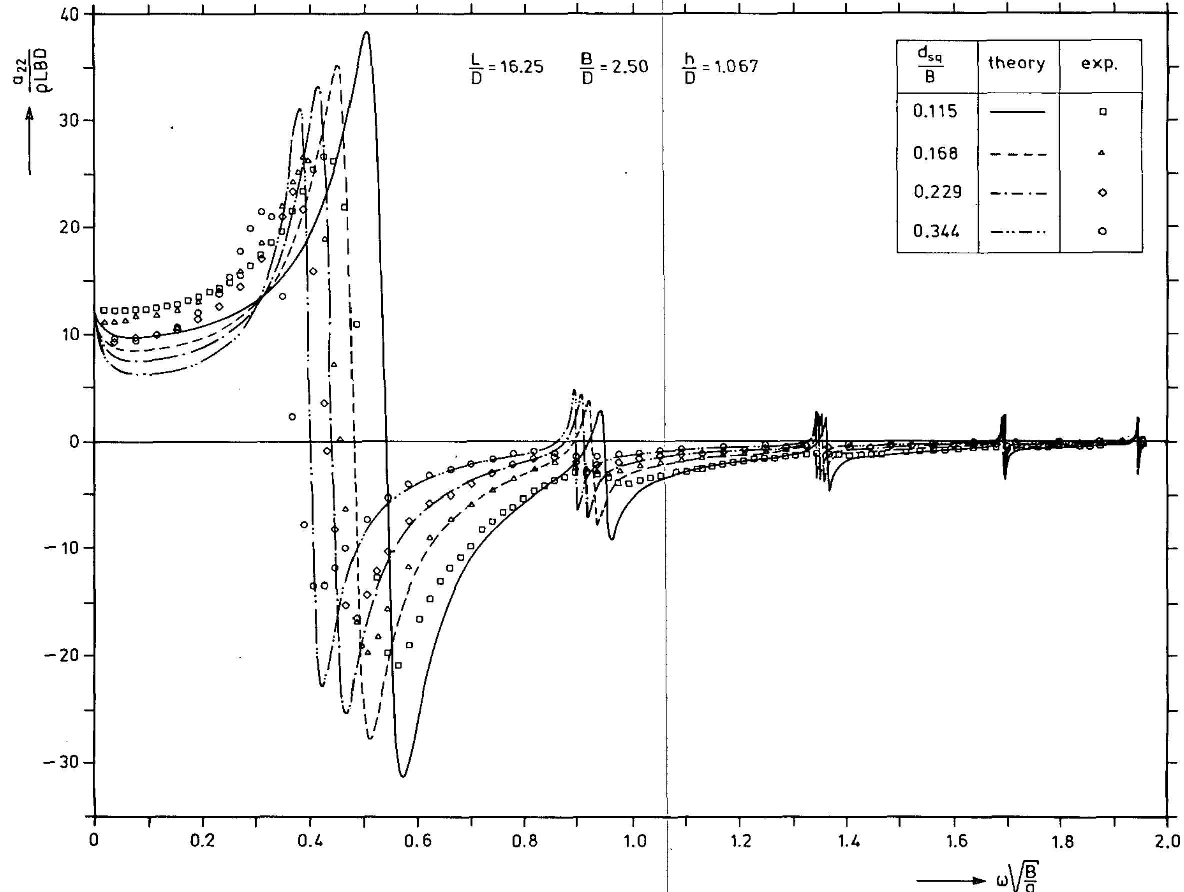

Fig. 4.3 - Added mass for swaying motion near a vertical wall (h/D = 1.067)

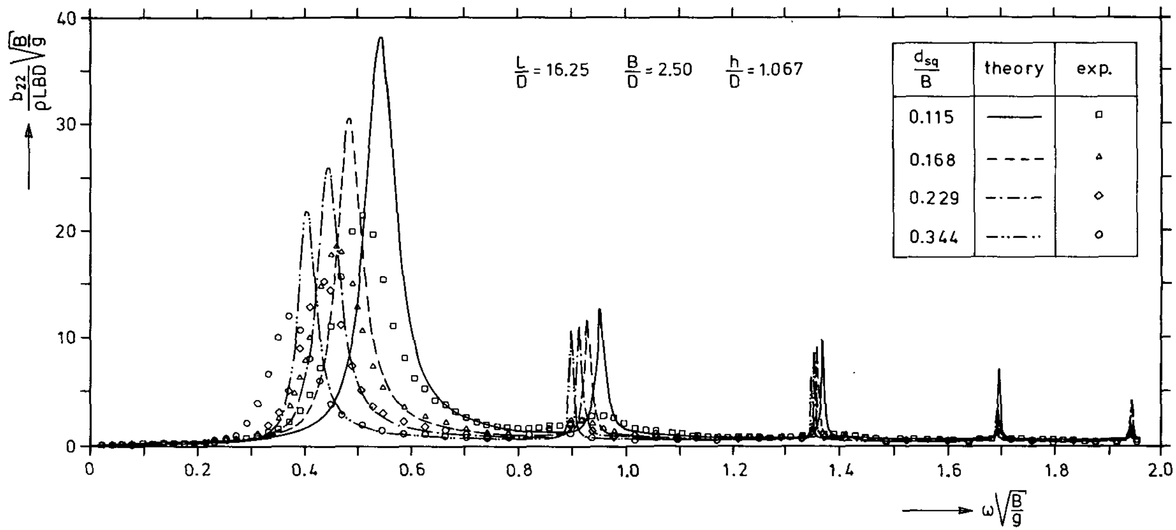

Fig. 4.4 - Sway damping force coefficient near a vertical wall (h/D = 1.067)

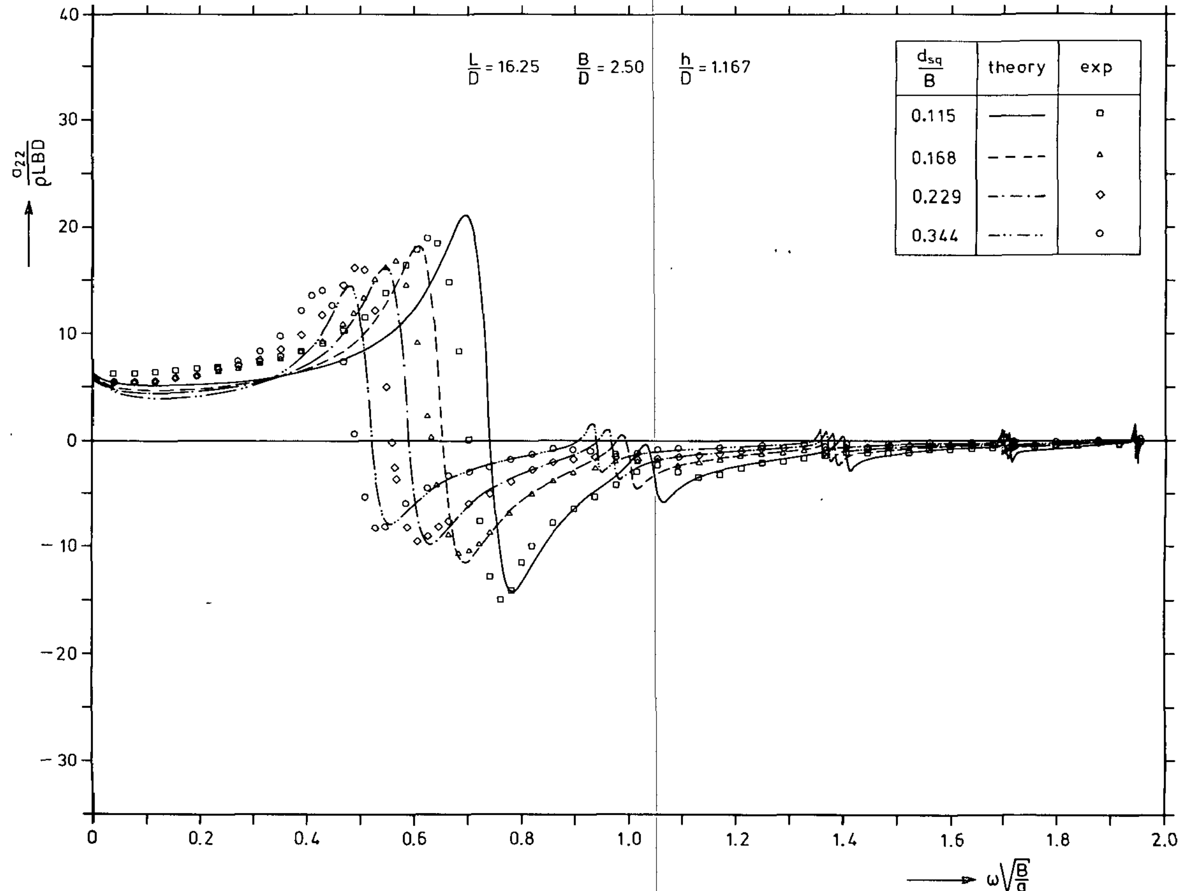

Fig. 4.5 - Added mass for swaying motion near a vertical wall (h/D = 1.167)

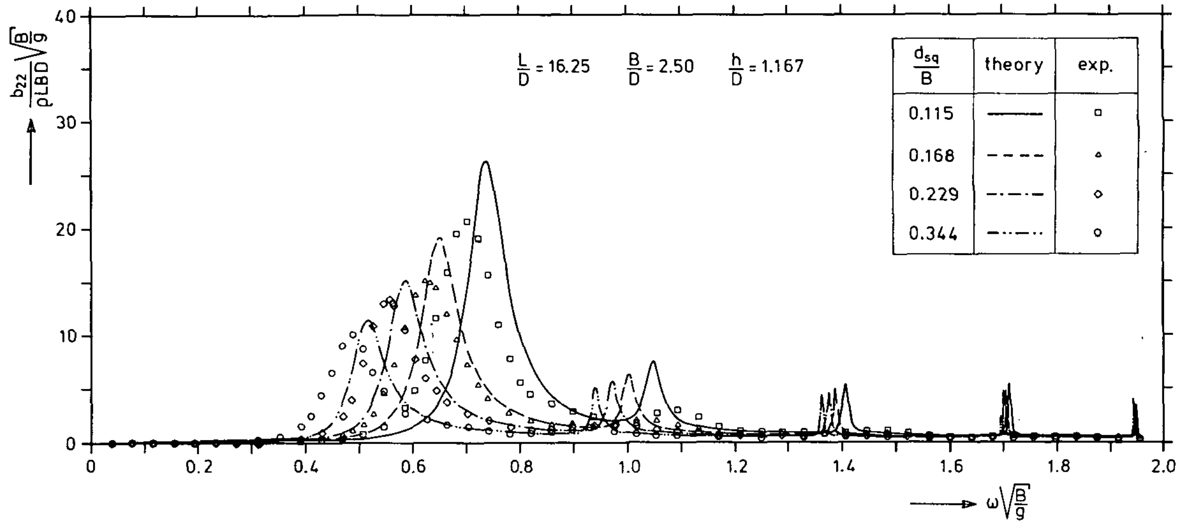

Fig. 4.6 - Sway damping force coefficient near a vertical wall (h/D = 1.167)

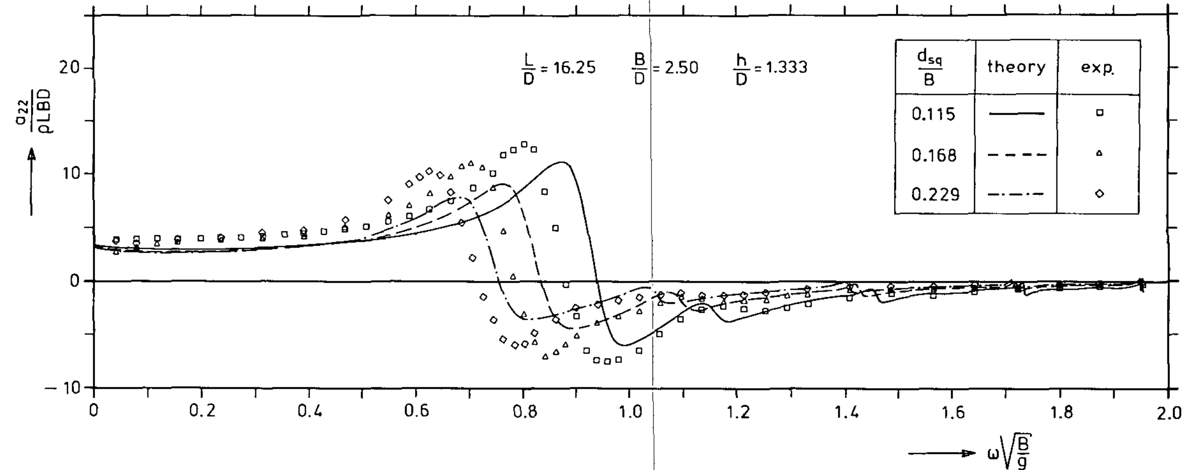

Fig. 4.7 - Added mass for swaying motion near a vertical wall (h/D = 1.333)

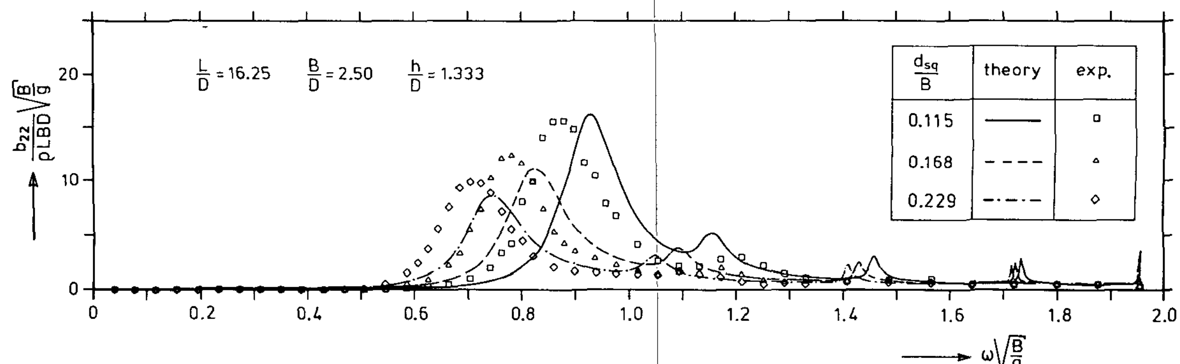

Fig. 4.8 - Sway damping force coefficient near a vertical wall (h/D = 1.333)

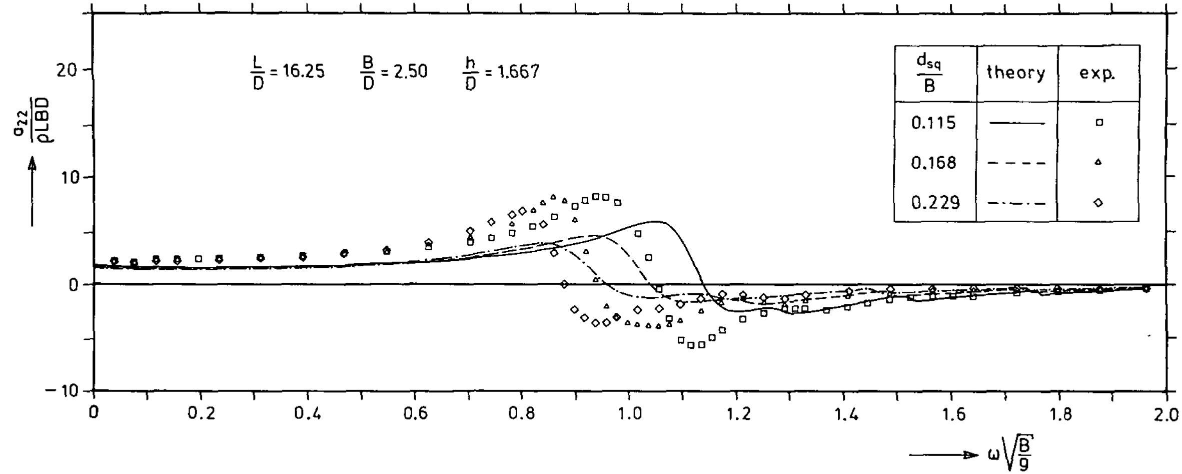

Fig. 4.9 - Added mass for swaying motion near a vertical wall (h/D = 1.667)

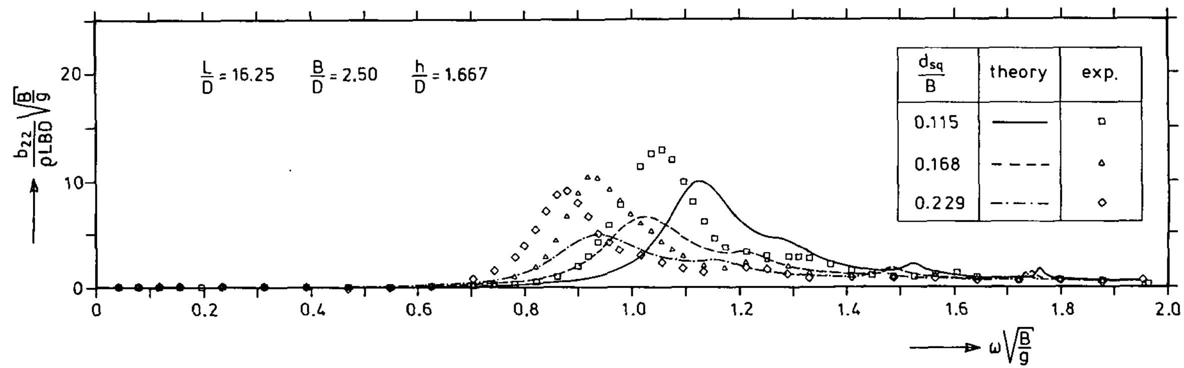

Fig. 4.10 - Sway damping force coefficient near a vertical wall (h/D = 1.667)

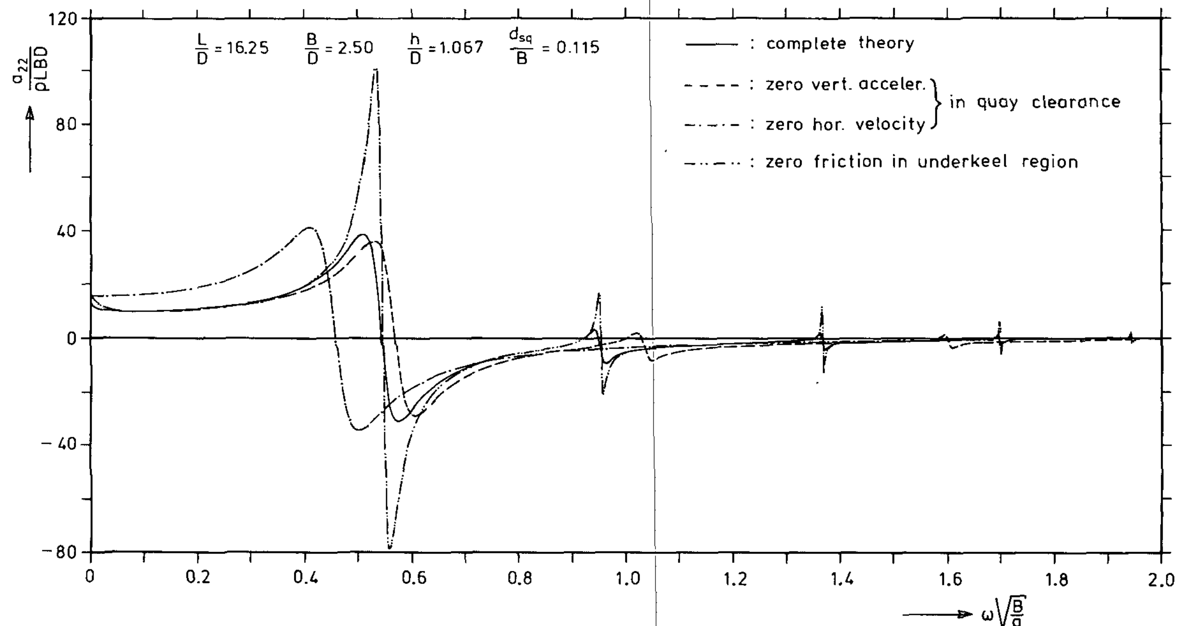

Fig. 4.11 - Added mass for swaying motion near a vertical wall (h/D = 1.067, d_{sq}/B = 0.115)

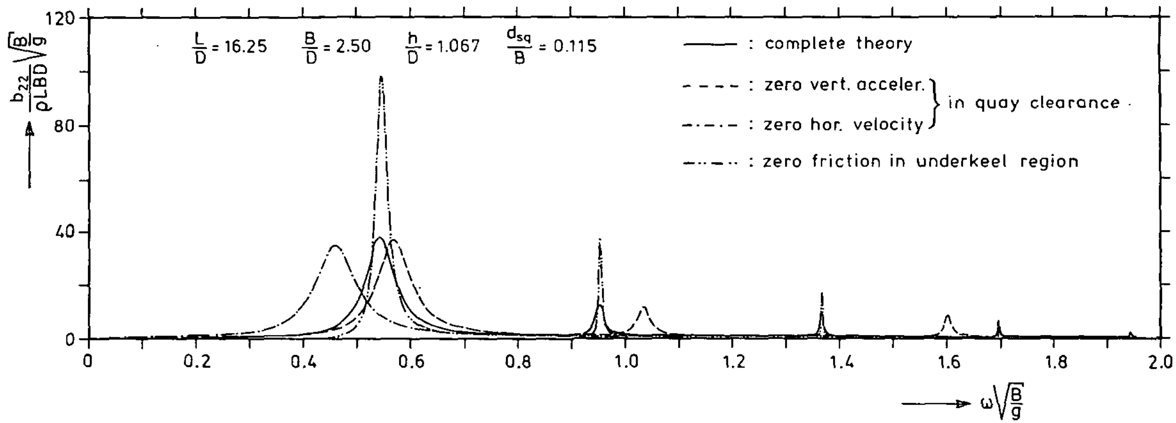

Fig. 4.12 – Sway damping force coefficient near a vertical wall ($h/D = 1.067$, $d_{sq}/B = 0.115$)

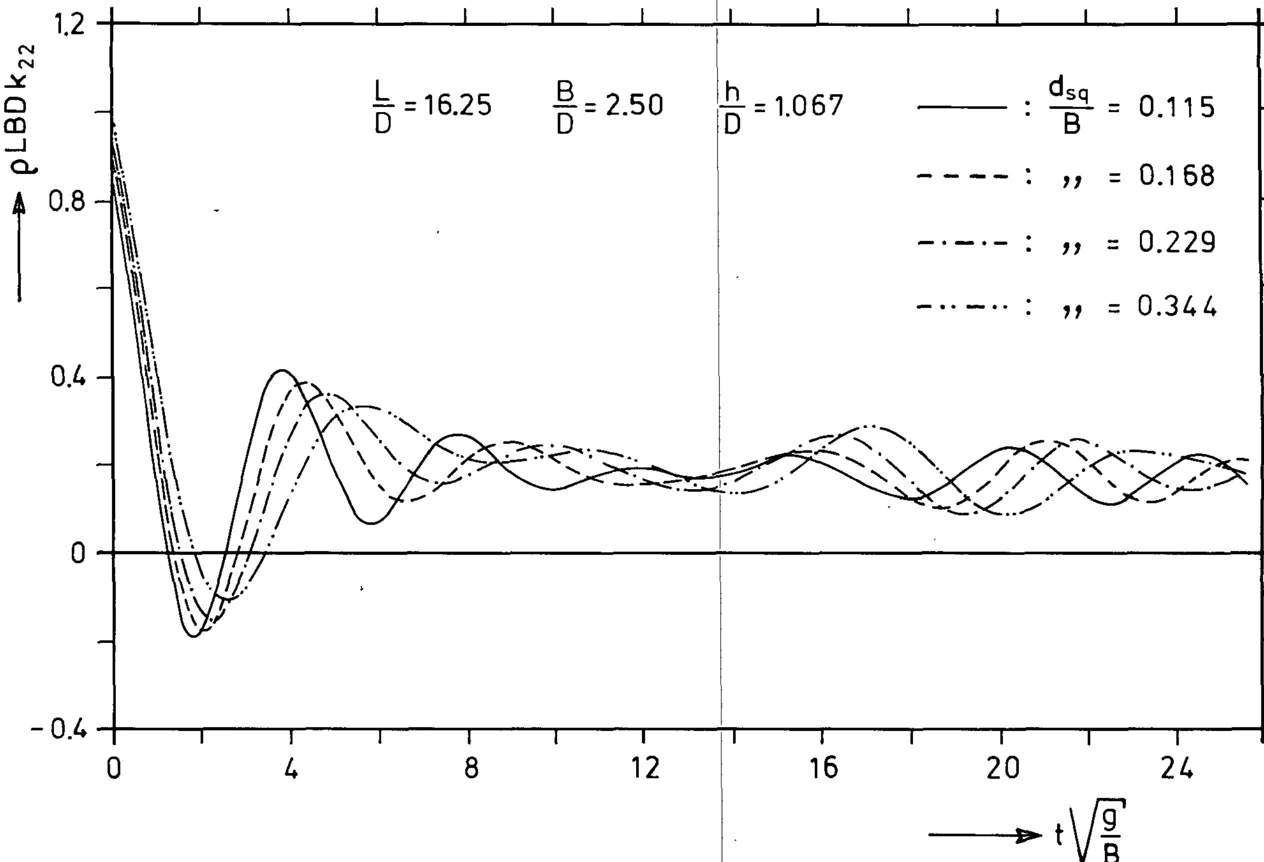

Fig. 4.13 - Impulse response function for sway motion near a vertical wall (h/D = 1.067)

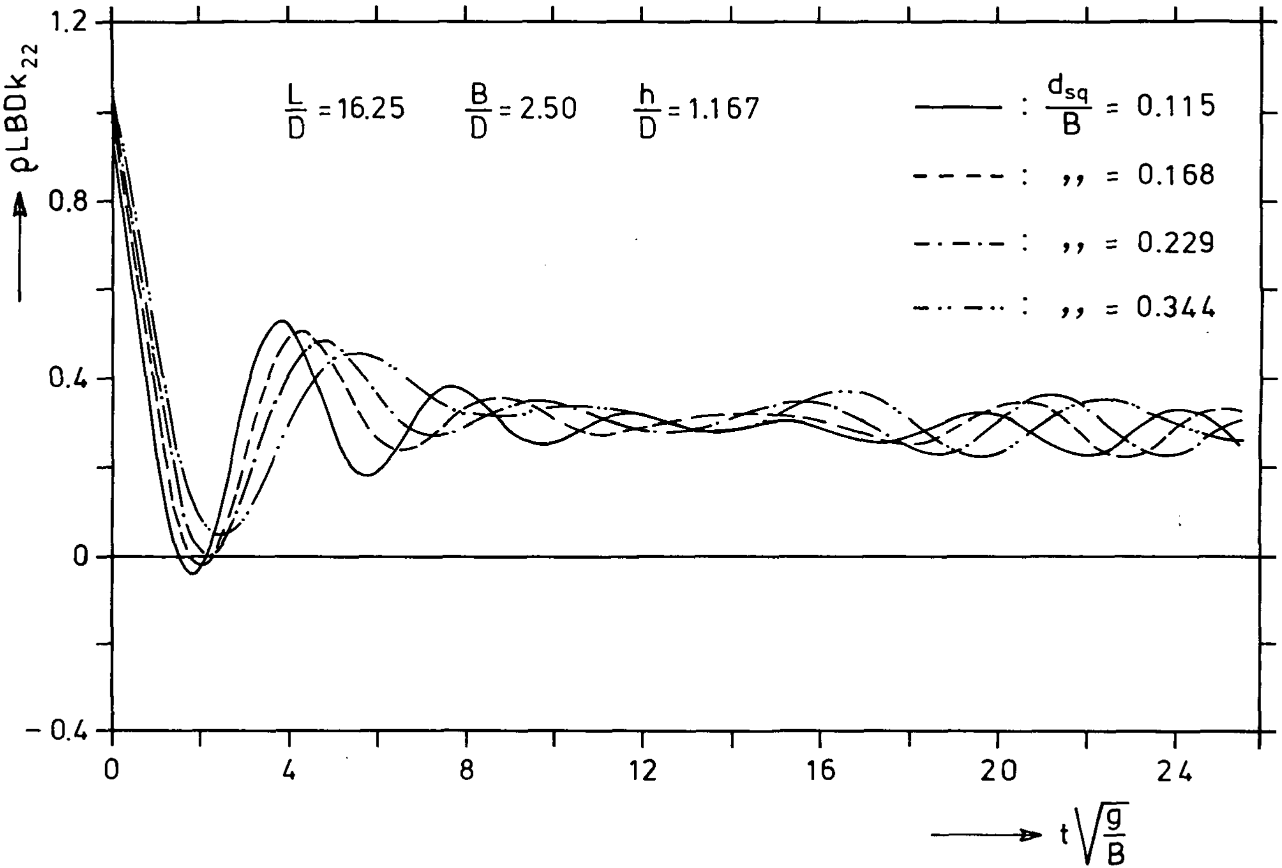

Fig. 4.14 - Impulse response function for sway motion near a vertical wall (h/D = 1.167)

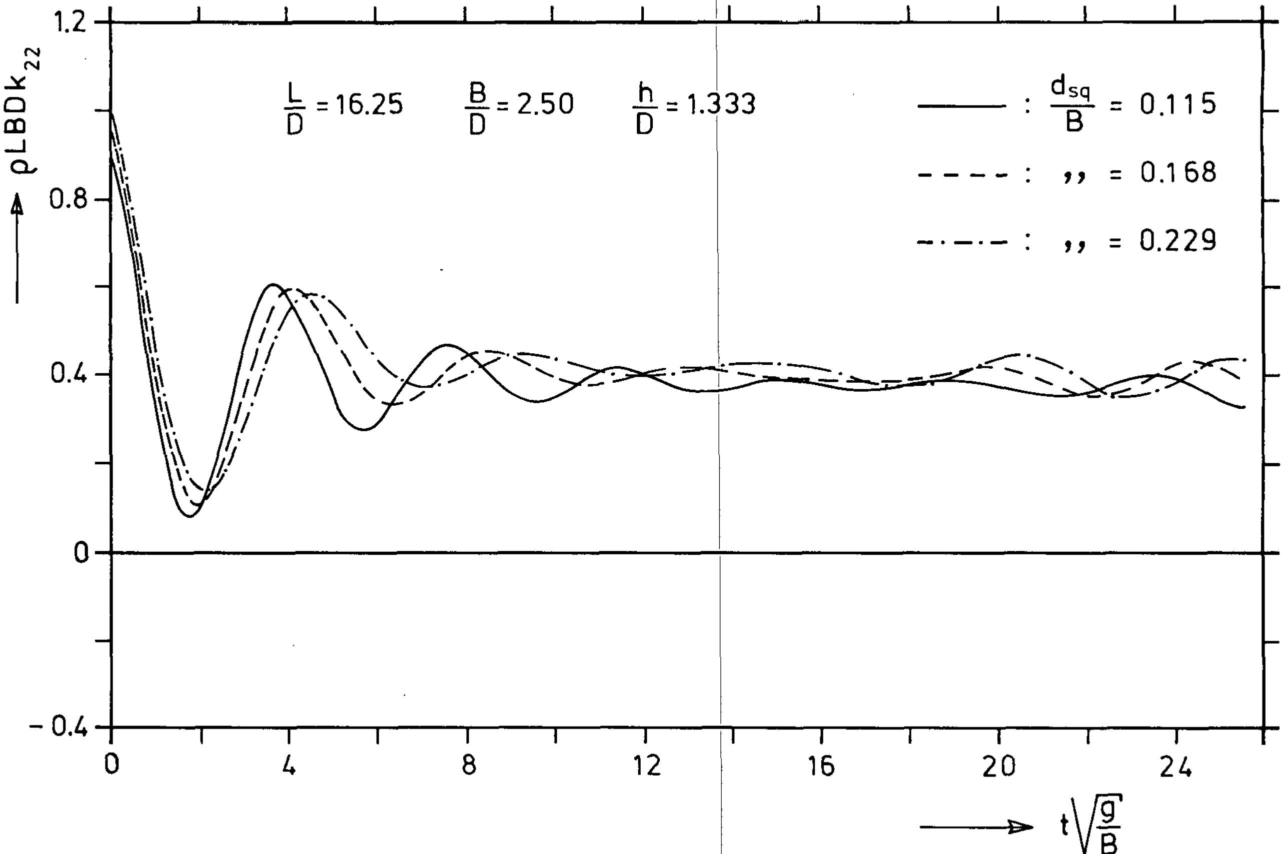

Fig. 4.15 - Impulse response function for sway motion near a vertical wall ($h/D = 1.333$)

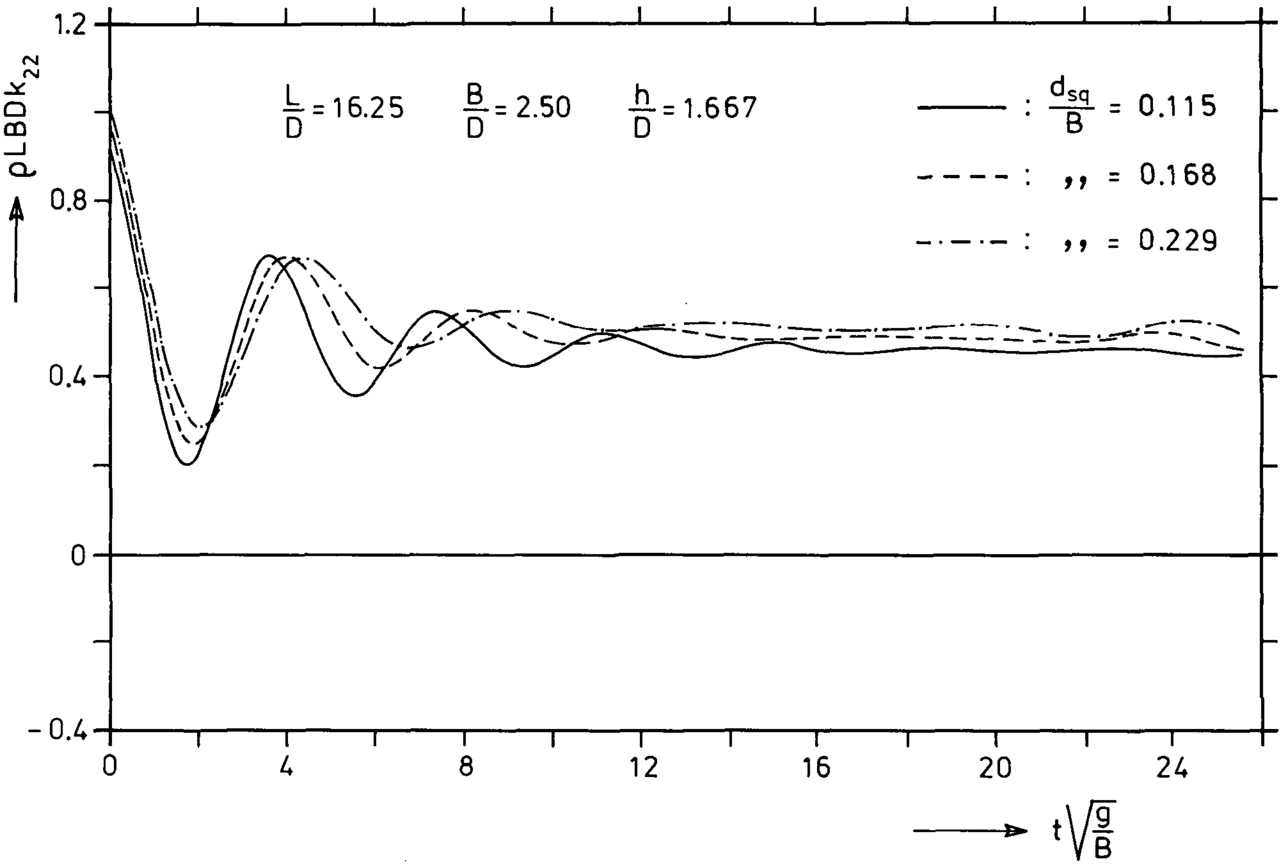

Fig. 4.16 - Impulse response function for sway motion near a vertical wall
(h/D = 1.667)

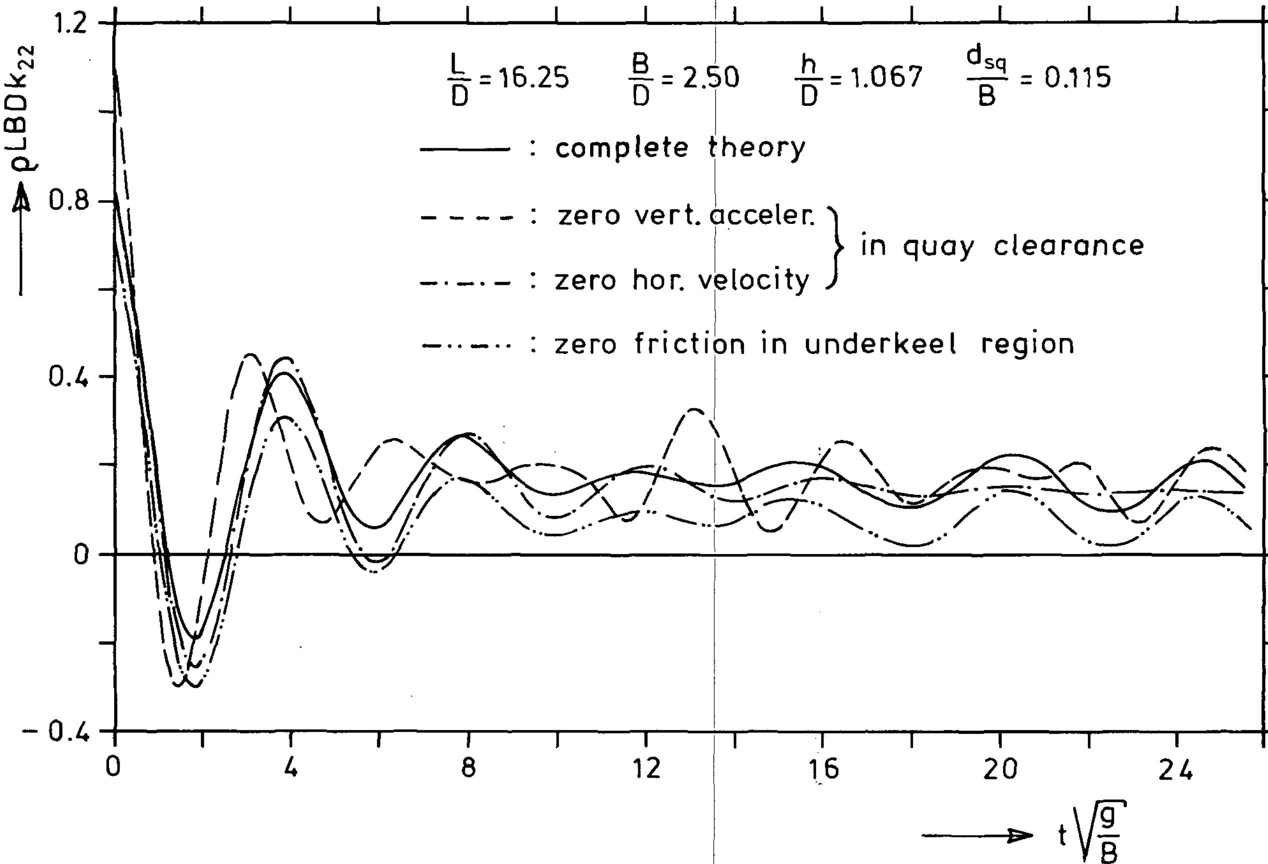

Fig. 4.17 - Impulse response function for sway motion near a vertical wall ($h/D = 1.067$, $d_{sq}/B = 0.115$)

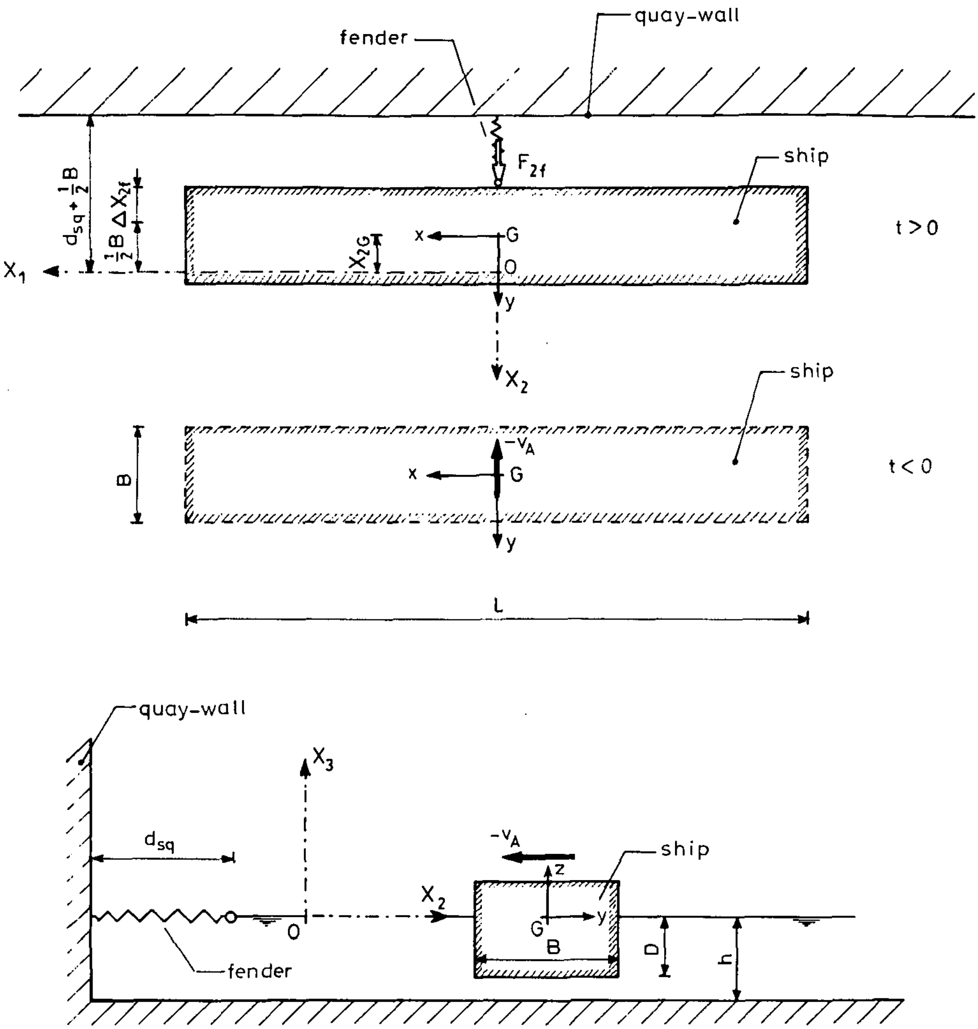

Fig. 4.18 - Plan and cross-section of closed berthing lay-out

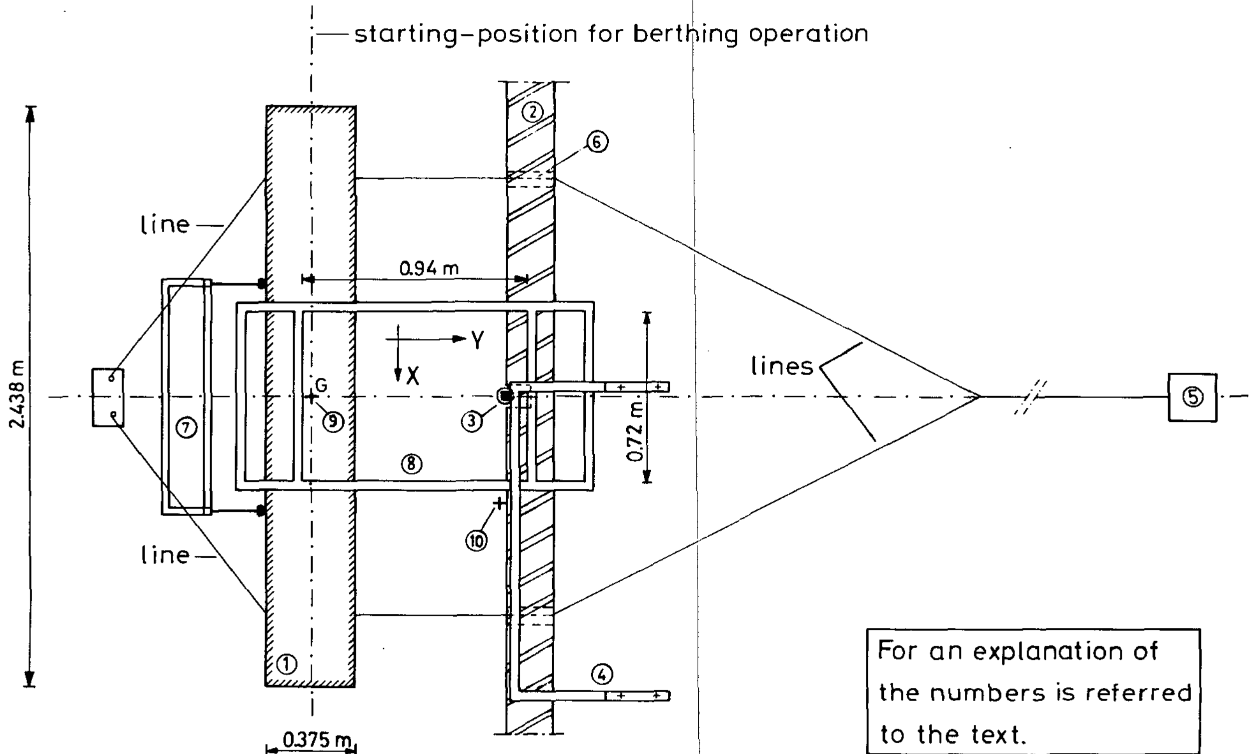

Fig. 4.19 - Plan of berthing lay-out for experiments: closed berth

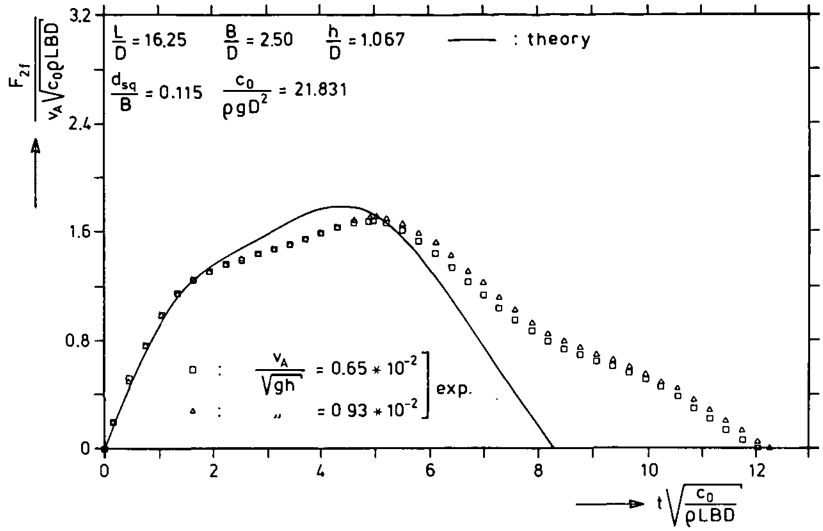

Fig. 4.20 - Time history of fender force: closed berth (i.r.f.-technique, h/D = 1.067)

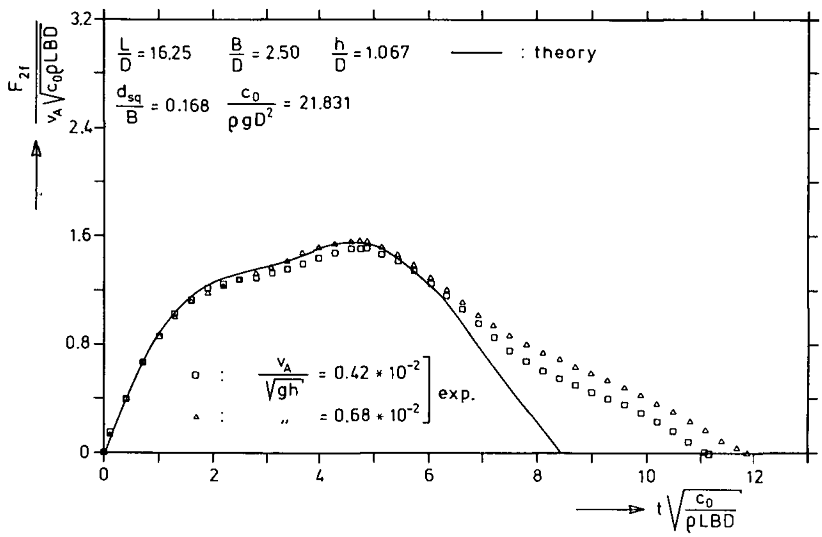

Fig. 4.21 - Time history of fender force: closed berth (i.r.f.-technique, h/D = 1.067)

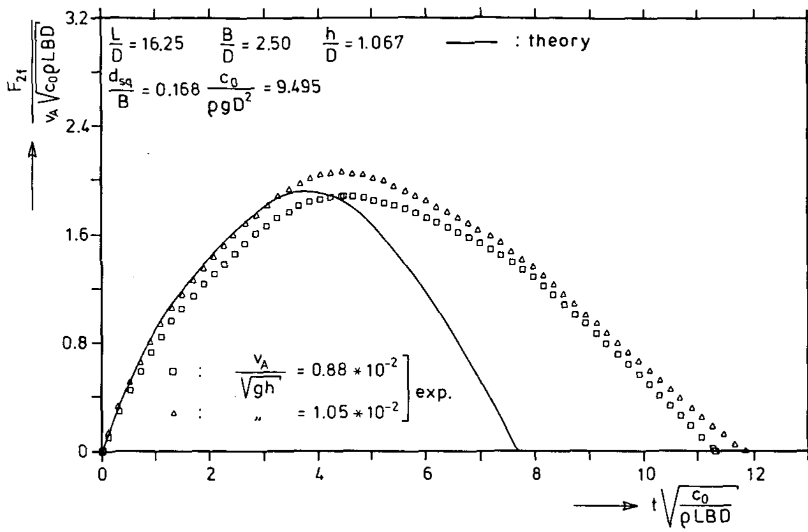

Fig. 4.22 - Time history of fender force: closed berth (i.r.f.-technique, h/D = 1.067)

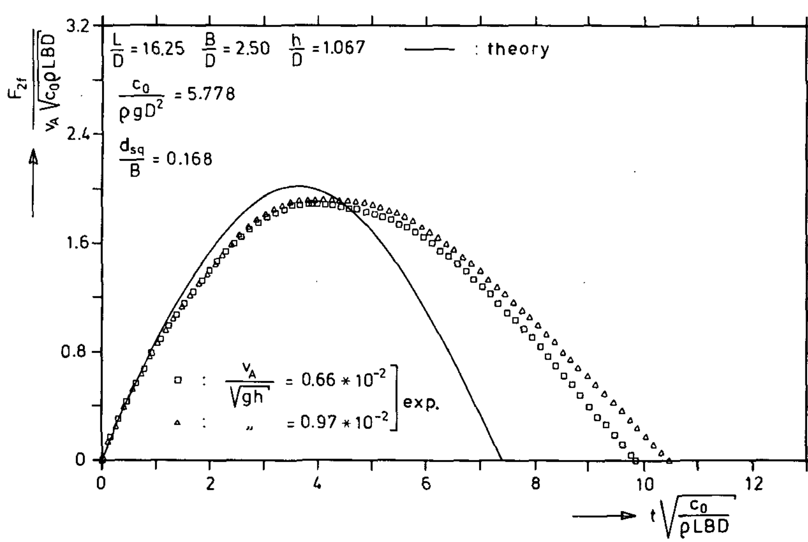

Fig. 4.23 - Time history of fender force: closed berth (i.r.f.-technique, h/D = 1.067)

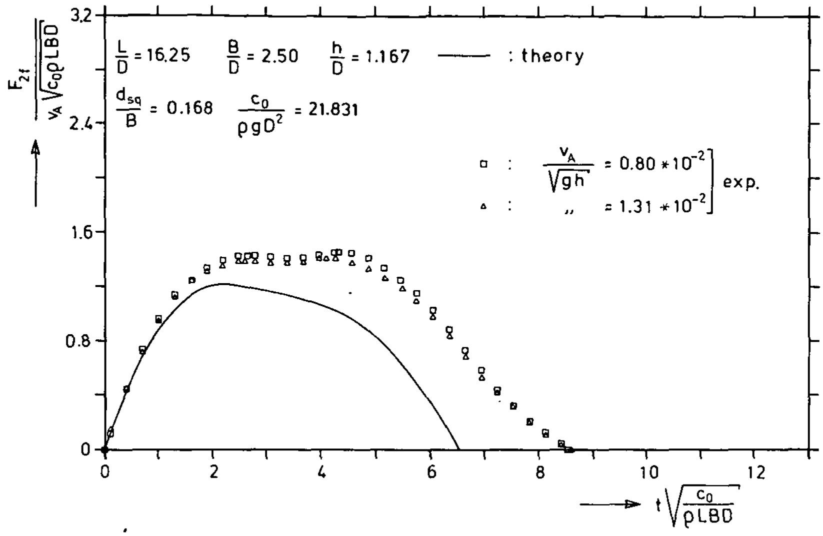

Fig. 4.24 - Time history of fender force: closed berth (i.r.f.-technique, h/D = 1.167)

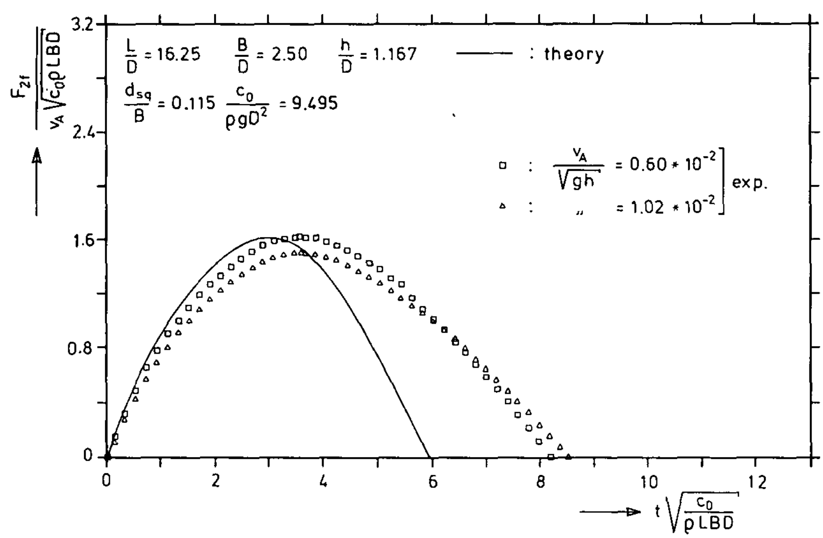

Fig. 4.25 - Time history of fender force: closed berth (i.r.f.-technique, h/D = 1.167)

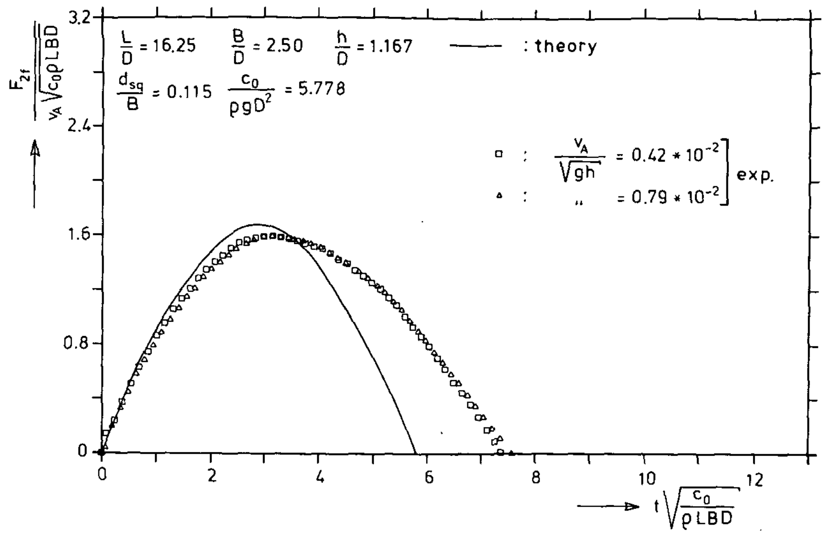

Fig. 4.26 - Time history of fender force: closed berth (i.r.f.-technique, h/D = 1.167)

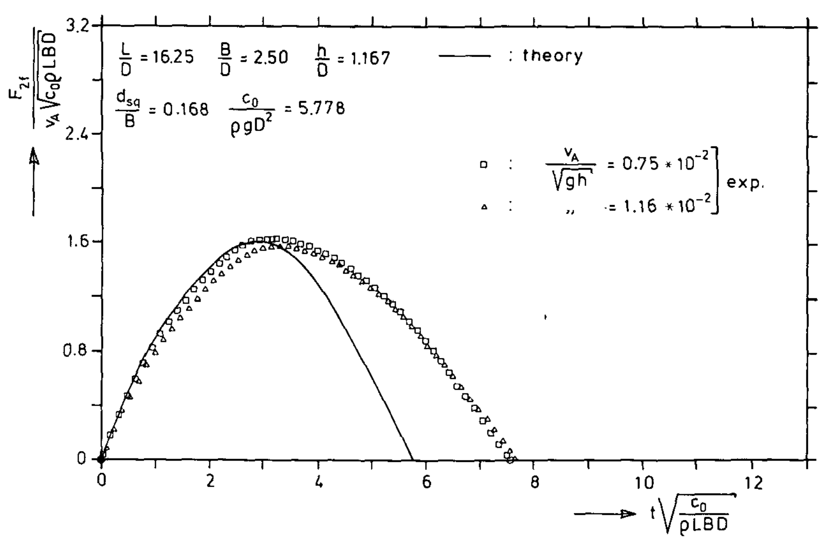

Fig. 4.27 - Time history of fender force: closed berth (i.r.f.-technique, h/D = 1.167)

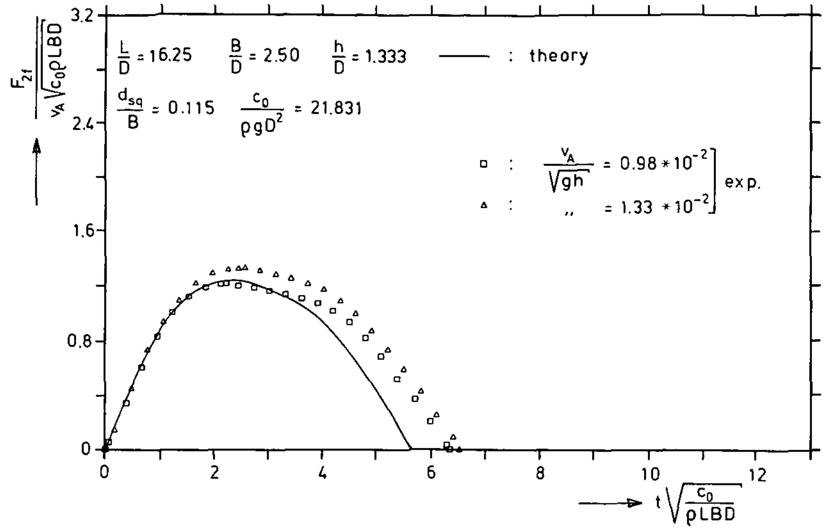

Fig. 4.28 - Time history of fender force: closed berth (i.r.f.-technique, h/D = 1.333)

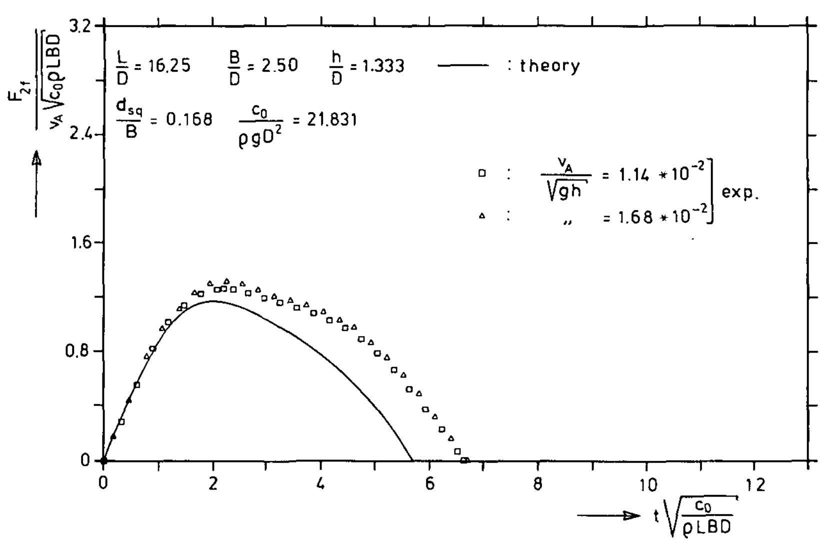

Fig. 4.29 - Time history of fender force: closed berth (i.r.f.-technique, h/D = 1.333)

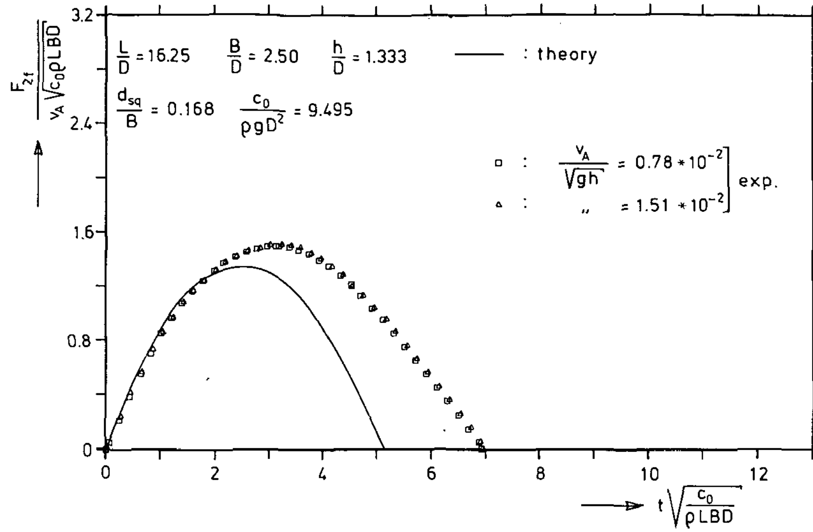

Fig. 4.30 - Time history of fender force: closed berth (i.r.f.-technique, h/D = 1.333)

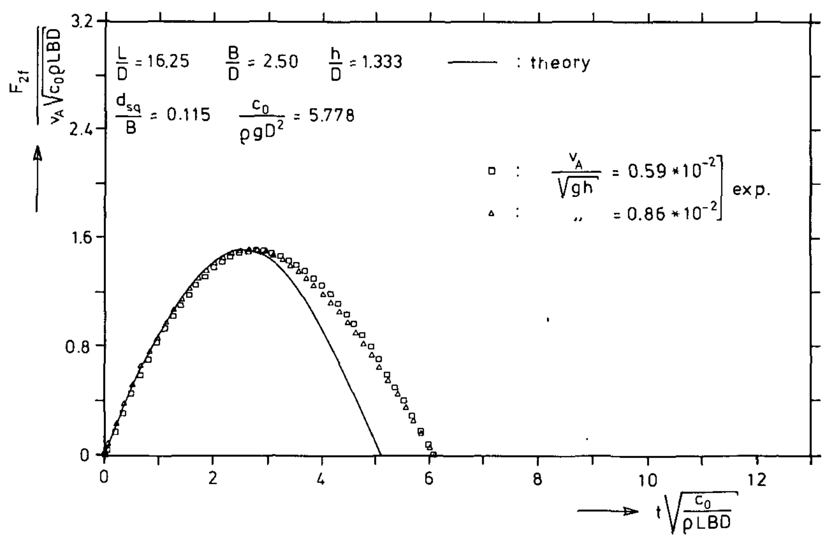

Fig. 4.31 - Time history of fender force: closed berth (i.r.f.-technique, h/D = 1.333)

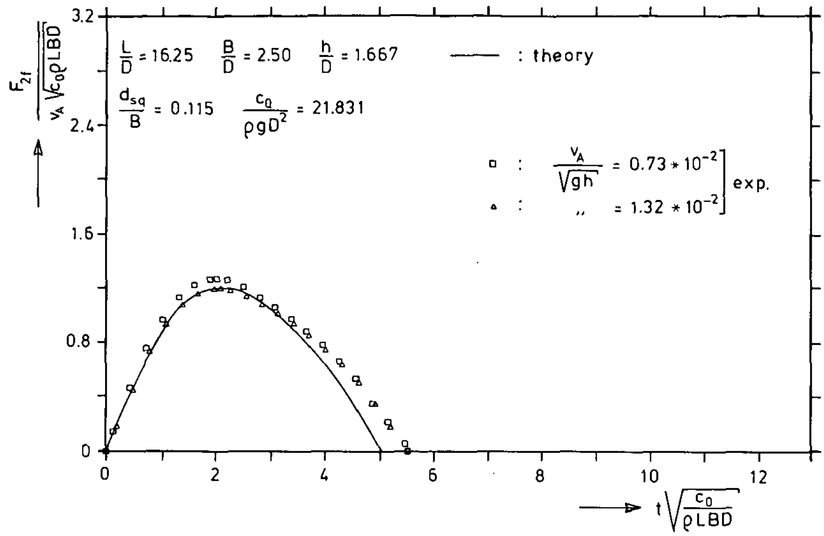

Fig. 4.32 - Time history of fender force: closed berth (i.r.f.-technique, h/D = 1.667)

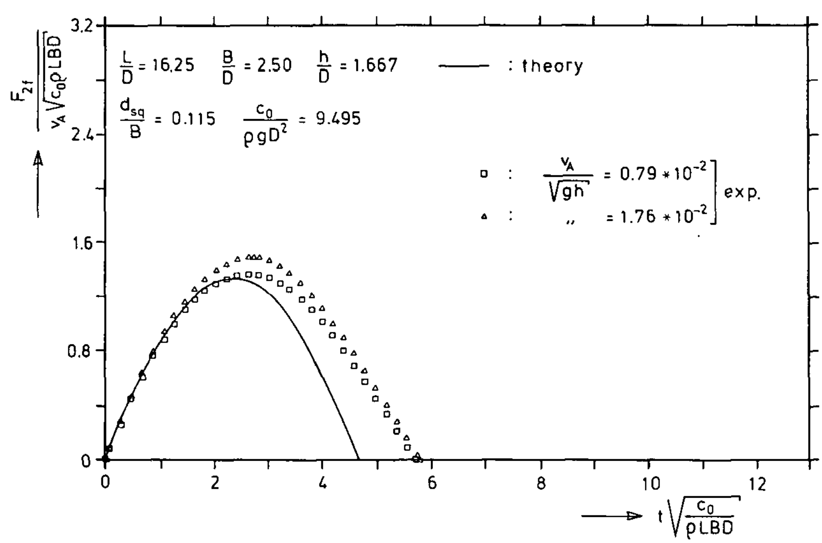

Fig. 4.33 - Time history of fender force: closed berth (i.r.f.-technique, h/D = 1.667)

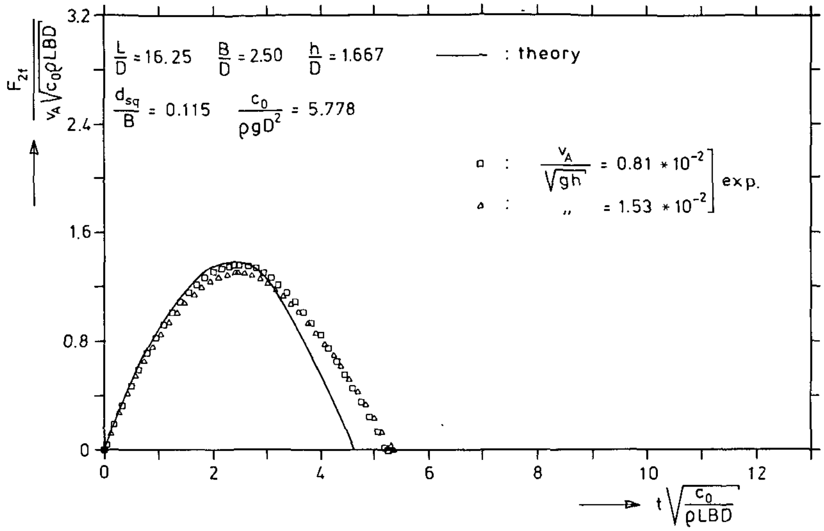

Fig. 4.34 - Time history of fender force: closed berth (i.r.f.-technique, h/D = 1.667)

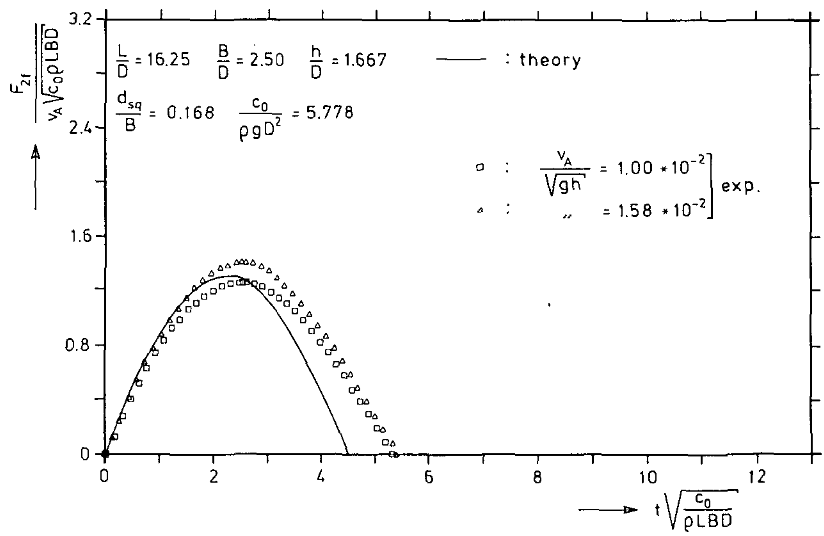

Fig. 4.35 - Time history of fender force: closed berth (i.r.f.-technique, h/D = 1.667)

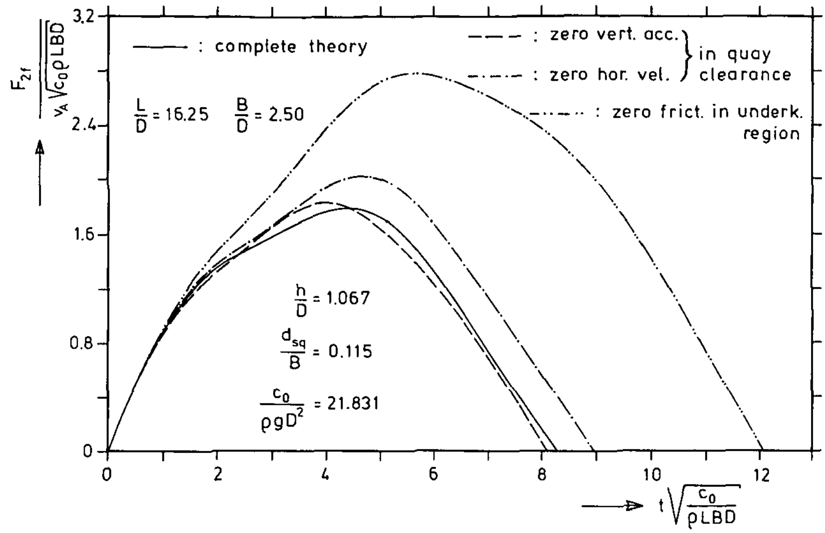

Fig. 4.36 - Time history of fender force: closed berth (i.r.f.-technique, h/D = 1.067)

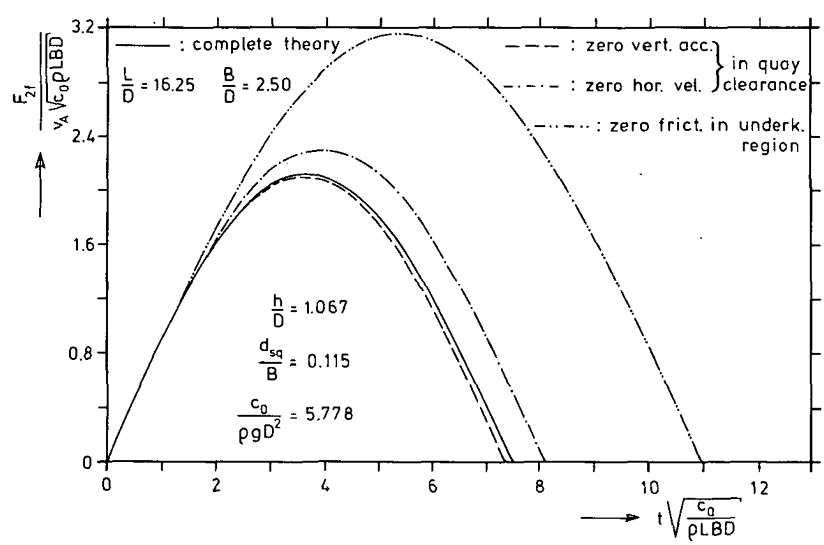

Fig. 4.37 - Time history of fender force: closed berth (i.r.f.-technique, h/D = 1.067)

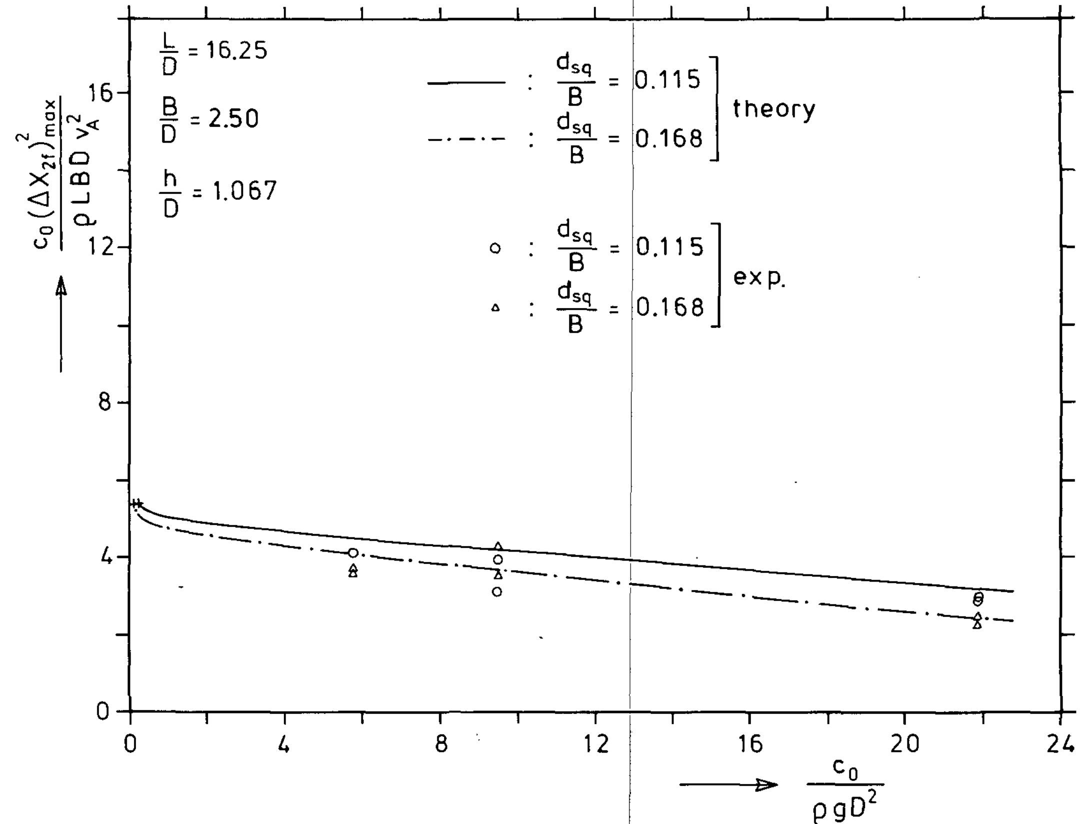

Fig. 4.38 - Influence of fender elasticity on absorbed energy: closed berth ($h/D = 1.067$)

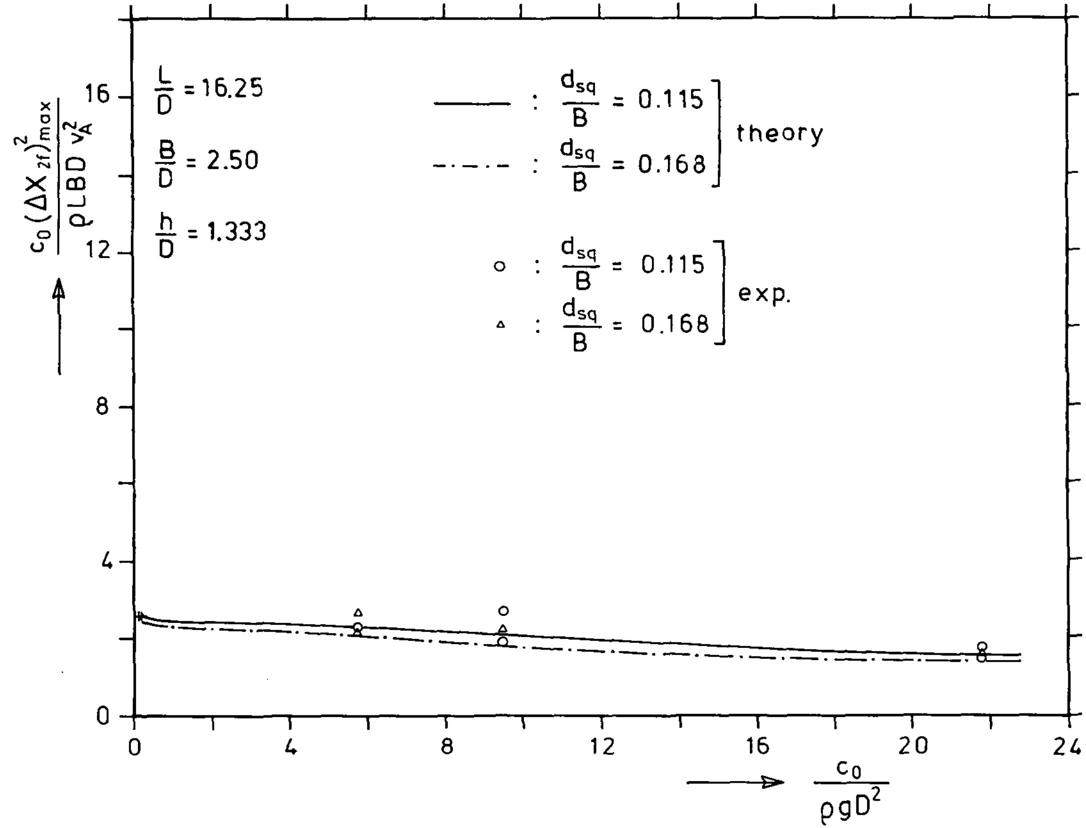

Fig. 4.39 - Influence of fender elasticity on absorbed energy: closed berth (h/D = 1.333)

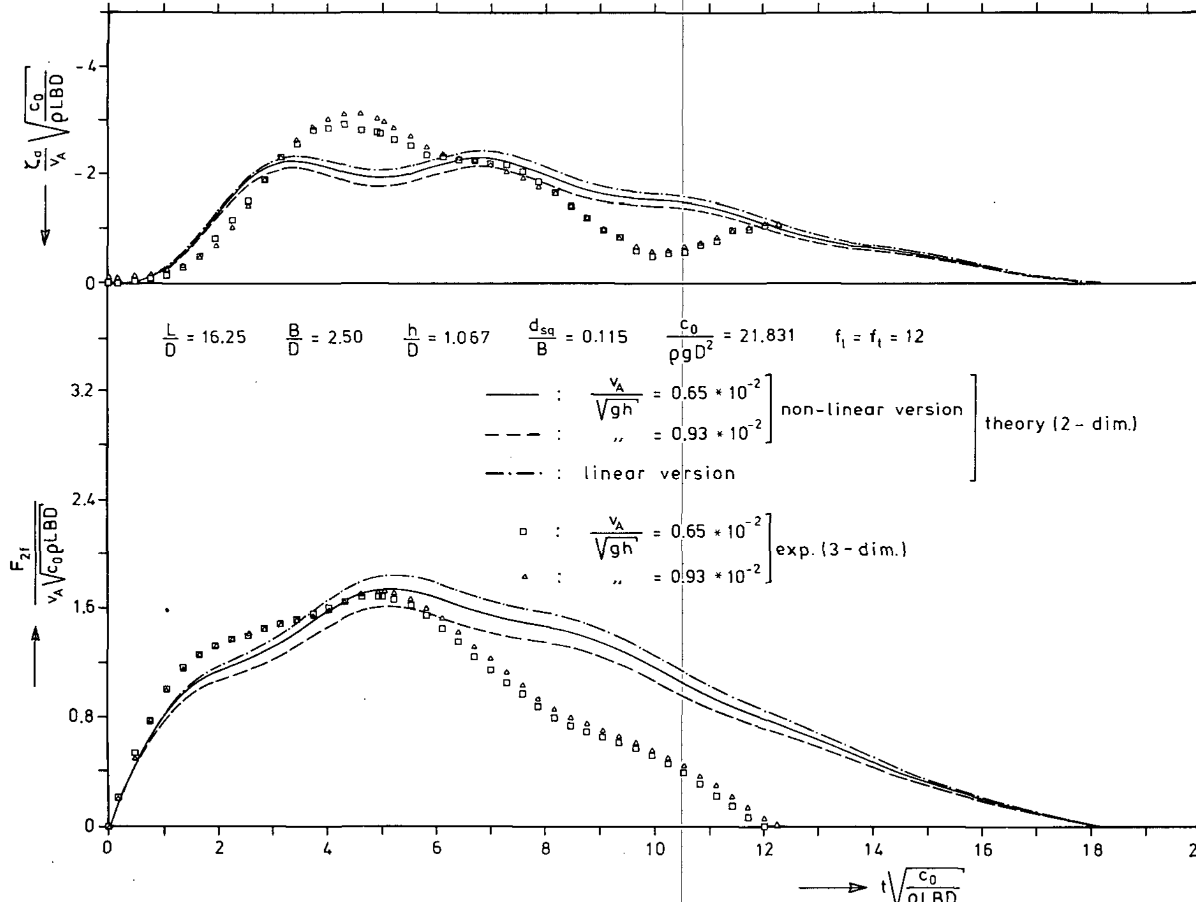

Fig. 4.40 - Time histories of fender force and water-surface elevation in quay clearance: closed berth (d.t.a., h/D = 1.067)

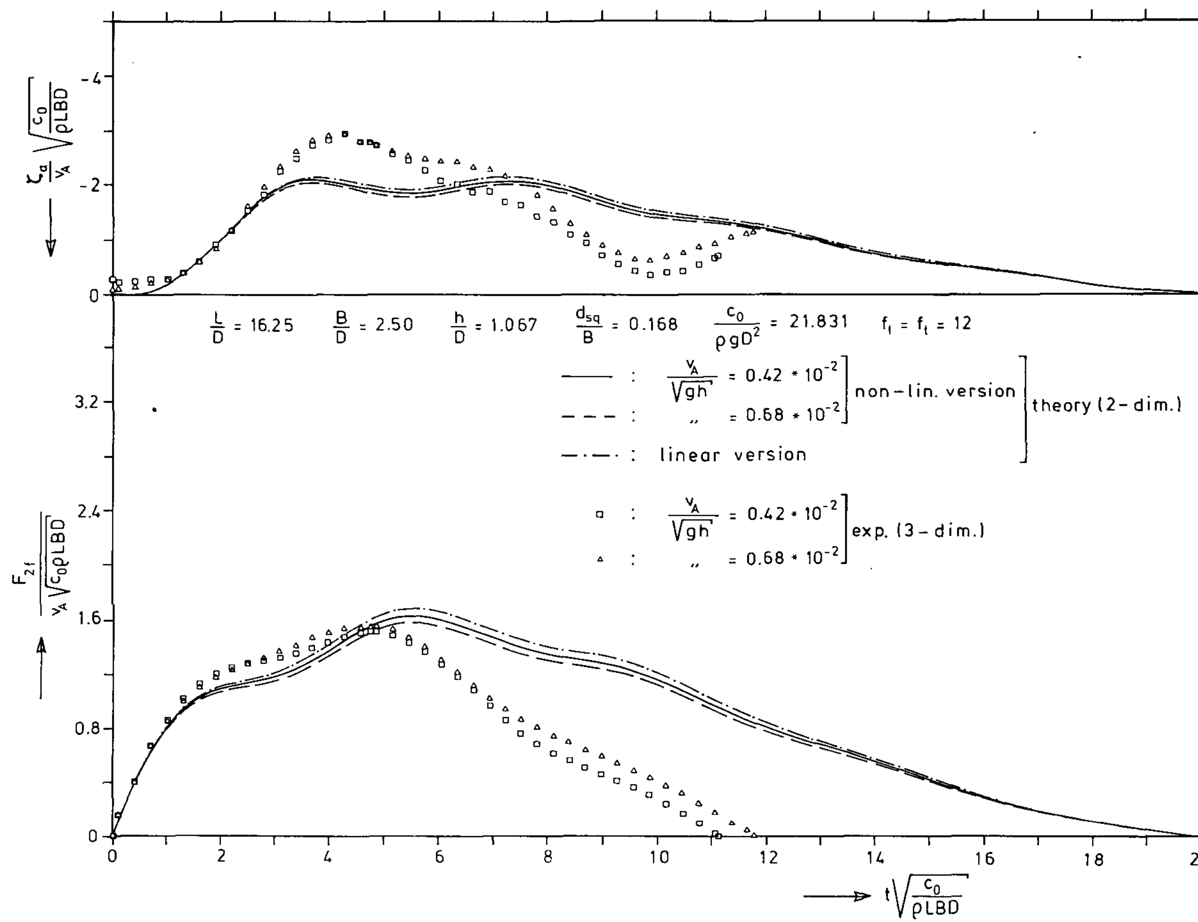

Fig. 4.41 - Time histories of fender force and water-surface elevation in quay clearance: closed berth (d.t.a., h/D = 1.067)

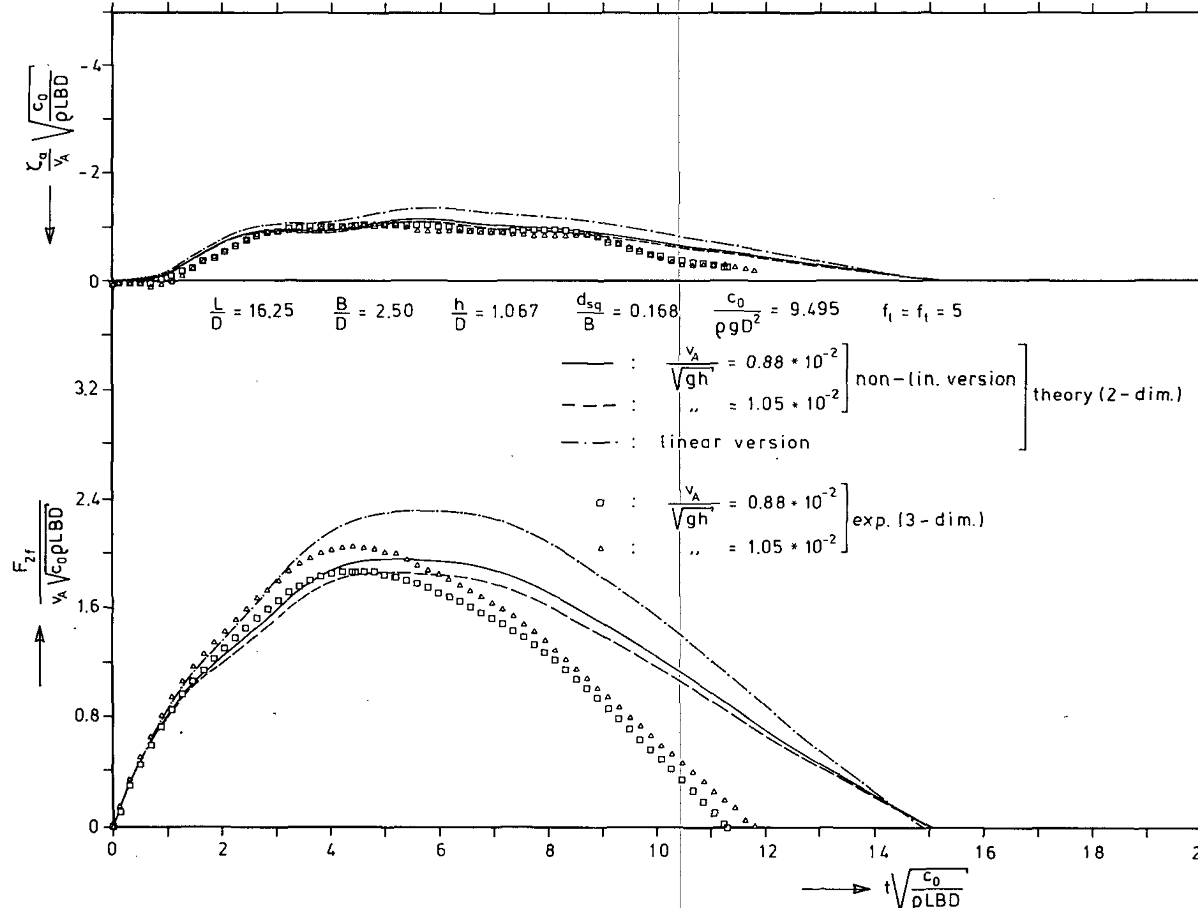

Fig. 4.42 - Time histories of fender force and water-surface elevation in quay clearance: closed berth (d.t.a., h/D = 1.067)

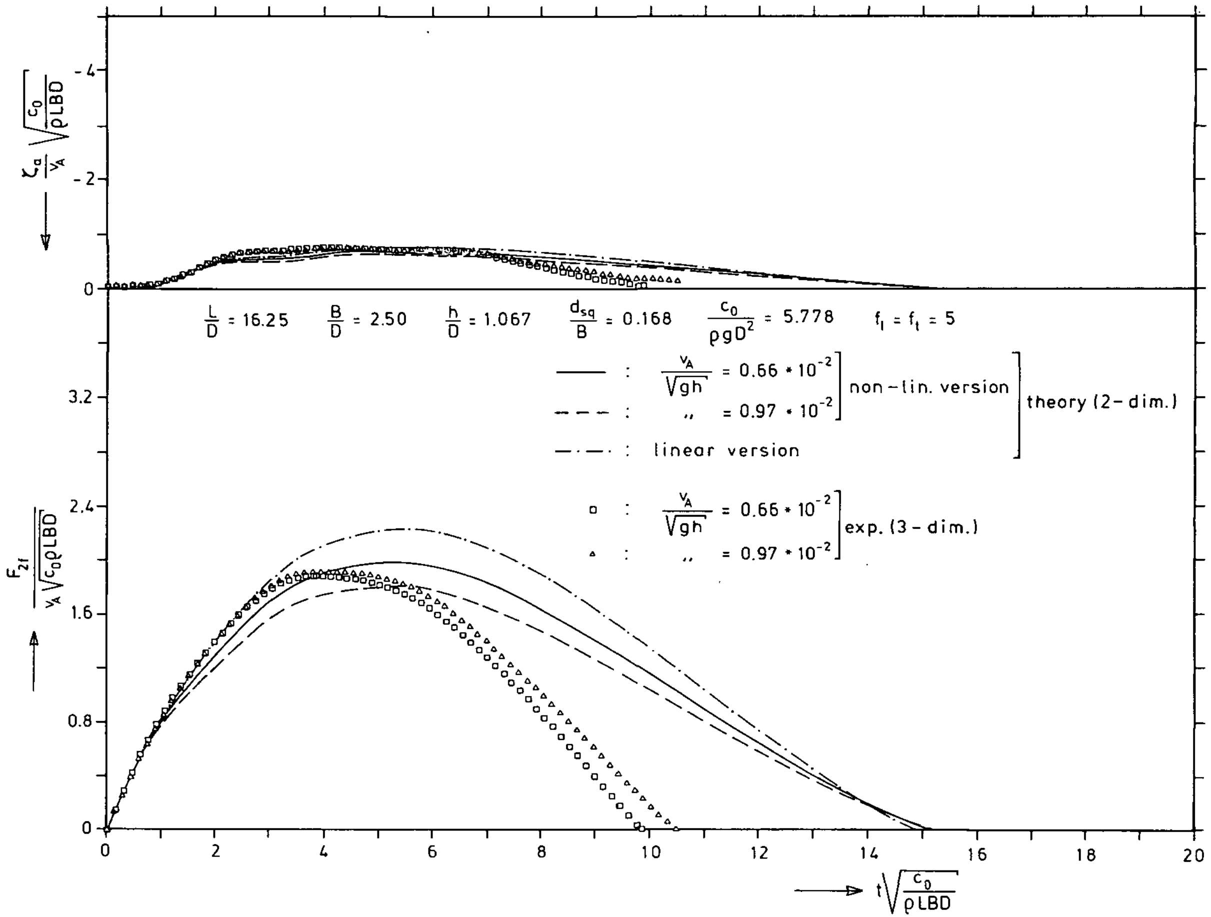

Fig. 4.43 - Time histories of fender force and water-surface elevation in quay clearance: closed berth (d.t.a., h/D = 1.067)

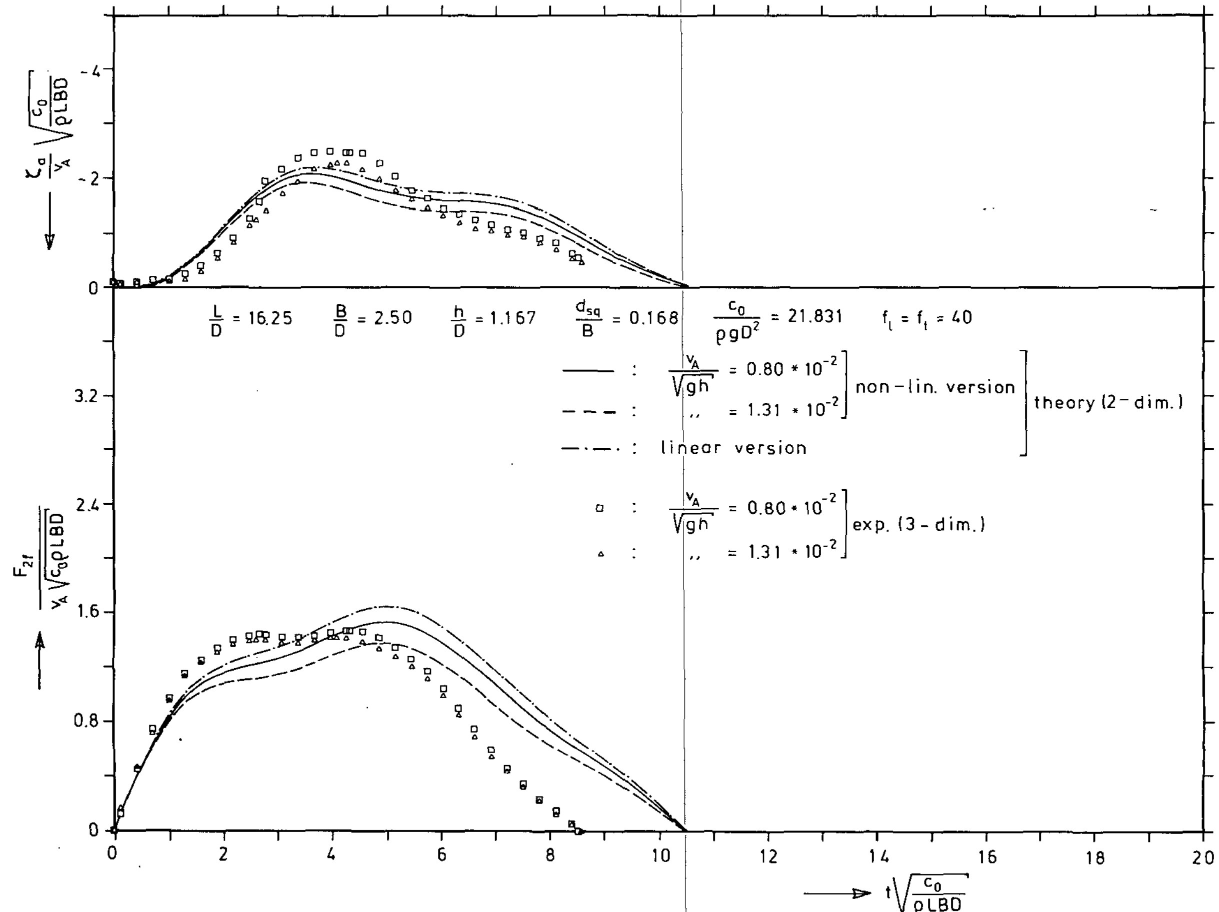

Fig. 4.44 - Time histories of fender force and water-surface elevation in quay clearance: closed berth (d.t.a., h/D = 1.167)

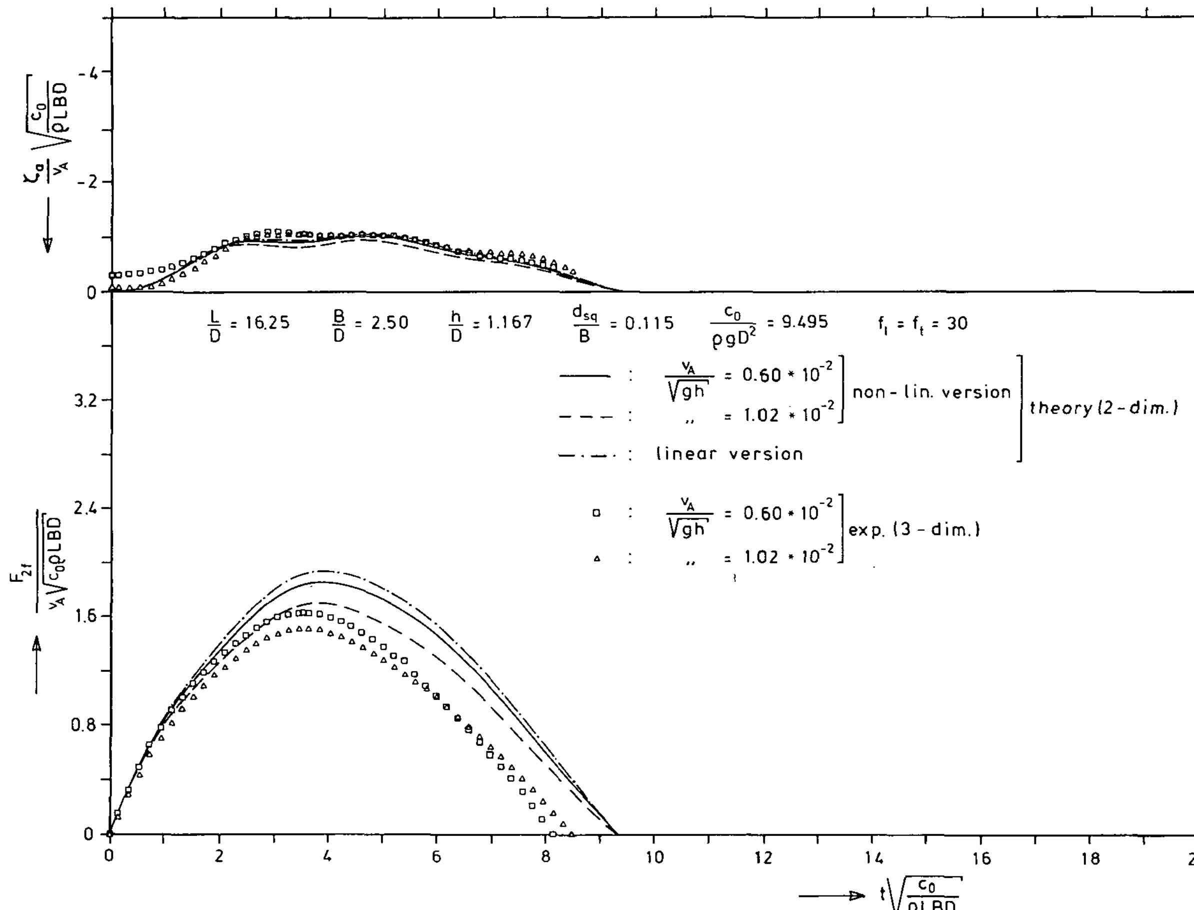

Fig. 4.45 - Time histories of fender force and water-surface elevation in quay clearance: closed berth (d.t.a., h/D = 1.167)

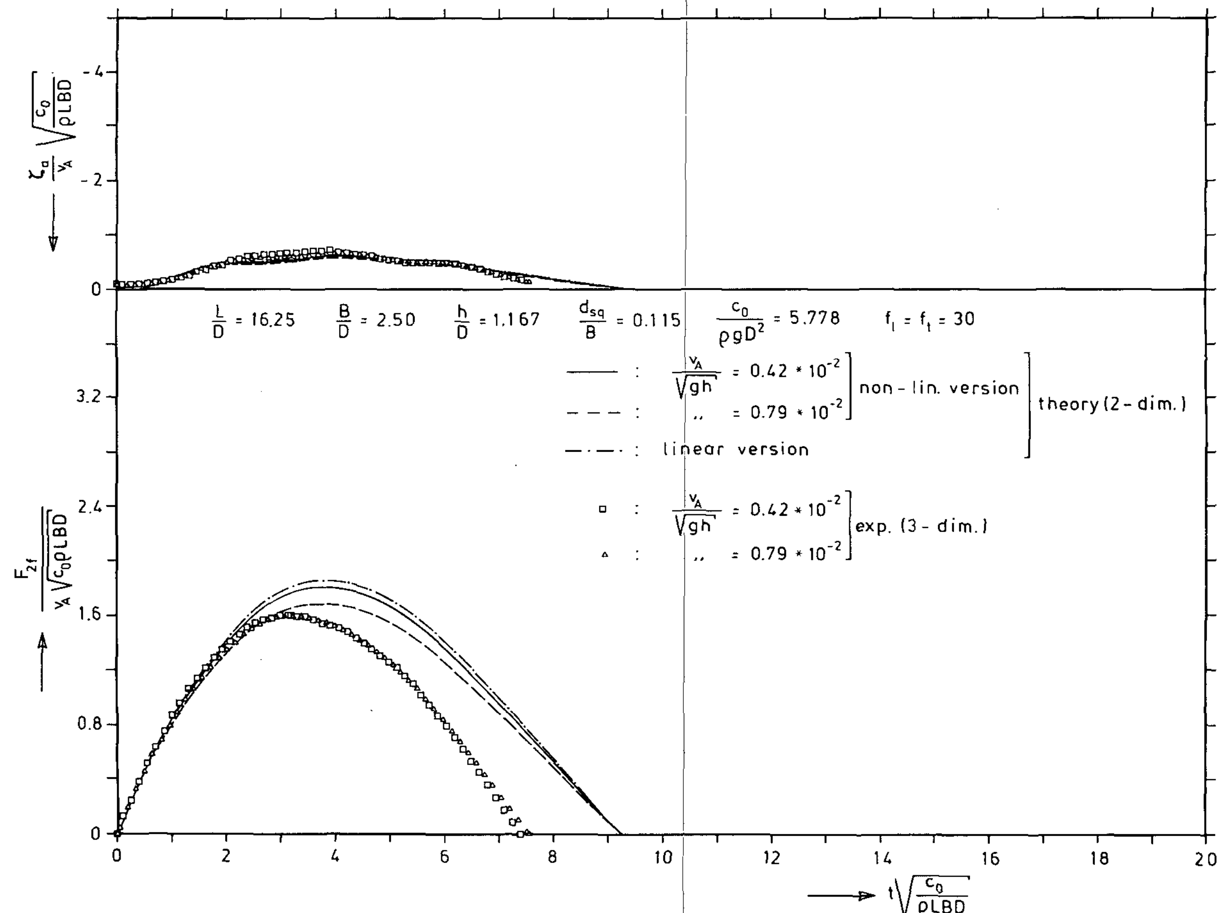

Fig. 4.46 - Time histories of fender force and water-surface elevation in quay clearance: closed berth (d.t.a., h/D = 1.167)

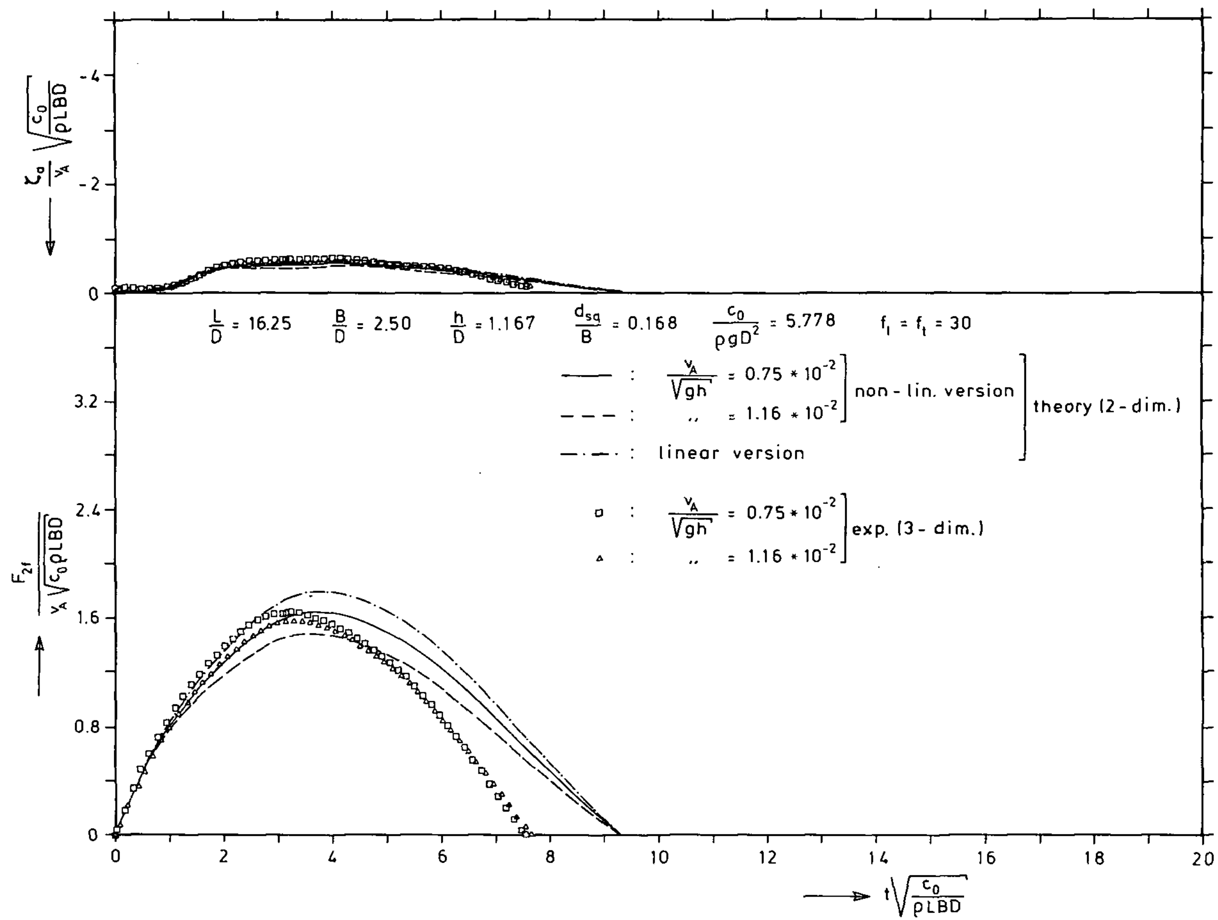

Fig. 4.47 - Time histories of fender force and water-surface elevation in quay clearance: closed berth (d.t.a., h/D = 1.167)

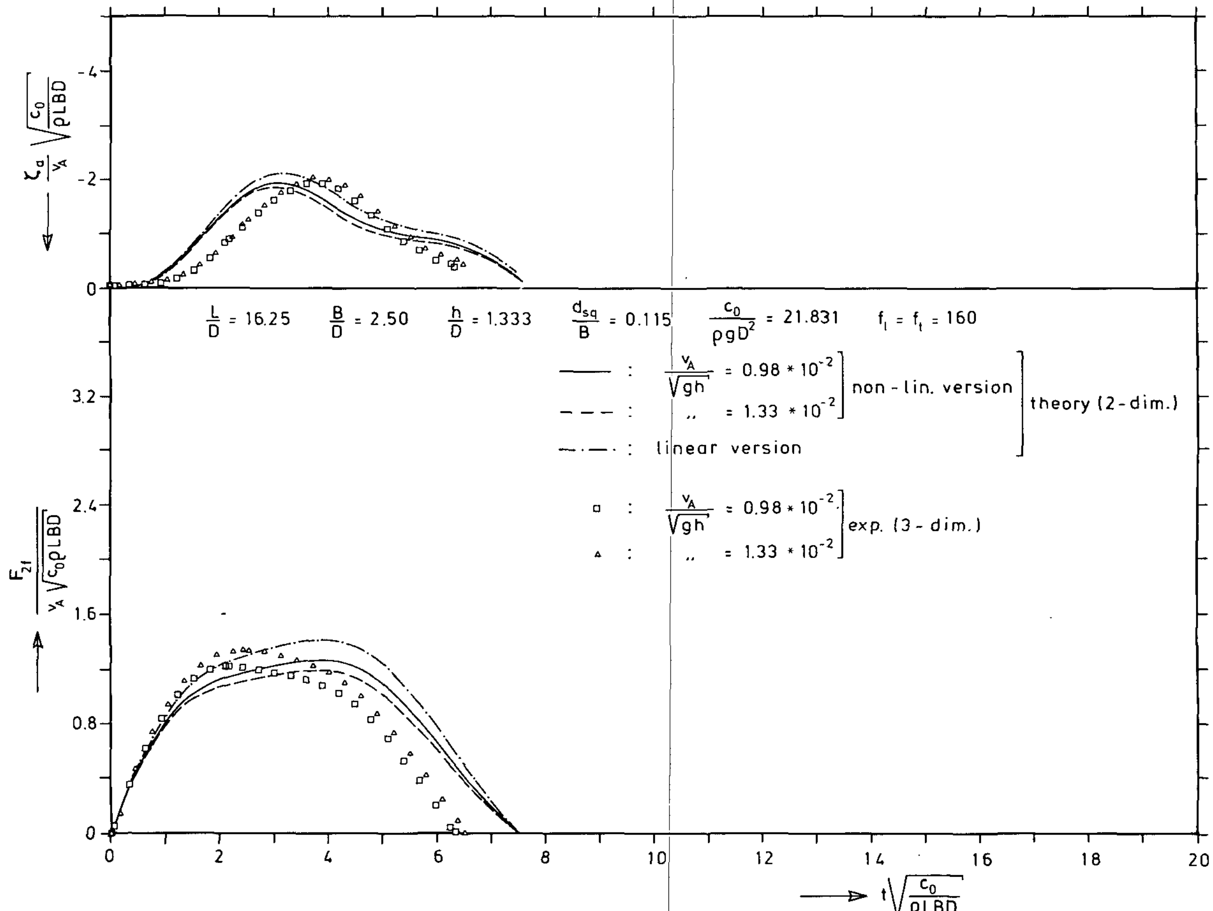

Fig. 4.48 - Time histories of fender force and water-surface elevation in quay clearance: closed berth (d.t.a., h/D = 1.333)

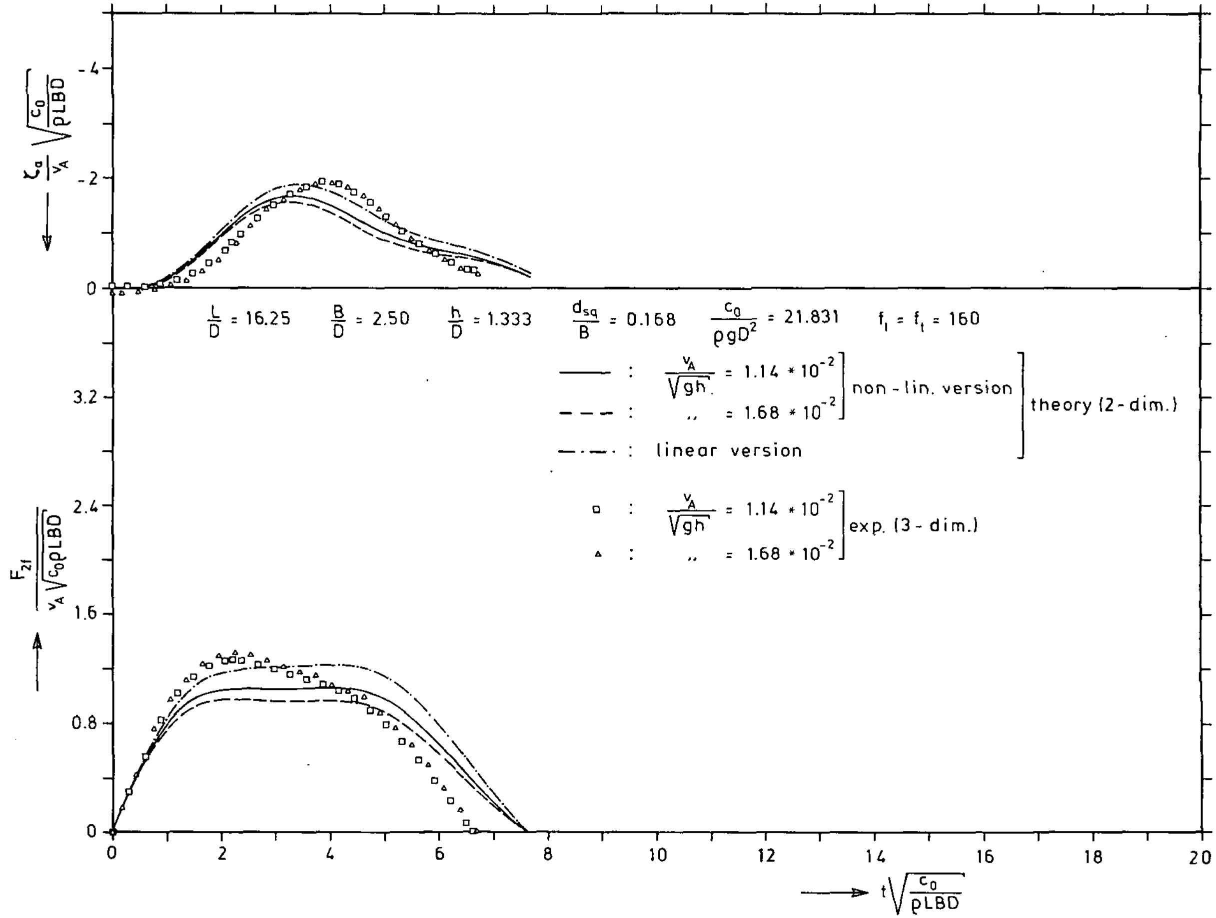

Fig. 4.49 - Time histories of fender force and water-surface elevation in quay clearance: closed berth (d.t.a., h/D = 1.333)

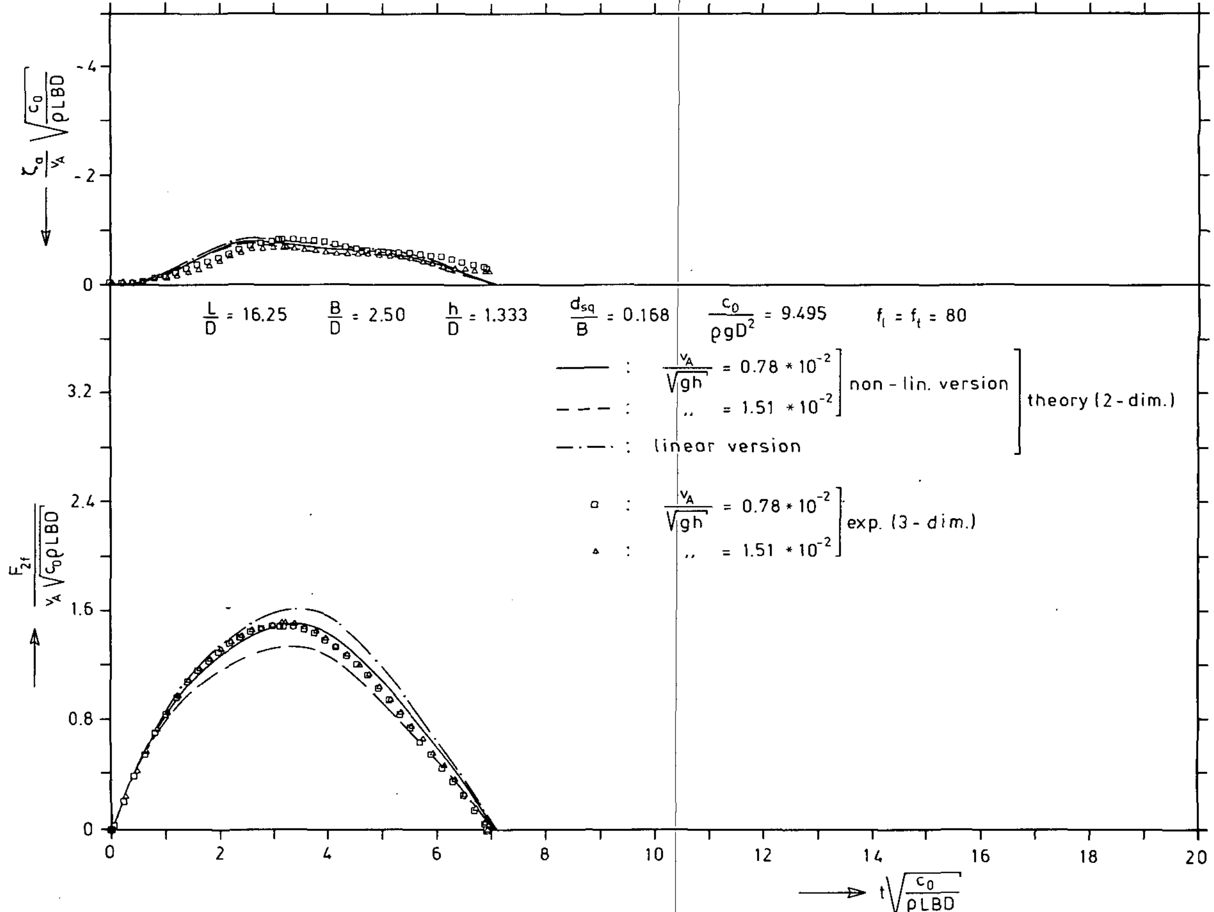

Fig. 4.50 - Time histories of fender force and water-surface elevation in quay clearance: closed berth (d.t.a., h/D = 1.333)

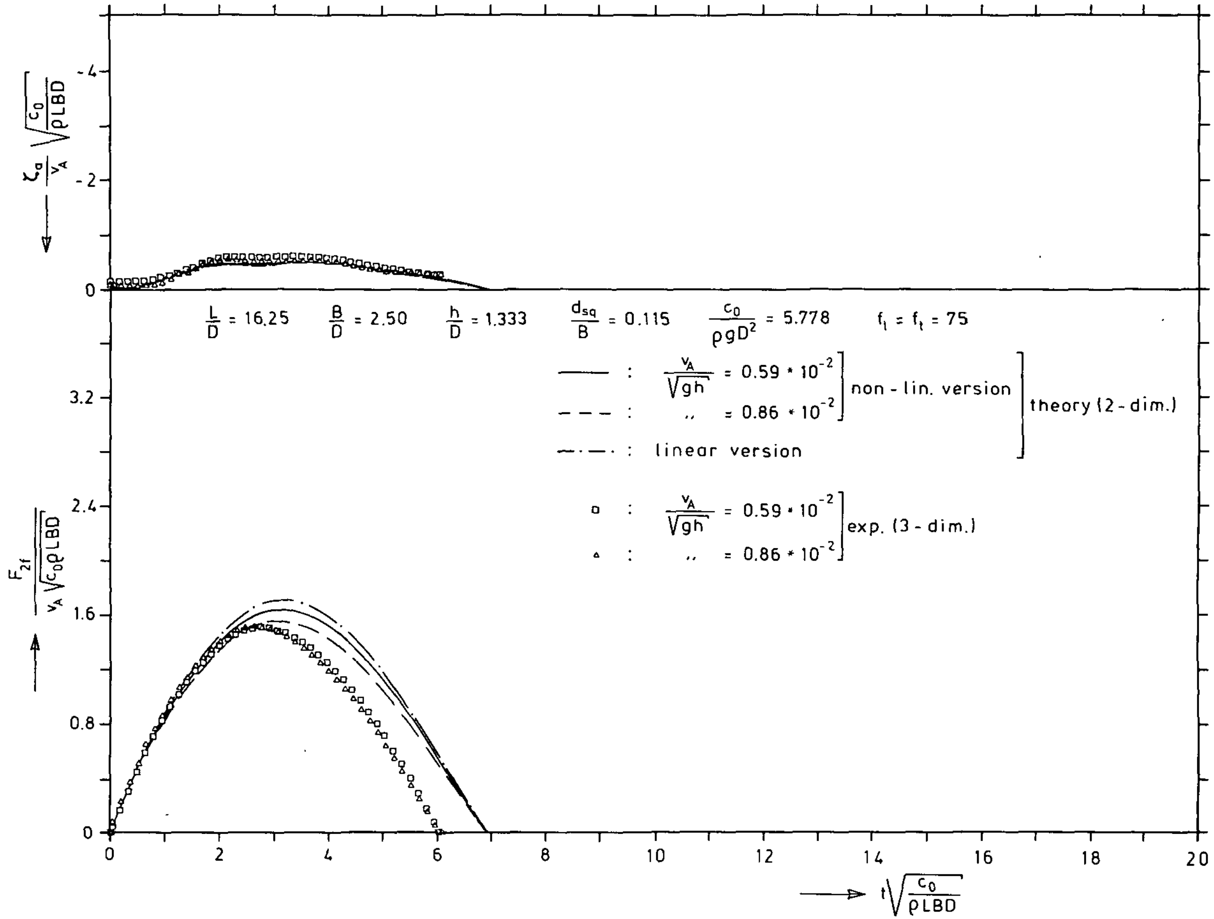

Fig. 4.51 - Time histories of fender force and water-surface elevation in quay clearance: closed berth (d.t.a., h/D = 1.333)

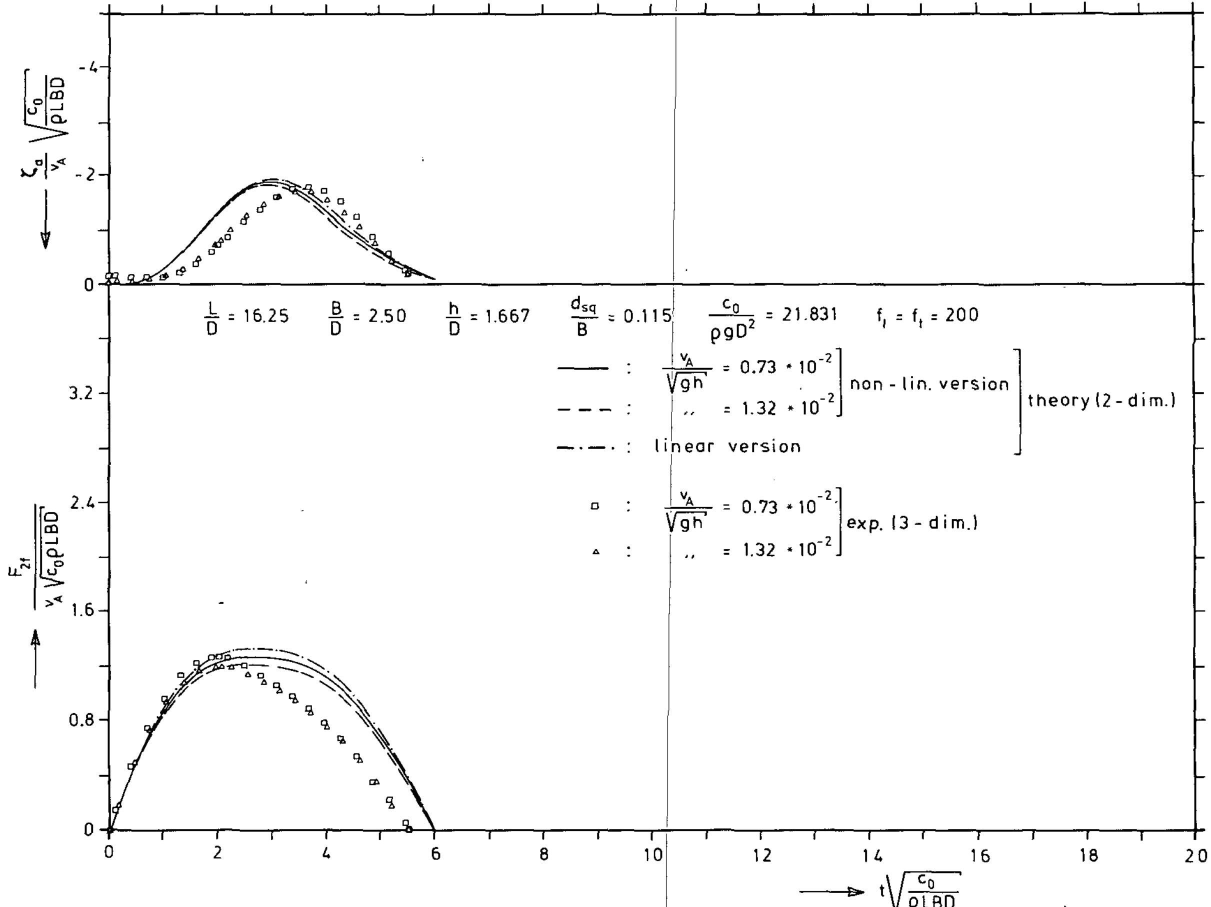

Fig. 4.52 - Time histories of fender force and water-surface elevation in quay clearance: closed berth (d.t.a., h/D = 1.667)

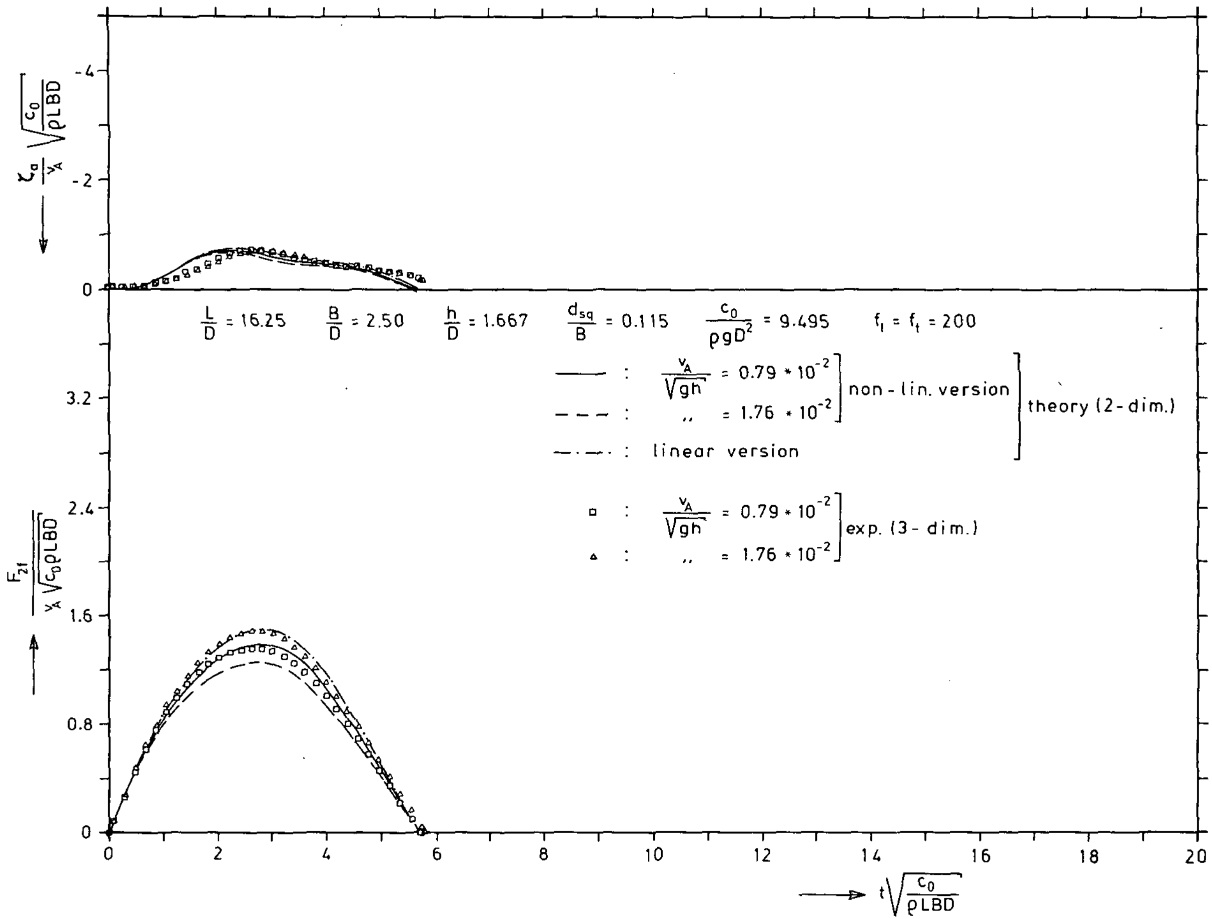

Fig. 4.53 - Time histories of fender force and water-surface elevation in quay clearance: closed berth (d.t.a., h/D = 1.667)

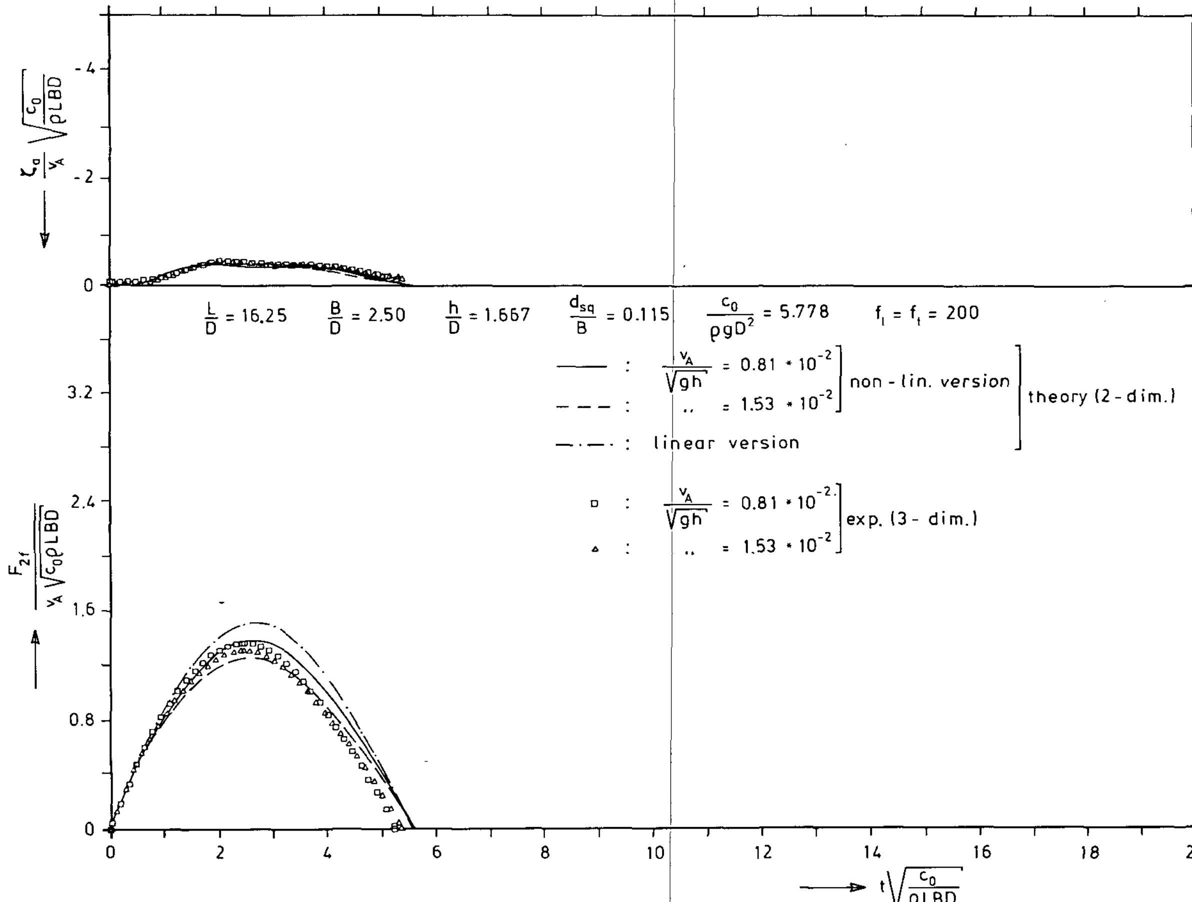

Fig. 4.54 - Time histories of fender force and water-surface elevation in quay clearance: closed berth (d.t.a., h/D = 1.667)

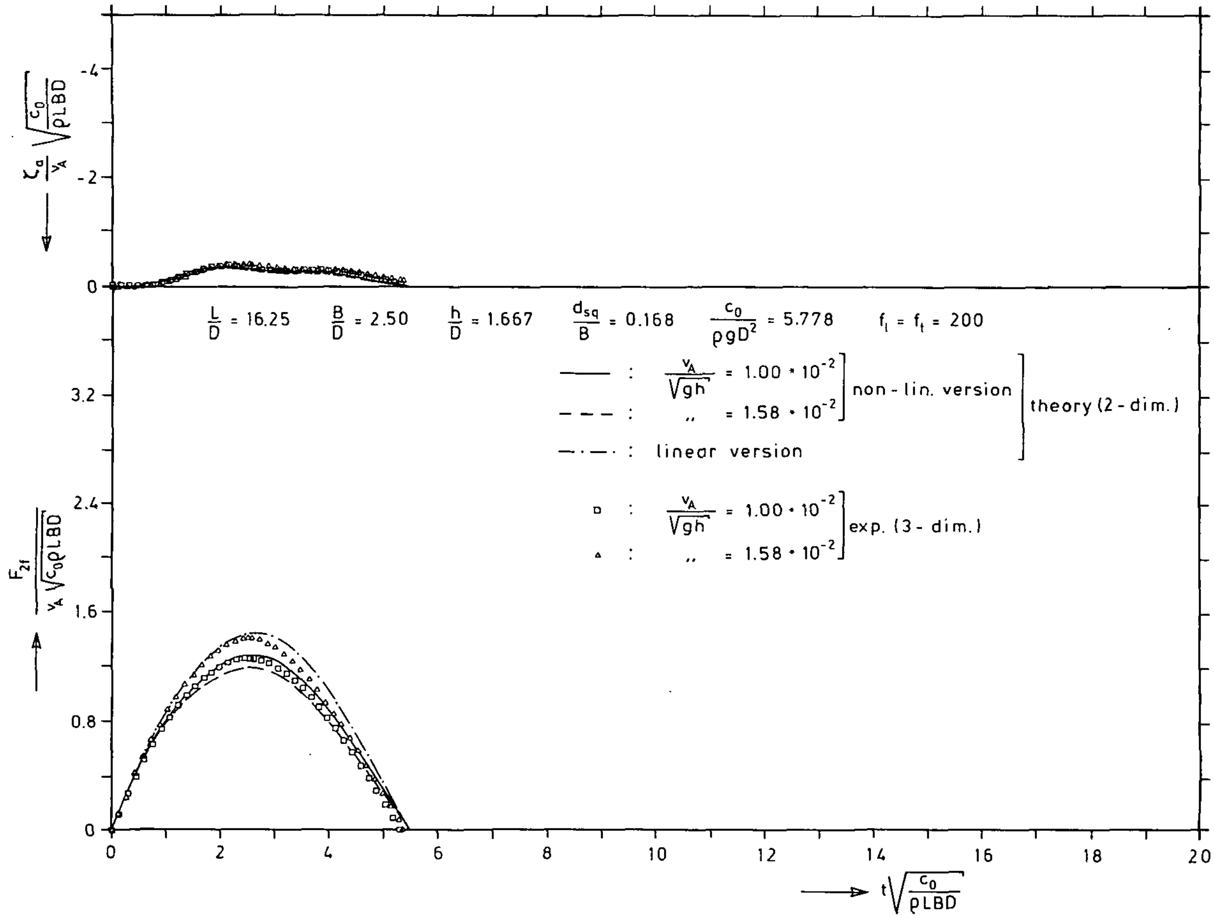

Fig. 4.55 - Time histories of fender force and water-surface elevation in quay clearance: closed berth (d.t.a., h/D = 1.667)

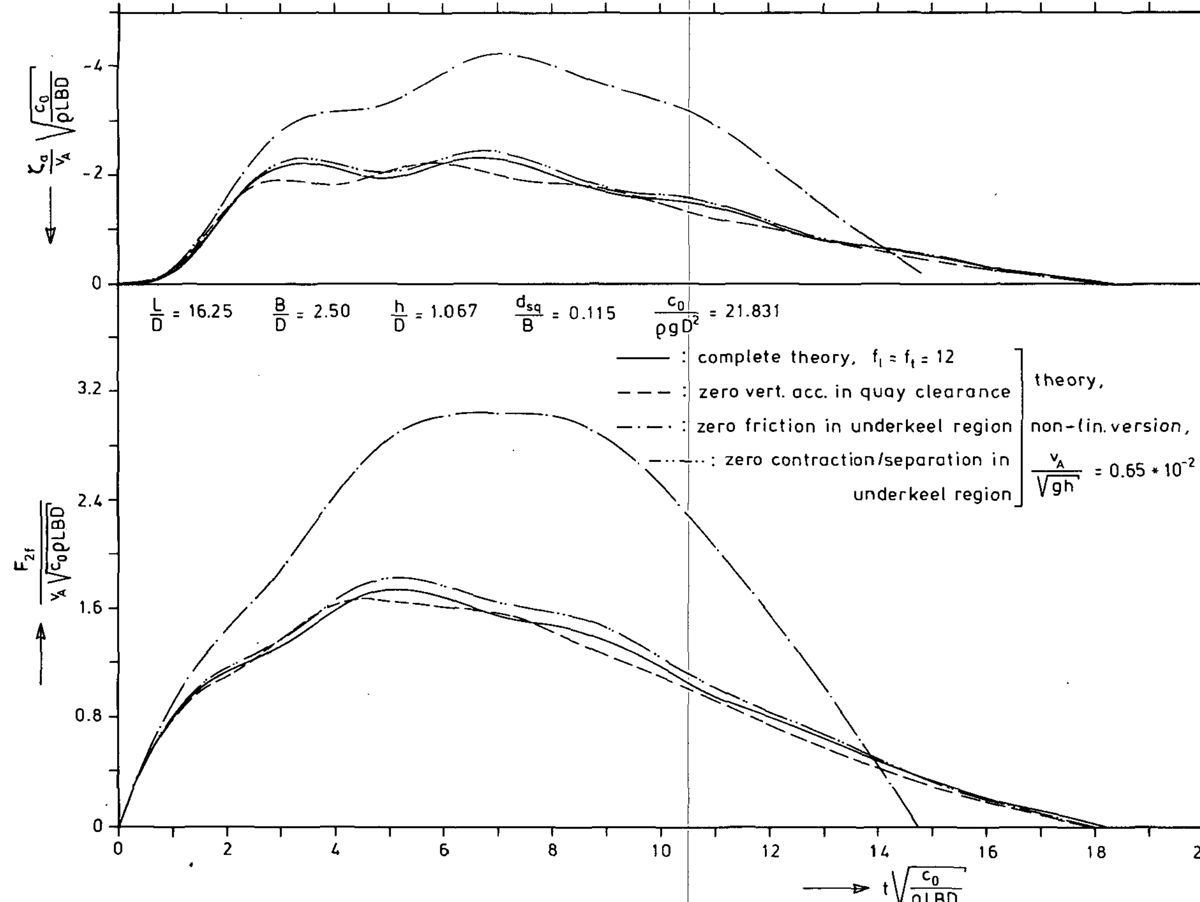

Fig. 4.56 - Time histories of fender force and water-surface elevation in quay clearance: closed berth (d.t.a., h/D = 1.067)

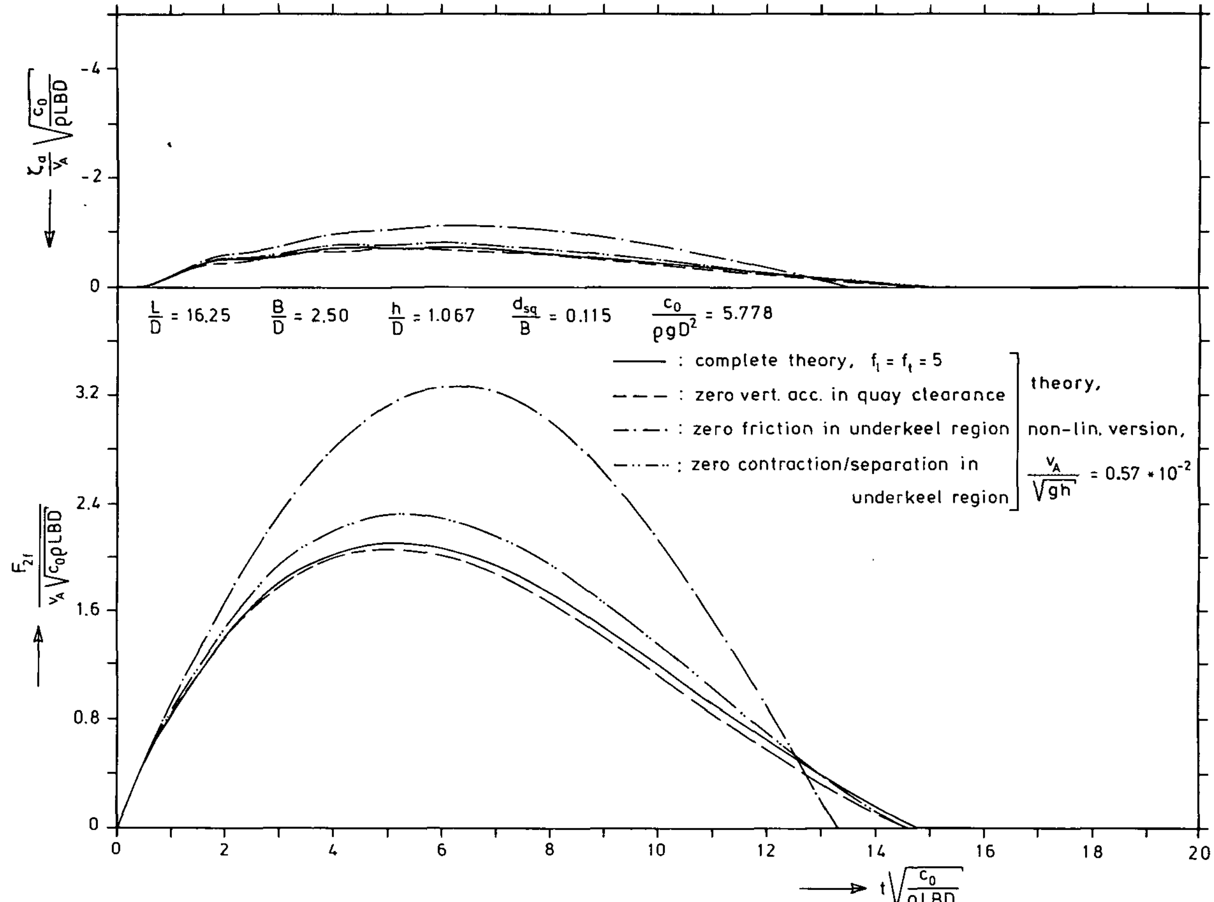

Fig. 4.57 - Time histories of fender force and water-surface elevation in quay clearance: closed berth (d.t.a., h/D = 1.067)

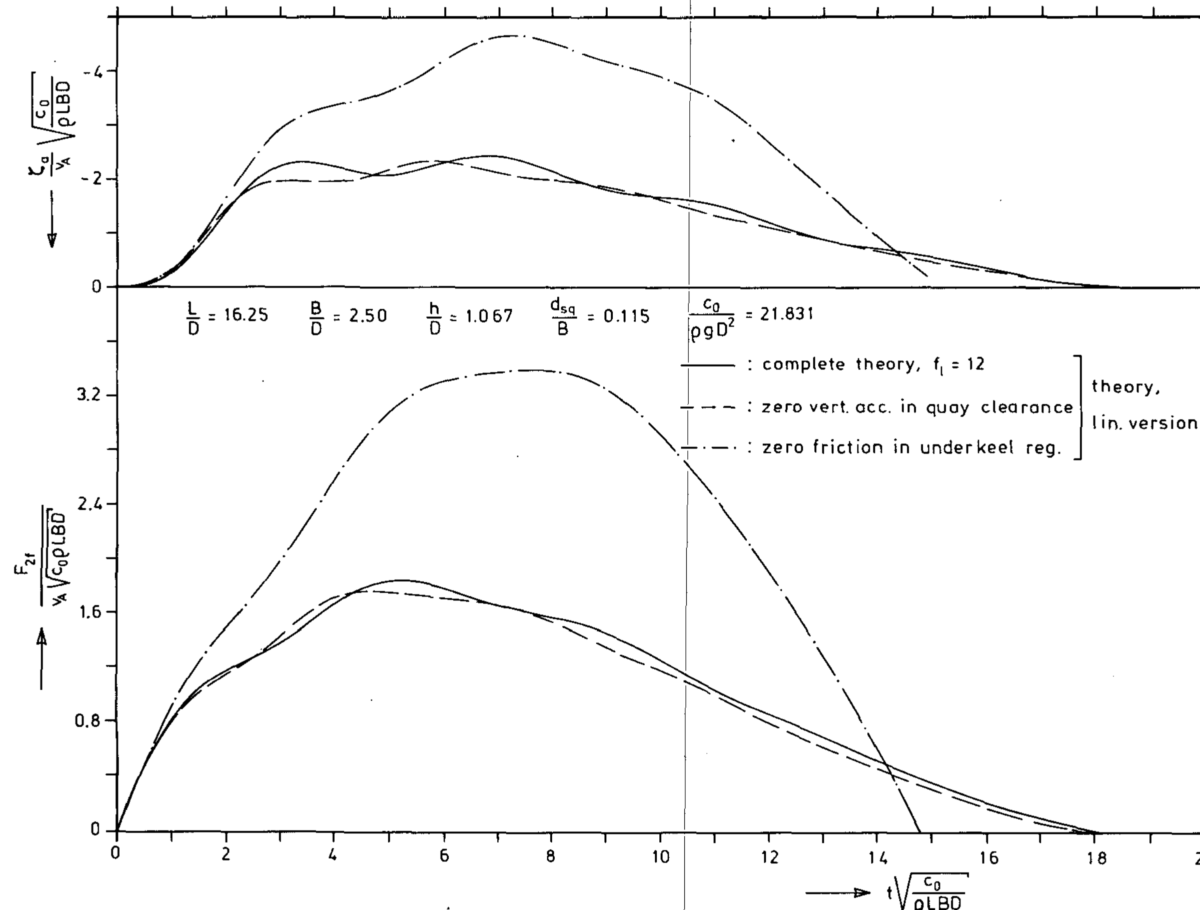

Fig. 4.58 - Time histories of fender force and water-surface elevation in quay clearance: closed berth (d.t.a., h/D = 1.067)

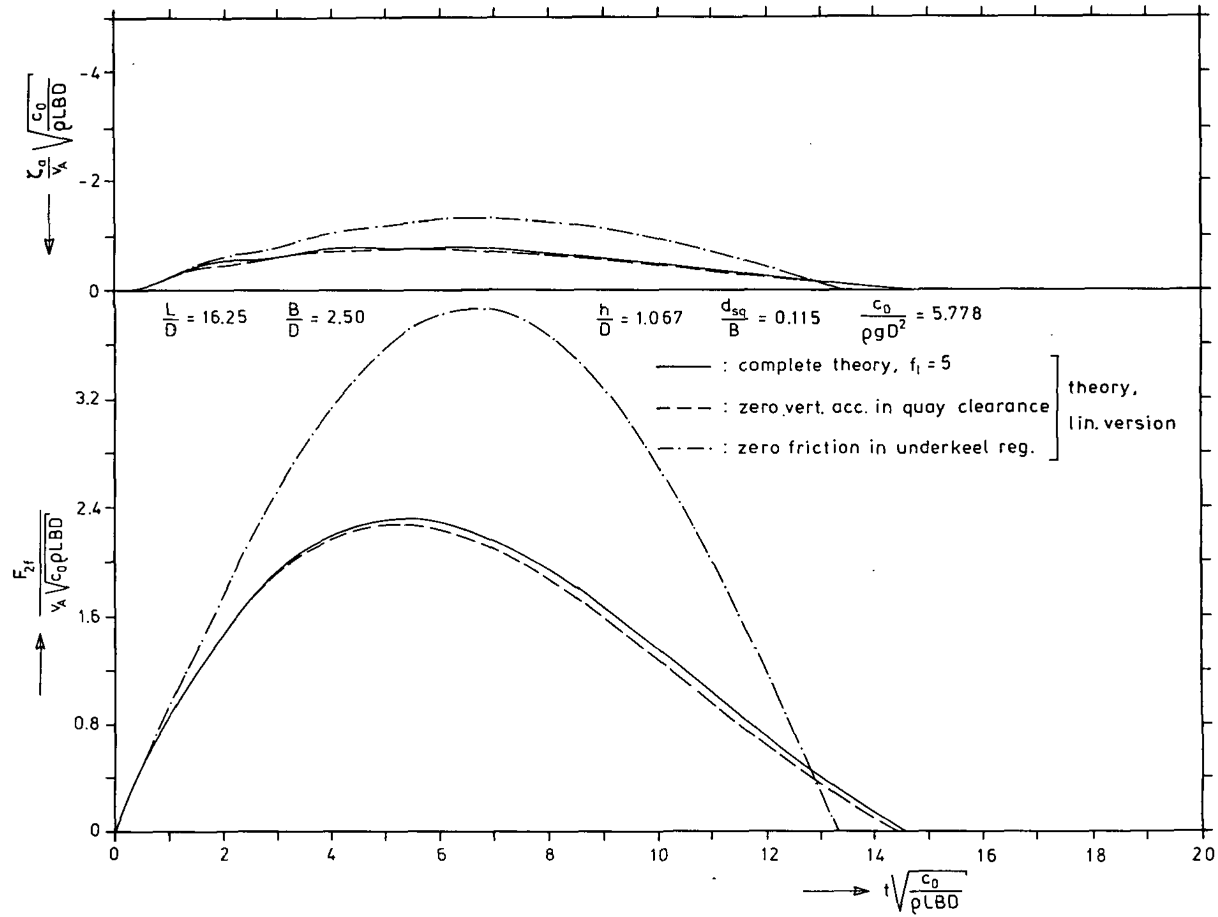

Fig. 4.59 - Time histories of fender force and water-surface elevation in quay clearance: closed berth (d.t.a., h/D = 1.067)

Appendix A: The stability of the linear ship-fluid system

The stability of the linear ship-fluid system can be defined as follows (see ref. [82]).

Suppose that a linear system is subjected to two different, arbitrary pulses (i.e. input signals) and thereupon, in both cases, is let to take its own course. Then this system is stable if, for $t \to \infty$, the difference of the two results (i.e. output signals) converges, and asymptotically stable if the difference for $t \to \infty$ tends to zero.

According to (2.17^b) it applies for the linear ship-fluid system in the time domain:

$$\dot{x}_j(t) = \sum_{i=1}^{6} \int_{-\infty}^{t} f_i(\tau)\, k_{ij}(t-\tau)d\tau \qquad , \qquad j = 1,2,\ldots,6 \quad . \qquad (2.17^b)$$

At the time $t = 0$ an arbitrary pulse in the i-direction is exerted upon the ship:

$$f_k(t) = \delta_{ik}\zeta_i\delta_i(t) \qquad ,$$

where δ_{ik} = Kronecker delta: $\delta_{ik} = 1$ for $k = i$, $\delta_{ik} = 0$ for $k \neq i$,

ζ_i = (arbitrary) coefficient specifying the magnitude of the pulse in the i-direction,

$\delta_i(t)$ = unit pulse (i.e. delta or Dirac function) in the i-direction.

Substitution of $f_k(t)$ into (2.17^b) yields:

$$\dot{x}_j(t)\Big|_I = \zeta_i \int_{-\infty}^{t} \delta_i(\tau)\, k_{ij}(t-\tau)d\tau = \zeta_i k_{ij}(t) \qquad \text{(case I)}.$$

Then, at the time $t = t_1$ ($t_1 \geq 0$) an other arbitrary pulse, also in the i-direction, is exerted upon the ship:

$$f_k(t) = \delta_{ik}\eta_i\delta_i(t-t_1) \qquad ,$$

where η_i = (arbitrary) coefficient specifying the magnitude of the pulse in the i-direction.

Substitution of this expression for $f_k(t)$ into (2.17^b) gives:

$$\dot{x}_j(t)\Big|_{II} = \eta_i \int_{-\infty}^{t} \delta_i(\tau-t_1)\ k_{ij}(t-\tau)d\tau = \eta_i k_{ij}(t-t_1) \qquad \text{(case II).}$$

The difference of these two results (i.e. output signals) can be written as:

$$\dot{x}_j(t)\Big|_{II} - \dot{x}_j(t)\Big|_{I} = \eta_i k_{ij}(t-t_1) - \zeta_i k_{ij}(t) \quad .$$

In case $t \to \infty$ the limit of this expression then yields:

$$\lim_{t\to\infty} \left\{\dot{x}_j(t)\Big|_{II} - \dot{x}_j(t)\Big|_{I}\right\} = \eta_i \lim_{t\to\infty} k_{ij}(t-t_1) - \zeta_i \lim_{t\to\infty} k_{ij}(t) \quad ,$$

which can be reduced to:

$$\lim_{t\to\infty} \left\{\dot{x}_j(t)\Big|_{II} - \dot{x}_j(t)\Big|_{I}\right\} = (\eta_i-\zeta_i)\ k_{ij}(\infty) \quad ,$$

since $\lim_{t\to\infty} k_{ij}(t-t_1) = k_{ij}(\infty)$.
The ship-fluid system now is stable in any case, if this limit does converge, i.e. if $k_{ij}(\infty)$ = constant:

- if $k_{ij}(\infty) = 0$, the system is asymptotically stable; the modes of motion (heave, roll and pitch) have a restoring force;
- if $k_{ij}(\infty)$ = constant $\neq 0$, the system is stable, the modes of motion (surge, sway and yaw) have no restoring force.

Appendix B: The behaviour of $k_{ii}(t)$ for $i = 1,2,6$ as $t \to \infty$

In order to give a physical interpretation as well as an explanation of the behaviour of the i.r.f. as t tends to infinity for ship motions without restoring force, it is started from a specific simplified case with the following features: the ship moves merely in the horizontal plane, $V_1, V_2 = 0$, the water is calm (no waves, no current) and has unrestricted horizontal dimensions, the ship motions (surge, sway and yaw) are uncoupled.
In case of uncoupled motions it can be written for the linear ship-fluid system in the time domain:

$$\dot{x}_i(t) = \int_{-\infty}^{t} f_i(\tau)\ k_{ii}(t-\tau)d\tau \quad . \tag{2.69}$$

Upon the ship now such a force (moment) is exerted, that it translates (rotates) with a constant velocity, viz.:

$$\dot{x}_i = v_{oi} U(t) \quad ,$$

where v_{oi} = constant velocity of the ship in the i-direction.
For $t > 0$ it then holds good:

$$v_{oi} = \int_{0}^{t} f_i(\tau)\ k_{ii}(t-\tau)d\tau \quad .$$

Taking the Laplace transform of this expression one obtains:

$$\frac{v_{oi}}{s} = L\{f_i(t)\}\ L\{k_{ii}(t)\} \quad , \quad Re[s] > Re[s_1] \quad ;$$

in doing so it is supposed that $L\{f_i(t)\}$ and $L\{k_{ii}(t)\}$ exist and that at least one of these Laplace transforms converges absolutely. If $L\{f(t)\}$ does exist and $f(t)$ has a limit for $t \to \infty$, then it holds (see ref. [87]):

$$\lim_{s \downarrow 0} sL\{f(t)\} = \lim_{t \to \infty} f(t) \quad .$$

Making use of this lemma one obtains:

$$\lim_{t \to \infty} f_i(t) = f_i(\infty) = \lim_{s \downarrow 0} sL\{f_i(t)\} \quad ,$$

or:

$$f_i(\infty) = \lim_{s \downarrow 0} \frac{v_{oi}}{L\{k_{ii}(t)\}} = \lim_{s \downarrow 0} \frac{v_{oi}}{\int_0^\infty k_{ii}(t)e^{-st}dt} = \frac{v_{oi}}{\int_0^\infty k_{ii}(t)dt} \quad .$$

Under the circumstances mentioned above a steady state will come into being for large values of t. In view of linearity only small displacements/rotations and velocities are considered. Waves which are generated in the beginning, have already travelled away from the ship for large values of t. Separation of flow and vortex shedding, which do occur in reality and produce a resistance that is proportional to certain (positive) power of the velocity, have to be neglected in this linearized approach. Now two possibilities are to be discerned, viz. the fluid is inviscid and the fluid shows a (linear) viscous behaviour.

If the fluid is considered to be inviscid, it can be stated that the resulting force (moment) upon the ship for large values of t must equal zero, so:

$$f_i(\infty) = 0 = \frac{v_{oi}}{\int_0^\infty k_{ii}(t)dt} \quad ,$$

from which it follows that $\int_0^\infty k_{ii}(t)dt \to \infty$, in other words, this integral does not converge absolutely. This implies $k_{ii}(\infty) > 0$, i.e. the ship -after getting a pulse at t = 0- will maintain a final velocity larger than zero. One thing and another can be illustrated as follows: let

$$f_i(t) = \delta_i(t) \quad ,$$

then it holds good that

$$\dot{x}_i(t) = \int_{-\infty}^{t} \delta_i(\tau)\, k_{ii}(t-\tau)d\tau = k_{ii}(t) \quad ,$$

and consequently:

$$\dot{x}_i(\infty) = k_{ii}(\infty) \quad .$$

Therefore, as the ship at constant (rotational) velocity does not encounter any resistance, and as it 'forgets' its original (rotational) velocity with respect to the water, it generally will keep -after a pulse- in the long run a constant (rotational) velocity; this implies $k_{ii}(\infty)$ = constant $\neq 0$ for i = 1,2,6.

In case of viscous effects from the fluid it must hold good that $f_i(\infty)$ = constant $\neq 0$, so that ${}_0\int^{\infty} k_{ii}(t)dt$ does converge absolutely. This implies $k_{ii}(\infty) = 0$, i.e. the ship -after getting a pulse at t = 0- slows down until its velocity equals zero.

Appendix C: Two direct methods to determine $k_{ii}(t)$ for i = 1,2,6

C.1. Method using both Fourier and Laplace transforms

By combining (2.26[d]) with (2.26[e]) and putting $c_{ii} = 0$, the f.r.f. or harmonic transfer function of the linear ship-fluid system for the case of uncoupled, horizontal motions can be written as:

$$K_{ii}(\omega) = \frac{1}{\{m_{ii} + a_{ii}(\omega)\}i\omega + b_{ii}(\omega)} \quad . \tag{C.1}$$

Since -according to (2.41)- $a_{ii}(0)$ = constant $\neq 0$ and $b_{ii}(0) = 0$, $K_{ii}(\omega)$ contains a singularity (i.e. a pole) for $\omega = 0$. By means of (2.41) it is to be derived that in the neighbourhood of this pole $K_{ii}(\omega)$ behaves as:

$$K_{ii}(\omega)\Big|_{\omega \downarrow 0} = \frac{1}{m_{ii} + a_{ii}(0)} \frac{1}{i\omega} \quad . \tag{C.2^a}$$

If there should be further any poles, these probably lie in the left half-plane; the presence of hydrodynamic damping points that way. From a physical point of view this pole means that in case of a translation (rotation) in the horizontal plane with constant (rotational) velocity -i.e. $\omega = 0$- no force (moment) is required. According to (2.25[a]) the f.r.f. $K_{ii}(\omega)$ is the Fourier transform of the i.r.f. $k_{ii}(t)$. Now $K_{ii}(\omega)$ has a pole for $\omega = 0$, and this indicates that $k_{ii}(t)$ is not absolutely integrable. For the determination of $K_{ii}(\omega)$ therefore no use can be made of an ordinary Fourier transform and it has to be passed on to the Laplace-transform technique. Hereby it has to be borne in mind that the Fourier transform is to be considered as a special case of the Laplace transform.

Suppose that the pole in $K_{ii}(\omega)$ can be isolated and that $K_{ii}(\omega)$ can be written as:

$$K_{ii}(\omega) = K_{ii}^{(p)}(\omega) + K_{ii}^{(r)}(\omega) \quad , \tag{C.3}$$

with, according to (C.2[a]),

$$K_{ii}^{(p)}(\omega) = K_{ii}(\omega)\Big|_{\omega \downarrow 0} \quad , \tag{C.2^b}$$

where $K_{ii}^{(p)}(\omega)$ = part of $K_{ii}(\omega)$ containing the pole for $\omega = 0$,

$K_{ii}^{(r)}(\omega)$ = part of $K_{ii}(\omega)$ without poles.

As $K_{ii}^{(r)}(\omega)$ does not contain poles, this function can be treated with ordinary Fourier-transform techniques. $K_{ii}^{(p)}(\omega)$ is purely imaginary, consequently $Re[K_{ii}(\omega)] = Re[K_{ii}^{(r)}(\omega)]$, so that $Re[K_{ii}(\omega)]$ is not influenced by isolating the pole. Because of the pole for $\omega = 0$ $k_{ii}(t)$ cannot be determined as being the inverse Fourier transform of $K_{ii}(\omega)$; however, the determination of $k_{ii}(t)$ as the inverse Laplace transform of the transfer function is possible. By replacing $i\omega$ in (C.3) and (C.2^{a,b}) with $s = \lambda + i\omega$, $K_{ii}(\omega)$ can be transformed into:

$$K_{ii}(s) = \frac{1}{m_{ii} + a_{ii}(0)} \frac{1}{s} + K_{ii}^{(r)}(s) \quad , \tag{C.4}$$

where $K_{ii}(s)$ = Laplace transform of $k_{ii}(t)$ = transfer function for the i-direction in response to a force excitation in the i-direction,

$K_{ii}^{(r)}(s)$ = part of $K_{ii}(s)$ without poles.

Taking the inverse Laplace transform of $K_{ii}(s)$ one obtains:

$$k_{ii}(t) = \frac{1}{2\pi i} \int_{c-i\infty}^{c+i\infty} K_{ii}(s)\, e^{st} ds =$$

$$= \frac{1}{m_{ii} + a_{ii}(0)} U(t) + \frac{1}{2\pi i} \int_{c-i\infty}^{c+i\infty} K_{ii}^{(r)}(s)\, e^{st} ds \quad ,$$

where c = real constant.

$K_{ii}^{(r)}(s)$ does not contain poles in the right half-plane. Therefore the integral on the right-hand side of the above expression can be written as an inverse Fourier transform (to that end s is replaced by $i\omega$):

$$k_{ii}(t) = \frac{1}{m_{ii} + a_{ii}(0)} U(t) + \frac{1}{2\pi} \int_{-\infty}^{\infty} K_{ii}^{(r)}(\omega)\, e^{i\omega t} d\omega \quad . \tag{C.5}$$

Further,

$$K_{ii}^{(r)}(\omega) = Re[K_{ii}^{(r)}(\omega)] + i\, Im[K_{ii}^{(r)}(\omega)] = Re[K_{ii}(\omega)] + i\, Im[K_{ii}^{(r)}(\omega)] \quad ,$$

substitution of which into (C.5) yields:

$$k_{ii}(t) = \frac{1}{m_{ii}+a_{ii}(0)} U(t) + \frac{1}{2\pi} \int_{-\infty}^{\infty} \{Re[K_{ii}(\omega)]\cos(\omega t) - Im[K_{ii}^{(r)}(\omega)]\sin(\omega t)\}d\omega +$$

$$+ \frac{i}{2\pi} \int_{-\infty}^{\infty} \{Re[K_{ii}(\omega)]\sin(\omega t) + Im[K_{ii}^{(r)}(\omega)]\cos(\omega t)\}d\omega .$$

$k_{ii}(t)$ is a real function of t; as a result it applies

$$\int_{-\infty}^{\infty} Re[K_{ii}(\omega)]\sin(\omega t)\, d\omega = - \int_{-\infty}^{\infty} Im[K_{ii}^{(r)}(\omega)]\cos(\omega t)\, d\omega \quad \text{for all } t,$$

so that

$$k_{ii}(t) = \frac{1}{m_{ii}+ a_{ii}(0)} U(t) + \frac{1}{2\pi} \int_{-\infty}^{\infty} Re[K_{ii}(\omega)]\cos(\omega t)\, d\omega +$$

$$- \frac{1}{2\pi} \int_{-\infty}^{\infty} Im[K_{ii}^{(r)}(\omega)]\sin(\omega t)\, d\omega \quad .$$

Since $k_{ii}(t) \equiv 0$ for $t < 0$ (see (2.18)), the second term on the right-hand side is an even function and the third term an odd function of t, it must hold good that:

$$\int_{-\infty}^{\infty} Re[K_{ii}(\omega)]\cos(\omega t)\, d\omega = - \int_{-\infty}^{\infty} Im[K_{ii}^{(r)}(\omega)]\sin(\omega t)\, d\omega \quad ,$$

by means of which $k_{ii}(t)$ can be written as:

$$k_{ii}(t) = \frac{1}{m_{ii}+ a_{ii}(0)} U(t) + \frac{1}{\pi} \int_{-\infty}^{\infty} Re[K_{ii}(\omega)]\cos(\omega t)\, d\omega \quad .$$

Generally it holds that $Re[K_{ii}(\omega)]$ is an even function of ω (see (2.25[a])), so that $k_{ii}(t)$ finally becomes:

$$k_{ii}(t) = \frac{1}{m_{ii}+ a_{ii}(0)} U(t) + \frac{2}{\pi} \int_{0}^{\infty} Re[K_{ii}(\omega)]\cos(\omega t)\, d\omega \quad . \tag{C.6}$$

On account of (C.1) $Re[K_{ii}(\omega)]$ now has the form

$$Re[K_{ii}(\omega)] = \frac{b_{ii}(\omega)}{\{m_{ii}+ a_{ii}(\omega)\}^2\omega^2 + b_{ii}^2(\omega)} \tag{C.7}$$

and is therefore -in this approach- identical to $Re[H_{ii}(i\omega)]$ (see (2.64)). Likewise it holds good that:

$$\frac{1}{m_{ii} + a_{ii}(0)} = \alpha_{ii} \quad . \tag{2.65}$$

Introducing the unit step function $U(t)$ in order to satisfy the causality condition (2.18), $k_{ii}(t)$ then can be written as:

$$k_{ii}(t) = \left\{\alpha_{ii} + \frac{2}{\pi} \int_0^{\infty} Re[H_{ii}(i\omega)]\cos(\omega t)\, d\omega\right\} U(t) \quad . \tag{C.8}$$

It is easily to be seen that (C.8) is equivalent to the i.r.f. as represented by the set of expressions (2.67), (2.66), (2.64) and (2.65).

C.2. Formal method using Laplace transforms

As indicated in the foregoing, it generally holds good that the transfer function of a linear system is identical to the Laplace transform of the i.r.f. (see also refs. [79, 80]).
The harmonic transfer function or f.r.f. of the linear ship-fluid system in case of uncoupled, horizontal motions again is written as (C.1). It has been shown that $K_{ii}(\omega)$ contains a pole for $\omega = 0$. If in (C.1) $i\omega$ is replaced by $s = \lambda + i\omega$, it can be passed on to the Laplace notation. The transfer function $K_{ii}(s)$ then takes the form:

$$K_{ii}(s) = \frac{1}{\{m_{ii} + a_{ii}(s)\}s + b_{ii}(s)} \quad , \tag{C.9}$$

and the i.r.f. $k_{ii}(t)$ -through the inverse Laplace transform of $K_{ii}(s)$-

$$k_{ii}(t) = \frac{1}{2\pi i} \int_{c-i\infty}^{c+i\infty} K_{ii}(s)\, e^{st} ds \quad . \tag{C.10}$$

The integrand of this integral has a pole for $s = 0$. This means that in (C.10) $c = 0$ and that the path of integration is formed by a semi-circle around the origin -situated in the right half-plane and with radius $r \downarrow 0-$, plus the respective positive and negative imaginary axis connected to that.
Now $k_{ii}(t)$ can be written as the sum of three integrals:

$$k_{ii}(t) = \frac{1}{2\pi i}\left(I_I + I_{II} + I_{III}\right) \quad , \tag{C.11}$$

where

$$I_I = \lim_{r\downarrow 0} \int_{-i\infty}^{-ir} K_{ii}(s)\, e^{st} ds \quad ,$$

$$I_{II} = \lim_{r\downarrow 0} \int_{r} K_{ii}(s)\, e^{st} ds \quad ,$$

$$I_{III} = \lim_{r\downarrow 0} \int_{ir}^{i\infty} K_{ii}(s)\, e^{st} ds \quad ,$$

with $K_{ii}(s)$ according to (C.9).
In the integral I_{II} s can be represented by $s = re^{i\phi}$, where $r = |s|$ and $\phi = \arg(s)$; then $ds = ire^{i\phi}d\phi$, so that I_{II} changes into:

$$I_{II} = \lim_{r\downarrow 0} \int_{-\frac{\pi}{2}}^{\frac{\pi}{2}} \frac{e^{tre^{i\phi}}}{\{m_{ii} + a_{ii}(re^{i\phi})\}re^{i\phi} + b_{ii}(re^{i\phi})}\, ire^{i\phi} d\phi =$$

$$= i \int_{-\frac{\pi}{2}}^{\frac{\pi}{2}} \frac{\lim_{r\downarrow 0} e^{tre^{i\phi}}}{\lim_{r\downarrow 0} a_{ii}(re^{i\phi}) + m_{ii} + \lim_{r\downarrow 0} \frac{b_{ii}(re^{i\phi})}{re^{i\phi}}}\, d\phi \quad .$$

On the analogy of (2.41) it can be written for small values of r:

$$\left.\begin{aligned} a_{ii}(s) &= a_{ii}(re^{i\phi}) = a_{ii}(0) + a_{ii}^{(2)}r^2e^{2i\phi} + O(r^4) \quad , \\ b_{ii}(s) &= b_{ii}(re^{i\phi}) = \qquad\qquad b_{ii}^{(2)}r^2e^{2i\phi} + O(r^4) \quad , \end{aligned}\right\} \text{for } r \to 0 \quad ,$$

from which it follows:

$$\lim_{r\downarrow 0} a_{ii}(re^{i\phi}) = a_{ii}(0) \; , \qquad \lim_{r\downarrow 0} \frac{b_{ii}(re^{i\phi})}{re^{i\phi}} = \lim_{r\downarrow 0} b_{ii}^{(2)} re^{i\phi} = 0 \quad .$$

Besides it holds good that

$$\lim_{r \downarrow 0} e^{tre^{i\phi}} = 1 \quad .$$

Substitution of one thing and another into the expression for I_{II} yields:

$$I_{II} = i \int_{-\frac{\pi}{2}}^{\frac{\pi}{2}} \frac{1}{m_{ii} + a_{ii}(0)} \, d\phi = \frac{\pi i}{m_{ii} + a_{ii}(0)} \quad .$$

In the integral I_{III} it applies $s = i\omega$, $ds = id\omega$ and $\omega > 0$, so that I_{III} takes the form:

$$I_{III} = \lim_{r \downarrow 0} \int_{r}^{\infty} \frac{ie^{i\omega t}}{\{m_{ii} + a_{ii}(i\omega)\}i\omega + b_{ii}(i\omega)} \, d\omega \quad .$$

In the integral I_I it applies $s = -i\omega$, $ds = -id\omega$ and $\omega > 0$, so that I_I takes the form:

$$I_I = - \lim_{r \downarrow 0} \int_{\infty}^{r} \frac{ie^{-i\omega t}}{-\{m_{ii} + a_{ii}(-i\omega)\}i\omega + b_{ii}(-i\omega)} \, d\omega =$$

$$= - \lim_{r \downarrow 0} \int_{r}^{\infty} \frac{ie^{-i\omega t}}{\{m_{ii} + a_{ii}(-i\omega)\}i\omega - b_{ii}(-i\omega)} \, d\omega \quad ;$$

$a_{ii}(i\omega)$ and $b_{ii}(i\omega)$ are even functions of ω, so that I_I becomes:

$$I_I = - \lim_{r \downarrow 0} \int_{r}^{\infty} \frac{ie^{-i\omega t}}{\{m_{ii} + a_{ii}(i\omega)\}i\omega - b_{ii}(i\omega)} \, d\omega \quad .$$

For $(I_I + I_{III})$ it then can be derived:

$$I_I + I_{III} = \lim_{r \downarrow 0} 2i \int_{r}^{\infty} \frac{\omega\{m_{ii} + a_{ii}(i\omega)\} \sin(\omega t) + b_{ii}(i\omega) \cos(\omega t)}{\{m_{ii} + a_{ii}(i\omega)\}^2\omega^2 + b_{ii}^2(i\omega)} \, d\omega \quad .$$

With $s = i\omega$ it follows from (C.9):

$$\frac{b_{ii}(i\omega)}{\{m_{ii} + a_{ii}(i\omega)\}^2\omega^2 + b_{ii}^2(i\omega)} = \mathrm{Re}[K_{ii}(\omega)] \quad ,$$

$$\frac{\omega\{m_{ii} + a_{ii}(i\omega)\}}{\{m_{ii} + a_{ii}(i\omega)\}^2\omega^2 + b_{ii}^2(i\omega)} = - \mathrm{Im}[K_{ii}(\omega)] \quad .$$

Substitution of the results obtained so far into the expression for $k_{ii}(t)$ (C.11) yields:

$$k_{ii}(t) = \frac{1}{2}\frac{1}{m_{ii}+a_{ii}(0)} + \frac{1}{\pi}\lim_{r\downarrow 0}\int_r^{\infty}\{Re[K_{ii}(\omega)]\cos(\omega t) - Im[K_{ii}(\omega)]\sin(\omega t)\}d\omega =$$

$$= \frac{1}{2}\frac{1}{m_{ii}+a_{ii}(0)} + \frac{1}{\pi}\int_0^{\infty} Re[K_{ii}(\omega)]\cos(\omega t)d\omega - \frac{1}{\pi}\int_0^{\infty} Im[K_{ii}(\omega)]\sin(\omega t)d\omega \ .$$

As $k_{ii}(t) \equiv 0$ for $t < 0$ (see (2.18)), the first two terms on the right-hand side are even functions of t and the third term is an odd function of t, it must hold good that:

$$-\frac{1}{\pi}\int_0^{\infty} Im[K_{ii}(\omega)]\sin(\omega t)d\omega = \frac{1}{2}\frac{1}{m_{ii}+a_{ii}(0)} + \frac{1}{\pi}\int_0^{\infty} Re[K_{ii}(\omega)]\cos(\omega t)d\omega \quad ,$$

substitution of which into the above expression for $k_{ii}(t)$ finally gives:

$$k_{ii}(t) = \frac{1}{m_{ii}+ a_{ii}(0)} + \frac{2}{\pi}\int_0^{\infty} Re[K_{ii}(\omega)]\cos(\omega t)d\omega \quad . \tag{C.12}$$

In this approach, again $Re[K_{ii}(\omega)] = Re[H_{ii}(i\omega)]$, while at the same time (2.65) applies. Adding the unit step function U(t) in order to satisfy the causality condition (2.18), $k_{ii}(t)$ then takes a form identical to (C.8).

Appendix D: Outline of solution of mixed boundary-value problem

The (first order) velocity potential $\Phi(x_2,x_3,t)$ has to satisfy the equation of Laplace:

$$\nabla^2\Phi = \frac{\partial^2\Phi}{\partial x_2^2} + \frac{\partial^2\Phi}{\partial x_3^2} = 0 \quad \text{in } R \quad , \tag{3.2}$$

subject to the boundary conditions:

$$\frac{\partial^2\Phi}{\partial t^2} + g\,\frac{\partial\Phi}{\partial x_3} = 0 \quad \text{on} \quad x_2 \geqq \tfrac{1}{2}B \quad , \quad x_3 = 0 \quad , \tag{3.4}$$

$$\frac{\partial\Phi}{\partial x_2} = \{U(x_3+D) - U(x_3)\}\dot{x}_2 + \{U(x_3+h) - U(x_3+D)\}v_b \quad \text{on} \quad x_2 = \tfrac{1}{2}B \quad , \tag{3.5}$$

$$\frac{\partial\Phi}{\partial x_3} = 0 \quad \text{on} \quad x_2 \geqq \tfrac{1}{2}B \quad , \quad x_3 = -h \quad , \tag{3.6}$$

$$\Phi(x_2,x_3,t)\Big|_{x_2\to\infty} \longrightarrow \text{outgoing dispersive wave,} \tag{3.7}$$

and the supplementary condition

$$\Phi(x_2,x_3,t) \ , \ \Phi^1(x_2,x_3,t) \qquad \text{being finite in } R, \tag{3.8}$$

where R is defined by:

$$\left.\begin{array}{l} x_2 > \tfrac{1}{2}B \quad , \quad -h \leqq x_3 \leqq 0 \quad , \\ x_2 = \tfrac{1}{2}B \quad , \quad -D \leqq x_3 \leqq 0 \quad , \quad -h \leqq x_3 < -D \quad , \end{array}\right\} R \tag{3.3}$$

and $x_2(t)$ and $v_b(t)$ are prescribed according to

$$x_2(t) = -i\hat{x}_2 e^{i\omega t} \quad , \tag{3.9}$$

$$v_b(t) = \hat{v}_b e^{i(\omega t-\theta)} \quad , \tag{3.10}$$

respectively; further

$$v = \frac{\partial \Phi}{\partial x_2} \quad , \quad w = \frac{\partial \Phi}{\partial x_3} \quad . \tag{3.1}$$

The determination of $\Phi(x_2,x_3,t)$ from the expressions above may be considered as an extension of the work dealt with in ref. [96].

Due to the linearity of the problem the velocity potential $\Phi(x_2,x_3,t)$ can be conceived as being composed of the velocity potential $\Phi_s(x_2,x_3,t)$ resulting from the motion of the ship only, and the velocity potential $\Phi_{kc}(x_2,x_3,t)$ resulting from the motion of the mass of water in the keel clearance:

$$\Phi(x_2,x_3,t) = \Phi_s(x_2,x_3,t) + \Phi_{kc}(x_2,x_3,t) \quad ; \tag{D.1}$$

each single velocity potential must satisfy the Laplacian and relevant boundary conditions; the subscripts s and kc indicate that the quantity concerned relates to the motion of the ship and the motion of the mass of water in the keel clearance, respectively. $\Phi(x_2,x_3,t)$, and consequently $\Phi_s(x_2,x_3,t)$ and $\Phi_{kc}(x_2,x_3,t)$, are simple-harmonic functions of time t; therefore the sinusoidal time-dependence may be factored out:

$$\Phi_{s,kc}(x_2,x_3,t) = \phi_{s,kc}(x_2,x_3)\, T_{s,kc}(t) \quad , \tag{D.2}$$

where $\phi_{s,kc}(x_2,x_3)$ = harmonic function of place,

$$\left.\begin{aligned} T_s(t) &= e^{i\omega t} \quad , \\ T_{kc}(t) &= e^{i(\omega t-\theta)} \quad , \end{aligned}\right\} \text{ i.e. simple-harmonic functions of time.}$$

Substitution of (D.2) into (3.2), (3.4), (3.6) and (3.8) yields:

$$\nabla^2\phi_{s,kc} = 0 \quad \text{in } R \quad , \tag{D.3}$$

$$\phi_{s,kc} - \frac{g}{\omega^2}\frac{\partial \phi_{s,kc}}{\partial x_3} = 0 \quad \text{on} \quad x_2 \geq \tfrac{1}{2}B \ , \ x_3 = 0 \quad , \tag{D.4}$$

$$\frac{\partial \phi_{s,kc}}{\partial x_3} = 0 \quad \text{on} \quad x_2 \geq \tfrac{1}{2}B \ , \ x_3 = -h \quad , \tag{D.5}$$

$$\phi_{s,kc} \ , \ \phi^1_{s,kc} \qquad \text{being finite in } R, \tag{D.6}$$

respectively.

The Laplacian (D.3) is solved by means of separation of variables, i.e. $\phi_{s,kc}(x_2,x_3)$ is supposed to be of the form

$$\phi_{s,kc}(x_2,x_3) = Y_{s,kc}(x_2)\, Z_{s,kc}(x_3) \quad , \tag{D.7}$$

where $Y_{s,kc}(x_2)$ = function of x_2 only,
$Z_{s,kc}(x_3)$ = function of x_3 only;
then (D.3) changes into:

$$\frac{1}{Y_{s,kc}} \frac{d^2 Y_{s,kc}}{dx_2^2} = - \frac{1}{Z_{s,kc}} \frac{d^2 Z_{s,kc}}{dx_3^2} = \alpha^2 \quad , \tag{D.8}$$

where α^2 = constant of separation.
The solution of the expressions in (D.8) reads as:

$$\left.\begin{aligned} Y_{s,kc}(x_2) &= Ae^{\alpha x_2} + Be^{-\alpha x_2} \quad , \\ Z_{s,kc}(x_3) &= Ce^{i\alpha x_3} + De^{-i\alpha x_3} \quad , \end{aligned}\right\} \tag{D.9}$$

where A, B, C, D = constants of integration.
Starting from the general assumption that α is a constant complex quantity, written as $\alpha = \alpha_r + i\alpha_i$ with $Re[\alpha] = \alpha_r$, $Im[\alpha] = \alpha_i$, it can be shown that merely the three following cases have to be considered:

I : $\alpha = 0$, i.e. $\alpha_r = \alpha_i = 0$,

II : $\alpha = \alpha_r$, i.e. $\alpha_i = 0$,

III : $\alpha = i\alpha_i$, i.e. $\alpha_r = 0$.

Using $\alpha = \alpha_r + i\alpha_i$ (D.9) can be written as:

$$\left.\begin{aligned} Y_{s,kc}(x_2) &= (Ae^{\alpha_r x_2} + Be^{-\alpha_r x_2})\cos(\alpha_i x_2) + i(Ae^{\alpha_r x_2} - Be^{-\alpha_r x_2})\sin(\alpha_i x_2) \quad , \\ Z_{s,kc}(x_3) &= (De^{\alpha_i x_3} + Ce^{-\alpha_i x_3})\cos(\alpha_r x_3) - i(De^{\alpha_i x_3} - Ce^{-\alpha_i x_3})\sin(\alpha_r x_3) \quad . \end{aligned}\right\} \tag{D.10}$$

Introduction of the supplementary condition (D.6) then yields:

$$Z_{s,kc}(x_3) \quad , \quad \frac{dZ_{s,kc}}{dx_3} \quad \text{being finite on} \quad -h \leq x_3 \leq 0 \quad , \tag{D.11^a}$$

and

$$Y_{s,kc}(x_2) \quad , \quad \frac{dY_{s,kc}}{dx_2} \quad \text{being finite on} \quad x_2 \geq \tfrac{1}{2}B \quad , \tag{D.11^b}$$

$$\text{if} \begin{cases} \text{either} \quad \alpha_r = 0 \quad \text{(cases I and III, respectively),} \\ \text{or, both} \quad \alpha_r > 0 \quad \text{and} \quad A = 0 \quad \text{(case II),} \\ \text{or, both} \quad \alpha_r < 0 \quad \text{and} \quad B = 0 \quad \text{(case II).} \end{cases}$$

Introducing the boundary conditions (D.5) and (D.4) into the three above-mentioned cases successively and using (D.7), it is obtained:

I : for $\alpha = 0$: $\quad \phi_{s,kc}(x_2,x_3) = 0$ (i.e. the zero-solution);

II : for $\alpha = \alpha_r$: $\quad$ if $\alpha_r > 0$, $\quad \phi_{s,kc}(x_2,x_3) = K_1 e^{-\alpha_r x_2} \cos\{\alpha_r(x_3+h)\}$

$$\text{with} \quad \omega^2 = -g\alpha_r \tan(\alpha_r h) \ ,$$

and if $\alpha_r < 0$, $\quad \phi_{s,kc}(x_2,x_3) = K_2 e^{\alpha_r x_2} \cos\{\alpha_r(x_3+h)\}$

$$\text{with} \quad \omega^2 = -g\alpha_r \tan(\alpha_r h) \ ;$$

III: for $\alpha = i\alpha_i$: $\quad \phi_{s,kc}(x_2,x_3) = \{E \cos(\alpha_i x_2) + iF \sin(\alpha_i x_2)\} \cosh\{\alpha_i(x_3+h)\}$

$$\text{with} \quad \omega^2 = g\alpha_i \tanh(\alpha_i h) \ ,$$

where K_1, K_2, E, F = constants of integration.
With regard to case II it has to be noted that the equation
$\omega^2 = -g\alpha_r \tan(\alpha_r h)$
contains two series of real roots for α_r with the same absolute values but opposite signs:

$$\left.\begin{array}{lll} \text{for} \ \alpha_r > 0 \ \text{it holds:} & \alpha_r = +m_1, +m_2, \ldots, +m_n, \ldots \\ \text{for} \ \alpha_r < 0 \ \text{it holds:} & \alpha_r = -m_1, -m_2, \ldots, -m_n, \ldots \end{array}\right\}$$

with $m_n > 0$, arranged in order of increasing magnitude. The complete solution for case II is composed of linear combinations of:

$$K_1 e^{-\alpha_r x_2} \cos\{\alpha_r(x_3+h)\} \quad \text{and} \quad K_2 e^{\alpha_r x_2} \cos\{\alpha_r(x_3+h)\}$$

for the respective values of α_r, and can be written as:

$$\phi_{s,kc}(x_2,x_3) = \sum_{n=1}^{\infty} C_n e^{-m_n x_2} \cos\{m_n(x_3+h)\} \quad , \tag{D.12^a}$$

where C_n = constant of integration

and

$$m_n = \text{positive roots of } \omega^2 = -gm_n \tan(m_n h) \quad , \quad m_1 < m_2 < \cdots < m_n < \cdots \quad . \tag{3.12^b}$$

Similarly, with regard to case III, the equation

$\omega^2 = g\alpha_i \tanh(\alpha_i h)$

contains two real roots with the same absolute values but opposite signs:

$\alpha_i = \pm\, m_0 \quad , \quad m_0 > 0 \quad .$

The complete solution for case III is composed of a linear combination of

$$\{E \cos(\alpha_i x_2) + iF \sin(\alpha_i x_2)\} \cosh\{\alpha_i(x_3+h)\}$$

for the respective values of α_i, and can be written as:

$$\phi_{s,kc}(x_2,x_3) = \{A \cos(m_0 x_2) + iB \sin(m_0 x_2)\} \cosh\{m_0(x_3+h)\} \quad , \tag{D.12^b}$$

where

$$m_0 = \text{positive root of } \omega^2 = gm_0 \tanh(m_0 h) \quad . \tag{3.12^a}$$

(3.12^a) and (3.12^b) are the expressions for the wave numbers: m_0 is the usual wave number and m_n satisfies $(n - \frac{1}{2})\pi < m_n h < n\pi$.

The solution for $\phi_{s,kc}(x_2,x_3)$ which satisfies the Laplacian (D.3), the boundary conditions (D.4) and (D.5) and the supplementary condition (D.6), consists of a linear combination of the solutions for the respective cases I, II and III, viz. (D.12^a) and (D.12^b), and reads as:

$$\phi_{s,kc}(x_2,x_3) = \{A \cos(m_0 x_2) + iB \sin(m_0 x_2)\} \cosh\{m_0(x_3+h)\} + \\ + \sum_{n=1}^{\infty} C_n e^{-m_n x_2} \cos\{m_n(x_3+h)\} \quad . \tag{D.13}$$

On account of (D.2) it then can be written:

$$\Phi_{s,kc}(x_2,x_3,t) = \left[\{A\cos(m_0x_2) + iB\sin(m_0x_2)\}\cosh\{m_0(x_3+h)\} + \right.$$

$$\left. + \sum_{n=1}^{\infty} C_n e^{-m_nx_2}\cos\{m_n(x_3+h)\}\right] T_{s,kc}(t) \quad . \quad (D.14)$$

Applying boundary condition (3.7) to the above expression (D.14) one obtains:

$$\Phi_{s,kc}(x_2,x_3,t) = \left[C_0\cosh\{m_0(x_3+h)e^{-im_0x_2} + \right.$$

$$\left. + \sum_{n=1}^{\infty} C_n e^{-m_nx_2}\cos\{m_n(x_3+h)\}\right] T_{s,kc}(t) \quad , \quad (D.15)$$

where C_0 = constant of integration.

According to (D.1) the velocity potential $\Phi(x_2,x_3,t)$, satisfying the equation of Laplace (3.2) plus the boundary conditions (3.4), (3.6) and (3.7) and the supplementary condition (3.8) now becomes:

$$\Phi(x_2,x_3,t) = i\,\frac{\omega}{m_0}\,(A_0 + B_0e^{-i\theta})\cosh\{m_0(x_3+h)\}e^{i(\omega t - m_0x_2 + \frac{m_0B}{2})} +$$

$$-\sum_{n=1}^{\infty}\frac{\omega}{m_n}\,(A_n + B_ne^{-i\theta})e^{-m_nx_2 + \frac{m_nB}{2}}\cos\{m_n(x_3+h)\}e^{i\omega t} \quad , \quad (3.11)$$

where A_0, B_0, A_n, B_n = (so far unknown) constants of integration.

Substitution of $\Phi(x_2,x_3,t)$ as formulated by (3.11) into boundary condition (3.5) as well as substitution of $x_2(t)$ and $v_b(t)$ according to (3.9) and (3.10), respectively, gives the result (supposing $\omega \neq 0$):

$$(A_0 + B_0e^{-i\theta})\cosh\{m_0(x_3+h)\} + \sum_{n=1}^{\infty}(A_n + B_ne^{-i\theta})\cos\{m_n(x_3+h)\} =$$

$$= \hat{x}_2\{U(x_3+h) - U(x_3)\} + \frac{\hat{v}_b}{\omega}\,e^{-i\theta}\{U(x_3+h) - U(x_3+D)\} \quad . \quad (D.16)$$

On account of Weierstrass' theorem the series

$$\sum_{n=1}^{\infty}(A_n + B_ne^{-i\theta})\cos\{m_n(x_3+h)\}$$

is supposed to be uniformly convergent on the closed interval $-h \leq x_3 \leq 0$; as a consequence, this series can be differentiated and integrated term by term. The factors $(A_0 + B_0 e^{-i\theta})$ and $(A_n + B_n e^{-i\theta})$ in (D.16) may be considered as the coefficients of $\cosh\{m_0(x_3+h)\}$ and $\cos\{m_n(x_3+h)\}$, respectively. Resolution of the right-hand side of (D.16) on $-h \leq x_3 \leq 0$ into terms conformable to its left-hand side is, generally, only possible if the series of even functions:

$$\cosh\{m_0(x_3+h)\},\ \cos\{m_1(x_3+h)\},\ \cos\{m_2(x_3+h)\},\ldots,\ \cos\{m_n(x_3+h)\},\ldots \tag{D.17}$$

is complete on this interval. With regard to this point the line is taken that the functions (D.17) form a complete series (basis) on $-h \leq x_3 \leq 0$. Besides the functions (D.17) are orthogonal on $-h \leq x_3 \leq 0$. The so far unknown constants of integration A_0, B_0, A_n and B_n in (3.11) then can be determined by applying the principle of orthogonality to (D.16) on $-h \leq x_3 \leq 0$. To that end (D.16) is multiplied by $\cosh\{m_0(x_3+h)\}$ and $\cos\{m_m(x_3+h)\}$ $(m = 1,2,\ldots,n,\ldots)$, respectively, and subsequently integrated over the interval in question, yielding:

$$(A_0 + B_0 e^{-i\theta}) \int_{-h}^{0} \cosh^2\{m_0(x_3+h)\}dx_3 +$$

$$+ \sum_{n=1}^{\infty} (A_n + B_n e^{-i\theta}) \int_{-h}^{0} \cosh\{m_0(x_3+h)\}\cos\{m_n(x_3+h)\}dx_3 =$$

$$= \hat{x}_2 \int_{-h}^{0} \{U(x_3+h) - U(x_3)\}\cosh\{m_0(x_3+h)\}dx_3 +$$

$$+ \frac{\hat{v}_b}{\omega} e^{-i\theta} \int_{-h}^{0} \{U(x_3+h) - U(x_3+D)\}\cosh\{m_0(x_3+h)\}dx_3$$

and

$$(A_0 + B_0 e^{-i\theta}) \int_{-h}^{0} \cosh\{m_0(x_3+h)\}\cos\{m_m(x_3+h)\}dx_3 +$$

$$+ \sum_{n=1}^{\infty} (A_n + B_n e^{-i\theta}) \int_{-h}^{0} \cos\{m_m(x_3+h)\}\cos\{m_n(x_3+h)\}dx_3 =$$

$$= \hat{x}_2 \int_{-h}^{0} \{U(x_3+h) - U(x_3)\}\cos\{m_m(x_3+h)\}dx_3 +$$

$$+ \frac{\hat{v}_b}{\omega} e^{-i\theta} \int_{-h}^{0} \{U(x_3+h) - U(x_3+D)\} \cos\{m_m(x_3+h)\} dx_3 \quad .$$

Using (3.12^a) and (3.12^b) it can be verified that:

$$\int_{-h}^{0} \cosh\{m_0(x_3+h)\} \cos\{m_n(x_3+h)\} dx_3 = 0 \quad \text{for all } n \quad ,$$

and

$$\int_{-h}^{0} \cos\{m_m(x_3+h)\} \cos\{m_n(x_3+h)\} dx_3 \begin{cases} = 0 & \text{if} \quad n \neq m \ , \\ \neq 0 & \text{if} \quad n = m \ . \end{cases}$$

By means of these relations it finally can be derived for A_0, B_0, A_n and B_n:

$$\frac{A_0}{\hat{x}_2} = A_0' = 2 \frac{\sinh(m_0 h) - \sinh\{m_0(h-D)\}}{m_0 h + \sinh(m_0 h) \cosh(m_0 h)} \quad , \tag{3.13a}$$

$$\frac{A_n}{\hat{x}_2} = A_n' = 2 \frac{\sin(m_n h) - \sin\{m_n(h-D)\}}{m_n h + \sin(m_n h) \cos(m_n h)} \quad , \tag{3.13b}$$

$$\frac{B_0 \omega}{\hat{v}_b} = B_0' = \frac{2 \sinh\{m_0(h-D)\}}{m_0 h + \sinh(m_0 h) \cosh(m_0 h)} \quad , \tag{3.14a}$$

$$\frac{B_n \omega}{\hat{v}_b} = B_n' = \frac{2 \sin\{m_n(h-D)\}}{m_n h + \sin(m_n h) \cos(m_n h)} \quad , \tag{3.14b}$$

respectively; the superscript ' indicates that the quantity concerned is dimensionless.

The velocity potential $\Phi(x_2,x_3,t)$ now has been fully defined: $\Phi(x_2,x_3,t)$ as formulated by (3.11) satisfies the Laplace equation (3.2) plus the set of boundary conditions (3.4), (3.5), (3.6) and (3.7) and the supplementary condition (3.8); the respective real coefficients (i.e. constants of integration) A_0, A_n, B_0 and B_n figuring in (3.11) are represented by ($3.13^{a,b}$) and ($3.14^{a,b}$), the wave numbers m_0 and m_n are given by (3.12^a) and (3.12^b), respectively.

Appendix E: Determination of $a_{22}(\omega), b_{22}(\omega)$ using a long-wave approximation for the motion of the water in case of unrestricted horizontal dimensions

This appendix presents a simplified approach to determine the hydrodynamic sway coefficients for a schematized ship on shallow water with unrestricted horizontal dimensions.

Use is made of a long-wave approximation for the motion of the water, in which -even in case of a small keel clearance- no account is taken of the circulation of water around 'bow' and 'stern'. Therefore, in addition to the fact that this approach is subject to the restrictions of the long-wave theory, it has to be considered as basically one-dimensional. Application of the long-wave approximation further implies that the expressions for $a_{22}(\omega)$, $b_{22}(\omega)$ to be derived only hold true for low (circular) frequencies.
The hydrodynamic sway coefficients are determined for the same (schematized) ship and for the same shallow water depths as in Section 3. The assumptions and simplifications as stated in Section 1.3.4 do also apply in this appendix.

The schematized ship is supposed to have merely a lateral velocity (i.e. in the sway direction) $\dot{x}_2(t)$. Let the heights of the generated long waves in region c (i.e. on port-side) and in region a (i.e. on starboard-side) be η_c and η_a, respectively (see fig. E.1); η_a and η_c are assumed to be very small with respect to the water depth: $\eta_a \ll h$, $\eta_c \ll h$.
Neglecting friction effects in the regions a and c and assuming that the waves propagate without distortion, the velocities of propagation can be represented by $c_w = \sqrt{gh}$. In conformity with the long-wave theory the (horizontal) fluid velocities under the long waves in region a and region c (i.e. v_a and v_c, respectively) are supposed to be uniformly distributed in the vertical plane and parallel to $\dot{x}_2$; this also holds good at a (very) short distance from the ship's wall. The velocities in the undisturbed fluid region are equal to zero. Further it is supposed that the velocities in the underkeel clearance, v_b, are horizontal and parallel with $\dot{x}_2$, and that they are distributed uniformly over the height.

From the long-wave theory it can be derived that in the fluid regions a and c the following respective expressions hold good:

$$\left.\begin{aligned} -\eta_a c_w + v_a(h - \eta_a) &= 0 \quad , \\ v_c(h + \eta_c) - \eta_c c_w &= 0 \quad . \end{aligned}\right\}$$

As both $\eta_a \ll h$ and $\eta_c \ll h$, v_a and v_c can be written as:

$$v_a = \frac{g}{c_w}\eta_a \quad , \quad v_c = \frac{g}{c_w}\eta_c \quad . \tag{E.1}$$

Applying the law of conservation of mass on starboard-side, c.q. port-side of the ship, one obtains:

$$\left.\begin{aligned} v_a(h - \eta_a) &= v_b(h - D) + \dot{x}_2(D - \eta_a) \quad , \\ v_c(h + \eta_c) &= v_b(h - D) + \dot{x}_2(D + \eta_c) \quad . \end{aligned}\right\}$$

It is assumed that the water depth h and the draught of the ship D are of the same order of magnitude; therefore, both $\eta_a \ll D$ and $\eta_c \ll D$, so that the above expressions become:

$$\left.\begin{aligned} v_a h &= v_b(h - D) + \dot{x}_2 D \quad , \\ v_c h &= v_b(h - D) + \dot{x}_2 D \quad , \end{aligned}\right\} \tag{E.2}$$

respectively.

Application of the law of conservation of momentum to the mass of water underneath the ship yields (per unit length), incorporating laminar friction:

$$\rho B(h - D)\dot{v}_b = -\rho g(h - D)(\eta_a + \eta_c) - 2\gamma B(v_b - \tfrac{1}{2}\dot{x}_2) \quad . \tag{E.3}$$

Let the velocity $\dot{x}_2$ be the result of an external force $f_2(t)$ acting upon the schematized ship in the sway direction. The equation of motion of the ship then can be represented by

$$\rho LBD\ddot{x}_2 = -\rho g(D - \eta_a)L(\eta_a + \eta_c) - \tfrac{1}{2}\rho gL(\eta_a + \eta_c)^2 + \gamma BL(v_b - \dot{x}_2) + f_2(t) \quad ,$$

or,

$$\rho LBD\ddot{x}_2 = -\rho gDL(\eta_a + \eta_c) + \gamma BL(v_b - \dot{x}_2) + f_2(t) \quad . \tag{E.4}$$

Elimination of v_a and v_c from (E.1) and (E.2) yields:

$$\eta_a + \eta_c = \frac{2}{c_w}\{v_b(h - D) + \dot{x}_2 D\} \quad .$$

Substituting this expression into (E.3) and (E.4) one obtains

$$\dot{v}_b + \frac{2g(h-D)}{Bc_w} v_b + \frac{2gD}{Bc_w} \dot{x}_2 + \frac{2\gamma}{\rho(h-D)} (v_b - \frac{1}{2} \dot{x}_2) = 0 \tag{E.5}$$

and

$$\ddot{x}_2 + \frac{2g(h-D)}{Bc_w} v_b + \frac{2gD}{Bc_w} \dot{x}_2 - \frac{\gamma}{\rho D} (v_b - \dot{x}_2) = \frac{1}{\rho LBD} f_2(t) \quad , \tag{E.6}$$

respectively. Confining oneself to the pure sway mode of motion as represented by

$$\{m_{22} + a_{22}(\omega)\}\ddot{x}_2 + b_{22}(\omega)\dot{x}_2 = f_2(t) \quad , \tag{3.29^b}$$

---

where $m_{22} = \rho LBD$,
it can be stated that again $x_2(t)$, $v_b(t)$ and γ have the respective form:

$$x_2(t) = -i\hat{x}_2 e^{i\omega t} \quad , \tag{3.9}$$

$$v_b(t) = \hat{v}_b e^{i(\omega t - \theta)} \quad , \tag{3.10}$$

$$\gamma = \rho\sqrt{\nu\omega} \quad . \tag{3.20^a}$$

By substitution of these expressions for $x_2(t)$, $v_b(t)$ and γ into (E.5) and subsequently equating the real and imaginary parts it can be derived

$$\tan(\theta) = \frac{C_1}{C_2} \tag{E.7}$$

and

$$\frac{\hat{v}_b}{\omega\hat{x}_2} = \frac{C_3}{\sqrt{C_1^2 + C_2^2}} \quad , \tag{E.8}$$

where

$$C_1 = \frac{\omega B h}{2 D c_w} \quad , \tag{E.9^a}$$

$$C_2 = \frac{h-D}{D} + \frac{B\sqrt{\nu\omega}}{c_w D}\,\frac{h}{h-D} \quad , \tag{E.9^b}$$

$$C_3 = -1 + \frac{B\sqrt{\nu\omega}}{2 c_w D}\,\frac{h}{h-D} \quad . \tag{E.9^c}$$

Elimination of $f_2(t)$ from (E.6) and (3.29^b) yields:

$$a_{22}(\omega)\ddot{x}_2 + b_{22}(\omega)\dot{x}_2 = \rho LBD\left\{\frac{2g(h-D)}{Bc_w}\, v_b + \frac{2gD}{Bc_w}\,\dot{x}_2 - \frac{\gamma}{\rho D}(v_b - \dot{x}_2)\right\} \quad . \tag{E.10}$$

Substituting $x_2(t)$, $v_b(t)$ and γ according to (3.9), (3.10) and (3.20^a), respectively, into (E.10) and making use of (E.7) and (E.8) it is obtained in a similar way as above:

$$a_{22}(\omega) = \rho LBD\,\frac{h}{D}\,\frac{C_3^2 C_4}{C_1^2 + C_2^2} \quad , \tag{E.11^a}$$

$$b_{22}(\omega) = \rho LBD\,\frac{2c_w}{B}\left(1 + C_3 C_4 - \frac{C_2 C_3^2 C_4}{C_1^2 + C_2^2}\right) \quad , \tag{E.12^a}$$

where

$$C_4 = \frac{h-D}{h} \quad . \tag{E.9^d}$$

For $\omega \to 0$ the respective sway added-mass and sway damping force coefficient become

$$a_{22}(0) = \rho LBD\,\frac{D}{h-D} \quad , \tag{E.13}$$

$$b_{22}(0) = 0 \quad ; \tag{E.14}$$

in these expressions the friction in the keel clearance does not play a part. Neglecting the underkeel friction (i.e. $\nu = 0$) $a_{22}(\omega)$ and $b_{22}(\omega)$ take the form

$$a_{22}(\omega) = \rho LBD\,\frac{h-D}{D}\,\frac{4gD^2}{\omega^2 B^2 h + 4g(h-D)^2} \quad , \tag{E.11^b}$$

and

$$b_{22}(\omega) = \rho LBD \frac{2c_w}{B} \frac{\omega^2 B^2 D}{\omega^2 B^2 h + 4g(h-D)^2} \quad . \tag{E.12b}$$

In case of zero keel clearance (i.e. $h \to D$) the underkeel friction effect can be left out of consideration. The hydrodynamic sway coefficients then are derived to be:

$$a_{22}(\omega)\Big|_{h\to D} = 0 \quad , \tag{E.15}$$

$$b_{22}(\omega)\Big|_{h\to D} = 2\rho Lhc_w \quad . \tag{E.16}$$

At the risk of labouring the obvious it is noted yet that there can only be question of a pure long-wave approximation if $\omega \simeq 0$; formally the expressions derived above apply for $\omega << 2\pi\sqrt{g/h}$.

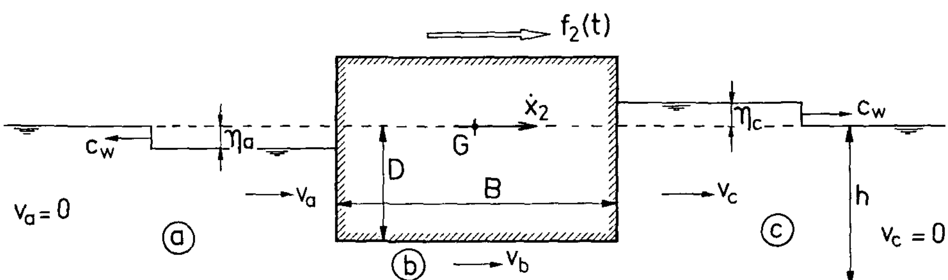

Fig. E.1 - Definition sketch for sway motion on horizontally unrestricted water (long-wave approximation)

Appendix F: Complementary remarks on $a_{ii}(\omega), b_{ii}(\omega)$ for $i = 1,2,6$ in case of horizontally unrestricted water

F.1. Sway added-mass at zero frequency

For $\omega = 0$ the values of $a_{22}(\omega)$ from Section 3.2.1.5 and Appendix E, respectively, can be compared with those from ref. [103]. In all three of the cases use is made of a (two-dimensional) strip approach. The values are presented in dimensionless form in the table below. The agreement between the respective results is considered to be satisfactory.

$\frac{a_{22}(0)}{\rho LBD}$	ref. [103]	Sect. 3.2.1.5	App. E	
	2-D pot. theory	2-D pot. theory	1-D long-w. appr.	
$\frac{h}{D} = 1.333$	3.968	3.955	2.992	$\frac{L}{D} = 16.25$
$\frac{h}{D} = 1.167$	6.850	7.087	5.972	$\frac{B}{D} = 2.50$

F.2. Sway added-mass at high frequencies

Concerning the (special) problem of determining the sway added-mass at high frequencies work has been done with regard to its relevance to ship vibrations. Reference is made to ref. [88] where an excellent review is given of published data. In ref. [89] experimentally sway added-masses are determined for $\omega \to \infty$ by means of an electric analogon, taking into account the influence of a restricted water depth; the results apply to the case of zero forward and transverse speed on water with unrestricted horizontal dimensions; the sway added-masses are given per unit length for ships with rectangular cross-sections. On basis of the data from ref. [89] the following (dimensionless) added mass for the swaying motion at high frequencies is predicted:

$$\frac{a_{22}(\omega)}{\rho LBD} \simeq 0.35 \quad \text{for } \omega \to \infty \quad . \tag{F.1}$$

For comparison the following table with data from Section 3.2.1.5 is provided:

$\frac{h}{D}$	$\frac{a_{22}(\infty)}{\rho LBD}$
1.333	0.356
1.167	0.377
1.000	0.433

The agreement of these data with those from ref. [89] is satisfactory.

F.3. Hydrodynamic damping force coefficients at high frequencies

Generally it holds good that the hydrodynamic coefficient of the damping force approaches asymptotically to zero with increasing frequency. To investigate this asymptotic behaviour for $\omega \to \infty$ a two-dimensional approach may be used.

The relation between the damping coefficient and the amplitude of the radiated waves at infinity in case of a ship on water with unrestricted horizontal dimensions at zero forward and transverse speed is given in ref. [90] to be (per unit length):

$$b''_{ii}(\omega) = \frac{\rho g^2}{\omega^3} R_i^2(\omega) \quad , \tag{F.2}$$

where $R_i(\omega)$ = ratio of the amplitude of the radiated waves at infinity to the amplitude of the (ship) motion in the i-direction = wave making coefficient for (ship) motion in the i-direction;

the superscript $''$ indicates that the quantity concerned is given per unit length.

For shallow water the bottom has to be horizontal.

When the ship is approximated by a vertical barrier extending to the (sea) bottom (thus ignoring the keel clearance, which is permissible if the wave length is small compared with the draught of the ship), the behaviour of the damping coefficients for horizontal motions at high frequencies can be determined from refs. [96] and [104]. For the surge and sway modes of motion the ship then may be regarded as a piston-type wave maker. According to refs. [96] and [104], respectively, the wave-making coefficient has the form:

$$R_i(\omega) = \frac{2\,\sinh^2(m_0h)}{m_0h + \sinh(m_0h)\,\cosh(m_0h)} = \frac{2\{\cosh(2m_0h) - 1\}}{2m_0h + \sinh(2m_0h)} \quad , \quad i = 1,2, \tag{F.3}$$

where m_0 is given according to (3.12^c). At high frequencies it holds good that $m_0 = \omega^2/g$. For the surge and sway modes of motion the wave-making coefficient approaches to a constant value when $\omega \to \infty$:

$$R_i(\omega) = 2 \quad , \quad \omega \to \infty \quad , \quad i = 1,2 \quad . \tag{F.4}$$

Consequently, for high frequencies the surge and sway damping force coefficients can be approximated by (per unit length):

$$b''_{ii}(\omega) = \frac{4\rho g^2}{\omega^3} \quad , \quad \omega \to \infty \quad , \quad i = 1,2 \quad . \tag{F.5}$$

On account of the fact that

$$b_{ii}(\omega) = L\,b''_{ii}(\omega) \quad , \tag{F.6}$$

the sway damping force coefficient becomes for high frequencies:

$$b_{22}(\omega) = \frac{4\rho g^2 L}{\omega^3} \quad , \quad \omega \to \infty \quad . \tag{F.7}$$

According to (3.34^b) it holds good for the yaw damping moment coefficient $b_{66}(\omega)$ that particularly at high frequencies:

$$b_{66}(\omega) = \frac{1}{12}L^2 b_{22}(\omega) \quad , \quad \omega \to \infty \quad . \tag{3.34^b}$$

In general form the hydrodynamic damping force coefficients for horizontal motions at high frequencies now can be represented by:

$$b_{ii}(\omega) = \frac{q_i}{\omega^3} \quad , \quad \omega \to \infty \quad , \quad i = 1,2,6 \quad , \tag{F.8}$$

where q_i = constant in approximative expression for $b_{ii}(\omega)$ in case $\omega \to \infty$; q_i is dependent on the mode of motion, but independent of the water depth. If the hydrodynamic damping force coefficients for horizontal motions are known from $\omega = 0$ to $\omega = \omega_1$ -where ω_1 represents a certain (circular) frequency-, then it is possible to choose the values of the constant q_i such that the high-frequency approximations correspond with the known parts of the damping curves.

According to (3.43) the sway damping force coefficient in case of zero keel clearance is:

$$b_{22}(\omega)\Big|_{h\to D} = 2\rho L \frac{\omega}{m_0^2} \frac{2\sinh^2(m_0 h)}{m_0 h + \sinh(m_0 h)\cosh(m_0 h)} \quad . \tag{3.43}$$

For high frequencies this expression changes into:

$$b_{22}(\omega)\Big|_{h\to D} = \frac{4\rho g^2 L}{\omega^3} \quad , \quad \omega \to \infty \quad , \tag{F.9}$$

which expression is identical to (F.7).

For high frequencies the sway damping force coefficient in dimensionless form is:

$$\frac{b_{22}}{\rho LBD}\sqrt{\frac{B}{g}} = \frac{4g^2}{BD}\sqrt{\frac{B}{g}}\ \frac{1}{\omega^3} \quad , \quad \omega \to \infty \quad . \tag{F.10}$$

In Section 3.2.3.1 values for $b_{22}(\rho LBD)^{-1}(B/g)^{1/2}$ are presented as function of $\omega(B/g)^{1/2}$ with h/D as parameter. From these it appears that:

- in case of large values of $\omega(B/g)^{1/2}$ (say $\omega(B/g)^{1/2} > 3.9$) $b_{22}(\rho LBD)^{-1}(B/g)^{1/2}$ becomes independent of h/D, and
- for $\omega(B/g)^{1/2} > 2.8$, independent of h/D, (F.10) makes a good approximation for the (dimensionless) sway damping force coefficient.

F.4. Hydrodynamic yaw coefficients

From the experimental results as presented in Section 3.2.3.2 it appears that the added mass-moment of inertia for the yawing motion is not very dependent on the frequency, at least for the frequency range considered in the experiments (i.e. for low values of ω). In other words, the influence of the free surface of the fluid seems to play a minor part. Also the influence of the water depth is not very important. One thing and another seems to justify an approximation of the added mass-moment of inertia for the yawing motion -certainly for lower frequencies- by means of the relevant value for 'infinite' water. The concept of 'infinite' water has to be understood as follows: the fluid domain has unrestricted horizontal dimensions, there is neither in-

fluence of a bottom, nor of a free surface (no waves). This implies that $a_{66}(\omega)$ = constant and $b_{66}(\omega) = 0$.
In the following table expressions are given for the added mass-moment of inertia per unit length (= a''_{66}) in case of three elementary forms:

		a''_{66}	reference
I	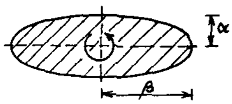	$\frac{1}{8}\pi\rho(\alpha^2-\beta^2)^2$	see ref. [98]
II	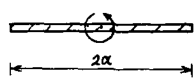	$\frac{1}{8}\pi\rho\alpha^4$	see ref. [98]
III	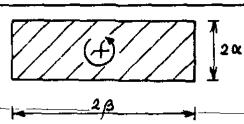	coeff. $*$ $\pi\rho\beta^4$ coeff. = $f(\frac{\alpha}{\beta})$	see ref. [105]

Application of these respective expressions for a''_{66} to the schematized ship (model) as used yields successively:

	I, II, III applied to schematized ship					
	α	β	coeff.	a''_{66} kg m	$a_{66} = a''_{66} * D$ kg m^2	$\frac{a_{66}}{\frac{1}{12}L^2\rho LBD}$
I	$\frac{1}{2}B$	$\frac{1}{2}L$	--	826.74	123.93	1.823
II	$\frac{1}{2}L$	--	--	867.40	130.02	1.912
III	$\frac{1}{2}B$	$\frac{1}{2}L$	$\frac{\alpha}{\beta} = \frac{B}{L} = 0.154$ coeff. $\simeq$ 0.149	1033.94	154.99	2.280

In case of a ship harmonically oscillating on shallow water the influence of the (three-dimensional) end effects (i.e. the circulation of water around bow and stern) decreases with increasing frequency. In behalf of the determination of $a_{66}(\omega)$ and $b_{66}(\omega)$ then use can be made of the (two-dimensional) strip theory, i.e.:

$$a_{66}(\omega) = \frac{1}{12}L^2 a_{22}(\omega) \quad , \qquad (3.34^a)$$

and

$$b_{66}(\omega) = \frac{1}{12}L^2 b_{22}(\omega) \quad , \qquad (3.34^b)$$

for the higher frequencies.

To close this appendix -for the sake of completeness- three more references concerning hydrodynamic coefficients have to be mentioned: ref. [106] deals with an analogue procedure for the determination of the virtual mass, in ref. [107] the viscosity of the fluid is taken into account in case of an axially oscillating spheroid and ref. [108] gives a review of added masses and fluid inertial forces.

Appendix G: Numerical evaluation of the i.r.f. $k_{ii}(t)$ for i = 2,6

On account of Section 2.5.2 and (2.67) the expression to be used for the numerical calculation of $k_{ii}(t)$ reads as:

$$\left.\begin{aligned} k_{ii}(t) &= \frac{2}{\pi}\int_0^\infty \mathrm{Re}\left[K_{ii}(\omega)\right]\cos(\omega t)d\omega \quad \text{for} \quad t > 0 \quad , \\ k_{ii}(0) &= \frac{1}{2}\, k_{ii}(0^+) \quad , \\ k_{ii}(t) &\equiv 0 \quad \text{for} \quad t < 0 \quad , \end{aligned}\right\} \tag{G.1}$$

where according to (2.66)

$$\mathrm{Re}\left[K_{ii}(\omega)\right] = \mathrm{Re}\left[H_{ii}(i\omega)\right] + \pi\alpha_{ii}\delta(\omega) \tag{G.2}$$

with -see (2.64)-

$$\mathrm{Re}\left[H_{ii}(i\omega)\right] = \frac{b_{ii}(\omega)}{\{m_{ii} + a_{ii}(\omega)\}^2\omega^2 + b_{ii}^2(\omega)} \tag{G.3}$$

and

$$\alpha_{ii} = k_{ii}(\infty) = \frac{1}{m_{ii} + a_{ii}(0)} \quad . \tag{2.65}$$

Using (G.2) and (2.65), (G.1) can be put into the form:

$$\left.\begin{aligned} k_{ii}(t) &= k_{ii}(\infty) + \frac{2}{\pi}\int_0^\infty \mathrm{Re}\left[H_{ii}(i\omega)\right]\cos(\omega t)d\omega \quad \text{for} \quad t > 0 \quad , \\ k_{ii}(0) &= \frac{1}{2}\, k_{ii}(0^+) \quad , \\ k_{ii}(t) &\equiv 0 \quad \text{for} \quad t < 0 \quad . \end{aligned}\right\} \tag{G.4^{a,b,c}}$$

Suppose now that the hydrodynamic coefficients $a_{ii}(\omega)$ and $b_{ii}(\omega)$ are known (by calculation and/or measurements) from $\omega = 0$ to $\omega = \omega_M$. (G.4^a) then can be written as:

$$k_{ii}(t) = k_{ii}(\infty) + \frac{2}{\pi}\int_0^{\omega_M} \mathrm{Re}\left[H_{ii}(i\omega)\right]\cos(\omega t)d\omega + \frac{2}{\pi}\int_{\omega_M}^{\infty} \mathrm{Re}\left[H_{ii}(i\omega)\right]\cos(\omega t)d\omega \quad . \tag{G.5}$$

Since along the closed interval $[0, \omega_M]$ $a_{ii}(\omega)$ and $b_{ii}(\omega)$ -and consequently $\mathrm{Re}[H_{ii}(i\omega)]$- are known in discretizised form, the first integral in (G.5) can be solved numerically. The solution of this integral can be represented by:

$$\int_0^{\omega_M} \mathrm{Re}\left[H_{ii}(i\omega)\right]\cos(\omega t)d\omega = I_M(t) + R_M(t) \quad , \tag{G.6}$$

where $I_M(t)$ = result of numerical integration along the closed interval $[0, \omega_M]$,

$R_M(t)$ = discretization error (i.e. process error) in consequence of the numerical process of integration along $[0, \omega_M]$.

Although for high circular frequencies $a_{ii}(\omega)$ might be equated to $a_{ii}(\infty)$ = constant and an estimate of $b_{ii}(\omega)$ is available (see Appendix F), an analytical solution of the second integral in (G.5) is probably not possible because of the complicated form of its integrand: only a rough estimate can be made. Therefore $I_M(t)$ has to be used as approximation for the integral in (G.4^a). On account of the behaviour of $a_{ii}(\omega)$ and $b_{ii}(\omega)$ one obtains by majorating the second integral in (G.5):

$$\left| \int_{\omega_M}^{\infty} \mathrm{Re}\left[H_{ii}(i\omega)\right]\cos(\omega t)d\omega \right| < \frac{b_{ii}(\omega_M)}{\{m_{ii} + a_{ii}(\omega_M)\}^2\omega_M^2} \int_{-\frac{\pi}{2t}}^{+\frac{\pi}{2t}} \cos(\omega t)d\omega =$$

$$= \frac{b_{ii}(\omega_M)}{\{m_{ii} + a_{ii}(\omega_M)\}^2\omega_M^2}\,\frac{2}{t} \quad ; \tag{G.7}$$

this expression can be regarded as an estimate for the error which arises by truncating the (numerical) process of integration (i.e. the truncation error). To provide that the result of the numerical calculation of the first integral in (G.5) -i.e. $I_M(t)$- represents a sufficiently accurate and reliable solution for the integral in (G.4^a), it can be stated that the following condition must be fulfilled:

$$\frac{2}{\pi}\left[R_M(t) + \frac{b_{ii}(\omega_M)}{\{m_{ii} + a_{ii}(\omega_M)\}^2\omega_M^2}\,\frac{2}{t}\right] \ll \left\{k_{ii}(\infty) + \frac{2}{\pi} I_M(t)\right\} \quad . \tag{G.8}$$

For convenience' sake in the following $\mathrm{Re}[H_{ii}(i\omega)]$ is represented by the general form:

$$f(\omega) = \mathrm{Re}[H_{ii}(i\omega)] \quad .$$

Suppose that $a_{ii}(\omega)$ and $b_{ii}(\omega)$ -and therefore $f(\omega)$- are given in a discretizised form at the abscissas

$$\omega = \omega_0, \omega_1, \cdots\cdots, \omega_M \quad ,$$

with successive intervals

$$(\Delta\omega)_n = \omega_n - \omega_{n-1} = \omega_{n+1} - \omega_n \quad , \quad n = 1,3,5,\cdots\cdot,M-1 \quad ,$$

where the subscript n indicates a running index representing a real, positive, odd integer, and the subscript M represents a real, positive, even integer. Then (G.6) can be written as:

$$I_M(t) + R_M(t) = \int_0^{\omega_M} f(\omega)\cos(\omega t)d\omega = \sum_{n=1,3,\cdots}^{M-1} \int_{\omega_{n-1}}^{\omega_{n+1}} f(\omega)\cos(\omega t)d\omega \quad .$$

Let for $\omega = \omega_{n-1}, \omega_n, \omega_{n+1}$ the values of $f(\omega)$ be represented by f_{n-1}, f_n and f_{n+1}, respectively.
Applying the Lagrange three-point interpolation formula for equally spaced abscissas on the closed interval $[\omega_{n-1}, \omega_{n+1}]$, $f(\omega)$ can be approximated by (see fig. G.1 and ref. [109]):

$$f(\omega)\Big|_{n-1,n,n+1} \simeq y_{n-1,n,n+1}(\omega) = a_n\omega^2 + b_n\omega + c_n \quad ,$$

$$\text{where} \quad a_n = \frac{f_{n-1} - 2f_n + f_{n+1}}{2\{(\Delta\omega)_n\}^2} \quad ,$$

$$b_n = -2a_n\omega_n - \frac{f_{n-1} - f_{n+1}}{2(\Delta\omega)_n} \quad ,$$

$$c_n = a_n\omega_n^2 + \omega_n\frac{f_{n-1} - f_{n+1}}{2(\Delta\omega)_n} + f_n \quad .$$

The discretization error on the interval $[\omega_{n-1}, \omega_{n+1}]$ as a consequence of this approximation for $f(\omega)$ is (see ref. [109]):

$$E_{n-1,n,n+1}(\omega) = (\omega - \omega_{n-1})(\omega - \omega_n)(\omega - \omega_{n+1}) \frac{1}{3!} \frac{d^3 f(\xi)}{d\omega^3} \quad ,$$

with $\omega_{n-1} \leq \omega \leq \omega_{n+1}$, $\omega_{n-1} \leq \xi \leq \omega_{n+1}$.

On the interval $[\omega_{n-1}, \omega_{n+1}]$ $f(\omega)$ then can be written as:

$$f(\omega)\Big|_{n-1,n,n+1} = y_{n-1,n,n+1}(\omega) + E_{n-1,n,n+1}(\omega) \quad ,$$

from which it follows:

$$\int_{\omega_{n-1}}^{\omega_{n+1}} f(\omega)\cos(\omega t)d\omega = \int_{\omega_{n-1}}^{\omega_{n+1}} y_{n-1,n,n+1}(\omega)\cos(\omega t)d\omega +$$

$$+ \int_{\omega_{n-1}}^{\omega_{n+1}} E_{n-1,n,n+1}(\omega)\cos(\omega t)d\omega \quad .$$

$$\int_{\omega_{n-1}}^{\omega_{n+1}} y_{n-1,n,n+1}(\omega)\cos(\omega t)d\omega = \int_{\omega_{n-1}}^{\omega_{n+1}} (a_n\omega^2 + b_n\omega + c_n)\cos(\omega t)d\omega =$$

$$= \frac{1}{t^2}\{(2a_n\omega_{n+1} + b_n)\cos(\omega_{n+1}t) - (2a_n\omega_{n-1} + b_n)\cos(\omega_{n-1}t)\} +$$

$$+ \frac{1}{t}\{(f_{n+1} - a_n \frac{2}{t^2})\sin(\omega_{n+1}t) - (f_{n-1} - a_n \frac{2}{t^2})\sin(\omega_{n-1}t)\} \quad .$$

$$\int_{\omega_{n-1}}^{\omega_{n+1}} E_{n-1,n,n+1}(\omega)\cos(\omega t)d\omega =$$

$$= \int_{\omega_{n-1}}^{\omega_{n+1}} (\omega - \omega_{n-1})(\omega - \omega_n)(\omega - \omega_{n+1}) \frac{1}{3!} \frac{d^3 f(\xi)}{d\omega^3}\cos(\omega t)d\omega \quad ;$$

let $\left.\dfrac{d^3f(\xi)}{d\omega^3}\right|_{max}$ be the maximum value of $\dfrac{d^3f(\xi)}{d\omega^3}$ on $\left[\omega_{n-1}, \omega_{n+1}\right]$ and suppose it distributed uniformly at the same time; then it holds good:

$$\int_{\omega_{n-1}}^{\omega_{n+1}} E_{n-1,n,n+1}(\omega)\cos(\omega t)d\omega \leqq$$

$$\leqq \frac{1}{3!}\left.\frac{d^3f(\xi)}{d\omega^3}\right|_{max}\int_{\omega_{n-1}}^{\omega_{n+1}}(\omega-\omega_{n-1})(\omega-\omega_n)(\omega-\omega_{n+1})\cos(\omega t)d\omega \quad ,$$

with

$$\frac{1}{3!}\left.\frac{d^3f(\xi)}{d\omega^3}\right|_{max}\int_{\omega_{n-1}}^{\omega_{n+1}}(\omega-\omega_{n-1})(\omega-\omega_n)(\omega-\omega_{n+1})\cos(\omega t)d\omega =$$

$$= \frac{1}{t^2}\{\cos(\omega_{n+1}t)-\cos(\omega_{n-1}t)\}\left[2\{(\Delta\omega)_n\}^2-\frac{6}{t^2}\right]\frac{1}{3!}\left.\frac{d^3f(\xi)}{d\omega^3}\right|_{max} +$$

$$- 3(\Delta\omega)_n\frac{2}{t^3}\{\sin(\omega_{n+1}t)+\sin(\omega_{n-1}t)\}\frac{1}{3!}\left.\frac{d^3f(\xi)}{d\omega^3}\right|_{max} \quad .$$

For $I_M(t)$ and $R_M(t)$ now it can be written:

$$I_M(t) = \sum_{n=1,3,\cdots}^{M-1}\int_{\omega_{n-1}}^{\omega_{n+1}} y_{n-1,n,n+1}(\omega)\cos(\omega t)d\omega \quad , \tag{G.9}$$

$$R_M(t) \leqq \sum_{n=1,3,\cdots}^{M-1}\left|\frac{1}{3!}\left.\frac{d^3f(\xi)}{d\omega^3}\right|_{max}\int_{\omega_{n-1}}^{\omega_{n+1}}(\omega-\omega_{n-1})(\omega-\omega_n)(\omega-\omega_{n+1})\cos(\omega t)d\omega\right| \quad , \tag{G.10}$$

respectively. With respect to the evaluation of

$$\left.\frac{d^3f(\xi)}{d\omega^3}\right|_{max}$$

the following has to be remarked. In the numerical calculation this term was taken to be the maximum out of the values of:

$$\frac{d^3f(\omega)}{d\omega^3}$$

at the three respective abscissas $\omega = \omega_{n-1}, \omega_n, \omega_{n+1}$, calculated numerically by means of a five-point formula for equally spaced abscissas (see ref. [109]).

Since in $f(\omega) = \mathrm{Re}\left[H_{ii}(i\omega)\right]$ -with $\mathrm{Re}\left[H_{ii}(i\omega)\right]$ according to (G.3)- $a_{ii}(0)$ = constant $\neq 0$ and $b_{ii}(0) = 0$, $f(0)$ takes an indeterminate form. With (2.41) $f(0)$ can be approximated by:

$$f(0) = \mathrm{Re}\left[H_{ii}(0)\right] \simeq \lim_{\omega \to 0} \frac{b_{ii}^{(2)}\omega^2 + \ldots}{\{m_{ii} + a_{ii}(0) + a_{ii}^{(2)}\omega^2 + \ldots\}^2 \omega^2 + \{b_{ii}^{(2)}\omega^2 + \ldots\}^2} =$$

$$= \frac{b_{ii}^{(2)}}{\{m_{ii} + a_{ii}(0)\}^2} \quad .$$

Making use of the expressions derived above, now -for $t > 0$- the numerical calculation can be carried out: $k_{ii}(t)$ is calculated from:

$$k_{ii}(t) = \frac{1}{m_{ii} + a_{ii}(0)} + \frac{2}{\pi} I_M(t) \quad ,$$

with $I_M(t)$ according to (G.9), while the truncation error and the discretization error, except for the factor $\frac{2}{\pi}$, are estimated by means of the expressions (G.7) and (G.10), respectively.

It is obvious that the numerical procedure described above is not suited to calculate the value of $k_{ii}(t)$ at the time $t = 0$. At $t = 0$ for the numerical integration a Simpson routine (see ref. [109]) was applied along the same range of frequencies as used in the case with $t > 0$. A valuation could be made for the discretization error (see ref. [109]). It was not possible to give an estimate for the truncation error.

<u>Supplementary note</u>

The value of $k_{ii}(0^+)$ $(i = 2,6)$ as calculated above can be checked c.q. approximated in a rather simple way.

Suppose that the uncoupled motions of the schematized ship are described by the equation(s) of motion:

$$M_{ii}\ddot{x}_i(t) = f_i(t) \quad , \quad i = 1,2,\ldots,6 \quad ,$$

where $M_{ii} = m_{ii}$ + added mass(-moment of inertia), representing the 'mass effect'.

It is assumed that within a very short length of time the (hydrodynamic) damping of the ship-fluid system may be neglected. For $t < t_0$ there is a state of rest. At the point of time $t = t_0$ the ship is subjected to a unit pulse in the i-direction:

$$f_i(t) = \zeta_i\delta_i(t-t_0) \quad , \quad \zeta_i = 1 \quad , \quad t_0 > 0 \quad .$$

The equation(s) of motion then become(s):

$$M_{ii}\ddot{x}_i(t) = \delta_i(t-t_0) \quad .$$

Taking the Laplace transform of this expression one obtains:

$$M_{ii}\left[sL\{\dot{x}_i(t)\} - \dot{x}_i(0^+)\right] = e^{-t_0 s} \quad .$$

Since $\dot{x}_i(0^+) = 0$ this yields:

$$L\{\dot{x}_i(t)\} = \frac{1}{M_{ii}}\,\frac{1}{s}\,e^{-t_0 s} \quad .$$

According to (2.69) it holds good for uncoupled ship motions:

$$\dot{x}_i(t) = \int_{-\infty}^{t} f_i(\tau)\,k_{ii}(t-\tau)d\tau \quad , \quad i = 1,2,\ldots,6 \quad .$$

With $f_i(t) = \zeta_i\delta_i(t-t_0)$, $\zeta_i = 1$ it can be derived by taking the Laplace transform of this expression (see also Appendix B):

$$L\{\dot{x}_i(t)\} = L\{k_{ii}(t-t_0)\}$$

with $\dot{x}_2(t) = k_{ii}(t-t_0) = 0$ for $t < t_0$.
Therefore it can be written:

$$L\{k_{ii}(t-t_0)\} = \frac{1}{M_{ii}}\,\frac{1}{s}\,e^{-t_0 s} \quad ,$$

from which it follows by taking the inverse Laplace transform:

$$k_{ii}(t-t_0) = \frac{1}{M_{ii}} U(t-t_0) \quad .$$

Replacing $t-t_0$ by t the i.r.f. finally takes the form:

$$k_{ii}(t) = \frac{1}{M_{ii}} U(t) \quad .$$

As small lengths of time correspond with high (circular) frequencies, it applies:

$$M_{ii} = m_{ii} + a_{ii}(\infty) \quad ,$$

so that

$$k_{ii}(0^+) = \frac{1}{m_{ii} + a_{ii}(\infty)} \quad .$$

This expression can be used to check the values of $k_{ii}(0^+)$ as calculated above for the cases $i = 2$ and $i = 6$.

Concerning the values of $a_{22}(\infty)$ and $a_{66}(\infty) = \frac{1}{12}L^2 a_{22}(\infty)$ it is referred to Appendix F.

For comparison the values of $(m_{ii} + a_{ii}(\infty))^{-1}$ as well as the values of $k_{ii}(0^+)$ as calculated for the distinct cases are presented in dimensionless form in the table on the next page.

Generally the agreement between the respective results is considered to be satisfactory. The discrepancy between $(m_{ii} + a_{ii}(\infty))^{-1}$ and $k_{ii}(0^+)$ as calculated 'three-dimensionally' can be declared from the way in which the hydrodynamic coefficients $a_{ii}(\omega), b_{ii}(\omega)$ in the lower-frequency range were modified with respect to their original two-dimensional values, and from the fact that the two-dimensional values of $a_{ii}(\infty)$ were maintained.

	$\frac{\rho LBD}{m_{22}+a_{22}(\infty)}$	theor. (2-dim.); $\rho LBD\ k_{22}(0^+)$	theor. with modif. a_{22}, b_{22} (3-dim.); $\rho LBD\ k_{22}(0^+)$
$\frac{h}{D} = 1.333$	0.738	0.738	0.810
$\frac{h}{D} = 1.167$	0.726	0.726	0.790

	$\frac{m_{66}}{m_{66}+a_{66}(\infty)}$	theor. (2-dim.); $m_{66}k_{66}(0^+)$	theor. with modif. a_{66}, b_{66} (3-dim.); $m_{66}k_{66}(0^+)$
$\frac{h}{D} = 1.333$	0.678	0.678	0.784
$\frac{h}{D} = 1.167$	0.665	0.665	0.782

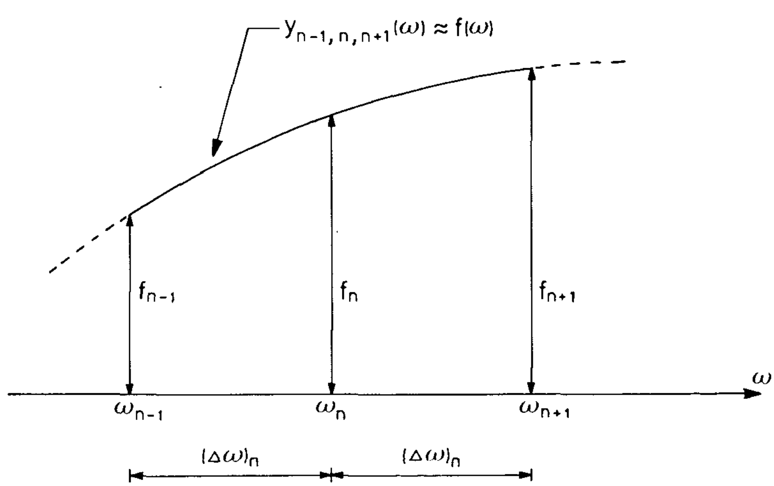

Fig. G.1 - Definition sketch for evaluation of integral (G.6)

Appendix H: Determination of $k_{22}(t)$ using a long-wave approximation for the motion of the water in case of unrestricted horizontal dimensions

In case of zero underkeel friction (E.5) and (E.6) take the form

$$\dot{v}_b + \frac{2g(h-D)}{Bc_w} v_b + \frac{2gD}{Bc_w} \dot{x}_2 = 0 \tag{H.1}$$

and

$$\ddot{x}_2 + \frac{2g(h-D)}{Bc_w} v_b + \frac{2gD}{Bc_w} \dot{x}_2 = \frac{1}{\rho LBD} f_2(t) \quad , \tag{H.2}$$

respectively. Elimination of v_b from these two expressions then yields:

$$\dddot{x}_2 + \frac{2c_w}{B} \ddot{x}_2 - \frac{1}{\rho LBD} \dot{f}_2(t) - \frac{1}{\rho LBD} \frac{2g(h-D)}{Bc_w} f_2(t) = 0 \quad ; \tag{H.3}$$

(H.3) has to be considered as the equation of motion in the sway direction of ship and water combined. It applies to ship motions considered from an initial state of rest as well as with respect to a given uniform motion (on which the transient $\dot{x}_2$ may be superimposed). It is obvious that this long-wave approximation for the motion of the water actually is based on a one-dimensional concept for flow and wave-radiation.

For $t < 0$ there is a state of rest. At the time $t = 0$ the ship is subjected to a unit pulse in the sway direction:

$$f_i(t) = \zeta_i \delta_i(t) \quad , \quad \zeta_i = 1 \quad , \quad i = 2 \quad .$$

In case of uncoupled motions it can be written for the sway motion of the linear ship-fluid system in the time domain (see (2.69)):

$$\dot{x}_i(t) = \int_{-\infty}^{t} f_i(\tau)\, k_{ii}(t-\tau)d\tau \quad , \quad i = 2 \quad .$$

From the last two equations it can be derived:

$$\dot{x}_2(t) = k_{22}(t) \quad ,$$

with $\dot{x}_2(t) = k_{22}(t) = 0$ for $t < 0$.

Now (H.1) and (H.2) can be written as:

$$\dot{v}_b + \frac{2g(h-D)}{Bc_w} v_b + \frac{2gD}{Bc_w} k_{22}(t) = 0$$

and

$$\dot{k}_{22}(t) + \frac{2g(h-D)}{Bc_w} v_b + \frac{2gD}{Bc_w} k_{22}(t) = \frac{1}{\rho LBD} \delta_2(t) \quad ,$$

respectively. Taking the Laplace transforms of these two expressions one obtains:

$$sL\{v_b(t)\} + \frac{2g(h-D)}{Bc_w} L\{v_b(t)\} + \frac{2gD}{Bc_w} L\{k_{22}(t)\} = 0$$

and

$$sL\{k_{22}(t)\} + \frac{2g(h-D)}{Bc_w} L\{v_b(t)\} + \frac{2gD}{Bc_w} L\{k_{22}(t)\} = \frac{1}{\rho LBD} \quad ;$$

elimination of $L\{v_b(t)\}$ yields:

$$L\{k_{22}(t)\} = \frac{1}{\rho LBD} \frac{1}{s} \{1 - \frac{2gD}{Bc_w} \frac{1}{s + \frac{2c_w}{B}}\} \quad .$$

By taking the inverse Laplace transform of this expression one obtains for the i.r.f. for the sway motion:

$$k_{22}(t) = (\alpha_0 + \beta_0 e^{-\gamma_0 t}) U(t) \quad , \tag{H.4}$$

where $\alpha_0 = \frac{1}{\rho LBD} \frac{h-D}{h}$, $\beta_0 = \frac{1}{\rho LBD} \frac{D}{h}$, $\gamma_0 = \frac{2c_w}{B}$.

The i.r.f. for the sway motion as calculated from (H.4), is presented in figs. 3.10 and 3.11 as a broken line.

Appendix I: Criterion for convergence of computational scheme in case of 'centric impact' to linear fender

For the case of a berthing operation in which $X_{1f} = -e_0 = 0$ the motion of the schematized ship represents a 'centric impact' (i.e. no rotation) and is given to be -according to ($3.59^{a,b}$)-:

$$\dot{X}_{1G}(t) = 0 \quad , \quad \dot{X}_{2G}(t) = v_A + \dot{x}_2(t) \quad , \tag{I.1}$$

with

$$\dot{x}_2(t) = \int_0^t f_2(\tau)\, k_{22}(t-\tau)d\tau \quad . \tag{3.51^b}$$

In (3.51^b) $f_2(t)$ is the reaction force of the linear fender; on account of (3.49), (3.50^a) and (3.60^a) $f_2(t)$ can be written as:

$$f_2(t) = -c_0 \Delta X_{2f}(t) \quad , \quad \Delta X_{2f}(t) \geqq 0 \quad . \tag{I.2}$$

Combination of (I.1), (3.51^b) and (I.2) yields for the motion of the ship:

$$\dot{X}_{2G}(t) = v_A - c_0 \int_0^t \Delta X_{2f}(\tau)\, k_{22}(t-\tau)d\tau \quad . \tag{I.3}$$

During the contact between ship and fender the displacement of the ship's centre of gravity $X_{2G}(t)$ equals the deflexion of the fender $\Delta X_{2f}(t)$.
For clearness' sake the following simplified notations are used:

$$\dot{X}_{2G}(t) = V(t) \quad , \quad \Delta X_{2f}(t) = \Delta Y(t) \quad , \quad k_{22}(t) = k(t) \quad ;$$

(I.3) then takes the form:

$$V(t) = v_A - c_0 \int_0^t \Delta Y(\tau)\, k(t-\tau)d\tau \quad . \tag{I.4}$$

The calculation of (I.4) is carried through according to the iteration procedure as described in Section 3.4.2, using equidistant time steps Δt. It is supposed that the contact between ship and fender has a length of time $N\Delta t$, where N is a real positive integer.

Let $t = n\Delta t$, $\tau = l\Delta t$,

with $n = 1,2,3,\ldots,N$, $l = 1,2,3,\ldots,n$;

then $V(t) = V(n\Delta t) = V_n$, $V_0 = v_A$,

$\Delta Y(\tau) = \Delta Y(l\Delta t) = \Delta Y_l$, $\Delta Y_0 = 0$, $\Delta Y_N = 0$,

$k(t-\tau) = k(n\Delta t - l\Delta t) = k\{(n-l)\Delta t\} = k_{n-l}$.

In these expressions is:

n,l = real positive integer -when used as subscript it represents a number of time steps Δt and indicates that the quantity concerned must be taken at the point of time $t = n\Delta t$, $\tau = l\Delta t$, respectively.

Suppose that the calculation of (I.4) has arrived to the point of time $t-\Delta t$; in the iteration procedure for point of time t the m^{th}-approximation of V_n then can be written as:

$$V_n^{(m)} = v_A - c_0 \sum_{l=1}^{n} \frac{1}{2}\Delta t(\Delta Y_{l-1}\, k_{n-l+1} + \Delta Y_l\, k_{n-l}) =$$

$$= v_A - c_0 \sum_{l=1}^{n-1} \frac{1}{2}\Delta t(\Delta Y_{l-1}\, k_{n-l+1} + \Delta Y_l\, k_{n-l}) - \frac{1}{2} c_0\Delta t(k_1\Delta Y_{n-1} + k_0\Delta Y_n) \quad ;$$

the superscript (m) indicates that in the iteration procedure the m^{th}-approximation is taken of the quantity concerned.

The approximation used for ΔY_n is:

$$\Delta Y_n = \Delta Y_{n-1} + \frac{1}{2}\Delta t\{V_n^{(m-1)} + V_{n-1}\} \quad .$$

Elimination of ΔY_n from the last two equations yields:

$$V_n^{(m)} = v_A - c_0 \sum_{l=1}^{n-1} \frac{1}{2}\Delta t(\Delta Y_{l-1}\, k_{n-l+1} + \Delta Y_l\, k_{n-l}) +$$

$$- \frac{1}{2} c_0\Delta t\ \Delta Y_{n-1}\ (k_0 + k_1) - \frac{1}{4} c_0\Delta t^2\ k_0\{V_n^{(m-1)} + V_{n-1}\} \quad .$$

In a completely analogous way it applies for the $(m-1)^{th}$-approximation of V_n:

$$V_n^{(m-1)} = v_A - c_0 \sum_{l=1}^{n-1} \frac{1}{2} \Delta t(\Delta Y_{l-1}\ k_{n-l+1} + \Delta Y_l\ k_{n-l}) +$$

$$- \frac{1}{2} c_0 \Delta t\ \Delta Y_{n-1}(k_0 + k_1) - \frac{1}{4} c_0 \Delta t^2\ k_0 \{V_n^{(m-2)} + V_{n-1}\} \quad .$$

Now it can be written:

$$V_n^{(m)} - V_n^{(m-1)} = - \frac{1}{4} c_0 \Delta t^2\ k_0 \{V_n^{(m-1)} - V_n^{(m-2)}\} \quad .$$

The iteration procedure for the calculation of V_n converges if:

$$\frac{\left|V_n^{(m)} - V_n^{(m-1)}\right|}{\left|V_n^{(m-1)} - V_n^{(m-2)}\right|} < 1 \quad , \quad \text{i.e. if} \quad \left|- \frac{1}{4} c_0 \Delta t^2\ k_0\right| < 0 \quad ;$$

in other words the computational scheme in case of a 'centric impact' to a linear fender is convergent if:

$$\Delta t < 2\sqrt{\frac{1}{c_0 k_0}}$$

with $k_0 = k_{22}(0^+)$.

Appendix J: Determination of berthing operations in case of an open berth using a long-wave approximation for the motion of the water

In case of an undamped, linear fender -using a long-wave approximation for the motion of the water- analytical expressions can be derived for the relevant quantities figuring in berthing to an open structure. If in the same situation the fender has a non-linear characteristic, generally, the relevant quantities can only be determined by means of a numerical approach.

For a plan and cross-section of the open berthing lay-out reference is made to fig. 3.14.

J.1. Centric impacts

In case of a centric impact the following relations apply:

$$\psi(t) = 0 \quad , \quad X_{2G}(t) = \Delta X_{2f}(t) \quad , \quad F_{2f}(t) = f(\Delta X_{2f}) \quad .$$

For an undamped, linear fender the reaction force in the fender then can be written as (see (3.60^a)):

$$F_{2f}(t) = \begin{cases} 0 & \text{for} \quad X_{2G}(t) < 0 \quad , \\ -c_0 X_{2G}(t) & \text{for} \quad X_{2G}(t) \geq 0 \quad . \end{cases} \tag{J.1}$$

The purely lateral motion of the schematized ship (i.e. in the sway direction) during its contact with the fender can be represented by (I.1):

$$\dot{X}_{1G}(t) = 0 \quad , \quad \dot{X}_{2G}(t) = v_A + \dot{x}_2(t) \tag{I.1}$$

with

$$\dot{x}_2(t) = \int_0^t f_2(\tau)\, k_{22}(t-\tau)d\tau \quad ; \tag{3.51^b}$$

in (3.51^b) $f_2(t) = F_{2f}(t)$, with $F_{2f}(t)$ according to (J.1); $k_{22}(t)$ is represented by (H.4):

$$k_{22}(t) = (\alpha_0 + \beta_0 e^{-\gamma_0 t})\, U(t) \quad , \tag{H.4}$$

where $\alpha_0 = \frac{1}{\rho LBD}\frac{h-D}{h}$, $\beta_0 = \frac{1}{\rho LBD}\frac{D}{h}$, $\gamma_0 = \frac{2c_w}{B}$.

Substitution of these respective expressions for $\dot{x}_2(t)$, $f_2(t)$ and $k_{22}(t)$ into (I.1) yields:

$$\dot{X}_{2G}(t) = v_A - c_0 \int_0^t X_{2G}(\tau)\{\alpha_0 + \beta_0 e^{-\gamma_0(t-\tau)}\}U(t-\tau)d\tau \quad . \tag{J.2}$$

The integro-differential equation (J.2) can be solved in two ways, which both, naturally, lead to the same result: in the first approach use is made of Laplace transforms, in the second approach (J.2) is transformed into an ordinary differential equation.

Taking the Laplace transform of (J.2) it can be derived, since $X_{2G}(0^+) = 0$:

$$L\{X_{2G}(t)\} = v_A \frac{s + p_0}{s^3 + p_0 s^2 + q_0 s + r_0} \quad , \quad Re[s] > 0 \quad , \tag{J.3}$$

where $p_0 = \gamma_0 = \frac{2c_w}{B}$,

$q_0 = (\alpha_0 + \beta_0)c_0 = \frac{c_0}{\rho LBD}$,

$r_0 = \alpha_0 \gamma_0 c_0 = \frac{2c_w}{B}\frac{c_0}{\rho LBD}\frac{h-D}{h}$.

As the denominator of the right-hand side of the above expression generally has three (different) roots, this right-hand side can be separated into a sum of partial fractions; $X_{2G}(t)$ then can be determined by taking the inverse Laplace transform of each summand separately.

By differentiating (J.2) two times with respect to t one obtains, using the expression for $k_{22}(t)$ according to (H.4):

$$\dddot{X}_{2G}(t) + p_0 \ddot{X}_{2G}(t) + q_0 \dot{X}_{2G}(t) + r_0 X_{2G}(t) = 0 \quad . \tag{J.4}$$

(J.4) is a linear homogeneous ordinary differential equation of the third order with constant real coefficients.

N.B. As could be expected -since $X_{2G}(0^+) = \ddot{X}_{2G}(0^+) = 0$ and $\dot{X}_{2G}(0^+) = v_A$-, solution of (J.4) by way of the Laplace-transform technique leads to an expression for $L\{X_{2G}(t)\}$ which is identical to (J.3).

Let the general solution of (J.4) be represented by

$$X_{2G}(t) = \sum_{m=1}^{3} C_m e^{w_m t} \quad ,$$

where m = subscript representing a real positive integer, $m = 1,2,3$,

C_m = constant of integration;

w_m represents the roots of the characteristic equation:

$$w^3 + p_0 w^2 + q_0 w + r_0 = 0 \quad . \tag{J.5}$$

Generally this equation has three different roots, either three real roots, or one real root plus two roots which are complex conjugated.

The quantity $X_{2G}(t)$ now is determined by solving (J.4); the initial conditions read as:

$$X_{2G}(0) = 0 \quad , \quad \dot{X}_{2G}(0) = v_A \quad , \quad \ddot{X}_{2G}(0) = 0 \quad . \tag{J.6}$$

(J.5) is a cubic equation with real coefficients; for the determination of its roots it is referred to ref. [110].

Let $w_m = \xi_m - \frac{p_0}{3} = \xi_m - \frac{1}{3}\frac{2c_w}{B}$;

ξ_m then satisfies the cubic equation with real coefficients:

$$\xi^3 + a_0\xi + b_0 = 0 \quad ,$$

where $a_0 = \frac{1}{3}(3q_0 - p_0^2) = \frac{1}{3}\left(3\frac{c_0}{\rho LBD} - \frac{4c_w^2}{B^2}\right)$,

$$b_0 = \frac{1}{27}(2p_0^3 - 9p_0q_0 + 27r_0) = \frac{2}{27}\frac{c_w}{B}\left(\frac{8c_w^2}{B^2} - 9\frac{c_0}{\rho LBD} + 27\frac{c_0}{\rho LBD}\frac{h-D}{h}\right) \quad .$$

On account of the values for ρ, g, L, B, D, h and c_0 as applied, it holds good that:

$$\frac{b_0^2}{4} + \frac{a_0^3}{27} > 0 \quad ,$$

or, in other words, there is one real root (ξ_1) and there are two roots (ξ_2 and ξ_3) which are complex conjugated; the roots ξ_1, ξ_2 and ξ_3 read as:

$$\xi_1 = A_c + B_c \quad , \qquad \xi_2 = -\frac{A_c + B_c}{2} + \frac{A_c - B_c}{2} i\sqrt{3} \quad ,$$

$$\xi_3 = -\frac{A_c + B_c}{2} - \frac{A_c - B_c}{2} i\sqrt{3} \quad ,$$

where $A_c = \sqrt[3]{-\frac{b_0}{2} + \sqrt{\frac{b_0^2}{4} + \frac{a_0^3}{27}}}$, $B_c = \sqrt[3]{-\frac{b_0}{2} - \sqrt{\frac{b_0^2}{4} + \frac{a_0^3}{27}}}$;

A_c and B_c are real constants.
The roots w_1, w_2 and w_3 of (J.5) now can be written as:

$$w_1 = P \quad , \qquad w_2 = R + iQ \quad , \qquad w_3 = R - iQ \quad ,$$

where $P = A_c + B_c - \frac{1}{3}\frac{2c_w}{B}$,

$$Q = \frac{A_c - B_c}{2}\sqrt{3} \quad ,$$

$$R = -\frac{A_c + B_c}{2} - \frac{1}{3}\frac{2c_w}{B} \quad .$$

By means of the initial conditions (J.6) it can be derived for the constants of integration C_1, C_2 and C_3:

$$C_1 = \frac{-v_A(w_2 + w_3)}{(w_1 - w_2)(w_1 - w_3)} = - v_A \frac{2R}{(P-R)^2 + Q^2} = -2v_A S \quad ,$$

$$C_2 = \frac{v_A(w_1 + w_3)}{(w_2 - w_3)(w_1 - w_2)} = v_A \frac{2QR - i(P^2 - R^2 + Q^2)}{2Q\{(P-R)^2 + Q^2\}} = v_A S - i v_A T \quad ,$$

and

$$C_3 = \frac{-v_A(w_1+w_2)}{(w_1-w_3)(w_2-w_3)} = v_A \frac{2QR + i(P^2-R^2+Q^2)}{2Q\{(P-R)^2+Q^2\}} = v_A S + i v_A T \quad ,$$

$$\text{where} \quad S = \frac{R}{(P-R)^2+Q^2} \quad , \quad T = S\,\frac{P^2-R^2+Q^2}{2QR} \quad .$$

For $X_{2G}(t)$ and $\dot{X}_{2G}(t)$ it then can be derived:

$$X_{2G}(t) = 2v_A\left[-Se^{Pt} + e^{Rt}\{S\cos(Qt) + T\sin(Qt)\}\right] \quad , \qquad (J.7^a)$$

$$\dot{X}_{2G}(t) = 2v_A\left[-PSe^{Pt} + e^{Rt}\{(RS+QT)\cos(Qt) - (QS-RT)\sin(Qt)\}\right] \quad , \qquad (J.7^b)$$

respectively.
The time histories of the fender forces as calculated from (J.1) and ($J.7^a$) for the respective spring rates c_0 and water depths h are presented in figs. 3.19 through 3.24 as broken lines.
In case of a fender which is damped and/or (non-)linear the real constant coefficients p_0, q_0 and r_0 generally become functions of $X_{2G}(t)$ and $\dot{X}_{2G}(t)$ (see (H.3)); an analytical solution of the berthing-ship problem then is only possible in very special cases. Making use of the i.r.f. for the sway motion, (H.4), in case of the non-linear fender the time history of the fender force is determined in the same way (i.e. numerically) as described in Sections 3.4.1 and 3.4.2; for the respective water depths h and lateral speeds of approach v_A the results are presented in figs. 3.25 through 3.28 as broken lines.

J.2. Eccentric impacts

In addition to the assumptions and simplifications as made in Section 1.3.4 the following is supposed to apply.

- The angle of rotation of the ship's longitudinal axis of symmetry around the OX_3-axis during the contact between ship and fender, i.e. $\psi(t)$, remains (very) small.
- The point of contact between ship and fender does not move along the ship's hull during the deflexion of the fender; i.e. $\overline{AG} = e_0$, when there is contact between ship and fender.

The two above assumptions are affirmed by the results presented in Section 3.4.4.3.

- Regarding the motion of the schematized ship in the sway direction, the hydrodynamic effects are taken into account by means of a long-wave approximation for the motion of the water.
- With respect to the rotation of the schematized ship in the horizontal plane, the hydrodynamic effects are only taken into account by means of a constant added mass-moment of inertia for the yawing motion; the (hydrodynamic) damping is neglected. For a justification of this assumption reference is made to Appendix F, Section F.4.

The resulting simplified approach then -just as in Section 3.4.1- amounts to a formulation related to an $ox_1x_2x_3$-co-ordinate system travelling along with the given initial velocity v_A and without rotation; this implies that the additional forces due to the actual rotation of the $ox_1x_2x_3$-system are neglected.

The equation of motion of ship and water combined for the x_2-direction reads as (see Appendix H):

$$\dddot{x}_2 + \frac{2c_w}{B}\ddot{x}_2 - \frac{1}{\rho LBD}\dot{f}_2(t) - \frac{1}{\rho LBD}\frac{2g(h-D)}{Bc_w}f_2(t) = 0 \quad . \tag{H.3}$$

Using the strip-theory concept, (H.3) can simply be transformed into a similar expression describing the rotation of the schematized ship in the horizontal plane, just by substituting.

$$x_2 = x_6 \quad , \quad \rho LBD = m_{66} \quad \text{with} \quad m_{66} = \frac{1}{12}L^2\, m_{22} \quad , \quad f_2(t) = f_6(t) \quad :$$

$$\dddot{x}_6 + \frac{2c_w}{B}\ddot{x}_6 - \frac{1}{m_{66}}\dot{f}_6(t) - \frac{1}{m_{66}}\frac{2g(h-D)}{Bc_w}f_6(t) = 0 \quad . \tag{J.8}$$

However, for reasons of simplicity, as equation of motion for the x_6-direction a choice is made for:

$$M_{66}\ddot{\psi} = f_6(t) \quad , \tag{J.9}$$

where $M_{66} = m_{66}$ + yaw added mass-moment of inertia;
M_{66} has to be considered as a constant.

As $\overline{AG} = e_0$ and $\psi(t)$ remains (very) small during the contact between ship and fender, the motion of the (schematized ship in the x_1-direction can be neglected, so that -after linearization of the terms containing $\psi(t)$- (3.59^{a,b}) can be written as:

$$\dot{X}_{1G}(t) \approx 0 \quad , \quad \dot{X}_{2G}(t) = v_A + \dot{x}_2(t) \quad . \tag{J.10}$$

The resulting force and moment, as acting in and about the ship's centre of gravity are:

$$\left.\begin{aligned} f_2(t) &= F_{2f}\cos(\psi) \quad , \\ f_6(t) &= -\overline{AG}\ F_{2f}\cos(\psi) \quad , \end{aligned}\right\} t \geqq 0 \quad . \tag{3.50^{a,b}}$$

For an undamped, linear fender the reaction force in the fender has the form:

$$F_{2f}(t) = \begin{cases} 0 & \text{for} \quad \Delta X_{2f}(t) < 0 \quad , \\ -c_0 \Delta X_{2f}(t) & \text{for} \quad \Delta X_{2f}(t) \geqq 0 \quad . \end{cases} \tag{3.60^{a}}$$

Combination of (H.3), (J.10), (3.50^{a}) and (3.60^{a}) and subsequent linearization of the terms containing $\psi(t)$ yields as equation of motion for the translation:

$$\dddot{X}_{2G}(t) + \frac{2c_w}{B}\ddot{X}_{2G}(t) + \frac{c_0}{\rho LBD}\frac{d}{dt}\Delta X_{2f}(t) + \frac{2g(h-D)}{Bc_w}\frac{c_0}{\rho LBD}\Delta X_{2f}(t) = 0 \quad . \tag{J.11}$$

Similarly from (J.9), (3.50^{b}) and (3.60^{a}) it can be derived for the equation of motion for the rotation:

$$M_{66}\ddot{\psi}(t) = e_0 c_0 \Delta X_{2f}(t) \quad . \tag{J.12}$$

The relation between $X_{2G}(t)$ and $\Delta X_{2f}(t)$ reads in linearized form as (see 3.48)):

$$X_{2G}(t) = \tfrac{1}{2}B + \Delta X_{2f}(t) + e_0\tan\{\psi(t)\} - \tfrac{1}{2}B\cos\{\psi(t)\} \quad .$$

From this expression it can be derived for small values of $\psi(t)$:

$$\left.\begin{array}{ll} X_{2G} = \Delta X_{2f} + e_0\psi \quad , & \dot{X}_{2G} = \frac{d}{dt}\Delta X_{2f} + e_0\dot{\psi} \quad , \\ \ddot{X}_{2G} = \frac{d^2}{dt^2}\Delta X_{2f} + e_0\ddot{\psi} \quad , & \dddot{X}_{2G} = \frac{d^3}{dt^3}\Delta X_{2f} + e_0\dddot{\psi} \quad . \end{array}\right\} \tag{J.13}$$

Elimination of X_{2G} from (J.11) and (J.13) yields:

$$\left[\frac{d^3}{dt^3} + \frac{2c_w}{B}\frac{d^2}{dt^2} + \frac{c_0}{\rho LBD}\frac{d}{dt} + \frac{2g(h-D)}{Bc_w}\frac{c_0}{\rho LBD}\right]\Delta X_{2f} + e_0\dddot{\psi} + \frac{2c_w}{B}e_0\ddot{\psi} = 0 \quad ;$$

eliminating ψ from this expression by means of (J.12) one obtains:

$$\left[\frac{d^3}{dt^3} + p_0\frac{d^2}{dt^2} + q_0\frac{d}{dt} + r_0\right]\Delta X_{2f} = 0 \quad , \tag{J.14}$$

where $p_0 = \frac{2c_w}{B} \quad , \quad q_0 = c_0\left(\frac{1}{\rho LBD} + \frac{e_0^2}{M_{66}}\right) \quad ,$

$$r_0 = c_0\,\frac{2c_w}{B}\left(\frac{h-D}{h}\,\frac{1}{\rho LBD} + \frac{e_0^2}{M_{66}}\right) \quad .$$

(J.14) is a linear homogeneous ordinary differential equation of the third order with constant real coefficients; its initial conditions are:

$$\Delta X_{2f}(0) = 0 \quad , \quad \left.\frac{d}{dt}\Delta X_{2f}(t)\right|_{t=0} = v_A \quad , \quad \left.\frac{d^2}{dt^2}\Delta X_{2f}(t)\right|_{t=0} = 0 \quad . \tag{J.15}$$

(J.14) has the same form as (J.4); the same holds for the initial conditions (J.15) and (J.6).

N.B. Starting from Appendix F, Section F.4, for the yaw added mass-moment of inertia a value is chosen which is two times the mass-moment of inertia of the ship around the Gz-axis; this implies that $M_{66} = 3m_{66}$.

On account of the values for ρ, g, L, B, D, h, m_{66}, e_0 and c_0 as applied, it holds good that:

$$\frac{b_0^2}{4} + \frac{a_0^3}{27} > 0 \quad ,$$

where $a_0 = \frac{1}{3}(3q_0 - p_0^2) = c_0\left(\frac{1}{\rho LBD} + \frac{e_0^2}{M_{66}}\right) - \frac{4c_w^2}{3B^2}$,

$$b_0 = \frac{1}{27}(2p_0^3 - 9p_0q_0 + 27r_0) =$$

$$= \frac{2}{27}\frac{c_w}{B}\left(\frac{8c_w^2}{B^2} - 9\frac{c_0}{\rho LBD} + 27\frac{c_0}{\rho LBD}\frac{h-D}{h} + 18c_0\frac{e_0^2}{M_{66}}\right) \quad ;$$

consequently the solution of (J.14) has the same form as that of (J.4). So,

$$\Delta X_{2f}(t) = 2v_A\left[-Se^{Pt} + e^{Rt}\{S\cos(Qt) + T\sin(Qt)\}\right] \quad , \tag{J.16}$$

where the basic formulae for P, Q, R, S and T are identical to those in Section J.1; the same holds for the quantities A_c, B_c, a_0, b_0 and p_0; only q_0 and r_0 have a different form. Elimination of $\Delta X_{2f}(t)$ from (J.12) and (J.16) yields:

$$\ddot{\psi}(t) = 2v_A\frac{e_0c_0}{M_{66}}\{-Se^{Pt} + Se^{Rt}\cos(Qt) + Te^{Rt}\sin(Qt)\} \quad . \tag{J.17}$$

The initial conditions of this ordinary differential equation of the second order are:

$$\psi(0) = 0 \quad , \quad \dot{\psi}(0) = 0 \quad . \tag{J.18}$$

Now $\psi(t)$ can be determined by direct integration of (J.17) with respect to time; the two constants of integration are eliminated by using the initial conditions (J.18). In doing so one obtains for $\psi(t)$:

$$\psi(t) = 2v_A\frac{e_0c_0}{M_{66}}\left[-\frac{S}{P^2}e^{Pt} + \frac{TR^2+2RSQ-TQ^2}{(R^2+Q^2)^2}e^{Rt}\sin(Qt) + \frac{SR^2-2TQR-SQ^2}{(R^2+Q^2)^2}e^{Rt}\cos(Qt) + \right.$$

$$\left. + \left(\frac{S}{P} - \frac{SR-TQ}{R^2+Q^2}\right)t + \left\{\frac{S}{P^2} - \frac{SR^2-2TQR-SQ^2}{(R^2+Q^2)^2}\right\}\right] \quad . \tag{J.19}$$

According to (J.13) $X_{2G}(t)$ reads as:

$$X_{2G}(t) = \Delta X_{2f}(t) + e_0\psi(t) \quad . \tag{J.20}$$

Since $\Delta X_{2f}(t)$ and $\psi(t)$ are given by (J.16) and (J.19), respectively, $X_{2G}(t)$ now can be determined.
The time histories of the fender forces, the angles of rotation and the translations of G as calculated from (J.16) and (3.60^a), (J.19) and (J.20), for the respective water depths h and values of e_0 are presented in figs. 3.31 through 3.38 as broken lines.

Appendix K: Hydrodynamic coefficients for sway motion near a vertical wall: specific cases

In some specific cases the hydrodynamic coefficients for pure swaying near a vertical wall can be written in a rather simple and direct form. The respective expressions are to be derived from (4.44) and (4.46) through ($4.49^{a,b}$) and presented below.

I - Zero friction in underkeel region: $\alpha_1 = 0$,
- zero horizontal velocity of fluid in quay clearance: $f_{u_a} = 0$ (i.e. strip theory);

$$\frac{a_{22}(\omega)}{\rho LBD} = -\frac{1}{3}A_0 + A_1 \frac{\omega^4 A_2 - \omega^2 A_3 + A_4}{\omega^4 A_5 + \omega^2 A_6 + A_7} , \qquad \text{(K.1)}$$

$$\frac{b_{22}(\omega)}{\rho LBD}\frac{c_w}{g} = \frac{D}{B}\frac{\omega^4 A_1^2}{\omega^4 A_5 + \omega^2 A_6 + A_7} , \qquad \text{(K.2)}$$

with $A_0 = \frac{1}{2} f_{w_a} \frac{D^2}{Bd_{sq}}$,

$$A_1 = 1 + \frac{1}{2} f_{w_a} \frac{Dh}{Bd_{sq}} \frac{h-D}{h} ,$$

$$A_2 = \frac{1}{2} f_{w_a} \frac{D^2}{Bd_{sq}} \left\{1 + f_{w_a} \frac{Dh}{Bd_{sq}} \frac{h-D}{h}\right\} ,$$

$$A_3 = \frac{c_w^2}{Bh}\frac{D}{d_{sq}}\left[1 - \frac{d_{sq}}{B}\frac{h-D}{h}\left\{1 - \frac{3}{2} f_{w_a} \frac{Dh}{d_{sq}^2}\right\}\right] ,$$

$$A_4 = \frac{c_w^2}{Bh}\frac{c_w^2}{Bd_{sq}}\frac{D}{d_{sq}}\frac{h-D}{h} ,$$

$$A_5 = \left\{1 + f_{w_a} \frac{Dh}{Bd_{sq}} \frac{h-D}{h}\right\}^2 ,$$

$$A_6 = \frac{h-D}{h}\frac{c_w^2}{B^2}\left[\frac{h-D}{h} - 2\frac{B}{d_{sq}}\left\{1 + f_{w_a} \frac{Dh}{Bd_{sq}} \frac{h-D}{h}\right\}\right] ,$$

$$A_7 = \left\{\frac{h-D}{h}\frac{c_w^2}{Bd_{sq}}\right\}^2 \quad ,$$

$$a_{22}(0) = \rho LBD\left\{\frac{D}{h-D} + \frac{1}{3} f_{w_a} \frac{D^2}{Bd_{sq}}\right\} \quad , \tag{4.48^b}$$

$$b_{22}(0) = 0 \quad , \tag{4.49^b}$$

$$a_{22}(\infty) = \frac{1}{12} f_{w_a} \rho LBD \frac{D^2}{Bd_{sq}} \left\{4 + f_{w_a} \frac{Dh}{Bd_{sq}} \frac{h-D}{h}\right\}\left\{1 + f_{w_a} \frac{Dh}{Bd_{sq}} \frac{h-D}{h}\right\}^{-1} \quad , \tag{K.3}$$

$$b_{22}(\infty) = \rho LBD \frac{g}{c_w} \frac{D}{B} \left\{1 + \frac{1}{2} f_{w_a} \frac{Dh}{Bd_{sq}} \frac{h-D}{h}\right\}^2\left\{1 + f_{w_a} \frac{Dh}{Bd_{sq}} \frac{h-D}{h}\right\}^{-2} \quad , \tag{K.4}$$

$$f_{w_a} = \left.\begin{array}{lll} 0 & : & \text{zero} \\ +1 & : & \text{non-zero} \end{array}\right\} \text{vertical acceleration of fluid in quay clearance.}$$

II - Zero friction in underkeel region: $\alpha_1 = 0$,
- zero vertical acceleration of fluid in quay clearance: $f_{w_a} = 0$,
- non-zero horizontal velocity of fluid in quay clearance: $f_{u_a} = 1$;

$$\frac{a_{22}(\omega)}{\rho LBD} = c_w\omega\{S_1(S_4-1) - S_0S_5\} + S_2S_4 + S_3S_5 + \\ - d_{sq}\omega^2\{S_0(S_4-1) + S_1S_5\} \quad , \tag{K.5}$$

$$\frac{b_{22}(\omega)}{\rho LBD}\frac{c_w}{g} = \frac{h}{c_w}\,\omega\left[c_w\omega\{S_0(S_4-1) + S_1S_5\} + S_3S_4 - S_2S_5 + \\ - d_{sq}\omega^2\{S_1(S_4-1) - S_0S_5\}\right] \quad , \tag{K.6}$$

with $$S_0 = \frac{Dd_{sq}c_w^2(h-D)}{\omega^4 d_{sq}^2 B^2 h^2 + \omega^2 d_{sq} c_w^2 (h-D)\{d_{sq}(h-D)-2Bh\} + c_w^4(h-D)^2} \quad ,$$

$$S_1 = \frac{c_w D\{\omega^2 d_{sq} Bh - c_w^2(h-D)\}}{\omega^4 d_{sq}^2 B^2 h^2 + \omega^2 d_{sq} c_w^2 (h-D)\{d_{sq}(h-D)-2Bh\} + c_w^4(h-D)^2}\frac{1}{\omega} \quad ,$$

$$S_2 = \frac{Dc_w^2(h-D)}{c_w^2(h-D)^2 + \omega^2B^2h^2} \quad ,$$

$$S_3 = \frac{BDhc_w\omega}{c_w^2(h-D)^2 + \omega^2B^2h^2} \quad ,$$

$$S_4 = \frac{\alpha \sinh(\alpha L) + \beta \sin(\beta L)}{\frac{1}{2}L(\alpha^2+\beta^2)\{\cosh(\alpha L) + \cos(\beta L)\}} \quad ,$$

$$S_5 = \frac{\alpha \sin(\beta L) - \beta \sinh(\alpha L)}{\frac{1}{2}L(\alpha^2+\beta^2)\{\cosh(\alpha L) + \cos(\beta L)\}} \quad ,$$

$$\alpha = \sqrt{-\frac{1}{2}a + \frac{1}{2}\sqrt{a^2+b^2}} \quad ,$$

$$\beta = \sqrt{\frac{1}{2}a + \frac{1}{2}\sqrt{a^2+b^2}} \quad ,$$

$$a = \omega^2\left[\frac{1}{c_w^2} - \frac{Bh(h-D)}{d_{sq}\{c_w^2(h-D)^2 + \omega^2B^2h^2\}}\right] \frac{c_w^2}{gD} \quad ,$$

$$b = \omega \frac{c_w(h-D)^2}{d_{sq}\{c_w^2(h-D)^2 + \omega^2B^2h^2\}} \frac{c_w^2}{gD} \quad ,$$

$$a_{22}(0) = \rho LBD \frac{D}{h-D} \quad , \tag{K.7}$$

$$b_{22}(0) = 0 \quad , \tag{4.49^b}$$

$$\left.\begin{array}{lll} a_{22}(\infty) = 0 & \text{for} & \omega \neq \\ a_{22}(\infty) \to \pm\infty & \text{for} & \omega = \end{array}\right\} (2n-1)\pi \frac{\sqrt{gD}}{L} \quad , \quad n \to \infty \quad , \tag{K.8}$$

$$\left.\begin{array}{lll} b_{22}(\infty) = \rho LBD \frac{gD}{Bc_w} & \text{for} & \omega \neq \\ b_{22}(\infty) \to +\infty & \text{for} & \omega = \end{array}\right\} (2n-1)\pi \frac{\sqrt{gD}}{L} \quad , \quad n \to \infty \quad . \tag{K.9}$$

Appendix L: Analytical determination of $k_{22}(t)$ near a vertical wall applying strip theory

Starting from the set of linearized equations (4.21), (4.31) and (4.32) the i.r.f. for the sway motion near a vertical wall can be determined analytically, if the following simplification is introduced: the horizontal velocity in the quay clearance, $\breve{u}_a(x_1,t)$, is left out of consideration, which implies independence of x_1 (i.e. strip theory). The expression (4.21) then leads to the identity $0 \equiv 0$, and -with $f_2(t)$ according to (4.51)- (4.31) and (4.32) change into:

$$a_2\ddot{x}_2 + a_1\dot{x}_2 + b_2\ddot{\zeta}_a + b_1\dot{\zeta}_a + b_0\zeta_a = 0 \qquad \text{(L.1)}$$

and

$$c_2\ddot{x}_2 + c_1\dot{x}_2 - d_2\ddot{\zeta}_a - d_1\dot{\zeta}_a - b_0\zeta_a = \frac{1}{\rho LBD}\zeta_2\delta_2(t-t_0) \quad , \quad \zeta_2 = 1 \quad , \qquad \text{(L.2)}$$

respectively, where

$$a_2 = \frac{D}{d_{sq}}\left\{\frac{d_{sq}}{h-D} + \frac{1}{2}f_{w_a}\frac{D}{B}\right\} \quad , \qquad a_1 = \frac{1}{2}\alpha_1\frac{g(h+D)}{c_w(h-D)} \quad ,$$

$$b_2 = \frac{d_{sq}}{h-D} + f_{w_a}\frac{D}{B} \quad , \qquad b_1 = \frac{gd_{sq}}{Bc_w}\left\{1 + \alpha_1\frac{B}{h-D}\right\} \quad , \qquad b_0 = \frac{g}{B} \quad ,$$

$$c_2 = 1 - \frac{1}{6}f_{w_a}\frac{D^2}{Bd_{sq}} \quad , \qquad c_1 = \frac{1}{2}\alpha_1\frac{c_w}{D} \quad ,$$

$$d_2 = \frac{1}{2}f_{w_a}\frac{D}{B} \quad , \qquad d_1 = \frac{gd_{sq}}{Bc_w}\left\{1 - \frac{1}{2}\alpha_1\frac{B}{D}\right\} \quad .$$

Laplace transformation of (L.1) and (L.2) yields:

$$a_2\left[sL\{\dot{x}_2(t)\} - \dot{x}_2(0^+)\right] + a_1L\{\dot{x}_2(t)\} + b_2\left[s^2L\{\zeta_a(t)\} - s\zeta_a(0^+) - \dot{\zeta}_a(0^+)\right] +$$

$$+ b_1\left[sL\{\zeta_a(t)\} - \zeta_a(0^+)\right] + b_0L\{\zeta_a(t)\} = 0 \quad ,$$

$$c_2\left[sL\{\dot{x}_2(t)\}-\dot{x}_2(0^+)\right] + c_1L\{\dot{x}_2(t)\} - d_2\left[s^2L\{\zeta_a(t)\} - s\zeta_a(0^+) - \dot{\zeta}_a(0^+)\right] +$$

$$- d_1\left[sL\{\zeta_a(t)\} - \zeta_a(0^+)\right] - b_0L\{\zeta_a(t)\} = \frac{1}{\rho LBD}\,\zeta_2 e^{-t_0 s} \quad ,$$

with $\dot{x}_2(0^+) = 0 \quad , \quad \zeta_a(0^+) = 0 \quad , \quad \dot{\zeta}_a(0^+) = 0 \quad .$

Elimination of $L\{\zeta_a(t)\}$ from these two equations leads to the following expression for $L\{\dot{x}_2(t)\}$:

$$L\{\dot{x}_2(t)\} = \zeta_2 A\, F(s) e^{-t_0 s} \quad , \quad \zeta_2 = 1 \quad , \tag{L.3}$$

where

$$A = \frac{1}{\rho LBD}\,\frac{b_2}{\alpha_3} \quad ,$$

$$F(s) = \frac{s^2 + p_1 s + q_1}{s^3 + p_0 s^2 + q_0 s + r_0} \quad ,$$

with

$$p_0 = \frac{\alpha_2}{\alpha_3} \quad , \quad q_0 = \frac{\alpha_1}{\alpha_3} \quad , \quad r_0 = \frac{\alpha_0}{\alpha_3} \quad ,$$

$$p_1 = \frac{b_1}{b_2} \quad , \quad q_1 = \frac{b_0}{b_2} \quad ,$$

$$\alpha_0 = b_0(a_1 + c_1) \quad ,$$

$$\alpha_1 = a_1d_1 + a_2b_0 + b_0c_2 + b_1c_1 \quad ,$$

$$\alpha_2 = a_1d_2 + a_2d_1 + b_1c_2 + b_2c_1 \quad ,$$

$$\alpha_3 = a_2d_2 + b_2c_2 \quad .$$

The denominator of F(s) can be factorized. To that end the cubic equation with real coefficients

$$s^3 + p_0 s^2 + q_0 s + r_0 = 0$$

is considered; for the determination of its roots it is referred to ref. [110] and Appendix J. Let these roots be represented by

$$s_m = \xi_m - \frac{p_0}{3} \quad , \quad m = 1,2,3 \quad ,$$

where s_m = certain complex number;
then ξ_m satisfies the following cubic equation with real coefficients:

$$\xi^3 + a_\alpha \xi + b_\alpha = 0 \quad ,$$

where

$$a_\alpha = \frac{1}{3}(3q_0 - p_0^2) \quad ,$$

$$b_\alpha = \frac{1}{27}(2p_0^3 - 9p_0 q_0 + 27r_0) \quad .$$

Then it generally holds good that

$$\xi_1 = A_c + B_c \quad , \quad \xi_2 = \varepsilon A_c + \varepsilon^2 B_c \quad , \quad \xi_3 = \varepsilon^2 A_c + \varepsilon B_c \quad ,$$

with

$$A_c = \sqrt[3]{-\frac{b_\alpha}{2} + \sqrt{K_\alpha}} \quad , \quad B_c = \sqrt[3]{-\frac{b_\alpha}{2} - \sqrt{K_\alpha}} \quad ,$$

$$K_\alpha = \frac{b_\alpha^2}{4} + \frac{a_\alpha^3}{27} \quad ,$$

$$\varepsilon = -\frac{1}{2}\left(1 - i\sqrt{3}\right) \quad , \quad \varepsilon^2 = -\frac{1}{2}\left(1 + i\sqrt{3}\right) \quad , \quad \varepsilon^3 = 1 \quad .$$

By means of the real quantity K_α three cases can be distinguished with respect to the roots ξ_1, ξ_2 and ξ_3:

I : $K_\alpha > 0$, i.e. there is one real root (ξ_1) and there are two roots (ξ_2 and ξ_3) which are complex conjugated:

$$\xi_1 = A_c + B_c \quad , \quad \xi_2 = -\frac{A_c + B_c}{2} + \frac{A_c - B_c}{2}\, i\sqrt{3} \quad ,$$

$$\xi_3 = -\frac{A_c + B_c}{2} - \frac{A_c - B_c}{2}\, i\sqrt{3} \quad ;$$

II : $K_\alpha = 0$, i.e. there are three real roots of which two (ξ_2 and ξ_3) are equal:

$$\xi_1 = 2\sqrt[3]{-\frac{b_\alpha}{2}} \quad , \quad \xi_2 = \xi_3 = -\sqrt[3]{-\frac{b_\alpha}{2}} \quad ;$$

III: $K_\alpha < 0$, i.e. there are three different real roots:

$$\xi_1 = 2(r_\alpha)^{1/3}\cos(\tfrac{\phi}{3}) \quad , \quad \xi_2 = 2(r_\alpha)^{1/3}\cos\left(\frac{\phi+2\pi}{3}\right) \quad ,$$

$$\xi_3 = 2(r_\alpha)^{1/3}\cos\left(\frac{\phi+4\pi}{3}\right) \quad ,$$

with

$$r_\alpha = \sqrt{-\frac{a_\alpha^3}{27}} \quad , \quad \phi = \arccos\left(-\frac{b_\alpha}{2r_\alpha}\right) \quad .$$

The inverse Laplace transform of (L.3) can be written as

$$\dot{x}_2(t) = \zeta_2 A\ f(t-t_0)\ U(t-t_0) \quad , \quad \zeta_2 = 1 \quad ,$$

where $f(t) = L^{-1}\{F(s)\}$ = inverse Laplace transform of $F(s)$.
With (4.52) this yields

$$k_{22}(t-t_0) = A\ f(t-t_0)\ U(t-t_0) \quad .$$

Replacing $t-t_0$ by t the i.r.f. finally takes the form

$$k_{22}(t) = A\ f(t)\ U(t) \quad . \tag{L.4}$$

What now remains to be done is a further specification and elaboration of the three distinct cases in order to find appropriate expressions for the function $f(t)$.

Case I : $K_\alpha > 0$, i.e. s_1 is real, s_2 and s_3 are complex conjugated;

$$F(s) = \frac{s^2 + p_1 s + q_1}{s^3 + p_0 s^2 + q_0 s + r_0} = \frac{D_1}{s-s_1} + \frac{D_2}{s-s_2} + \frac{D_3}{s-s_3} \quad ;$$

$$s_1 = P_1 \quad , \quad s_2 = R_1 + iQ_1 \quad , \quad s_3 = R_1 - iQ_1 \quad ,$$

$$P_1 = A_c + B_c - \frac{p_0}{3} \quad , \quad Q_1 = \frac{A_c - B_c}{2}\sqrt{3} \quad , \quad R_1 = -\frac{A_c + B_c}{2} - \frac{p_0}{3} \quad ;$$

$$f(t) = L^{-1}\{F(s)\} = D_1 e^{s_1 t} + D_2 e^{s_2 t} + D_3 e^{s_3 t} \quad ;$$

$$D_1 = \frac{-p_1 s_1 - q_1 - s_1^2}{(s_1 - s_2)(s_3 - s_1)} = \frac{P_1^2 + p_1 P_1 + q_1}{(P_1 - R_1)^2 + Q_1^2} \quad , \quad e^{s_1 t} = e^{+P_1 t} \quad ,$$

$$D_2 = \frac{-p_1 s_2 - q_1 - s_2^2}{(s_1 - s_2)(s_2 - s_3)} = \frac{1}{2}(M + iN) \quad , \quad e^{s_2 t} = e^{R_1 t} e^{iQ_1 t} \quad ,$$

$$D_3 = \frac{-p_1 s_3 - q_1 - s_3^2}{(s_2 - s_3)(s_3 - s_1)} = \frac{1}{2}(M - iN) \quad , \quad e^{s_3 t} = e^{R_1 t} e^{-iQ_1 t} \quad ,$$

$$M = -\frac{P_1(p_1 + R_1) + P_1 R_1 - R_1^2 - Q_1^2 + q_1}{(P_1 - R_1)^2 + Q_1^2} \quad ,$$

$$N = \frac{(P_1 - R_1)\{q_1 + R_1(p_1 + R_1)\} - Q_1^2\{(p_1 + R_1) + P_1\}}{Q_1\{(P_1 - R_1)^2 + Q_1^2\}} \quad .$$

The i.r.f. now can be written as:

$$k_{22}(t) = A\left[D_1 e^{+P_1 t} + \{M\cos(Q_1 t) - N\sin(Q_1 t)\}e^{+R_1 t}\right] U(t) \quad . \qquad \text{(L.5)}$$

Case II : $K_\alpha = 0$, i.e. s_1, s_2 and s_3 are real, $s_2 = s_3$;

$$F(s) = \frac{s^2 + p_1 s + q_1}{s^3 + p_0 s^2 + q_0 s + r_0} = \frac{D_4}{s-s_1} + \frac{D_5}{s-s_2} + \frac{D_6}{(s-s_2)^2} \quad ;$$

$$s_1 = 2\sqrt[3]{-\frac{b_\alpha}{2}} - \frac{p_0}{3} \quad , \quad s_2 = -\sqrt[3]{-\frac{b_\alpha}{2}} - \frac{p_0}{3} \quad ;$$

$$f(t) = L^{-1}\{F(s)\} = D_4 e^{s_1 t} + D_5 e^{s_2 t} + D_6 t\ e^{s_2 t} \quad ;$$

$$D_4 = \frac{s_1^2 + p_1 s_1 + q_1}{(s_2 - s_1)^2} \quad ,$$

$$D_5 = \frac{s_2^2 - 2s_1 s_2 - p_1 s_1 - q_1}{(s_2 - s_1)^2} \quad ,$$

$$D_6 = \frac{s_2^2 + p_1 s_2 + q_1}{s_2 - s_1} \quad ;$$

This leads to an i.r.f. of the form:

$$k_{22}(t) = A\{D_4 e^{s_1 t} + D_5 e^{s_2 t} + D_6 t\ e^{s_2 t}\}\ U(t) \quad . \tag{L.6}$$

Case III: $K_\alpha < 0$, i.e. s_1, s_2 and s_3 are real and different from one another;

$$F(s) = \frac{s^2 + p_1 s + q_1}{s^3 + p_0 s^2 + q_0 s + r_0} = \frac{D_1}{s-s_1} + \frac{D_2}{s-s_2} + \frac{D_3}{s-s_3} \quad ;$$

$$s_1 = 2(r_\alpha)^{1/3}\cos\left(\frac{\phi}{3}\right) - \frac{p_0}{3} \quad , \quad s_2 = 2(r_\alpha)^{1/3}\cos\left(\frac{\phi+2\pi}{3}\right) - \frac{p_0}{3} \quad ,$$

$$s_3 = 2(r_\alpha)^{1/3}\cos\left(\frac{\phi+4\pi}{3}\right) - \frac{p_0}{3} \quad ;$$

$$f(t) = L^{-1}\{F(s)\} = D_1 e^{s_1 t} + D_2 e^{s_2 t} + D_3 e^{s_3 t} \quad ;$$

$$D_1 = \frac{-p_1 s_1 - q_1 - s_1^2}{(s_1 - s_2)(s_3 - s_1)} \quad ,$$

$$D_2 = \frac{-p_1 s_2 - q_1 - s_2^2}{(s_1 - s_2)(s_2 - s_3)} \quad ,$$

$$D_3 = \frac{-p_1 s_3 - q_1 - s_3^2}{(s_2 - s_3)(s_3 - s_1)} \quad ;$$

The corresponding i.r.f. then becomes:

$$k_{22}(t) = A\left(D_1 e^{s_1 t} + D_2 e^{s_2 t} + D_3 e^{s_3 t}\right) U(t) \quad . \tag{L.7}$$

A specific, simple case arises when -besides the horizontal velocity- also the vertical acceleration in the quay clearance and the underkeel friction effect are left out of consideration. This implies in (L.1) and (L.2) $f_{w_a} = 0$ and $\alpha_1 = 0$. The three cases which can be distinguished with respect to the sign of the characteristic quantity K_α now lead to the following expressions for $k_{22}(t)$.

Case I : $K_\alpha > 0$, i.e. $d_{sq} < 4B$; (L.5) then reduces to:

$$k_{22}(t) = \frac{1}{\rho LBD} \left[1 - \frac{D}{h} + \frac{D}{h}\{\cos(r_2 t) - \frac{r_1}{r_2} \sin(r_2 t)\} e^{-r_1 t}\right] U(t) \quad , \tag{L.8}$$

where $r_1 = \frac{c_w}{2B}$, $r_2 = r_1 \sqrt{\frac{4B}{d_{sq}} - 1}$.

Case II : $K_\alpha = 0$, i.e. $d_{sq} = 4B$; (L.6) now takes the form:

$$k_{22}(t) = \frac{1}{\rho LBD} \left\{1 - \frac{D}{h} + \frac{D}{h}(1 - r_1 t) e^{-r_1 t}\right\} U(t) \quad . \tag{L.9}$$

Case III: $K_\alpha < 0$, i.e. $d_{sq} > 4B$; (L.7) then becomes:

$$k_{22}(t) = \frac{1}{\rho LBD} \left\{1 - \frac{D}{h} + \frac{D}{h} \frac{1}{r_3 - r_4} \left(r_3 e^{-r_3 t} - r_4 e^{-r_4 t}\right)\right\} U(t) \quad , \tag{L.10}$$

where $r_3 = r_1\left\{1 + \sqrt{1 - \frac{4B}{d_{sq}}}\right\}$, $r_4 = r_1\left\{1 - \sqrt{1 - \frac{4B}{d_{sq}}}\right\}$.

Appendix M: Estimation of the main frequencies figuring in the time history of ship berthing at a closed structure

The mathematical approach in the time domain to ship berthing at a closed structure can be represented by (4.58) and (4.59) with $f_2(t)$ given by (4.65) and initial conditions (4.66); in this, $X_0(t)$ and $Y_0(t)$ stand for the underkeel friction effect and are modelled in conformity with ($4.60^{b,c}$) and ($4.61^{b,c}$), respectively; further $Z_0(t)$ is according to (4.62) and $\lambda_b = 1.44$. Linearization of this set of equations with regard to terms containing combinations of x_2 and $\dot{\zeta}_a$ and/or their respective derivatives yields

$$\frac{D}{d_{sq}}\left\{\frac{d_{sq}}{h-D} + \frac{1}{2}f_{w_a}\frac{D}{B}\right\}\ddot{x}_2 + f_1\frac{6\nu}{(h-D)^2}\frac{h+D}{h-D}\dot{x}_2 +$$

$$+\left\{\frac{d_{sq}}{h-D} + f_{w_a}\frac{D}{B}\right\}\ddot{\zeta}_a + \frac{gd_{sq}}{Bc_w}\left\{1 + 2f_1\frac{6\nu}{(h-D)^2}\frac{Bh}{c_w(h-D)}\right\}\dot{\zeta}_a + \frac{g}{B}\zeta_a = 0 \qquad \text{(M.1)}$$

and

$$\left\{1 - \frac{1}{6}f_{w_a}\frac{D^2}{Bd_{sq}}\right\}\ddot{x}_2 + f_1\frac{6\nu}{(h-D)^2}\frac{h}{D}\dot{x}_2 +$$

$$-\frac{1}{2}f_{w_a}\frac{D}{B}\ddot{\zeta}_a - \frac{gd_{sq}}{Bc_w}\left\{1 - f_1\frac{6\nu}{(h-D)^2}\frac{Bh}{c_wD}\right\}\dot{\zeta}_a - \frac{g}{B}\zeta_a = -\frac{c_0}{\rho LBD}x_2 \qquad ; \qquad \text{(M.2)}$$

$f_2(t)$ was introduced into (4.59) with the restriction that only moments of time are considered during which there is contact between ship and fender, i.e. $x_2(t) \leq 0$. As expected the respective left-hand sides of (M.1) and (M.2) are identical to those of (L.1) and (L.2), on the understanding that α_1 has been replaced by $f_1\alpha_1$ with α_1 given by (4.9) and γ according to (3.20^b). Elimination of ζ_a from (M.1) and (M.2) leads to:

$$G_4\ddddot{x}_2 + G_3\dddot{x}_2 + G_2\ddot{x}_2 + G_1\dot{x}_2 + G_0x_2 = 0 \qquad , \qquad \text{(M.3)}$$

where

$$G_0 = \frac{g}{B}\frac{c_0}{\rho LBD} \qquad ,$$

$$G_1 = \frac{c_0}{\rho LBD}\,\frac{gd_{sq}}{Bc_w} + f_1\,\frac{6\nu}{(h-D)^2}\,\left\{\frac{2d_{sq}}{h-D}\,\frac{c_0}{\rho LBD} + \frac{g}{B}\left(\frac{h}{D} + \frac{h+D}{h-D}\right)\right\} \quad ,$$

$$G_2 = \frac{g}{B}\left(\frac{h}{h-D} + \frac{1}{3}f_{w_a}\,\frac{D^2}{Bd_{sq}}\right) + \frac{c_0}{\rho LBD}\left(\frac{d_{sq}}{h-D} + f_{w_a}\,\frac{D}{B}\right) +$$

$$+ f_1\,\frac{6\nu}{(h-D)^2}\,\frac{gd_{sq}}{Bc_w}\left(\frac{h}{D} + \frac{h+D}{h-D}\right) + \frac{d_{sq}}{D}\left\{f_1\,\frac{6\nu}{(h-D)^2}\right\}^2 \quad ,$$

$$G_3 = \frac{gd_{sq}}{Bc_w}\left(\frac{h}{h-D} + \frac{1}{3}f_{w_a}\,\frac{D^2}{Bd_{sq}}\right) + f_1\,\frac{6\nu}{(h-D)^2}\,\frac{d_{sq}}{D}\,\frac{h+D}{h-D} +$$

$$+ f_1 f_{w_a}\,\frac{6\nu}{(h-D)^2}\,\frac{h}{B}\left\{1 + \frac{2}{3}\,\frac{D^2}{h(h-D)}\right\} \quad ,$$

$$G_4 = \frac{d_{sq}}{h-D} + f_{w_a}\,\frac{D}{B} + \frac{1}{3}f_{w_a}\,\frac{D^2}{Bd_{sq}}\left(\frac{d_{sq}}{h-D} + \frac{1}{4}f_{w_a}\,\frac{D}{B}\right) \quad .$$

Expression (M.3) is a linear, homogeneous, ordinary differential equation of the fourth order with constant, real, positive coefficients. Its solution can be written as the sum of four exponential functions. The fact that the fender is linear plays an important part in the process of linearization. The characteristic equation of (M.3) reads as:

$$G_4\chi^4 + G_3\chi^3 + G_2\chi^2 + G_1\chi + G_0 = 0 \quad , \qquad \text{(M.4)}$$

where χ_m = root of fourth-degree characteristic equation (m = 1,2,3,4).
Now let

$$G_0, G_1, G_2 \gg G_3, G_4 \quad .$$

Then in (M.3) a 'main (second-order) system' can be distinguished of the form

$$G_2\ddot{x}_2 + G_1\dot{x}_2 + G_0 x_2 = 0 \quad , \qquad \text{(M.5)}$$

with (circular) frequency $\sqrt{\dfrac{G_0}{G_2} - \dfrac{G_1^2}{4G_2^2}}$

and damping constant $\frac{G_1}{2G_2}$;
its characteristic equation becomes:

$$G_2\kappa^2 + G_1\kappa + G_0 = 0 \quad ,$$

where κ_m = root of second-degree characteristic equation (m = 1,2).
Supposing that (M.5) represents a weakly damped system, i.e.

$$\frac{G_1}{2G_2} < \sqrt{\frac{G_0}{G_2}} \quad ,$$

it can be stated that two out of the four roots of (M.4) are in the proximity of:

$$\kappa = -\frac{G_1}{2G_2} \pm i\sqrt{\frac{G_0}{G_2} - \frac{G_1^2}{4G_2^2}} \quad . \tag{M.6}$$

These two roots in question can be approximated by

$$\chi = (1+\varepsilon)\kappa \quad , \tag{M.7}$$

where ε = small (complex) parameter, $|\varepsilon| < 1$.
Substitution of this expression for χ into (M.4) yields

$$G_4(1+\varepsilon)^4\kappa^4 + G_3(1+\varepsilon)^3\kappa^3 + G_2(1+\varepsilon)^2\kappa^2 + G_1(1+\varepsilon)\kappa + G_0 = 0 \quad . \tag{M.8}$$

With the orders of magnitude of (G_0,G_1,G_2) and (G_3,G_4) supposed to be in the proportion 1 to ε, (M.8) can be simplified to be:

$$G_4\kappa^4 + G_3\kappa^3 + G_2(1+2\varepsilon)\kappa^2 + G_1(1+\varepsilon)\kappa + G_0 = 0 \quad , \tag{M.9}$$

from which it follows

$$\varepsilon = -\frac{G_0+G_1\kappa+G_2\kappa^2+G_3\kappa^3+G_4\kappa^4}{2G_2\kappa^2+G_1\kappa} \quad . \tag{M.10}$$

Eliminating κ and ε from (M.7) by means of (M.6) and (M.10) χ_1 and χ_2 can be written as:

$$\chi_1 = (1+\varepsilon)\kappa_1 = -\beta_I + i\omega_I \quad , \quad \chi_2 = (1+\varepsilon)\kappa_2 = -\beta_I - i\omega_I \quad , \tag{M.11}$$

where

$$\beta_I = \frac{G_1}{2G_2}\left\{1 - \frac{G_3}{G_1}\left(\frac{G_0}{G_2} - \frac{G_1^2}{G_2^2}\right) + 2\frac{G_4}{G_2}\left(\frac{G_0}{G_2} - \frac{G_1^2}{2G_2^2}\right)\right\} \quad , \tag{M.12^a}$$

$$\omega_I = \sqrt{\frac{G_0}{G_2} - \frac{G_1^2}{4G_2^2}} + \frac{\frac{G_1G_3}{2G_2}\left(\frac{3G_0}{G_2} - \frac{G_1^2}{G_2^2}\right) + G_4\left(\frac{G_1^4}{2G_2^4} - \frac{2G_0G_1^2}{G_2^3} + \frac{G_0^2}{G_2^2}\right)}{\sqrt{4G_0G_2 - G_1^2}} \quad ; \tag{M.12^b}$$

as expected χ_1 and χ_2 are complex conjugated. ω_I represents a (circular) frequency corresponding with a period time $T_I = 2\pi/\omega_I$, and β_I is a damping constant. Half the period time, i.e. $T_I/2$, now has to be considered as an approximation for the duration of time of the contact between ship and fender. It has to be noted that the respective values of β_I and ω_I are higher than those of the damping constant and circular frequency of the 'main (second-order) system' represented by (M.5). The pair of roots χ_1 and χ_2 defines the following quadratic equation:

$$(\chi-\chi_1)(\chi-\chi_2) = \chi^2 + (1+\varepsilon)\,\frac{G_1}{G_2}\,\chi + (1+2\varepsilon+\varepsilon^2)\,\frac{G_0}{G_2} =$$

$$\simeq \chi^2 + (1+\varepsilon)\,\frac{G_1}{G_2}\,\chi + (1+2\varepsilon)\,\frac{G_0}{G_2} \quad ,$$

since $\varepsilon^2 << 1$. The remaining two roots of the characteristic equation (M.4) now are determined by the fraction

$$\frac{G_4\chi^4+G_3\chi^3+G_2\chi^2+G_1\chi+G_0}{\chi^2+(1+\varepsilon)\frac{G_1}{G_2}\chi+(1+2\varepsilon)\frac{G_0}{G_2}} =$$

$$= G_4\chi^2 + \left\{G_3-(1+\varepsilon)\frac{G_1G_4}{G_2}\right\}\chi + \left\{G_2-(1+2\varepsilon)\frac{G_0G_4}{G_2} - (1+\varepsilon)\frac{G_1G_3}{G_2} + (1+\varepsilon)^2\,\frac{G_1^2G_4}{G_2^2}\right\} \quad ,$$

with

$$\text{remainder} = \{-\varepsilon G_1-(1+2\varepsilon)\frac{G_0G_3}{G_2} + (1+\varepsilon)(1+2\varepsilon)\frac{2G_0G_1G_4}{G_2^2} + (1+\varepsilon)^2\,\frac{G_1^2G_3}{G_2^2} + - (1+\varepsilon)^3\,\frac{G_1^3G_4}{G_2^3}\}\chi +$$

$$+ \{-2\varepsilon G_0 + (1+2\varepsilon)^2\,\frac{G_0^2G_4}{G_2^2} + (1+\varepsilon)(1+2\varepsilon)\frac{G_0G_1G_3}{G_2^2} + - (1+2\varepsilon)(1+\varepsilon)^2\,\frac{G_0G_1^2G_4}{G_2^3}\} \quad .$$

Taking into account the order of magnitude of (G_0,G_1,G_2) and (G_3,G_4) these expressions can be written as:

$$\frac{G_4\chi^4+G_3\chi^3+G_2\chi^2+G_1\chi+G_0}{\chi^2+(1+\varepsilon)\frac{G_1}{G_2}\,\chi+(1+2\varepsilon)\frac{G_0}{G_2}} = G_4\chi^2 + \{G_3 - \frac{G_1G_4}{G_2}\}\chi + \{G_2 - \frac{G_0G_4+G_1G_3}{G_2} + \frac{G_1^2G_4}{G_2^2}\} \quad ,$$

$$\text{remainder} = \{-\varepsilon G_1 - \frac{G_0G_3}{G_2} + \frac{2G_0G_1G_4}{G_2^2} + \frac{G_1^2G_3}{G_2^2} - \frac{G_1^3G_4}{G_2^3}\}\chi +$$

$$+ \{-2\varepsilon G_0 + \frac{G_0^2G_4}{G_2^2} + \frac{G_0G_1G_3}{G_2^2} - \frac{G_0G_1^2G_4}{G_2^3}\} \quad .$$

With the remainder supposed to be small with respect to the denominator of the above fraction the reduced form of the characteristic equation (M.4) becomes:

$$G_4\chi^2 + \{G_3 - \frac{G_1G_4}{G_2}\}\chi + \{G_2 - \frac{G_0G_4+G_1G_3}{G_2} + \frac{G_1^2G_4}{G_2^2}\} = 0 \quad . \tag{M.13}$$

Assuming that (M.13) represents the characteristic equation of a weakly damped system, i.e.

$$\frac{1}{2}\left(\frac{G_3}{G_4} - \frac{G_1}{G_2}\right) < \frac{1}{G_2}\sqrt{\frac{G_2^3 - G_2(G_0G_4+G_1G_3) + G_1^2G_4}{G_4}} \quad ,$$

its damping constant and (circular) frequency are

$$\beta_{II} = \frac{1}{2}\left(\frac{G_3}{G_4} - \frac{G_1}{G_2}\right) \quad , \tag{M.14^a}$$

$$\omega_{II} = \sqrt{\left(\frac{G_0}{G_2} - \frac{G_1^2}{4G_2^2}\right) + \frac{G_2}{G_4} - 2\left(\frac{G_0}{G_2} - \frac{G_1^2}{2G_2^2}\right) - \frac{G_3}{2G_4}\left(\frac{G_1}{G_2} + \frac{G_3}{2G_4}\right)} \quad , \tag{M.14^b}$$

respectively. The values of β_{II} and ω_{II} have to be conceived as approximations. Dependent on the values of the respective input quantities the (circular) frequency ω_{II} may be discerned as a fast(er) oscillation with period time $T_{II} = 2\pi/\omega_{II}$ on the time histories of the fender force and the water-surface elevation in the quay clearance.

Appendix N: Estimation of the shear stress in the underkeel region in case of transient fluid motion

Consider the two-dimensional motion of a viscous fluid, under pressure, between two horizontal, fixed, parallel walls. Let the lower wall coincide with the x_2-axis of a just as well fixed, rectangular ox_2x_3-co-ordinate system. The linearized boundary-layer equations as related to the lower wall then read (see ref. [98]):

$$\frac{\partial p}{\partial x_3} = 0 \quad \text{in the boundary layer,} \tag{N.1}$$

$$\frac{\partial v}{\partial t} = -\frac{1}{\rho}\frac{\partial p}{\partial x_2} + \nu \frac{\partial^2 v}{\partial x_3^2} \quad , \tag{N.2}$$

$$\frac{\partial v}{\partial x_2} + \frac{\partial w}{\partial x_3} = 0 \quad . \tag{N.3}$$

Expression (N.1) states that, when proceeding normally to the wall, the pressure does not vary and is equal to the pressure just outside the boundary layer.
The horizontal scale is supposed to be much larger than the vertical scale, which implies

$$\frac{\partial w}{\partial x_3} = 0 \quad , \quad w = 0 \quad ,$$

so that $v = v(x_3,t)$.

When $v = v(x_3,t)$ and $p = p(x_2,t)$ are supposed to be uniformly convergent, Laplace transformation of (N.2) with respect to t leads to

$$sV - v(x_3,0^+) = -\frac{1}{\rho}\frac{\partial P}{\partial x_2} + \nu \frac{\partial^2 V}{\partial x_3^2} \quad , \tag{N.4}$$

where $V = V(x_3,s)$ and $P = P(x_2,s)$ are the unilateral, one-dimensional Laplace transforms of $v(x_3,t)$ and $p(x_2,t)$, respectively, with respect to t. Assuming a state of rest for $t \leqq 0$, it applies $v(x_3,0^+) = 0$, so that (N.4) can be put into the form

$$\frac{\partial^2 V}{\partial x_3^2} - \frac{s}{\nu}V = \frac{1}{\rho\nu}\frac{\partial P}{\partial x_2} \quad , \tag{N.5}$$

which has as its solution

$$V(x_3,s) = A(s)e^{x_3\sqrt{\frac{s}{\nu}}} + B(s)e^{-x_3\sqrt{\frac{s}{\nu}}} - \frac{1}{\rho s}\frac{\partial P}{\partial x_2} \quad ; \tag{N.6}$$

$A(s)$ and $B(s)$ are constants of integration.
The condition at the outer edge of the boundary layer -implying that its thickness is considered to be relatively small- reads as

$$\frac{\partial V}{\partial x_3} = 0 \quad \text{for} \quad x_3 \to \infty \quad , \tag{N.7^a}$$

and yields $A(s) = 0$; the condition at the wall is that of adherence,

$$V(x_3,s) = 0 \quad \text{for} \quad x_3 = 0 \quad , \tag{N.7^b}$$

leading to

$$B(s) = \frac{1}{\rho s}\frac{\partial P}{\partial x_2} \quad .$$

In this way (N.6) eventually becomes:

$$V(x_3,s) = \frac{1}{\rho}\frac{\partial P}{\partial x_2}\left\{\frac{1}{s}e^{-x_3\sqrt{\frac{s}{\nu}}} - \frac{1}{s}\right\} \quad . \tag{N.8}$$

Taking the inverse Laplace transform of (N.8) one obtains:

$$v(x_3,t) = \frac{1}{\rho}U(t)\int_0^t \frac{\partial p(x_2,\tau)}{\partial x_2}\left[\operatorname{erfc}\left\{\frac{x_3}{2\sqrt{\nu(t-\tau)}}\right\} - 1\right]d\tau \quad . \tag{N.9}$$

$v(x_3,t)$ as given by (N.9) is the transient horizontal flow velocity in the boundary layer; the influence of the viscosity is represented by the complementary error function, indicated as erfc, in the integrand. It has to be noted that indeed $v(x_3,0) = 0$, since it holds good that $\operatorname{erfc}(z) \to 0$ as $z \to \infty$.
Therefore the influence of the viscosity is small as

$$\frac{x_3}{2\sqrt{\nu t_*}} >> 1 \qquad ,$$

where t_* represents a time scale. The boundary-layer thickness then has an order of magnitude amounting to $2\sqrt{\nu t_*}$. With respect to the underkeel region this implies that condition (N.7[a]) is satisfied for $x_3 \approx \frac{1}{2}(h-D)$, if

$$\frac{4\sqrt{\nu t_*}}{h-D} << 1 \qquad ;$$

in that case the boundary layer developing at the lower wall does not enter into the upper part of the keel clearance (and vice versa).

The horizontal retarding force on a fluid lamina, per unit area, can be derived to be:

$$\rho\nu \frac{\partial v}{\partial x_3} = -\sqrt{\frac{\nu}{\pi}}\, U(t) \int_0^t \frac{\partial p(x_2,\tau)}{\partial x_2} \frac{\exp\{-\frac{x_3^2}{4\nu(t-\tau)}\}}{\sqrt{t-\tau}} d\tau \qquad ; \qquad \text{(N.10)}$$

for $x_3 = 0$ this yields at the rigid lower wall:

$$\rho\nu \left.\frac{\partial v}{\partial x_3}\right|_{x_3=0} = -\sqrt{\frac{\nu}{\pi}}\, U(t) \int_0^t \frac{\partial p(x_2,\tau)}{\partial x_2} \frac{1}{\sqrt{t-\tau}} d\tau \qquad . \qquad \text{(N.11)}$$

Now (N.11) might be applied as an expression for the shear stress at the fluid-wall interfaces in the underkeel region in case the water motion has a transient character. This implies that, by way of example,

$$\left.\tau_{2,b}\right|_{bottom} = \rho\nu \left.\frac{\partial v}{\partial x_3}\right|_{x_3=0} \qquad . \qquad \text{(N.12)}$$

In order to give a simple idea of the transient behaviour of the shear stress, (N.11) and (N.12) are used to make a rough estimate for its actual value at the bottom boundary of the underkeel region. On account of (4.7[a,b]) the pressure gradient in the integrand of (N.11) might be approximated in the first instance by

$$\frac{\partial p(x_2,\tau)}{\partial x_2} \simeq \frac{\partial p_b}{\partial x_2} \simeq -\rho\,\frac{\partial \bar{v}_b}{\partial t} \simeq -\rho\,\frac{\bar{v}_{b*}}{t_*} \quad ,$$

where t_* now represents the time scale of the variation $\bar{v}_{b*}$ of $\bar{v}_b$; $\bar{v}_{b*}$ is supposed to be independent of τ. Since

$$\int_0^t \frac{1}{\sqrt{t-\tau}}\,d\tau = 2\sqrt{t} \simeq 2\sqrt{t_*} \quad ,$$

it then can be written:

$$\tau_{2,b}\Big|_{\text{bottom}} \simeq \frac{2\rho\bar{v}_{b*}}{\sqrt{\pi}}\sqrt{\frac{\nu}{t_*}} \quad , \tag{N.13}$$

which bears out that the more transient the underkeel fluid motion is, the larger the shear stress at a solid boundary. This is quite unlike the corresponding situation of steady, viscous, pressure flow between two parallel plates, with fully developed boundary layers, where it holds (see Section 3.2.1.3)

$$\tau_{2,b}\Big|_{\text{bottom}} = \gamma\bar{v}_b \quad , \quad \gamma = \frac{6\rho\nu}{h-D} \quad .$$